GROUND SUBSIDENCE STUDY REPORT
CONCORAN SUBSIDENCE BOWL

San Joaquin Valley, California

Prepared for:

California High Speed Rail Authority

Prepared by:

Amec Foster Wheeler Environment & Infrastructure, Inc.
180 Grand Avenue, Suite 1100
Oakland, California 94612

December 2017

Project No. 8715180680

GROUND SUBSIDENCE STUDY REPORT
CORCORAN SUBSIDNECE BOWL
California High-Speed Rail Project
San Joaquin Valley, California
Agreement No. HSR 14-31

December 2017
Project 8715180680

This report was prepared by the staff of Amec Foster Wheeler and their subconsultants under the supervision of the Engineers whose seal and signatures appear hereon.

The findings, recommendations, specifications, or professional opinions are presented within the limits described by the client, in accordance with generally accepted professional engineering and geologic practice. No warranty is expressed or implied.

Michael L. Rucker, PE
Associate Geotechnical Engineer
Amec Foster Wheeler Environment & Infrastructure, Inc.

Chin Man Mok, PhD, PE, GE, PG
Principal Engineer
GSI Environmental, Inc.

REGISTERED PROFESSIONAL ENGINEER
JAMES B. FRENCH
No. 2018
Exp. 6/30/2018
GEOTECHNICAL
STATE OF CALIFORNIA

James B. French, PE, GE
Principal Engineer and Project Manager
Amec Foster Wheeler Environment & Infrastructure, Inc.

TABLE OF CONTENTS

Page

TABLE OF CONTENTS
(Cont'd)

TABLE OF CONTENTS
(Continued)

TABLE OF CONTENTS
(Cont'd)

TABLE OF CONTENTS
(Continued)

TABLE OF CONTENTS
(Cont'd)

TABLES (EMBEDDED WITHIN TEXT)

TABLES AT END OF TEXT

TABLE OF CONTENTS
(Continued)

FIGURES EMBEDDED WITHIN TEXT

TABLE OF CONTENTS
(Cont'd)

PLATES

TABLE OF CONTENTS
(Continued)

TABLE OF CONTENTS
(Cont'd)

LIST OF APPENDICES

GROUND SUBSIDENCE STUDY REPORT
CONCORAN SUBSIDENCE BOWL
California High-Speed Rail Project
San Joaquin, California

ES.0 EXECUTIVE SUMMARY

The Amec Foster Wheeler Environment & Infrastructure, Inc. (AFW) team has performed a Ground Subsidence Study (GSS) for the California High-Speed Rail Authority (Authority), along and near to the portions of the proposed California High-Speed Rail Alignment (HSR Alignment) that will lie within the San Joaquin Valley (SJV) and Antelope Valley of California. The purpose of this study has been to evaluate the impact that subsidence may have on future HSR infrastructure and train performance. Our team has included AFW and our major subconsultant GSI Environmental, Inc. (GSI), and with assistance from Earth Mechanics, Inc. (EMI) and Moore Twining Associates, Inc. (MTA).

This GSS report focuses on the Corcoran Subsidence Bowl in the southern SJV. Much of Construction Package 2-3 (CP 2-3) and the northern portion of Construction Package 4 (CP 4) lie within the Corcoran Subsidence Bowl. The potential impacts of subsidence along other portions of the HSR Alignment, notably along Highway 152 (referred to herein as the El Nido subsidence bowl), and in Antelope Valley, are discussed in Appendices D and E, respectively.

ES.1 HISTORICAL SUBSIDENCE

ES.1.1 Background (see Section 3.0)

Over at least the past 90 years, groundwater drawdown due to groundwater withdrawals has induced subsidence over large areas within the SJV. Plate ES-1 is a map showing the observed subsidence from 1926 to 1970 and from 2007 to 2010, along the proposed HSR Alignment.

The Corcoran Subsidence Bowl sits in the Southern SJV between the Fresno and Bakersfield alluvial fans. Prior to the population growth and development of large-scale farming in the Southern SJV, the area to the west of the HSR Alignment was covered by the historical Tulare Lake, located in the topographically lowest region of the hydrologic basin at the time. Starting in the latter half of the 1800s, the lake has been dried up by farmers to create arable land. Although the former lakebed has been developed into agricultural land, flooding still periodically occurs in this area.

According to the United States Geologic Survey (USGS), subsidence in the SJV has been observed during much of the last century; from 1926 to 1970, there was as much as 28 feet of subsidence near Mendota to the northwest, and 14 feet in the Pixley portion of the Corcoran Subsidence Bowl area to the east of the HSR Alignment, as shown on Plate ES-1 with the

subsidence contour lines (subsidence from this time period is referred to as “1900s Historical Subsidence” in this report). During the same period, 1900s Historical Subsidence along the HSR Alignment in the Tulare Lake area may have been about 4 to 6 feet.

Following development of state and federal water projects, surface water became readily available and groundwater extraction was reduced, and subsidence due to groundwater drawdown was temporarily slowed or stopped. However, in the past 10 to 25 years, groundwater pumping has once again been increasing, with associated resumption and acceleration of groundwater drawdown and associated subsidence; this was exacerbated during a moderate to severe drought from Winter 2007 through Fall 2009, and a severe to exceptional drought from Winter 2012 through Fall 2016. The colors on Plate ES-1 show the magnitudes and patterns of subsidence from 2007 to 2010, which exceeded an average of 8 inches per year according to analyses by the Jet Propulsion Laboratory (JPL). Profiles of historical subsidence along the HSR Alignment, as well as profiles of induced changes in slope and vertical curvature, are presented on Plate ES-2. Toward the end of the recent drought, annual subsidence rates of 1 to 1½ feet have been observed near Corcoran in 2015-2016 (as shown in Figure 5-3). Groundwater pumping and drawdown, and consequent subsidence, are anticipated to continue into the future at least until sustainable groundwater pumping is achieved. Due to inelastic soil behavior, subsidence is mostly irreversible even if groundwater pumping decreases and groundwater level recovers.

The HSR Alignment for CP 2-3 passes nearly through the center of the Corcoran Subsidence Bowl, and the northern portion of Construction Package 4 (CP 4) lies within the southern portion of the Corcoran Subsidence Bowl. Further to the north, the El Nido Subsidence Bowl is located near Highway 152, in an area of future HSR contracts and extending south to the northern portion of Construction Package 1 (CP 1); subsidence in this area is addressed in Appendix D. Subsidence is also occurring along the HSR Alignment in Antelope Valley, which is addressed in Appendix E.

It has been recognized at least since the Fall of 2013 that subsidence in the SJV had the potential to impact the HSR (RDP 2015).

Due to uncertainties associated with subsidence, the Authority directed prospective Contractors for CP 2-3: “Unless directed otherwise by the Scope of Work, for bidding purposes assume that subsidence from groundwater pumping is not an impact to the project area” (Authority 2014a, Section 6.6.7) The Authority indicated they would then adjust design parameters if needed through design variances based on findings from a Ground Subsidence Study (GSS) to be developed under a separate contract. The GSS was also to provide the Authority with recommendations for future ground subsidence monitoring and mitigation measurements. This GSS report is a product of that study.

ES.1.2 Subsidence and Topographic Data

Observed broad areal subsidence data is available for three historical periods: (1) the USGS published a map showing the subsidence between 1926 and 1970 (Plate ES-1); (2) the JPL produced digital subsidence data between 2007 and 2010 based on their estimation using the Interferometric Synthetic Aperture Radar (InSAR) technology (also on Plate ES-1); (3) the JPL also provided digital subsidence data between 2015 and 2016 based on their interpretation of the Sentinel satellite InSAR data. The highest rates of subsidence were observed between 2015 and 2016 due to heavy groundwater pumping towards the end of a severe 4-year drought. Past subsidence is discussed in Section 5.0.

InSAR technology can identify changes in ground surface elevation, but it does not provide information about absolute elevations. There are several available elevation or topographic information sources: (1) The National Map published on-line by the USGS (2016) covers the entire SJV[1] and in the Corcoran area generally represents elevations from surveys made in the 1920s; (2) a 1966 survey of the Tulare Lake Basin by the U.S. Coastal and Geodetic Survey with updates based on 1982-83 floods (Summers Engineering, Inc., 1969, 1992); (3) a 2008 topographic data developed by the U.S. Army Corps of Engineers (USACE) based on Light Detection and Ranging (LiDAR) and IFSAR covering most of the Tulare Lake flood zone delineated by the Federal Emergency Management Agency (FEMA); and (4) 2015 LiDAR data collected by the CP 2-3 Contractor for a few-mile-wide strip along the proposed HSR Alignment. In addition, (6) in August and December of 2016, the AFW team collected additional topographic data along a network of roads overlapping the 2008 LiDAR coverage using Real Time Kinematic (RTK) Geographic Information System (GPS) equipment mounted on a vehicle (see Appendix C). We then developed a 2016 Digital Elevation Model (DEM) by synthesizing these various sources using a project-developed calculation method (see Sections 5.0 and 6.0).

ES.2 FORECASTING MAGNITUDES, RATES, AND PATTERNS OF FUTURE SUBSIDENCE

For the HSR, subsidence occurring after construction affect HSR structures, guideways, and track alignment, so we developed forecasts of future magnitudes, rates, and patterns of future subsidence as summarized below and further discussed in Section 6.0.

In 2014, the State of California legislature passed the Sustainable Groundwater Management Act (SGMA), which requires that local agencies in critically over-drafted groundwater sub-basins throughout the State prepare Groundwater Sustainability Plans (GSPs) by 2020, and to have implemented these plans by 2040. One key component to be addressed by GSPs in subsiding areas will be control of ground subsidence. Thus, it is anticipated that subsidence

[1] As described later in the text, the 2013 DEM is based on the 2009 National Elevation Dataset, but in the Corcoran area, the elevations have not been updated appreciably since 1928.

will likely continue until groundwater over-draft becomes controlled in the future and "sustainable" groundwater pumping is achieved. In this GSS, subsidence impact evaluation was based on the assumption of 20 years of subsidence projected from 2016. Several approaches to forecasting were considered.

The USGS is in the process of updating its Central Valley Hydrogeological Model (CVHM) for simulating regional groundwater flow and subsidence. The USGS provided us with an interim version of the model to explore the possibility of locally refining the model for use in forecasting future subsidence at adequate spatial and temporal resolutions in the vicinity of the HSR Alignment. However, following discussions with the USGS, it was agreed that making the necessary modifications should not be included in the scope of this GSS. This is further discussed in Section 4.2.

For this GSS, future subsidence forecasts were developed based on extrapolations or projections from observed historical subsidence. Three subsidence scenarios were developed based on extrapolations of various recent observed rates of subsidence, looking forward for the 20-year period from 2016 to 2036. The subsidence rate has been observed to be generally accelerating over the past 10 years, likely due to several factors, such as increasing groundwater extraction rates and decreasing natural recharge under recent drought conditions. Observed maximum subsidence along the HSR Alignment from 1926 to 2010 has been about 17 feet (for an average of about 2.5 in/yr, although the variability within this time frame is not well-known). At various time over the past ten years, maximum rates of subsidence in the Corcoran Subsidence Bowl have averaged about 8 in/yr from 2007 to 2010; 12 in/yr from 2010 to 2015; and 20 in/yr from 2015 to 2016. For our forecasting, Scenario A (or 2036a) was based on an extrapolation of the subsidence rates calculated from the 2007-2010 InSAR data provided by the JPL. It represents a period of less severe subsidence in the past 10 years. Scenario B (or 2036b) was based on an extrapolation of the subsidence rates we computed from the estimated changes in topographic surfaces between 2008 and 2016, which represents average rates over the past 10 years. Scenario C (or 2036c) was based on the subsidence rates calculated from the 2015-2016 InSAR data provided by JPL. It represents a period of generally faster subsidence towards the end of a severe 4-year drought. Based on these three scenarios and the estimated 2016 ground surface elevation, we developed three scenarios of the forecast 2036 ground surface topography. Profiles along the HSR Alignment of forecast subsidence, change in slope, and change in curvature for each of these scenarios are shown on Plate ES-3. Our approach to evaluating past and forecast subsidence are further discussed in Sections 5.0 and 6.0, respectively.

ES.3 EVALUATION OF POTENTIAL SUBSIDENCE IMPACTS TO THE CALIFORNIA HIGH-SPEED RAIL (SEE SECTION 7.0)

Rapid and large-magnitude subsidence poses several potential concerns to the HSR, including (1) changes in slopes, vertical curvature, horizontal curvature, and twist; (2) development of fissures or compaction faults; and (3) changes in floodplains and site drainage. Because subsidence varies spatially, differential subsidence will induce changes in vertical slopes and curvature along the HSR tracks. Similarly, differential horizontal displacement transverse[2] to the tracks will induce horizontal curvature, which will result in changes to vertical and transverse centripetal (and centrifugal as inertial counterpart) accelerations in the trains. Induced changes in ground slopes can affect overland flow and stream flow. Vertical deformation of the ground surface can change the location and shape of the topographically lowest region in a hydrologic basin. Thus, subsidence can affect site drainage characteristics as well as the location and extent of floodplains and flood depths. Differential subsidence also causes stresses and strains in the subsurface soils. Excessive strains can generate fissures and compaction faults.

The AFW team performed groundwater and geomechanical modeling using finite element software to evaluate the potential impacts of groundwater extraction from a hypothetical single well on the horizontal and vertical changes in slopes and curvatures induced along a straight and level HSR Alignment (Section 4.0). The calculated curvatures and accelerations represent potential incremental components due to subsidence caused by groundwater extraction, regardless of whether the design HSR Alignment is initially straight or curved. The model was based on an idealized subsurface profile representative of a typical condition in the Corcoran area. The modeling results indicate that drawdown-induced differential subsidence, slopes, strains, and curvatures are anticipated to generally be within tolerable limits for the HSR, with some cautions to be kept in mind, such as: local subsurface heterogeneity may result in actual impacts to the HSR being greater than indicated by this study of a hypothetical condition; differential subsidence could induce strains and stresses in viaduct structures; and preexisting faults or fissures may be reactivated by future subsidence.

The AFW team performed evaluations of the potential impacts of subsidence on drainage characteristics in the Corcoran area and floodwater storage in the historical Tulare Lake area.

These various modes of impact are further summarized in the following sections.

[2] In this report, “transverse” refers to the direction perpendicular to the direction of the track. “Radial” refers to the direction away from or toward the well. “Horizontal” refers to any horizontal direction without respect to specific direction.

ES.3.1 Induced Changes in Vertical Slopes (See Sections 4.0 & 5.0)

The *Design Criteria* (e.g., Authority 2012) for the HSR allows track slopes of up to 1.5 percent. Based on our modeling and our subsidence forecasting, we forecast that, apart from local anomalies, maximum values of induced change in slope (i.e., differential subsidence) will be on the order of 0.002 (or 0.2 percent) over the next 20 years, well below the maximum allowable track gradient from the *Design Criteria.* However, if maximum differential subsidence steepens a portion of the track that is already at or near the maximum allowed by the *Design Criteria*, the results could potentially exceed the allowable by a small amount. Also, if maximum differential subsidence approaches or exceeds these values at a HSR viaduct, significant stresses could be induced in the structure, and local concentrations of differential subsidence could result in even greater strain. These potential conditions should be considered by the viaduct designers.

ES.3.2 Induced Changes in Vertical Curvature (See Sections 4.0 & 5.0)

The *Design Criteria* allows induced accelerations of up to 0.05g, where g is the acceleration due to gravity. Induced changes in vertical acceleration of the passing train is directly related to the induced vertical curvature or radius of curvature. Induced change in vertical curvature is the rate at which the induced change in vertical slope varies over distance. Curvature is typically reported in units of 1/feet (or $feet^{-1}$), and calculated in the U.S. as feet/foot per foot. The reciprocal of the curvature is the radius of curvature, typically reported in units of feet. At the HSR design speed, this corresponds to a curvature of no more than about 1.2E-05 ft^{-1}. Our forecasts based on 20-year extrapolations from recent subsidence rates suggests future changes in vertical curvature could be in the range of up to 5E-06 ft^{-1}, on the order of 40 percent of the maximum allowable. Site conditions differing from what was assumed in the calculations, or local concentrations of strain, could result in greater changes in curvature than these calculated forecasts. It is possible that changes in curvature will increase the design curvature built into the track at specific locations, which could result in a need to perform track regrading to restore the track curvature to design limits.

ES.3.3 Induced Horizontal Displacement and Curvature (See Sections 4.1 & 7.1)

Because the subsurface behaves as a continuum, vertical subsidence will also result in horizontal movement of the ground surface, with maximum horizontal displacements on the order of 1/7 to 1/4 of the maximum vertical displacements caused by a single well when pumping from the deeper or shallower aquifers, respectively. Thus, the induced changes in horizontal accelerations are anticipated to be below the allowable upper limits. Under some conservative assumptions of adverse conditions, the highest induced changes in accelerations may approach or slightly exceed the allowable limits. It is possible that changes in curvature will increase the design curvature built into the track at specific locations, which could result in a need to perform track realignment to restore the track curvature to design limits.

We do not anticipate that super-elevation or twist limits will be exceeded. However, if induced horizontal curvature exceeds allowable limits, modifications to track super-elevation might be necessary to compensate for the induced curvature. Although we do not anticipate that induced twist will be a critical parameter, this should be further evaluated if more refined InSAR or other subsidence data becomes available in the future.

ES.3.4 Subsidence-Induced Fissures and Faults (See Section 8.5)

Although subsidence-induced fissures are infrequent in the SJV, at least three fissures have occurred in the mid-1900s, located in the Corcoran Subsidence Bowl about 3½, 5½, and 9 miles from the future HSR Alignment. The likelihood of such fissures occurring beneath or immediately adjacent to the HSR Alignment in the future is considered to be relatively low, but not negligible. If a future fissure were to develop beneath or adjacent to a HSR guideway, it could lead to distortion to or lack of support for the track, requiring interruption of normal services for mitigation or repair work.

One occurrence of subsidence-induced faulting is known to have occurred in the SJV, at the Pond-Poso Creek Fault about 2 miles from the proposed HSR Alignment. In our opinion it is unlikely that any such faulting would occur except in the general vicinity of the Poso Creek Fault, and possibly at the shoulders (edges) of the general Corcoran Subsidence Bowl in the vicinities of Deer Creek and perhaps Hanford. If such faulting were to occur along the HSR Alignment, it would likely occur slowly and could be accommodated by monitoring and periodic ballast releveling.

ES.3.5 Subsidence-Induced Changes to Floodplains (See Section 7.2)

The current FEMA flood zones within the Corcoran Subsidence Bowl appear to have been delineated based on topographic information at least 30 years ago, prior to the more-recent increases in subsidence rates and magnitudes. Subsidence has already modified, and will continue to modify, drainage and floodplain patterns to some extent in the vicinity of the HSR Alignment, in a potentially adverse manner with respect to the concerns of the HSR. Areas evaluated for potential floodplain changes within the Corcoran Subsidence Bowl include the FEMA floodplain features along river channels that cross the HSR Alignment in the vicinity of four creeks: the Cross Creek crossing near Hanford; the Tule River crossing a short distance south of Corcoran; the Deer Creek crossing about 16 miles south of Corcoran; and the Poso Creek crossing a short distance south of the Kern County line.

The Tulare Lake flood zone is the topographically lowest region in the hydrologic basin. The HSR Alignment passes along the east edge of the historical Tulare Lake, which prior to the late 1800s was the largest body of fresh water west of the Mississippi River. The limits of the historical Tulare Lake generally roughly coincide with the current FEMA floodplain in general. However, the areas of greatest and most rapid recent subsidence in the Corcoran Bowl are roughly along the HSR Alignment near the eastern edge of the historical Tulare Lake. As a

consequence, the 2009 USACE estimate of the 100-year Tulare Lake floodplain was already shifted to the east of the FEMA outline such that more of the HSR Alignment is within the anticipated floodplain, and ongoing subsidence is expected to continue this trend.

Our initial screening calculations indicated the need for further evaluation of three of the river crossings and the Tulare Lake flood zone that could be impacted by subsidence. FLO2D modeling was performed to assess the flood zones and flood depths in these regions using the three scenarios (2036a, 2036b, and 2036c) of forecast 2036 ground surface profiles. Forecast profiles along the HSR Alignment are shown on Plate ES-3. The results indicated that: at the Cross Creek crossing, subsidence would not induce substantial change to the associated floodplain; at the Deer Creek crossing, the flood zone would shift northward toward the Tule River Crossing, and the length of the flood zone along the HSR Alignment would increase; and at the Poso Creek crossing, flood patterns are not expected to be significantly changed by subsidence. Based on an estimated 100-year flood volume of approximately 1.65 million acre-feet, the FLO2D results indicated that this flood zone would become more oblong in shape, with the lowest region shifting eastward toward the HSR Alignment. This flood zone will likely merge with the Deer Creek and Tule River flood zones; the resulting flood depth along the HSR Alignment could potentially be more than 16 ft, and the length of the HSR Alignment within the modified flood zone could potentially be more than 20 miles.

The DWR has indicated that a large portion of the water in the Tulare Lake Basin comes from the Kings River; Austin (2012) reported that 49% of the floodwaters in the Tulare Lake Basin during the floods of 1983 came from the Kings River. Some of the water from the Kings River is routed to flow by gravity through a series of canals and sloughs toward the north and into the San Joaquin River drainage, and the remainder is routed through other canals and sloughs toward the south and into the Tulare Lake basin. There is apparently a “pinch point” near Tranquility, with a limit in the flow capacity toward the north. Apparently with modifications to these sloughs and canals and appurtenant facilities, and with proper floodwater coordination, most of the Kings River water could be safely routed to flow by gravity to the north. However, currently there is no entity responsible for or with authority to study or implement such a coordination effort, nor is there funding in place for any improvements,

Federal, State, and local flood agencies are aware of the potential issues in the Tulare Lake flood zone. To alleviate the issues, they are considering alternative ways of storing or routing the drainage to reduce the volume of surface water flow into the historical Tulare Lake flood zone. It is anticipated that these mitigation measures, if properly designed and implemented, could reduce future Tulare Lake flooding and, consequently, decrease the flood depth along the HSR Alignment and the length of the alignment that might be impacted by flood in this region. We recommend that the Authority lend their support to these efforts.

ES.4 FUTURE SUBSIDENCE MONITORING

Available information regarding recent patterns of subsidence in the Corcoran Subsidence Bowl is remarkably detailed compared to what might have been possible just a few decades ago. However, the "noise" in the most useful available data sources (e.g., L-band InSAR produced by JPL for the 2007-2010 period; a comparison of the RFP topo with the 2015 LiDAR by the CP 2-3 contractor; a comparison of the 2008 LiDAR by the USACE and the 2016 RTK performed by AFW; and Sentinel InSAR processed by JPL for the 2014-2015 and 2015-2016 periods), and the uncertainty associated with projecting these subsidence rates forward 20 years, are great enough that it is difficult to exclude the possibility that small-scale subsidence anomalies may be present and of a magnitude that could impact the HSR ride-ability and comfort. For this reason, additional monitoring and higher resolution InSAR analysis may be appropriate. In addition, a comprehensive subsidence and settlement monitoring program to differentiate subsidence from HSR construction settlement is also recommended in Sections 9.0, and 10.4.

ES.5 CONCLUSIONS AND RECOMMENDATIONS

In most locations, subsidence is not expected to cause significant impacts to the HSR performance. However, several potential risks remain. Therefore, recommendations are provided regarding instrumentation and monitoring, and design and mitigation considerations are presented regarding future hazards from induced differential subsidence, curvature, fissures and faults, and changes in flood patterns (Section 10.0).

Viaducts in subsiding areas should consider the possible impact of forecast differential subsidence. To accommodate anticipated levels of racking, single-span bridges may be more robust than multi-span bridges.

Regarding flooding of the Tulare Lake and the impact this could have on the HSR, as alluded to above in Section ES.3.5, a flood-management solution seems to be possible to this flooding hazard, although there is currently no allocated funding or a lead entity. We recommend that the Authority investigate this potential solution to Tulare Lake basin flood management in coordination with other interested parties, and work to bring about its implementation to the extent this is feasible. In addition, there is some uncertainty about whether the depth of flow at river crossings may increase slightly if there is no Tulare Lake flooding; to account for this, near crossing we recommend adding the values given to account for uncertainty in Section 10.3.

CORCORAN SUBSIDENCE BOWL FINAL REPORT
(DRAFT FOR REVIEW)

Ground Subsidence Study
California High-Speed Rail Project
San Joaquin Valley, California

1.0 INTRODUCTION

The Amec Foster Wheeler Environment & Infrastructure, Inc. (AFW) team performed a Ground Subsidence Study (GSS) for the California High-Speed Rail Authority (Authority), along and near to the portions of the proposed California High-Speed Rail Alignment (HSR Alignment) that will lie within the San Joaquin Valley (SJV) and Antelope Valley of California. The purpose of this study is to evaluate the impact that subsidence may have on future HSR infrastructure and train performance. Our team includes AFW and our major subconsultant GSI Environmental Inc. (GSI), with assistance from Earth Mechanics, Inc. and Moore Twining Associates, Inc.

This GSS report focuses on the Corcoran Subsidence Bowl in the southern SJV. The Corcoran Subsidence Bowl includes much of Construction Package (CP) 2-3 and the northern portion of CP 4. Appendices to this report consider potential impacts of subsidence along other portions of the HSR Alignment, notably along Highway 152 (sometimes referred to herein as the El Nido subsidence bowl), and in Antelope Valley.

1.1 BACKGROUND AND HISTORY

Over at least the past 90 years, groundwater drawdown due to groundwater extraction has induced subsidence over large areas within the SJV. Plate 1-2 is a map showing the observed subsidence from 1926 to 1970 and from 2007 to 2010, with the proposed HSR Alignment.

The Corcoran Subsidence Bowl sits in the Southern SJV between the Fresno and Bakersfield alluvial fans. Although these two alluvial fans are comprised largely of granular soils with limited compressibility and subsidence potential, the Corcoran Subsidence Bowl is generally underlain by more fine-grained and compressible lacustrine soils. Prior to the population growth and development of large-scale farming in the Southern SJV, the area to the west of the HSR Alignment was covered by the historical Tulare Lake, located in the topographically lowest region of the hydrologic basin at the time. Starting in the second half of the 1800s, the lake has been dried up by farmers to create arable land. In addition, up-stream dams and water diversion structures were constructed to provide water supply storage and to regulate flows in some streams draining to this area. Although the former lakebed has been developed into agricultural land, flooding still periodically occurs in this area.

Following the drying up of Tulare Lake, the groundwater phreatic surface initially remained high in the area, but it has been steadily drawn down over the years, with wells extending deeper;

new wells are now commonly on the order of 1000 to 1500 feet (ft) deep. With lowering of the groundwater phreatic surfaces, groundwater pore pressures are lowered. Soil particles consequently feel increased pressure and the soil structure is compressed, resulting in ground subsidence.

According to the United States Geologic Survey (USGS), subsidence has been observed during the last century, with as much as 28 feet near Mendota to the northwest, and 14 feet in the Corcoran Subsidence Bowl area east of the HSR Alignment occurring between 1926 and 1970, as shown in Plate 1-1 (shown by the subsidence contour lines). During that period, subsidence along the HSR Alignment in the Tulare Lake area may have been about 4 to 6 feet.

Following development of state and federal water projects, surface water became readily available, groundwater extraction was reduced, and subsidence due to groundwater drawdown was temporarily slowed or stopped. However, in the past 10 to 25 years, groundwater pumping has been accelerating, with associated resumptions and accelerations of groundwater drawdown and associated subsidence; this was exacerbated during the severe drought from fall 2011 to fall 2015. Plate 1-1 also shows the magnitudes and patterns of subsidence from 2007 to 2010 (shown by the color shading), which exceeded an average of 8 inches per year according to analyses by the Jet Propulsion Laboratory (JPL). Profiles of historical subsidence along the HSR Alignment, as well as profiles of induced changes in slope and vertical curvature, are presented on Plate 1-2. Toward the end of the recent drought, annual subsidence rates of 1 to 1½ feet were observed over a 12½ -month period near Corcoran in 2015-2016. Groundwater pumping and drawdown, and consequent subsidence, are anticipated to continue into the future at least until sustainable groundwater pumping is achieved. Due to inelastic soil behavior, subsidence is mostly irreversible even if groundwater pumping decreases and groundwater levels recover.

The HSR Alignment for the Design-Build CP 2-3 passes nearly through center of the Corcoran Subsidence Bowl, and the northern portion of CP 4 lies within the southern portion of the subsidence bowl. Further to the north, the El Nido Subsidence Bowl is located near Highway 152, in an area of future HSR contracts and extending south to the northern portion of CP 1.

It has been recognized at least since the fall of 2013 that subsidence in the SJV had the potential to impact the HSR (RDP 2015). The Authority's original strategy for addressing ground subsidence included a three-step approach to be taken with each selected Design-Build Contractor (Contractor):

1. The Contractor would perform subsidence studies and propose design parameters and design implement approaches, which would be included in their Design Baseline Report (DBR).
2. The Authority would review and approve the Contractor's DBR.

3. Upon completion of the Contractor's subsequent design, the Contractor would develop and implement an instrumentation and monitoring program to record the occurrence and distribution of subsidence, and to document impacts to the HSR tracks and facilities as a result of subsidence, for future use by the Authority.

Because subsidence was considered to be relatively minor with the CP 1 area (which was the first construction package to be advertised and awarded), this original approach to subsidence was workable. However, during the bidding phase for CP 2-3, this strategy was found to be problematic as became evident with inquiries from prospective bidders for the CP 2-3 contract. It was noted that:

- Literature reviews indicated that subsidence studies normally take years to complete, which would not allow the contractors to meet the tight construction schedule.
- The known area of subsidence covered more than one construction package. It was suggested that it would be more cost-efficient and program-consistent to have one entity to conduct the studies for the entire area.
- Requesting a Contractor to propose design parameters for their own design could introduce potential conflicts of interest for the contract.
- The multi-step approach would leave major uncertainties regarding the appropriate scope of work to account for subsidence, and the uncertain scope would make it difficult or impossible to provide consistent and competitive. In other words, this approach caused a great problem of biddability, and any winning bid would likely be challenged.

With the above concerns in mind, the Authority removed the subsidence study from the CP 2-3 scope of work and requested prospective Contractors: "Unless directed otherwise by the Scope of Work, for bidding purposes assume that subsidence from groundwater pumping is not an impact to the project area." The Authority indicated they would then adjust design parameters if needed through design variances based on findings from a statewide GSS to be developed under a separate contract. The GSS was also to provide the Authority with recommendations for future ground subsidence monitoring and mitigation measurements. This GSS report is a product of that study.

1.2 SCOPE OF GROUND SUBSIDENCE STUDY

In the broadest sense, ground subsidence simply means that the ground is moving downward. There are five primary mechanisms or types of potential subsidence in the SJV:

1. Groundwater drawdown-induced subsidence, which may occur in compressible alluvial layers (especially clayey soils) as groundwater is withdrawn.
2. Hydrocompaction, which may occur when artificially-placed fill or loose alluvial deposits are initially wetted.
3. Subsidence due to oil and gas extraction.
4. Tectonic subsidence due to tectonic plate movement.
5. Drainage and oxidation of organic soils and peat.

The scope of the current GSS has focused on subsidence induced by groundwater extraction, or more technically, the lowering of the groundwater phreatic surface due to groundwater extraction (Type 1 subsidence from the above list). However, the other types of potential subsidence are briefly summarized in this report in Section 8.7 (hydrocompaction, tectonic, oil and gas, and peat); and are mentioned in Sections 8.6.1.5 and 8.6.2.3 (oil and gas extraction); 9.7 (tectonic activity, and oil and gas extraction); and 9.8.2 (tectonic activity).

The purpose of this report is to present the findings, evaluations, and recommendation developed for this GSS. The main body of this report presents the results of our study in the Corcoran Subsidence Bowl; appendices address subsidence in the El Nido Subsidence Bowl and in Antelope Valley, and provide additional background and detail.

1.3 GROUND SUBSIDENCE STUDY APPROACH

For this GSS, subsidence and its anticipated impacts to the HSR were evaluated using the following methods:

1. Studied available information relevant to subsidence in the Corcoran Subsidence Bowl. Sources of information include the following:
    a) Literature regarding subsidence in the SJV and elsewhere.
    b) InSAR data of subsidence in the SJV.
    c) Topographic or elevation data, from the USGS 2009 National Elevation Dataset; Light Detection and Ranging (LiDAR) and IFSAR from the U.S. Army Corps of Engineers (USACE); long-term continuous Global Positioning System (CGPS) sources (see Appendix B); and project-specific surveys using both GPS and LiDAR technologies.
    d) Observations of subsidence as reported by local water and infrastructure agencies.
    e) Performed a Real-time Kinematic (RTK) GPS survey of the Corcoran Subsidence Bowl to develop current (2016) topographic elevations.
2. Developed forecasts of subsidence by extrapolating historical rates and patterns of subsidence for 20 years into the future.
3. Performed a numerical analysis of the drawdown from a hypothetical single well with a profile representative of conditions in the SJV.
4. Evaluated the possibility of refining the USGS's updated Central Valley Hydrogeologic Model (CVHM-mod) for subsidence forecasting along the HSR Alignment.
5. Performed flood modeling to evaluate potential change in flood zones and depths in comparison with available Federal Emergency Management Agency (FEMA) and USACE flood zones for the Corcoran Subsidence Bowl area.

AFW evaluated the information gathered or developed from each of these various sources with respect to the California High-Speed Train Project Design Criteria (*Design Criteria)* and how subsidence may affect the HSR performance.

This report presents a summary of our findings and evaluations, along with recommendations regarding design considerations, instrumentation and monitoring, and maintenance.

1.4 DEFINITIONS

The following definitions apply to words as used within this report:

1. **Subsidence**: Downward movement of the ground surface in response to lowering of groundwater levels (in unconfined aquifers) or phreatic levels (in unconfined or confined aquifers).
2. **Differential Subsidence**: Difference in the magnitude of subsidence across a distance between two points. This is a dimensionless value, being measured in terms of length per length (e.g., feet subsidence per foot of horizontal offset). It may also be thought of as the first derivative of subsidence. It may be termed "induced slope", "induced gradient", or "induced grade".
3. **Induced Curvature**:
   a) Induced vertical curvature is the rate of change of gradient that has been created or induced by differential subsidence. It has units of 1/Length (e.g., $feet^{-1}$ or $miles^{-1}$). It may also be thought of as the second derivative of subsidence.
   b) Similarly, induced horizontal curvature is the rate of change in horizontal direction that has been induced by differential horizontal displacement associated with vertical subsidence (this will be discussed in Section 4.1 on modeling of subsidence from drawdown around a single well.
4. **Radius of curvature**: the reciprocal of curvature, in units of length (e.g., feet or miles).
5. **Induced Acceleration**: Forcing a vehicle (e.g., a high-speed train) to follow a curved path results in an acceleration orthogonal to travel path. The magnitude of acceleration is equal to $A = V^2/R$, where A is acceleration, V is the velocity of the vehicle, and R is the radius of curvature. This equation holds for either vertical or horizontal curves.
6. **Super-elevation or Cant**: The sideways slope of the tracks, i.e., the difference in elevation of the two rails, divided by the distance between the rails. As with the slope, this is a dimensionless value.
7. **Twist**: The rate of change in super-elevation or cant.
8. **Settlement**: For this GSS, the term "settlement" is reserved for downward movement of the ground surface (or structure) in response to a load added at the ground surface (e.g., placement of an embankment or a structural footing". This is distinguished from subsidence: both are downward movement, but the mechanisms are different.
9. **Digital Elevation Model (DEM)**: A numerical elevation model for use in Geographic Information System (GIS) or Computer Aided Design (CAD) software. A DEM may represent the ground surface (either past, present, or forecast future; it may be made from measured or computed elevations), or it may represent the areal distribution of subsidence: e.g., the colored representation of subsidence on Plate 1-1 represents a DEM of subsidence values.

10. **Fissure (or sometimes Earth Fissure)**: When local differential subsidence results in convex-upward change in curvature of the ground, tensile stresses are likely to develop. A crack or fissure may initiate when these strains approach 200 to 600 microstrain. Earth fissures start out as small cracks and may not be visible at the ground surface. They may grow and widen from surface water flowing into the crack, softening and eroding material on the sides of the crack, in some cases leading to gullies or trough-like depressions.
11. **Fault (or Subsidence-Induced Fault, or Compaction Fault)**: Existing faults or other features can create an obstruction to horizontal groundwater flow, such that groundwater can be drawn down differentially on either side of the fault, leading to differential subsidence. When drawdown and consequent subsidence are significantly greater on one side of the fault, differential strains may localize into a subsidence-induced normal fault, with abrupt vertical offset occurring across a fairly short distance. (In this context, "subsidence" refers to the settlement of the ground surface, whereas "compaction" refers to the volumetric compression of the underlying soil.)
12. **Water of Compaction**: A one-time source of water wells that causes significant subsidence as it is drawn out of and causes compaction of fine-grained water bearing deposits. This water is permanently mined from the groundwater reservoir aquifer system, and can represent a significant percentage of total pumpage (Lofgren 1975). Water of Compaction is especially characteristic in confined aquifers.

2.0 SOURCES OF INFORMATION

2.1 CATEGORIES OF AVAILABLE INFORMATION

This section presents the sources of information used in this GSS. Categories of information include the following:

1. Personal communications
2. Interviews with stakeholders
3. Topographic and Subsidence Data along HSR Alignment
   i) Survey and LiDAR Data
   ii) Global Positioning System
   iii) InSAR
   iv) Satellite Altimetry
   v) HSR and nearby Geotechnical Data
4. Groundwater Elevations
5. On-line Databases
   i) TOPEX/Poseidon
   ii) Jason-1
   iii) Jason-2

6. Available Literature
    i) Groundwater in California: California Department of Water Resources
    ii) US Geological Survey Water-Supply Papers
    iii) US Geological Survey Professional Papers – Central California
    iv) US Geological Survey Open-File Reports
    v) General Subsidence and Earth Fissuring
    vi) High-Speed Rail Subsidence
    vii) Conference Proceedings (hard copies in Phoenix AFW office)
    viii) Subsidence and Earth Fissuring Literature – Central California
    ix) Mechanics of Subsidence and Earth Fissuring
    x) Subsidence and Earth Fissure Characterization and Measurements
    xi) InSAR for Subsidence and Earth Fissuring
    xii) Subsidence and Earth Fissuring in Las Vegas Valley and Nevada
    xiii) Subsidence and Earth Fissuring in Arizona
    xiv) Miscellaneous

2.2 PERSONAL COMMUNICATIONS

AFW has spoken with USGS scientists working on subsidence in the SJV, and an academician who has studied and published works on the geology of the southern SJV.

2.2.1 Ms. Michelle Sneed

Early in this investigation, we spoke with Ms. Michelle Sneed, a hydrologist with the USGS, and currently the USGS's specialist regarding subsidence in the SJV. Ms. Sneed has been leading the USGS's subsidence studies in this area.

Because of Ms. Sneed's extensive involvement with subsidence studies in the SJV, we asked her observations of subsidence impact on infrastructure, as well as her opinion regarding the potential for groundwater drawdown-induced subsidence to cause future fissures or faults in the SJV, and the risk these pose for the future HSR.

2.2.2 Dr. Tom Holzer

We spoke with Dr. Tom Holzer, PhD, a research geologist with the USGS, and editor of the USGS's *Man-Induced Land Subsidence* published in 1984, to which he contributed the chapter "Ground Failure Induced by Groundwater Withdrawal from Unconsolidated Sediment." Dr. Holzer was also the author of "Faulting Caused by Groundwater Level Declines, San Joaquin Valley, California," in *Water Resources Research*, Vol. 16, No. 6 (published in 1980), and numerous other subsidence and ground failure related publications.

Because of Dr. Holzer's long history of being involved with subsidence-induced ground deformations, including in the SJV, we asked his opinion regarding the potential for groundwater drawdown-induced subsidence to cause future fissures or faults in the SJV, and the risk these may have on the future HSR.

2.2.3 Dr. Claudia Faunt

We spoke with Dr. Claudia Faunt, PhD, a hydrologist with the USGS, and currently the USGS's Project Chief regarding the CVHM of the SJV. Dr. Faunt has been leading the USGS's efforts to update and recalibrate CVHM and provided the AFW team with interim versions of CVHM (referred to herein as CVHM-mod) and supporting files and documentation.

2.2.4 Dr. Randall Hanson

We spoke with Mr. Randall Hanson, PhD, a hydrologist with the USGS, and currently the USGS's Lead Developer of the Farm Package (FMP2) utilized in the CVHM-mod of the SJV. Dr. Hanson has provided the AFW team with insight on how the FMP2 works within CVHM-mod.

2.2.5 Dr. Jason Saleeby

We have communicated with Dr. Jason Saleeby, PhD, retired professor from the California Institute of Technology, who has done extensive tectonic research in the region, including publications with mapped locations for 'Corcoran Clay Faults' (Saleeby and Foster 2004, Saleeby et al. 2013). Discussions included identification of original source material for Saleeby's publications and resulted in AFW reviewing and utilizing seismic reflection data (Miller 1999) that informed Saleeby. Corcoran clay fault (CCFs) and other tectonic structure described by Saleeby are important to the understanding of the sub-surface geologic characterization and areas where earth fissures, compaction faults, and other concentrations of horizontal and/or vertical displacement could occur.

2.3 INTERVIEWS WITH STAKEHOLDERS

2.3.1 Overview

During interviews with stakeholders, a few reported that subsidence has caused subtle changes in gradient of some gravity-flow canals, and there has been some distress to well casings that have risen up out of the ground due to subsidence.

In addition, ongoing vertical-offset creep has been observed where the Pond-Poso Creek Fault crosses Peterson Road, leading to periodic maintenance to smooth the resulting bump in the road (see Plate 1-1 for location of Pond-Poso Creek Fault).

Otherwise, no agency has been found that has identified subsidence-induced distress to roads, bridges, railroads, buildings, or pipelines. (It may be noted that some relatively subtle distress to at least one roadway has been caused by subsidence-induced movement of the Pond-Poso

Creek Fault, where the Kern County Department of Public Works performs periodic maintenance as needed. In addition, some bridges have required jacking up due to changes to canal hydraulics caused by subsidence, but subsidence has not directly caused distress to the bridge structures.)

It may also be noted that there could be subsidence-induced distresses to infrastructure that has not been identified as such. A number of agencies indicated they are not specifically looking for signs of subsidence, although most water agencies have begun doing so, as has the California Department of Transportation (Caltrans).

For this GSS, interviews were conducted with various entities with responsibility for infrastructure in the SJV to assess the impact of subsidence on infrastructure. Entities contacted include private companies with long, linear infrastructure such as railroads and pipeline companies as well as State and local public agencies.

2.3.2 Railroads

In January or early February of 2016, Mr. Frank Vacca of the Authority interviewed representatives of Burlington Northern-Santa Fe Railroad and Union Pacific Railroad regarding any impacts subsidence may have had on their operations or maintenance activities. In short, both BNSF and UPRR indicated that:

- They do regular track maintenance including ballast releveling, but they have not noticed any increases or changes to maintenance that is attributed to subsidence.
- They do not have any plans or budget set aside to perform increased monitoring or maintenance in response to subsidence.

2.3.3 Agencies in San Joaquin Valley

2.3.3.1 State Agencies

2.3.3.1.1 Department of Water Resources

Mr. John Curless of the Department of Water Resources (DWR) Division of Engineering indicated that there has been up to 6 feet of subsidence on the California Aqueduct near Milepost 163, since its construction in the mid-1960s through 1973; this is about 29 miles west of the town of Corcoran on the HSR Alignment (the approximate location is shown on Plate 1-1). The subsidence has resulted in cracking of the canal lining. DWR has performed repeated surveys along the Aqueduct from 1967 to the present. Mr. Curless indicated that the survey data was being compiled, but has not yet been published.

Ms. Jeanine Jones of the DWR indicated that DWR believes subsidence has contributed to ongoing maintenance needs for the California Aqueduct over its life, but that they have not identified or tracked how much has been attributable to subsidence. They have also needed to raise ("jack up") several bridges over the California Aqueduct as a consequence of subsidence,

and that several local irrigation districts have needed to raise canal levees or raise ("jack up") bridges over canals on account of changes to canal hydraulics caused by subsidence (but note that subsidence did not directly cause structural damage to the structures), but she was not aware of anyone tracking these efforts as being subsidence related.

Ms. Jones noted that subsidence forecasting is very difficult, as is evaluating future subsidence-impacted flood patterns. She said it may be possible to at least partially mitigate Tulare Lake flooding if various agencies could coordinate management of flood waters, but at this time, there is no agency responsible for or with authority to study or implement such a coordination effort.

It is the opinion of the DWR Operations and Management group that subsidence contributed to channel incision and scour that led to the I-5 Arroyo Pasajero bridge failure which resulted in loss of life.

Ms. Jones indicated that DWR flood personnel believe subsidence has been responsible for recent scour areas at the Avenue 21 bridge along the Eastside Bypass, which they are currently concerned about. Mr. Farley indicated that this is an area where subsidence has resulted in loss of freeboard for the Eastside Bypass Canal, which means that floodwaters flow deeper and wider than originally designed. At the bridge, the abutment appears to constrict the flow, resulting in turbulence and consequent erosion of the levees just down steam from the bridge (see Figure 2-1).

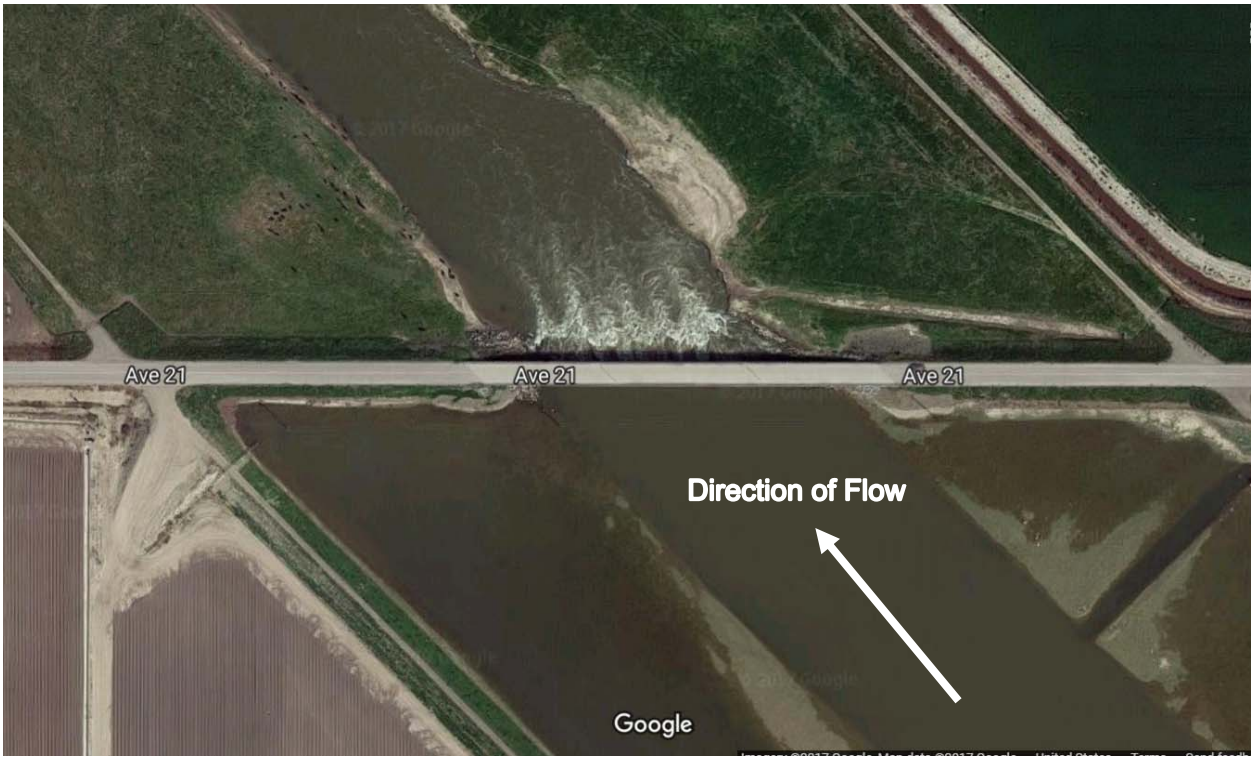

Figure 2-1: Eastside Bypass Flood Flows at Avenue 21 Bridge

Mr. Greg Farley of the DWR noted that a large portion of the water that enters the Tulare Lake basin comes from the Kings River. Some of the water from the Kings River is routed through a series of canals and sloughs (e.g., Murphy Slough, Fresno Slough, and James Bypass) toward the north and into the San Joaquin River drainage, and the remainder is routed through other canals and sloughs to the south (e.g., South Fork Kings River) and into the Tulare Lake basin. There is apparently a "pinch point" near Tranquility, with a limit in the flow capacity toward the north. Apparently with modifications to these sloughs and canals and appurtenant facilities, and with proper flood water coordination, most of the flood waters that may now enter Tulare Lake could be safely routed to the north. However, there is currently no agency responsible for or with authority to study or implement such a coordination effort, nor is there funding available for the improvements.

2.3.3.1.2 Caltrans Office of Structure Investigations - North

Caltrans Office of Structure Investigations - North is responsible for the investigation, evaluation, work recommendations, and documentation of all city, county, state, and federal bridges in northern California, including the SJV. In October 2015, Mr. Erol Kaslan, PE (Chief, Structures Investigations – North) indicated that the Office was aware of the subsidence issue in the SJV and had performed inspections of bridges to look for evidence of movement and had found none.

In November 2017, Mr. Kaslan said they still had not found any evidence of subsidence having had any impact on any of their structures. (He did note that the word "subsidence" occurred in some inspection records, but it was used to describe foundation settlement, not "subsidence" as the terms is used in this GSS report.) We also spoke with several inspectors who concurred with Mr. Kaslan's summary, including Messrs. Andy Corker, Rick Jorgensen, and Ryan Odell.

2.3.3.1.3 Caltrans District 6

Caltrans District 6 is responsible for maintenance of over 2,000 miles of State Routes in Madera, Fresno, Tulare, Kings and Kern Counties, including State Route 198 that runs perpendicular to the proposed HSR Alignment in Hanford. Mr. John Liu, Deputy Director for District 6, was not aware of any subsidence or settlement that has impacted bridges or roadways.

2.3.3.1.4 Caltrans District 10

Caltrans District 10 is responsible for maintenance of over 3,500 lane miles of State Routes in eight counties, including State Route 152 in Merced County that runs parallel to the proposed HSR Alignment. Ms. Sam Haack, Deputy Director for District 10, was not aware of any subsidence or settlement that has impacted bridges or roadways.

2.3.3.2 Local Public Works Agencies

Local agencies include city and county public works departments and water agencies.

2.3.3.2.1 Kings County Department of Public Works

Mr. Kevin McAlister, Public Works Director for Kings County, indicated that the County maintains pipelines, canals, ditches, roadways, levees and basins. He is not aware of any subsidence or settlement that has impacted County infrastructure.

2.3.3.2.2 City of Hanford Public Works

Mr. Lou Camara, Public Works Director for the City of Hanford, indicated that the City maintains pipelines, wells, roadways, and basins. He indicated that two of the City's wells collapsed approximately 5 years ago and that the well collapses may have been related to subsidence.

2.3.3.2.3 City of Corcoran Public Works

Mr. Baldo Rodriguez, Public Works Director for the City of Corcoran, indicated that the City maintains streets, curb/gutter, and underground utilities. He is not aware of any subsidence or settlement that has impacted City infrastructure. He also indicated that the City had recently asked their surveying consultant to reshoot City benchmarks and compare the results with previous readings, in part due to information from local irrigation districts that high levels of subsidence had occurred in the area. Mr. Rodriguez was not sure that he could share the results of their surveying and stated that a formal request would need to be made with the City Manager/City Attorney.

2.3.3.2.4 City of Wasco Public Works

Mr. Bob Wren, Public Works Director for the City of Wasco, indicated that the City maintains storm, sanitary sewer, and water pipelines; seven wells; roadways; and eight retention basins. He is not aware of any subsidence or settlement that has impacted City infrastructure.

2.3.3.3 Water and Power Entities

The following water agencies in the SJV were interviewed.

2.3.3.3.1 San Luis Canal Company

San Luis Canal Company (SLCC) consists of approximately 45,000 acres of productive farmland between the cities of Los Banos and Dos Palos in Merced County. Mr. Chase Hurley, General Manager, indicated that SLCC maintains pipelines, wells, canals, ditches, roadways, levees, and basins. Impacts to infrastructure due to subsidence include a San Joaquin diversion structure (intake) that has lost about 50 cubic feet per second (cfs) capacity. No cracking or distress to the structure has been noted. At the bottom end of the Temple Orchard Canal, the water is lapping onto the County road and periodic earthwork is required. Future headworks

diversion repair is estimated at $15 million for a new pumping facility. In conjunction with USBR monitoring for subsidence is performed at the river diversion structure from headworks east to Red Top and at the Temple Orchard Canal system 1 to 2 times per year.

2.3.3.3.2 Central California Irrigation District

The Central California Irrigation District (CCID) is one of the largest irrigation districts in the Central Valley, serving more than 143,000 acres of farmland. Mr. Chris White, General Manager, indicated that CCID maintains pipelines, wells, canals, ditches, roadways, levees, and basins. Mr. White indicated that there has been 6 ft of subsidence between 2008 and 2013 in the Red Top area. Impacts to infrastructure due to subsidence include loss of channel flow capacity.

2.3.3.3.3 Kaweah Delta Water Conservation District

The Kaweah Delta Water Conservation District (KDWCD) is located in the south-central portion of the SJV and lies in portions of both Tulare and Kings Counties. The total area of the District is about 340,000 acres with approximately 255,000 acres located in the western portion of Tulare County and the remaining, 85,000 acres, in the northeastern portion of Kings County. Mr. Larry Dotson, Senior Engineer, indicated that KDWCD maintains basins and natural channels. He is not aware of any subsidence or settlement that has impacted KDWCD infrastructure.

2.3.3.3.4 Lakeside Irrigation District

Mr. Shaun Corley, Manager of the Lakeside Irrigation District (LID), indicated that LID maintains pipelines, canals, ditches, and basins. He is not aware of any subsidence or settlement that has impacted LID infrastructure. He is only aware of a Caltrans study of subsidence along the Highway 198 corridor.

2.3.3.3.5 Corcoran Irrigation District

Mr. Gene Kilgore, Manager of the Corcoran Irrigation District (CID), indicated that CID maintains pipelines, wells, canals, ditches, roadways, levees, and basins. He is not aware of any subsidence or settlement that has impacted CID infrastructure. He indicated that CID had to put in a lift station and start pumping to get flow out of a subsided area south of the Tule River. Mr. Kilgore said that Dustin Fuller with Cross Creek Flood Control/Tulare Lake Drainage District may have some information on subsidence.

2.3.3.3.6 Tulare Lake Basin Water Storage District

Mr. Jacob Westra, Assistant Manager of the Tulare Lake Basin Water Storage District (TLBWSD), indicated that TLBWSD maintains two lateral pipelines that are laterals off of the California Aqueduct. He is not aware of any subsidence or settlement that has impacted TLBWSD infrastructure.

2.3.3.3.7 Lower Tule River and Pixley Irrigation Districts

The Lower Tule River Irrigation District and the Pixley Irrigation District (PID) supply supplemental water for district-wide crop irrigation to more than 125,000 acres in the Central Valley of California. Mr. Eric Limas, Assistant Manager, indicated that both districts maintain pipelines, wells, canals, ditches, roadways, levees, and basins. Mr. Limas indicated that a few of the ditches, mostly in the Pixley Irrigation District area, need to be operated with a higher water level to maintain the same flow rate, but they have not observed cracking or other distress to structures that can be attributed to subsidence.

2.3.3.3.8 Alpaugh Irrigation District

Mr. Bruce Howarth, General Manager of the Alpaugh Irrigation District (AID), indicated that AID maintains pipelines, 18 wells extending to depths of 1,500 ft below ground surface (bgs), canals, ditches, roadways, levees, and basins, including a large water storage reservoir. Mr. Howarth indicated that a canal and reservoir have experienced settlement at the location of the proposed HSR Alignment. Mr. Howarth indicated that the east end of the reservoir has settled differentially such that 3 to 4 ft of water no longer drains from that end upon emptying the reservoir. Mr. Howarth said that Dragados, a CP 2-3 Contractor, has knowledge of this settlement.

2.3.3.3.9 Shafter-Wasco Irrigation District

Mr. Dana Munn, General Manager of the Shafter-Wasco Irrigation District (SWID), indicated that SWID maintains wells and pipelines. He is not aware of any subsidence or settlement that has impacted SWID infrastructure. He indicated that Semitropic Water District has a subsidence monitoring well.

2.3.3.3.10 Rosedale-Rio Bravo Water Storage District

Rosedale encompasses approximately 44,000 acres of lands, of which approximately 27,500 are in irrigated agriculture, with an additional 7,500 acres developed in residential, commercial and industrial. Mr. Zach Smith, Operations Manager of the Rosedale-Rio Bravo Water Storage District (RRBWSD), indicated that RRBWSD maintains 15 miles of canals, 5 miles of pipelines, 25 wells, and multiple basins and levees. He is not aware of any subsidence or settlement that has impacted RRBWSD infrastructure.

2.3.3.3.11 Oildale Mutual Water Company

Oildale Mutual Water Company (OMWC) supplies water to 8,000 retail customers in the Oildale area. Mr. Doug Nunneley, General Manager, indicated that OMWC maintains wells and pipelines. He is not aware of any subsidence or settlement that has impacted OMWC infrastructure.

2.3.3.3.12 Arvin-Edison Water Storage District

A representative of the Arvin-Edison Water Storage District (AEWSD) indicated that AEWSD maintains pipelines, wells, canals, levees, and basins. AEWSD is not aware of any subsidence or settlement that has impacted their infrastructure. AEWSD established a subsidence monitoring network in 2012, but no further monitoring of the network points has been performed.

2.3.3.3.13 Pacific Gas & Electric Company (PG&E)

A representative of PG&E indicated that transmission lines and pipelines are not normally impacted until differential subsidence is severe, and so far, they have not observed any differential subsidence severe enough to impact their transmission lines or pipelines.

2.3.3.4 Summary of Findings from Agencies in San Joaquin Valley

Near the town of Pond there has been ongoing subsidence-induced vertical offset of the Pond-Poso Creek Fault, averaging perhaps on the order of 0.4 inches per year, but maxing out at about 1 inch per year, which has required periodic maintenance of the road pavement.

AID pond dikes appear to have settled differentially. Although it is not clear how much of this total or differential settlement may be the result of settlement in response to the surcharge weight of the pond dikes, and how much the result of differential subsidence due to groundwater drawdown, it is likely that groundwater drawdown-induced subsidence has at least contributed to the differential settlement. We are not aware any corresponding road damage in this area. We are aware of three canals in the Alpaugh vicinity where subsidence has caused sufficient flattening of gradients that modifications to the canals were required. One canal owned by AID required adding two ft of freeboard to the embankment. A nearby canal owned by the Angiola Water District and the Homewood Canal both required construction of a new lift station to correct gradient changes. The locations of the three modifications to the canals in relation to the HSR Alignment are shown on Figure 2-2.

Figure 2-2: Locations of Nearby Canals Affected by Subsidence

Photographs of the lift stations on the Angiola Water District canal and the Homewood Canal are included on Figures 2-2 and 2-3, respectively.

Figure 2-3: New Angiola Lift Station

Figure 2-4: New Homeland Lift Station Location

CCID is also experiencing flattening of gradients of sufficient magnitude that a new lift station may be required. We are aware that about 6 miles south of the town of Dos Palos (and about 13 miles south of the HSR Alignment), the Delta Mendota Canal has experienced cracking in several locations of the concrete lining that is suspected to be the result of buckling caused by differential ground subsidence. Also in this area, differential subsidence has caused changes to the canal hydraulics such that the soffit of the Russell Avenue Bridge over the Delta Mendota Canal is about 3 ft closer to the top of water in the canal than it was immediately following construction. When the canal is running full, water is at the bridge soffit, and walls have been constructed along the bridge and adjacent canal to keep the bridge from being overtopped by canal water.

Besides these findings, roads, bridges, pipelines, and buildings appear to generally be performing quite well, and besides impacts related to changes in drainage and canal hydraulics, there has been very little observed or reported consequences of groundwater drawdown induced subsidence.

2.3.4 High-Speed Rail In Other Countries

2.3.4.1 France

We interviewed Mr. Dominique Rulens, formerly of Systra (the French firm that has been responsible for much of the design of high-speed rail lines in France). He indicated that the French do not have high-speed rail lines in areas of rapid subsidence, at least in part because groundwater withdrawal is controlled by regulation. On the other hand, they have recently tested high-speed trains on ballasted track to speeds up to 357 miles per hour (mph), and they operate commercially with passengers in France up to 200 mph (Rulens 2016).

2.3.4.2 China

Several papers presented in November 2015 at the Ninth International Symposium on Land Subsidence (NISOLS) in Japan included reference land subsidence and its effects on high-speed rail (HSR) infrastructure in China. Mr. Ken Fergason, PG, with AFW, had the opportunity to meet with and discuss land subsidence and its effects on HSR with several of the authors of these papers, and these discussions generally contained more detail in regard to the effects of land subsidence on HSR systems than was discussed in the oral/poster presentations and the corresponding published papers.

Discussions that Mr. Fergason had as well as subsequent emails are summarized below. It is noted that English is not the first language of the individuals spoken to and that some of the information discussed below has a certain degree of uncertainty due to the potential of information becoming lost in translation.

Two presentations mentioned impacts to an HSR system in central China that were in the final stages of construction and nearing full operation. Additional impacts to rail infrastructure, including subways, were mentioned. It was indicated that the design of the HSR system, route of the track, and speed of the train were all impacted due to land subsidence and earth fissuring within the Fenwei Basin.

Mr. Fergason had discussions with Dr. Chaoying Zhao from Chang'an University who researches land subsidence and earth fissuring in China and whose research identified the issue of land subsidence and its impacts on the HSR system in the Fenwei Basin. Discussions were somewhat general since Dr. Zhao does not work directly for the HSR system and are summarized below.

- Dr. Zhao stated that land subsidence and earth fissuring led to the route of the planned HSR system to be changed, in some locations the design was changed from viaducts to embankments because of subsidence concerns, and there were plans to reduce train speeds to approximately 60 to 80 mph in certain areas effected by land subsidence and earth fissuring.
- Land subsidence totals and rates are similar to those of Taiwan: totals of 5 to 6 ft and annual rates of 3 to 4 inches per year.
- They generally control induced track curvature so as to keep vertical accelerations under 0.05g. He did not report on rates of subsidence.

2.3.4.2.1 Xi'an Metro in the Province of Shaanxi, China

The city of Xi'an (the capital of Shaanxi Province in China) has a subway known as the Xi'an Metro (or the Xi'an Subway). This rail system is not high-speed (top speed of 50 mph [railway-technology.com 2017]), but it is in an area that is subject to subsidence-induced fissures and faulting that cross the metro alignment.

In personal communication between Mr. Fergason of AFW, and Qiangbing Huang and Jianwei Qiao of the Department of Geological Engineering at Chang'an University, in Xi'an, China, we were provided a copy of a presentation they gave on November 10, 2015, titled *Ground Fissure: A Great Challenge to Metro Project in Xi'an, China*. In this presentation, they indicated that:

Xi'an is well known for its unique geological [hazards]: ground fissures [note that their use of the term "fissure" seems to include both fissures as well as faults, as we use the terms]. These ground fissures have destroyed buildings, bridges, roads, pipelines, and other infrastructure, and in the past 20 years have caused enormous damage of up to 161.9 billion RMB [$24 billion US]. These ground fissures not only restrict the efficient use of the urban construction land and the development of Xi'an City, but also are a serious threat on the construction of Xi'an Metro.

There appears to be a number of subsidence-induced faults that cross the Metro line, with potential offsets over the life of the project (100 years) of about 6 to 20 inches. To evaluate the potential impact to their Metro tunnels, they performed numerical modeling and large-scale testing, which indicated the tunnel could be damaged if offsets exceeded about 8 inches. To mitigate, they developed flexible tunnel joints, increased the tunnel strength, and increased the tunnel diameter in areas of anticipated offset. Additional tunnel waterproofing was implemented, as was a monitoring program to warn of crack development.

2.3.4.2.2 Beijing Plain, China

Recent publications from China have indicated recognition that land subsidence presents a potential hazard to HSR in the Beijing Plain of China. Published subsidence rates range up to about 5 inches per year for the last few years. A 2015 study recommends that groundwater pumping be prohibited near HSR tracks. A more comprehensive evaluation of the effects of land subsidence on infrastructure, including HSR, is currently being conducted by Professor Chen Mi of Capital Normal University (China), Professor Li Zhenhong of Newcastle University (United Kingdom [UK], and Spanish engineer Roberto Tomás of the University of Alicante (Spain). Mr. Fergason has contacted Dr. Tomás who indicated that research is ongoing and they hope to publish results in 2017.

2.3.4.3 Taiwan

Information regarding subsidence along the Taiwan high-speed rail was provided by Cheinway Hwang, Chair Professor of the National Chiao Tung University and Convener of the Civil and Hydraulic Engineering Program of the Ministry of Science and Technology in Taipei, Taiwan, and his colleagues. Mr. Fergason spoke with Prof. Hwang at the NISOLS meeting in Japan. In addition, Prof. Hwang and several colleagues (YW "Jacky" Chen, Ricky Kao, and YS Cheng) gave a presentation to the AFW team, the Authority, and the RDP, in San Francisco in December 2016.

2.3.4.3.1 Presentations by and Conversations with Prof. Cheinway Hwang et al. at NISOLS Meeting

Monitoring is being performed using several technologies, including level surveys; multi-layer magnetic extensometers; CGPS; monitoring wells; differential InSAR (DInSAR); persistent scatterer InSAR (PSInSAR); temporary coherent point InSAR (TCPInSAR); gravimetry; and satellite altimetry. Numerical modeling analysis is also being performed.

Where subsidence was observed, or was suspected to be likely to occur, public policy has prohibited groundwater pumping within 1 mile of the high-speed rail alignment, and/or tracks were supported on viaducts. This apparently has been generally effective in reducing or eliminating most significant subsidence. Where subsidence or other forms of subsidence is still occurring along viaducts, they use leveling jacks at each bent, and relevel the viaduct spans on a periodic basis.

**In addition to groundwater drawdown-induced subsidence, one example was provided where a road embankment was constructed beneath a high-speed rail viaduct, not far from one of the viaduct bents. In this location, settlement induced by the weight of the embankment fill caused tilting and possibly settlement of the viaduct bent. To mitigate, the embankment was removed from the vicinity of the high-speed rail viaduct, and replaced by a viaduct highway designed to avoid causing settlement of the high-speed rail foundations.

They also performed satellite altimetry modeling in the California SJV, processing data from October 1992 through February 2015. They presented preliminary graphs of subsidence a short distance south of Hanford during the NISOLS meeting, and published a final version in June 2016[3], showing about 5 ft of subsidence over this period of about 23 years, for an average rate of about 2.6 inches per year. However, their rates began at about 1.8 inches per year from 1992, and accelerated to about 4.3 inches per year by about 2010. (Note that this compares reasonably well with a JPL InSAR rate of about 5 to 6 inches per year from 2007 through 2010 in this general area.)

2.3.4.3.2 December 2015 Meeting with Professor Cheinway Hwang and his Team

Prof. Hwang and team confirmed their normal use in Taiwan of the 1/1000 (= 0.1 percent [%]) “angular deflection” criteria.

There was also discussion of mitigation that was performed at one location where a highway embankment crossed the HSR Alignment and induced local subsidence that rotated at least one pier and produced unacceptable movement. In response, Cheinway indicated the highway

[3] Hwang, Cheinway, YuandeYang, Ricky Kao, Jiancheng Han, Devin L. Galloway, Michelle Sneed, Wei-Chia Hung, C. K. Shum, Yung-Sheng Cheng, Fei Li, 2016. “Time-varying land subsidence detected by radar altimetry: California, Taiwan and north China,” in *Scientific Reports*. June 21.

embankment had been removed and replaced with a viaduct supported on deep foundations. (Note that this was not a drawdown-induced subsidence mechanism, but rather conventional settlement under a surface load.)

A presentation by Prof. Hwang and his team indicated that the following subsidence monitoring methods are used in Taiwan, including for the THSR. These include:

- GPS – some continuous stations, and GPS campaigns including permanent antenna mounting points to minimize setup error.
- InSAR – starting with what they call DInSAR (classical), then PSInSAR, and now TCPInSAR (Temporarily Coherent Point InSAR) methods developed in Hong Kong. TCPInSAR may be worth investigating further for the HSR.
- Compaction extensometer – considerable time was spent on this topic. A multipoint system has been developed in Taiwan, where a single well can have up to 25 magnetic rings that are placed outside of a plastic (non-conductive) casing, and detected electro-magnetically. Using an Invar tape to lower and raise a ring-detecting sonde in the well, an effective accuracy of 1 millimeter (mm) can be achieved. The method has been used with Invar tape lengths up to 300 meters. Example data sets were presented. There was a discussion of subsidence depths in SJV for HSR. Subsidence depths up to 500 meters may be relevant; at a minimum, compaction extensometer depths need to get at least well below the Corcoran clay unit, which appears doable with the 300m tape.
- Gravity meter – research is progressing on using gravity meter methods to measure subsidence. Gravity measurements are much faster than GPS survey. The idea is to use change in gravity to indirectly measure subsidence. Among other variables, the magnitude of gravitational force is a function of the gravity meter's distance from the center of the earth, and the depth to groundwater. Multiple variables effect gravity measurements. Although under some conditions gravity meters may be useful especially as a screening tool to identify where GPS measurements may be needed, it seemed to be recognized that with large potential and unknown changes in depths to groundwater, it may not be an applicable methodology for the HSR.

Prof. Hwang then presented results of satellite-based "radar altimetry" they had performed for parts of Taiwan, and also for the SJV. Satellite radar altimetry measurements are feasible along radar satellite track paths. A subsidence history was presented for satellite tracks passing between Hanford and Corcoran using the TOPEX/Poseidon satellite data for the years 1992-2002, the Envisat satellite data for the years 2002-2010; the Jason-1 satellite for the years 2002-2009, and the Jason-2 satellite for the years 2008 to 2015 satellite). These historical satellite tracks generally seemed to be oriented approximately north-northeast to south-southwest, or south-southeast to north-northwest, and hence at discrete locations they cross the HSR Alignment. The results of this historical altimetry study were published in 2016 (Hwang et al, 2016), are summarized in Section 2.3.4.3. Subsidence profiles for extended time periods could be developed at other locations along the satellite tracks, and may be of interest where they may be near the HSR Alignment.

Prof. Hwang said that in Taiwan they have not noticed horizontal ground movement toward wells accompanying vertical subsidence, but they not been specifically looking for it as they are primarily doing one-dimensional subsidence modeling.

They noted that they have more plastic and less brittle soil than SJV, and have not seen fissuring, although they understand the Chinese have seen fissures, especially in the north, in drier climates than Taiwan.

After his presentation and general discussions, Cheinway led a brief discussion of responses to a few questions that had been prepared prior to the meeting. The questions are shown below, with answers in square brackets.

- Question: Currently, there is an abundant amount of information available about land subsidence and earth fissures. However, this information is widely scattered among different governmental agencies, educational institutions, private consultants, and local freight/rail companies. Is there any integrated, inter-operable online data library set up in Taiwan or China for use by the geoscience research community?
    - *[Response: No formal collection exists, but data and publications from much of the world are readily available, except that there are some limits to access to Chinese data. Cheinway indicated he does not attend geotechnical conferences, so there may be more he is not aware of in that field.]*
- Question: Since land subsidence and earth fissures are a hot topic for research in Taiwan and China, is there any partnering set up among universities to share research data and reduce duplication of efforts in research work?
    - *[Response: They have not seen fissuring; see above discussion.]*
- Question: As research and data acquisition techniques are advancing with time, has a risk analysis approach been incorporated into publications and mapping products? (Tom)
    - *[Response: Others in Taiwan are addressing risk, but not his group.]*
- Question: What is the rate of grade change (either measured as percent of grade change in 100 ft (or meter) or measured as the vertical radius) caused by subsidence?
    - *[Response: The presentation noted that a general change of grade of 0.001 is considered to be an upper limit for acceptable grade change for the THSR. They anticipate embankments will perform better than viaducts in areas with differential subsidence. Cheinway also cautioned that adjacent or crossing embankments from other infrastructure could cause problems in response to load-induced settlement.]*

2.3.4.3.3 Communications with Wei-Chia (Kelvin) Hung, PhD

Additional information was provided by Wei-Chia (Kelvin) Hung, PhD. Dr. Hung is the owner and manager of Green EECC, who performs land subsidence monitoring for the Taiwan HSR Corporation. Information shared by Dr. Hung is summarized below.

- Total maximum documented land subsidence in Taiwan that has occurred in the recent past is over 5 ft with recent maximum rates of around 2.5 inches per year.

- Compressible geologic units are present to depths of approximately 700 ft as documented by vertical extensometers, and much of the land subsidence is occurring due to withdrawal from confined alluvial aquifers below depths of 200 ft.
- Land subsidence in Taiwan is largely seasonal with more groundwater withdrawal (and subsidence) occurring in the dry season, and rebound of groundwater levels and some rebound of land subsidence occurring in the wet season.
- This amount of land subsidence has caused significant effects to the HSR system, including slowing the trains down and localized reconstruction of the system.
- The HSR system is largely constructed on viaducts and to accommodate the land subsidence, the equivalent of “hydraulic jacks” have been installed to raise and lower the tracks to accommodate for vertical movement due to land subsidence.
- Horizontal deformation has been observed and causes the track to “sway back and forth” throughout the year. They had no way to accommodate for this horizontal movement.
- The government of Taiwan has prohibited groundwater withdrawal within approximately 1 mile of the HSR tracks to prevent horizontal and other deformation from ground subsidence.
- Internet searches of “land subsidence Taiwan high-speed rail” return many articles that discuss the problems and the high costs that have been incurred as a result of land subsidence.

2.3.5 Summary

Owners and operators of infrastructure in the SJV were interviewed to ascertain how their infrastructure had been impacted by subsidence (if at all, or if they knew), how they were monitoring for such impacts (if at all), and what mitigation measures had been implemented (if any). Several consultants with existing HSR systems in other countries were also interviewed with the same general questions.

In general, subsidence has not had a significant impact on most infrastructure, with a few notable exceptions, including the following:

- One road near the community of Pond has required ongoing maintenance due to ongoing differential movement across the Pond-Poso Creek Fault (averaging on the order of 0.4 inches per year, with maximum observed rates on the order of 1 in/year);
- Dikes around one water storage pond near Alpaugh have experience differential settlement, likely due to a combination of groundwater drawdown-induced subsidence and settlement in response to the weight of the dikes being placed over compressible soils.
- A small number of canal owners have reported changes in gradient to a degree that it has noticeably impacted flow (in at least two locations requiring construction of a lift station), and concrete linings have cracked, apparently due to differential subsidence. In one location, a low spot in the canal resulted in deeper flows, leading to a need to raise the banks of the canal and construct walls along a bridge to keep water from the pavement that was at or below maximum water level.

- In Taiwan, groundwater pumping has been regulated within about 1 mile of the HSR Alignment to reduce subsidence, and adjustable jacks have been added to viaducts to allow adjustment on a periodic basis.
- In China, in subsiding areas, tracks have been supported on embankments with ballast rather than on viaducts, and train speeds have been reduced.

2.4 TOPOGRAPHIC AND SUBSIDENCE DATA ALONG HSR ALIGNMENT

Survey activity in the SJV has included project survey monuments at approximately 2-mile intervals along the HSR Alignment completed in 2010 and repeated in early 2015. This survey provided evidence that significant subsidence is occurring in the SJV. Detailed surveys covering a portion of the HSR Alignment were completed using Light Detection and Ranging (LiDAR) in 2008 and RTK GPS survey in 2016. Over that time period of 8 years, these surveys are of sufficient detail to provide quantifiable local subsidence information, with measurement constraints or 'noise.' LiDAR and RTK surveys are considered to have insufficient precision for normal subsidence monitoring; however, these measurements are of sufficient precision to provide valuable information for the portion of the SJV with up to 9 ft of subsidence, including possible areas of compaction faulting (clay faults).

2.4.1 2008 LiDAR Survey from U.S. Army Corps of Engineers

In support of a dam break analysis for Success Dam in the Sierra Nevada Foothills east of the HSR, an airborne LiDAR survey of the SJV from Success Dam west to the Tulare Lakebed was completed under the direction of USACE (2009) in July 2008. This LiDAR survey encompassed the HSR Alignment from about Allensworth (south of Deer Creek) north through the town of Corcoran. Elevation results were processed and reported to a scale of 10-foot by 10-foot pixels across the surveyed area.

2.4.2 2016 RTK Survey

In support of flood analyses for the HSR Alignment, AFW performed an RTK GPS survey in August 2016. The objective of this survey was to provide up-to-date elevation information to adjust the USACE 2008 LiDAR SJV elevations to account for differential subsidence since 2008 that could modify patterns of flooding. Surveying was performed using a vehicle-mounted RTK receiver station and the Caltrans CGPS Station CRCN in Corcoran as the RTK base station. The receiver station vehicle was driven 700 miles on local roads in the SJV with RTK measurements taken at interval of about 50 to 60 ft along those roads while the vehicle was in motion. A total of about 76,000 RTK points were acquired; elevations were also acquired at Project benchmarks and other selected benchmarks.

2.4.3 Other Recent Surveys

Repeat surveys of HSR Project benchmarks in 2010 and 2015 have provided static GPS verification of subsidence in the SJV. At typical spacing distances of about 2 miles, these

measurements provide no information on local differential subsidence. Several Continuous Global Position Survey (CGPS) stations in the SJV provide point-specific detailed subsidence histories for the last several years extending to before the current drought conditions. A LiDAR survey of the HSR Alignment by Dragados in 2015 provides additional coverage of the Project area. Its relevance is limited since the 2016 RTK survey provides newer measurements of subsidence to compare with the 2008 LiDAR.

2.4.4 Interferometric Synthetic Aperture Radar (InSAR)

Farr et al. (2015) at JPL provided satellite-based L-band InSAR classical interferometry for the Central Valley. This work was performed for the California DWR, and appears to have been focused on DWR infrastructure. Starting with the 6/21/2007 scene, classical interferometric results were obtained for the following dates: 9/21/2007, 11/6/2007, 12/22/2007, 2/6/2008, 3/23/2008, 5/8/2008, 8/8/2008, 6/26/2009, 9/26/2009, 12/27/2009, 3/29/2010, 5/14/2010, and 12/30/2010. Two L-band scenes were needed to provide coverage for the Central Valley. The western scene covers the California Aqueduct and areas with extensive historical subsidence measurements and studies. The scene appears to have relatively 'smooth' results which may, at least in part, be the result of extensive post-processing smoothing or other operations having been applied to the classical interferometric information. The eastern scene has interferometric results that exhibit considerable small-scale roughness relative to the western scene. This implies that the classical interferometric results may be less smoothed by post-processing operations.

More recent InSAR has been provided by JPL (Farr et al., 2015; 2017) to increase coverage of much of the SJV from 2014 to 2016. JPL used Canadian Radarsat-2 satellite C-band radar for coverage for the period May 3, 2014 to January 22, 2015, and the European Space Agency Sentinel-1A satellite C-band radar for coverage for the period May 7, 2015 to September 10, 2016.

2.5 AVAILABLE LITERATURE

Relevant literature related to groundwater drawdown and subsidence is listed in Section 12.0.

3.0 HISTORY AND MECHANISMS OF GROUND SUBSIDENCE

3.1 INTRODUCTION

3.1.1 San Joaquin Subsidence History

Over at least the past 90 years, groundwater drawdown due to groundwater extraction has induced subsidence over large areas within the SJV. Plate 1-1 is a map showing the observed subsidence from 1926 to 1970 and from 2007 to 2010.

The Corcoran Subsidence Bowl sits in the Southern SJV between the Fresno and Bakersfield alluvial fans. Prior to the population growth and development of large-scale farming in the

Southern SJV, the area to the west of the HSR Alignment was covered by the historical Tulare Lake, located in the topographically lowest region of the hydrologic basin at the time. Starting in the latter half of the 1800s, the lake has been dried up by farmers to create arable land. Although the former lakebed has been developed into agricultural land, flooding still periodically occurs in this area.

According to the USGS, subsidence has been observed during much of the last century, with as much as 28 ft occurring near Mendota to the northwest, and 14 ft in the Pixley portion of the Corcoran Subsidence Bowl area to the east of the HSR Alignment, as shown on Plate 1-1. During this period, subsidence along the HSR Alignment in the Tulare Lake area may have been about 4 to 6 ft.

Following development of state and federal water projects, surface water became readily available and groundwater extraction was reduced and subsidence due to groundwater drawdown was temporarily slowed or stopped. However, in the past 10 to 25 years, groundwater pumping has once again been accelerating, with associated resumptions and accelerations of groundwater drawdown and associated subsidence; this was exacerbated during the severe drought from fall 2011 to fall 2015. Plate 1-1 also shows the magnitudes and patterns of subsidence from 2007 to 2010, which exceeded an average of 8 inches per year according to analyses by the JPL. Profiles of historical subsidence along the HSR Alignment, as well as induced changes in slope and vertical curvature, are presented on Plate 1-2. Toward the end of the recent drought, annual subsidence rates of 1 to 1½ ft have been observed near Corcoran in 2015-2016. Groundwater pumping and drawdown, and consequent subsidence, are anticipated to continue into the future at least until sustainable groundwater pumping is achieved. Due to inelastic soil behavior, subsidence is mostly irreversible even if groundwater pumping decreases and groundwater levels recover.

3.1.2 Subsidence and Topographic Data

Observed broad areal subsidence data is available for three historical periods. The USGS published a map showing the subsidence between 1926 and 1970 (Plate 1-1). The JPL produced digital subsidence data between 2007 and 2010 based on their estimation using the Interferometric Synthetic Aperture Radar (InSAR) technology (also on Plate 1-1). Recently, the JPL also provided digital subsidence data between 2015 and 2016 based on their interpretation of the Sentinel satellite InSAR data. The highest rates of subsidence were observed between 2015 and 2016 due to heavy groundwater pumping towards the end of a severe 4-year drought. Past subsidence is discussed in Section 5.0.

InSAR data indicates the changes in ground surface elevation, but it does not provide information about absolute elevation. Available elevation or topographic information includes:

The National Map published on-line by the USGS (2016) covers the entire SJV[4] and in the Corcoran area generally represents elevations from surveys made in the 1920s; a 1966 survey of the Tulare Lake Basin by the U.S. Coastal and Geodetic Survey with updates based on 1982-1983 floods (Summers Engineering, Inc., 1969, 1992); 2008 topographic data developed by the USACE based on Light Detection and Ranging (LiDAR) and IFSAR covering most of the Tulare Lake flood zones delineated by the FEMA; and 2015 LiDAR data collected by the CP 2-3 Contractor for a few-mile-wide strip along the proposed HSR Alignment. In August and December of 2016, the AFW team collected additional topographic data along a network of roads overlapping the 2008 LiDAR coverage using RTK GPS equipment mounted on a vehicle. A 2016 DEM was then developed by synthesizing these various sources using a project-developed calculation method (see Section 6.0).

3.1.3 HSR Contracting Strategy Regarding Subsidence

The HSR Alignment for the Design-Build CP 2-3 passes nearly through center of the Corcoran Subsidence Bowl located, and the northern portion of CP 4 lies within the southern portion of the Corcoran Subsidence Bowl. Further to the north, the El Nido Subsidence Bowl is located near Highway 152, in an area of future HSR contracts and extending south to the northern portion of CP 1; subsidence in this area is addressed in Appendix D. Subsidence is also occurring along the HSR Alignment in Antelope Valley, which is addressed in Appendix E.

It has been recognized at least since the fall of 2013 that subsidence in the SJV had the potential to impact the HSR (RDP 2015).

Due to uncertainties associated with subsidence, the Authority directed prospective Contractors for CP 2-3: “Unless directed otherwise by the Scope of Work, for bidding purposes assume that subsidence from groundwater pumping is not an impact to the project area.” The Authority indicated they would then adjust design parameters if needed through design variances based on findings from a statewide GSS to be developed under a separate contract. The GSS was also to provide the Authority with recommendations for future ground subsidence monitoring and mitigation measurements. This GSS report is a product of that statewide study.

3.1.4 Soil Consolidation Mechanisms

When a soil is subjected to compressive effective stress, the resulting volumetric strain is a function of the effective stress divided by the modulus (or stiffness) of the soil. In general, the modulus of a sandy or gravelly soil is an order of magnitude greater than the modulus of a clayey soil, so that for a given change in effective stress, the volume change in a clay will be an order of magnitude greater than in a sandy or gravelly soil. Soil stiffness or compressibility are

[4] As described later in the text, the 2013 DEM is based on the 2009 National Elevation Dataset, but in the Corcoran area, the elevations have not been updated appreciably since 1928.

nonlinear parameters, with the modulus increasing with increasing stress. If “effective stresses” exceed what the soil has previously experienced, compression occurs along a “virgin” compression range, as shown in Figure 3-1.

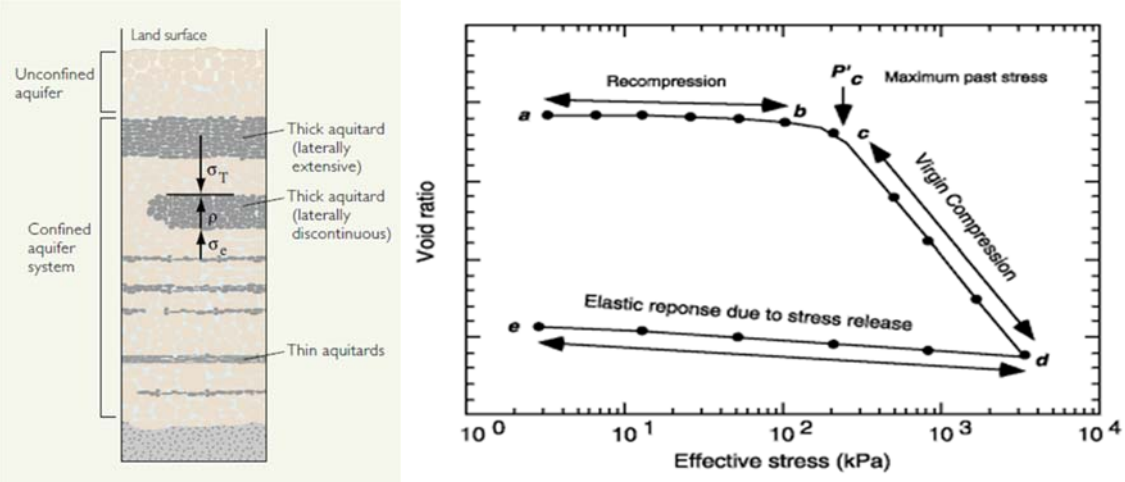

Figure 3-1: Basic schematic of aquifer system (Galloway et al.1999), and nonlinear consolidation behavior of soils, especially aquitards. Water of compaction is removed during virgin compression.

In a saturated soil, because the modulus of water is much greater than the modulus of a soil, water is squeezed out from the soil pore spaces for the soil to undergo volumetric compression. In a gravel, the hydraulic conductivity is fast enough that soil compression can also occur quite rapidly as long as there is a path for water to be squeezed out. A sandy soil is similar but somewhat slower because the hydraulic conductivity may still be relatively higher (although it slows with decreasing grain size). A coarse sand may have a hydraulic conductivity 1 to 2 orders of magnitude smaller than a relatively fine gravel, and a fine or silty sand may have a hydraulic conductivity another 1 to 3 orders of magnitude smaller. A clayey soil may have a hydraulic conductivity value of another 2 to 3 orders of magnitude smaller than a fine sand, or maybe 4 to 8 orders of magnitude smaller than a medium to fine gravel. Thus, when a clayey soil is compressed, it may take a long time for the water to drain out and the soil to finally consolidate.

The high-permeability coarse-grained soils in an aquifer allow for groundwater to travel with relative ease so that it can both be removed (e.g., via pumping) and be recharged (e.g., when water at a higher pore pressure in adjacent materials is available). Pumping from aquifers lowers the hydrostatic pressure in the aquifer pore water, resulting in increases in the particle-to-particle “effective stresses” in the compressible fine-grained aquitard material (especially clays), causing them to undergo compression as they squeeze groundwater into adjacent coarse-grained aquifer materials. Because of irreversible loss of pore space (compaction) during compression, the original storage volume generally cannot subsequently be recovered. The compaction resulting from soil compression is manifested at the ground surface as land

subsidence. Subject to the same pumping rate, a well in a more permeable aquifer system produces smaller drawdown at the well but a larger radius of influence.

A schematic overview of aquifer system components and basic consolidation behavior in the Corcoran Subsidence Bowl is presented in Figure 3-1. The aquifer system consists of a shallow unconfined aquifer and a deeper confined aquifer separated the thick Corcoran clay. , The Corcoran Clay Member of the Tulare Formation is the principal low-permeability soil zone in the SJV that creates a confined aquifer system. The approximate depth to the Corcoran clay along the HSR Alignment and within the Corcoran subsidence bowl is shown on Figure 3-2. The deeper aquifer consists of interbedded layers of low permeability aquitards and permeable soils. The recharge coming from the Sierran foothills is the major inflow to the aquifer system. Poland et al. (1975) have noted that “the areas in which subsidence has been appreciable coincide generally with the areas in which groundwater is withdrawn chiefly from confined aquifer systems” (e.g., from below the Corcoran Clay). Bertoldi et al. (1991) reported that by 1991, an estimated 100,000 high-capacity wells (typically greater than 1,000 gallons per minute [gpm]) were in operation in the Central Valley. They also report that typical large capacity water wells of that era had perforated zones extending above and below the Corcoran Clay, and thus permitted significant local flow paths between underlying deeper confined aquifers and shallower unconfined aquifers.

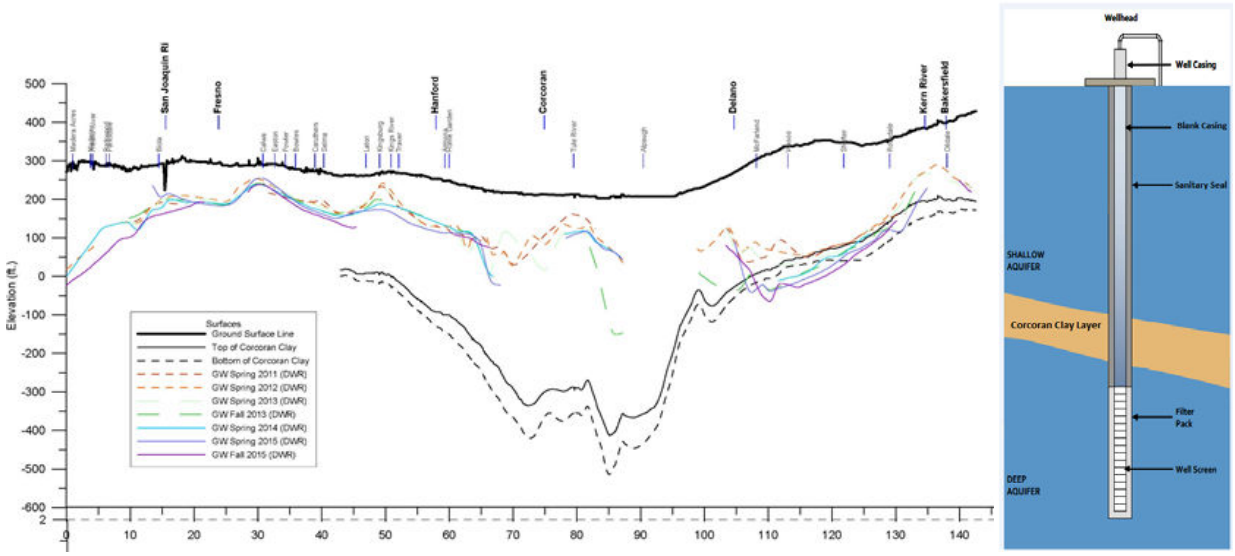

Figure 3-2: Typical elevation along HSR Alignment of the Corcoran Clay, the principal confining horizon in the SJV, and a typical modern water well configuration into the deep aquifer system. Earlier water wells commonly were screened in both the shallow and deep aquifer systems.

While the Tulare Lake was present and the groundwater was high, all of the underlying soils were submerged such that at any depth, any soil particle only felt the buoyant weight of the soil above. After the Tulare Lake was drained about 100 years ago. shallow groundwater was utilized for agricultural and domestic uses. Once groundwater was lowered, the soil particle

below the water table in the shallow aquifer felt the unit weight of the soils above the water table and would consolidate accordingly. The drawdown in the shallow aquifer resulted in upward hydraulic gradient across the Corcoran Clay between the shallow and deep aquifers. The Corcoran clay provided a barrier to water being squeezed out of the underlying soils. Over time, deeper soils would eventually feel the reduction in pore pressure and would consolidate accordingly, resulting in consequent subsidence of the ground surface.

With the quantity of available groundwater diminishing in the upper aquifers (above the Corcoran clay), wells have been drilled deeper, now often extending to depth of 1000 to 1500 ft or more. While in the past these wells punctured this aquitard and not only allowed the water to escape, but (of course) accelerated the drainage process by actively pumping. This pumping results in pressure decreases in the pore water with corresponding increases in the pressure the individual soil particles feel from the overlying soil particles, leading to consolidation. Removal of water from the aquifer system, by pumping or other means, is a primary cause of subsidence in confined aquifers; the lost water may be termed “water of compaction.”

Due to low permeability of compressible clayey soil, the pore pressure within the aquitard layers respond slowly to the pore pressure decrease in the sandy aquifer materials, resulting in delayed subsidence responses.

Given the regional-scale of groundwater extraction and land subsidence in the Central Valley, and the relative paucity of reliable data regarding soil strata, pumping quantities (and rates), and subsidence patterns, quantitative analysis of land subsidence is challenging to say the least. Complexities of groundwater and land subsidence modeling are addressed in Section 4.0.

3.1.5 Settlement vs. Subsidence

3.1.5.1 Introduction

In this section, to distinguish between Subsidence and Settlement, the term “Subsidence” will be used to designate downward movement of the ground surface in response to groundwater withdrawal and lowering of the groundwater level; this results in an increase in the effective stresses within the soil below the original top of groundwater and a corresponding compression of the soil. On the other hand, the term “Settlement” will be used to designate downward movement of the ground surface in response to the imposition of new loads at or near the ground surface, that which occurs beneath new fill embankments or structural footings.

New loads that will lead to Settlement include conventional or mechanically stabilized earth (MSE) embankments, structures on shallow foundations, or structures on deep foundations. Settlement will be the greatest directly beneath the embankments or structures, but the ground surface beyond the edges of embankments or foundations will also settle to a diminishing degree with increasing distance from the loaded area.

Significant subsidence along the HSR Alignment in Section CP 2-3 is primarily a deep phenomenon occurring in pumped aquifers below the Corcoran Clay, although shallower pumping may be encountered in some locations.

3.1.5.2 Contractual Background

By contract, each design-build contractor (Contractor) is responsible for limiting post-construction Settlement to the values identified in the project *Design Criteria*. On the other hand, the Contractors are not responsible for the consequences of Subsidence. It therefore is contractually important to be able to distinguish the causes of downward (and possibly lateral) ground displacement between Subsidence and Settlement.

3.1.5.3 Subsidence

Subsidence occurs as a result of the lowering of groundwater or phreatic levels, sometimes termed groundwater drawdown. Most commonly, groundwater drawdown may be broadly regional, or it may occur somewhat more locally, such as with a conical area around a water pumping well (possibly several hundred to several thousand feet in diameter around the well), as depicted in Figure 3-3 (see Section 4.0 for additional discussion). The pattern of groundwater drawdown may also be affected by zones of groundwater recharge (e.g., along rivers or streams or near recharge ponds). Groundwater flow is also affected by the geometry and properties of aquifers and aquitards, and the relative continuity or discontinuity of these zones. However, in general in the SJV, spatial variability of groundwater or phreatic levels is relatively gentle. As a consequence, the spatial variability of Subsidence, or the magnitude of “differential Subsidence,” is also generally relatively gentle, and any induced changes in the slope of the ground surface are relatively gentle with a relatively broad spatial distribution.

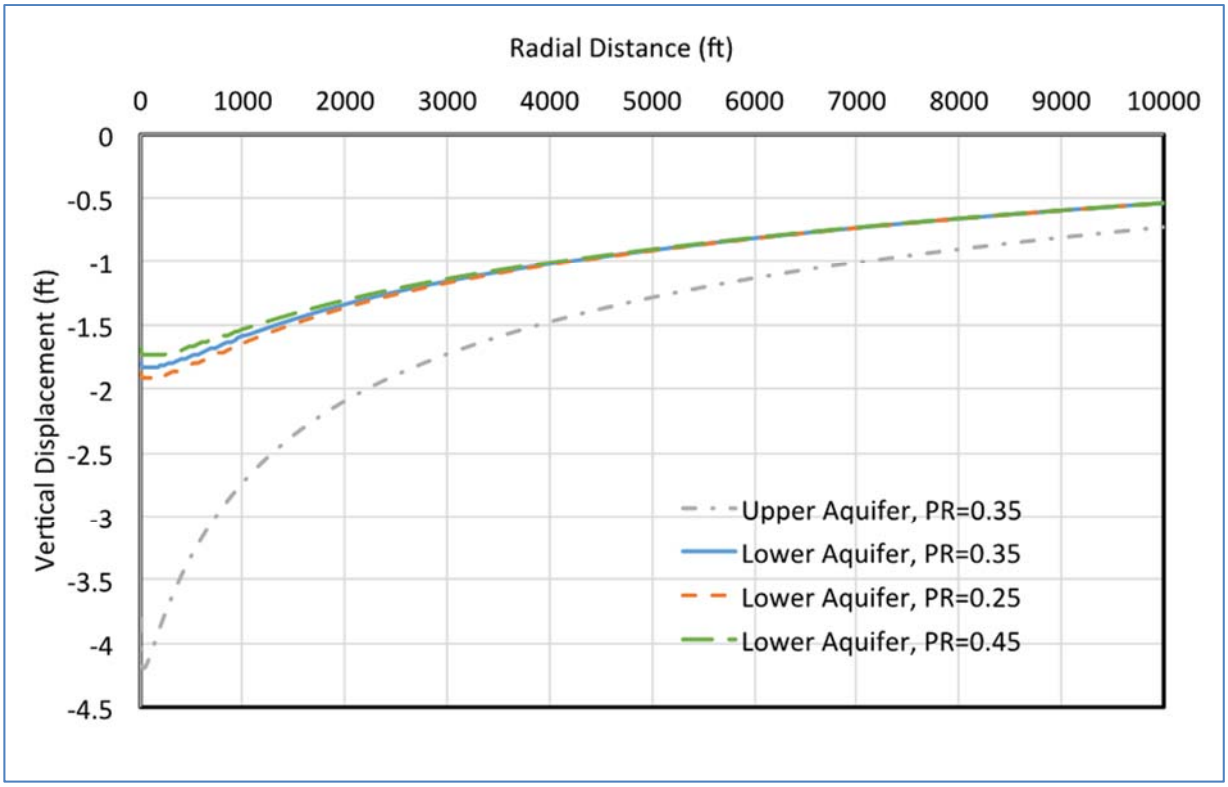

Figure 3-3: Modeled subsidence profiles along radial direction after 20 years of groundwater extraction

3.1.5.4 Settlement

Placement of new loads, such as embankments or structures, also increases stresses in the soils beneath these loads to a depth equal to one to a few times the width over which the load is applied. Where soil stress is increased in more compressible soils such as geologically-young and/or saturated clays, consolidation of the soils results, leading to Settlement of the ground surface and of the overlying new embankment or structure. Because the stress increase spreads laterally beneath the load, beyond the simple footprint of the applied load as “pressure bulbs” as depicted in Figure 3-4, the ground surface for a short distance beyond the edge of the applied load also settles, although the magnitude of Settlement attenuates relatively rapidly beyond the edge of the load.

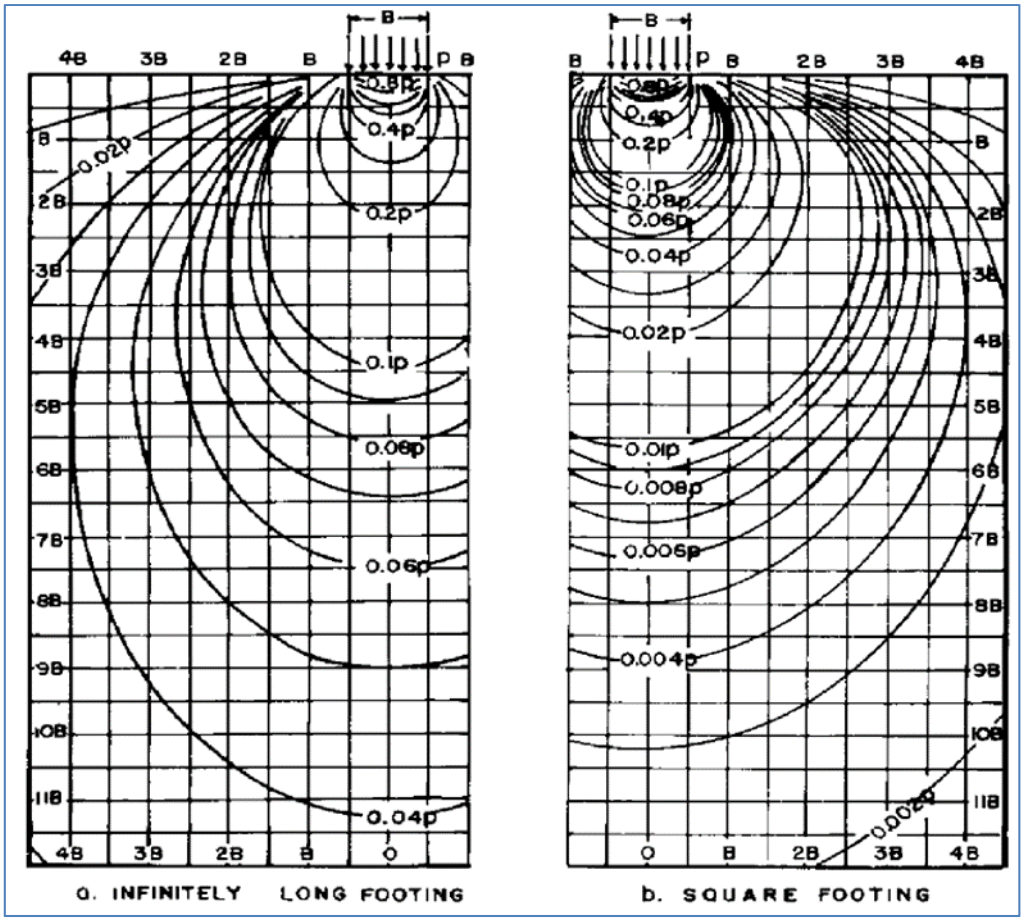

Figure 3-4: Vertical stress contours below footing or embankment. From Navy Design Manual 7.01: Soil Mechanics, 1986.

For illustrative purposes, the schematic pattern of Settlement beneath and beyond a hypothetical embankment, placed over clayey soils with relatively shallow groundwater, is shown on Figure 3-5.

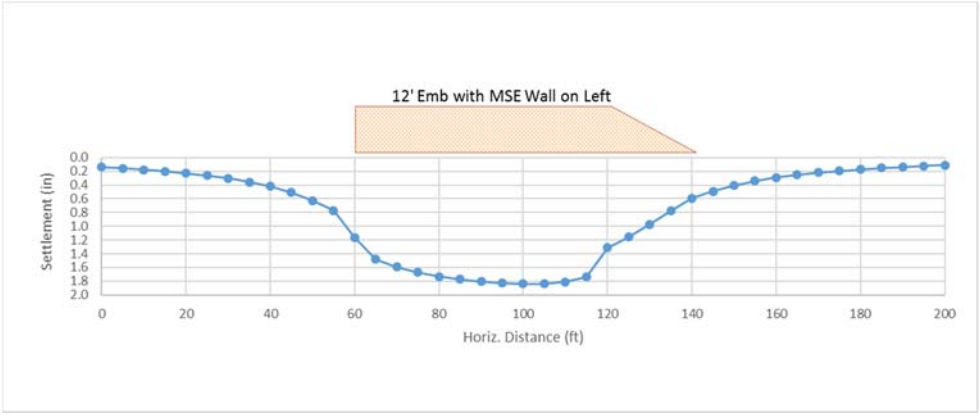

Figure 3-5: Conceptual Settlement Profile Under Generic 12-ft Embankment

3.1.5.4.1 Relative Predictability of Subsidence and Settlement Values

Reliable prediction of Subsidence requires knowledge of the deep subsurface profile (possibly extending down to 1,000 to 2,000 ft or more), including spatial distribution of material types; properties (e.g., compressibility, hydraulic conductivity) of these materials; the stress history throughout the profile; current groundwater conditions; and future groundwater drawdown (related to future groundwater use and recharge conditions). Because soils as deep as several thousand feet appear to be contributing significantly to currently ongoing Subsidence, knowledge of the soil profile and groundwater conditions would ideally extend to these depths.

Currently, with the limited information regarding variability of subsurface profiles and future groundwater drawdown, the best method of prediction may be to assume that something similar to past rates and patterns of Subsidence will continue into the future. However, this does not take into account changes in land use or groundwater extraction, or complexities in subsurface geology. When it is completed and well-calibrated, use of the CVHM-mod (discussed in Section 4.2) is expected to improve subsidence predictions. Also, predictions may be improved with more detailed subsidence information, from sources such as on-ground monitoring, or higher resolution InSAR (e.g., X-band Cosmo-SKYMED), and ongoing improvements in knowledge of groundwater extraction and drawdown.

Relatively reliable prediction of Settlement requires a knowledge of the subsurface profile to the depth of interest (i.e., one to a few times the width of the applied load, so on the order of a few tens to maybe somewhat more than 100 ft), including spatial distribution of material types, properties (e.g., compressibility, hydraulic conductivity) of these materials, and the stress history throughout the profile.

Within the SJV, in general, prediction of Settlement is simpler and more reliable than prediction of Subsidence for reasons described in the preceding sections and summarized as follows:

- Depth of interest for Settlement is much less, so it is easier to define the soil profile.
- For Settlement, the magnitude and distribution of applied load is generally known with very good level of accuracy, whereas for Subsidence, the increased stresses are a result of changes in groundwater and phreatic levels, which are difficult to determine particularly to the great depths of several thousand feet that contribute to Subsidence.
- The areal distribution of Settlement is generally relatively simple to determine with knowledge of the load distribution and soil properties within a depth equal to one to a few times the width of the embankment, whereas the areal distribution of Subsidence is very broad and difficult to delineate because it is affected by the changes in groundwater and phreatic levels as well as material properties and stratification patterns that are present to very great depths.

Although prediction of Settlement is simpler than prediction of Subsidence, both Settlement and Subsidence can be measured with relative ease as discussed in the following sections.

3.1.5.5 Distinguishing Settlement from Subsidence

Figure 3-5 provides insight regarding how to distinguish Subsidence from Settlement. In general, with Settlement, the pattern of ground deformation is greatest beneath the loaded area and attenuates rapidly with distance from the edge of the loaded area. On the other hand, the pattern of Subsidence-induced ground deformation will not display any particular similarity to the shape of the loaded area. Although it is possible that general trends of Subsidence could coincidentally roughly follow the pattern of embankment or structure loading, differential Subsidence patterns will still almost certainly be more gentle and subtle than Settlement patterns, and Settlement patterns will almost certainly be much more “locked-in” to the spatial distribution of the embankment or structure loading patterns.

Total ground deformations can be assumed to be approximately the additive superposition of Subsidence and Settlement. We are not aware of any condition where there would be a significant synergistic (or antagonistic) relationship between Subsidence and Settlement, in which the occurrence of Settlement would significantly increase (or decrease) the magnitude of Subsidence, or where the occurrence of Subsidence would significantly increase (or decrease) the magnitude of Settlement. In other words, Subsidence and Settlement are independent variables.

3.1.5.6 Recommendations

Recommendations will involve some combination of instrumentation and/or monitoring. Methodologies to be considered are discussed in the following subsections. The final selection of what methodologies to implement is further discussed in Sections 9.0 and 10.0.

3.1.5.6.1 Survey Control Points

To monitor Settlement, survey control points must be established outside of the limits of significant Settlement. In order to assure that survey points are set back far enough, we recommend that the Contractor develop representative cross-section profiles of anticipated Settlement similar to Figure 3-5, depicting the calculated pattern and magnitudes of Settlement beneath and near embankments (including conventional trapezoidal embankments as well as MSE wall-retained embankments and other fills) and structurally-loaded areas (including footings most importantly). Settlement of the ground around deep foundation elements is expected to be minor, but this should be confirmed by the Contractor)

Where available data suggests Subsidence is occurring at a significant rate, control points themselves may be subject to significant subsidence. Therefore, control points should be checked periodically during and following construction to determine the rate of Subsidence. We recommend that the surveys be repeated frequently enough that the Subsidence between readings is not more than about 0.1 to 0.2 ft.

Immediately following construction of any significant embankment or structure, the tops of the embankments and structures should be surveyed to establish a baseline, and then periodically following construction. The survey should be repeated frequently enough that the Subsidence between readings is not more than about 0.1 to 0.2 ft.

3.1.5.6.2 InSAR

Baseline InSAR observations may be processed and evaluated for the HSR Alignment prior to construction, and updated during and following construction to evaluate patterns of ground deformation near embankments and structures, as well as deformation of the tops of completed embankments and structures. InSAR may also be performed at the end of the contract to evaluate rates of Subsidence and Settlement.

In order to achieve the most meaningful InSAR results, processing of the relevant scenes may be performed as they become available. In any case, although Subsidence or Settlement rates may not be needed as frequently as scenes are captured, the more frequently-spaced data points provide much better accuracy and reliability of interpreted values, and fewer or smaller areas lost to decorrelation.

We tentatively suggest that X-band will provide the best resolution (3 m pixels) and accuracy, at least along roads and other hard features such as buildings. C-band may also be considered but we anticipate it will not be significantly cheaper and the quality of data will be diminished and the pixel size will be coarser. It may be advantageous to find areas where C-band also provides similar result to X-band.

Although in principle it may be possible to make use of InSAR processing performed by government agencies, we recommend considering whether a private InSAR contractor should be retained to assure timely completion of image processing that adequately covers the areas of interest. We believe that it could work to have the InSAR contractor be retained by either the Contractor or by the Authority. In either case, the results of the InSAR evaluations should be made available to both parties.

3.1.5.6.3 LiDAR Survey

A professionally provided LiDAR survey of the CP 2-3 HSR Alignment has been performed by the CP 2-3 Contractor. We recommend that a similar survey be performed after the end of construction, shortly before the contractor is to turn the site over to the Authority.

3.2 GEOLOGIC SETTING

3.2.1 Physiography

The Corcoran Bowl is located in the south portion of the Great Valley Geomorphic Province (the southern portion of the Great Valley is commonly referred to as the San Joaquin Valley [SJV]). The topography of the Great Valley is relatively flat, bordered by the Pacific Coast Range to the

west, the Klamath Mountains and Cascade Range to the north, the Sierra Nevada to the east, and San Emigdio and Tehachapi mountains to the south.

The SJV is an asymmetric structural trough that is filled with sediments up to 30,000 ft thick. Deposition in the valley was mainly marine until the middle to late Pliocene epoch (approximately 3.4 to 2.6 million years ago [Ma]) when the valley's seas retreated and were replaced by freshwater rivers and lakes. Alluvial fan deposits in the SJV were derived from the erosion of the South Coast Ranges and the Sierra Nevada. Along the eastern margin of the SJV, a series of predominantly non-marine Tertiary clastic deposits rest upon granite and metamorphic basement rocks of the southwestward-tilted Sierran block. Bedding within these sediments generally dip gently southwestward beneath the alluvial deposits which cover most of the valley floor. During the Ice Ages of 2.58 Ma to 11,700 years ago, many cycles of glacial advance and retreat across the Sierra Nevadas generated the dominant material to fill the valley underlying the HSR Alignment. Alluvium ranged from punctuated mega-flood events depositing coarse alluvium to lacustrine fines carried by seasonal flows deposited in lakebeds. From before about 760 to 615 thousand years ago (Ka, for kilo-annum), the Pleistocene Corcoran Lake extended from the Sacramento-San Joaquin Delta to the foot of the Tehachapi Mountains. By about 615 Ka, continuing basin deposition and local and regional tectonics changed surface water flow to substantially drain the lake to the north. Alluvial filling of the ancient Corcoran Lake area proceeded until, with continuing development of the Kings River alluvial fan through the Pleistocene to the present, only the historical Tulare Lake remained, covering about 440,000 acres by the early 1800s. The approximate extent of historical Tulare Lake is shown on Figure 3-6.

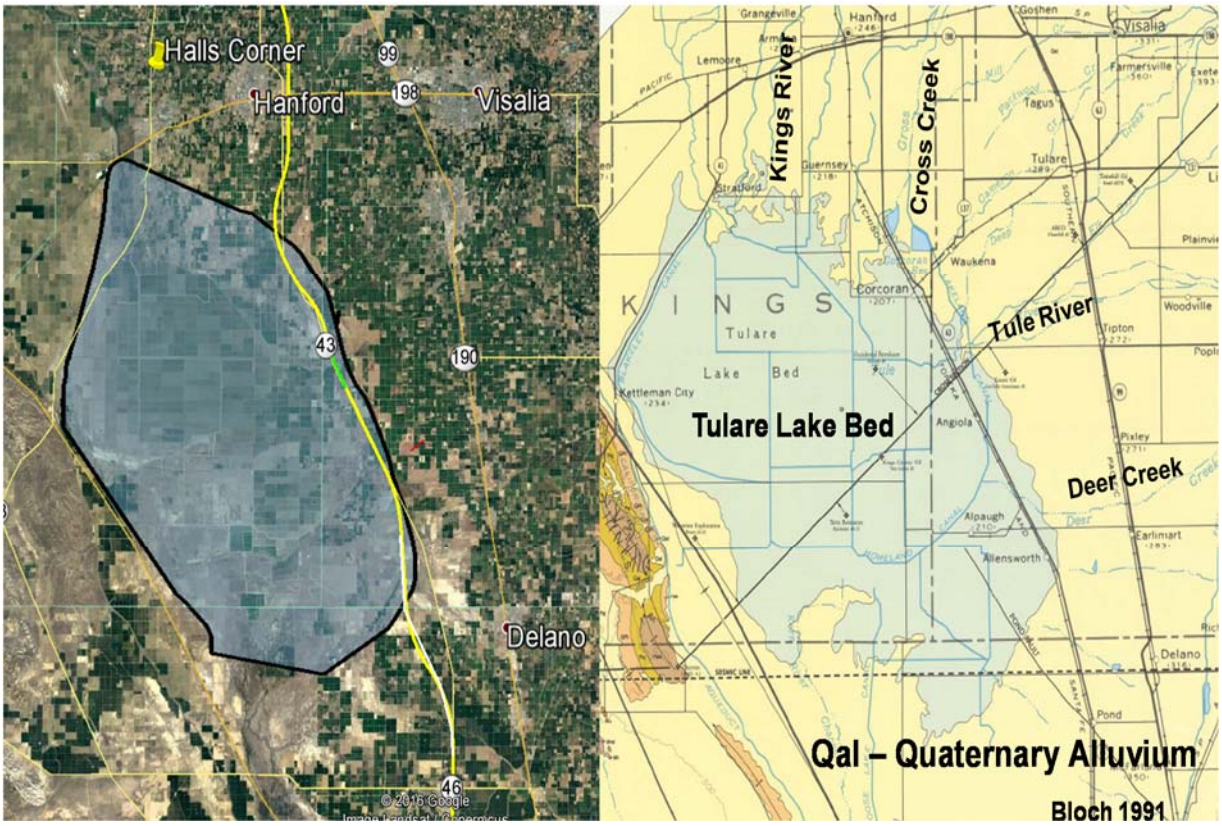

Figure 3-6: Rough Outline of Historical Tulare Lake (after Paul, 2007) and Local Geology (Bloch 1991)

The local geology of the Corcoran Bowl area is a mixture of alluvium that consists of alluvial fan and basin deposits. A geologic map showing the extent of Quaternary Alluvium is included in Figure 3-6.

3.2.1.1 Basin Alluvium and Subsidence-related Alluvium Behavior

Basin alluvium and typical parameters relevant to subsidence (as well as compaction faulting and earth fissuring) may be generalized into three groups or classes. The boundaries or interfaces of these alluvium groups or classes become locations where differential stresses and strains become concentrated, and compaction faults or earth fissures are more likely to develop. General alluvium facies relevant to subsidence and earth fissuring characterization are:

- **Proximal-type** – the material that is deposited primarily near the bedrock exposures at the base of the mountains, at high energy drainages and on steeper basin slopes; it is usually relatively coarse-grained. Material behavior tends to be dominated by coarse materials (gravels and sands). The high energy needed to transport coarse particles may provide densification during the deposition process, so that the coarse-grained alluvium tends to be relatively incompressible. Compressibility tends to be relatively minor and, due to high permeabilities, relatively rapid. Within the SJV, the Fresno area exemplifies proximal-type coarse-grained alluvium behavior.

- **Medial-type** – the intermediate material between the proximal and distal facies. Material behavior tends to be dominated by the interconnectivity of coarser and finer material lenses and horizons. In this heterogeneous alluvium, the higher permeability coarse-grained alluvium fraction provides drainage to the more compressible fine-grained alluvium fraction. Although total compressibility for a given thickness of heterogeneous alluvium tends to be less than that for fine-grained alluvium, it tends to occur much more rapidly, perhaps over years to decades. Within the SJV, the Corcoran and Pixley areas exemplify medial-type heterogeneous alluvium behavior.
- **Distal-type** / **lacustrine** – the material that is deposited primarily in the center of the basin farthest from the bedrock exposures; it is usually fine-grained. Material behavior tends to be dominated by fines (silts and clays). Fine-grained alluvium is generally deposited at low energy, especially in lake (lacustrine) environments; in-place density and compressibility of this alluvium tends to be a function of its effective-stress history. The Tulare Lakebed exemplifies massive lacustrine alluvium behavior.

Figure 3-7 presents a generalized geologic profile of the aquifer systems showing relative positions of these alluvium types through the southern SJV. Given the great depths and thicknesses of basin alluvium within the SJV, and availability of historical geophysical well logs both for oil exploration and groundwater development, electrical well logs provide a practical means to assess compaction characteristics (which can lead to subsidence) of compressible aquifer systems (Miller el al., 1971). Typical material property parameters corresponding to these fresh water alluvium types (Rucker el al., 2015) that impact subsidence behavior are as follows:

- **Fine-grained alluvium,** composed primarily of clays and silts, has relatively low resistivity (typically <10 ohm-meter [ohm-m]) and is very compressible. Water of compaction (Lofgren 1975) is stored in the fine-grained alluvium. But having very low permeability, it tends to have very slow compression (depending also on layer thickness, with thicker more homogeneous zones compressing slower than thinner or more interbedded zones compressing more rapidly) occurring perhaps over decades to centuries.
- **Heterogeneous alluvium** has a moderate resistivity (typically 10 to ~25-30 ohm-m) and is composed of inter-lensing and/or inter-fingering of fine-grained and coarse-grained alluvium. The high permeability coarse-grained alluvium fraction provides drainage to the highly compressible fine-grained alluvium fraction. Although total compressibility for a given thickness of heterogeneous alluvium may be less than that for fine-grained alluvium, it occurs much more rapidly, perhaps over years to decades.
- **Coarse-grained alluvium** generally has a high resistivity (typically greater than ~25 to 30 ohm-m) and is composed primarily of sands and gravels. The high energy needed to transport coarse particles may provide densification during the deposition process, so that coarse-grained alluvium is relatively incompressible. Coarse-grained alluvium compaction tends to be minor and, due to high permeabilities, rapid.

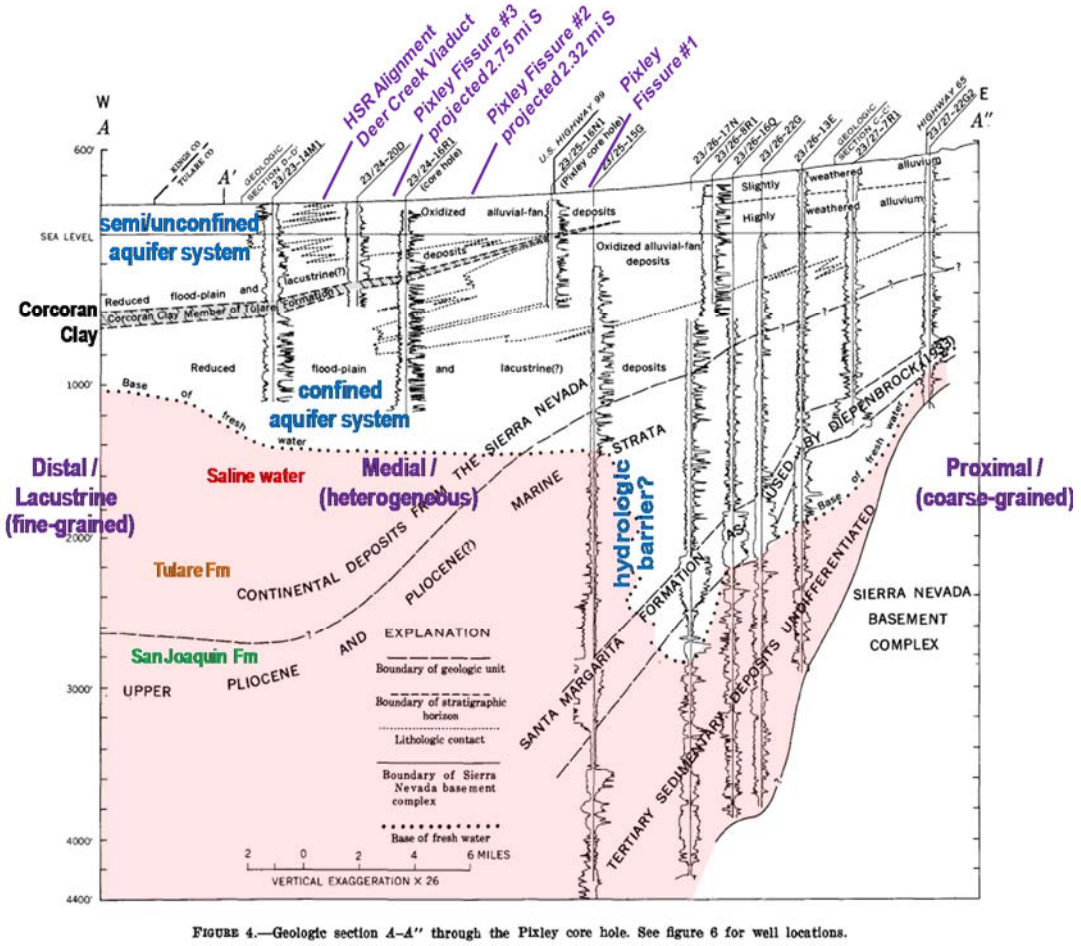

FIGURE 4.—Geologic section A–A'' through the Pixley core hole. See figure 6 for well locations.

Figure 3-7: SVJ west to east geologic profile through HSR Deer Creek Viaduct and Pixley Fissures (from Lofgren & Klausing, 1969; see Plate 8-1 for profile location)

As an aquifer system, the geometrically complex alluvial stratigraphy within the Tulare Formation is challenging to quantitatively characterize and parameterize. Faunt et al. (2009; USGS PP 1766) described how, for developing the Central Valley Hydrologic Model (CVHM), the SJV basin alluvium aquifer system is discretized into more than 20,000 one-mile square cells with 10 layers generally increasing with thickness. Five layers are below Corcoran Clay, two layers represent the Corcoran Clay, and three layers are above the Corcoran Clay. Alluvium (Tulare Formation) texture is simplified, after extensive database construction of information on about 8,500 well and driller logs, and statistical analysis, into percentage of coarse-grained material in 50-foot thick layers in the cells, and ultimately in each cell layer. The overall distribution of averages of the percent coarse-grained deposits above, below, and beyond the edge of the Corcoran Clay within the Tulare Formation aquifer system in Tulare Basin are shown numerically and graphically on Plate 3-1. Various possible relationships between percentage coarse-grained deposits and aquifer system hydraulic conductivity, as well as trends of potential subsidence behavior, are also illustrated on Plate 3-1. Where the Corcoran Clay is present, an overall mean of 35% coarse-grained texture is estimated within the Tulare

Formation below the Corcoran Clay (Faunt et al.2009, Table A2). Where the Corcoran Clay is absent, an overall mean of 47% coarse-grained texture for the relevant Tulare Formation is estimated for Kings County, and an overall mean of 41% coarse-grained texture is estimated for the relevant Tulare Formation in Tulare and Kern Counties. At a 1-mile lateral cell dimension, 5 layers covering many climatic cycles of deposition (discussed in the following sections) through up to about 2,000 ft of the lower Tulare Formation, the CVHM is unable to model fine details of structure between coarse and fine-grained alluvial materials within the Tulare Formation implied by Miller (1999).

Although about 8,500 well and driller logs were utilized to develop the CVHM, little of that information extended to depths within the lower Tulare Formation. On page 26 of PP 1766 (Faunt, 2009) describing the CVHM, it is stated that:

> *"For depth intervals with less than approximately 1,000 texture values (depth intervals greater than 550 ft), the number of driller logs likely is insufficient to represent the average percentage of coarse-grained texture at a given depth."*

To improve characterization of the deeper portions of the Tulare Formation, another information source is available. Historical geophysical oil and gas well log data has recently become accessible online through the State of California Department of Conservation Division of Oil, Gas and Geothermal Resources (DOGGR) website. Although oil and gas wells have typically been cased to depths of several hundred feet, DOGGR provides detailed characterization, primarily formation resistivity and spontaneous potential, through the deeper portions of the Tulare Formation; most of the well logs extend to far greater depths. Occasionally, a more complete suite of geophysical logs is available. Plate 3-2 presents an example of a suite of geophysical logs with a description of available geotechnical parameters, and a resistivity log at an historical USGS corehole. Geotechnical laboratory testing has also performed on samples from that corehole. Dry density unit weight, porosity and void ratio results are plotted beside the resistivity log and the lithologic description. Resistivity logs presented on plates for this report are color coded with blue (less than 10 ohm-m), green (10 to about 30 ohm-m), and red (higher than 30 ohm-m). This color coding is similar in nature to the USGS color coding system used to represent percentage coarse-grained deposits as shown on Plate 3-1.

3.2.2 Geologic History of SJV Relevant to Subsidence along HSR Alignment

Prior to and during the Pleistocene Epoch (Quaternary Period), tectonic forces, including uplift of the Sierra Nevada, Coastal and Transverse Ranges, and folding, faulting and flexure of the Pacific and North American Plates were shaping the deep basin of the SJV (Miller 1999). Saleeby et al. (2012, 2013) posit that in Pliocene-Quaternary time, the Tulare Basin portion of the SJV (encompassing the HSR Projects CP-1 from about Madera [to the north] to the north part of CP-4 at Pond-Poso Creek Fault) has undergone anomalous tectonic subsidence. This anomalous tectonic subsidence would have enhanced alluvium deposition into the Tulare Basin,

including deposition of the Tulare Formation during Quaternary time. The tops of the Santa Margarita Formation, and contemporary McClure Formation have been dated at about 7 Ma, which is when these shallow marine deposits would have been at approximately sea level. Current depths to the top of the 7 Ma deposits along parts of the HSR Alignment are summarized in Table 3-1, and are consistent with current depths shown in Figure 12 of Saleeby et al. (2013). Current depths to the 7 Ma deposits are about 6,000 feet at the Tule River Viaduct in the Tulare Basin south of Corcoran in the southern SJV. Current depths to the 7 Ma deposits are only 2,200 feet at the El Nido subsidence bowl about 80 miles to the north-northwest of Corcoran (in Township T13E-R10S) around Highway 152 south of El Nido. The youngest named marine deposits are the San Joaquin Formation dated to about 2.5 Ma (Scheirer et al., 2007) identified in the southern and central SJV, the 2.5 Ma marker beds in the upper San Joaquin Formation are at typical depths of 2,500 to 3,000 feet south of Corcoran in the southern SJV. Deposits in the northern SJV above (younger than) the Santa Margarita Formation have not been named.

Depths to bottom of freshwater aquifers, typically in the Tulare Formation and other Quaternary deposits younger than 2.5 million years (Ma), are summarized in Table 3-1. Freshwater may be present to depths ranging from below 1,500 feet to about 2,500 feet in the Tulare Basin south of Corcoran, and appears to become shallower to the north. At the northern Subsidence Bowl near Highway 152, fresh water may be present only to typical depths of about 1,000 feet. Bottom of fresh water extends more than 1,000 feet into permeable (high resistivity) layers and horizons into, and perhaps below, the marine San Joaquin Formation east of US Highway 99 and the Pixley Fissure No. 1 east of the HSR Alignment (see Figure 3-7). The potential for faulting, and thus a potential hydrologic barrier, in the vicinity of Pixley Fissure No. 1 is discussed in Section 8.5.3.

Saleeby et al. (2012, 2013) also posit that a “delamination hinge” at the top of the earth’s upper mantle (depth about 30 km) defines a boundary between tectonic deep anomalous subsidence (at the Tulare Basin) and deep anomalous uplift (as a delamination bulge at the southern Sierra Nevada Range). The approximate surface trace of this delamination hinge (Saleeby et al., 2013) is shown on Plate 8-1. It extends to the southeast along the western foothills of the Sierra Nevada south of the Stanislaus River to about the Kaweah River, where it turns to the south and then southwest in the southern Tulare Basin. The southernmost portion of the delamination hinge may be approximately coincident with the edge of recent subsidence indicated by InSAR (Plate 8-1), and appears to terminate at about the Pond-Poso Creek Fault in the vicinity of the HSR Alignment. Possible basin alluvium offset at the Pixley Fissure No. 1, discussed in Section 8.5.3, may be in the near vicinity of this delamination hinge. Saleeby et al. (2013) maps the northwestern extent of the Tulare Basin anomalous subsidence, also shown on Plate 8-1, to about Madera, northwest of Fresno.

3.2.2.1 Tulare Formation below Corcoran Clay

Within the Corcoran Subsidence Bowl, sediment compaction leading to land subsidence occurs primarily within the Tulare Formation. Researching basin alluvium stratigraphy driven by Pleistocene climate changes, Miller (1999, p 13) assessed the Tulare Formation using seismic reflection results, primarily below the Corcoran Clay, as controlled by available oil well geophysical logs. He noted that:

In this study area, the limits of vertical and horizontal seismic resolution are especially important to recognize in a geologic context. Terrestrial deposits range in size from alluvial fans with lateral continuity less than 1 km, to lake deposits that persist for distances over 100 km. Fluvial sand bodies and overbank mud deposits range from less than 100 m wide in isolated meander-belts to more than 10 km in braid-plains and strandline lacustrine sand deposits...

> "*In general Pleistocene lake levels rose and fell more frequently and with greater amplitude than sea level (Morrison, 1968), resulting in high aspect ratio lacustrine deposits, that allows seismic stratigraphy to resolve a time scale of deposition that is comparable to the frequency of exogenic climate cycles (Table 1.1). As a result, deltas were individually small and frequent deposits due to cyclic lake-level flooding and erosional truncation. The widespread paleosurfaces of erosion and local deposition, as well as lacustrine flood deposits provide the event stratigraphy that is critical to chronostratigraphic seismic reflections, as the coarse resolution of seismic stratigraphy merges discontinuous fluvial and alluvial deposits.*"

Miller's "exogenic climate cycles" are the Milankovitch astronomical forcing cycles that have operated on 100,000-year cycles over the last 1 Ma, and on 41,000-year cycles from 2.6 to 1 Ma (Lisiecki and Raymo 2005). Each climatic cycle would have encompassed glacial advance and retreat in the Sierra Nevada watershed draining into the SJV, with resulting relatively continuous fine-grained alluvial deposition and rare (such as 10,000+ year return interval flooding) pulses of discontinuous coarse-grained alluvium deposition in the lower portions of the SJV basin. Forty or more such climate cycles would have driven alluvial deposition in the SJV from the start of the Pleistocene to the start of deposition of the Corcoran Clay, and another half dozen cycles would have driven alluvial deposition overlying the Corcoran clay. Each climate cycle would have presented opportunities for individual small delta and other coarse-grained deposits to be erosionally truncated and encased within lacustrine and other fine-grained deposits. A significantly disconnected aquifer system, where many small coarse-grained aquifers are largely contained (encased) within a fine-grained honeycomb-type lattice of aquitards, could likely have developed within large portions of the Tulare Formation in the medial and especially distal portions of the SJV. Connectivity between these small aquifers may be limited to significantly inhibited. These medial and distal alluvial zones tend to underlie the Corcoran Clay.

3.2.2.2 Corcoran Clay Member

The Corcoran Clay Member of the Tulare Formation extends as a continuous lacustrine deposit for about 6,600 square miles (6,568 cells in the CVHM) underlying the central portion of the SJV at typical depths of about 200 to 300 ft at its edges up to about 800 ft in the Tulare Lake area. For the CVHM, an overall mean of 26% coarse-grained texture was estimated for its layers. Thickness of the Corcoran Clay Member ranges from feathering to about 20 ft near its edges to over 100 ft towards its center. Its chronology is constrained by the Long Valley Caldera event (Izett el al., 1988), currently dated at 0.76 Ma (Miller 1999) as indicated by the underlying Bishop Ash layer (Croft 1972). The Bishop ashfall (Izett et al.1988) encompassed SJV to about 10 miles northwest of Madera; it appears that the ashfall zone encompasses the portion of the SJV subject to significant historical and current subsidence. After the event, it is inevitable that Bishop Ash that blanketed the western Sierras in various stages of weathering, would have continued to be transported into and deposited in the Pleistocene Corcoran Lake. Corcoran Lake drained about 0.6 Ma as a hydrologic outlet developed to the north towards the incipient San Francisco Bay (Bartow 1991). Page (1983) reported the Friant Pumice Member dated to 0.618 to 0.612 Ma may overlie the Corcoran clay. As a continuous deposit including very low permeability fines, it is anticipated that the Corcoran Clay effectively sealed the underlying Tulare Formation alluvium into a confined aquifer system with materials having high porosities, high water contents and limited compaction consistent with an effective stress regime starting at the lakebed. With no or severely inhibited avenues of escape, trapped pore waters in the confined aquifer system supported additional loading on the alluvial column as hundreds of feet of deposition proceeded after Corcoran Lake drained. The release of that trapped ‘water of compaction’ below the Corcoran Clay by deep groundwater pumping contributes to rapid, large-magnitude compaction within the SJV confined aquifers and resulting subsidence.

3.2.2.3 Tulare Formation above Corcoran Clay

After drainage system changes and the emptying of Corcoran Lake by about 0.6 Ma, Tulare Formation basin alluvium continued to be deposited in the Central Valley. It is anticipated that deposition patterns continued to be driven primarily by Pleistocene climatic conditions and patterns as glaciation continued to advance and retreat across the Sierra Nevadas. Pleistocene lakes continued to form in the lowest portions of the basin and deposit confining clay lakebeds (Croft 1972) of much smaller scale than the Corcoran Clay. However, unlike the aquifer systems below the Corcoran Clay, the aquifer systems above the Corcoran Clay are anticipated to generally be semi-confined to unconfined. It is also anticipated that continued development of the large alluvial fan where the Kings River enters the SJV helped to build the northern edge of the Tulare Lake Basin. Above the Corcoran Clay, 43% (Tulare and Kern Counties) to 46% (Kings County) coarse-grained texture is estimated within the Tulare Formation above the Corcoran Clay (Faunt el al., 2009, Table A2). Where the Corcoran Clay is absent, an overall mean of 47% coarse-grained texture for the relevant Tulare Formation was estimated for Kings

County, and an overall mean of 41% coarse-grained texture is estimated for the relevant Tulare Formation in Tulare and Kern Counties. At a 1-mile lateral cell dimension and modeled 3 layers covering about 6 climatic cycles through up to about 300 to 700 ft of the upper Tulare Formation, the CVHM is unable to model fine details of structure between coarse and fine-grained alluvial materials within the Tulare Formation.

3.2.3 Historical Tulare Lake

Into the mid-1800s, the historical Tulare Lake was the largest freshwater lake west of the Mississippi River, covering up to about 440,000 acres when full. During the late 1800s, the lake began to disappear and dried up as surface water formerly feeding the lake was diverted for agriculture; eventually, the lakebed was developed into agricultural land. Groundwater still remained close to the ground surface in shallow aquifers, and was artesian in lower confined aquifers located below the Corcoran Clay; contours of Corcoran Clay thickness are shown on Figure 3-8.

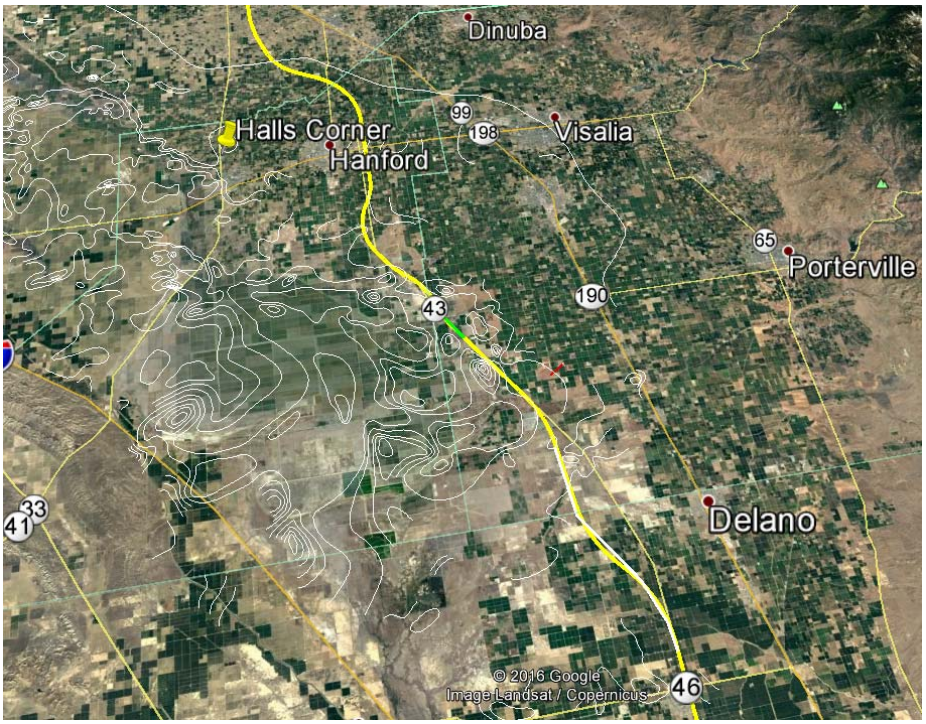

Figure 3-8: Contours of Corcoran Clay Thickness

3.2.4 Historic and Recent Subsidence in the San Joaquin Valley

Historical subsidence has been observed in the SJV since the 1920s, as documented in the work directed by Joseph Poland (Ireland et al., 1984, etc.). His contours of subsidence between about 1926 and 1970 are reproduced on Plate 1-1, which indicates subsidence of up to about 28 ft over this 44-year period, for an average rate of about 7½ inches per year near Mendota. In

the Corcoran Bowl area, along the HSR Alignment, the maximum subsidence was of about 6 or 7 ft, for an average rate of about 1½ to 2 inches per year.

Beginning in the 1990s, satellite altimetry (Hwang et al., 2016; see Figure 3-9 below) indicates subsidence rates near the HSR Alignment may have been about:

1.8 inches per year from 1992 to 2002 (TOPEX/Poseidon Satellite)
2.6 inches per year from 2002 to 2010 (ENVISAT Satellite)
2.5 inches per year from 2002 to 2009 (JASON-1 Satellite)
4.3 inches per year from 2008 to 2015 (JASON-2 Satellite)

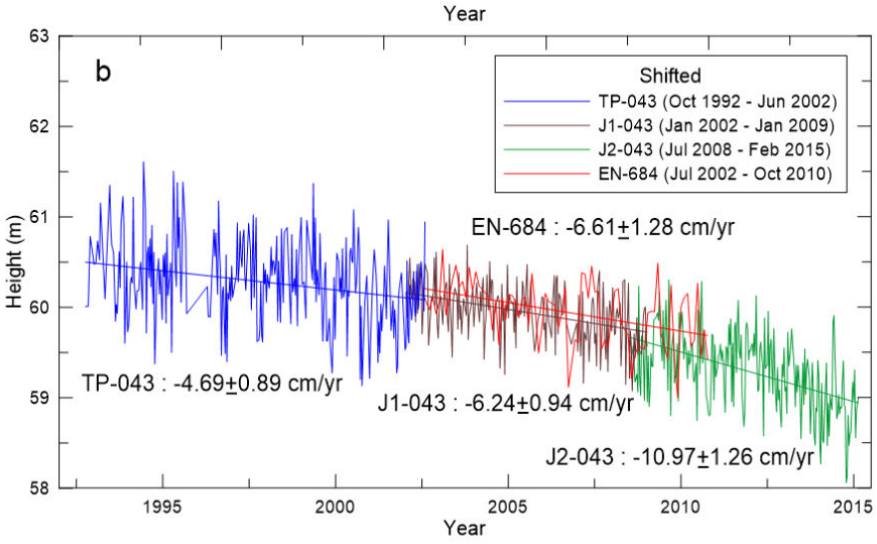

Figure 3-9: Subsidence from Satellite Altimetry (from Hwang et al., 2016)

Subsidence along the HSR Alignment in the Corcoran Bowl from June 21, 2007 through December 30, 2010, was estimated by the National Aeronautics and Space Administration's (NASA's) JPL using the ALOS L-band InSAR to be about 2¼ ft over this 3.5-year period, for an average rate about nearly 8 inches per year.

GPS-based survey data from along the CP 2-3 of the HSR between about 2010 and late 2015 indicated about 5½ ft of subsidence over this 5+ year period, for an average rate about 12 inches per year.

Subsidence along the HSR Alignment in the Corcoran Bowl from May 7, 2015, through May 25, 2016, was estimated by the NASA's JPL using the Sentinel C-band InSAR to be about 16 inches over this 1.05-year period, for an average rate about 15 inches per year.

A comparison of USACE LiDAR data from 2008, Dragados LiDAR data from 2015, and AFW RTK GPS data from 2016 indicates similar rates of subsidence. Other details of our methods of estimating rates and areal patterns of subsidence are presented in Sections 5.0 and 6.0.

This available data gives a general introduction to the rates of subsidence in the Corcoran subsidence Bowl over the past 90 years, with a general pattern of acceleration being apparent.

3.3 FORECAST GROUNDWATER USE AND GROUND SUBSIDENCE

In 2014, the California State Senate passed the Sustainable Groundwater Management Act (SGMA), which requires that local agencies in critically over-drafted groundwater sub-basins in the SJV prepare "sustainable" groundwater management plans by 2020, and implement these plans by 2040.

As discussed in Section 6.2, for this GSS, AFW assumed that as 2040 approaches, groundwater drawdown will gradually taper towards zero in order to meet the requirements of SGMA. AFW has made the assumption that subsidence rates observed over a range of periods within the past 10 years will continue over the next 20 years. This assumption may be somewhat conservative if groundwater use gradually moves towards the requirements of sustainability before that time, but may be unconservative if groundwater use continues at its current rate, or continues to accelerate as it has recently been doing. Details of forecast subsidence scenarios are presented in Section 6.2. In overview:

1. Scenario A (or 2036a) assumes that subsidence rates observed from 2007 to 2010 will continue for 20 years (generally the slowest estimate of the three scenarios).
2. Scenario B (or 2036b) assumes that subsidence rates observed from 2008 to 2016 will continue for 20 years.
3. Scenario C (or 2036c) assumes that subsidence rates observed from May 2015 to May 2016 will continue for 20 years (generally the fastest estimate of the three scenarios).

The original plan for this GSS was to utilize physical-based groundwater modeling coupled with subsidence calculations to forecast a range of assumptions about land use and water use (including both groundwater and surface water). The modeling was to be based on a calibration and refinement of the USGS's updated CVHM-mod. However, as further discussed below, the CVHM-mod is still being calibrated by the USGS, and our attempt to further calibrate an interim version of the model provided by the USGS for HSR application was not successful. Therefore, subsidence forecasting was based almost solely on extrapolations of recently-observed subsidence rates. CVHM-mod modeling is further discussed in Section 4.2.

3.3.1 Evaluation of Potential Subsidence Impacts to the California High-Speed Rail

Rapid and large-magnitude subsidence poses several potential concerns to the HSR that have been the subject of this GSS, including: changes in slopes, vertical curvature, horizontal curvature, and twist; fissures; compaction faults; and changes in floodplains and site drainage. Groundwater withdrawals have been inducing ground subsidence. Differential subsidence will induce changes in vertical slopes and curvature along the HSR tracks. Similarly, differential

horizontal displacement transverse[5] to the tracks will induce horizontal curvature, which will result in changes to vertical and transverse centripetal (and centrifugal as inertial counterpart) accelerations in the trains. Induced changes in vertical slopes can affect overland flow and stream flow. Vertical deformation of the ground surface can change the location and shape of the topographically lowest region in a hydrologic basin. Thus, subsidence can affect site drainage characteristics as well as the location and extent of floodplains and flood depths. Differential subsidence also causes stresses and strains in the subsurface soils. Excessive strains can generate fissures and compaction faults.

These potential impacts are discussed in the following chapters.

3.4 CONTRACTUAL CONSIDERATION

By contract, each Contractor is responsible for controlling and mitigating any adverse impacts related to settlement, but not for impacts related to subsidence. Therefore, for contractual reasons, it is important to be able to distinguish between post-construction subsidence and settlement. This is further discussed in Sections 3.1.5, 9.3, and 10.4.

4.0 NUMERICAL MODELING OF SUBSIDENCE AND GROUNDWATER DRAWDOWN

We performed numerical analysis of subsidence from drawdown around a hypothetical single well with subsurface conditions representative of the Corcoran Subsidence Bowl area. The pumping rate assigned to the well is typical of the total average groundwater extraction in well(s) in a one square mile region. This consideration is conservative because distributing this pumping rate to multiple wells will produce less severe localized subsidence, displacements, slopes, and curvatures on HSR Alignment. The results are presented in Section 4.1. We also attempted to perform numerical analyses of areal subsidence in the SJV by further refining an updated version of the USGS's CVHM-mod. However, this exercise did not produce meaningful results; the process is described in Section 4.2.

4.1 MODELING OF SUBSIDENCE FROM DRAWDOWN AROUND SINGLE WELL

4.1.1 Introduction

As introduced in Section 3.0, subsidence has been occurring along portions of the HSR Alignment in the SJV in response to groundwater withdrawals from pumping wells since at least the early 1900s. Groundwater withdrawals slowed in the latter portion of the 1900s when surface water became more available from the California State Water Project, with a corresponding slowing of subsidence. However, groundwater withdrawals from pumping wells have increased over the past 10 to 20 years or so, with a corresponding resumption and

[5] In this report, "transverse" refers to the direction perpendicular to the direction of the track. "Radial" refers to the direction away from or toward the well. "Horizontal" refers to any horizontal direction without respect to specific direction.

acceleration of subsidence. In the Corcoran area, maximum subsidence rates have reached a foot or more per year, among the fastest in the world. An overview of subsidence in the SJV is shown on Plate 1-1, and a profile of historical subsidence along the HSR Alignment is shown on Plate 1-2.

The hydraulic stress due to groundwater withdrawal from a well causes pore pressure / phreatic head in the subsurface alluvial aquifer system to drop. The farther away from the well screen, the smaller is the phreatic head drop. As withdrawal continues over time, the phreatic head drop increases and propagates outward from the well, creating an influence cone surrounding the well. In an unconfined aquifer system, pressure head drop causes groundwater drawdown and creates a drawdown cone centered at the well.

Figure 4-1: Local subsidence bowl developed using data acquired from June 2007 to December 2010 with a maximum subsidence of 36 inches, and 18 to 21 inches around its periphery, in the vicinity of the HSR Alignment. InSAR data from Farr et al., 2015.

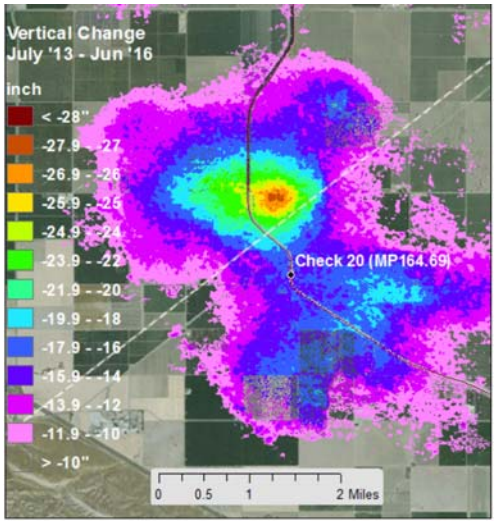

Figure 4-2: Local subsidence bowl developed from July 2013 to June 2016 with a maximum subsidence of 28 inches and 10 inches around its periphery adjacent to the California Aqueduct. InSAR data from Farr et al., 2017

Pore pressure reduction results in an increase in effective stresses in the subsurface continuum, causing changes in three-dimensional strains, leading to ground subsidence and horizontal displacement. Examples of apparent single-well subsidence signatures derived from InSAR are presented in Figures 4-1 and 4-2. Excessive strains could potentially lead to cracking and fissures. The induced strains vary spatially and with depth in the vicinity of a pumping well, creating non-uniform horizontal displacement in addition to vertical subsidence at the ground surface. Available horizontal displacement monitoring data in the field has been limited (Burbey el al., 2006). Subsidence and horizontal displacement vary spatially; so all displacements will be

associated with some degree of differential displacements. For this simplified analysis, we assumed homogeneous but vertically anisotropic conditions in which differential subsidence and horizontal displacement will create a subsidence cone centered at the well and will lead to a change in the slope and super-elevation along the proposed HSR Alignment. For non-homogeneous conditions, they will not be concentric or regular, but we consider these simplifications to be reasonable for understanding general patterns of subsidence.

If a groundwater extraction well is located within approximately 3000 ft from a straight and leveled HSR Alignment, differential transverse[6] displacement within the differential subsidence cone will induce vertical slopes and curvature along the HSR tracks. The track will dip down into this cone to a low point at the nearest approach to the well, and then rise as it travels away from the well. With this dip and climb back out, there is a series of three curving sections of the vertical alignment: convex up, concave up, and convex up. Similarly, there are three curving sections of the horizontal alignment. If the well is to the left of the line of travel, the horizontal curves will be to the left, the right (near then nearest approach), and to the left (straightening back out while leaving the vicinity of the well).

4.1.2 Rail Performance

Rail performance may be evaluated in terms of safety and of passenger comfort. Both of these are addressed in the project *Design Criteria.* At the design speeds for the HSR, rail performance is very sensitive to changes in the track geometry, particularly in terms of vertical and horizontal curvature, which create vertical and horizontal accelerations, and super-elevation (felt as twist and a change in horizontal curvature or horizontal acceleration).

Vertical and horizontal curvatures will result in vertical and transverse centripetal (and centrifugal as inertial counterpart) accelerations in the trains[7]. The induced accelerations are equal to the velocity squared divided by the radius of curvature, or $A = V^2/R$. According to the project *Design Criteria*, “ride comfort (smoothness of ride) shall be achieved with lateral and vertical acceleration values equal to or less than 0.05g and 0.045g (i.e., 5% and 4.5% of gravitational acceleration [g]), respectively, for the maximum design speeds (of 250 mph).” Therefore, the purpose of this current modeling study has been to calculate accelerations associated with the curvatures induced by differential subsidence near a hypothetical single well. For the design speed of 250 mph, the relationship between acceleration and the radius of curvature is shown on Figure 4-3 below.

---

[6] “Transverse” refers to the direction perpendicular to the direction of the track. “Radial” refers to the direction away from or toward the well. “Horizontal” refers to any horizontal direction without respect to specific direction.

[7] “Acceleration” refers to the centripetal accelerations induced by the incremental vertical or horizontal curvature of the tracks that results from groundwater extraction-induced differential displacement; the constant downward acceleration of gravity is ignored.

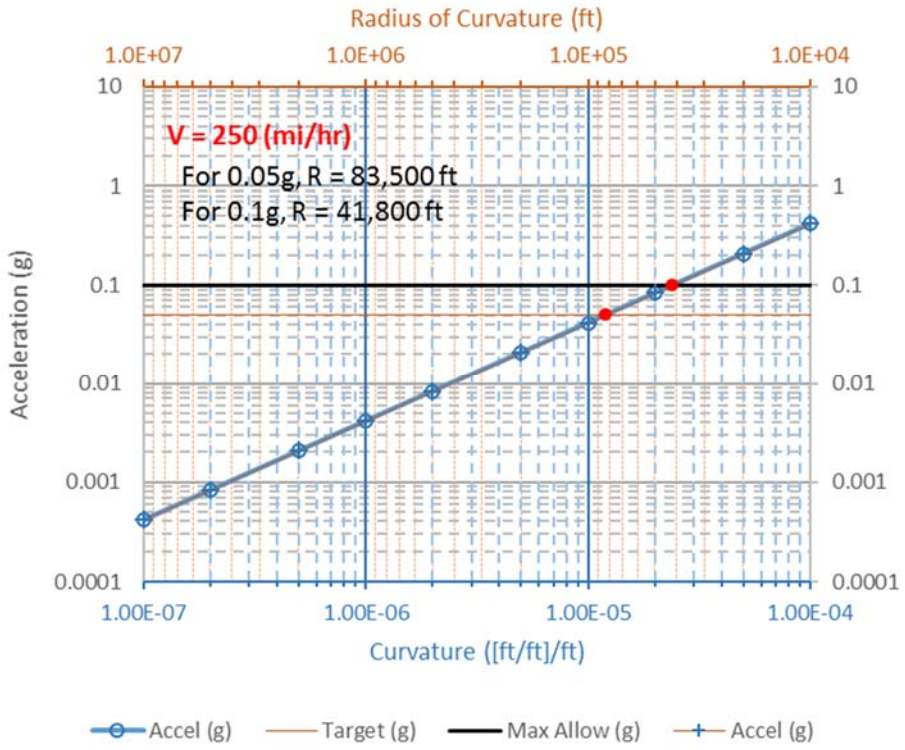

Figure 4-3: Acceleration as a Function of Radius of Curvature at Design Speed

4.1.2.1 Vertical Curves

Vertical curves should limit induced acceleration to 0.045 times the acceleration of gravity ("g") to the extent possible, and to 0.10g in any case. In addition, any designed vertical curve should have a minimum curve length of 875 ft (to avoid a sense of bumpiness or vertical oscillations). "Bounciness" may also be a concern with respect to passenger comfort.

4.1.2.2 Horizontal Curves

Horizontal curves should limit radius of curvature as a function of the design speed based on a lateral acceleration limit of 0.05g (maximum unbalanced super-elevation of 3 inches, per the *Design Criteria,* Section 4.4.5.3). In addition, superelevation should be matched to the design velocity and radius of curvature by the following equations (*Design Criteria,* Section 4.4.5.1):

$$R = 4\ V^2_{max} / (Ea + Eu) \qquad \text{Eq. 4-1}$$

Where R = minimum radius of curvature in feet

V = train velocity in mph

Ea = actual (designed & constructed) superelevation in inches (6 inches max.)

Eu = unbalanced superelevation in inches (3 inches max)

For ballasted HSR track placed on an embankment, any transverse ground movement that is induced by differential subsidence will impose horizontal curvature on the track. Based on preliminary findings from our ongoing numerical analysis of subsidence around a hypothetical well, it appears these horizontal curvatures will be quite gentle and not likely to need more than ¼ inch of superelevation ("Ea" in equation 4-1) to balance the curvature. To put this in perspective, for an assumption of straight track with no designed/constructed superelevation, unbalanced superelevation of 3 inches results in an allowable minimum curve radius of about 83,000 ft at a design speed of 250 mph. Such magnitudes of induced horizontal curvature likely could only occur if faulting, tension cracks, or earth fissures were to develop along the HSR Alignment, which is considered unlikely.

Rigid elevated structures, or rigid sections of track subjected to horizontal displacement from differential subsidence, have been known to concentrate differential horizontal movement at structure or section joints (June 2012). Design-build teams should further evaluate this potential condition.

4.1.2.3 Other Considerations

Twist. In the UK, it has been found that excessive "twist" in the track can cause passenger discomfort or motion sickness. A twist of 1/400 is approximately the critical value.

Structures. Differential subsidence across HSR structures will induce stresses or angular distortion. Anticipated differential subsidence should be accounted for by the structural designers. In addition, structural designers should identify the magnitude of differential subsidence that could induce unacceptable stress or angular distortion levels.

Tensile Strain and Cracking. Differential subsidence could also cause tensile strains and cracking in brittle soils, and in lime- or cement-treated soils such as could be used to form the "treated subgrade" at the top of embankments and immediately below the ballast. Thus, in areas where the magnitude of subsidence is large, caution is advised in the selection of embankment materials.

4.1.3 Modeling Approach

4.1.3.1 Introduction

The AFW team used groundwater and geomechanical finite element modeling to compute the horizontal and vertical ground surface displacements caused by groundwater extraction from a hypothetical single well. The subsurface domain was idealized as a horizontally layered aquifer system representative of a hydrogeologic environment typical of the Corcoran area. The model was axisymmetric (considered radial and vertical directions only) and centered at the groundwater extraction well. The size of the finite elements was finer near the pumping well and it increased with distance from the well. The results of the axisymmetric modeling included

vertical and radial displacement; these were transformed to obtain the displacements in the vertical and transverse directions with respect to the HSR Alignment; these vertical and transverse displacements were then processed to calculate induced slope and curvature along originally straight and level HSR track alignment offset at a range of distances from the well.

The groundwater model was based on Darcy flow,

$$v = K \cdot \nabla h \qquad \text{Eq. 4-2}$$

where v is the apparent groundwater flow velocity (Darcy flux), K is the hydraulic conductivity tensor, and ∇h represents the gradient of h, where h is the phreatic head expressed as:

$$h = \frac{p}{\gamma_w g} + z \qquad \text{Eq. 4-3}$$

where p is the pore water pressure, γ_w is the density of water, g is the acceleration of gravi, and z is the elevation.

The relationship between changes in pore fluid pressure and compression of an aquifer system is based on Terzaghi's principle of effective stress,

$$\sigma_e = \sigma_T - \mathrm{p} \qquad \text{Eq. 4-4}$$

where effective or inter-granular normal stress (σ_e) is the difference between the total normal stress (σ_T) and the pore water pressure (p). A change in p causes a change in effective horizontal and vertical stresses. If the aquifer material is linearly elastic, the geomechanical constitutive behavior can be represented by,

$$\sigma' = C \cdot \epsilon \qquad \text{Eq. 4-5}$$

where ϵ is the strain tensor, σ' is the effective stress tensor, and C is the constitutive matrix in terms of the compressibility of the aquifer system skeleton, m_v, (or Young's modulus, E) and Poisson's ratio, ν. Under one-dimensional condition,

$$\frac{1}{m_v} = \frac{E \cdot (1-\nu)}{(1+\nu)(1-2\nu)} \qquad \text{Eq. 4-6}$$

Due to mass balance, the rate of change in pore volume in an aquifer system resulting from the change in strain equal to the divergence of the Darcy flux,

$$\nabla \cdot (\mathrm{K}\nabla \mathrm{h}) = \frac{\partial}{\partial t}\left(\epsilon_{xx} + \epsilon_{yy} + \epsilon_{zz}\right) \qquad \text{Eq. 4-7}$$

If q is the source/sink term representing the pumping rate, at the well screen,

$$\nabla \cdot (\mathrm{K}\nabla \mathrm{h}) - q = \frac{\partial}{\partial t}\left(\epsilon_{xx} + \epsilon_{yy} + \epsilon_{zz}\right) \qquad \text{Eq. 4-8}$$

If the tensile stress induced by groundwater extraction-induced subsidence is excessive, then earth fissures might occur within the tensile zones. Subsidence magnitude and fissure geometry

are closely related to the thickness and skeletal compressibility of fine-grained sediments within the aquifer system, and to stress history and water level changes.

We performed numerical modeling using a sequential or uncoupled approach. First, groundwater modeling was performed to compute the change in phreatic head/pore water pressure throughout the model domain at each time step due to groundwater extraction at a well. Subsequently, geomechanical modeling was performed to compute the displacement at the ground surface for each time step using the pore pressure computed previously by groundwater modeling. The results using a sequential approach are practically the same as those from a fully coupled approach shortly after the beginning of groundwater extraction. We also performed one coupled analysis to compare with the uncoupled analysis, which confirmed that the uncoupled approach produced displacements and stresses nearly identical to a coupled analysis.

4.1.3.2 Software Used

Finite-element analyses were performed for this evaluation to model the responses of the alluvial structure to the applied stresses resulting from changes in pore water pressure, and the resulting deformations. The numerical analyses were performed by using two finite element based computer programs SEEP/W and SIGMA/W developed by GeoSlope (2012). In SIGMA/W, both force and displacement boundary conditions are specified together with soil properties defined using effective stress parameters. In SEEP/W, head and flow boundary conditions together with hydraulic conductivity and volumetric water content functions are specified. An uncoupled analysis in essence involves solving the SIGMA/W equilibrium equations and seepage continuity equations separately. Sometimes, instead of solving the two sets of equations both at the same time, it is numerically advantageous to solve the SEEP/W transient flow equations first and then use the SEEP/W results in the equations as known hydraulic boundary conditions. The change in pore-pressures is calculated first and then the related volume change is computed for the previously computed pore-pressure changes. This is known as an uncoupled analysis.

4.1.3.3 Soil and Groundwater Assumptions Used

We assumed that the subsurface is composed of three hydrogeologic layers. The uppermost layer was 250 ft thick, representing the unconfined upper or shallow aquifer. The lowermost layer was 1210 ft thick, representing the confined lower or deep aquifer, which is the major water production unit in the SJV. The middle layer was 40 ft thick, simulating a “leaky” aquitard separating the shallow and deep aquifer.

For the numerical analysis, the parameters representing the alluvial system were Young’s modulus (E), saturated hydraulic conductivity (K) and coefficient of volume compressibility (M_v), which is related to the Young’s modulus and Poisson’s ratio. Selection of input parameter

values was based on typical ranges of the parameters in the region. Sensitivity analyses was performed with respect to Poisson's ratio and well screen intervals. In the analysis to estimate the sensitivity of horizontal displacement with respect to Poisson's ratio, the vertical compressibility was kept constant by also changing Young's modulus as a function of Poisson's ratio. Poisson's ratio values were varied from 0.35, which is expected to be close to the actual field value, to 0.25 and 0.45, which are, respectively, the upper and lower limits considered to be realistic.

The input parameters used in the model are given in Tables 4.1a and 4.1b. The initial groundwater table was assumed to be 50 ft below the surface. The pumping rate, Q, was assumed to be 500,000 cubic feet per day (2600 gpm). A constant-head boundary condition was used for a far-field head boundary condition (at a distance of 26,400 ft from the pumping well). Two different pumping scenarios were assumed. In first case, pumping was performed only from the lower aquifer, and in second case, pumping was performed from both upper and lower aquifers. The transient model was run for 100 years, and output was saved for 2 years, 20 years, and 100 years, and output was saved for 2 years, 20 years, and 100 years. The goal of the study was to estimate the long-term deformation. Since the parameters assumed in this model were selected to be representative of the average compressibility across an aquifer, the presence of locally low-permeability layers that contribute to delayed responses of the aquifer unit were not evaluated. As a result, the time scale of the deformation will likely be slower than simulated, although the simulated long-term deformations will be practically unaffected. In this study, the 2-year responses were already approaching the 20-year responses, which are almost the same as the 100-year responses (see Plate 4-1), so for simplicity, only the 20-year results are reported.

TABLE 4-1a
Input Parameters for Finite Element Model

Layer	Top	Bottom	Thickness	K_x	K_v	M_v
	(ft bgs)	(ft bgs)	(ft)	(ft/d)	(ft/d)	(1/psf)
Shallow	0	250	250	7	0.7	6.18E-07
Aquitard	250	290	40	0.1	0.01	1.14E-06
Deep	290	1500	1210	35	3.5	5.15E-07

TABLE 4-1b
Model Parameters for Sensitivity Analysis (varied Poisson's ratio and Young's Modulus to keep vertical compressibility constant)

Layer	Upper Aquifer	Aquitard	Lower Aquifer
Model 1			
Poisson's ratio	0.25	0.25	0.25
Young's Modulus (psf)	1.35E+06	7.32E+05	1.62E+06
Model 2			
Poisson's ratio	0.35	0.35	0.35
Young's Modulus (psf)	1.01E+06	5.47E+05	1.21E+06
Model 3			
Poisson's ratio	0.45	0.45	0.45
Young's Modulus (psf)	4.27E+05	2.32E+05	5.12E+05

4.1.3.4 Transformation to Deformation Along or Perpendicular to Track

The horizontal and vertical displacements at the ground surface were computed by an axisymmetric finite element model. We considered an initially straight and level HSR Alignment with the closest distance between the well and the alignment equal to "d". Consider a finite element node as shown on Figure 4-4. The radial coordinate in the axisymmetric model is r. The projected coordinate of the node at the ground surface on the HSR Alignment, x, can be computed in terms of r as:

$$x = x(r) = \sqrt{r^2 - d^2} \qquad \text{Eq. 4-9}$$

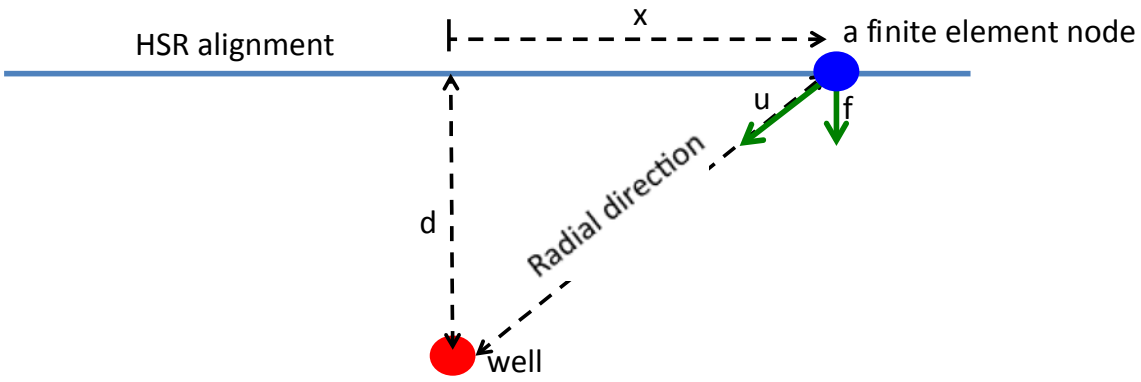

Figure 4-4: Projection of axisymmetric model results onto HSR Alignment

Let u(r) and w(r) be the radial and vertical displacements, respectively, at this surface node. The projection of the radial displacement, u, to the direction perpendicular or transverse to the HSR Alignment can be computed as the transverse displacement, f, by:

$$f = f(r) = u(r) \cdot \frac{d}{r} \qquad \text{Eq. 4-10}$$

After all finite element nodes on the ground surface are mapped and projected along the HSR Alignment, the transverse angular deviation of the HSR track from the initial alignment ($f' = \frac{df}{dx} = \frac{df}{dr} \cdot \frac{dr}{dx} = \frac{df}{dr} / \frac{dx}{dr}$) and horizontal curvatures ($f'' = \frac{df'}{dx} = \frac{df'}{dr} / \frac{dx}{dr}$) can be more conveniently computed by the finite difference method with unequal interval finite difference method (Figure 4-5).

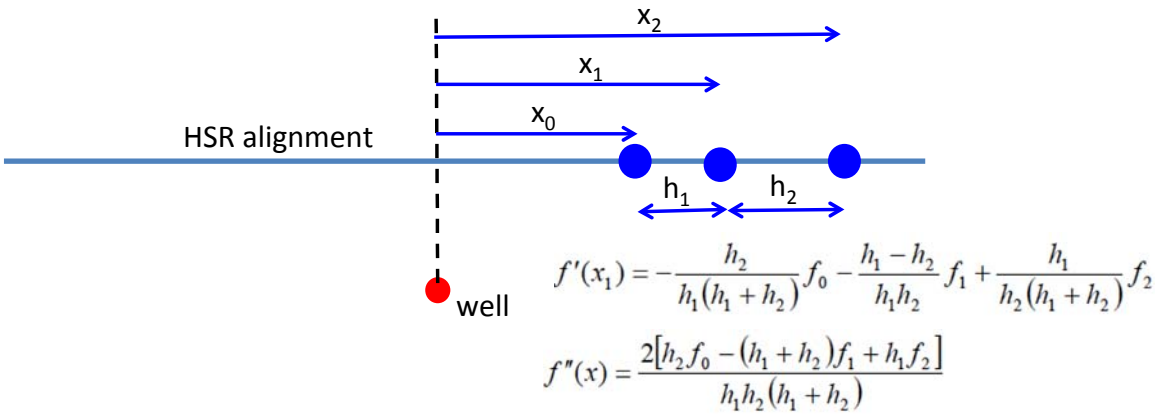

Figure 4-5: Unequal-interval finite difference computation of slopes and curvatures

Similarly, the vertical slope, *w'*, and vertical curvature, *w''*, can be computed by the finite difference method by replacing *f* in these equations with *w*.

4.1.4 Modeling Results

As discussed in Section 4.1, because the 2-year results were only a small amount less than the 20-year results, and the 100-year results were hardly different from the 20-year results, we only the 20-year results are reported. The modeling results for the 20-year responses are summarized in Table 4-2; additional details can be seen in Figures 4-6 through 4-16, as discussed in Section 4.1.5 All displacement, curvature, and acceleration results presented in these tables and figures were evaluated at the ground surface.

TABLE 4-2
Modeling results for modeled 20-year responses; 2-year responses are similar.

Groundwater Extraction Zones	Poisson's Ratio	Time Period	Well Distance from Tracks (ft)	Min Vert Radius of Curvature (ft)	Max Vert Acceleration (convex up = neg) (g)	Min Horiz Radius of Curvature (ft)	Max Horiz Acceleration (convex away from well = pos) (g)
300' to 400' (lower aquifer)	0.25	20 yrs	200 400 1,000	916,000 1,140,000 2,630,000	0.212% 0.171% 0.074%	4,620,000 3,170,000 4,610,000	0.042% 0.061% 0.042%
300' to 400' (lower aquifer)	0.35	20 yrs	200 400 1,000	1,060,000 1,280,000 2,900,000	0.184% 0.152% 0.067%	5,380,0003, 640,0005,2 30,000	0.036% 0.053% 0.037%
300' to 400' (lower aquifer)	0.45	20 yrs	200 400 1000	1,440,000 1,490,000 3,160,000	0.135% 0.131% 0.061%	7,810,0004, 480,0006,0 90,000	0.025% 0.043% 0.032%
100' to 200' (upper and lower aquifer)	0.35	20 yrs	200 400 1,000	82,700 203,000 926,000	2.347% 0.955% 0.210%	137,000 277,000 1,080,000	1.45% 0.70% 0.18%

4.1.4.1 Vertical Displacement and Curvature

Figure 4-6 shows the vertical displacement on the ground surface as a function of radial distance from the well in the axisymmetric model after 20 years of groundwater extraction for various cases of screen intervals (pumping from lower aquifer versus upper aquifer) and Poisson's ratio values. These curves represent the subsided profile along a straight alignment passing through the well location (i.e., equivalent to d = 0 ft on Figure 4-4).

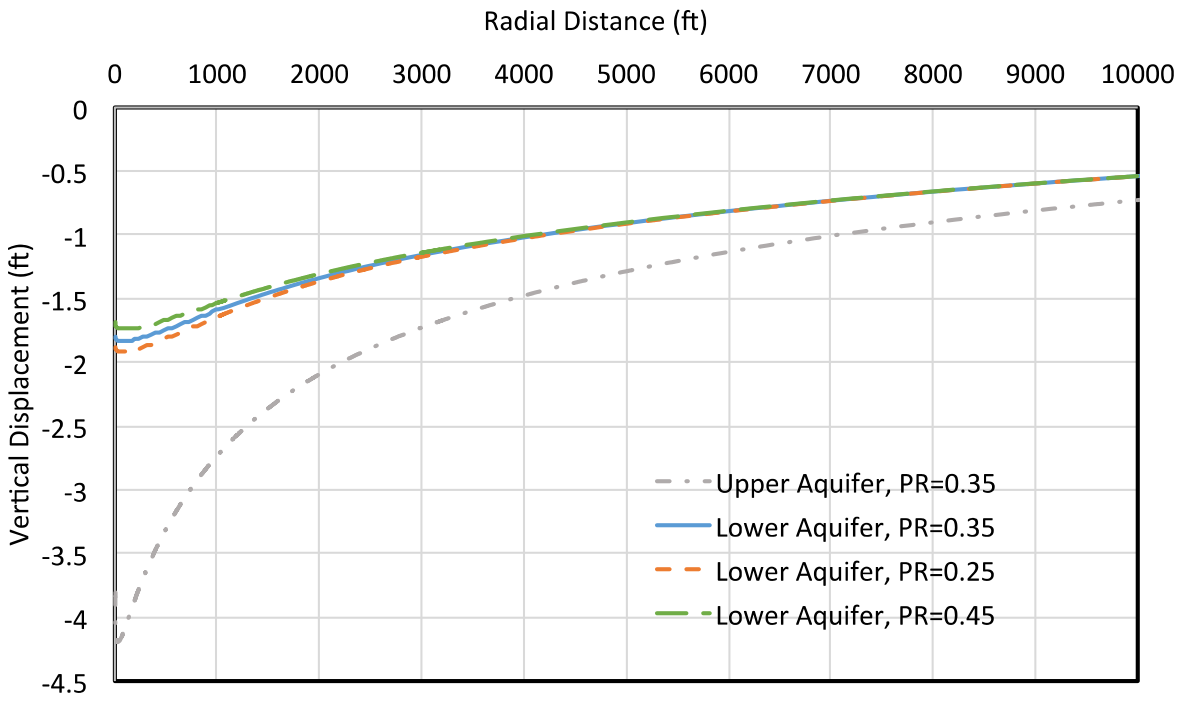

Figure 4-6: Subsidence profiles along radial direction after 20 years of groundwater extraction; subsidence profiles at 2 years of extraction are slightly smaller.

As can be seen, if groundwater is extracted from the lower aquifer, the subsided profiles for all values of Poisson's ratio are quite similar, although as Poisson's ratio increases from 0.25 to 0.45, the aquifer becomes slightly less compressible (when Poisson's ratio = 0.5, the material is incompressible). The boundary condition of zero radial displacement at the well center causes the vertical displacement at the well center (i.e., r = 0 ft) to be slightly less than the vertical displacement in the small region immediately away from the well. Although the differential subsidence in this region is small, the computed curvature in this small region is high since the distance is small. We believe that this locally large curvature is a numerical modeling artifact and it does not exist in reality. In addition, the rigidity of railroad track would smoothen small-scale differential displacement. Therefore, this local curvature near the center is ignored in our evaluation. Figure 4-6 also shows that groundwater extraction from the shallow aquifer causes approximately 2.5 times larger subsidence in comparison to groundwater extraction from the deep aquifer; it creates more abrupt subsidence profile near the well, producing a steeper subsidence cone.

Figure 4-7 shows the vertical displacement profile along the HSR Alignment at offset distances of 200 ft, 400 ft, and 1000 ft, respectively, from the well, for the case of groundwater extraction from the lower aquifer and Poisson's ratio of 0.35.

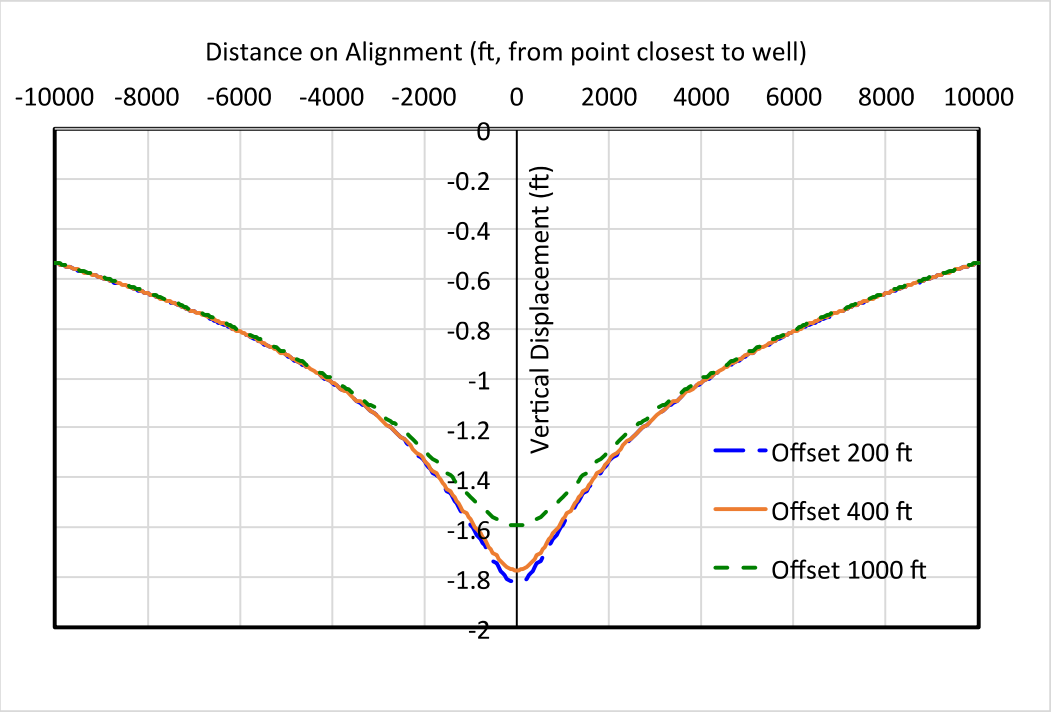

Figure 4-7: Vertical subsidence profiles along HSR Alignment due to pumping from lower aquifer; subsidence profiles at 2 years of extraction are slightly smaller.

The closer the well is to the HSR Alignment, the greater is the maximum vertical acceleration. This is depicted on Figure 4-8, which shows the vertical acceleration along the subsided rail alignment for train speed of 250 mph for the three representative alignment offset distances.

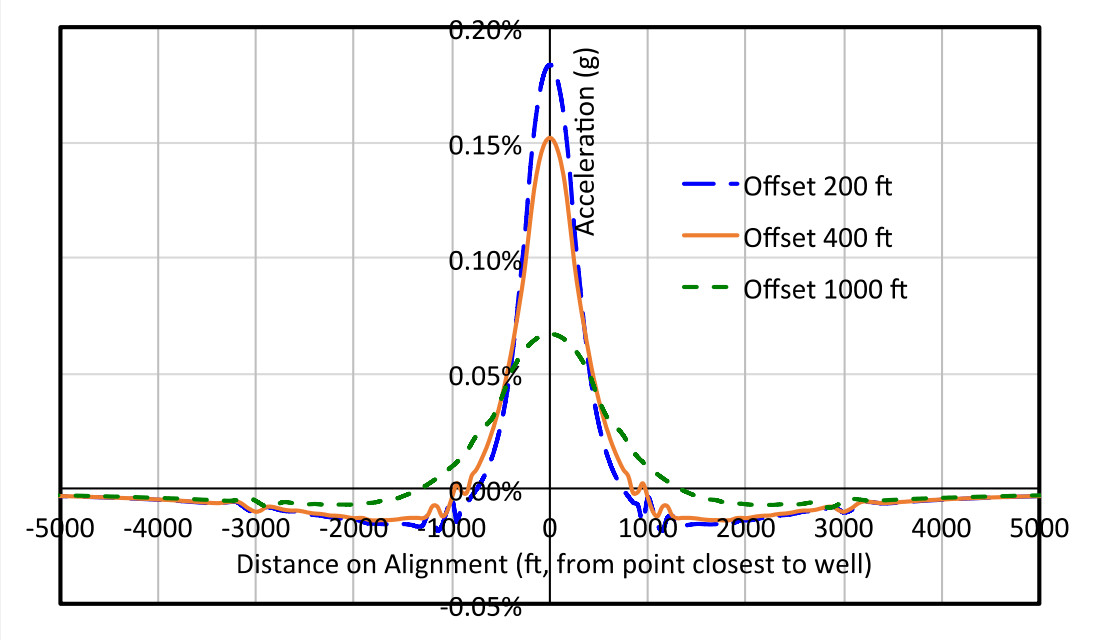

Figure 4-8: Vertical acceleration along the HSR Alignment due to pumping from lower aquifer

Figures 4-9 and 4-10 are similar plots for the case of groundwater pumping from the upper aquifer zone. In this case, the subsidence is larger than the subsidence in the case of groundwater pumping from the lower aquifer zone. In addition, the resulting differential subsidence is also larger. Since pumping from the upper aquifer produces a sharper subsidence cone, the subsidence magnitude and curvature drop off faster with offset distance than the case of pumping from the lower aquifer.

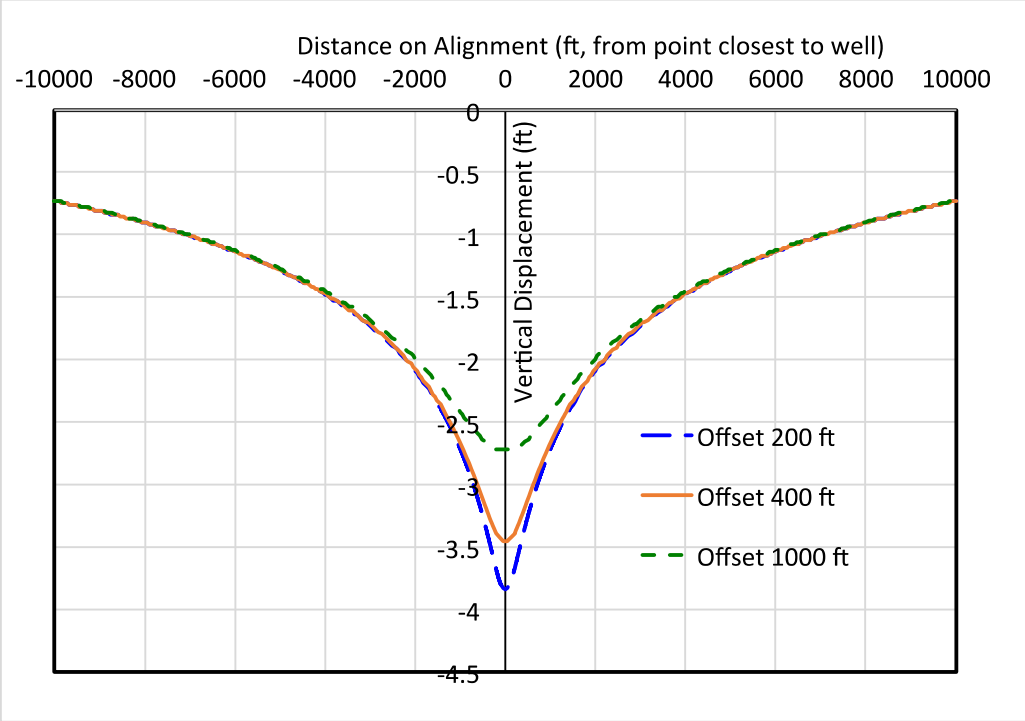

Figure 4-9: Vertical subsidence profiles along HSR Alignment due to pumping from upper aquifer

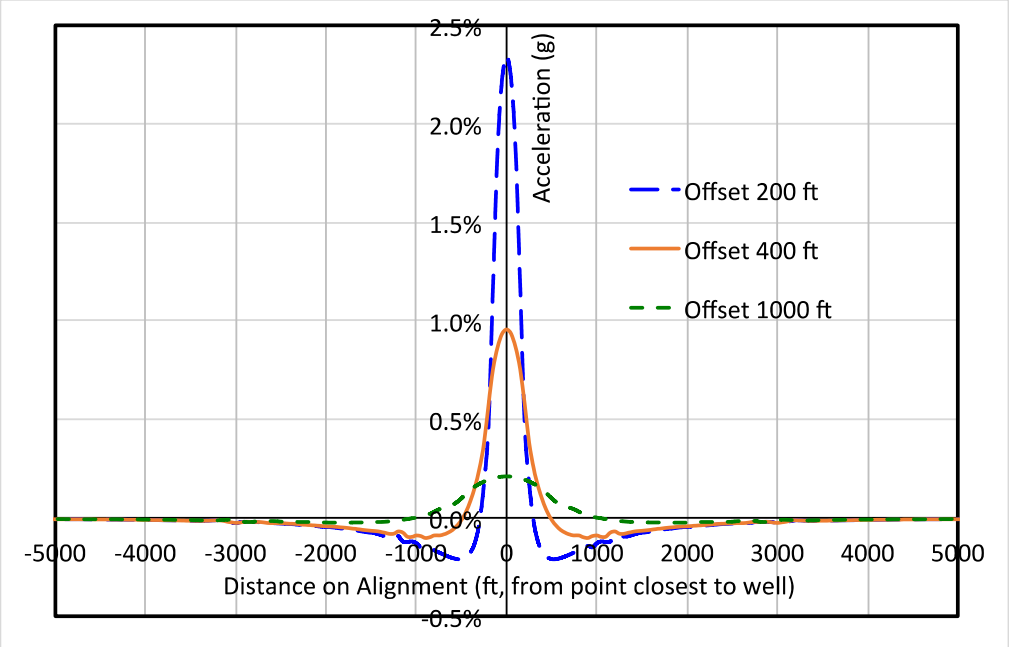

Figure 4-10: Vertical acceleration along HSR Alignment due to pumping from upper aquifer

4.1.4.2 Horizontal Displacement and Curvature

Figure 4-11 shows the radial displacement profile on the ground surface as a function of the radial distance from the well. Due to axisymmetry, there is no radial displacement at the location of the well. The radial displacement increases with radial distance to a maximum at approximately 1600 ft from the well for pumping from the lower aquifer. The radial displacement then decreases with increasing radial distance. The radial displacement depends slightly on Poisson's ratio.

Figure 4-11 also shows that groundwater extraction from the upper aquifer causes larger radial displacement in comparison to the case of groundwater extraction from the lower aquifer. In this case, the maximum radial displacement occurs at a radial distance of approximately 800 ft, which is closer to the well than when pumping from the lower aquifer.

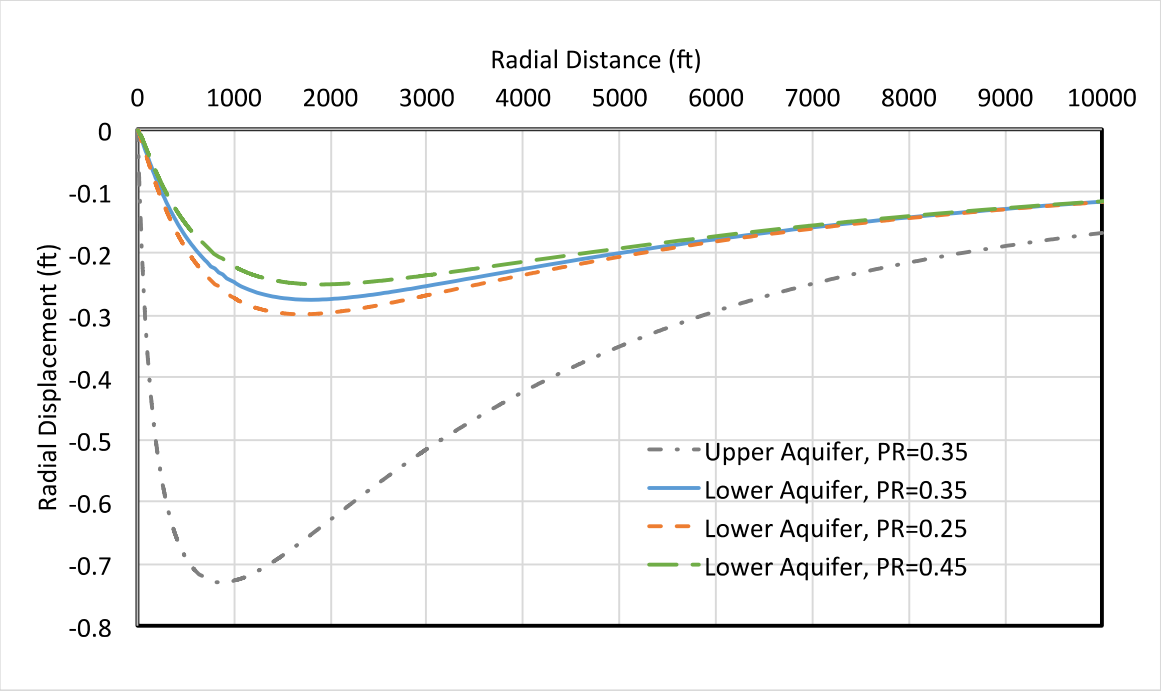

Figure 4-11: Radial displacement profiles after 20 years of groundwater extraction

If the rail alignment passes through the well location, there is no transverse displacement to the tracks. Figure 4-12 shows the profiles of transverse displacement along the rail alignment with offset distances of 200 ft, 400 ft, and 1000 ft. Figure 4-13 shows the horizontal acceleration for train speed of 250 mph for the same three offset distances.

For the case of pumping from the lower aquifer, the maximum radial displacement occurs at approximately 1600 ft from the well. Because the radial displacement is not a linear function of the radial distance from the well, the maximum induced horizontal curvature occurs with an offset distance different from the distance to the location of maximum radial displacement. As seen in Figure 4-13, the maximum induced horizontal curvature occurs at an offset distance of about 400 ft, which is smaller than the offset distance where maximum radial displacement occurs.

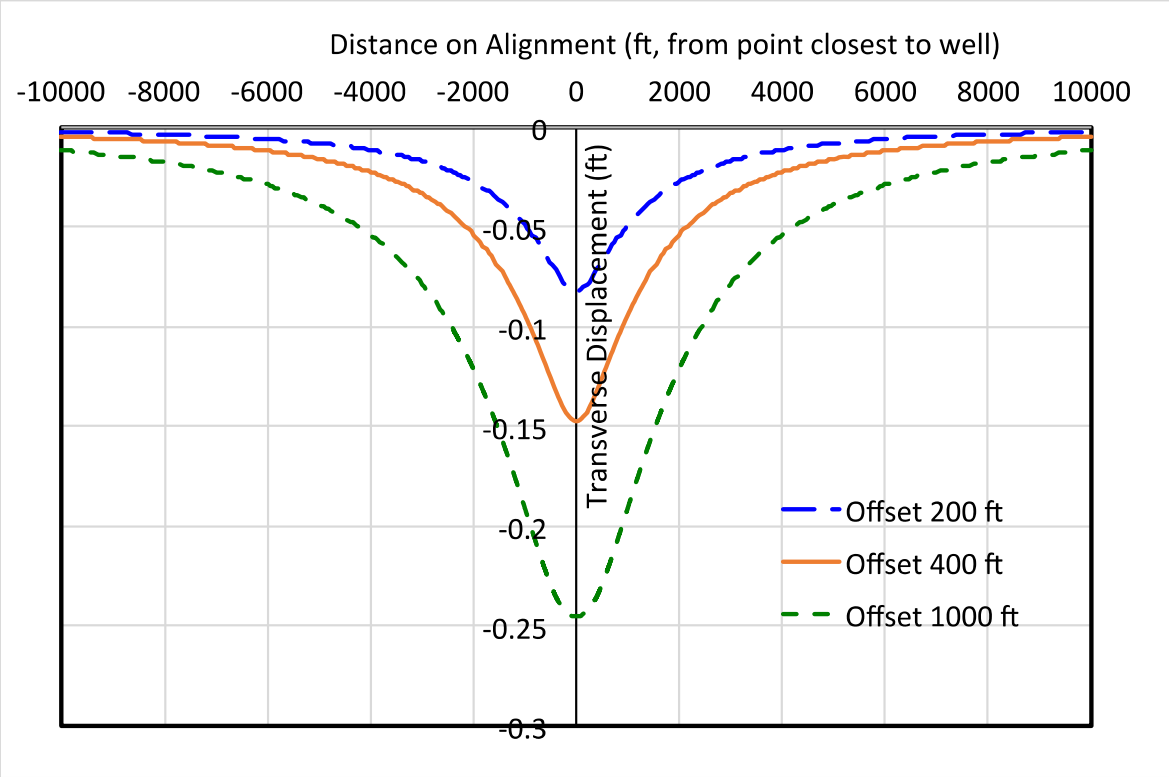

Figure 4-12: Transverse displacement profiles along HSR Alignment due to pumping from lower aquifer

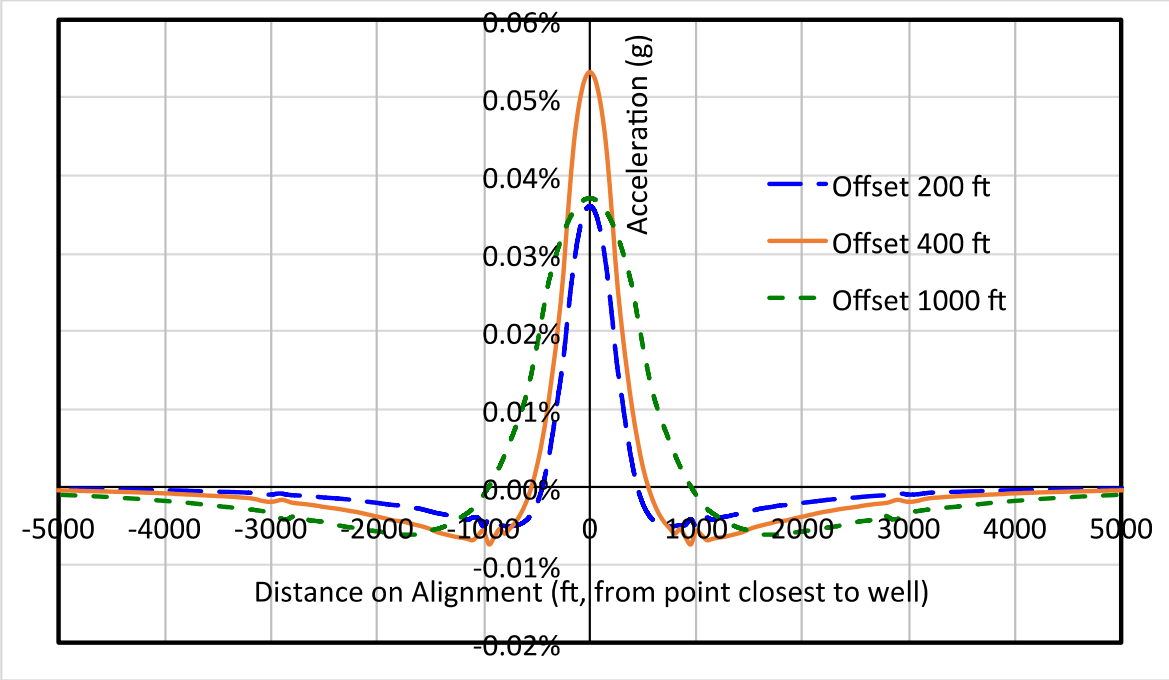

Figure 4-13: Horizontal acceleration along HSR Alignment due to pumping from lower aquifer

Figures 4-14 and 4-15 are similar plots for the case of groundwater pumping from the upper aquifer. In this case, the transverse displacements in Figure 4-14 are larger than the displacements for the case of groundwater pumping from the lower aquifer (Figure 4-12). Consequently, the resulting differential transverse displacements and accelerations (Figure 4-15) are also larger, they occur closer to the well, and then they drop off faster with increasing offset distance than in the case of pumping from the lower aquifer. As seen in Figure 4-15, the maximum curvature occurs when the offset distance is approximately 200 ft, compared to 400 ft in the case of pumping from the lower aquifer. Figure 4-11 shows that maximum radial displacement occurs at an offset distance of approximately 900 ft from the well. Maximum curvature occurs closer to the well than where maximum radial displacement occurs.

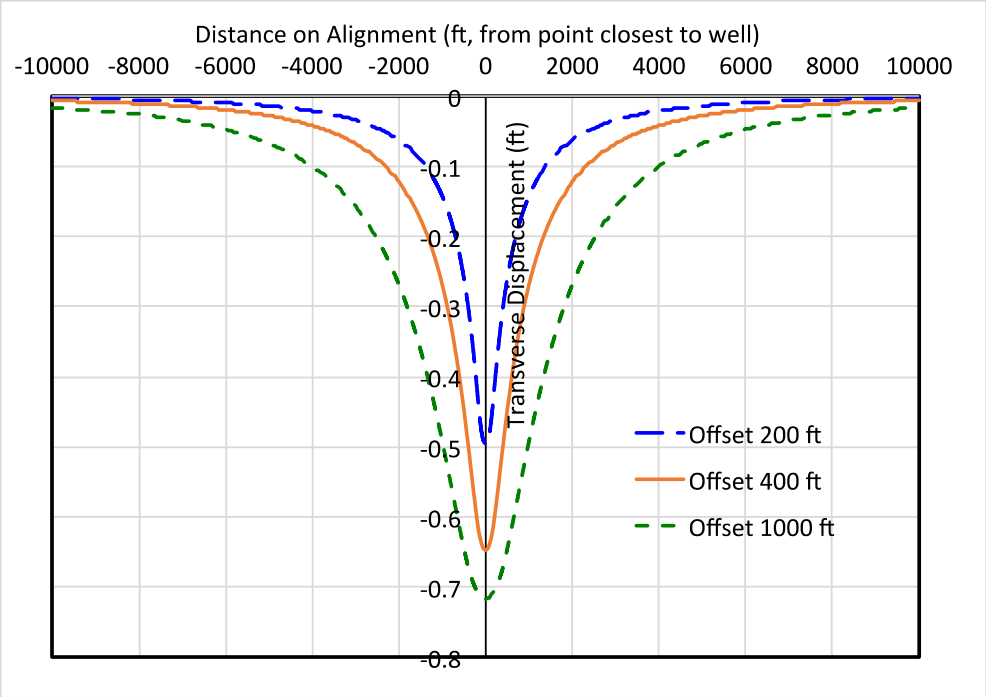

Figure 4-14: Transverse displacement profiles along HSR Alignment due to pumping from upper aquifer

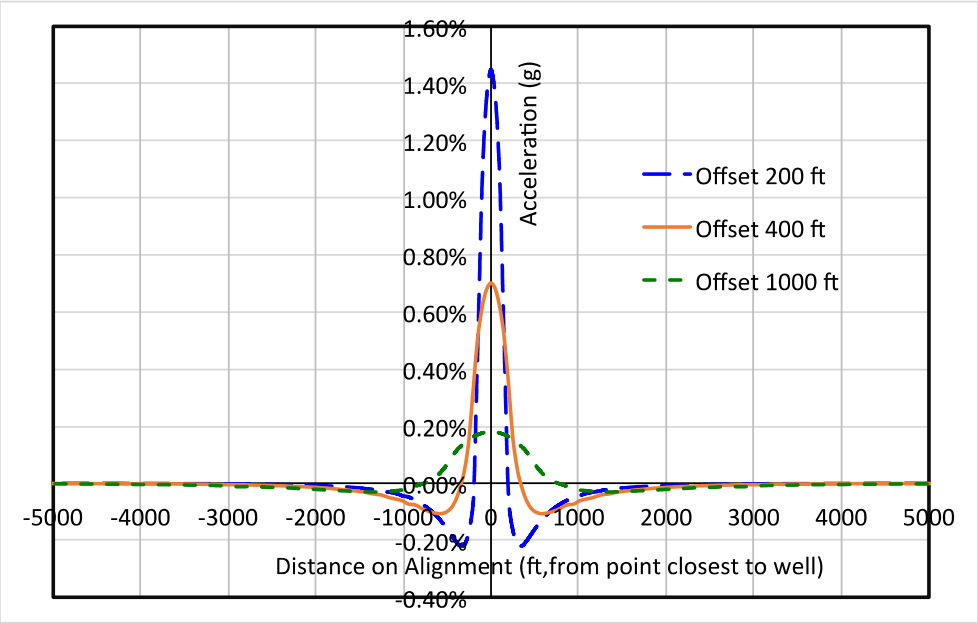

Figure 4-15: Horizontal acceleration along HSR Alignment due to pumping from upper aquifer

4.1.4.2.1 Ratio of Horizontal to Vertical Curvature

In the case of groundwater extraction from the lower aquifer, the maximum radial displacement is approximately one-seventh of the maximum vertical displacement. The ratio of maximum vertical curvature to the maximum horizontal curvature is approximately 4.

For groundwater extraction from the upper aquifer, the maximum transverse displacement is approximately one-sixth of the maximum vertical displacement, and the ratio of maximum vertical curvature to maximum horizontal curvature is approximately 1½.

4.1.4.3 Tensile Strains

Maximum tensile strains would be expected to be in a direction radial to a single well with the pattern shown in Figure 4-16.

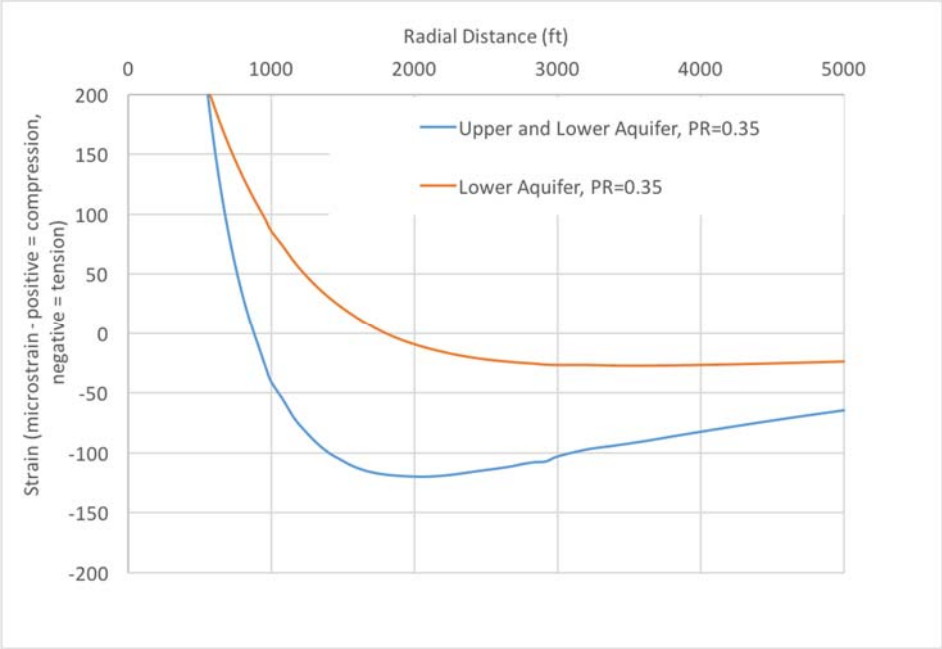

Figure 4-16: Subsidence-induced compressive or tensile strain vs distance from well

As shown in the Table 4.3, the modeled maximum tensile strain in a radial direction was about 28 microstrain (about 20 to 35 microstrain for a range of Poisson's ratios) when pumping from the lower aquifer, and about 120 microstrain when pumping from the upper and lower aquifer together. In general, tensile cracking is not anticipated to initiate below something on the order of 200 microstrain. Thus, tensile strains that would initiate tensile cracking were not observed in the cases analyzed; however, spatial variation in field subsurface conditions could result in locally-greater tensile strains than were modeled, which potentially could result in tensile cracking in some locations.

TABLE 4-3
Summary of maximum modeled tensile strain.

Groundwater Extraction Zones	Poisson's Ratio	Time Period	Max Subsidence at Well (ft)	Max Tensile Strain (microstrain)	Distance from Well of Maximum Strain
300' to 400' (lower aquifer)	0.25	20 years	1.91	33	2999
300' to 400' (lower aquifer)	0.35	20 years	1.83	28	3599
300' to 400' (lower aquifer)	0.45	20 years	1.74	22	3599

Groundwater Extraction Zones	Poisson's Ratio	Time Period	Max Subsidence at Well (ft)	Max Tensile Strain (microstrain)	Distance from Well of Maximum Strain
100' to 200' (upper aquifer) and 300' to 400' (lower aquifer)	0.35	20 years	4.20	120	2039

4.1.4.4 Parametric Analysis

Additional analyses were performed for 13 cases to evaluate the sensitivity of the model results under the same pumping rate to other parameters, including: aquifer compressibility, boundary conditions, horizontal hydraulic conductivity, and the vertical-to-horizontal hydraulic conductivity anisotropy ratio. The Poisson's ratio value was assumed to be 0.35 for all cases, and all cases were evaluated at 20 years (at 2 years the resulting subsidence and accelerations would be slightly less, and at 100 years, the results would be nearly unchanged). The maximum horizontal and vertical accelerations for these 13 cases are summarized in Table 4.4.

For the cases of pumping from the lower aquifer only, the following cases were evaluated:

- Simulation Cases 1 and 2: Both vertical and horizontal maximum induced accelerations increased with increased vertical soil compressibility (M_v). Doubling M_v resulted in approximately 35% and 25% increase in induced vertical and transverse accelerations, respectively.
- Simulation Cases 3 and 4: Both vertical and horizontal maximum accelerations increased with reduced horizontal hydraulic conductivity (K_x). Reducing K_x from 35 feet per day (ft/day) to 7 ft/day resulted in approximately 35% increases in vertical and horizontal acceleration by a factor of about 5, but induced accelerations still less than 1% g. In reality, if K_x were as low as 7 ft/day, the aquifer would have a smaller yield and the pumping rate at the well would likely be less than the rate modeled.
- Simulation Case 5: Both vertical and horizontal maximum accelerations were relatively insensitive to the vertical-to-horizontal hydraulic conductivity ratio.
- Simulation Cases 6 and 7: A higher initial water level resulted in lower maximum vertical accelerations. Lowering the initial water level from 50 ft to 100 ft increased the vertical maximum acceleration by approximately 50%. Horizontal acceleration was relatively insensitive to initial water level.
- Simulation Case 8: The boundary of the model is far enough such that the model results are not sensitive to modest changes in the distance to the model boundary.

For the cases of pumping simultaneously from both the upper and lower aquifers, the following cases were evaluated:

- Simulation Cases 9 and 10: Both vertical and horizontal accelerations increased with increased vertical soil compressibility (M_v). Doubling M_v resulted in approximately 50% increases in maximum vertical and horizontal accelerations.

- Simulation Cases 11 and 12: Both vertical and horizontal maximum accelerations increased with reduced K_x. Reducing K_x from 7 ft/day to 1 ft/day resulted in approximately double the maximum vertical and horizontal accelerations. (In reality, if K_x were as low as 1 ft/day, the aquifer would have a smaller yield and the pumping rate at the well would likely be less than the rate modeled.)
- Simulation Case 13: Raising the initial water level to the ground surface resulted in slightly lower maximum vertical accelerations.

TABLE 4-4

Summary of parametric study

Simulation Cases	Groundwater Extraction Zones	M_v (1/psf)	K_x (feet/day)	K_v/K_x	Initial Water Level Feet (BGS)	Boundary Conditions	Max. Vert. Accel (g)	Max. Hori Accel (g)
Base Case	**Deep**	**5.15E-7**	**35**	**0.1**	**50**	**Constant H**	**0.184%**	**0.053%**
1	Deep	1 .0 E-7	35	0.1	50	Constant H	0.088%	0.027%
2	Deep	1.0 E-6	35	0.1	50	Constant H	0.251%	0.066%
3	Deep	5.15E-7	70	0.1	50	Constant H	0.095%	0.021%
4	Deep	5.15E-7	7	0.1	50	Constant H	0.846%	0.230%
5	Deep	5.15E-7	35	0.02	50	Constant H	0.174%	0.051%
6	Deep	5.15E-7	35	0.1	0	Constant H	0.149%	0.048%
7	Deep	5.15E-7	35	0.1	100	Constant H	0.290%	0.049%
8	Deep	5.15E-7	35	0.1	50	H varies	0.157%	0.047%
Base Case	**Shallow and Deep**	**6.18E-7**	**7**	**0.1**	**50**	**Constant H**	**2.347%**	**1.449%**
9	Shallow and Deep	1.0 E-7	7	0.1	50	Constant H	0.540%	0.250%
10	Shallow and Deep	1.0 E-6	7	0.1	50	Constant H	3.618%	2.293%
11	Shallow and Deep	6.18E-7	20	0.1	50	Constant H	1.210%	0.696%
12	Shallow and Deep	6.18E-7	1	0.1	50	Constant H	4.820%	3.142%
13	Shallow and Deep	6.18E-7	7	0.1	0	Constant H	2.308%	1.425%

4.1.5 Evaluation and Discussion

The modeling results indicate that:

1. With similar magnitude of groundwater extraction, pumping from a shallow aquifer caused greater ground surface displacement than pumping from deeper zones, in both vertical and radial directions.
2. Maximum vertical displacement occurred at or near the well.

3. Maximum transverse displacement was located at approximately 1600 ft from the well for the case of groundwater extraction from the lower aquifer. When groundwater was extracted from the upper aquifer, maximum transverse displacement occurred at approximately 800 ft from the well.
4. In case of pumping from lower aquifer, the maximum transverse displacement was approximately one-seventh of the maximum vertical displacement. The maximum horizontal curvature was approximately one fourth of the maximum vertical curvature.
5. In case of shallow groundwater pumping, the maximum transverse displacement was on the order of one sixth of the maximum vertical displacement. The maximum horizontal curvature was approximately two-thirds of the maximum vertical curvature.
6. For pumping from the upper aquifer, the maximum induced vertical acceleration was less than 0.025 g and the maximum induced horizontal acceleration was less than 0.015 g. Calculated curvatures when pumping from the lower aquifer were much lower than this.
7. We expect that most heavy pumping in the SJV is primarily from deeper aquifers, similar to or deeper than our modeled “lower aquifer” cases, so we might expect observed subsidence patterns in the SJV would be similar to our modeled patterns for pumping from the lower aquifer, possibly with some areas still pumping from the upper aquifer. In our modeling, the differential subsidence between the well and 1 mile from the well, when pumping from the lower aquifer, or from both aquifers, was about 1 ft or 3 ft, respectively. The most pronounced subsidence cone observed in JPL InSAR results was centered about 1.5 miles to the northeast of the HSR Alignment, as shown on Plate 4-1; over the period of June 2007 to December 2010, local differential subsidence at this cone was about ¾ to 1¼ foot over a radius of about 1 mile, which appears to be bracketed by the magnitude of our modeling results. Plate 4-1 presents a comparison of modeled results vs. an InSAR-derived single-well subsidence cone.
8. Given the similarity in modeled results from 2 years to 20 years of modeled pumping (see Plate 4-1), it is anticipated that single well subsidence and curvature will develop rapidly, and may be essentially complete, within a relatively short period of a few years or less, at that well. It may further be inferred, that if the single well is permanently shut down, local subsidence and curvature might at least partially reverse as subsidence of the surrounding ground ’catches up’ with the previous single well subsidence cone.
9. Tensile strains that would initiate tensile cracking were not observed in the cases analyzed, but larger concentrations of strains and tensile cracking could occur under certain variable subsurface conditions. Thus, our modeling suggests tensile cracking would be expected to be uncommon but, in response to adverse subsurface variability, could occur. This is generally consistent with the fact that tensile cracking and resulting fissures have been uncommon but not unknown in the SJV. (This study did not rigorously or quantitatively address the possibility of spatially variable field conditions that could lead to subsidence-induced faults or ground fissures. Fissures are further addressed in Section 8.5.3 of this report.
10. Vertical subsidence is relatively insensitive to variations in Poisson’s ratio for a given vertical compressibility value. The results support that conventional modeling based on one-dimensional (vertical) compression (i.e., change in storage), such as the MODFLOW-family of codes, reasonably simulates the vertical subsidence, although it cannot model horizontal deformation.

11. This single-well subsidence model was developed to investigate sensitivity to various parameters based on a simplified subsurface profile with no lateral variability in the subsurface profile. Actual subsidence patterns will be effected by spatial variability of hydrogeologic parameters and the spatial relationship of multiple wells, which were not addressed in this simplified model.

The current modeling was performed to evaluate the ground deformation in response to pumping from a single well, but the effects of multiple wells can be approximated by superposition of the effects of individual wells. However, wells are typically spaced apart from each other to avoid significant interfering their individual production yields. We expect that it is relatively uncommon that wells be spaced closer than about 1300 ft and operating at the same time and at the same rate as modeled. Even if there are multiple extraction wells close to the HSR Alignment, their total production yield may not be significantly more than single-well extraction rates assumed in this modeling. If this is the case, the pumping will be distributed between multiple wells, the total vertical and radial or transverse displacement will be relatively unchanged or at least not significantly increased, while the differential vertical and radial or transverse displacement are expected to be relatively unchanged or slightly reduced; thus, total induced accelerations will not be significantly adversely impacted.

Even if we were to conservatively assume that there are two wells, with one on each side of the HSR Alignment, operating continuously at the same rate as modeled cases, the resulting maximum induced vertical acceleration will still be less than twice their individual values (i.e., it will still be less than 0.05 g). The induced maximum traverse accelerations individually by these two wells will be opposite in direction. Therefore, similar to the vertical accelerations, the maximum induced horizontal acceleration will be less than twice their individual values (, i.e., it will still be less than 0.03 g). Therefore, if there are multiple extraction wells close to the HSR Alignment, the total production yield will likely be significantly greater than the yield from the single-well extraction rate assumed in this modeling study. If it is the case, that the pumping will be distributed between multiple wells, the total vertical and radial or transverse displacement will not be relatively unchanged or at least not significantly increased, while the differential vertical and radial or transverse displacement are expected to be relatively unchanged or slightly reduced; thus, and the total induced accelerations will not be significantly impacted.

Based on our evaluations summarized in Plate 4-1 (and discussed in List Item 7 above), and as further discussed below in Section 8 (e.g., in the discussion of Plates 8-2, 8-3, 8-4, 8-9, and 8-10), it appears there may be some relatively small well-related local subsidence expression in the vicinity of the HSR Alignment, but the nearest more significant subsidence cone we observed was about 1.5 miles from the HSR Alignment. In conclusion, we anticipate that unless a large pumping well, screened in the upper aquifer and drawing groundwater down from within this aquifer, is located within several hundred feet of the HSR Alignment, the induced curvatures are expected to be relatively small, with induced accelerations within the *Design Criteria* limits. The results from parameter/sensitivity analysis support the conclusion.

4.2 CENTRAL VALLEY HYDROGEOLOGIC MODEL FOR HSR APPLICATION

The USGS previously created a Central Valley Hydrogeologic Model (CVHM) to evaluate the hydrologic impacts of regional-scale pumping and the resulting subsidence using a 1-mile spatial resolution (Faunt el al., 2010). The CVHM was a numerical model that was originally calibrated for the period from 1961 through 2003, ending shortly prior to when the most-recent accelerated subsidence in the SJV was widely recognized. In 2014, the USGS began the process of updating the CVHM based on data extending through 2013. Herein we will refer to the future updated model as the CVHM2. However, at this time, model revisions are still in progress and CVHM2 updating has not been completed.

The USGS provided the AFW team with an interim version of the model to explore the possibility of locally refining the model for use in forecasting subsidence at finer spatial and temporal resolutions in the vicinity of the HSR Alignment. However, following our preliminary review of this interim model and discussions with the USGS, it was agreed that making the necessary modifications should not be included in the scope of our GSS at this time.

Although the CVHM2 is not ready for use in forecasting subsidence for the HSR at this time, it could potentially be a valuable tool for evaluating groundwater drawdown and estimating subsidence at 1-mile resolution in the future following completion of calibration efforts by the USGS. If needed, a future version of the model could subsequently be refined and improved for areas relevant to the HSR at spatial and temporal resolutions appropriate for evaluation of flood zones and other subsidence induced impacts.

5.0 PAST SUBSIDENCE MAGNITUDES, RATES, AND PATTERNS

Subsidence appears to have been occurring slowly in the SJV for at least several million years as a part of progressive alluvial deposition in the area. More recently, subsidence in the Corcoran Subsidence Bowl has been re-initiated and/or accelerated since Tulare Lake was drained in the late 1800s, and with the general increasing of groundwater pumping from beneath the area to support grown in both agriculture and domestic water needs.

5.1 GEOLOGICAL ASPECTS OF SUBSIDENCE

As described in Section 3.2, subsidence is primarily occurring in compressible aquifer systems subject to extensive pumping within the SJV. Geologic forces and phenomena have controlled the distribution and, in some places (see Section 8.6.3.3 for further discussion), significant zones of inhibited connectivity between these aquifer systems that impact subsidence patterns, magnitudes and rates. The HSR Alignment passes primarily through the eastern portion of the SJV within the Corcoran Subsidence Bowl. Erosion of the Sierra Nevada Mountains during the Pleistocene Ice Ages is the primary source of eastern SJV basin aquifer system materials, and runoff from the Sierras is the dominant form of transport, placement and distribution of the eastern SJV aquifer system sediments.

Historical studies of subsidence from the 1920s to 1972 in the SJV led to the conclusion that:

> "*…the areas in which subsidence has been appreciable coincide generally with the areas in which ground water is withdrawn chiefly from confined aquifer systems…. Furthermore, the great increases in stress applied to the sediments in the ground-water reservoir by the intensive mining of groundwater have developed chiefly as increased seepage stresses on confined aquifer systems.*" (Poland et al., 1975)

The DWR recently published a new estimation of historical subsidence based on 1949 photogrammetry and 2005 NextMAP InSAR. As shown on Figure 5-1, the DWR has estimated that magnitudes of historical subsidence are up to 20 ft or more in the subsidence-prone areas around Corcoran and the southern SJV over this period. Initial review of the figure also shows a general agreement with other reports of subsidence, with patterns of minimal to minor subsidence closer to the Sierra Nevada mountain front and in the center of the historical Tulare Lake.

Several relatively isolated subsidence features are shown in the southern SJV. One such feature, located about 6 miles west-southwest of the HSR Alignment at Deer Creek, and 13 miles south of Tule River crossing, is coincident with part of the Trico Gas Field (shown on Plate 8-1). It is possible that significant historical subsidence may have resulted from hydrocarbon extraction. JPL 2007-2010 InSAR (Plate 8-15) shows continuing recent subsidence there at a rate of only about 1 inch per year. A second significant and relatively isolated subsidence feature, located 22 miles farther south, is positioned between the Semitropic and abandoned Buttonwillow gas and oil fields; those fields are 2 to 3 miles from that apparent subsidence feature. A few miles to the southwest, a third significant and relatively isolated subsidence feature, located adjacent to the California Aqueduct, has no associated oil or gas wells. Farther southwest, historical subsidence is indicated coincident with the South Belridge oil and gas field. Overall, this estimated historical subsidence map may be useful in filling some gaps in general trends within the historical subsidence record, but there is potential for significant disagreement with documented historical subsidence observations.

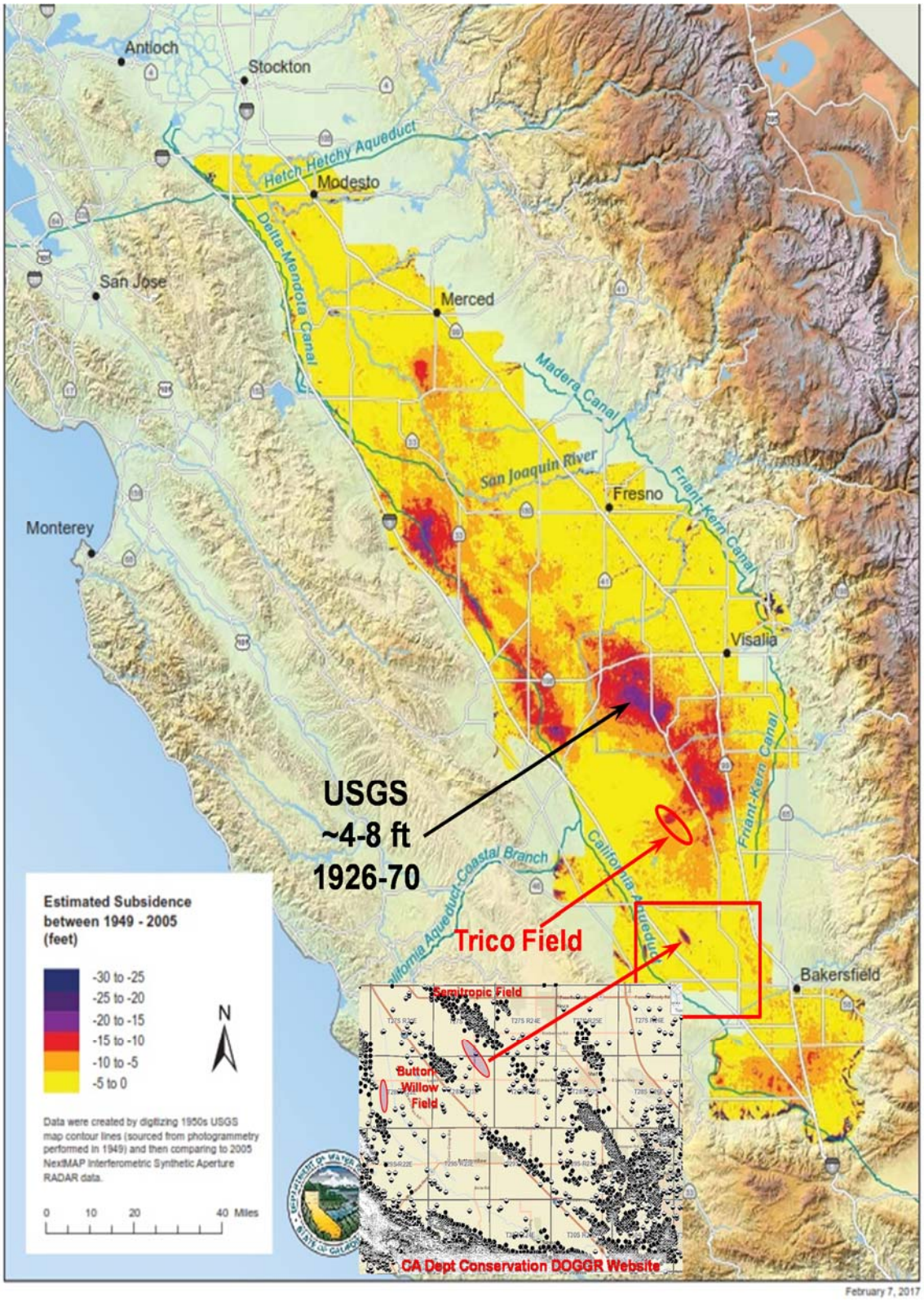

Figure 5-1: Estimated subsidence in the San Joaquin Valley 1949-2005 (DWR 2017)

Recent maximum subsidence rates and short-term magnitudes have equaled or exceeded maximum historical rates in the Corcoran Subsidence Bowl area of the SJV. Thus, it appears that in spite of the presence of thousands of large-diameter wells penetrating geologic confining beds and providing pathways of vertical hydraulic connection within the SJV alluvium aquifer system (Faunt, 2009, p 22), significant aquifer confinement is still present in some areas. Recent and continuing mining of groundwater within these confined aquifer zones is anticipated to be the primary driver of the current subsidence.

As shown in Figure 5-2, recent and historical subsidence magnitudes are small in the eastern portion of the SJV closest to the Sierra Nevada Range. Subsidence is anticipated to be minimal in the dense coarse alluvium of the basin proximal facies, and to proceed rapidly in the coarser medial facies of the basin alluvium due to relatively high aquifer system hydraulic conductivities. Except for a limited area along Highway 99 at the eastern edge of the Corcoran Subsidence Bowl, both historical and recent subsidence is small to negligible outside of the edge of the underlying Corcoran Clay Member the Tulare Formation.

Recent and historical subsidence magnitudes are also small in the Tulare Lakebed where lacustrine sediments may be subject to eventual significant subsidence, but where very low hydraulic conductivities are anticipated to cause subsidence to proceed very slowly, perhaps in geologic time. Water quality and well performance constraints may also limit the effectiveness of groundwater pumping in this area.

Relatively large-magnitudes of historical and recent subsidence have occurred in areas within the SJV where confined aquifer conditions are present (Poland et al., 1975). Such confined aquifer conditions are present beneath the Corcoran Clay within the zone of ashfall from the Long Valley Caldera event about 760,000 years ago. InSAR coverage provides an effective characterization of overall recent and ongoing subsidence in the Corcoran Subsidence Bowl. The concentration of large magnitude historical and recent subsidence between the Tulare Lakebed and the approximate edge of the Corcoran Clay is shown in Figure 5-2. Subsidence in (assumed) unconfined aquifer systems is evident in historical subsidence to the east of the Corcoran Clay. However, being measured at only a few surveyed profiles, that historical subsidence is poorly constrained. An abrupt increase in subsidence at the approximate edge of the Corcoran Clay is inferred by the existence and location of the Pixley Fissure. The Pixley Fissure is discussed in Section 8.5.3.

Dynamics of northward tectonic plate movements driving anomalous subsidence in the Tulare Basin as described by Saleeby et al. (2013) may further complicate understanding the strengths of basin materials subject to subsidence. Confinement of aquifers, especially those underlying the extensive Corcoran Clay, may cause the sediments to be in an undrained condition. Underlying lithospheric spreading due to tectonic plate movement might also be straining and dilating these undrained sediments into a state of (reduced) residual strength. If fluid

contributing to supporting the overlying basin material column is removed, as by pumping, the result may be an even greater magnitude of subsidence than due to aquifer confinement alone. Tape et al. (2009) present a theoretical analysis of horizontal ground velocity, strain rate, and dilation rate around a simplified model of the San Andreas Fault that includes the southern SJV area. Their model includes northward movements of 1 to 4 mm per year in the southern SJV, and strain and dilation rates up to 1E-7 per year extending about 20 to 30 miles from the modeled San Andreas Fault. Assuming that portions of the Tulare Basin sediments were subject to similar strains due to tectonic activity, and ”confinement” did not begin until 0.7 Ma , confined, undrained sediments may still have been subject to strains and dilation of several percent. Sediments confined at earlier times would have been subject to more strain and dilation. Areas of low basin sediment strengths are indicated where overall pressure or compression wave velocities (Vp) in parts of the Tulare Basin are as low as 6,200 to 6,400 ft per second (Plate 8-15). These overall velocities gradually increase (and sediment strength increases) to the north in the basin. It should be noted that historical maximum subsidence zones have been along the southwest edge of the basin where tectonic strains might have been concentrated. Smaller historical maximums at Pixley and Delano appear to straddle (be on either side of) the ”delamination hinge” inferred by Saleeby et al. (2013).

Some areas of significant historical subsidence have little current subsidence, and some areas of significant current subsidence had relatively less historical subsidence. These areas where recent and historical subsidence are not consistent may indicate changing groundwater pumping patterns from the early to mid-20th century to recent times. These apparent mismatches in historical to current subsidence rates are evidence that patterns of groundwater exploitation, as well as geologic conditions, control land subsidence.

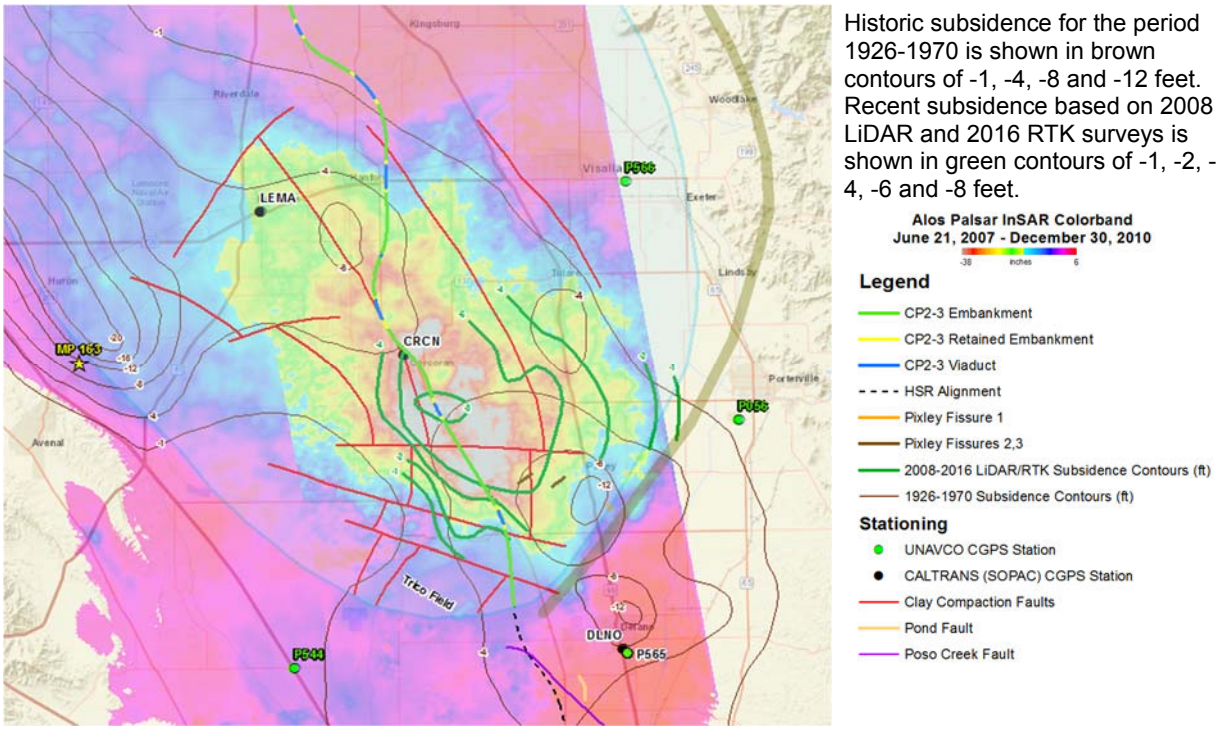

Figure 5-2: Summary of subsidence in Corcoran area of San Joaquin Valley.

5.2 OBSERVED GROUND ELEVATIONS AND LAND SUBSIDENCE

Historical subsidence from the 1900s measured using level survey profiles (Lofgren & Klausing 1969; Ireland el al., 1984) in the southeastern SJV were greatest to the east of the HSR Alignment. Figure 5-1 broadly summarizes the subsidence from 1926 to 1970 (shown by the shaded contours). Figures 5-1 broadly summarize subsidence from 1949 to 2005, and Figure 5-2 broadly summarizes subsidence from 1926 to 1970 (shaded contours) as well as from 2007 to 2010 (colors).

From 1926 through 1970, a local maximum subsidence of about 12 to 14 feet was documented near Pixley in the vicinity of Highway 99, near the edge of the underlying Corcoran Clay Member of the Tulare Formation. Subsidence was less than 4 feet in the Corcoran vicinity, and increased to roughly 6 feet both to the north and south along the HSR Alignment within the Corcoran Subsidence Bowl. Documented maximum subsidence rates up to about 0.9 feet per year in the general HSR Alignment vicinity occurred in the years 1948 through 1954. As surface water delivery systems were completed and demand for groundwater diminished, subsidence rates declined throughout the area. Through 2005, a maximum of about 10 to 15 feet of cumulative subsidence has been estimated in and to the southeast of Corcoran, and about 15 to 20 feet of cumulative subsidence has been estimated to the north and northwest of Corcoran.

5.2.1 Recent Ground Elevation Surveys

USGS topographic maps (e.g., the 2015 Corcoran Quadrangle, 7.5-minute Series) and the NAD2009 (based on NASA's Shuttle Radar Topography Mission [SRTM]) do not reflect current subsided elevations along the HSR Alignment in much of the Corcoran Subsidence Bowl. Recent survey work has provided a better understanding of current ground elevations, and documents recent land subsidence. Elevation of HSR monuments were established using static GPS methods at approximate 2-mile intervals along the HSR Alignment in 2010.

Resurvey of these HSR Alignment monuments in February 2015 identified maximum subsidence in exceedance of 5 ft near the Tule River about 3 miles south of Corcoran to essentially zero elevation change at about 27 miles north of Corcoran between 2010 to 2015.

In July 2008, a LiDAR topographic elevation survey was performed through a portion of the southeast SJV to support a USACE dam break analysis in the Tule River area to the Tulare Lakebed; this 2008 regional elevation survey included about 21 miles of the project alignment, from Corcoran to the north, to south of the Deer Creek Viaduct.

To develop relatively current topographic information, elevations were measured in August of 2016 using a vehicle-mounted RTK survey system driving on local roads throughout the area previously measured by LiDAR (Appendix C). These 2016 elevations, collected at typical intervals of 50 to 60 ft to an accuracy of a few tenths of a foot, provided a grid or "wireframe" onto which the continuous 2008 LiDAR elevation information could be draped, to create a surface representing the 2016 condition. This process is further described in Section 6.0.

5.2.2 Recent Land Subsidence Characterization

Ground subsidence in the Corcoran Subsidence Bowl between June 2007 and December 2010 is broadly summarized in Figure 5-2. Color banding in Figure 5-2 presents subsidence from June 2007 through December 2010 based on satellite-based InSAR. Maximum subsidence within the subsidence bowl during that time is interpreted to be about 3.2 ft (38 inches) with a maximum average subsidence rate of about 0.9 ft per year.

More-recent InSAR starting in 2014 has documented an increase in subsidence rates through the southern SJV. Using Radarsat-2 satellite data from May 3, 2014, through January 22, 2015, a maximum of 13 inches of subsidence south of Corcoran was reported by Farr et al. (2015).

Using Sentinel-1 satellite data from March 2015 to September 2016, a maximum of 22 inches of subsidence was reported in the Corcoran area by Farr et al. (2017). JPL has also developed a subsidence map based on Sentinel-1 data for the period of May 2015 to May 2016 as shown on Figure 5-3 (Farr 2016).

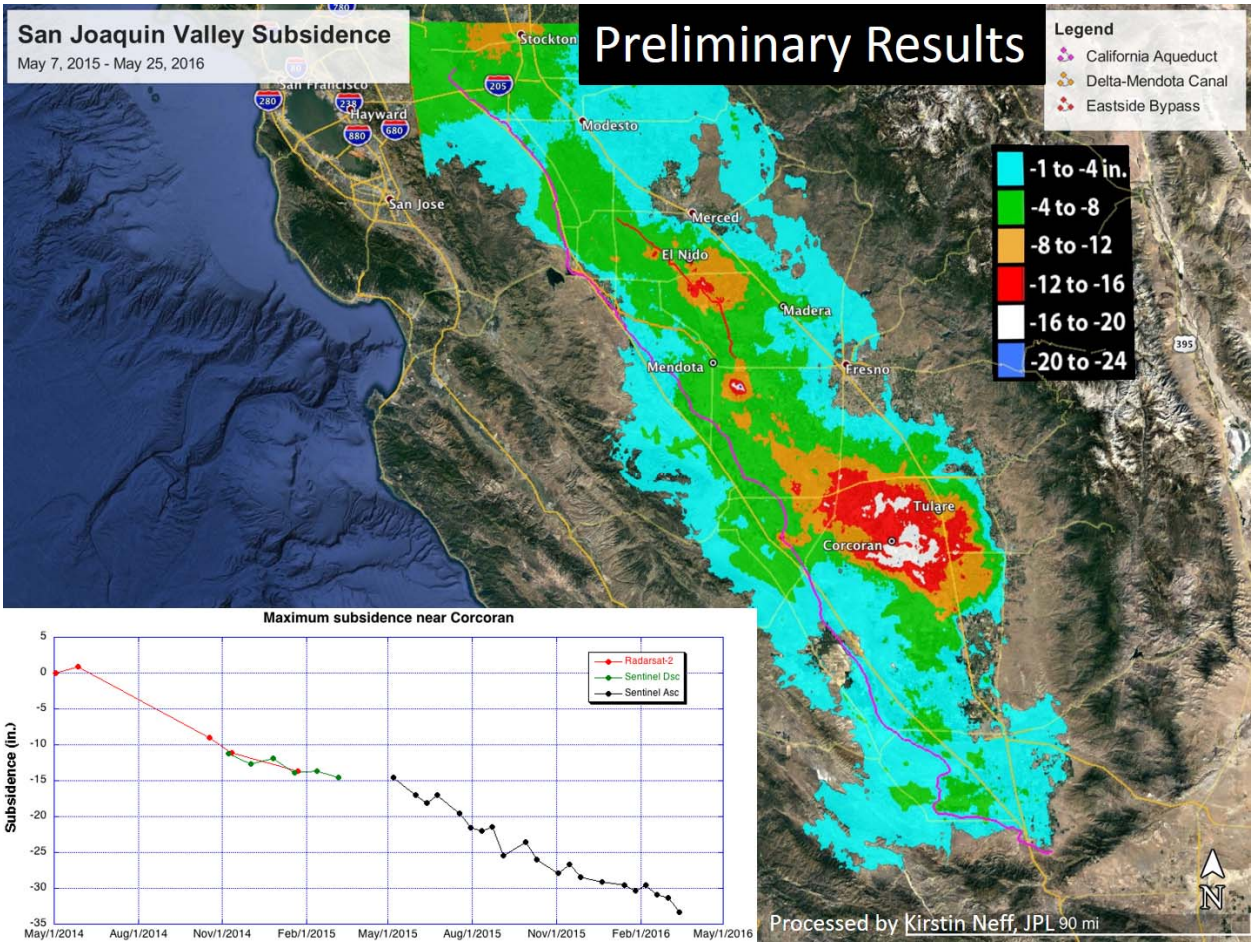

Figure 5-3: San Joaquin Valley Subsidence May 7, 2015 – May 25, 2016 (JPL). Also shows a plot of maximum subsidence near Corcoran for the period May 2014 through March 2016.

Recent subsidence in parts of the Corcoran Subsidence Bowl is so rapid that comparison of 2008 LiDAR and 2016 RTK elevations has provided effective subsidence characterization even though these methods are accurate to only a few tenths of a foot. The maximum subsidence measured from July 2008 to August 2016 (a period of about 8 years) by combination of LiDAR & RTK is greater than 9 ft (for an average of over 1 foot per year); this maximum subsidence occurred south of Corcoran at 144th Avenue, about 1 mile west of the HSR Alignment.

Recent subsidence in the Corcoran Subsidence Bowl is being measured using several independent technologies. Caltrans maintains CGPS station CRCN adjacent to Highway 43 just north of Corcoran (see Appendix A). A continuously operating static GPS survey station at location CRCN has documented a subsidence rate of about 1 foot per year since the beginning of 2013 at that location. Repeat static GPS survey by Caltrans at the CRCN location shows subsidence occurring prior to 2012. (This static GPS survey data contradicts the pre-2013 CRCN CGPS results but is consistent with the pattern of the CRCN CGPS results from 2013 to late 2015 and with other InSAR information, and we believe movement was actually occurring at

a similar rate before 2013.) Other CGPS stations in the area with several years of subsidence data, including subsidence pre-dating 2012, operated by either Caltrans or the Plate Boundary Observatory (PBO), are shown in Figure 5-2. These other CGPS stations include subsidence data predating 2012 that is summarized in Appendix A of this report. InSAR reported by Farr et al. (2015; 2017) indicates a very similar subsidence rate at the CRCN location in 2015 to 2016, somewhat faster than their reported subsidence rate from 2007 through 2010.

Subsidence calculated from the 2008 LiDAR and 2016 RTK surveys matches well with the InSAR, repeat survey, and CGPS subsidence trends at CRCN.

Finally, subsidence trends inferred from satellite altimetry results starting from 2000 to 2015 at a point in the Corcoran Subsidence Bowl in the vicinity of CRCN, presented by Hwang et al. (2016), are consistent with the subsidence trends indicated by the InSAR and survey information (Figure 5-4). These various subsidence measurements indicate that subsidence, which had been occurring prior to 2012, accelerated in about 2012 as drought conditions enveloped the SJV and persisted until the winter and spring of 2017.

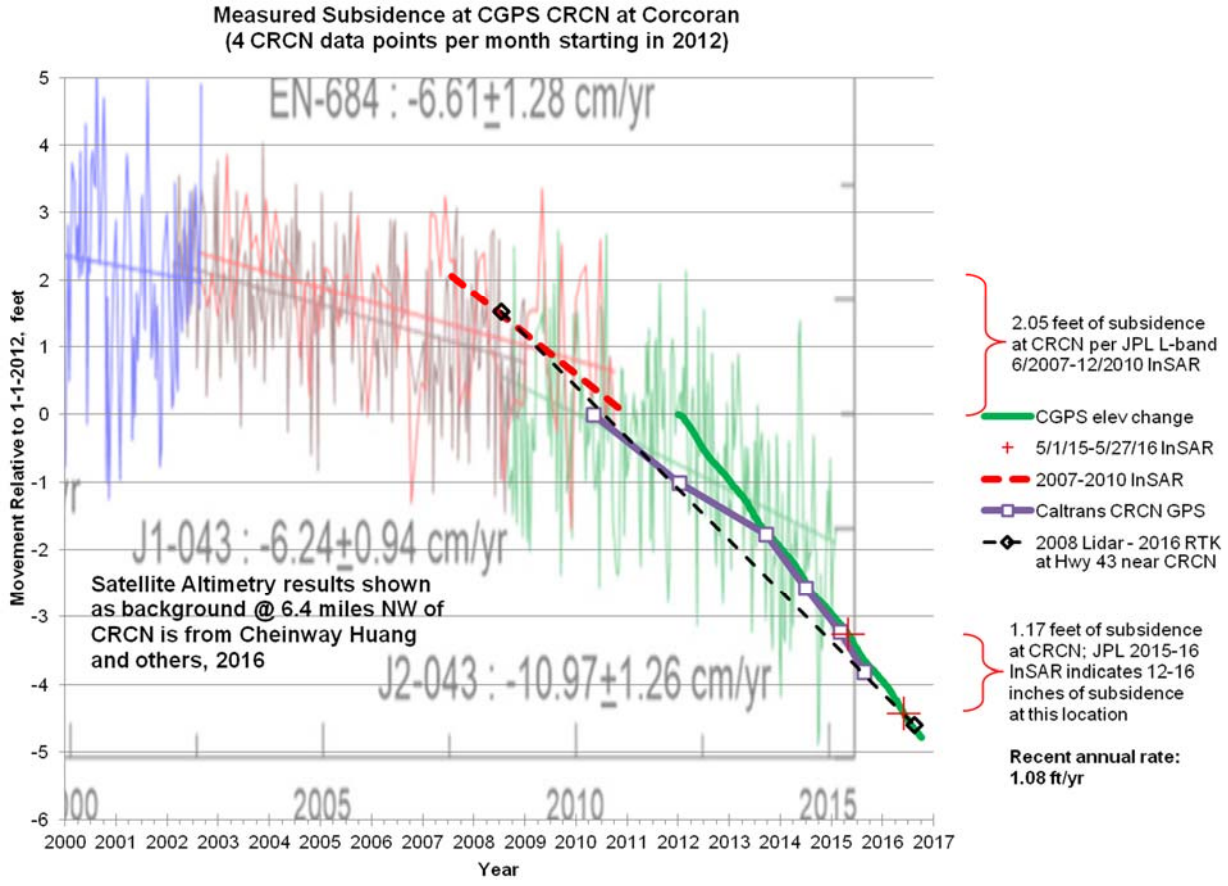

Figure 5-4: Comparison of various subsidence measurements in Corcoran area for 2007-2016

6.0 FORECASTING FUTURE SUBSIDENCE

For the HSR, future subsidence will be more important than historical subsidence, so we developed forecasts of future magnitudes, rates, and patterns of future subsidence as summarized below.

In 2014, the State of California legislature passed the SGMA, which became effective in 2015. SGMA requires that local agencies in critically over-drafted groundwater sub-basins in the SJV (such as the Tulare Lake Basin) prepare Groundwater Sustainability Plans (GSPs) by 2020, and implement these plans by 2040. Given the over 20-year window to reach sustainability, it is unlikely that there will be a significant decrease in groundwater extraction until well into this 20-plus year window. Hence, based on the rates and magnitudes of observed recent and ongoing subsidence (primarily due to excessive groundwater pumping), it appears likely that subsidence will continue for a number of years before groundwater overdraft is slowed and "sustainable" groundwater pumping is achieved. In this GSS, subsidence impact evaluation assumed 20 years of subsidence projection from 2016, i.e., through 2036.

Conceptually, prediction of future subsidence could be made by (1) a data-driven model that is based on extrapolation from historical subsidence rates, and/or (2) a hydrogeological or physically-based model that simulates the hydrologic process, hydrogeologic behaviors, and geomechanical deformation mechanism. As discussed below, there currently is no adequate hydrogeologic model available to reliably forecast subsidence in the Tulare Lake area, so for this GSS future subsidence has been estimated based on extrapolation from historical data. In any case, it should be recognized that uncertainties are inherent in all prediction models. It is therefore important that subsidence along the HSR Alignment be monitored in the future.

6.1 HYDROGEOLOGICAL-BASED MODELING OF SUBSIDENCE

As discussed above in Section 4.2, in 2009 the USGS released the CVHM, a groundwater and subsidence model of the entire SJV based on the USGS computer code MODFLOW. The purpose of the CVHM was to evaluate the hydrologic impacts of regional-scale pumping and the resulting subsidence at 1-mile resolution. However, the CVHM was only calibrated for the period from 1961 through 2003, ending prior to when the most-recent accelerated subsidence in the SJV was widely recognized.

In 2014, the USGS began the process of updating the CVHM to include data through 2013, adding new surface water routing (i.e., streamflow routing, or SFR), farm management (FMP2), and subsidence (SUB) packages, and converting the model to the new code MODFLOW-OWHM (One Water Hydrologic Model). The updated model, referenced herein as CVHM2, is currently undergoing calibration by the USGS.

One of the tasks for the AFW team has been to evaluate if the USGS model can be adopted and refined for use to predict future subsidence at adequate spatial and temporal resolutions in

the vicinity of the HSR Alignment. As discussed in Section 4.2 of this report, the USGS provided us with an interim version of the model to explore the possibility of locally refining the model for use in forecasting future subsidence at adequate spatial and temporal resolutions in the vicinity of the HSR Alignment. However, following preliminary evaluations and discussions with the USGS, it was agreed that making the necessary modifications should not be included in the scope of this GSS.

6.2 METHODS USED TO FORECAST SUBSIDENCE

For this GSS, future subsidence forecasts were developed based on the assumption that recent and ongoing subsidence patterns and rates will continue for 20 years into the future (i.e., from 2016 to 2036). The 2016 topographic elevations in the Corcoran Subsidence bowl have been estimated using statistical methods to integrate available topographic and subsidence data as presented in Section 7.2.5.1 of this report.

The subsidence rate has been observed to be generally accelerating over the past 10 years or more, likely due to several factors, including recent drought conditions, increasing groundwater extraction rates, etc.

Three reasonable scenarios of 20 years of subsidence in the Corcoran Subsidence Bowl were established using recent rate-of-subsidence trends:

- Scenario A (2036a): This was based on an extrapolation of the subsidence rates calculated from the 2007-2010 InSAR data provided by the JPL. It is thought to represent a lower bound for 20 years of subsidence. The extrapolation assumes this subsidence rate can be extrapolated by multiplying by about 6 times the InSAR-derived rate from 2007 to 2010. This represents relatively recent subsidence rates before the latest accelerations were observed beginning during the 4-year period between fall 2011 and fall 2015, which was the driest since record keeping began in 1895, and also pre-dating construction of numerous new wells over in recent years.
- Scenario B (2036b): An 8-year average rate is available between the 2008 LiDAR and the 2016 RTK elevations. This represents a relatively long-duration average of subsidence, during which the average rate was generally between that of the period of 2007 to 2010, and the period of 2015-2016. This magnitude of subsidence over about 8 years can be multiplied by about 2.5 to extrapolate it forward 20 years. We judge that this rate may be the most reasonable for the current forecast.
- Scenario C (2036c): We judge that a reasonable upper bound may be estimated by taking about 20 times the InSAR-derived rate from May 2015 to May 2016. This represents the subsidence toward the end of the severe drought conditions that have dominated the area from fall 2011 to fall 2015 and into the following year.

We also performed preliminary evaluation of the LiDAR data provided by the CP 2-3 Design-Build Contractor (Dragados, 2015a), and these elevations are presented on Plate 1-2. However, apparently because the methodology and/or resolution was different from other available data, using this data to evaluate induced changed in slope or curvature appeared to produce a large

amount of what we interpret to be “noise” that is an artifact of the methods used rather than an indication of actual changes in slopes or curvature.

6.3 RECOMMENDATIONS FOR FUTURE MONITORING & INSTRUMENTATION

Because forecasting using the above-described approach contains many uncertainties, we recommend that future subsidence be monitored. Preliminary and conceptual recommendations for monitoring current and future land subsidence for the project are presented in Sections 8.6.5, 8.6.6, and 10.4 of this report. GPS survey methods should be utilized to provide reliable and precise elevations at specific points along the project alignment. Satellite-based InSAR technologies and procedures are rapidly developing and could provide invaluable information regarding rates and patterns of subsidence. The Uninhabited Aerial Vehicle Synthetic Aperture Radar (UAVSAR) program operated by JPL for DWR (Farr el al., 2015, 2017) is beginning to demonstrate effective corridor subsidence monitoring capabilities. Finally, once the HSR is operational, inertial and other continuous on-train monitoring methods should be implemented and utilized to provide critical information concerning changing track geometries resulting from continuing subsidence.

7.0 POTENTIAL IMPACTS TO HSR SYSTEM

7.1 TECHNICAL CONSIDERATIONS

Conceptually, there are several ways in which subsidence could adversely impact the HSR. Each has been evaluated at least in a preliminary fashion as summarized in this report. For the discussion below, we have considered the forecast topography for the 2016 Scenarios A, B, and C. It should be noted that Scenarios A and C are based primarily on extrapolations of InSAR evaluations produced by JPL that have a significance amount of smoothing inherent in the JPL products. Scenario B is based on numerical extrapolations with less smoothing inherent in the initial topography calculations, but with a moderate amount of smoothing to the profile that was taken from the forecast topographic surface. Because of this, the steepness of induced change in slopes and curvature are much greater as reported for Scenario B than for Scenarios A or C, but this is likely just an artifact of the method of calculations and smoothing that were used. This raises a question about which might be more realistic: the induced changes in slope and curvature for Scenarios A and C (significantly less than for Scenario B), or is Scenario B more realistic. With the available data, it is difficult to form a reliable conclusion, as discussed below in Section 7.2.6, and future monitoring will be valuable in improving these forecasts. However, we generally believe that the induced changes in slope and curvature indicated by our modestly smoothed results Scenario B are likely to be conservative with the possible exception of local anomalies such as possible compaction faults or subsidence-induced fissures, as discussed in Sections 7.2.6.

7.1.1 Induced Changes in Slope

The maximum induced changes in slope are in the range of up to 0.13 percent for Scenarios A and C, and 0.43 percent for Scenario B. The HSR *Design Criteria* (Table 4-4) has recommended and maximum grades of 1.25% and 2.5%, respectively, for ballasted track. As such, there appears to be very little chance these values will be exceeded. However, these induced changes in slope are within the range that can produce ground cracking under some conditions. In addition, these levels of differential subsidence could induce significant stains and stresses into structures, and this possible hazard should be addressed by the project designers. Recommendations for monitoring the potential development of excessive differential subsidence are presented in Section 8.0, 9.0, and 10.0.

7.1.2 Induced Changes in Vertical Curvature

Vertical curvature must be limited to values that will not create an induced vertical curvature greater than 0.05 times the acceleration of gravity (g). With a design speed of 250 mph, this required a radius of curvature of at least 83,500 ft, i.e., a curvature not greater than an absolute value of 0.000012 (i.e., 1.20E-05) $feet^{-1}$(positive or negative, i.e., either concave or convex upward). As seen on Plate 1-2, we anticipate that over the 20 years following construction, the maximum induced changes in vertical curvature will be in the range of up to 2.5E-6 ft^{-1} for Scenarios A and C, and possibly as much as 1.8E-5 ft^{-1} for Scenario B. Note however that although these brief spikes in curvature in Scenario B would theoretically produce accelerations greater 0.05g at 250 mph, we believe these large values are likely caused by “noise” in the data and small-scale localized error in the data resulting from the numerical methods used to extrapolate the available data, and the actual values will be less than this, and that better data would indicate the actual induced vertical curvatures are much less. The value in collecting higher-quality or better-resolution InSAR or other data is addressed below in Section 9.0.

7.1.3 Induced Changes in Horizontal Curvature

Although we do not have any direct measurements of subsidence-induced horizontal curvature within the Corcoran Subsidence Bowl, the results of our single-well subsidence modeling indicated that the maximum induced horizontal accelerations for a train going 250 mph would be about 0.014g, corresponds to an unbalanced super-elevation of about 0.9 inches, which is less than the target maximum of 3 inches (*Design Criteria,* Section 4.4.5.4). Therefore, we do not anticipate that induced horizontal curvature will be a significant problem for the HSR in the Corcoran Subsidence Bowl, unless induced curvature is greater than anticipated. This has been further discussed in Section 4.1.

7.1.4 Induced Changes in Twist

Subsidence is not expected to directly affect twist significantly, apart from uncommon anomalies such as fissures or faults.

7.1.5 Fissures

In 1969, three fissures developed near Pixley, California, as discussed in Section 8.6, located about 3½, 5½, and 9 miles from the HSR Alignment. Tensile cracks developed undetected to depths of at least 55 ft, which was the maximum depth observable in a bucket-auger boring due to the presence of groundwater. Following flooding of the area in 1969, when the flood receded, a trough up to about 6 ft deep, 8 ft wide, and a ½ mile long had been formed. Although fissures are not common in the SJV, they have occurred in the past and there is reasonable chance they could occur in the future. Forecasting where and when they might occur is difficult, but they are more likely to occur in areas of greatest induced convex-upward change in curvature where tensile stresses are likely to develop, which could lead to tensile cracking and fissure formation if there is an available source of surface water. It is recommended to perform monitoring of surface subsidence, particularly toward the end of identifying locations along the HSR Alignment that exhibit significant convex upward change in curvature. Note that induced upwardly convex change in radius of curvature near Pixley was on the order of 2500 miles. Analysis of historical oil wells bracketing the Pixley Fissure indicates a possibility that this fissure may have developed over an unknown fault or other discontinuity deep in the alluvial basin material, which could have led to concentrated differential strains, as illustrated in Section 8.5.3. This is further discussed in Section 10.2.

7.1.6 Compaction Faulting

According to Holzer, between the 1950s and 1980, the Pond-Poso Fault developed about 10 inches of vertical offset (downward to the southwest), with a maximum rate of about an inch per year, as illustrated in Section 8.5.4. It is thought that it is still moving, but we are not aware of any recent measurements, although the county reports periodically repairing Peterson Road where it crosses the fault. This fault is thought to be related to the Poso Creek Fault, which crosses the HSR Alignment about 5 miles further north. If movement similar to what has been occurring near Pond were to occur near where the Poso Creek Fault crosses the HSR Alignment, it could cause distress to the guideways. This is further discussed in Section 10.2.

7.1.7 Floodplain Changes

It appears that the center of the Corcoran Subsidence Bowl may have already experienced 22 to 26 ft of subsidence over the past 90 years, which, in our opinion, has already altered the flood patterns from the FEMA floodplains which appear to have been developed in the 1980s. Ongoing subsidence will continue to change flood patterns. Based on our calculations, the approximate volume of water that FEMA assumed would collect in the Tulare Lake basin during a 100-year flood is about 1.65 million acre-feet (based on our back-calculation from the FEMA floodplain and the topography in the 1980s (approximate date of original FEMA calculation), which is approximately the same volume USACE assumed for a 100-year flood (based on our

back-calculation from the USACE 100-year floodplain [USACE 2010]). The resulting floodplain limits are shown in Figure 7-1 and discussed in the following text:

1. Based on this volume and the topography of the area from either the 1920s (USGS 1926) or the early 1980s (approximate date of original FEMA calculation), water from a 100-year flood would submerge ground adjacent to the HSR Alignment for a length of about 8 miles, with up to about 1 mile where water is higher than 4'-9" below the Top of Rail.
2. Repeating the same calculation for the calculated 2016 topography, we estimate that water from a 100-year flood would submerge ground adjacent to the HSR Alignment for a length of about 9 miles, with up to about 4 miles where water is higher than 4'-9" below the Top of Rail. A plan and profile of this case are shown in Figures 7-16(c) and 7-17(b), respectively.
3. Repeating the same calculation for Scenarios A through C for a range of calculated 2036 topographies, we estimate that water from a 100-year flood would submerge ground adjacent to the HSR Alignment for a length of about 20 to 22 miles, with up to about 6 to 10 miles where water is higher than 4'-9" below the Top of Rail, and 2 to 5 miles where water would be above the Top of Rail. Plans and profiles of these cases are shown in Figures 7-16(d) through (f), and 7-17(c) through (e), respectively (presented below in Section 7.2.5.3.3).

This is further discussed in Section 7.2.

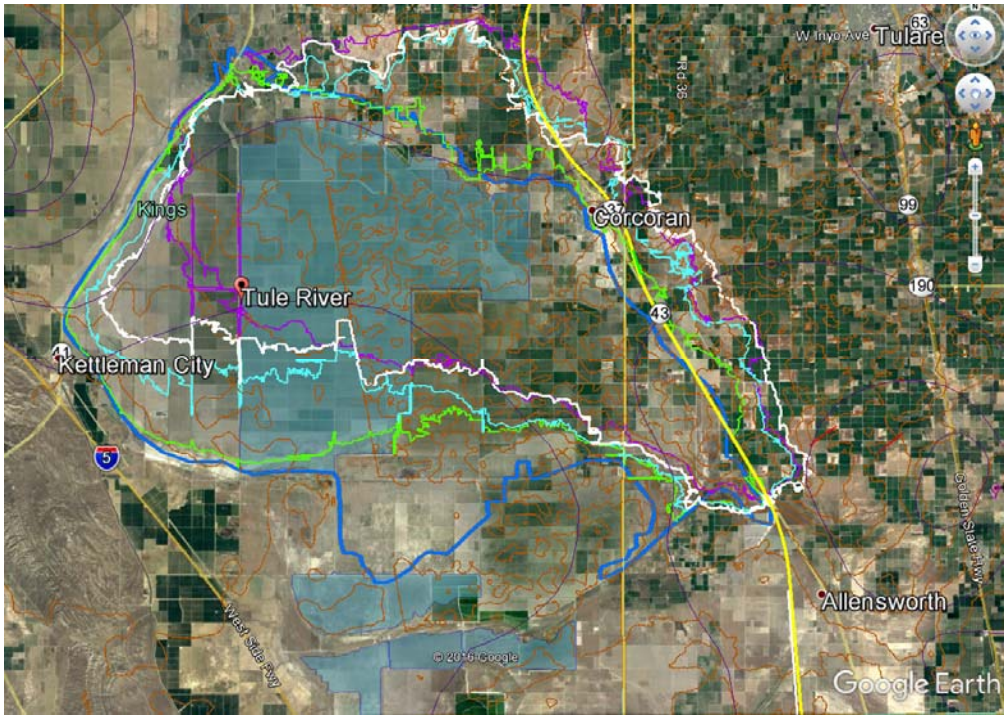

Figure 7-1: Current modeled extent of 100-year floodplains for various scenarios: FEMA in shaded zones; USACE 2009 outlined in royal blue; 2016 scenario in bright green; Scenario 2036a shown in bright blue; Scenario 2036b shown in white; Scenario 2036c shown in purple; HSR Alignment shown in yellow.

7.1.8 Operating Speed

HSR *Design Criteria* limits on-train accelerations induced by track curvature (vertical and horizontal) to 0.05g (where "g" represents the acceleration of gravity). Thus, for a design speed of 250 mph, this corresponds to a maximum curvature of about 1.2E-5 ft^{-1}, or a minimum radius of curvature of 84,000 ft. If combined curvature, including effects of initial design track configuration plus changes in curvature due to subsidence or other factors cause accelerations to exceed 0.05g, the track geometry would need to be realigned or the trains slowed.

Based on current forecasts, we anticipate subsidence could induce changes in acceleration of up to a couple percent g sometime over the next 20 years; anywhere these changes happen to additively correspond with locations of original design curvature, allowable accelerations may be exceeded, and modifications to track geometry or the slowing of trains may become necessary.

Local subsidence anomalies (such as subsidence-induced faults) could result in greater curvatures, but if this occurs, we anticipate it could be mitigated through modest ballast re-leveling.

7.1.9 Site Drainage

Although subtle changes in site gradients may usually have a minimal impact to performance of the HSR primary infrastructure or train performance, it may alter gradients along drainage ditches at the toes of the embankments or elsewhere. The *Design Criteria* requires a minimum longitudinal slope along the toe drainage ditches of 0.5%. Although the anticipated subsidence-induced changes in slope are generally much less than this (e.g., see changes in slope plotted on Plate 1-2), these changes could potentially impact flow gradients, which in turn could increase flow depths adversely. Because the exact locations where such changes may occur are not possible to reliably forecast, we believe it will be most appropriate to address this potential hazard by monitoring and as needed maintenance or mitigation.

Local subsidence anomalies (such as subsidence-induced faults) could impact drainage, but if this occurs, we anticipate it could be mitigated through local maintenance efforts.

7.2 SUBSIDENCE-INDUCED CHANGES TO FLOODPLAINS

7.2.1 Overview

Subsidence has already modified, and will continue to modify, drainage and floodplain patterns to some extent in the vicinity of the HSR Alignment, in a potentially adverse manner with respect to the concerns of the HSR. Areas evaluated for potential floodplain changes within the Corcoran Subsidence Bowl include the FEMA floodplain features along river channels that cross the HSR Alignment in the vicinity of: the Cross Creek crossing near Hanford; the Tule River crossing a short distance south of Corcoran; the Deer Creek crossing about 16 miles south of Corcoran; and the Poso Creek crossing a short distance south of the Kern County line.

In addition, the HSR Alignment passes along the east edge of the historical Tulare Lake, which prior to the late 1800s was the largest body of fresh water west of the Mississippi River. The Tulare Lake flood zone is the topographically lowest region in the hydrologic basin. The limits of the historical Tulare Lake generally roughly coincide with the current FEMA floodplain. However, the areas of greatest and most rapid recent subsidence in the Corcoran Bowl are roughly along the HSR Alignment near the eastern edge of the historical Tulare Lake. As a consequence, the 2009 USACE estimate of the 100-year Tulare Lake floodplain was already shifted to the east of the FEMA outline such that more of the HSR Alignment is within the anticipated floodplain, and ongoing subsidence is expected to continue this trend.

Our initial screening calculations indicated the need for further evaluation of three of the river crossings and the Tulare Lake flood zone that could be impacted by subsidence. FLO2D modeling was performed to assess the flood zones and flood depths in these regions using the three scenarios of forecast 2036 ground surface profiles. This FLO2D modeling indicated that: at the Cross Creek crossing, subsidence would not induce substantial change to the associated floodplain; at the Deer Creek crossing, the flood zone would shift northward toward the Tule River Crossing, and the length of the flood zone along the HSR Alignment would increase; and at the Poso Creek crossing, flood patterns are not expected to be significantly changed by subsidence.

Based on an estimated 100-year flood volume of approximately 1.65 million acre-feet, the FLO2D results indicated that this flood zone would become more oblong in shape, with the lowest region shifting eastward toward the HSR Alignment. This flood zone will merge with the Deer Creek and Tule River flood zones; the resulting flood depth along the HSR Alignment could potentially be more than 16 ft, and the length of the HSR Alignment within the modified flood zone could potentially be more than 20 miles.

The DWR has indicated that a large portion of the water in the Tulare Lake Basin comes from the Kings River; Austin (2012) reported that 49% of the floodwaters in the Tulare Lake Basin during the floods of 1983 came from the Kings River. Some of the water from the Kings River is routed to flow by gravity through a series of canals and sloughs toward the north and into the San Joaquin River drainage, and the remainder is routed through other canals and sloughs toward the south and into the Tulare Lake basin. There is apparently a “pinch point” near Tranquility, with a limit in the flow capacity toward the north. With modifications to these sloughs, canals and appurtenant facilities, and with proper floodwater coordination, most of the Kings River water could be safely routed to flow by gravity to the north. However, there is currently no agency responsible for or with authority to study or implement such a coordination effort, nor is there funding in place for any improvements.

Federal, State, and local flood agencies are aware of the potential issues in the Tulare Lake flood zone. To alleviate the issues, they are considering alternative ways of storing or routing

the drainage to reduce the volume of surface water flow into the historical Tulare Lake flood zone. It is anticipated that these mitigation measures would reduce the flood depth along the HSR Alignment and would decrease the length of the HSR Alignment that might be impacted by flood in this region. We recommend that the Authority lend their support to these efforts.

7.2.2 Hydrology Background

During rain events, surface water runs off along pathways of steepest gradient and accumulates in lowland areas. The depth of surface water flow at a location depends on the slope of the ground surface, ground surface roughness, and drainage discharging flux. Under extreme rainfall conditions in the Corcoran Subsidence Bowl area, the flow depths in some areas and the depths of water accumulation could become excessive, resulting in flooding. The footprints of the floodplains depend on the characteristics of rainfall events, ground surface topography, and land surface roughness. Streams and their overflowing banks primarily dictate the floodplains in the upstream areas along major drainage pathways. Overflowing banks and overland flow control the floodplains towards the downstream areas. The lowland floodplain footprints will follow the topographic contours corresponding to the flood elevation in the water accumulation storage area.

Ground subsidence over time causes progressive changes in ground surface topography. Consequently, the pathways of steepest gradient could change, causing changes in the characteristics of the resulting drainage network. The floodplains in the lowland storage areas could shift. The resulting footprints of the floodplain and flood elevation could change. Overland flow and stream flow are approximately proportional to the square root of the sloping gradient. In areas where the slope is steepened, surficial runoff velocities increase and could increase the chance of erosion. Associated with the increased velocities, floodplain footprints and flood depths generally become smaller. Travel time is shorter along a reach and flow accumulation starts sooner in downstream areas. Conversely, in areas where the slopes become gentler, surficial runoff velocities generally become slower, and floodplain footprints and flood depths generally increase. This could cause flow to back up in upstream areas.

The section of the HSR system covered in the Corcoran Subsidence Bowl passes through the area with the most rapid subsidence. By contract, the design-build contractors (Contractors) need to design the tracks and facilities such that there is at least 2 ft of clearance from the flood level corresponding to the 100-year flood event to the top of the embankment. The HSR system *Design Criteria* in relation to flood and drainage issues are summarized in Section 7.2.3. The Contractors are not responsible for impacts related to subsidence. FEMA flood maps were the basis for the floodplain requirements shown in the bidding documents. Currently, it is uncertain what DEMs FEMA has used to develop their flood zones. The project team has obtained flood zone information from FEMA, including the Hydrologic Engineering Center (HEC)-2 model input file for the Tule River flood plain, but available information has been limited. The HEC-2 file was

generated in 1984. The cross-sectional information in the model files indicates that the elevations were about 12 to 16 ft higher than recent LiDAR elevation data. There has been a concern that the areal extent and possibly the elevation or depth of floodplains could change due to subsidence in the Corcoran Subsidence Bowl, including along or near the HSR Alignment.

The AFW team has performed an evaluation of the potential changes in subsidence since the 1983 floods and the 1984 FEMA floodplain calculations were performed, and that 20 years of ongoing future ground subsidence could have on the areal extent and depth of the 100-year floodplain within the Corcoran Subsidence Bowl. Our evaluation was conducted in two stages. First, a preliminary screening level evaluation was performed by comparing the changes in topographic contours and drainage characteristics to identify if there are areas where floodplain change caused by ground subsidence will potentially have significant impacts on HSR design such that further evaluation would be needed (Section 7.2.4). Subsequently, for these identified areas needing further evaluation, numerical flood modeling was performed to quantify the potential flood zone changes (Section 7.2.5).

7.2.3 California High-Speed Rail System *Design Criteria*

7.2.3.1 General

CP 2-3 is currently the area of most pressing concern regarding subsidence and floodplain changes, because (1) this area is currently in the final design stages, and (2) among the areas of early construction (CP 1, CP 2-3, and CP 4), this is the area with the most rapid subsidence (CP 4 is in the southern edge of the Corcoran Subsidence Bowl where subsidence rates are less than they are a short distance to the north, but floodplain changes were evaluated that included the northern several miles of CP 4).

Floodplain and drainage requirements for CP 2-3 are presented in the *Design Criteria* (California High-Speed Train Project, Agreement No.: HSR 13-57, Design Criteria, Addendum No. 5, Rev. 2, dated October 9, 2014; the requirement for CP 4 are generally the same, so for simplicity, only the CP 2-3 *Design Criteria* are cited). Key elements of the *Design Criteria* state (Section 8.4.6):

> "*The proposed elevation of the track subballast (bottom) shall be a minimum of 2 feet higher than the 100-year Base Flood Elevation. Drainage facilities located within a floodplain shall be designed so that the proposed improvements will not result in the following:*
>
> - *Increase the flood flow rate or inundation hazard to adjacent upstream or downstream property*
> - *Raise the flood level of drainage way*
> - *Reduce the flood storage capacity or obstruct the movement of floodwater within a drainage way*

Refer to the Caltrans HDM General Aspects chapter for FEMA guidelines where encroachment on floodplains is anticipated."

Furthermore, Section 10.9.5.3 of the *Design Criteria* requires:

"*Where an embankment is located in a floodplain, the highest flood water level shall be evaluated from the 100-year flood. The embankment shall be, in addition to the drainage layer arrangement in Section 10.9.5.2, designed to protect the slopes within the highest water level with a layer of drainage layer and protection riprap as depicted on Figure 10-5. The drainage material shall be designed to comply with Sherard's filter criteria (Sherard et al., 1984 a & b). This layer shall extend up to the highest flood water level plus 2 feet and be underlain by a layer of geosynthetic membrane.*"

This required geometry is depicted graphically in Figure 10-5 of the *Design Criteria*.

7.2.3.2 Goals and Objectives

The project "Goals and Objectives" (Section 8.3 of the *Design Criteria*) states:

The following goals and objectives shall be considered in development of drainage design:

- *The CHSTP shall not adversely impact the existing floodplain of the area adjacent to the HST corridor.*
- *Ensure critical HST structures/facilities are protected against 100- and 500-year flood events. Critical HST structures/facilities, in this chapter, refers to HST structures/facilities that are critical to safe operation of HST system, refer to Section 8.6.7.*
- *Comply with regulatory requirements.*
- *Contain drainage within the Authority's right-of-way.*
- *Keep runoff from outside the Authority's right-of-way from entering into the Authority's right-of-way.*
- *To the extent that is reasonable and practical, avoid placement of third-party drainage access points from within the Authority's access controlled right-of-way.*

7.2.3.3 Hydrological Analyses

The "Hydrological Analyses" (*Design Criteria* Section 8.4) states that:

Hydrologic design and analysis shall conform to industry standards, codes, guidelines, and utilize applicable software. The criterion for each factor involved in hydrologic analysis to obtain optimum runoff calculations are outlined in this section. For criteria not included in this section, references shall be used as follows:

- *Caltrans HDM for rainfall hydrological analyses*
- *FHWA HDS-02 for criteria not found in Caltrans and for snowmelt analyses*

7.2.4 Preliminary Drainage Study and Floodplain Screening

We examined the HSR Alignment where it is in general proximity to (1) the areas where the JPL 2007-2010 InSAR and other data (see Section 5.0) shows a significant amount of ground subsidence, and (2) the floodplains delineated on FEMA floodplain map. We identified the following regions where we judged that HSR flooding might be impacted by subsidence such that flood screening should be performed: Cross Creek Crossing, Tule River Crossing, Deer Creek Crossing, Poso Creek Crossing, and Historical Tulare Lake (Figure 7-2).

We applied the ArcHydro package on the Esri ArcGIS platform to delineate the predominant drainage network in these areas using two DEMs that represent the recent and future ground surface topography. For this screening study, we used the 2013 DEM and downloaded from the USGS website (USGS DEM).[8] We approximated the ground subsidence in the next 20 years as six times the subsidence observed by the JPL between July 2007 and December 2010 (referred to as the JPL 2007-2010 subsidence). We considered the future DEM as computed by subtracting six times the JPL 2007-2010 subsidence from the USGS DEM.

The changes in major drainage pathways in each area were examined to evaluate the potential of changing flood zone locations or patterns. The topographic elevation contours were used to estimate the potential changes in vertical slopes along major drainage pathways and the resulting potential changes in surface water flux. The results of the preliminary screening evaluation for each area are summarized below:

- Cross Creek Crossing – The observed subsidence in the upstream area of the floodplain is small. Surface water generally flows toward the HSR Alignment downgradient of the floodplain in this area. The observed subsidence increases toward the downgradient area and the HSR Alignment. A significant amount of subsidence was observed in an area south of the FEMA floodplain and east of the HSR Alignment. The future topographic contours are more closely spaced in the upgradient drainage area, indicating an increase in slope and faster flow. The topographic slope in the upgradient area will increase by approximately 15 percent[9]. The resulting future discharge will be approximately 8% higher than the current discharge. In the downgradient area near the HSR Alignment, the change in slope is small and the subsidence is fairly uniform in this local area. It is anticipated that the future drainage flood depth caused by ground subsidence at the HSR Alignment in this area overall might not change significantly. There is an area south of the Cross Creek crossing where larger subsidence was reported by JPL. The ground subsidence might cause floodwater to flow toward this area and the water accumulation might potentially impact the HSR system. Further flood

[8] At the time of this early screening study, it was assumed that the USGS DEM would be representative of the relatively-recent ground surface topography. Since then, we have discovered that the elevations in this area have not been updated since the 1928 Corcoran Quad sheet (USGS 1928), which was based on 1926 field data. However, for screening purposes, this older data is considered adequate.

[9] In this discussion, the percent change refers to a percent of the pre-subsidence slope. For example, if an initial slope is 1%, and it steepens to 1.1%, this would be described herein as a 10% increase, because 1.1 is 10% greater than 1%.

analysis would be needed to evaluate the potential local changes in flood flow and its impacts.

- Tule River Crossing – The observed subsidence in the upstream area of the floodplain is small. Surface water generally flows toward the HSR Alignment downgradient of the floodplain in this area. The observed subsidence increases slightly toward the downgradient area and the HSR Alignment. The spacings of the current and future topographic contours are similar. The slope in the upgradient area will increase by approximately 12%. The resulting future discharge will be approximately 6% higher than the current discharge. In the downgradient area near the HSR Alignment, the change in slope is small. The subsidence is fairly uniform in this local area. It is anticipated that the future drainage flood depth caused by ground subsidence at the HSR Alignment in Area B overall might not change significantly.
- Deer Creek Crossing – The observed subsidence in the upstream area of the floodplain is small. Surface water generally flows toward Highway 99 downgradient of the floodplain in this area. Floodwater accumulates along Highway 99. The floodplain extends along northwest direction. The observed subsidence increases slightly toward the downgradient area and the HSR Alignment. The slopes increase in the upgradient area and decreases in the downgradient area. It indicates that the slopes in the upgradient area will increase by approximately 12%. The resulting future discharge rates will be approximately 6% higher than the current discharge rates. Similarly, the slope in the downgradient area will decrease by approximately 12%. The future discharge in the downgradient area will be approximately 6% lower than the current discharge. The topography downgradient is flat and drainage characteristics are sensitive to the subsidence profile. The ground subsidence might cause floodwater to flow northwest toward the Tule River Crossing along the HSR Alignment. In addition, this area is in close proximity to the Tulare Lake flood zone. The flood zones in this area will potentially be comingled in the future in close proximity to the HSR Alignment. Further flood analysis would be needed to evaluate the potential local changes in flood flow and its impacts.
- Poso Creek Crossing – No major changes in drainage paths and topographic slopes are observed, indicating that the associated floodplains will not be impacted by ground subsidence.
- Historical Tulare Lake – A significant amount of ground subsidence has occurred on the east side of the floodplain. The topographic contours and drainage networks indicate a change in storage profile in this area and a general spatial shift of the storage toward the downgradient area of the floodplains of Tule River Crossing and Deer Creek Crossing in the vicinity of the HSR Alignment. We estimated the future flood elevation and footprint of the future floodplain based on the future DEM and the resulting topographic contours. The results indicate that the future flood zones of the Tulare Lake, Tule River, and Cross Creek will potentially be comingled. Further detailed drainage analyses were performed.

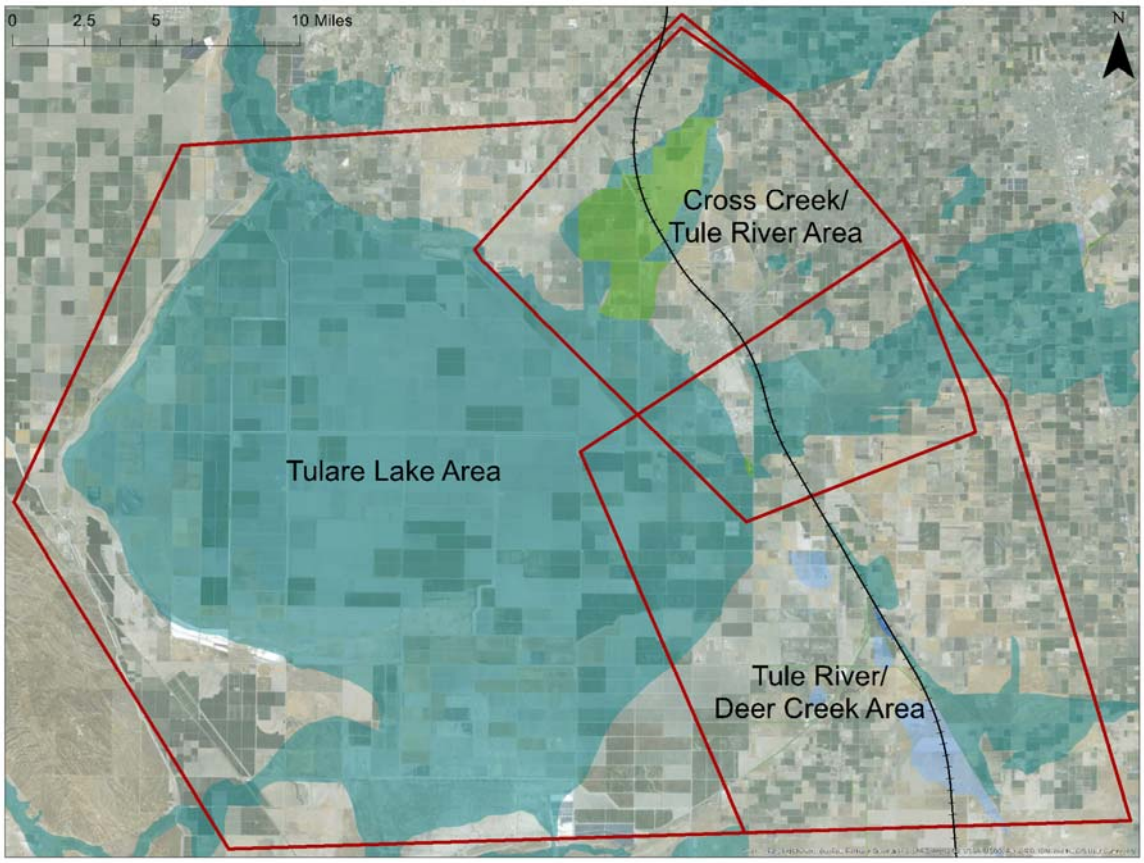

(a) FEMA flood zones associated with historical Tulare Lake, Cross Creek Crossing, Tule River Crossing, and Deer Creek Crossing

(b) Poso Creek Crossing

Figure 7-2: Flood zones evaluated

In summary, the results of the preliminary screening evaluation suggest that subsidence-induced floodplain changes are not likely to have significant impacts on the majority of the HSR Alignment. However, the AFW team identified two areas where the HSR might potentially be impacted, and more detailed flood analyses were performed. One is associated with localized subsidence observed near the floodplain for Cross Creek Crossing. The other is associated with the downgradient floodplain for the Deer Creek and potential co-mingling of the eastern portion of the Tulare Lake flood zone, the Tule River Crossing flood zone, and the Deer Creek Crossing flood zone.

7.2.5 Detailed Floodplains and Surface Drainage Study

The AFW team has performed detailed flood zone modeling using the commonly used commercial software FLO2D for the areas identified by the preliminary screening evaluation. Three models, referred to as the North Model, South Model, and Lake Model, as shown in Figure 7-2, were constructed. The North Model has a spatial resolution of 100 ft and was intended to capture the drainage flow in the flood zone of the Cross Creek Crossing for evaluating the potential impacts of the locally large subsidence observed by JPL south of the Crossing. The South Model has a spatial resolution of 100 ft and was intended to capture the drainage flow in the flood zone of the Deer Creek Crossing for evaluating the potential of flood zone shifting toward to the Tule River Crossing. The Lake Model has a spatial resolution of 200 ft and was intended to capture the retention storage of the Tulare Lake floodplain for evaluating the potential of co-mingling of the flood zones of Tulare Lake, Deer Creek Crossing, and Tule River Crossing. Three scenarios of future subsidence (Scenarios A, B, and C, as introduced in Section 6.2) were considered and each model was run for the three resulting scenarios of 2036 DEM. The three scenarios of 2036 DEM were constructed by subtracting the predicted future 20-year subsidence from the 2016 DEM. Section 7.2.5.1 presents the development of the three scenarios of the 2016 DEM, including a discussion on the USGS DEM data issues discovered during the course of the analysis. Section 7.2.5.2 presents the development of the 2036 DEM. Section 7.2.5.3 presents the models and the evaluation results.

7.2.5.1 Construction of 2016 DEM

During the course of the analyses, the AFW team discovered that the 2013 USGS DEM based on the 2009 National Elevation Dataset) appears to represent the 1920s ground surface topography and has not been substantially updated since then. LiDAR was used in 2015 to obtain elevation information within a band along the CP 2-3 HSR Alignment (referred to as 2015 LiDAR data). It was noticed that the USGS DEM is approximately 22 to 26 ft higher than the 2015 LiDAR data in portions of the model area that are near the center of the Corcoran

Subsidence Bowl. Available information from USGS indicated that various portions of the USGS DEM were compiled or constructed during a period ranging between 1999 and 2009. However, upon further investigation, additional information found suggests that the USGS DEM was based on USGS quad maps developed between 1946 and 1962, instead of the period between 1999 and 2009. Further details of these quad maps suggest that they were likely based on field information developed in the 1920s. We therefore refer to this DEM as the USGS 1926 DEM. A portion of this DEM is coarsely depicted in Figure 7-3a. The USGS has published the historical subsidence information for the period between 1926 and 1970 (referred to herein as 1900s Historical Subsidence) (Figure 7-3b). This Historical Subsidence was subtracted from the USGS 1926 DEM to create a DEM representative of the 1970 ground surface topography (referred to as the 1970 DEM).

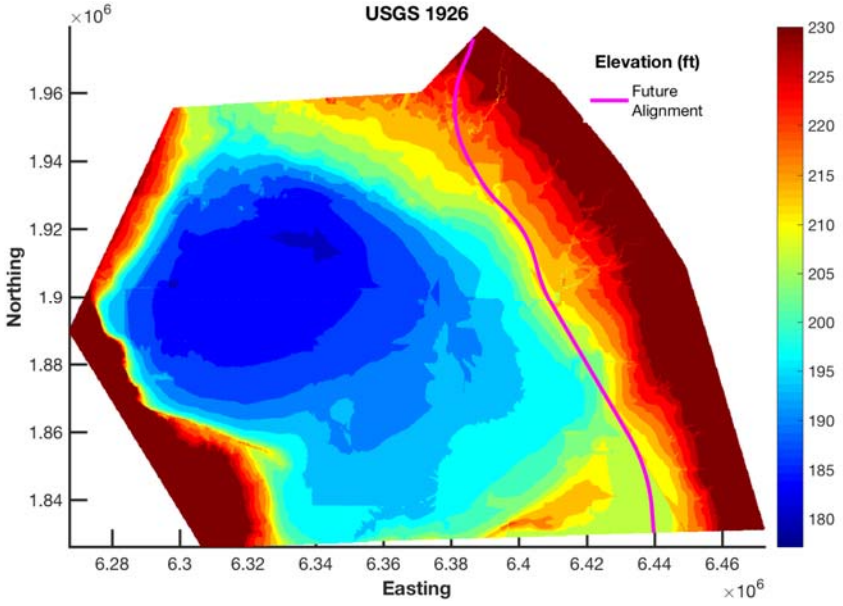

Figure 7-3a: 1926 Elevation data, provided by USGS

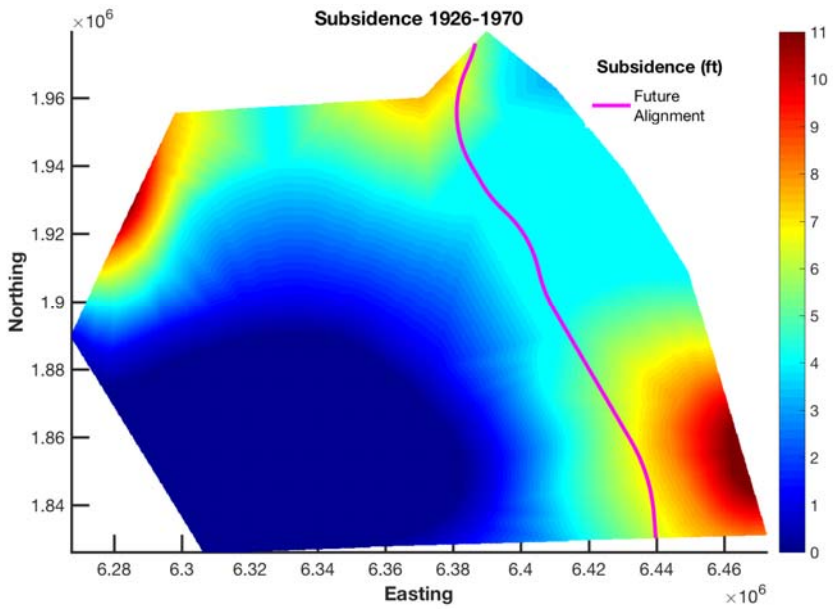

Figure 7-3b: Subsidence from 1926 to 1970, estimated

Figure 7-3: 1926 Elevation data and Subsidence from 1926 to 1970, estimated

A survey of the area of interest based on satellite IFSAR was conducted in 2004. However, data had insufficient resolution and poor quality and therefore was only used in this study where LiDAR topography was not available.

In July 2008, an airborne LiDAR (light detection and ranging) survey was conducted by Towill Inc. for hydrologic studies of the floodplain below Lake Success Dam. The elevations are coarsely depicted in Figure 7-4.

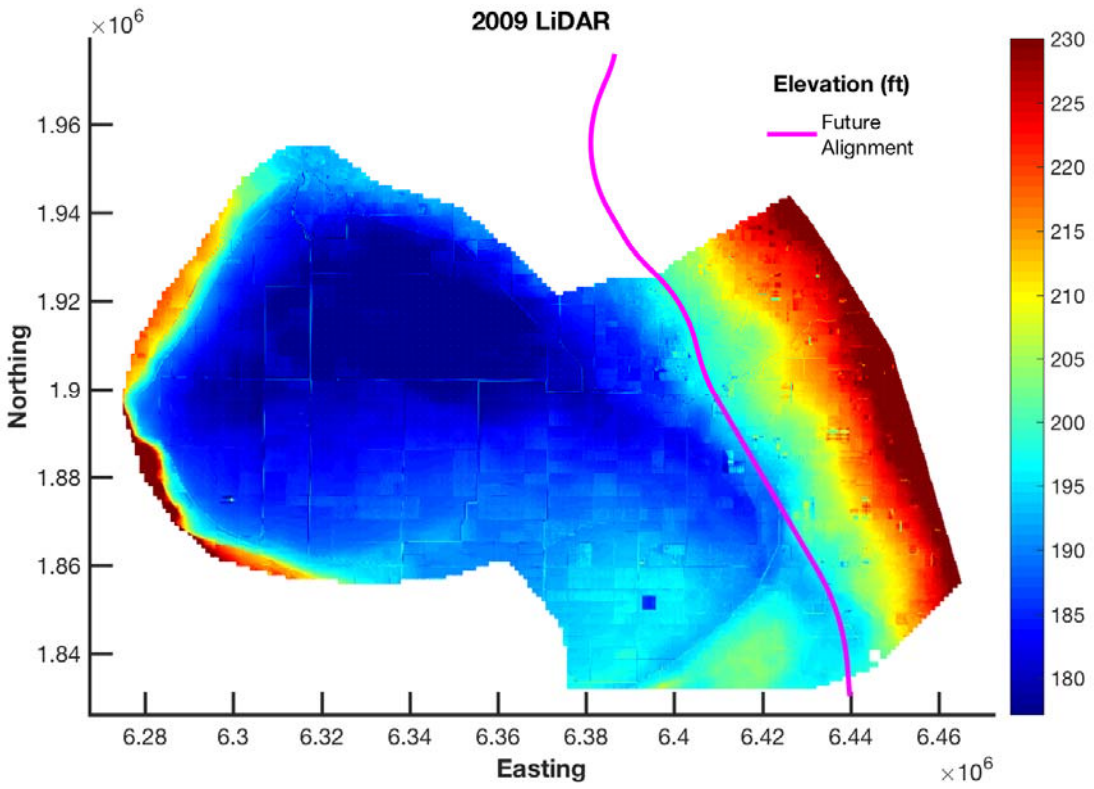

Figure 7-4: 2008 Elevation data (LiDAR)

In October 2015, an airborne LiDAR survey along section CP 2-3 was conducted by Towill Inc. for the California High-Speed Rail Authority. The elevations are coarsely depicted in Figure 7-5.

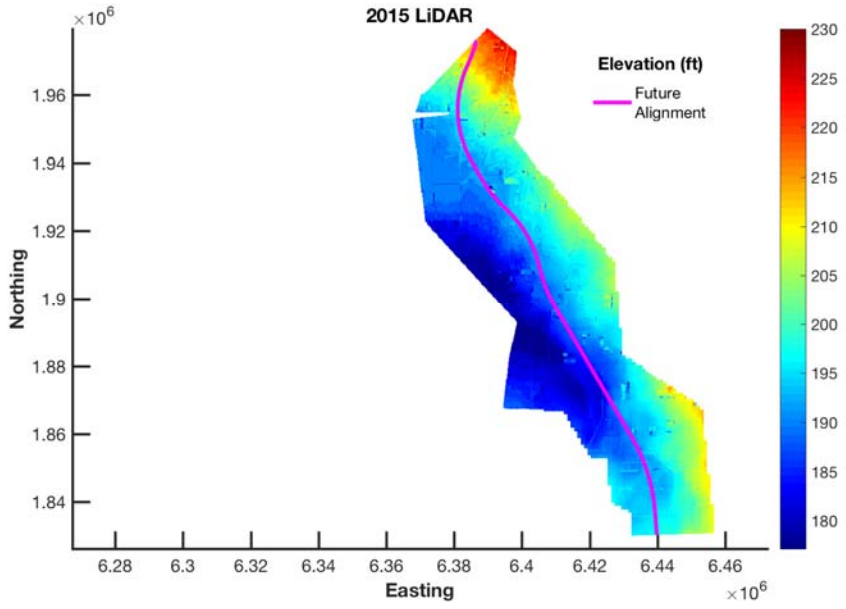

Figure 7-5: 2015 Elevation data along CP 2-3 (LiDAR)

The most recent elevation data originates from global positioning system (GPS) data enhanced with an RTK Global Positioning System (GPS) survey. This RTK survey was performed by AFW in August and December 2016. The RTK GPS device was mounted on a vehicle to allow quick data collection of a large area. The elevation data are plotted in Figure 7-6.

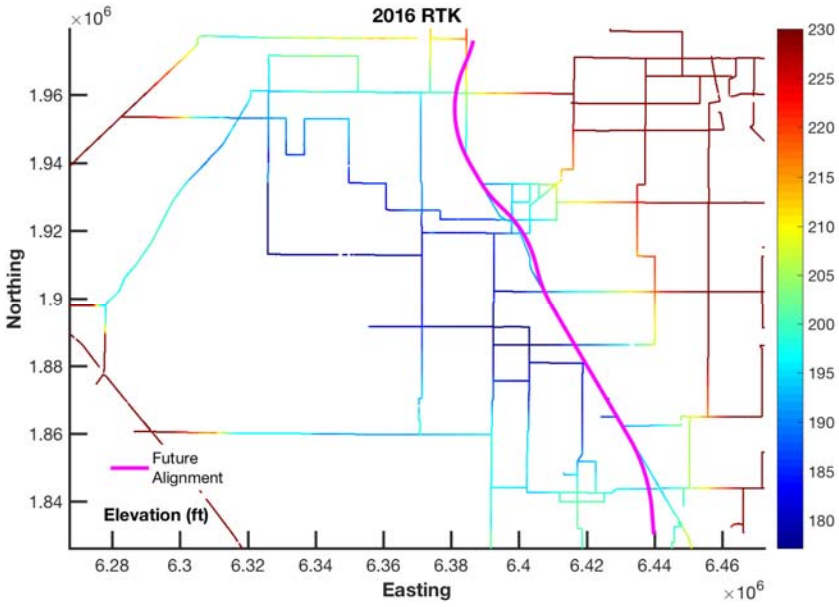

Figure 7-6: 2016 Elevation data (RTK)

NASA's JPL evaluated the subsidence in the SJV using satellite-based InSAR data gathered between June 2007 and December 2010. The subsidence, ranging up to about 3 ft, is depicted in Figure 7-7.

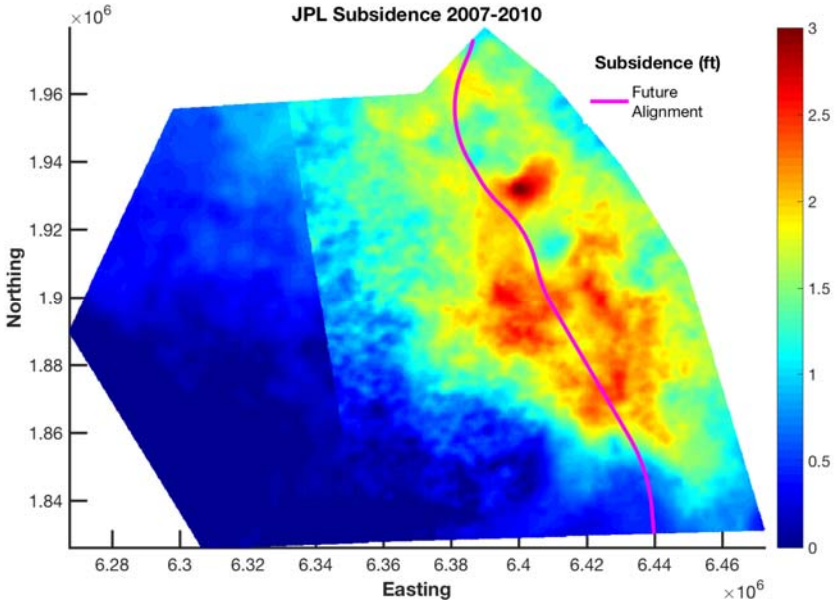

Figure 7-7: Subsidence from 2007 to 2010 (Farr el al., 2015)

The 2016 RTK data, 2015 LiDAR DEM, 2008 LiDAR DEM, 1926 USGS DEM, 2007-2010 JPL subsidence data, and USGS 1926-1970 subsidence data were integrated using statistical methods to create an estimated 2016 DEM (Figure 7-8).

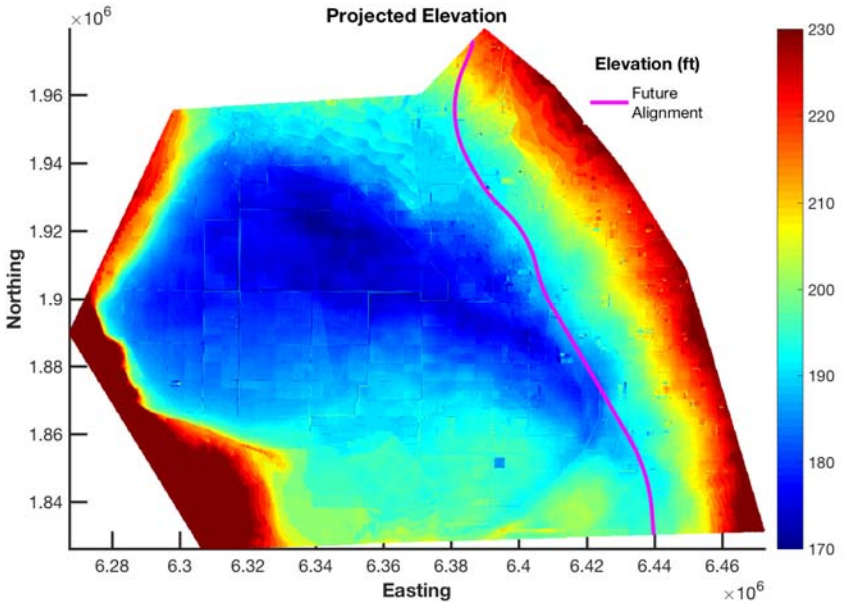

Figure 7-8: Estimated 2016 DEM

7.2.5.2 Construction of 2036 DEMs

Three subsidence scenarios were considered based on extrapolations of various recent observation data looking forward for the period of 2016 to 2036. The subsidence rate has been observed to be accelerating in the past 10 years.

7.2.5.2.1 Scenario A

For Scenario A, the 20-year subsidence was calculated based on the average annual subsidence rate from the 2007-2010 JPL InSAR data. It represents a period of less severe subsidence from the beginning of the past 10 years. The estimated 2016 DEM was lowered or "subsided" by an amount equal to the JPL 2007 to 2010 subsidence multiplied by a factor of 5.67 to extrapolate out for 20 years. The result from this projection method is plotted in Figure 7-9.

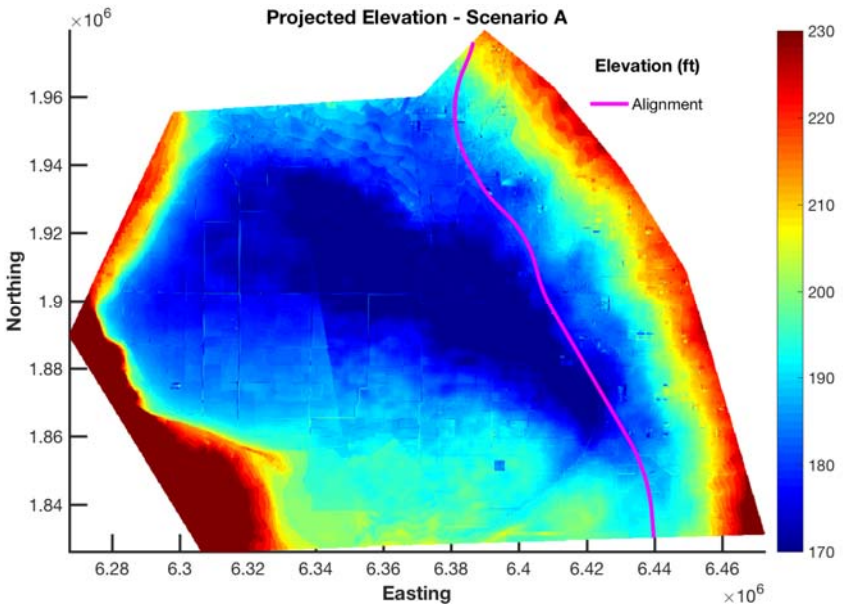

Figure 7-9: Projected 2036 Elevation based on 2007-2010 JPL subsidence (Scenario A)

7.2.5.2.2 Scenario B

For scenario B, the 20-year subsidence was calculated based on the average subsidence rate computed from the estimated changes in topographic surfaces between 2008 and 2016, which represents an average condition in the past approximately 8 years. The 2008 DEM was generated in a similar statistical approach as the 2016 DEM by integrating the available topographic and subsidence information. The estimated 2016 DEM was then lowered or "subsided" by an amount equal to the approximately 8-year subsidence between the generated 2008 and 2016 multiplied by 2.47 to extrapolate out for 20 years. Figure 7-10 shows the 2008 DEM, and Figure 7-11 shows the 2036 DEM for Scenario B.

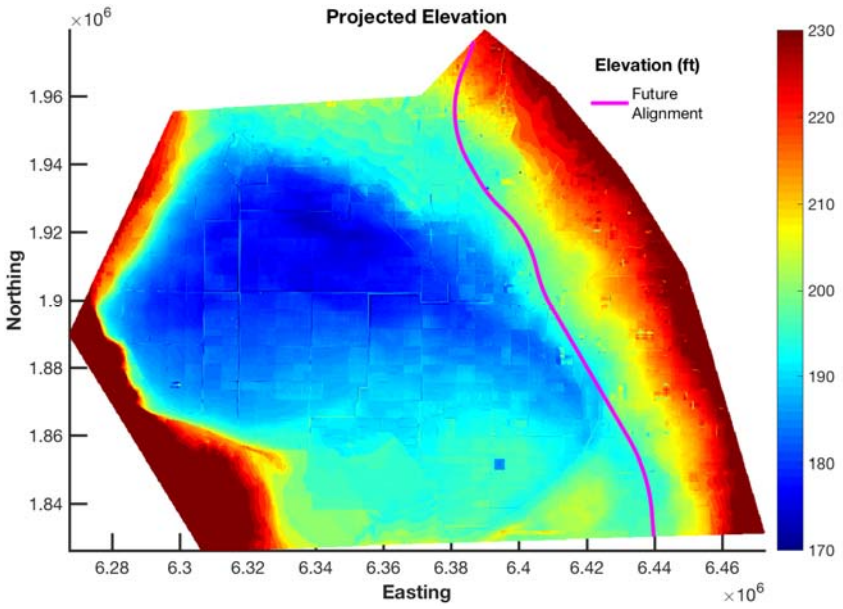

Figure 7-10: Estimated 2008 DEM

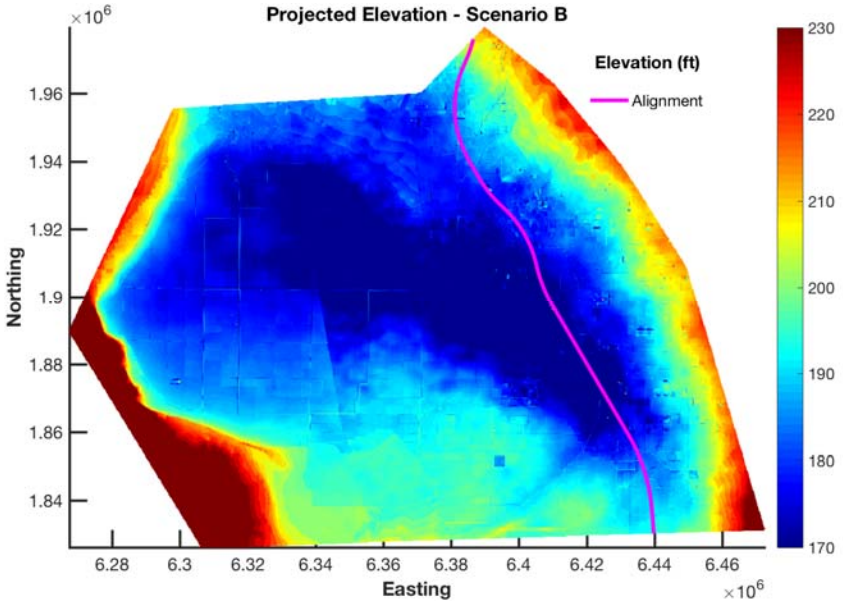

Figure 7-11: Projected 2036 Elevation based on 2008-2016 subsidence (Scenario B)

7.2.5.2.3 Scenario C

Scenario C was based on the annual subsidence rate calculated from May 7, 2015, to May 21, 2016 subsidence data provided by JPL. It represents a period of faster subsidence because this period was toward the end of a severe drought. This approximately 1.04-year subsidence was multiplied by a factor of 19 to extrapolate out for 20 years. Figure 7-12 shows the 2015-2016 JPL subsidence data. Figure 7-13 shows the resulting 2036 DEM (Scenario C)

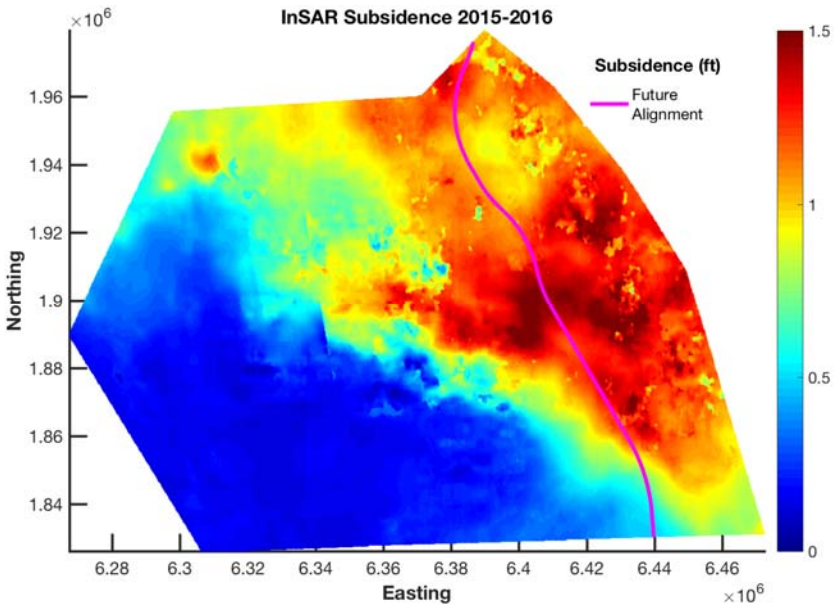

Figure 7-12: Subsidence from 2015 to 2016 (Farr el al., 2017)

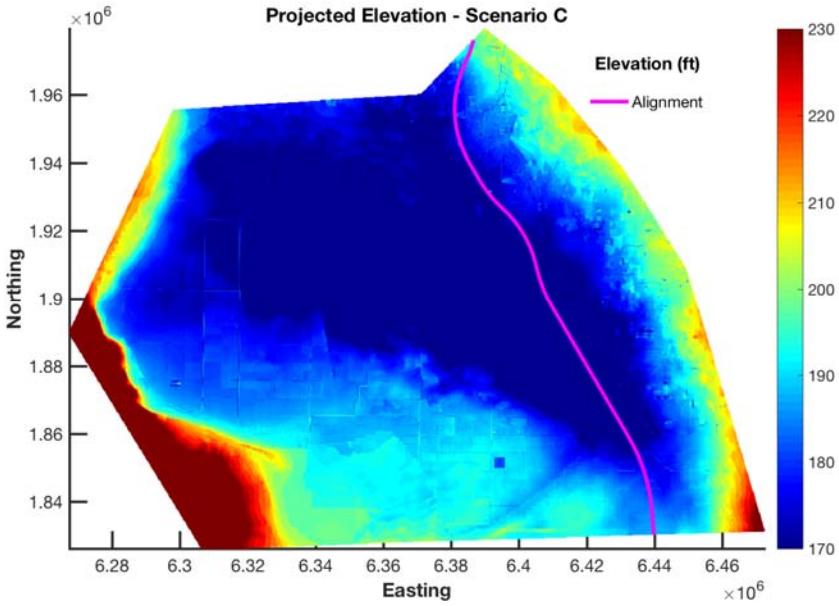

Figure 7-13: Projected 2036 Elevation based on 2015-2016 JPL subsidence (Scenario C)

7.2.5.3 FLO2D Modeling

The models simulate a 100-year storm lasting 72 hours (3 days) while the total simulation time is 108 hours (4.5 days). The inflows are based on the FEMA Flood Insurance Study. The model was run for each of the DEMs generated for the 2036 elevation scenarios, while the parameters (inflows, outflows, etc.) remained unchanged. For the Lake Model, an initial storage volume was

specified such that the total volume of water stored in the Tulare Lake flood zone at the end of the simulation is approximately 1.65 million acre-feet. (This value of 1.65 million acre-feet was estimated based on calculating the pond volume for the FEMA Tulare Lake footprint based on the 1980s topographic surface that FEMA used in their floodplain calculation, and calculating the pond volume for the USACEs Tulare Lake 100-year flood footprint based on the 2009 topographic surface that they used in their floodplain calculation; both methods gave very similar numbers.)

- Cross Creek: 19,200 cfs (17,681 cfs in model)
- Tule River: 20,500 cfs (19,838 cfs in model)
- Deer Creek: 3,470 cfs (6,069 cfs in model)
- Close to HSR Alignment: 2,500 cfs (8,095 cfs in model)
- 7627 cfs for 100Yr flood at Success Dam. At upstream boundary, model inflow is 20,500 cfs.
- Tule River peak flow at HSR Alignment 2,500 cfs

7.2.5.3.1 North Model

The water depth is defined as the forecast water elevation minus the forecast ground elevation before project grading activities. The maximum water depths throughout the modeling period are shown on Figures 7-14a through 7-14f for all DEM scenarios. The water depth at the Cross Creek Crossing appears to decrease from 4 ft to around 3 ft between 2008 and 2036. At the Tule River crossing, the water depth appears to increase from around 3 ft to around 4 ft for Scenario B. It is not expected to change significantly for Scenarios A and C as the location of the maximum water depths relative to the HSR Alignment do not change substantially.

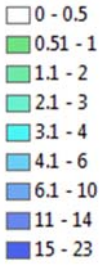

Figure 7-14 (a): Water Depth legend (ft)

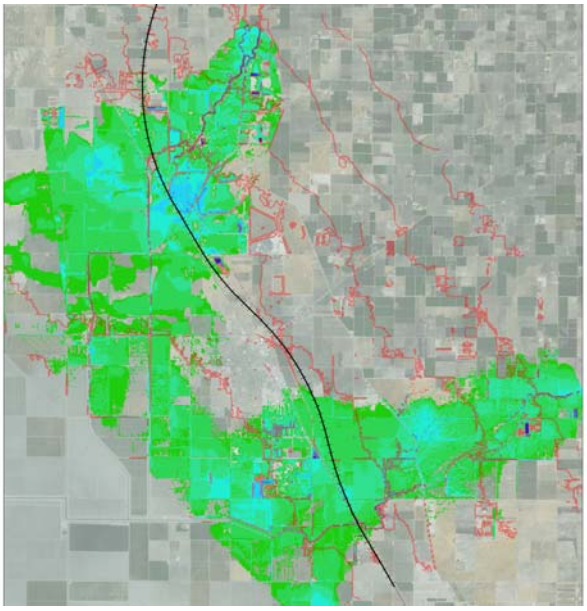

Figure 7-14 (b): 2008

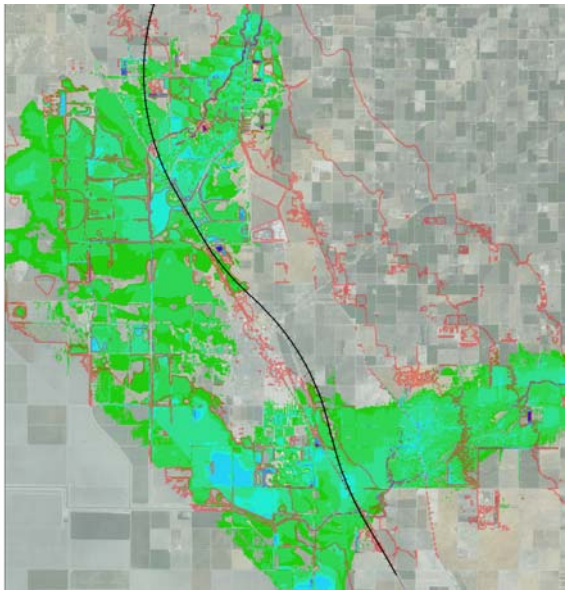

Figure 7-14 (c): 2016

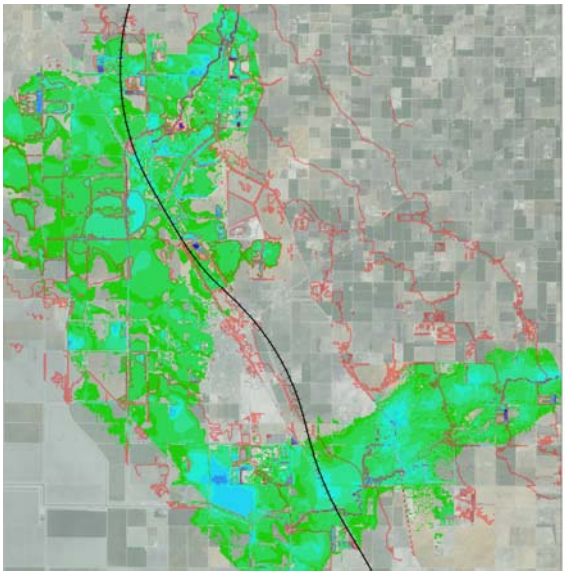

Figure 7-14 (d): 2036 Scenario A

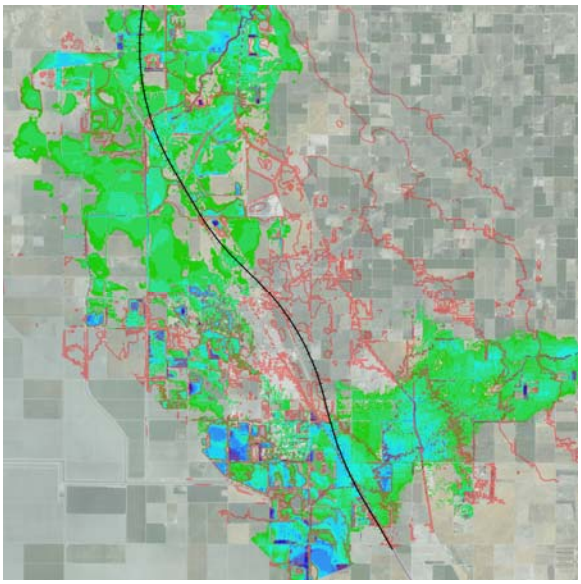

Figure 7-14 (e): 2036 Scenario B

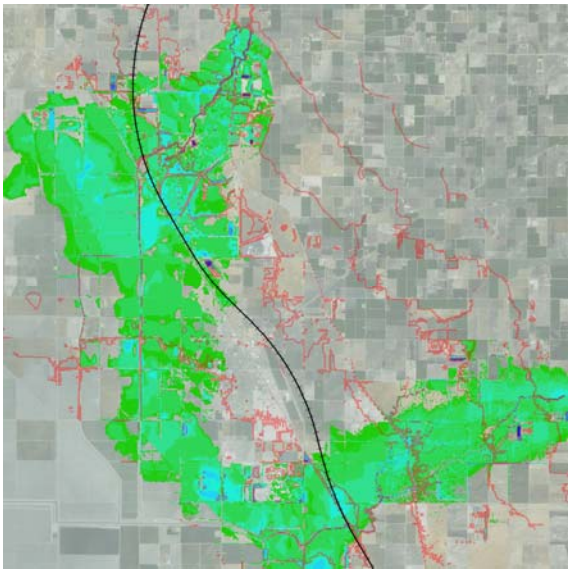

Figure 7-14 (f): 2036 Scenario C

Figure 7-14. Maximum water depth for 100-year flood and topographic contours close to HSR Alignment, North Model

7.2.5.3.2 South Model

The maximum water depths during the modeled 100-year storm for the different times and future scenarios are shown on Figures 7-15a through 7-15f. The flood zone at the Deer Creek Crossing clearly moves north over time and the floodplain shape elongates along the HSR Alignment. The maximum depth remains constant at about 3 ft.

Figure 7-15 (a): Water Depth legend (ft)

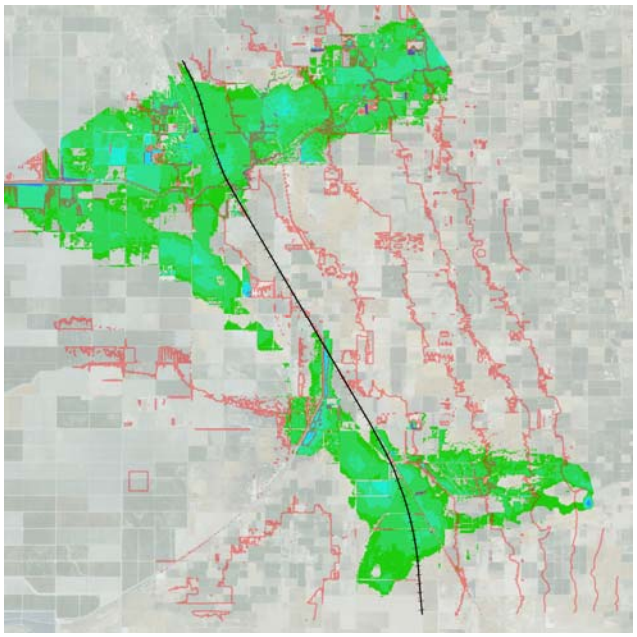

Figure 7-15 (b): 2008

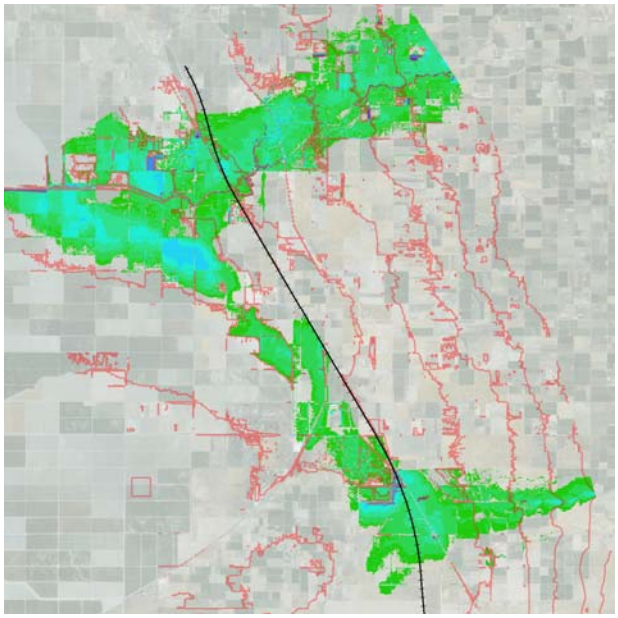

Figure 7-15 (c): 2016

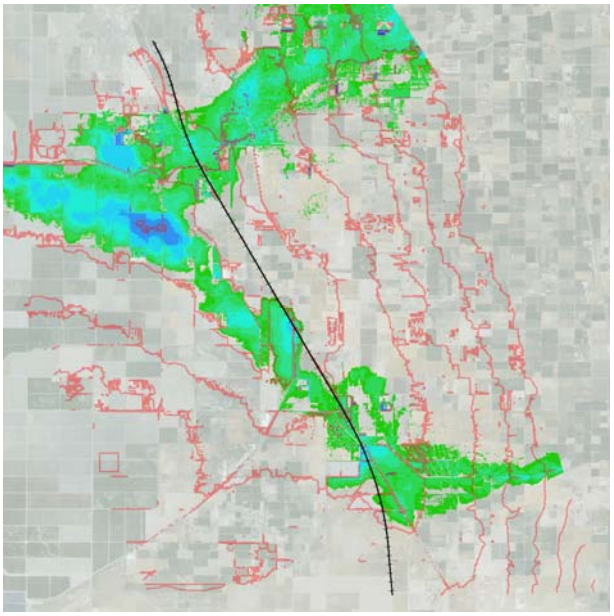

Figure 7-15 (d): 2036 (Scenario A)

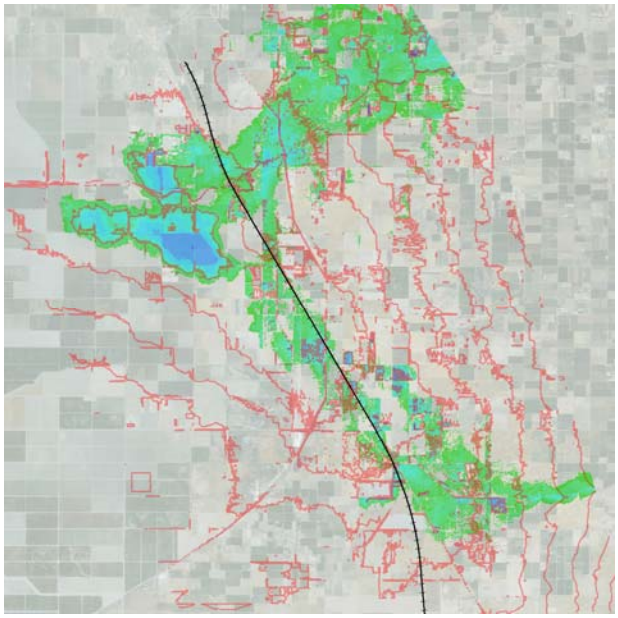

Figure 7-15 (e): 2036 scenario B

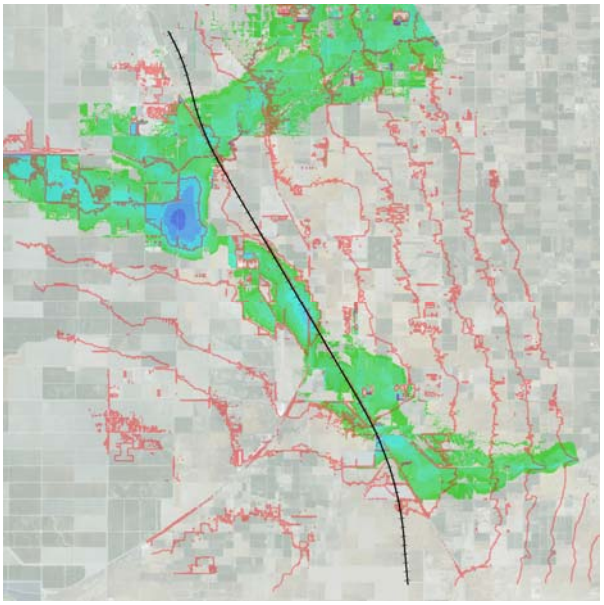

Figure 7-15 (f): 2036 Scenario C

Figure 7-15. Maximum water depth for 100-year flood and topographic contours close to HSR Alignment, South Model

7.2.5.3.3 Lake Model

Because subsidence is greater near the eastern side of the Tulare Lake flood zone, the lakebed is progressively tilting toward the east, (toward the HSR Alignment). This changes the shape of the flooded area from oval to more elongated, as the maximum water depth from the flood simulations show in Figure 7-16 (a through f). Profiles taken along the HSR Alignment (Figure 7-17 (a through e) show that between 2008 and 2036; the depth of water above the ground surface along the HSR Alignment increases through the years for both the maximum and final (post-storm steady state) stormwater elevation, and the affected length along the HSR also increases. By 2036, the maximum depth for the 100-year flood is forecast to be 16 ft, 20 ft, and 17 ft for Scenarios A, B, and C, respectively. The flood elevations at the end of the model simulations were determined, based on the approximate total stormwater volume in the historical Tulare Lake of 1.65 million acre-feet. They are shown in Figure 7-18.

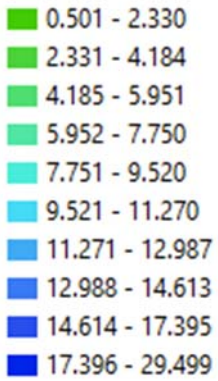

Figure 7-16 (a): Water Depth Legend (ft)

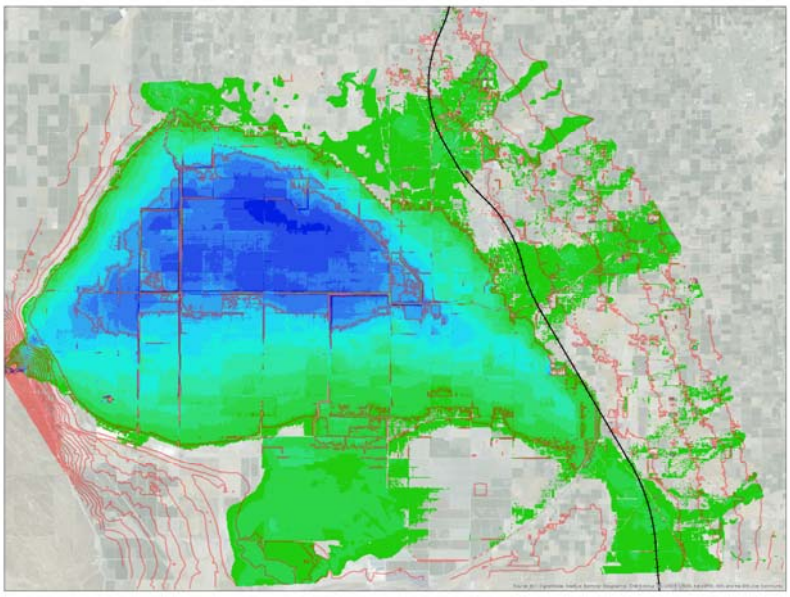

Figure 7-16 (b): 2008

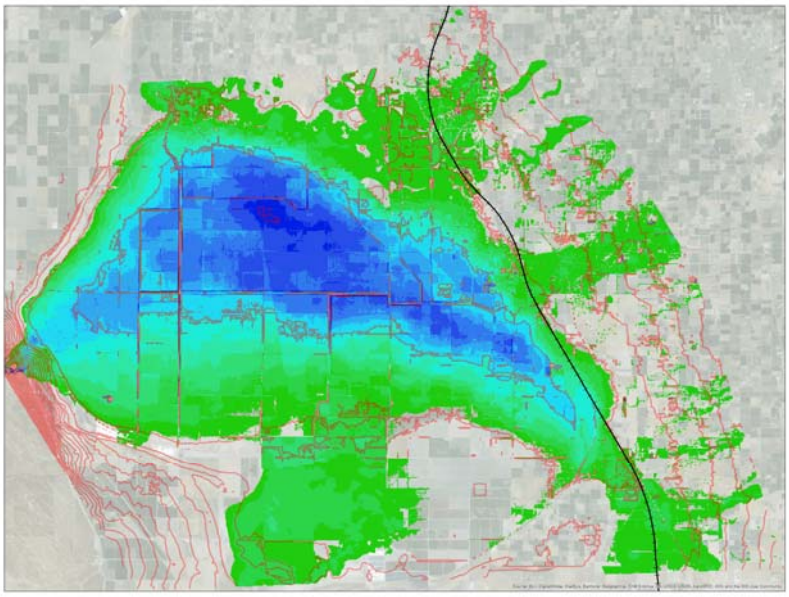

Figure 7-16 (c): 2016

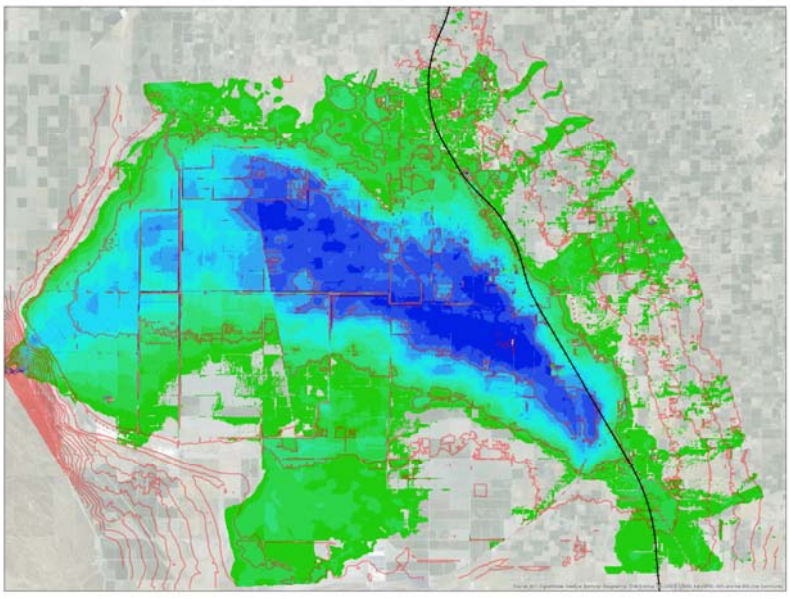

Figure 7-16 (d): 2036 Scenario A

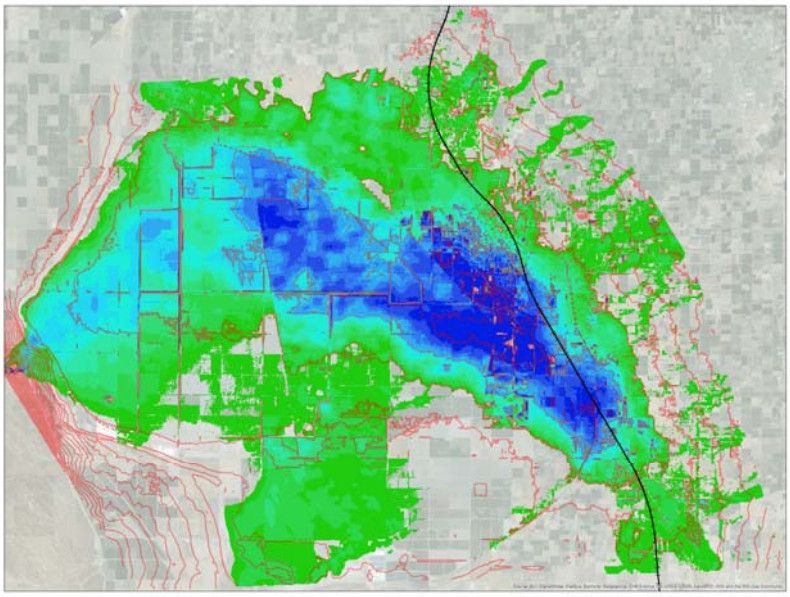

Figure 7-16 (e): 2036 Scenario B

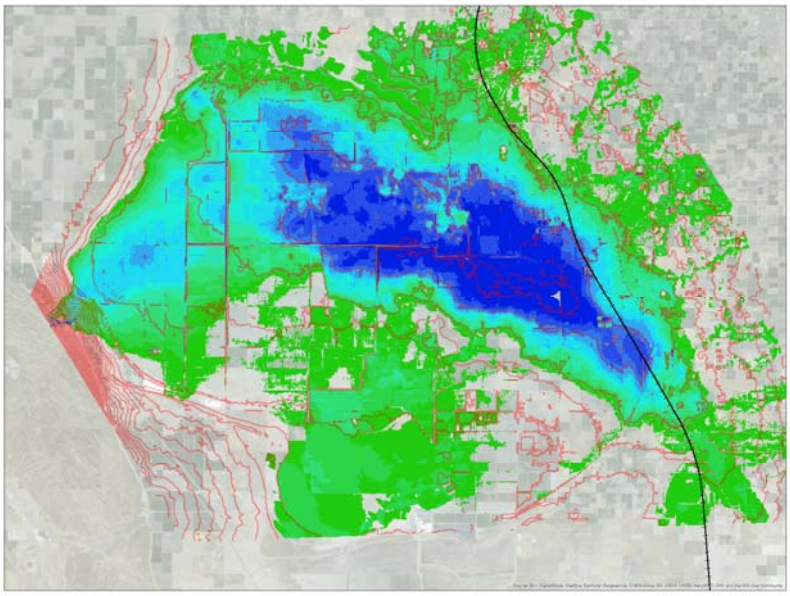

Figure 7-16 (f): 2036 Scenario C

Figure 7-16. Maximum water depth for 100-year flood and topographic contours close to HSR Alignment, Lake Model

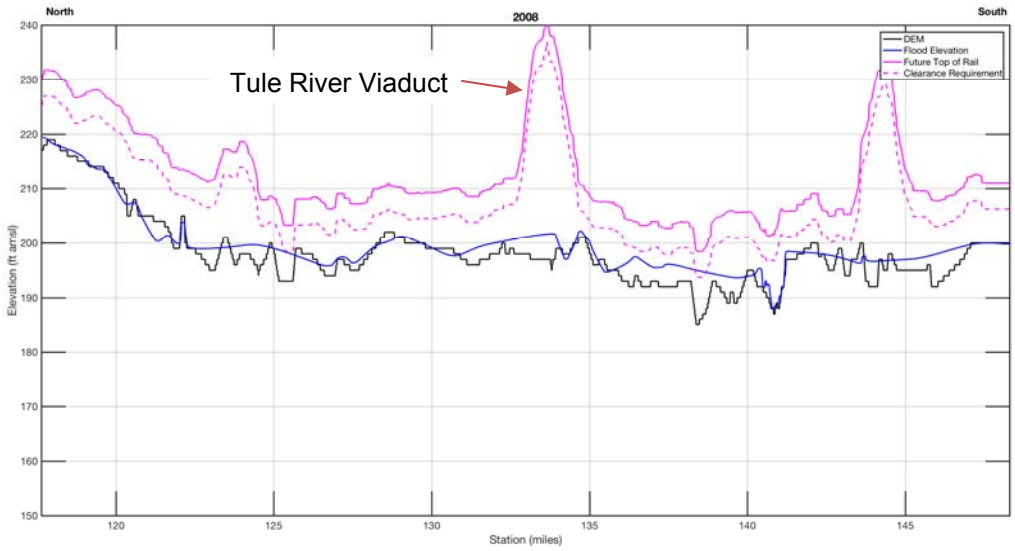

Figure 7-17(a): Tulare Lake Model 2008 along HSR Alignment. The DEM line is the modeled subsided ground surface.

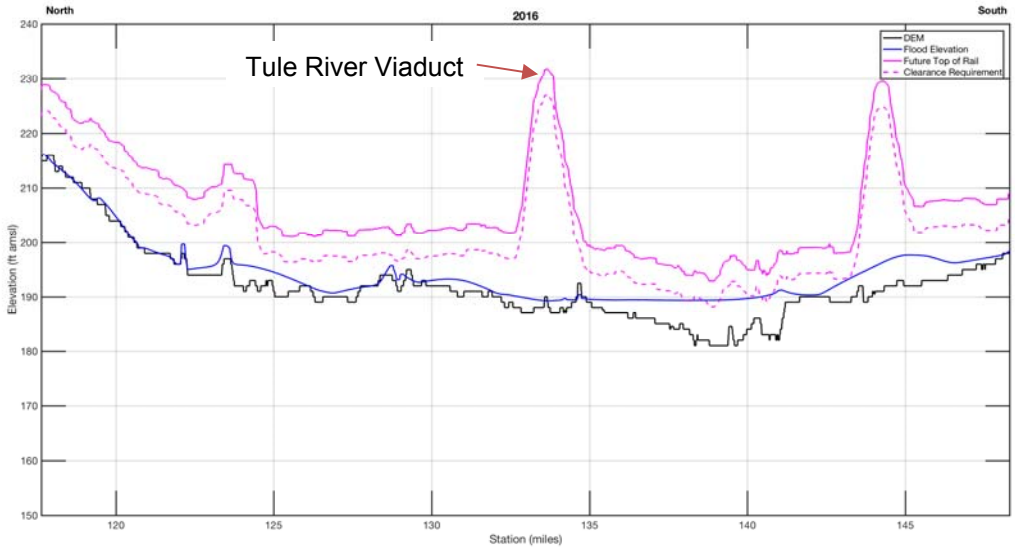

Figure 7-17(b): Tulare Lake Model 2016 along HSR Alignment. The DEM line is the modeled subsided ground surface.

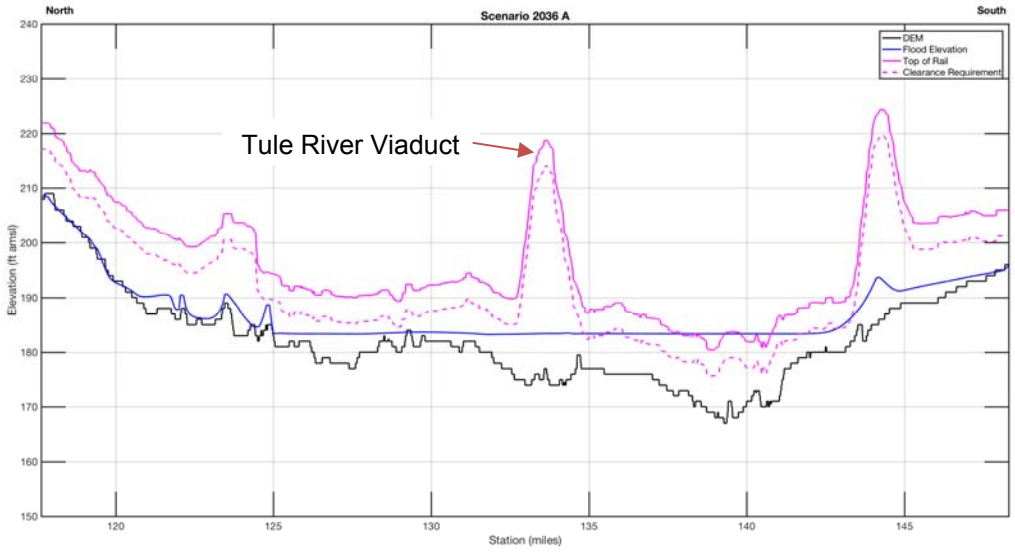

Figure 7-17(c): Tulare Lake Model 2036 Scenario A along HSR Alignment. The DEM line is the modeled subsided ground surface.

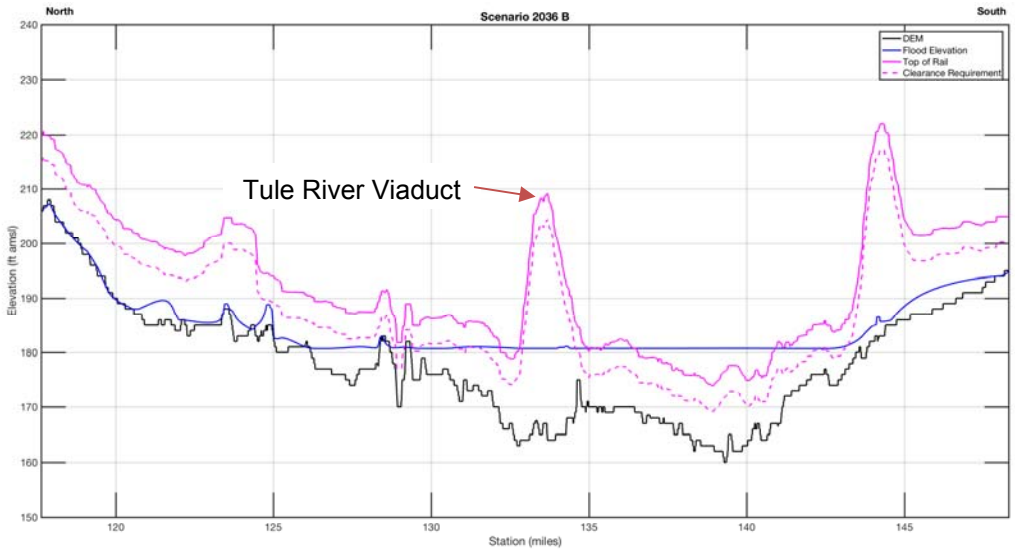

Figure 7-17(d): Tulare Lake Model 2036 Scenario B along HSR Alignment. The DEM line is the modeled subsided ground surface.

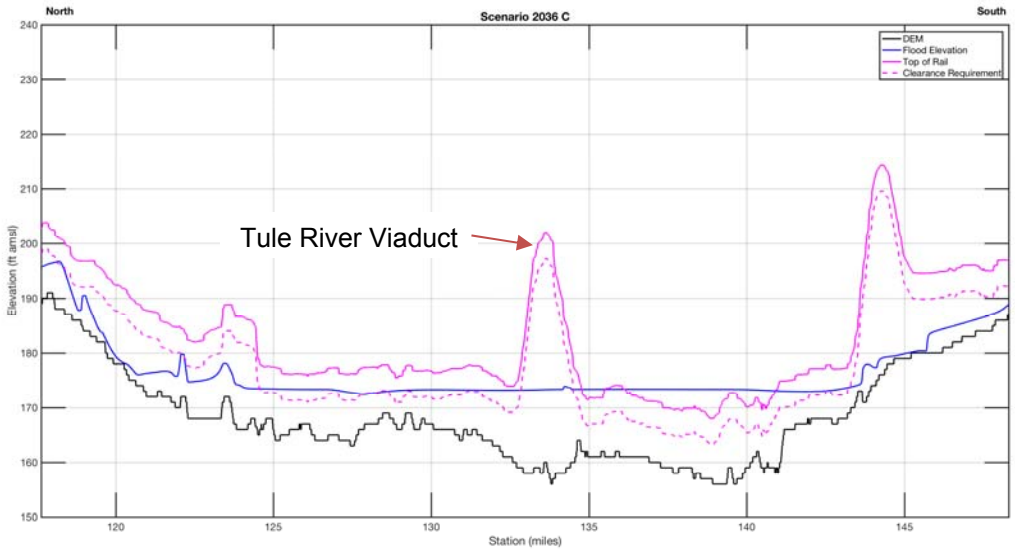

Figure 7-17(e): Tulare Lake Model 2036 Scenario C along HSR Alignment. The DEM line is the modeled subsided ground surface.

Figure 7-17. Ground surface and flood elevation profiles along HSR Alignment in the Tulare Lake area

Because the flood elevation is almost a level surface within the Tulare Lake flood zone (with a slight gradient downward from areas of inflow), the Tulare Lake flood elevations (shown in Table 7-1) are dictated primarily by the volume of floodwater entering the flood zone. Figure 7-18 shows the curves relating the flood elevation and flood volume for the evaluation period.

Table 7-1
Storm Water Volumes and Flood Elevations of the historical Tulare Lake for a 100-yr flood.

Year	Scenario	Lake Volume (acre-feet)	Lake Stage Elevation (NAVD88)
2008		1.62E+06	191.75
2016		1.64E+06	189.45
2036	A	1.66E+06	183.3
2036	B	1.66E+06	180.79
2036	C	1.65E+06	173.3

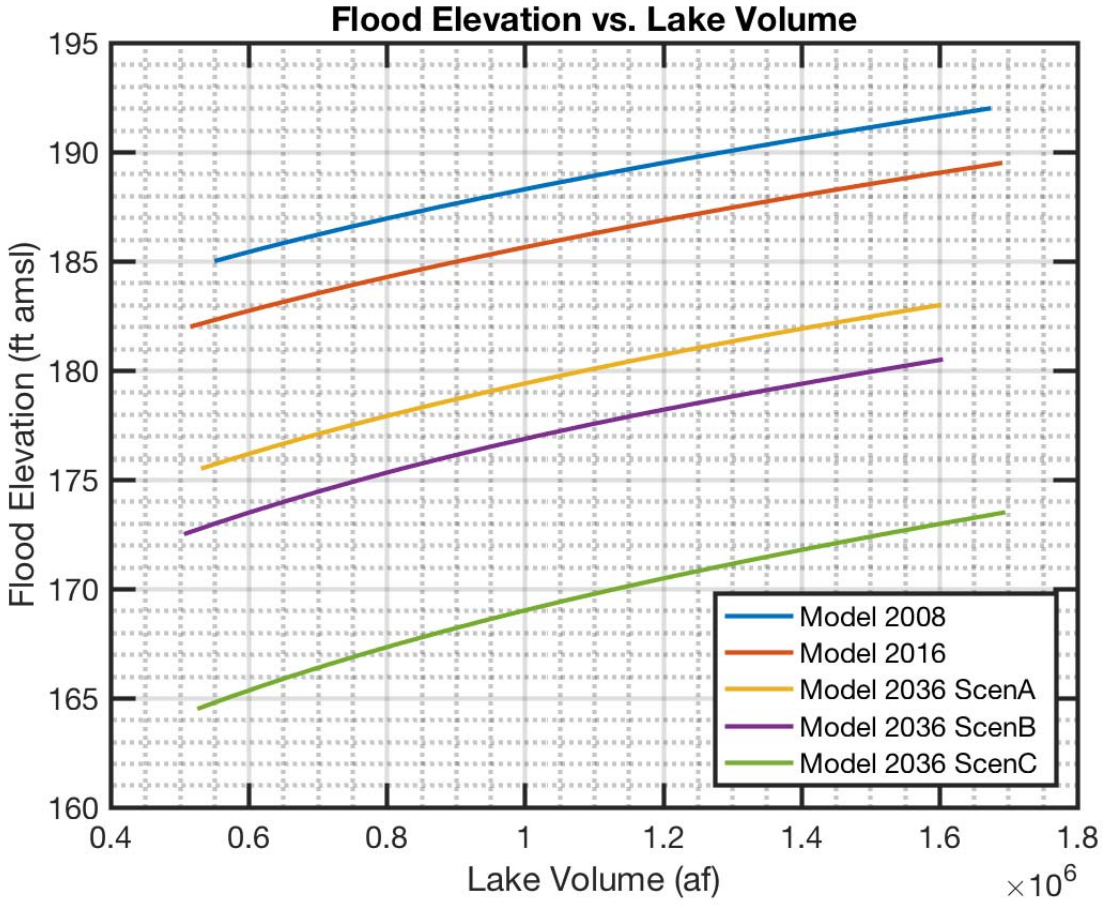

Figure 7-18: Estimated Storage Volume and Water Level Relationships in Tulare Lake Flood Zone

7.2.6 Conclusions Regarding Floodplain Impacts and Recommended Mitigation Approaches

7.2.6.1 Changes related to Tulare Lake

We recommend the Authority work with other agencies and stakeholders to coordinate control of floodwaters entering the Tulare Lake basin: we believe this is the only viable mitigation alternative. With implementation of appropriate flood control measures such as would be required to prevent a major filling of Tulare Lake basin to protect areas such as the community of Corcoran and the Corcoran State Prison, Tulare Lake flooding will not pose a threat to the HSR Alignment.

Other measures we considered include raising the track grade, by using either long viaducts or taller embankments, above the anticipated flood levels, or creating floodwalls or levees to protect the Alignment. Raising the track grade with long viaducts would be technically feasible but very expensive. Similarly, raising the track grade with taller embankments, or constructing floodwalls or levees to protect the Alignment, would require large increases in land acquisition, which would cause major schedule delays as well as high construction cost increases.

7.2.6.2 Changes associated with River Crossings

Floodplain changes related to river crossings without the influence of a flooding Tulare Lake are relatively modest. In general, it appears the existing floodplain limits for CP 2-3 or CP 4 may not need to be modified to accommodate changes associated with river crossings if Tulare Lake flooding can be controlled as discussed in Section 7.2.6.1.

8.0 REMAINING UNCERTAINTIES AND POTENTIAL RESPONSES

In order to confidently design the HSR, it would be most useful if the rates and patterns of future subsidence were well-known. Forecasts of future subsidence along the Corcoran subsidence bowl portion of the HSR Alignment have been developed based on extrapolations of relatively recent historic subsidence rates, as described above in Section 7.2.5.2. However, these forecasts are approximate at best, and significant uncertainty remains regarding both rates and patterns of future subsidence, as well as other factors, all of which the subject in this section.

Plate 8-1 presents the map overview of subsidence in the SJV, with locations of cross sections discussed throughout this Section 8.0.

8.1 PAUCITY OF QUANTITATIVE DATA FOR LOCALIZED DIFFERENTIAL SUBSIDENCE

It appears that in almost all locations of the Corcoran Subsidence Bowl, the overall or average induced slopes and curvatures, calculated after partially smoothing the apparent noise in the data, are generally not anticipated to be greater than can be accommodated by ballasted embankments and structural viaducts.

However, current InSAR data based on L-band satellite imagery has pixel sizes on the order of 250 ft, and significant data smoothing has presumably been performed to fill in areas of decorrelation. Where 2008 USACE LiDAR and 2016 RTK is available along the eastern portion of the Tulare Lakebed, comparable measurement sample distances are about 50 to 60 feet (as shown on Plate 8-2), but significant data smoothing is still needed. Although the overall or average slopes and curvatures are not expected to be greater than can be accommodated by the HSR, there is still a possibility that local anomalies, such as fissures or faults, may result in localized concentrations of strain and differential settlement that could constitute challenges to the HSR. Examples of such potential local anomalies are presented on Plates 8-3 8-4, 8-5, 8-6, 8-7, 8-8, 8-9, 8-10 and 8-11.

Understanding recent ground subsidence patterns would provide a useful tool for better-predicting future subsidence patterns. One approach would be to perform an evaluation of X-band InSAR data using an approach that combines the best satellite imagery with benefits of classical InSAR and the benefits of PSInSAR. Images can be as frequent as weeks apart, with 1 m pixel sizes and often with sub-centimeter vertical precision.

8.2 LACK OF THOROUGH HYDROGEOLOGICAL DATA AND MODEL

As discussed above, thorough hydrogeological data incorporated into a thorough and calibrated model should, in concept, be able to improve forecasting abilities. However, we expect that the large scale of the area involved, and the great depth of soil and groundwater contributing to subsidence, will continue to create challenges to reliable hydrogeological monitoring.

In addition, there are large uncertainties associated with water balance – how much groundwater will be removed from the ground, and how much recharge will occur.

Nevertheless, because of the potential improvements in predictive abilities that a complete hydrogeological model may provide, continuing to monitor progress in the calibration of the CVHM2 by the USGS is recommended.

8.3 UNCERTAINTIES REGARDING FUTURE GROUNDWATER DRAWDOWN

Subsidence is directly related to groundwater drawdown. In theory, SGMA is expected to require future groundwater use to be sustainable; presumably this would mean that groundwater drawdown would at least greatly slow if not actually come to a stop (except for annual or possibly longer cycles of rising and falling groundwater levels). Uncertainties associated with groundwater drawdown including many factors, particularly the following:

1. SGMA Implementation. Depending on how SGMA is implemented and enforced (or not), groundwater drawdown may continue unabated for some number of years, or may rapidly be slowed or stopped. How this plays out will have a significant impact on subsidence along the HSR Alignment.
2. Climate/Climate Change. Future temperature and precipitation patterns both in the valley and in the Sierras to the east may have a significant impact on how much groundwater is pumped.
3. Land Use. Continued agricultural development in the region will continue to have a significant impact on groundwater use.
4. Variability of Deep Groundwater Level Measurements. As of this time, there is limited coordinated information about deep groundwater levels. Without this information, it will be difficult to improve hydrogeological-based subsidence modeling.

For instance, measured water levels starting in 2005 at four deep wells located about six miles northwest of Corcoran are plotted in Figure 8-1. These wells are oriented in a west to east line that ranges from about 0.6 miles to 2 miles west of the HSR Alignment. Depths and construction details of these wells are currently unknown. Similarity in measured depths to groundwater prior to 2013, including groundwater level variations greater than 100 ft for all four wells, with some measured elevations being 100 ft to 150 ft below sea level, is consistent with completion of these wells in the deep confined aquifer system below the Corcoran clay. Measured water levels in these four wells are similar to each other to within about 20 ft from 2005 through early 2013. After 2013, the water levels at these four wells diverge from each other and show groundwater level differences up to 100 to over 200 ft.

It should be further noted that this is an example of significant data uncertainty in a critical area for subsidence impacting the HSR. It is not known if the information in Figure 8-1 illustrates a quality control issue in the process of collecting, reporting, and archiving the groundwater level data, or a radical departure from anticipated groundwater level behaviors. HSR subsidence monitoring may need dedicated (especially deep) groundwater piezometer wells and / or access to available (especially deep) groundwater wells to be able to independently verify relevant groundwater levels along the HSR Alignment.

Overall, due to uncertainties about groundwater levels, our primary evaluation of subsidence patterns was based on observations of ground surface elevation changes rather than correlations with groundwater drawdown patterns.

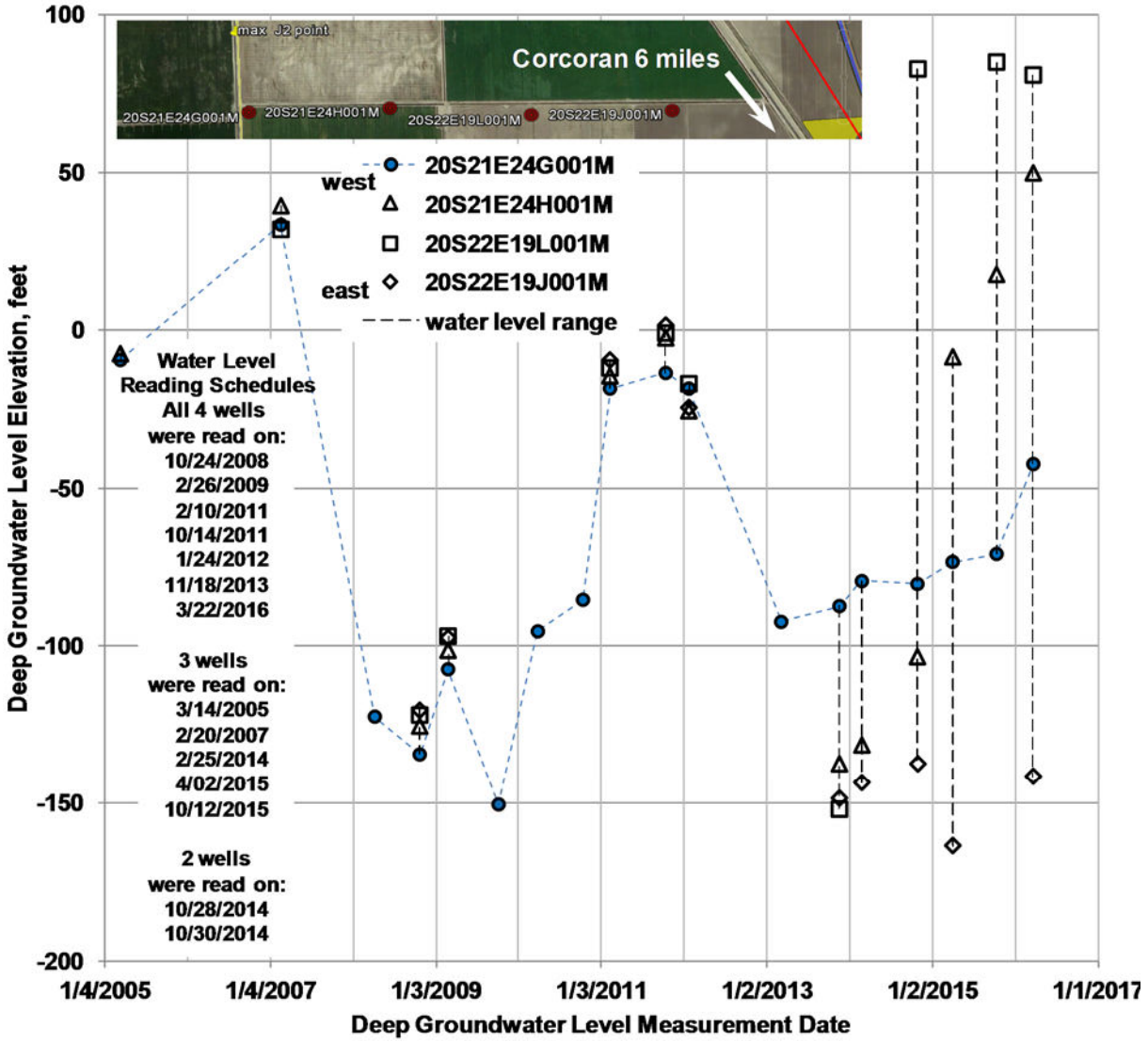

Figure 8-1: Measured deep groundwater levels since 2005 at four wells northwest of Corcoran

Effective mechanistic modeling of past subsidence and prediction of future subsidence requires confidence in understanding the groundwater levels and groundwater level changes driving subsidence. Currently, as shown in Figure 8-1, groundwater levels may vary radically over relatively short distances, such that in at least some critical areas, understanding of groundwater levels may be very uncertain.

8.4 Past and Ongoing Groundwater Drawdown and Subsidence in the San Joaquin Valley

During much of the 20th century, groundwater pumping was rapid through much of the SJV, with significant drawdown of groundwater levels over broad areas. This led to as much as 28 ft of subsidence, which is shown by the 1900s Historical Subsidence contours on Plate 8-1. With the development and completion of the California state water project, surface water became

plentiful and easier to obtain than groundwater; groundwater extraction and subsidence greatly slowed or possibly stopped.

Recent changes in economics and land use have resulted in the planting of many acres of orchards either in previously uncultivated areas or in areas previously cultivated with seasonal row crops. As a result of the high water demands of orchards, groundwater extraction has re-accelerated and subsidence has been occurring at rates even greater than in the last century (although in somewhat different areas, as seen on Plate 8-1).

8.4.1 Current and Ongoing Subsidence

Current and ongoing subsidence is discussed in Section 5.0. As seen on Plate 8-1, it appears that the rate of subsidence in the center of the Hanford-Corcoran bowl was about 2½ to 3 ft over a period of about 3½ years, between 2007 and 2010, or just under an average of 1 foot per year during that period. Between about September 2010 and July 2015 (just under 5 years), ground-based survey of monuments along the HSR Alignment for CP 2-3 indicated subsidence of up to about 5½ ft (Authority 2014, and DFJV 2015), for an average maximum rate just over 1 foot per year. The combination of 2008 USACE LiDAR and 2016 AFW RTK provides detailed subsidence information along selected roadways through the SJV to the east of Tulare Lake, as and shown on Plates 8-3 and 8-4. During this 8-year period, a maximum of over 9 ft of subsidence, just south of Corcoran, has been documented. Differential subsidence, including discrete locations of ground tension-inducing slope changes, likely compaction zones, and local subsidence features likely induced by single wells or small well groups, are interpretable. Differential subsidence features that have been interpreted from comparing the 2008 LiDAR and 2016 RTK results are summarized in Table 8-1 on Plate 8-11.

For 5½ months in 2014, from May through October, using C-band InSAR, JPL reported up about 10 inches of subsidence, or a rate of nearly 2 inches per month; if this rate were continuous it would amount to nearly 2 ft per year. However, it appears this rate, covering much of the growing season with presumed higher-than-average irrigation and groundwater pumping during the 3rd year of a severe drought, may have been faster than the average for the entire year. A separate review of C-band InSAR by Altamira for the whole of 2014 indicated about 1 foot of subsidence in the Corcoran-Hanford bowl.

Overall, it appears subsidence near the deepest portion of the Hanford-Corcoran bowl has averaged in the vicinity of 1 foot per year since at least 2006.

Review of CGPS instruments maintained by Caltrans suggests subsidence of a similar magnitude as documented by recent InSAR.

8.4.2 Anticipated Future Subsidence

As discussed in Section 5.0, it appears that subsidence in the center of the Hanford-Corcoran Subsidence Bowl over the past 10 years has averaged nearly 1 foot per year, possibly with some acceleration toward the 3rd or 4th year of the recent drought. Water use has been increasing in the past 10 to 20 years, and the trends show no sign of slowing (Marston & Konar 2017). However, based on the recent passage of the SGMA, we have assumed that by 2040 groundwater use will have become "sustainable," which we interpret will mean negligible to no ongoing groundwater drawdown beyond that time. We therefore consider it reasonable to anticipate that groundwater will continue to be drawn down at a steady or accelerating rate for the next 5 to 15 years such that subsidence may continue at a rate similar to or even accelerating beyond the recent rate during this period, but slowing and eventually stopping or nearly stopping after that. Thus, in rough terms, the area could subside about 10 ft in the next 10 years, and about 20 ft in the next 20 years.

These values will be a function in part of rainfall and land use/water use, which we anticipate could increase or decrease these rates by 25% to 50%.

8.4.3 Forecast Subsidence-Induced Slopes and Curvature

Forecast 20-year subsidence-induced changes in slopes and curvatures along the HSR Alignment have been calculated by extrapolating the JPL InSAR data from 2007 to 2010 (Scenario A); calculations of changes in topography from 2008 (based on USACE LiDAR) to 2016 (based on AFW RTK survey etc., as described in Appendix C) (Scenario B); and JPL InSAR data from 2015 to 2016 (Scenario C) are shown on Plate 8-17. (Note that Scenario B only includes the zone from about Corcoran to Deer Creek, which is the limits of the USACE 2008 LiDAR data.)

As an estimate, changes in slopes and curvatures may be expected to continue to increase for the next 10 to 20 years at a similar rate to the observed historical rates of the past 10 years. Thus, from Corcoran south to the Deer Creek Viaduct, it is anticipated that the current subsidence-induced slopes and slope changes over the next 10 to 20 years could increase by an additional 1.2 to 2.5 times the values shown on Plate 8-4. North of Corcoran and south of the Deer Creek Viaduct, it is expected that the current subsidence-induced changes in slopes and curvatures over the past 10 years could be as much as 3 times the values shown on Plate 1-2 for a 3½ year period. Future changes over the next 20 years could be greater than the amount observed for 2007 to 2010 (JPL), 2008 to 2016 (USACE and AFW RTK), and 2015 to 2016 (JPL) by factors of 6, 2.5, and 19, respectively, shown on Plate 8-17.

Because future subsidence impacts from existing wells will likely broaden and smooth out somewhat, these projections of changes in slopes and curvatures may be moderately to quite conservative. On the other hand, future land use and water use are difficult to forecast, as is

future rainfall. Construction of future wells may accelerate subsidence and locally cause increases in changes to slopes and curvature. Also, local variability in pumping rates or subsurface stratification (such as the PCF or the Corcoran Clay acting as possible groundwater barriers) could cause local increases.

8.5 FLOODWATER MANAGEMENT IN THE TULARE LAKE BASIN

There is currently little coordination of floodwater management in the Tulare Lake Basin, so there is limited understanding of likely flood potentials. A flood-management solution seems to be possible to this flooding hazard, although there is currently no allocated funding or a lead entity. It is our understanding that there is an informal group of interested parties who are currently discussing these topics. Because resolving these flood concerns is a matter of vital interest to the Authority, and we recommend that they take steps to support these coordination efforts.

8.6 SUBSIDENCE-INDUCED FISSURES AND FAULTS

Earth fissures generally result from differential compaction (subsidence) due to groundwater withdrawal in unconsolidated to semi-consolidated sediments such as basin alluvium. Differential subsidence is typically a result of changes in compressible material thickness (such as rapid increase in bedrock depth at basin edges) or basin material lithologic changes (such as fines to coarse sediments at edges of significant lacustrine deposits) Holzer (1984) classifies earth fissures as tensile ground failures and compaction faults as shear failures. He further reports that horizontal displacements across uneroded earth fissures are typically less than a few centimeters, whereas fault offsets as much as 1.5 ft have been measured.

Although fissures caused by groundwater drawdown-induced subsidence are infrequent in the SJV, subsidence has resulted in at least three fissures in the mid-1900s, located about 3½, 5½, and 9 miles from the future HSR Alignment. If a future fissure were to develop beneath or adjacent to a HSR guideway (conventional or MSE embankment), it could lead to distortion of the track, requiring slow-down or interruption of service until the track could be realigned.

Given that current subsidence rates in the Hanford-Corcoran Subsidence Bowl are greater now than when the historical fissures developed, and that the total magnitudes of recent subsidence are likely approaching and almost certainly will exceed 1900s Historical Subsidence, it is possible that new fissures will develop in this area in the future. In project communications, Tom Holzer and Michelle Sneed of the USGS each concurred on this opinion.

On the other hand, it is also generally recognized that there are not likely to be a large number of new fissures in this area, and therefore the likelihood of such fissures occurring beneath or immediately adjacent to the HSR Alignment is considered to be relatively low, but not negligible.

Assuming future fissures do develop, it is likely that the preceding tensile strains and tensile cracks will develop relatively slowly. Such cracks could then enlarge relatively rapidly in the event of flooding or heavy rainfall (see Plate 8-12 for pictures of historic erosion-enlarged fissures).

Regarding the potential risk due to fissures, during the formation of tensile stresses and tensile cracks beneath or adjacent to the HSR Alignment, the risk to HSR embankments could include the development of tensile cracks in the embankment. Initially, this may not lead to any deterioration of the track, but if left unchecked, heavy rainfall (or flooding if this portion of the HSR Alignment is in a floodplain) could result in erosion or crack collapse that could lead to the development of significant depression or settlement of the trackbed, and in a worst-case scenario, partial erosion of the embankment.

Similar to potential cracks in the embankment, if ground cracks are left unchecked, heavy rainfall (or flooding if this portion of the HSR Alignment is in a floodplain) could result in erosion or crack collapse that could lead to development of significant depression of the ground beneath the embankment. If this is left unchecked, the depression could propagate upward toward the trackbed.

Assuming future fissures do develop, it is likely that the preceding tensile strains and tensile cracks would develop relatively slowly. Such cracks could then enlarge relatively rapidly in the event of flooding or heavy rainfall. The risk (albeit a relatively low risk) that fissure development may pose to the HSR may be reduced to an acceptable level by monitoring and, in the event that differential subsidence induces tensile strains that are observed or suspected to be high, or tensile cracks are observed or otherwise detected, taking appropriate mitigation measures as discussed in the following sections.

Based on the rates and magnitudes of observed recent and ongoing subsidence, it appears possible that at least a limited number of fissures could develop in the future in the SJV. At this time, it is not possible to predict the locations where such fissures will develop, but using a variety of future ongoing monitoring methods combined with some understanding of underlying hydrogeologic conditions, it should be possible to identify locations that exhibit significant convex upward-induced curvature, which could be associated with an increased likelihood of fissure development as tensile ground strains gradually develop over time. If these areas are then monitored with increased attention, it should be possible to identify cracks or incipient fissures before they significantly affect the rail and to perform mitigation so as to maintain track safety and to maintain and/or restore the track to the original *Design Criteria*.

8.6.1 Sources of Information Regarding Subsidence-Induced Fissures and Faults

8.6.1.1 Literature Review

Key relevant literature reviewed includes the following:

- Holzer (1978, 1979, 1980, 1984), Jachens and Holzer (1979, 1982), and Holzer and Pampeyan (1981) provide several insights into subsidence and earth fissure behavior. Several case studies of subsidence-induced fault movement are represented, including movement at the Pond-Poso Creek fault in the vicinity of the HSR Alignment (Holzer 1980) and exploratory drilling, characterization (including geophysical logging) and fault movement monitoring at the Picacho fault in south-central Arizona (Holzer 1978).
- Holzer and Pampeyan (1981) reported that earth fissuring at four sites (including Arizona, California, and Nevada) developed fissures when there was convex upward change in curvature with tensile strain rates on the order of 100 to 700 microstrain per year.
- Jachens and Holzer (1979, 1982) concluded that earth fissuring occurred at horizontal tensile strains in the range of 200 to 2000 microstrain, with most in the range of 200 to 600 microstrain. Multiple investigations by AFW (Plate 8-13) have confirmed these to be reasonable ranges.
- Guacci (1978) documented historical observations and a significant field exploration program from 1974, of the 1969 Pixley Fissure (see Fissure 1 on Plate 8-1), with passing mention of the other two nearby fissures from the similar time frame.
- USGS textural model. The textural model from the USGS CVHM-mod was used to assess rough stratigraphic profiles along the HSR Alignment with a few transverse stratigraphic profiles, including one through the location of the Pixley Fissure (Plate 8-14).
- Holzer (1980) presents an investigation and evaluation of the subsidence-induced Pond-Poso Creek Fault (PPCF), which is located a short distance from the HSR Alignment (Plates 8-1 and 8-5).
- Miller (1999) presents historical seismic reflection profiles in critical areas of the HSR Alignment and provides insight into the character of relevant basin alluvium structure (Plates 8-5 and 8-15).
- State of California DOGGR files are available on the web, with images of historical oil and gas well geophysical logs, primarily electrical resistivity logs (e-logs), which provide detailed data to characterize basin alluvium for subsidence potential at select well locations. An overview of relevant e-log results and interpretations for subsidence characterization is presented on Plate 8-16.

8.6.1.2 Personal Communications

Early in the investigation, prior to acquisition and analysis of 2008 LiDAR and 2016 RTK survey results that have identified some specific locations of tensile ground strain resulting from recent and current subsidence, AFW spoke with Ms. Michelle Sneed, a hydrologist with the USGS (Section 2.2.1), and with Dr. Thomas Holzer, a research geologist with the USGS (Section 2.2.2). They were both asked, given current subsidence rates, about the potential for groundwater drawdown-induced subsidence to cause future fissures or faults in the SJV, and the risk these pose for the future HSR. Current subsidence rates in the Corcoran Subsidence

Bowl are greater now than when the historical Pixley Fissures developed, and the total magnitudes of recent subsidence is likely approaching and almost certainly will exceed 1900s Historical Subsidence. Given these current conditions, both concurred that it is possible that new fissures could develop in this area in the future.

We have also communicated with Dr. Jason Saleeby (Section 2.2.5) concerning mapped locations for "Corcoran Clay Faults" (Saleeby and Foster, 2004, Saleeby et al., 2013). Discussions included identification of original source material for Saleeby's publications and resulted in AFW reviewing and utilizing seismic reflection data (Miller 1999) that informed Saleeby. CCFs and other tectonic structures described by Saleeby are important to the understanding of the sub-surface geologic characterization and areas where earth fissures, compaction faults, and other concentrations of horizontal and/or vertical displacement could occur.

8.6.1.3 Recent Survey Measurements in SJV: LiDAR

Until an effective history of InSAR coverage for the SJV at appropriate resolutions and sufficient time-scales is built up, characterization of differential subsidence in the SJV capable of discerning incipient earth fissure and compaction fault development will be limited to other surveys. Relevant surveys through the HSR Alignment area are discussed in Section 2.4. Repeat surveys of HSR benchmarks (typically at spacings of about 2 miles) in 2010 and 2015 provided static GPS corroboration of InSAR-derived subsidence rates in the SJV.

Detailed surveys of a portion of the HSR Alignment were completed using LiDAR in 2008 and RTK survey in 2016. Over that period of 8 years, enough subsidence has accumulated that these surveys can show sufficient detail to interpret quantifiable local subsidence information, with measurement constraints or "noise," as shown on Plates 8-3 and 8-4. Interpreted potential current tensile strain zones identified from the LiDAR and RTK surveys are summarized in Table 8-1 (presented on Plate 8-11). LiDAR and RTK surveys are considered to have insufficient precision for normal subsidence monitoring; however, these measurements are of sufficient precision to provide valuable information for the portion of the SJV with up to 9 ft of subsidence, including possible areas of compaction faulting (clay faults). Using the available information, these plates show our interpretation of what we consider to be reasonable and mostly likely in terms of subsidence, differential subsidence, and ground curvature. However, we note that such interpretation work is an imprecise science, and future observations and data may call for revising these interpretations.

8.6.1.4 Past Amec Foster Wheeler Experience

AFW has performed subsidence and earth fissure assessment and mitigation work with particular emphasis on dams and embankments associated with flood control retention (flood retarding structure [FRS]) or storage where earth fissures can be a geo-hazard safety risk and

differential subsidence can impact facility operations (e.g., AMEC [2009, 2011a, 2011b, 2014a]; Fergason et al. [2015]; Keaton et al. [1998]; Panda et al [2015]; Rucker et al [1998, 2006, 2013, 2015]). Relevant concepts derived from this work are shown on Plates 8-13 and 8-16. Plate 8-13 provides a conceptual summary of differential subsidence leading to earth fissuring and results of modeling on various projects relating tensile ground strain to change in slope of subsidence about a point of fixity. For the HSR, Plate 8-16 summarizes components of compressible basin alluvium as characterized from e-logs, using a well located adjacent to the HSR Viaduct near Alpaugh as an example. Plates 8-3 and 8-4 provide interpretations of differential subsidence results in SJV, including a portion of the HSR Alignment.

Based on known and potential impacts of earth fissuring on flood retention structures and dams, current guidance for earth fissure risk zonation (AMEC 2014a) is summarized in Table 8-2. These guidelines can be applied to other large-scale and linear infrastructure, such as HSR.

Table 8-2
Guidance for Earth Fissure Risk Zonation for Flood Control Dams, Levees, Channels and Basins (AMEC 2014a)

Risk Category	Definition	Mitigation
High	Region where earth fissures are present at this time and likely to continue in the future.	Avoidance and / or significant engineered remedial solutions.
Moderate	Region that has experienced significant differential subsidence* in the past **and** where future additional significant differential subsidence* could lead to earth fissure formation.	Consider avoidance or implement engineered remedial efforts such as structural elements and / or subsidence and earth fissure monitoring.
Low-Moderate	Region that has experienced significant differential subsidence* in the past **or** could experience future significant differential subsidence*; likelihood is less than for moderate risk zone.	Subsidence and earth fissure monitoring.
Low	Region that has not experienced significant differential subsidence* in the past and is not expected to experience significant differential subsidence* in the future.	Typical dam safety monitoring and maintenance.

* Significant differential subsidence is differential subsidence resulting in large-scale ground tensile strains greater than 0.02% (200 microstrain), which we have found typically to correspond to a change in slope about a point greater than 0.05%.

8.6.1.5 Literature Regarding Earth Fissuring Due to Oil Extraction

Land subsidence is also occurring in areas within the greater SJV due to extraction of oil and gas, which also extracts significant amounts of groundwater. Earth fissures have been reported in some of these oil and gas fields (such as Lost Hills oil field).

Conditions in these areas are site-specific as the geologic and pumping conditions are typically different from other areas in the SJV. However, the presence of earth fissures does show that where significant land subsidence occurs in areas with susceptible geologic conditions within the SJV, earth fissures are possible. Specific references detailing earth fissures are sparse as they typically occur within local news outlets or regulator reporting, but land subsidence in these areas has been documented in several studies, including Borchers and Carpenter (2014), and Fielding et al. (1998).

8.6.2 Summary History of Subsidence-Induced Fissures

8.6.2.1 Overview of Conditions Leading to Subsidence-Induced Fissures

Ground fissures are features associated with subsidence in some parts of the world, including Southern California (Antelope Valley, Mohave Desert, Coachella), Arizona, Nevada, Mexico, China, and elsewhere.

Where they are common, several conditions are generally present:

5. Local differential subsidence results in convex upward change in curvature of the ground, which leads to tensile stresses in the ground. For fissures to initiate, these strains generally approach 200 to 600 microstrain (0.02% to 0.06%).
6. Subsidence-induced change in slope of the ground (percent slope change) commonly approaches 0.05% to 0.15%, and that change in slope of about 0.05% to 0.15% is typically sustained over a distance of at least 1000 to 2000 ft. The development of tensile strains is caused by this change in slope. A summary of the typical relation between tensile strain and change in slope is shown on Plate 8-13. This relationship has been empirically determined through comparison of finite-element modeled differential subsidence and strains at earth fissure and potential earth fissure sites in Arizona and Northern Nevada (Plate 8-13). It has been presented by Rucker et al. (2013) in relation to earth fissure impacts on dam safety.
7. There is commonly a relatively thick layer of unsaturated, slightly moist, weakly cemented material above the saturated compressible layer, and it is the convex upward flexure of this overlying layer that results in tensile stresses developing near the ground surface.
8. The surficial soils that are most susceptible to piping erosion are those that have at least some cementation or cohesion that enable the tension crack to stay open without initially collapsing. In order to adequately concentrate tensile stresses for fissures to develop, there needs to be a rapid change in the thickness of the underlying compressible layer, and this change must normally occur within several hundred feet, possibly to about

1,000 ft, of the ground surface. This is often a result of a rising of the bedrock beneath the compressible layer along the flank of an alluvial basin (e.g., McMicken Dam in Arizona, or Coachella) or buried bedrock peak within the alluvium (e.g., Antelope Valley, Hawk Rock at Powerline Dam FRS in Apache Junction, Arizona). Rapid variation in alluvium compressibility across facies changes (i.e., changes in the alluvial strata) is also a cause of earth fissuring (e.g., Cochise, Arizona, Olive Avenue at Loop 303 Freeway west of Glendale, Arizona). The fissure near Pixley (Plates 8-1, 8-12, and 8-14) is in an area of shallowing alluvium as shown on Plate 8-18. However, review of historical oil well e-logs (Plates 8-19 and 8-20) indicates that an abrupt offset in the alluvium facies may be coincident with the Pixley Fissure; this will be discussed further in Section 8.5.3.2.

9. Where earth fissuring occurs due to differential subsidence at alluvium facies changes, the fissuring typically occurs where the nature of alluvium materials change, from coarse-grained to heterogeneous or fine-grained (Rucker et al. 2015). Coarse-grained alluvium tends to have relatively low compressibility, leading to minor compression that occurs rapidly due to high permeability. Heterogeneous alluvium tends to consist of inter-bedded coarse and fine materials. The fine-grained materials are more compressible, while the interbedded coarser-grained material may allow relatively rapid drainage of the fine-grained lenses and layers; thus, significant subsidence can occur relatively rapidly (scale of years) in heterogeneous alluvium. However, unless the finer alluvium is drained by wells or coarser beds, it may take decades to centuries for pore pressures to fully dissipate and subsidence to end. A north-south geologic profile (Plate 8-21) and seismic reflection profile (Plate 8-15) provide insight into the geometries of the basin alluvium. The seismic reflection profile indicates the presence of relatively steeply dipping features within the compressible basin alluvium that may have the effect of cutting off or limiting lateral groundwater flow; such features can be anticipated to behave as facies changes that may enhance differential subsidence.

It has been hypothesized that, before fissures become visible at the ground surface, cracks may commonly start near the top of groundwater and propagate up to the ground surface. Alternatively, the possibility of cracks initiating at the ground surface is consistent with engineering mechanics of a beam or plate in flexure, where tensile strains would be largest near the ground surface. A buried ground crack may remain undetected for some time as surficial soils bridge over this subsurface feature. Indirect evidence of the incipient fissure can include vegetative lineaments visible in aerial photography and animal burrowing activity concentrated in the incipient fissure area. If sheet flow, or runoff from heavy rains, or flooding expose the crack, they may cause erosion and lead to collapse of the crack walls or erosion of material from the crack. This can lead to relatively rapid production of a visible fissure at the ground surface, possibly within hours or days.

The single-well groundwater and geomechanical modeling, discussed in Section 4.0, indicates that strains developed around a single well are not expected to be adequate to initiate fissuring.

Subsidence features have been identified that are consistent with behavior around a single well or small group of wells, which are shown on Plates 8-3, 8-4, 8-9 and 8-10, and are summarized in Table 8-1 (presented on Plate 8-11).

8.6.2.2 San Joaquin Valley Fissures (Pixley & Vicinity)

Three significant fissures have been identified and mapped in the SJV in the late 1960s, all in what is known as the "Pixley Subsidence Bowl." These three fissures were located about 3½, 5½, and 9 miles east of the HSR Alignment, as shown on Plate 8-1. Guacci (1978) has thoroughly investigated and described the eastern-most of these fissures, which is known as the Pixley Fissure; for purposes of discussion in this report, it is referred to as the Pixley Fissure No. 1. The locations of the other two are shown by Guacci but AFW is not aware of detailed descriptions of them; pictures of each of the three Pixley Fissures (provided by Tom Holzer) are shown on Plate 8-12.

The Pixley Fissure No. 1 (Plate 8-14) was first observed following floodwaters receding from the area of the fissure. The surface expression was initially reported to be about ½ mile long, up to about 8 ft in width, and up to about 6 ft in depth. At the time of Guacci's investigation in 1974, 5 years after the original appearance of the Pixley Fissure in 1969, the fissure had changed shape somewhat through the process of ongoing slumping and erosion, and was a maximum width of about 12 ft, with maximum surface relief of about 3.4 ft.

When the Pixley Fissure No. 1 occurred on the sides of the Pixley Subsidence Bowl (Fissure 1 on Plate 8-1), there had been as much as 14.2 ft of subsidence near the center of the Pixley Bowl. This subsidence occurred over the preceding half century, with up to 0.7 ft per year in the years leading up to the fissure. At the location of the Pixley Fissure, mapped subsidence was on the order of 9 ft. A first approximation of the maximum subsidence-induced slope tilt in the vicinity was on the order of 0.04% (or 400 microradians) based on the very coarse interpolation between contours of subsidence from the USGS, with convex-upward change in ground curvature at the location of the Pixley Fissure, as seen on Plates 8-1 and 8-14. Historical level surveys between 1942 and 1964 (Plate 8-14) document slope change of about 0.04% along the survey profile 3 miles north and about 2 miles east of the fissure. The orientation of differential subsidence relative to the survey profile is unknown; actual slope change could have been larger than the measured differential subsidence. Furthermore, this historical (and available) subsidence profile information lacks sufficient detail to infer a subsurface condition or feature that would contribute to localized differential subsidence and ground strain concentration where fissuring could be anticipated.

Using historical oil well e-logs in the Pixley Fissure No. 1 area, a profile of the deep basin alluvium across the fissure has been developed as shown on Plates 8-19 and 8-20. A possible significant offset, down to the west, in the basin profile is interpreted in the very near vicinity of the fissure. Offset of about 400 ft at a depth of about 3,500 ft, and about 150 ft at a depth of

1,500 ft, is shown on Plate 8-19. Possible offset of about 150 ft in the basin alluvium to depths at least as shallow as 700 ft is also apparent. Such an offset is a likely mechanism to isolate lateral effects of groundwater pumping and induce localized significant differential subsidence with more significant localized slope change than the 0.04% estimated from published information. Thus, this apparent offset is a likely contributor to the development of the Pixley Fissure No. 1. It is possible that the fissure could be associated with compaction faulting; this will be discussed further in Section 8.5.4 of this report.

Very little is known of the other fissures in the area (Fissures 2 and 3 on Plate 8-1) except for the photographs shown on Plate 8-12 and their approximate locations as shown by Guacci (1978). As can be seen from the Pixley Bowl subsidence contours (Plate 8-1), the subsidence-induced ground slope is significantly less than at the Pixley Fissure. Cross Section A-A' (Plate 8-18) and local e-log cross sections on Plates 8-19 and 8-20 suggest there may be relatively abrupt facies changes underlying the general area of at least Pixley Fissure No. 1, and perhaps all three fissures, which could have led to concentrations of strain and subsequent fissure development. Otherwise, it is not completely clear what led to their development in those specific locations and orientations.

The general 2008 to 2016 west to east differential subsidence profile across the eastern SJV documented on Plate 8-3 indicates the potential for multiple locations with large subsidence-induced ground tension. Eventually, continued tensile strain development capable of initiating earth fissures could be anticipated throughout the area during extended periods of large differential subsidence. It should be noted that calculated slope changes on Plate 8-3 (as well as Table 8-1 (presented on Plate 8-11), and other plates where 2008 LiDAR and 2016 RTK elevation data are utilized) are for slope change along the axis of the roads used for the RTK survey. Where the strike of a slope change is at an angle to a road, the actual slope change magnitude, which would be determined on the actual slope dip orientation, will be larger.

8.6.2.3 Fissures in Other Locations

Fissures have developed in a number of other locations in Southern California (including Antelope Valley, the Mojave Desert, Edwards Air Force Base, west of Chino, and near Coachella), as well as Arizona, Nevada, and China.

Fissures caused frequent damage to a runway at Edwards Air Force Base, with short shutdowns during repairs each time, until the runway was abandoned.

Recent fissures have been attributed to hydrocompaction in response to leakage from the California Aqueduct about 4 miles south of Buttonwillow, California.

Recent fissures thought to be associated with oil and gas extraction have been identified about 8 miles southwest of Lost Hills, California. Other fissures related to oil and gas extraction have

been identified in the past century in the southern end of the SJV (not in the vicinity of the HSR Alignment).

Ground fissuring related to subsidence has affected roadways and other infrastructure in the Chino basin in southern California. Between the 1940s and the time the groundwater basin was adjudicated in 1978, groundwater levels in an area south of Chino declined by approximately 130 ft. In 1973, fissures were observed extending north and south from a paved road and reportedly caused a slight depression and cracking across the roadway. Land use in the area at that time was predominantly agricultural, and other damage to roads or infrastructure may have occurred but have gone unreported. Although groundwater levels generally stabilized or recovered after 1978, a shift in pumping to deeper aquifer zones resulted in renewed subsidence and fissuring in the early 1990s. Fissuring and distress at that time damaged buildings and manifested as linear cracks or depressions in roadways, curbs, gutters, sidewalks, and a parking lot.

8.6.3 Subsidence-Induced and Subsidence-Enhanced Faults

In some cases, existing faults can create a groundwater block, such that groundwater can be draw down differentially across the fault, leading to differential subsidence across the fault, and in some cases the differential strains can localize into a normal fault.

8.6.3.1 Pond-Poso Creek Fault (PPCF)

Tom Holzer of the USGS (1980) mapped one location where this condition was noted in the 1970s near the town of Pond, about 2 miles east of the future HSR Alignment. Pictures of this fault are included on Plate 8-5. Vertical-offset faulting of about 8 inches was observed across a very narrow zone in an exploratory trench across the fault scarp located about 0.5 – 1.5 miles from the preexisting Poso Creek Fault (PCF) and over a length of about 2 miles, as shown on Plate 8-1. This was called the Pond-Poso Creek Fault (PPCF). The movement reportedly crept fairly slowly, rather than abruptly such as would occur during seismic fault slip. In a very limited monitoring program in 1977 to 1979, Holzer (1980) measured vertical displacement across the fault up to about 30 mm, of which up to about 25 mm occurred over a period of 4 months. Smith (1983) reports that apparent vertical offset along the westernmost Pond Fault, based on seismic reflection geophysics through the area, is about 250 feet at a depth of 3,600 feet, about 100 feet at a depth of 1,760 feet, about 50 feet at a depth of 875 feet, and about 35 feet at a depth of 250 feet. The deeper of these offsets is somewhat smaller than, but consistent with, the deep interpreted offsets at the Pixley Fissure. Offset at the Pond Fault is also apparent in seismic reflection Line 116 (Plate 8-5) as presented in Miller (1999).

Although the PPCF is located about 2 to 2.5 miles from the HSR Alignment, the PCF continues to the northwest and crosses the HSR Alignment about 4 ½ miles northwest of the PPCF.

The vertical offset mapped by Holzer (1980) as subsidence-induced movement on the preexisting Pond-Poso Creek Fault is the only documented example of this type of movement in the SJV.

However, the PCF intersects the HSR Alignment about 5 miles northwest of the PPCF. Subtle aspects of the 2007 to 2010 InSAR settlement pattern in this area (Plate 8-5) have been evaluated and are consistent with a potential for recent or ongoing subsidence-induced differential movement from 2007 to 2010 with magnitude up to about 2 inches across the PPC area in the vicinity of the HSR Alignment. Continuing monitoring of subsidence in that area over a period of several years may provide more conclusive evidence of presence or absence of subsidence related displacements in this area.

8.6.3.2 Potential Faulting at Pixley Fissure No. 1

Using historical oil well e-logs in the Pixley Fissure No. 1 area, a profile of the deep basin alluvium across the fissure has been developed as shown on Plates 8-19 and -20. As shown on Plate 8-19, a possible significant offset, down to the west, in the basin profile is interpreted in the very near vicinity of the fissure. An apparent offset of about 150 feet in the Tulare Formation basin alluvium aquifer system, down to the west, at depths at least as shallow as 700 feet is apparent on Plate 8-19. That offset of about 150 feet is also interpreted at a depth of 1,500 feet, roughly at the top of the San Joaquin Formation, with an age of about 3.4 Ma (Miller 1999) underlying the Tulare Formation. Plate 8-20 shows the apparent offset is increased to about 400 feet, down to the west, at a depth of about 3,500 feet where the top of the Santa Margarita Formation (age 7 Ma) is interpreted. Such an offset, active for the last several million years, is a likely mechanism to isolate lateral effects of groundwater pumping and induce localized significant differential subsidence; a possible hydrologic barrier is implied in the depths to saline water as shown in Figure 3-7 of Section 3.2 of this report.

8.6.3.3 Corcoran Clay Faults – Other Geologic Conditions Leading to Significant Differential Subsidence and Potential Compaction Faulting

Near surface geologic material properties may control surface and near-surface erosional behavior of earth fissures, but the geology and geometry of the alluvium aquifers and aquitards from which groundwater is pumped controls the differential subsidence that drives earth fissure development. Geologic and geometric conditions in the basin alluvium Tulare Formation associated with the ancestral Tulare Lake may favor the development of significant differential subsidence in response to extensive groundwater pumping. There is uncertainty in the understanding of the mechanics of earth fissure development as well as these geologic conditions. For example, Budhu (2008) describes various theories and mechanisms for earth fissure initiation, including explanations of initiation ranging from the shallow alluvial profile (based on tensile strain) to the deeper alluvial profile above the groundwater table (based shear strain). Uncertainty surrounds possible fault features presented by Saleeby and Foster (2004);

these have been designated CCF as shown on Plates 8-1 and 8-3. It is not known if these CCFs, if present, have the potential to behave similarly to fault structures within the basin alluvium and enhance the potential for earth fissure development. Offsets in the depth to the Corcoran clay, as shown on Plate 8-21, have long been documented. Some of the CCFs appear to radiate from the ancient Tulare Lakebed area, while other CCFs might be coincident with possible ancient Tulare Lake shorelines. Assuming that locations of CCFs are correct, CCFs intercepting seismic reflection Line 133 (Miller 1999) are shown on Plate 8-15; possible CCF traces through the alluvium have been inferred in the Plate 8-15 reflection profile to follow changes in depth of seismic reflectors. Variations in depths to the Corcoran clay are also apparent in alluvium characterization developed from e-log profiles in the Alpaugh and Deer Creek area (Plates 8-6 and 8-7). CCFs might reflect significant changes in alluvium profile depths rather than actual faults within the compressible alluvium. Changes in depth to the top of the Corcoran Clay horizon are anticipated to be consistent with these changes in alluvium profile depth. Such changes in alluvium profile depths are likely sufficient to generate groundwater barriers that isolate lateral connectivity of aquifers subject to groundwater pumping and contribute to enhancement of differential subsidence. E-logs in the Hanford area (Plate 8-22) have not provided similar information regarding the Corcoran clay in that area.

At least some of the relatively steeply dipping features in the seismic reflection profile Line 133 (Plate 8-15) are described by Miller (1999) as examples of progradation: pulses of coarse-grained terrestrial deposition as deltas into the ancient lake. Fine-grained lakebed deposition occurred between these pulses of coarse-grained deposition. Plate 8-6 presents oil well e-logs (wells 371, 362 and 363) with deposits below depths of 1,000 feet of coarse-grained (high resistivity) alluvium with thicknesses of 20 to 100 feet alternating with similar thicknesses of fine-grained (low resistivity) alluvium. These e-log patterns are consistent with steeply dipping structure features apparent in seismic Line 133 between miles 17 to 20 and miles 20 to 25 on Plate 8-15. It appears that the dip of the alluvium progradation fabric along the HSR Alignment in the vicinity of Corcoran is generally southwest to south-southwest toward the more continuous lacustrine deposits of ancient Tulare Lake. That dip orientation may define the direction of interrupted groundwater flow; overall basin aquifer connectivity may be much greater in the direction of the progradation fabric strike orientation. InSAR subsidence patterns shown on Plates 8-1 and 8-8 indicate that differential subsidence may be more significant in the direction of the dip of the progradation structure within the alluvium. This anisotropic orientation within the basin alluvium may enhance the potential for differential subsidence and earth fissure development in some areas of very large and very rapid subsidence.

8.6.4 Preliminary Evaluation of Future Hazard and Risk to the HSR due to Subsidence-Induced Fissures or Faults

8.6.4.1 General

For the current discussion, “hazard” may be understood as the likelihood of a subsidence-induced fissure or fault occurring beneath or adjacent to the HSR Alignment. “Risk” may be understood as the probability that such an event will cause reduction in performance or loss to the HSR, and the level of this performance reduction or loss.

Detailed quantification of historical subsidence along the HSR Alignment is lacking, with just InSAR ((2007-2010 and 2014-2016) and comparative topography (e.g., LiDAR [USACE in 2008, Dragados in 2015] and IFSAR [USACE in 2008] vs. RTK [AFW in 2016]) datasets for relatively recent periods, up to several years, being available. Therefore, location-specific estimations of recent localized ground strains are just beginning to become feasible. Magnitudes and distribution of historical and current tensile strains in the basin alluvium are unknown. Given that caveat, and given the lack of documented earth fissures along the HSR Alignment, earth fissure risk along the HSR Alignment is anticipated to be low, based on the guidance presented in Table 8-2. Only effective monitoring of subsidence can assure that future areas of tensile ground strain will be identified as subsidence continues, and thus the future risk can be managed. Exceptions to low earth fissure risk zones are specific areas where a low-moderate rating may be appropriate due to specific geologic conditions. Low-moderate risk locations may include portions of the shoulders of the large subsidence zone indicated by L-band InSAR, (in the vicinity of viaducts near Hanford and Alpaugh, see Plate 8-8), or more specifically indicated by combined LiDAR with RTK, and the HSR Alignment crossing of the Poso Fault alignment. These and other areas of fissure risk might be observed to change over time as effective future monitoring provides specific information concerning localized differential subsidence. Over time, a continuation of recent differential subsidence trends may increase risk rating to ‘moderate’ in some locations. Earth fissure hazard and risk does not encompass possible impacts of differential subsidence on specific structures such as viaducts and retained embankments.

The risk associated with subsidence-induced fissures in the SJV has been, and still is, generally considered to be relatively low if effective monitoring of subsidence provides assurance that zones of significant differential subsidence are not developing over time along the HSR Alignment. Because of large magnitudes of subsidence occurring rapidly along portions of the HSR Alignment, it does not seem prudent to consider this risk to be negligible, as further discussed below.

8.6.4.2 Subsidence-Induced Fissures

First, regarding the hazard level, at least three subsidence-induced fissures have been documented about 3½, 5½, and 9 miles from the HSR Alignment; see Plate 8-3 and Table 8-1 (presented on Plate 8-11) for recent differential subsidence conditions in the general area of these historical fissures. Given that current subsidence rates in the Hanford-Corcoran Subsidence Bowl are greater now than when the historical fissures developed, and that the total magnitudes of recent subsidence are likely approaching and almost certainly will exceed 1900s Historical Subsidence, it is possible that new fissures will develop in this area in the future. Tom Holzer and Michelle Sneed of the USGS each concurred on this opinion.

On the other hand, it is also generally agreed that is not likely there will be a large number of new fissures in this area, and therefore the likelihood of such fissures occurring beneath or immediately adjacent to the HSR Alignment is considered to be relatively low, but not negligible. Distortion of the track at differential subsidence magnitudes below the threshold for earth fissure development may begin to impact comfort of the high-speed train ride before ground strains reach the point of initiating earth fissures.

Assuming future fissures do develop, it is likely that the preceding tensile strains and tensile cracks will develop relatively slowly. Such cracks could then enlarge relatively rapidly in the event of flooding or heavy rainfall. This condition could be of special concern in areas where flood inundation for extended periods of time is anticipated.

In the relatively unlikely event of earth fissure development along the HSR Alignment, the risk to HSR embankments could include the development of tensile cracks in the embankment and negative impact on train rides at high-speed. Initially, this may not lead to any deterioration of the track, but if left unchecked (unmitigated), heavy rainfall (or flooding if this portion of the HSR Alignment is in a floodplain) could result in erosion or crack collapse that could lead to development of significant depression or settlement of the trackbed.

Similar to potential cracks in the embankment, if ground cracks are left unmitigated, heavy rainfall (or flooding if this portion of the HSR Alignment is in a floodplain) could result in erosion or crack collapse that could lead to the development of significant depression of the ground beneath the embankment. If this is left unchecked, the depression could propagate upward toward the trackbed.

The risk (albeit a relatively low risk) that the fissure may pose to the HSR may be reduced to an acceptable level by monitoring and, in the event that tensile strains are observed to be high or tensile cracks are observed, taking appropriate mitigation measures as discussed in the following sections.

8.6.4.3 Hazard and Risk to the HSR from Subsidence-Induced Faults

Regarding the hazard level for subsidence-induced faulting along the HSR Alignment, one occurrence of subsidence-induced faulting is known to have occurred in the SJV, at the PPCF as mapped by Holzer (1980) about 0.5 – 1.5 miles northeast from the preexisting PCF (Plate 8-5). It is unlikely that any such faulting would occur except in the general vicinity of the PCF, and possibly at the shoulders (edges) of the general Corcoran Subsidence Bowl in the vicinities of Deer Creek and perhaps Hanford. We do not believe that available information can rule out the possibility of future subsidence-induced faulting in the vicinity of the PCF or the subsidence bowl shoulders (edges), including where it crosses the HSR Alignment.

If such faulting were to develop, the differential movement would be expected to be relatively slow, with similar rates of subsidence to other areas within the Hanford Corcoran Bowl, but this differential could be concentrated within a relatively narrow zone. However, as with the PPCF, which was located about 0.5 – 1.5 miles from the preexisting PCF, it may be difficult to anticipate where such differential movement may occur with currently-available information.

Regarding the potential risk due to faulting, the concentrated strains could result in a “bump” developing in the tracks. We anticipate that potential rate of differential movement will be relatively slow, so any such “bump” would develop slowly. If left unchecked it could potentially impact rider comfort or, eventually, require slowing of trains for safety.

The risk (albeit a relatively low risk) that a potential fault may pose to the HSR may be reduced to an acceptable level by monitoring and, in the event differential movement is observed, taking appropriate mitigation measures as discussed in the following sections.

8.6.5 Feasible Monitoring Approaches for Potential Fissures and Faults

The following represents a preliminary discussion of monitoring with respect to fissure and fault considerations. These and other aspects of monitoring will be addressed in Section 9.0. The following Table 8-3 lists methods that may be useful in monitoring conditions that may correspond to potential fissure development.

For any monitoring methods, proper implementation will be needed, along with criteria to evaluate critical observed values and a plan for how to report and respond to the observations.

Table 8-3 Feasible Monitoring Approaches

Method	Potential Value to Fissure Prediction or Identification	Useful Regarding:							
		Subsidence	Slope	Curvature	Tensile Strain	Crack Formation at Depth	Groundwater Levels	Visible Expression	Horizontal Displacement
InSAR	Good resolution of vertical deformation; need to consider relative pros/cons of L-band, C-band, or X-band	++	++	++	+				
UAVSAR	Good resolution of vertical and horizontal deformation; will require contracting for each flight	++	++	++	++				
LiDAR	Expensive for each date flown, but good resolution	++	++	++	+			+	
Optical Survey	Need to initially establish network of close-spaced (50-100 foot) monuments or control points, then labor-intensive for each reading of network. Vertical sensitivity better than GPS	++	++	+	+			+	
GPS	Need to initially establish monuments or control points, then labor-intensive for each reading.	++	++	++	+++				+++
CGPS	Relatively expensive for installation at single location; good to use available CGPS to calibrate InSAR or UAVSAR. Capable of real-time monitoring. Accuracy of InSAR may be improved with addition of Radar Transponders paired with CGPS (or GPS) stations	+++							
Piezometer	Consider standpipe or vibrating wire (expensive installation, labor-intensive to read unless remote reporting included). Water levels not directly relevant to HSR, but water level monitoring data is a key to understanding and predicting subsidence. Can be capable of real-time monitoring.						+++		

Method	Potential Value to Fissure Prediction or Identification	Useful Regarding:							
		Subsidence	Slope	Curvature	Tensile Strain	Crack Formation at Depth	Groundwater Levels	Visible Expression	Horizontal Displacement
Borehole Tilt Meter	Show angular tilt of near-surface ground, but this may be different from ground-surface tilt due to potential shear strains. Very high sensitivity, first indicator to identify movement or trend changes**.** Relatively expensive for single location, but may be useful where critical area is identified. Capable of real-time monitoring.	+	+	+	+				++
Tape Extensometer	Useful at location and in direction established. Primarily deployed as a monument array (typical 50-100-foot spacing) across feature when other evidence indicates imminent earth fissure development or after earth fissure is identified. Labor-intensive to read. Use with optical survey.				+				+++
Fiber Bragg Grating	Need to confirm capabilities.				+?				
Optic Interferometric Extensometer	Need to confirm capabilities.				++?				
Instrumented Train	With accelerometers and tilt meters, it may be possible to monitor track vertical and horizontal curvature. Need to confirm sensitivity.		++	++					+++
Seismic Refraction	May identify crack presence (or, when repeated over time, initiation) at depth before visible at surface IF crack location is spanned by geophones. Labor intensive geophysical operation, usually applied when other evidence indicates potential or imminent earth fissure development.					+++			

Method	Potential Value to Fissure Prediction or Identification	Useful Regarding:							
		Subsidence	Slope	Curvature	Tensile Strain	Crack Formation at Depth	Groundwater Levels	Visible Expression	Horizontal Displacement
Passive Geophone	May identify crack initiation at depth before visible at surface IF crack location is spanned by phones and seismic energy propagation is properly oriented.					+			
Precision electronic horizontal extensometer	Expensive / very expensive for measuring movement across known specific earth fissure location. Real-time monitoring capable.				++				+++
Trench or test pit	Confirm presence or absence of earth fissuring by observing and mapping trench or pit sidewalls. Destructive test, Occupational Safety and Health Administration regulations on work in trench							+++	
Direct Inspection	Look for signs of distress, etc.							++	

Description of rating system:

'+' Limited data quality and/or limited usefulness for indicated parameter.

'++' Good data quality and usefulness for indicated parameter.

'+++' Very good data and very useful for indicated parameter.

* Note that real-time monitoring will require remote telecommunications (wireless or wired) along HSR Alignment.

It should be noted that only some of the instrumentation and monitoring methods summarized above are relevant or suitable to real-time monitoring. Potential real-time monitoring methods include CGPS, remote piezometers, borehole tiltmeters, electronic (including optical) strain measurement methods and single-point horizontal electronic extensometers. Real-time subsidence monitoring networks have been applied or are in use; one example is a monitoring system to warn of subsidence that could indicate impending collapse of an abandoned brine

cavern in Carlsbad, New Mexico (AMEC 2014b). Piezometers, borehole tiltmeters, pressure gauges and a near real-time micro-seismicity network are part of this system.

8.6.6 Potential Mitigation Approaches for Future Fissures and Faults

Procedures have been developed to assess the potential for identification and assessment, and for mitigation of subsidence and earth fissuring for various situations and facilities. An example is the *Procedural Documents for Land Subsidence and Earth Fissures* (AMEC 2011a) prepared for the Flood Control District of Maricopa County for flood control structures. Mitigation at these structures, either on an expedited basis for an unsafe dam condition (Interim Dam Safety Mitigation), or during design to address anticipated future conditions, is addressed utilizing a failure mode and effects analysis structure. Mitigations have also been designed at locations where earth fissures intercept roadway alignments and other infrastructure; the mitigation effort is scaled to the risk at these facilities.

8.6.6.1 General

If fissures are to develop, they are expected to be in response to slow buildup of tensile strains, followed by crack initiation and propagation (initially the crack is likely to be no more than 1/8 to 1 inch wide, based on the investigation of the Pixley Fissure No. 1 [Guacci, 1978]), and then rapid enlargement in response to flooding or rainfall that causes piping, collapse, and erosion.

Depending upon situation details, appropriate mitigation of a potential fissure or fault condition may range from characterization with likely enhanced monitoring to engineered construction or reconstruction. It is likely that the most important mitigation action concerning potential development of an earth fissure will be to keep surface water away from the zone of significant ground tension and possible cracks, to fill any cracks that are noted, and then prevent surface water from accessing those cracks.

Regarding the hazard level for subsidence-induced faulting along the HSR Alignment, one occurrence of subsidence-induced faulting is known to have occurred in the SJV, at the PPCF about 0.5 – 1.5 miles northeast from the preexisting Poso Creek Fault. In our opinion it is unlikely (although not impossible) that any such faulting would occur except in the general vicinity of the Poso Creek Fault (i.e., possibly within about 1.5 miles, as with the Pond-Poso Creek Fault), and at the shoulders of the Corcoran Subsidence Bowl near Deer Creek to the south and Hanford to the north. We do not believe that available information can rule out the possibility of future subsidence-induced faulting in the vicinity of the Poso Creek Fault, including where it crosses the HSR Alignment.

If such faulting were to develop, the differential movement would be expected to be relatively slow, possibly on the order of 0.2 to 1 inch per year, and this differential could be concentrated within a relatively narrow zone. However, as with the Pond-Poso Creek Fault, which was located about 0.5 – 1.5 miles from the preexisting Poso Creek Fault, it may be difficult to

anticipate exactly where such differential movement may occur with currently available information. The risk (albeit a relatively low risk) that a potential fault may pose to the HSR may be reduced to an acceptable level by monitoring and, in the event differential movement is observed, taking appropriate mitigation measures. Proper monitoring of local differential subsidence (e.g., InSAR, UAVSAR, surveys, etc.) and instrumented train vertical accelerations should be able to identify any developing condition before it becomes a problem. Mitigation will likely consist primarily of track releveling.

Regarding the potential risk due to faulting, the relatively concentrated strains could result in a "bump" developing in the tracks. AFW anticipates that potential rate of differential movement will be relatively slow, so any such "bump" would develop slowly. If left unchecked it could potentially impact rider comfort or, eventually, require slowing of trains for safety.

8.6.6.2 Guideways

In general, the HSR guideways (including embankments and MSE walls) through subsiding areas will be constructed with ballasted track on embankments. This will allow re-ballasting to maintain or reestablish appropriate grades and superelevations.

Where convex-upward change in ground curvature or tensile strains are observed to be approaching what may be critical values, it may initially be appropriate to increase monitoring frequency or precision, possibly by adding methods. For instance, if InSAR is the primary monitoring method being used to track subsidence and an area of high curvature or tensile strains is noted, adding Brillouin Optical Time-Domain Reflectometry (BOTDR) may be a useful supplement to the InSAR; alternatively, ascending and descending passes of InSAR may be analyzed for horizontal ground displacements to evaluate tensile strains; ground-based extensometers may be added in the critical locations, the spacing of monuments may be made more frequent, and passive geophones may be added to search for areas of crack development at depth.

If tensile cracks are identified, it may be appropriate to mitigate these by pressure grout injection. Mitigation should include means to prevent surface water from accessing the area of tensile cracking.

If ground fissures or compaction faults are discovered beneath or immediately adjacent to the HSR Alignment, they should be immediately evaluated for present safety as well as for the likelihood of expansion that could impact track safety. If distortions in the track are identified, it may be necessary to slow trains accordingly in that area, or to temporarily halt service until safety can be confirmed or restored.

Ground fissures mitigation options should be carefully evaluated by appropriate Authority personnel or consultants. Mitigation may include pressure grout injection or other forms of embankment repair.

8.6.6.3 Viaducts

If there are signs of critical tensile strains or if convex upward change in ground curvature is observed during monitoring in the vicinity of any viaduct (particularly those supported by deep foundations), appropriate Authority personnel or consultants should immediately be notified and the condition should be evaluated for the possibility that induced slopes, a compaction fault, or a fissure could affect the foundation performance.

We anticipate that viaduct proposed for in a location with more than 0.1 to 0.25% induced slope change forecast for the next 20 years may need to account for this anticipated strain in the design. Possible design measures may include:

1. Use ballasted viaducts to allow for ballast releveling to smooth the train ride.
2. Use adjustable bent supports that can be adjusted to counteract or smooth differential subsidence. This has been implemented in the Taiwan high-speed rail.
3. Increase ductility or flexibility of structures to be able to accommodate anticipated strain.

If a viaduct will be located in an area where there is a potential for compaction faulting to develop, means to adjust or maintain flexibility in viaduct structural connections to mitigate larger differential subsidence may be needed.

- As illustrated in Plates 8-8 and 8-9, it tentatively appears that such a situation may be developing at the Deer Creek Viaduct.
- Currently-available information is insufficient to assess (or to rule out) whether a similar situation may be present at proposed viaduct locations in the Hanford area.

In each of these locations, monitoring by additional instrumentation (such as optical survey and perhaps tape extensometry, see Sections 9.7 and 9.8) would likely be sufficient to provide data over a period of one to a few years to better-assess this potential.

8.7 OTHER SUBSIDENCE OR SETTLEMENT MECHANISMS

Although this GSS has focused on Subsidence induced by groundwater drawdown, other causes of subsidence or settlement may occur within the SJV, as discussed in the following subsections.

8.7.1 Hydrocompaction

Hydrocompaction refers to the volumetric compression of loose dry soils that may occur upon initial wetting. It may refer to two different scenarios:

1. Clayey fills that are placed dry of optimum moisture (as defined by ASTM D 1557) may contain a flocculated structure of clay particles. This structure can be somewhat metastable and collapse or partially collapse when the soil is wetted, which may occur due to percolation of surface water such as from rainfall, irrigation, or landscape watering, or submersion such as within flood plains or in the first filling of an earth dam.

2. This potential can be largely mitigated by compacting soils at a high-enough water content, by using primarily granular soils, or (where viable) by preventing future wetting.
3. Wind-deposited loess or debris-flow deposited clayey soils may initially be in a very loose and potentially metastable soil structure, which can be subject to collapse or partial collapse on wetting.
4. Although relatively uncommon in alluvial soils, the potential for wind-deposited soils with collapse potential should be investigated within some areas of the HSR Alignment.
5. Similarly, loose deposits from debris flows are not likely to be present in most of the SJV, but they are known to be present in some locations along the western edge of the SJV/eastern flanks of the coast range where they about the SJV. Soils in these areas should be evaluated for this form of hydrocompaction or collapse.

Recommendations to address hydrocompaction should be developed and implemented by each design-build contractor.

8.7.2 Oil and Gas Extraction

Subsidence due to extraction of oil and gas has been known to occur within the SJV, primarily to the southwest of Bakersfield, and to a lesser extent to the north of Bakersfield (Bawden et al., 2003; Fielding et al., 1998). It is not thought to be a major factor along the HSR Alignment.

8.7.3 Tectonic Subsidence

As tectonic plates move, they may have both horizontal (primary) and vertical (secondary) components of movement. Where one plate abuts another plate, differential movement often gives rise to the formation of faults where the slippage occurs. Faults may also occur within a plate when vertical or lateral stresses exceed the strength of the plate material and the plate breaks in to separate blocks. The potential for fault offset is being evaluated under a separate study for the Authority and is not further evaluated for this GSS.

Away from faults, tectonic movement has the potential to cause ground drift in horizontal or vertical directions. In general, the magnitude of tectonic movement is small enough that it only becomes relevant to transportation infrastructure at the locations of fault crossings. This is thought to be the case in the SJV; one study of satellite-based GPS records that includes the southern SJV indicates that the area may be subsiding slowly, on the order of 2 mm per year or less (Howell et al., 2016). We do not anticipate that this movement will cause distress to the HSR project.

8.7.4 Organic Soils and Peat

Peat and soils with a high organic content may lead to ground subsidence through two primary mechanisms:

1. The peat or organic soil structure is by nature quite compressible, and when stresses increase (e.g., due to construction of an embankment or structure above them, or due to

groundwater drawdown), they will compress or lose volume, and the ground above will settle or subside.

2. Peat or other organic soils are biodegradable; when they are exposed to oxygen in the air, they will decay and actually lose mass through off-gassing of carbon dioxide. Most peats and organic soils are formed below water in lakes, rivers, or bays. As long as they stay submerged, oxidation tends to be fairly slow, but if groundwater is lowered such that they are exposed to air, they may decay relatively quickly, potentially leading to very large magnitude subsidence.

Peat and other organic soils are not likely to be present in most of the HSR Alignment. However, the design-build contractors should evaluate the possibility of their presence, particularly near river crossings, ponds, or marshy areas and develop recommendations to mitigate any potential hazards that are identified.

9.0 INSTRUMENTATION AND MONITORING OPTIONS

Effective characterization and monitoring of subsidence along the HSR Alignment and vicinity is of critical importance. Aspects of monitoring and instrumentation for monitoring are addressed below and in Appendix B. The immediate reason for monitoring subsidence and associated horizontal movement will be to better understand the causes, rates, magnitudes, and areal distribution of past and ongoing subsidence in order to better forecast future subsidence and how this may impact the HSR. By alerting HSR operators to developing adverse conditions due to subsidence so that mitigation measures (appropriate to the developing conditions) can be implemented before such conditions impact operations, instrumentation and monitoring will provide a means of reducing the risk of potential adverse impacts related to subsidence. Future monitoring will inform operators of any potential developing conditions where changes in track geometry or subsurface conditions may call for increased monitoring, and/or mitigation measures.

Preliminary recommendations addressing monitoring and evaluation methods, as well as management and distribution of monitoring results, are provided for pre-construction, during-construction, post-construction, and operational phases of the HSR project in Appendix B. Methodologies discussed include visual inspection and reconnaissance, survey (including optical and GPS survey methodologies and integration with other survey networks), InSAR, UAVSAR, LiDAR, satellite altimetry, high-resolution aerial imagery, groundwater elevations, tape extensometers, electric horizontal extensometers, compaction extensometers, borehole tiltmeters, seismic methods, fiber optic cable-based strain measurements, and instrumented trains.

In general, differential subsidence along the HSR Alignment will change the slope and superelevation of the rail; horizontal ground movement is expected to develop along with the vertical subsidence, which will change the alignment of the rail. On the other hand, if subsidence were uniform everywhere (i.e., a hypothetical situation in which there was no differential

subsidence between locations), it might not have a significant impact on the HSR. In reality, subsidence will never be completely uniform, so all subsidence will be associated with some degree of differential subsidence. Instrumentation and monitoring are intended to provide documented quantification of subsidence. Subsidence, induced slope, and induced curvature profiles along the HSR Alignment have been addressed in Section 4.1 of this report. Monitoring will provide the information necessary to apply means of reducing the risk of potential adverse impacts related to subsidence.

In the context of monitoring, “hazard” is used to indicate any source of potential damage, and “risk” is used to mean the probability or chance that this potential damage could actually occur. Future monitoring will inform the Authority and its consultants or operators of any potential developing conditions where changes in track geometry or subsurface conditions may call for increased monitoring and/or mitigation measures.

Monitoring will include evaluations of pre-construction (including past records such as survey data archived satellite InSAR imagery, etc.), during construction, post-construction and operation phases.

9.1 DATUMS FOR ELEVATION REFERENCING

In the vicinity of the Corcoran Subsidence Bowl, three potential classes of datums for elevation referencing could be considered, each with its own advantages and limitations. These three classes of datums include: (1) GPS-based observations using GEOID09 and CGPS ellipsoid heights; (2) reference to a “stable bedrock site” such as in the Sierra foothills; or (3) points established in the “firm” (although possibly subsiding) ground in the vicinity of the HSR Alignment. The implications of datum selection to the HSR design and construction control will be discussed below in Section 9.1.4.

9.1.1 GEOID09 and CGPS Ellipsoid Heights as Datums

For the HSR project, control points have been established at approximately 2-mile intervals along the length of the HSR Alignment. Within CP 2-3, these control points were field located in 2010 to 2011 as documented in a Record of Survey and Control Monument Data published in 2014 (Authority 2014b). As noted in this document, these control points elevations were determined as follows:

> “The orthometric height was determined by two, one-hour GPS observations, using GEOID09 and CGPS ellipsoid heights.”

Although these control points were accurately located at the time of their field-survey, some of them have been subsiding by as much as a foot per year through late 2015 (e.g., see Dragados 2015b), but by as much as 20 inches during the period of May 2015 to May 2016. Thus, many of the control points located within the Corcoran Subsidence Bowl were field-surveyed in 2010

to 2011, but by the time they were published in 2014, some of these control points may have subsided by as much as 3 feet or more in elevation from the published elevations. By fall 2015, some points had settled more than 5 feet (Dragados 2015b).

GPS readings are generally related to the GEOID09 and the ellipsoid; however, GPS readings may be corrected based on apparent elevations of nearby CGPS stations. If these CGPS stations are not regularly updated to account for subsidence, they may provide misleading data.

9.1.2 Control Points in "Stable Bedrock"

Although much of the ground along CP 2-3 is subsiding, bedrock in the Sierra foothills to the east are not. However, the entire Pacific Tectonic Plate is moving to the northwest at a rate of about 14 mm/yr. (Note that this tectonic drift includes the "stable" bedrock of the foothills as well as the SJV.) For any survey control points, whether in the foothills or the SJV, this tectonic drift should be accounted for in controlling locations along the HSR Alignment.

9.1.3 Control Points on "Firm Ground" near HSR Alignment

Survey control traditionally measures location (horizontal and vertical) with reference to an agreed-upon, defined, and stable datum consisting of a physical feature (such as a pipe or block of concrete) anchored in "stable" ground. Normally control points can be established as the project datums in the general vicinity of the project, and then survey locations can refer back to these control points as assumed stable locations.

However, within the Corcoran Subsidence Bowl, the ground surface is subsiding by as much as a foot or more per year, although the magnitude and rate varies somewhat irregularly along the HSR Alignment. If project elevations were to be related to the nearest control point, the actual constructed elevation of the project would be lower by as much as a foot for each year after the original design grades were established.

In addition, if each control point were to be used to control construction grades for the portion of the alignment that is nearest to it, there would be a point of discontinuity at the location where elevation control was transferred to the next control point, unless measures are taken to taper this transition.

9.1.4 Implications of Subsidence on Datum Selection

The concern to the HSR project may be described by considering a hypothetical Point A along the CP 2-3 alignment, near the center of the Corcoran Subsidence Bowl. For simplicity of arithmetically illustrating the issue, assume the original surveyed elevation was 200 ft at Point A in 2010. Let's say the preliminary design as was included in the RFP called for 5-ft-tall embankment, to Elev 205. However, by the time the RFP was released in 2014, Point A may have subsided to Elev 196, and by the time the CP 2-3 Contractor was beginning to prepare final design (say in 2015) Point A may have subsided to Elev 195. By the time they began

embankment construction (say 2018) Point A might have been at Elev 192, by the time they completed construction (say 2019) it might have been at Elev 191, and by the time they were ready to turn it over to the Authority (say 2020) it may have been at Elev 190.

If the original target embankment grade was held to Elev 205 based on the GEOID09 and GPS ellipsoid:

- At the time the final design was beginning in 2015, the embankment would appear to need to be 10 feet tall (rather than the original 5 feet) to reach Elev 205, but if it were built 10 feet tall, the final elevation in 2020 would be Elev 200 (rather than 205).
- If the embankment were built to Elev 205 at the end of construction in 2019, it would need to be 14 feet tall, but a year later when it is turned over to the Authority it would be Elev 204 (1 foot too low), although it would be 14 feet tall (9 feet taller than originally intended).
- In anticipation of forecast subsidence, the embankment could be built to Elev 206 in 2019, so that it would be at (approximately) 205 in 2020 (to the extent the rate of subsidence could be forecast reliably). However, over the next several years it would continue to subside, until it might be only Elev 195 in 2030.

9.1.5 Recommended Approach to Survey Control for Design and Construction

Because of the problems associated with trying to tie the design elevations to GEOID09 elevations, we recommend that local “subsiding” or “moving” control points be established (perhaps those monuments that were set for the RFP [Authority 2014b]), and that each be defined as the project datum in a piecewise fashion (e.g., each to serve as the project datum for the for the portion of the alignment nearest to it).

To solve the problem of grade discontinuity at each location where transferring control from one control point to the next, the construction survey control should taper the elevation adjustments in a linear faction between each pair of control points.

Because this sort of construction survey control is non-standard, non-intuitive, and complicated, the Design-Build Contractor should develop a comprehensive plan for how to calculate, implement, and control quality for the layout of the survey control, particularly the tapering between adjacent control points that are subsiding at differing rates.

9.1.6 Recommended Approach to Survey Monitoring of Subsidence

Although construction control should be based on local control points, some of which will be known to be subsiding on an on-going basis, subsidence monitoring should be tied to and reported in relation to GEOID09 elevations so that actual magnitudes and rates of subsidence will be reliably tracked.

Surveying for construction control and surveying for subsidence monitoring should be coordinated and correlated.

9.2 GLOSSARY OF SELECT TERMS RELATED TO INSTRUMENTATION AND MONITORING

The following list presents working definitions of select significant words related to monitoring.

- **Subsidence:** subsidence is used to refer to lowering of the ground surface caused by withdrawal of groundwater.
- **Settlement:** settlement is used to refer to lowering of the ground surface caused by loading from embankments, foundations, or other sources.
- **Accuracy:** How close a measurement is to the quantity's true value.
- **Precision:** The reproducibility or repeatability of the measurement.
- **Real-Time Monitoring:** System in which an automated measurement, data collection, and data transmission system provides access to data on an on-going basis, very shortly after the measurement is made.
- **Instrumentation:** To install instruments that will enable measurement of parameters relevant to subsidence.
- **Monitor:** Watch closely in order to observe, record, or detect. Monitoring may be used to determine if a process is starting to approach a limit (e.g., if the subsidence-induced slope change is approaching a value that may be significant for railroad curvature or for fissure formation).
- **Measurement:** The act of quantifying the actual traits of something, such as a magnitude of subsidence. Measurement could be used to determine the actual value of the characteristic in question. Measurement is often a key component of monitoring.

9.3 PARAMETERS TO MONITOR

This section presents a list of parameters that can be monitored for, with brief definitions and the relative importance of each parameter.

9.3.1 Subsidence and Settlement

Subsidence is the primary subject of this report, but Settlement induced by factors other than groundwater drawdown is discussed due to the need to distinguish it from Subsidence.

Subsidence itself has or is directly related to several parameters:

- **Magnitude:** measure of how much the ground has subsided overall, or during the period under discussion.
- **Rate:** how fast the subsidence is occurring per time interval, e.g., typically per month or per year.
- **Differential subsidence or subsidence-induced slope:** the rate at which subsidence changes across a horizontal distance, e.g., typically reported in feet per foot, percent, or radians.
- **Subsidence-induced superelevation change, cant (in the UK), or tilt:** differential subsidence in the direction transverse to the rail.

- "**Twist**" or "**cant gradient**" or "**superelevation gradient**" is the rate of cant change per unit length of track.
- **Subsidence-induced vertical curvature:** the rates at which differential subsidence changes across a horizontal distance, e.g., typically reported in (feet per foot) per foot. Vertical change in curvature may be convex upward or concave upward.
- **Radius of curvature:** Reciprocal of vertical curvature, typically reported in feet or miles.
- **Vertical acceleration:** Vertical acceleration is induced when a train travels through a vertical curve with the acceleration being equal to V^2/R where V is the velocity of the train and R is the radius of curvature. Generally reported in fractions or percent of gravity (or "g").
- **Subsidence-induced horizontal curvature:** analogous to vertical curvature, differential horizontal ground movement associated with subsidence will subtly change the alignment of the tracks. The horizontal curvature is the rate at which the alignment changes with distance along the tracks, e.g., typically reported in (feet per foot) per foot, or radians per foot. Vertical curvature may be to the right or to the left.
- **Radius of curvature:** Reciprocal of vertical curvature, typically reported in feet or miles.
- **Horizontal acceleration:** Horizontal acceleration is induced when a train travels through an induced horizontal curve, with the acceleration being equal to V^2/R where V is the velocity of the train and R is the radius of curvature. Generally reported in fractions or percent of gravity (or "g").
- **"Bumpiness":** this can result from regular or random changes in subsidence, which generally results from variations in subsurface stratigraphy and/or groundwater drawdown, and varying prior stress histories of the compressible soils. (This likely will be best monitored by analyzing the fluctuating or undulating accelerations of an instrumented train passing over track where variable differential subsidence is occurring.)

Horizontal movement often accompanies differential subsidence (e.g., see Section 4.0).

Horizontal movement has or is associated with the following properties:

- **Differential horizontal movement** occurs because horizontal movement is not uniform everywhere. This can lead to:
    - **Tensile strain**, where the soils is being stretched horizontally. This is typically reported in strain units of percent strain or microstrain. (Strain is differential movement divided by the length over which the differential movement occurs. Percent strain or microstrain are units of strain multiplied by 100 or by 1,000,000, respectively.) However, it must be understood that typical measurements of 'tensile strain' using GPS survey or extensometry are actually measurements of displacements between discrete points; such measurements do not account for concentration of strain in discrete zones between measurement points.
    - **Compressive strain**, where the soil is being compressed horizontally.
- **Horizontal curvature** occurs when there is differential horizontal movement. Horizontal curvature is typically reported as its reciprocal, i.e., as the horizontal radius of curvature, in units of feet or miles.

- **Cracks or tensile cracks:** In soils capable of exhibiting tensile strength, these can develop when tensile strains exceed the small capacity of a soil to stretch, typically on the order of 100 to 700 microstrain. For survey monuments spaced at distances of 1,250 feet, 100 to 700 microstrain represents an increase in distance between adjacent monuments of about 1 to 8 inches.
- **Earth fissure** gullies can develop when water is allowed to flood or flow through open tensile cracks, resulting in collapse of the crack and/or erosion of material from the crack. This can cause a significant fissure or ground depression along the alignment of the crack. Earth fissure gullies can also exhibit vertical displacement similar to compaction faults.
- **Subsidence-induced compaction faults** can develop when differential subsidence is significant in the location of a preexisting plain of weakness, typically a preexisting fault. The preexisting fault may also function as an aquitard, leading to a significant difference in the groundwater elevation across a narrow distance, which can in turn cause localized differential subsidence.

9.3.2 Groundwater Levels

As detailed in Section 4.0 and elsewhere in this report, subsidence is an effect of excessive groundwater withdrawals resulting in compaction of unconsolidated and semi-consolidated materials that form aquifer systems in basin alluvium. Compaction occurs primarily in fine-grained soils (aquitards) within the basin aquifer system, although coarse-grained soils (aquifers) contribute minor amounts of compaction. However, the connectivity of coarse-grained soils within an aquifer system, and the rate at which the fine-grained soils can be drained by the coarse-grained soils, provide the means for groundwater to drain from the fine-grained soils and thus control rates of subsidence. Excessive groundwater withdrawals remove water of compaction from aquitards within the aquifer system that results in inelastic compaction and land subsidence. Thus, although groundwater levels do not directly impact the HSR, they are significant because of their link to subsidence. The following parameters include groundwater levels.

9.3.2.1 Groundwater Aquifer Level Measurement

Groundwater withdrawals are the driving factor of the ongoing subsidence. Most of the groundwater that is being extracted is from lower aquifers, typically below the Corcoran clay. A limited amount of pumping is still occurring in upper aquifers where groundwater conditions may range from unconfined to confined. Groundwater monitoring should include upper and lower aquifers and a range of depth in the lower aquifers.

Manual readings performed on a regular schedule may provide adequate monitoring at some wells; wells located at critical or selected representative locations should be equipped with automatic groundwater level monitoring pressure transducers for remote, real-time monitoring of those groundwater levels that are the driving mechanism of subsidence. Specific

recommendations for water level monitoring wells will be made after an inventory of available existing wells has been performed.

It is anticipated that there may be existing irrigation wells within the HSR Alignment right of way; such existing wells at relevant locations that are screened at appropriate depths should, if suitable, be re-purposed as groundwater level monitoring sites. Such re-purposing would require access to construction information and may require downhole video logging and/or inspection(s) of the well condition.

9.3.2.2 Shallow Groundwater Level Measurement

Shallow groundwater level measurements and monitoring are more relevant to addressing construction settlement issues rather than subsidence. Since settlement caused by construction will need to be separated from subsidence, shallow groundwater level measurements will be a relevant portion of the overall construction as well as the subsidence monitoring program. It is anticipated that piezometers and shallow monitoring wells will be installed as part of the geotechnical investigation and construction monitoring program; information from that monitoring should be incorporated into the subsidence monitoring program.

9.4 SETTLEMENT CAUSED BY CONSTRUCTION ACTIVITIES, ETC.

Settlement will also be caused by the placement of new loads over compressible soils. New loads may include conventional or MSE embankments, structures on shallow foundations, or structures on deep foundations. Settlement will be the greatest directly beneath the embankments or structures, but ground beyond the edge of embankments or foundations will also settle, to a diminishing degree with increasing distance from the loaded area.

Based on historical data from the Pixley Extensometers Site as shown on Plate 9-1, significant subsidence along the HSR Alignment in Section CP 2-3 is primarily a deep phenomenon occurring in pumped aquifers below the Corcoran clay: for instance, during the early 1960s, about 97 percent of the subsidence resulted from compaction of soils deeper than 355 feet bgs. This historical behavior at the Pixley site is consistent with the recent land subsidence behaviors measured at CGPS P564 and summarized in Figure 9-1 below. In contrast to subsidence, settlement of the constructed HSR facilities will primarily be a shallow phenomenon. Assuming an isotropic soil material, Boussinesq equation based analysis of a continuous (strip) loading indicates that the stress bulbs encompassing 80%, 90% and 95% of surface loading (stress = 0.2q, 0.1q and 0.05q) extend to depths of about 2.5, 4 and 5.6 times the width of the load, respectively. The lateral extent of these stress bulbs from the load centerline is about 1, 1.4 and 2 times (respectively) the load width.

Influences of settlement in SJV basin materials, visualized as stress bulbs (Plate 9-1), are anticipated to remain above the Corcoran clay (where present), except where loading may be very wide and/or the Corcoran clay relatively shallow. Therefore, monitoring of settlement

should be focused on the HSR facilities and monitoring of subsidence should be offset from the ground-loading stress bulbs induced by those facilities. Determination of minimum offsets for subsidence monitoring points should account for the geometry, primarily the width, of the adjacent HSR facility or facilities. Minimum offset distances will also be influenced by changes in material strength with depth in the basin materials that modify distribution of stress and strain in the soil. In some locations, survey monitoring should extend beyond the limits of the HSR property, in which case appropriate permissions will need to be arranged.

9.5 FLOODPLAIN LEVELS

Design floodplain elevations were included in the contract documents, but because of ground subsidence these floodplains are likely to change and should be reevaluated and modified as appropriate. It must be understood that the magnitude and distribution of future subsidence has the potential to significantly alter the areal extend and depth of floodplains.

Review of available elevation data for the area around the HSR Tule River Viaduct shows significant inconsistencies in elevations over time (Plate 9-2). This could be caused by accumulation of historical and current subsidence that has not been accounted for in current floodplain mapping as discussed in Section 7.2 of this report. An existing network of benchmarks in the National Geodetic Survey (NGS) database (NGS 2016) documents that elevations at specific benchmarks were measured and recorded, mostly in the 1960s and 1970s. These benchmarks are commonly distributed at approximate 1-mile spacing through the basin. This network of existing (NGS recorded) benchmarks may be resurveyed using RTK GPS methods (typical accuracy of 20 mm plus 2 parts per million [ppm] distance from base station) to verify current elevations to assess floodplains with potential to impact the HSR Alignment. In critical areas, this survey may need to extend for several miles beyond the HSR Alignment. As subsidence continues in the future, RTK survey of portions of the NGS benchmark network should be incorporated into the annual monitoring program to assess whether flood risk at vulnerable points on the HSR Alignment is changing over time.

9.6 ANTICIPATED MOVEMENTS

Monitoring methods and frequencies of measurements need to be appropriate for the movement magnitudes and rates being measured. Accuracy and precision of movement measurement methods impose constraints on applicable measurement methods and upon measuring schedules (time between measurement readings). Anticipated ranges of ground movements to be monitored are discussed below.

- Vertical subsidence rates vary widely across the HSR Alignment. L-band InSAR (2007 to 2010), C-band InSAR (2014-2015), and several CGPS sites (2005 to 2016) indicate annual subsidence rates ranging from nil to about 1 foot per year or more. Furthermore, there is a distinct seasonal component to the subsidence rates as groundwater levels in the deeper confined aquifers below the Corcoran Clay Unit vary with groundwater

pumping that is tied to the seasons. Historical deep groundwater levels below the Corcoran clay have varied seasonally by as much as 60 to over 100 feet, while shallower water levels have varied by much smaller magnitudes (Lofgren and Klausing 1969). These seasonal groundwater level variations may result in an approximate sinusoidal component of up to about 1.5 inches to the vertical subsidence rate. That cyclical magnitude may represent elastic compression and rebound within the deeper alluvium; the elastic compression is maximum during the summer pumping period and the elastic rebound is maximum during the non-pumping winter period. Areas with relatively little inelastic subsidence currently occurring may still have cyclical elastic compression and rebound. An example CGPS time history is shown in Figure 9-1, and example time histories of subsidence at other CGPS sites are shown in Appendix A.

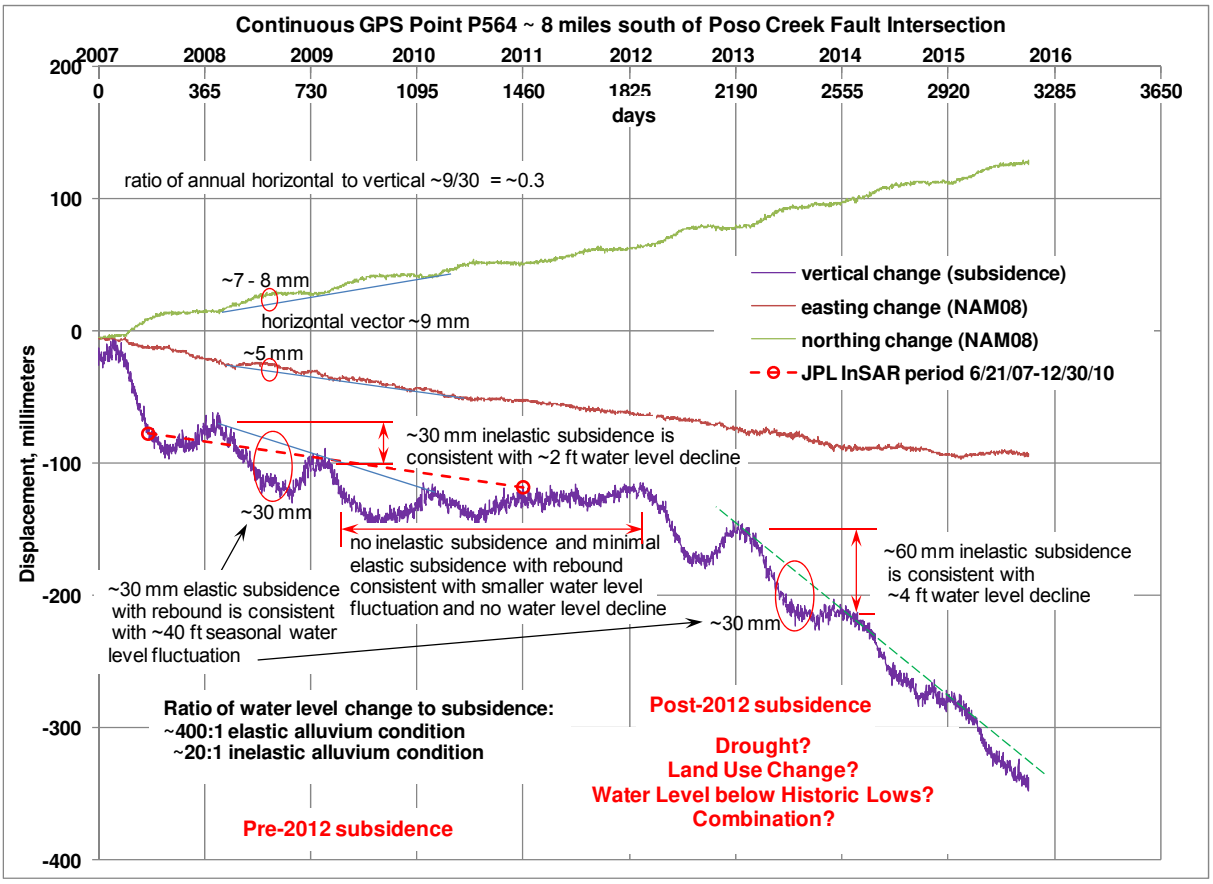

Figure 9-1: Example subsidence and northwest creep magnitudes and rates to be monitored

- Subsidence-induced horizontal ground movements may be anticipated where differential vertical subsidence occurs. Based on case studies (Burbey el al., 2006; Carpenter 1994) and modeling presented in Section 4.0 of this report, local horizontal ground movements may be up to as much as 10% to 30% of the local differential vertical subsidence, such as at a local subsidence cone around a pumping well. During periods of pumping and local subsidence (typically greatest in spring and summer), horizontal ground movements will tend to be toward the pumping well; during periods of less pumping (typically fall and winter), if subsidence rebound occurs, it may be accompanied by horizontal ground movements away from the well. Anticipated local horizontal

movements may typically be less than an inch. Horizontal movement (due to cycles of subsidence and rebound) may be cyclical as shown in the plot for CGPS Station P305 in Appendix A, or cyclical plus accumulative as shown in the plot for CGPS Station P056 in Appendix A.

- Differential horizontal ground movement greater than an inch may indicate developing ground strains, which could be associated with or lead to a possible compaction fault, tension crack, or earth fissure.
- Tectonic horizontal ground movement is also occurring, by which the North American Plate is moving to the northwest. CGPS data suggests the area appears to be moving horizontally toward the northwest at a rate of about 14 mm per year. Rates of movement may vary along the HSR Alignment in response to variations in the underlying tectonic movement; the SJV is near the boundary of the North American Plate marked by the San Andreas Fault just to the southwest. This tectonic horizontal movement will need to be accounted for in GPS measurements where the survey measurement frame of reference is not fixed to the ground.
- Anticipated "settlement" under the HSR embankments is independent of groundwater drawdown-induced land subsidence. As discussed in Section 3.1.5 of this report, the stresses induced by HSR embankments cause compression of relatively shallow soils and thereby induce settlement, but significant stress increments are not expected to extend more than two to three times the embankment width, whereas subsidence generally originates much deeper, such as below the Corcoran clay.
- Survey control monuments should be located as far away as is practical from the HSR embankments to minimize the potential for influences of embankment-induced settlement on subsidence measurements.

9.7 SUBSIDENCE FROM TECTONIC ACTIVITY AND OIL AND GAS EXTRACTION

Recent analysis of movement of the EarthScope PBO CGPS array (Howell el al., 2016; Grabowski 2016) indicates that the velocity of current vertical tectonic movement in the SJV ranges between about 2 mm per year upward at the San Andreas Fault to the west and the Sierra Nevada Mountains to the east, to about 1 to 2 mm per year downward in the SJV valley floor. Recent historical subsidence has been documented (Fielding el al., 1998) at the Lost Hills oil field to the southwest of the HSR Alignment. Short term very rapid rates of subsidence, up to about 1 mm/day, were interpreted from InSAR in the mid to late 1990s. Additionally, a review of aerial photographs shows signs of ground cracks or other linear features that may represent earth fissuring in the vicinity of the Lost Hills oil field, but these are far enough from the HSR Alignment that they need not be concern to the HSR. Being localized at the southwest edge of the SJV, the Lost Hills subsidence has no direct impact on the HSR Alignment. The HSR Alignment passes near the old Trico Field in the vicinity of Alpaugh and the Poso Creek Fault. As is shown in Figure 5-2, relatively minimal subsidence is currently occurring in the Trico Field area. Other oil fields are located in the area around Bakersfield (Bawden et al.2003) that may have experienced land subsidence in the past or present.

Contributions of tectonic and oil and gas extraction activity to subsidence appear to be minimal through the CP 2-3 Section of the HSR Alignment.

9.8 METHODS FOR MEASURING AND MONITORING SUBSIDENCE AND RELATED PARAMETERS

A number of methods are available for measuring and monitoring subsidence and the related parameters described in Section 9.2. The methods considered relevant are introduced in the following subsections. Table 9-1 summarizes each of the relevant methods, and for each method identifies:

- Capabilities and limitations;
- Whether data collection is continuous or intermittent;
- The project phase during which it may be applicable, e.g., pre-construction, during construction, post-construction, or during operations;
- Whether data acquisition is automated and whether data can be linked to an automated database;
- Costs have not been developed for this phase of the GSS;
- Frequency of spacing has not been developed for this phase of the GSS; and
- What parameter or hazard of interest is being measured or monitored.

9.8.1 Visual Inspection and Reconnaissance

Visual ground reconnaissance should be performed in locations where other monitoring results suggest that further investigation is warranted. Example procedures for performing visual inspection and reconnaissance are outlined in *Procedural Document: Geological Reconnaissance of Photolineaments and Terrestrial Search for Earth Fissures* (AMEC 2011b), and *Suggested Guidelines for Investigating Land-Subsidence and Earth Fissure Hazards in Arizona* (ALSIG 2011). High-resolution aerial imagery should be reviewed prior to conducting field inspections or reconnaissances. Inspections and reconnaissances should document ground cracks, potholes, indications of vertical offset, or other features which may indicate ground deformation such as cracks, vertical strain, earth fissuring, or compaction faulting in the vicinity of the HSR Alignment. Locations where measurements indicate significant tensile strains may be developing should periodically be visually inspected.

Visual inspections should ideally be performed as close in time as practicable to the other field measurements included in the monitoring program. Locations and descriptions of cracks, potholes and other erosional features should be documented with sketches, maps and photographs, as appropriate, and should include information regarding locations, dimensions and orientations. Features should be marked with stakes, small flags or whiskers nailed into the ground and the locations of the features should be determined using a handheld GPS instrument.

Ground reconnaissance will also provide an opportunity to observe and assess the conditions of survey monuments. Any disturbances by vandalism, traffic, flooding, construction activities or other causes should be noted.

9.8.2 Survey Control

Survey performed at regular time intervals at an established array of permanent monuments forms the backbone of a land subsidence monitoring effort. GPS technology allows for effective measurement of both vertical and horizontal positions at resolutions and accuracies appropriate to subsidence monitoring. Other subsidence monitoring methods and activities will utilize the permanent GPS monument array for reference and validation while monitoring subsidence behavior in the time periods between GPS survey campaigns.

Optical Survey: This includes conventional surveying methods using total station methods. Repeat optical survey is especially effective for measuring differential vertical ground movements at closely spaced point distances (typically about 40 to 100-foot spacing) in areas of potential compaction faulting or earth fissuring. Results need to be corrected for subsiding benchmarks or possibly by using static GPS.

GPS Survey (Static and RTK): Use conventional static GPS methods for subsidence monitoring along the HSR Alignment. For greatest precision, GPS requires communication with ground stations to correct for atmospheric and other factors. It may be necessary to consider whether the reference ground stations are subsiding and how this may affect static GPS readings. Static GPS survey is typically capable of providing (between adjacent stationary receivers) 5 mm plus 1 ppm horizontal accuracy and 10 mm plus 1 ppm vertical accuracy using proper survey procedures and collecting simultaneous data using stationary receivers for sessions usually lasting 30 minutes to 4 hours (http://water.usgs.gov/osw/gps/). RTK GPS survey is much faster than static GPS. RTK is suitable for subsidence monitoring of floodplains that might impact the HSR Alignment. RTK survey is typically capable of providing (between stationary and roving receivers) 10 mm plus 2 ppm horizontal accuracy and 20 mm plus 2 ppm vertical accuracy using proper survey procedures (http://water.usgs.gov/osw/gps/).

CGPS: Make use of existing CGPS networks as discussed in Appendix A. Note that CGPS networks may use differing coordinate systems, although the more-important subsidence measurements (which are relative) should not depend on which coordinate system is used. Existing CGPS networks include the PBO that monitors crustal movement in the area. PBO CGPS points are located primarily around the periphery of the SJV to minimize impacts of subsidence on the tectonic movement measurements. CALTRANS maintains several CGPS stations in the SJV that may have application to this project. Typical standard deviations of daily data sets for relevant PBO CGPS stations around the SJV are 5 to 6 mm vertical and 1 to 2 mm horizontal.

Stationary Control Benchmarks: It is known that the basin through which the HSR Alignment passes is tectonically moving toward the northwest, while the ground surface is subsiding in a manner that may include vertical and possibly horizontal movements. It is suggested that a series of "stationary" control benchmarks (SCB) be established to provide 'current control' for GPS survey measurements on a continuous 'on-demand' basis. These SCBs would consist of Static GPS stations with permanently mounted GPS antenna to eliminate potential setup errors. The SCB stations would serve as network benchmarks for project GPS measurements so that CGPS control would be available for construction monitoring. If feasible, these stations might function as (or as an equivalent to) project-specific CGPS points.

Survey control is discussed more extensively in Section 9.1 above, and in the generic *Draft Conceptual Initial Subsidence Monitoring Plan* included as Appendix B.

9.8.2.1 Construction Control Points

It is our understanding that the construction packages will include the implementation of survey control points spaced frequently along the HSR Alignment (anticipated to be at every 1,250 feet along the HSR Alignment), staggered on the right and left sides. These should be incorporated into the subsidence monitoring program in two ways:

- Whenever regular surveys are made of these control points, the results should be entered into a subsidence database for processing and evaluation.
- During construction, it may be appropriate to supplement the frequency of readings for the sake of the subsidence study. Initially, these should be re-surveyed at least once each year. Depending on the results of these surveys and other data (such as InSAR, reconnaissances, etc.), it may be appropriate to either increase or relax the frequency.

9.8.3 Satellite and Aircraft Based Methods

9.8.3.1 InSAR

The use of repeat-pass InSAR to characterize the distribution and rate of regional ground subsidence is of profound significance in monitoring and managing the risks associated with ground subsidence and earth fissuring. Being validated by GPS monument array survey results, InSAR quantifies subsidence behaviors between GPS monuments and throughout the SJV beyond the immediate HSR Alignment. InSAR also provides critical subsidence quantification over shorter (typically monthly to quarterly) time periods than (typically annual) GPS survey, and thus provides an early warning of significant subsidence behaviors. Interferometry has the ability to detect and quantify minute changes in the elevation of terrain by comparing phase variances of satellite-based or aircraft-based, side-looking radar data between orbits of a similar trajectory. Several InSAR-based methodologies exist and may be useful to a given site depending on site conditions and available satellite-based or aircraft-based data. These methodologies include

traditional 2-pass InSAR, stacked 2-pass InSAR interpretations, and various persistent scatter (PS) InSAR methods and algorithms.

InSAR data can be analyzed by direct observation of interferograms, cross-sectional presentation of vertical change, and interactive three-dimensional presentation with contouring. Examples of current InSAR profile presentations in the Central Valley include SIR2013-5142 (Sneed el al., 2013); the technology is rapidly evolving and significant improvements will become available as the project proceeds. These analyses can be used in a variety of ways, such as to support lineament analysis and reconnaissance, to compare with survey data, and to be used as a calibration tool for subsidence modelling. InSAR data analysis is particularly useful for assessing changes in the location or rate of regional ground deformation and to help refine characterization of bedrock/alluvial interfaces and general lithologic variations in the deep alluvium (Rucker et al., 2013; Weeks and Panda, 2004). Results from InSAR will depend on the site's terrain, ground and vegetation conditions, and sources of potential ground disturbance due to cultural interference such as agriculture or construction site grading.

For satellite-based interferometry, frequency of InSAR imaging depends on which satellite is utilized, and can range from roughly 4 days to 1 month. Aircraft-based interferometry may be scheduled based on aircraft availability and budget constraints; aircraft-based interferometry is further discussed in the following section. The time required for processing the data into useful products can also vary. Capabilities exist to have results within hours of acquisition, giving it a near real-time quality, but more often the turn-around is weeks to months.

InSAR has distinct limitations. It is a highly processed product and represents an interpretive analysis of raw satellite-based or aircraft-based data from no less than two individual data sets. It suffers from both atmospheric and terrain influences that affect the quality of the image. Procedures used in processing the data reduce the impact of these atmospheric and terrain influences; however, the processing cannot correct the remaining constraint of decorrelation due to rapid changes in the ground surface. This phenomenon can be caused by extensive vegetation, plowing and crop changes in agricultural areas, or by urban development. Redundancy in the event of equipment failure is becoming less of an issue as more InSAR-application satellites become operational. The technologies and processing techniques applied to InSAR are constantly evolving and improving. Flexibility is an integral part of utilizing InSAR as a monitoring tool.

9.8.3.2 UAVSAR

JPL provides Uninhabited Aerial Vehicle Synthetic Aperture Radar (UAVSAR) using L-band technology (wavelength = 24 centimeters [cm]), flying out of Palmdale. After making multiple flights over a given area, interpreted vertical and possibly horizontal differences or movement can be calculated with a pixel size of about 20 ft x 20 ft. An introduction to the method is available on the JPL website at http://uavsar.jpl.nasa.gov/education/what-is-uavsar.html.

The advantage of UAVSAR over satellite-based InSAR is greater resolution or reduced pixel size and the possibility of greater horizontal resolution of deformation. A disadvantage is that each flight pass requires a project-specific plane launch to fly the desired alignment, compared to satellites that periodically pass over the site. On the other hand, data acquisition flight scheduling is more flexible since UAVSAR missions are not subject to orbital constraints. Being a research tool, acquisition, maintenance and operational cost of the UAV equipment and system is high per unit area of coverage. Redundancy or replacement of capability in case of equipment failure or UAVSAR program termination is unknown.

JPL's UAVSAR has been successfully used by California DWR for studying subsidence along the California Aqueduct (Farr et al. 2015).

9.8.4 LiDAR

LiDAR uses combined laser and radar technology to create a digital topographic database. It can be very effective for developing elevation or distance information over large areas; an important application for HSR may be to assist in resolving current elevation uncertainties caused by historical subsidence. For surveying, LiDAR instruments are commonly mounted on an airplane with GPS and inertial location control, which flies over the target area and captures the digital imagery in a primarily downward view where bare ground can best be imaged. Terrestrial LiDAR is limited for subsidence applications where bare ground is the optical target being measured. The primarily horizontal view severely limits optical access to bare ground where vegetation, berms and other ground obstructions can block the LiDAR line-of-sight view and leave large areas in shadow. However, terrestrial LiDAR performed on a regular schedule may be an effective tool for monitoring movements, especially lateral movements, of retained embankments and viaducts and other structural facilities where effective lines-of-sight are available.

In concert with GPS measurements at checkpoints, airborne LiDAR provides absolute elevations, unlike InSAR, which only provides relative elevations (i.e., displacement, subsidence, etc.). Airborne LiDAR accuracy is calculated from statistical comparisons to GPS elevation data. The statistics are a function of the density of the point cloud on the ground and the availability and number of bare ground checkpoints. (Examples: a minimum of 30 check points is specified in a Scope of Work for the National Oceanic & Atmospheric Administration [2009] Shoreline Mapping that calls for 15 cm [0.5 foot] overall vertical accuracy] to perform statistical analysis of the accuracy. A study to test very localized LiDAR mapping of Louisiana levees by Thatcher et al. [2013] utilizing airborne [600-meter-wide swath, 3.5 points per m^2] and mobile terrestrial [7.5-meter swath, 866 points per m^2] LiDAR reports a statistically-derived vertical accuracy of 0.05 meters [0.16 feet] for airborne and 0.023 meters [0.076 feet] relative to 20 project GPS reference check points. An offset of about 5 cm was noted in the levee study

between airborne and ground elevations; this difference was attributed to grass on the levees impacting terrestrial lines-of-sight.)

For HSR Alignment, elevations at the bare ground checkpoints would be surveyed using GPS; due to the rapid and ongoing subsidence along the HSR Alignment, a GPS survey should be performed concurrently with the LiDAR. In order to derive magnitudes or rates of subsidence from airborne LiDAR data, at least two images must be captured, separated by some period of time, and the differences must be calculated.

LiDAR was recently used to establish a baseline (as of November 2015) topographic surface for CP 2-3. AFW has not reviewed details of that survey concerning check points and other accuracy measures.

Potential disadvantages of LiDAR include the need to assess whether return signals are bare ground or vegetation, vehicles, or other features or objects. Cultural features such as existing railroad embankments, ditches and other constructions that behave as bare ground must be accounted for in interpretation and analysis of results. LiDAR is dependent on GPS elevations for calibration purposes, and in areas of rapid subsidence it will be important to know the date of GPS control point measurements.

LiDAR is a rapidly evolving technology. Near future applications may include drone-based measurement systems with significant reductions in cost and enhanced performance.

9.8.5 Satellite Altimetry

Satellite altimetry is a satellite-mounted radar technology that provides elevations along predetermined lines on the earth. Originally developed to measure the elevation of the ocean surface, it is equally applicable to ground elevations. Data from a combination of TOPEX/Poseidon (1992-2006), Jason-1 (2001-20013) and Jason-2 (2008-present), provide historical data along the lines shown in Figure 9-2. (Jason-3 launched January 17, 2016 and operational control was assumed by the National Oceanic and Atmospheric Administration (NOAA) in June 2016, but Jason-3 data was not used for the current GSS.)

Satellite altimetry provides a chronologically unbroken historical record of subsidence since 1993, but only along predetermined lines, as shown in Figure 3-9. These lines can be used to calibrate other data methods and to fill in data gaps along those predetermined lines, particularly with InSAR (e.g., 2010-2014) and to cross-check with nearby GPS and CGPS results. However, satellite altimetry data is difficult to process and the results are likely to be too “noisy” to be of great use for future HSR subsidence evaluations.

Red	Referenced oribt: Jason-3 (from 2016), Jason-2, Jason-1 (before February 2009), Topex/Poseidon (before August 2002). (Visu_J2J1TP_Tracks_GE_V3.kmz)
Lavendar	Jason-1 (after february 2009) and Topex/Poseidon (after September 2002). (Visu_J1TP_Interlaced_Tracks_GE_V3.kmz)
Orange	Envisat new orbit (theoretical tracks extension phase - beyond November 2010, not strictly repetitive). (Visu_ENN_Tracks_GE_NewOrbit.kmz)

Figure 9-2: Satellite altimetry lines providing historical subsidence information.

9.8.6 High-Resolution Aerial Imagery

High resolution orthorectified color aerial imagery provides the means to directly observe the conditions of the system. Imagery may ideally be acquired as color orthographic imagery with a minimum resolution of 0.33 feet. It is noted that multi-spectral imagery can offer enhanced capabilities. The aerial imagery should provide geodetic coordinates in feet in accordance with the appropriate survey datum utilized by the monitoring system.

9.8.7 Groundwater Elevations

Groundwater levels (elevations) should be directly monitored on a frequent basis (quarterly, monthly, or continuous) along a corridor approximately 10-20 miles on either side of the HSR Alignment. This can best be done using a dedicated network of piezometers (used to measure groundwater levels only) and monitoring wells (used to measure groundwater levels and collect groundwater samples). The deep aquifer-confining Corcoran clay underlies most of the CP 2-3 Section of HSR Alignment; its known extent under the HSR Alignment ranges from about Hanford to the north, to Wasco to the south. Where the Corcoran clay or other aquitards are present, the piezometers and monitoring wells should be located at selected depth intervals above and below the confining unit, including at distances from the HSR Alignment to provide a picture of where and at what depth groundwater levels are changing (declining) the most. These data may provide insight as to areas at risk of subsidence along the HSR Alignment.

9.9 SUPPLEMENTAL INSTRUMENTATION METHODS

If results of the general monitoring program identify locations of concern or specific additional data needs, additional instrumentation may be appropriate to better characterize the local ground behavior. For instance, tape extensometers (Section 9.9.1) or electronic extensometers (Section 9.9.2) provide horizontal differential ground movement information between closely spaced monitoring points (typically about 40 to 100-foot spacing) at specific locations of known or suspected significant tensile strain development indicated by general monitoring; optical survey of these same points provides corresponding vertical movement data. Borehole tiltmeters (Section 9.9.4) can provide bi-directional real-time monitoring of ground movements. Alluvium compaction behavior at depth, which in the SJV is typically related to compressible aquifer systems below the Corcoran clay or deeper units, can be performed using compaction extensometers (e.g., magnetic extensometers) as described in Section 9.9.3. Surface seismic refraction methods such as the one described in Section 9.9.5 can be used to assess the absence or presence of tensile cracking (incipient earth fissuring) in the shallow subsurface at locations of known or suspected significant tensile strain development.

9.9.1 Tape Extensometer

Tape extensometers are a standard tool for measuring horizontal ground displacement at monitoring point spacings of less than 60 to 100 feet. A monitoring point array must be constructed and protected over time for continuing measurements. When configured as quadrilaterals (4 points forming an approximate square), relative horizontal ground movement direction can also be determined. Measurements are taken manually, and temperature measurements and corrections are typically included in the data collection and analysis.

If survey or InSAR-based monitoring indicates a potential for developing significant horizontal tensile strains or visual observation of tensile strain conditions are observed in an area, tape

extensometry is recommended as a first stage of close-spaced horizontal monitoring. A tape extensometer array may be installed through the suspect area, and monitoring can be initiated to further isolate the location of tensile strain development. Repeat measurements indicate the presence and magnitude of horizontal movements through the array area, and isolates areas of anomalous horizontal movements and strain concentration between array points.

9.9.2 Electronic Horizontal Extensometer

Various versions of electronic horizontal extensometers can be fabricated for use at specific features of interest or impending ground failure at locations of interest. This class of instrumentation would only be deployed once the general monitoring system has indicated that a potential hazard is developing, and further investigation (such as manual tape extensometry or interpretation of a seismic anomaly) has identified a specific location for such instrumentation. Real-time monitoring capabilities can be incorporated into such extensometer systems.

9.9.3 Compaction Extensometer

Compaction extensometers with monitoring points set at the bottom of the Corcoran clay unit will verify whether subsidence is concentrated in the deeper confined aquifers, or whether subsidence is also occurring in the shallower strata (which could possibly result in greater potential to generate ground failure).

Recently, magnetic extensometers have become available and are likely to provide a much more cost-effective method of installing an extensometer than in the past. Within a single boring, numerous magnetic rings can be inserted into the soil surrounding the plastic casing so that the depth at which soil compression is occurring can be localized between each pair of magnetic rings.

In the past, the USGS has installed a limited number of compaction extensometers in available abandoned irrigation wells (as well as drilled dedicated wells for compaction extensometer installations) to monitor subsidence. Suitable locations for compaction extensometers may exist with existing wells that may lie within the Alignment Right of Way. If suitable existing wells at appropriate locations become available, compaction extensometers would improve understanding of subsidence processes in the event that ground displacement problems develop along the HSR Alignment. Continuous data collection with real-time remote data connectivity should be implemented.

Ideally a compaction extensometer site would be combined with a CGPS station to provide vertical and horizontal displacement data at the ground surface to complement specific depths of compaction from the compaction extensometers; in addition, groundwater levels at the site should be continuously monitored.

9.9.4 Borehole Tiltmeter

If future monitoring identifies any critical locations where hazards may be developing, highly sophisticated instrumentation such as an array of precision borehole tiltmeters may become appropriate to monitor very small and possibly dynamic ground movements. The need for such instrumentation would develop as the presence of currently unknown conditions, behaviors, or trends become identified in the standard monitoring evaluations.

9.9.5 Seismic Methods

Surface seismic methods are an established means of identifying the presence of anomalous ground conditions that may be present leading up to the development of an earth fissure (Rucker and Keaton 1998; Rucker and Holmquist 2006). It is standard practice to perform surface seismic profiling when significant tensile ground strains (e.g., above 50 to 100 microstrain) are identified by a general monitoring program. Utilizing a 24-channel engineering seismograph and sledge hammer energy source, the locations of possible discrete tensile cracks (incipient earth fissures) are inferred from interpretations of anomalous patterns of signal attenuation and/or time delays in signal first arrivals. When a seismic anomaly is identified that may represent a tensile crack, it is then standard practice to perform anomaly verification by test trenching with detailed inspection and trench logging.

9.9.6 Piezometers and Observation Wells

A limited number of shallow piezometers were installed and monitored as part of the HSR Geotechnical Baseline Investigation. Those installations that are still operable should be incorporated into the groundwater level monitoring network. Likewise, piezometers installed as part of the final geotechnical investigation and construction monitoring should become part of the groundwater monitoring network. It is anticipated that geotechnical and construction-related piezometers and observation wells will be installed in shallow aquifers (above the Corcoran clay where present) where subsidence is less likely to be an issue, and settlement is likely to be an issue. Therefore, shallow piezometric information may become a valuable component in separating out settlement from subsidence.

Monitoring the deeper aquifer systems, where subsidence is likely to be an issue, will require deep wells to reach those deeper aquifer systems. Installing new wells for monitoring the deeper aquifer systems would be very expensive; if such installations are made, they should be integrated with compaction extensometers. It is anticipated that there may be existing irrigation wells within the HSR Alignment right of way; such existing wells at relevant locations that are screened at appropriate depths should, if suitable, be re-purposed as groundwater level monitoring sites. Where the Corcoran clay or other aquitards are present, it is anticipated that such wells will primarily be screened in aquifer systems below the confining unit.

9.9.7 Fiber Optic Cable-Based Strain Monitoring

Fiber optic technologies provide means to measure strain in a fiber optic cable. In Fiber Bragg Grating (FBG) technology, an FBG sensitive to a specific light frequency is fabricated into a short section of fiber optic cable; the FBG responds to a small portion of the spectrum around that light frequency. Minute changes in distance within the FBG cause a minute frequency shift, which becomes a measure of strain. Many FBG sensors, tuned to different light frequencies, can be fabricated into an optical fiber and measured individually using the different light frequencies to which each of the FBGs is fabricated. The result is a fiber optic cable that is also a distributed strain sensor. Having specific fabrication requirements at specific locations on an optical fiber, FBG technology has a relatively high fabrication cost and limited potential for soil strain monitoring.

BOTDR, as described by Soga et al. (2008) and Soga (2014), utilizes minute changes in distance between imperfections within a fiber optic cable (reflecting light back through the cable to an analyzer) to measure strain while the travel time of the reflected light (time-domain reflectometry) measures the distance along the fiber optic cable. Thus, the entire fiber optic cable becomes a distributed strain sensor with usable lengths of several kilometers. Fiber optic cable systems with redundancy and protection have been developed for civil engineering applications. BOTDR may have tremendous potential for geotechnical monitoring, including strain distribution on drilled shafts and strain under retained embankments which would be associated with settlement. Geotechnical monitoring for settlement is needed to be able to separate settlement from subsidence at HSR Alignment structures, embankments and other facilities.

9.10 INSTRUMENTED TRAIN

With regard to track tilt or curvature, ultimately it is the accelerations on the train that are more important for passenger comfort and train safety. These accelerations can be detected and recorded with on-train instrumentation, including primarily accelerometers.

It is our understanding that the Authority will utilize an instrumented train equipped with accelerometers and gyroscopes that can monitor longitudinal vertical slope, curvature, and acceleration; and horizontal curvature as well as superelevation and twist. Instrumented trains are in use on Japanese high-speed railways with inspection trains covering the entire system every ten days, and car body acceleration being monitored daily, since 1964 (Tsunashima el al., 2012). Recent instrumentation described by Tsunashima et al. (2012) is installed on in-service trains to monitor track conditions (located by GPS) several times a day. Accelerometers are mounted in a train car body and an axle box with an on-board processing unit that downloads data to a control center in real time. Based on figures presented in Tsunashima et al. (2012), track displacement precision is in the sub-millimeter range.

It is our expectation that an instrumented train will run on most days in which the HSR is operational, and perhaps instrumentation may operate on all high-speed trains. Vehicle-based measurements of acceleration in three dimensions and other parameters will provide detailed information about track geometry. Comparison of these results over time will indicate relevant changes in track geometry over time. If the evaluation of this information indicates changes in track geometry, this information can be used to design either modifications in the monitoring program, or maintenance or mitigation measures, as appropriate.

9.11 EXISTING RECORDING OR MEASURING PROGRAMS

9.11.1 CGPS

There are two CGPS networks operating within the SJV, with stations at the locations shown in Figure 5-2 and Appendix A. This data is available to the public, but it only covers the specific locations of the CGPS stations. Relevant available CGPS data within the SJV is summarized in Appendix A.

9.11.2 InSAR and Satellite Altimetry

Several space agencies are regularly capturing InSAR scenes that cover the SJV. JPL has been and continues to process this data for L-band and is in the process of beginning to process C-band data as well. Their processed data has generally been made available to the public as time after processing has been completed, but the Authority may have little control over how quickly it becomes available, or possibly even whether the processing is performed for any given period. To improve the availability of processed InSAR results, independent consultants may be retained to perform this work, within several days to weeks in some cases.

Satellite altimetry data is also available, extending back to the early 1990s, along select lines within the SJV. The available lines are shown in Figure 9-2.

9.11.3 Existing Conditions or Baselines

9.11.3.1 Elevations

Existing elevations within CP 2-3 were originally established by ground survey control and benchmarks originally set by the Authority, a topographic survey performed in 2011 by the Authority, and recently updated by the CP 2-3 Contractor (Dragados Flatiron Joint Venture) by a re-survey of the benchmarks, and a new LiDAR-based topographic map.

Anticipated future elevations may be estimated by projecting recent subsidence rates forward from existing or recent elevations.

9.11.3.2 Subsidence Rates

Recent or near-current rates of subsidence may be estimated based on available survey, LiDAR, and InSAR; if available, satellite altimetry data may also be considered, although it is difficult to process and the results are likely to have too much “noise” to be of great value.

9.11.3.3 Groundwater

Baseline groundwater levels and piezometric heads have been developed by the USGS for their CVHM2 using a 1-mile -square cell size. These may be refined with local data if and when such data becomes available.

The California DWR also periodically publishes contour maps of the groundwater levels in the SJV, typically every 2 to 5 years. These maps are typically 2 to 3 years out of date when published.

9.12 DATA MANAGEMENT AND ACCESSIBILITY

A data management system should be designed and implemented to gather, process, interpret, store, and make available relevant data. This will be addressed in detail in future technical memoranda. In summary:

- Data will likely be gathered though both automated and manual methods.
- Data may be continuously gathered and episodically gathered.
- Once entered into the database, evaluations should be automated to the extent possible such that action levels are identified and notifications sent when any measurements approach or exceed pre-defined levels.
- Data and evaluation results should be readily available to appropriate Authority personnel and consultants via the internet.
- Data should be securely stored and adequately replicated to guard against data corruption or loss.

10.0 EVALUATIONS AND RECOMMENDATIONS

10.1 OVERVIEW

Although subsidence is expected to continue in the future until sometime after SGMA measures have been successfully implemented, in most locations, subsidence-induced changes in slope and curvature, and subsidence-induced faults and fissures, are not expected to significantly impact the HSR ride performance, although they may influence viaduct structural design. In any case, some level of potential risk remains, and therefore we believe the preliminary recommendations in this chapter should be finalized and implemented into the design and operations of the HSR.

In addition, changes to flood patterns along rivers are expected to change somewhat, and the limits of the Tulare Lake flood basin have already shifted, and will continue to shift, toward the east and, if not mitigated, will thereby deepen the floodwaters along the HSR Alignment. If not mitigated, flooding of the Tulare Lake could have a significant adverse impact on the HSR infrastructure.

This section is organized in the following subsections:

Subsection 10.2: Subsidence-Induced Changes in Slope and Curvature, and Faults and Fissures, which provides recommendations regarding changes to the ground slope and curvature, and the possibility of subsidence-induced faults or fissures developing along the HSR Alignment.

Subsection 10.3: Potential Flood Impacts, which provides recommendations regarding the potential for subsidence-induced changes to flood patters along rivers, and the potential for the Tulare Lake flood basin to impact the HSR Alignment.

Subsection 10.4: Monitoring and Maintenance Approach, which provides recommendations regarding measures to take during all phases of the project, from design through the operational period, to detect any developing problem soon enough that remedial maintenance can be performed to protect the HSR infrastructure.

10.2 SUBSIDENCE-INDUCED CHANGES IN SLOPE AND CURVATURE, AND FAULTS AND FISSURES

10.2.1 General Considerations

We recommend implementing an instrumentation and monitoring program to track subsidence and to respond if warning signs associated with subsidence-induced curvature, faults, or fissures are observed. Final instrumentation and monitoring recommendations will be developed in collaboration with the Authority, but our initial recommendations are summarized as follows.

1. Preliminary instrumentation and monitoring recommendations are provided in Section 9.0, and an example Monitoring Plan is presented in Appendix B. These measures are critical to look for the development of:
    a) Potential convex upward change in curvature where tensile stresses may lead to cracks and fissures.
    b) Potential localization of differential strains that could indicate a local subsidence-induced fault or a concentration of ground deformation, either of which could affect performance of infrastructure or train ride-ability.

c) Subtle differential subsidence or corresponding horizontal displacements that could prompt a re-leveling or realigning of the tracks, or maintenance to embankments or appurtenant improvements could be required.

2. We recommend including on-train instrumentation to monitor for changes in accelerations that could signal differential movement and changes in the track geometry.
3. We recommend that the remaining uncertainties described in Section 8.0 be addressed, and then final instrumentation and monitoring recommendations developed in coordination with the Authority.
4. Structural and civil designers should study the observed differential subsidence and take this into consideration in their designs.
5. In general, we anticipate that embankments and MSE walls will be able to tolerate the anticipated degree of differential subsidence.
   a) We anticipate viaducts may be able to accommodate displacement-length ratios of about 1/400 (0.25%); we anticipate differential subsidence will generally be less than this (the largest observed induced gradient in the InSAR data of historical subsidence was on the order of 0.02% along the HSR Alignment or 0.04% nearby, but 20-year extrapolations from InSAR data suggest induced slopes could be 0.13%; by comparison, the maximum induced gradient near the Pixley fissure was about 0.06%). (Our Scenario B forecasts suggest there could be up to 0.43% induced change in slope, but we believe this is primarily “noise” inherent in the method of analysis.)
   b) Due to the noisy nature of both the JPL InSAR and the RFP-to-LiDAR comparison, it is not possible to rule out localized differential settlements greater than these values. We anticipate that performing additional X-band InSAR could help resolve this area of uncertainty.
6. Measures described in Section 3.1.5.6 should be followed to enable distinguishing future subsidence from settlement.

10.2.2 Design Considerations

The project designers should review the forecast changes in elevations, slopes, curvature, and account for these in their design.

10.2.2.1 Subsidence-Induced Changes in Slope

Taiwan HSR has limited the induced change in slope to 1/1000, or 0.1%. This may be a reasonable value for many cases, but the actual value that is critical for design will be a function of whether that rail is supported by a guideway, a viaduct, or another structure.

For guideways consisting of embankments or retained fill, changes in slope within the range anticipated to occur in the Corcoran Subsidence Bowl are not expected to be a significant problem for the HSR. (However, associated changes in curvature, which may require maintenance, are addressed in the next subsection.)

Where viaducts are present, differential subsidence (or differential settlement from other causes) will induce angular distortion at each bent. Designers should consider the anticipated change in slope shown on Plate 8-17 and design structures to accommodate this amount of angular distortion (generally well-below 0.1%, but possibly somewhat greater) plus some increase for uncertainty.

In general, we anticipate that simple-span viaduct structures should be able to accommodate the anticipated changes in slope, but that multi-span post-tensioned viaducts may have difficulty if angular distortion is greater than about 0.025% to 0.05%.

In general, the design team (e.g., structural engineer or track engineer) should indicate the tolerable levels of angular distortion.

10.2.2.2 Subsidence-Induced Changes in Vertical Curvature

To hold the velocity-induced change in acceleration to less than 0.045g as required by the *Design Criteria*, the total track vertical curvature must be less than 1.08E-5, which corresponds to a radius of curvature being at least 93,000 feet. Thus, where there is no vertical curvature built-in to the design grade, the allowable change in vertical curvature can be up to ±1.08E-05. However, where vertical curvature is present in the design grade, the subsidence-induced allowable change in curvature may be more than or less than 1.08E-05, depending on the direction of the original curvature (i.e., concave-up or convex-up), and the direction of the induced change in curvature.

The change in vertical curvature can be monitored using on-train accelerometers, as well as by measurements of changes in the track geometry through any methods of measuring elevations, such as surveying, LiDAR, etc., or methods of measuring changes in elevation, such as InSAR.

Where changes in vertical accelerations are observed, it is expected that relatively minor ballast-releveling will be the appropriate and adequate mitigation. In general, raising the track grade will be preferable to lowering it, because lowering it would reduce ballast thickness to less than the design value. If the amount of ballast-raising is large, it may be necessary to take additional measures, such as adding training walls along the side of the embankment to retain the ballast, or possibly add stabilized material (e.g., cement- or asphalt-treated aggregates) for subballast or ballast.

10.2.2.3 Subsidence-Induced Changes in Horizontal Curvature

Horizontal curvature will be addressed in a manner similar to the approach for vertical curvature, except that the *Design Criteria* required velocity-induced change in acceleration of 0.05g, which corresponds to a maximum horizontal curvature of 1.2E-05 or a radius of curvature of at least 83,500 feet.

The change in horizontal curvature can be monitored using on-train accelerometers, as well as by measurements of changes in the track geometry through any methods of measuring horizontal position, such as surveying, LiDAR, etc.

Where changes in horizontal accelerations are observed, the track superelevation or horizontal alignment can be evaluated and adjusted as appropriate.

Viaducts should be designed to be structurally able to accommodate the forecast movement. Compared to multiple-span viaducts, single-span viaducts will likely be more able to tolerate accommodate differential subsidence between adjacent bents and their use should be considered. Because subsidence may impact track slopes and curvature, it may be appropriate to design a system that can be adjusted in the future. Consideration should be given to measures such as using ballasted track viaducts, or adjustable jacks on bridges as has been done in Taiwan.

For conventional embankment or MSE-supported guideways where ballasted track will be used, ballast releveling should be anticipated to adjust the track alignment in response to observed subsidence. In general, we anticipate that required re-ballasting may be limited to less than about 1 foot, but more could be required in areas of localized greater differential subsidence. Consideration should be given to how this increased ballast thickness could be accommodated on the top of the guideways, such as increasing the width of the top of embankment, or allowing for low retaining walls along the edge of the guideways.

10.2.2.4 Subsidence-Induced Changes in Cant or Twist

We anticipate that subsidence-induced changes to cant or twist will be secondary to changes in slope or curvature and can be detected by on-train sensors. We anticipate that normal maintenance activities, driven by other criteria, will be able to address concerns that arise.

10.3 POTENTIAL FLOOD IMPACTS

10.3.1 Tulare Lake Basin Flooding

If flood control hazards will be addressed by local, regional, state, and federal agencies, it may be that floodplain concerns associated with filling of the Tulare Lake basin will be essentially eliminated. However, although it is our understanding that interested agencies are currently engaged in discussions to address these hazards, flood mitigation actions have not yet been decided upon or initiated. This means that (1) these hazards have not yet been mitigated, and (2) is it not known yet how effectively these hazards will be mitigated, or even if they will be mitigated at all pending resolution of funding, jurisdictional, and technical considerations.

In areas that were originally identified (in the bid documents) as lying within a flood zone but where, due to subsidence-related changes in topography, the flood depth is forecast to become

deeper, or areas that will become a flood zone area, there may be several mitigation options, depending on how deep the flood zone is expected to be.

1. Increase riprap height to embankments in original flood zones, and add riprap in new flood zones.
2. Add embankment subdrains in new flood zones.
3. It may be necessary to add cross-embankment culverts to promote additional drainage as needed
4. The top of rail must be at least 4'-9" above the design flood elevation. Where flood depths will increase, it may be necessary to raise the embankment height to maintain the required height of rail above flood elevation.

10.3.2 River and Creek Flood Hazards

In the vicinity of several rivers or creeks that cross the HSR Alignment, floodplain uncertainty associated with uncertainty in existing and forecast topography can be accounted for by adding some margin of safety above the forecast flood elevation, as discussed below:

- Cross Creek: add margin of safety: 3 feet
  - Not highly sensitive to local small-scale details of existing topo
  - Major uncertainties:
    - Magnitude and configuration of future subsidence.
    - It is thought that flood levels will be less sensitive to local small-scale details of existing topography; uncertainty in larger-scale topography is also relevant.
    - Both sources of uncertainty may be handled by adding some margin to forecast levels.
- Tule River: add margin of safety: 3 feet
  - More localized issue that is more sensitive to uncertainty of forecast
  - Major uncertainties:
    - Forecast subsidence.
    - Existing topography (particularly localized conditions).
- Deer Creek: add margin of safety: 1.5 feet
  - Major uncertainties:
    - Sensitive to both local-scale and larger scale topographic uncertainty near the HSR Alignment.
    - Farther away, it is less sensitive to local details and larger scale topography is more important.
    - Note that the Deer Creek flood zone merges with the Tulare Lake Basin, and the maximum forecast water depths are already more than 10-15 ft in some locations.

10.3.3 Flood-Related Design Recommendations

To mitigate the potential for changes to the Tulare Lake flood hazard that may result as a consequence of subsidence, we recommend the Authority collaborate with appropriate stakeholders to improve control of flood inflows to the Tulare Lake basin. The potential changes to flood depths discussed in this report are great enough that we consider adequate routing of floodwater away from the Tulare Lake basin will be the most reasonable approach to mitigation for all stakeholders.

To account for the impact of subsidence on flooding at river and creek crossings and the associated uncertainty, we recommend the design flood elevations be increased by the levels indicated in the previous subsection, and the embankment design modified accordingly.

Floodplain changes related to river crossings are relatively modest. In general, it appears the existing floodplain limits for CP 2-3 may not need to be modified to accommodate changes associated with river crossings.

10.4 MONITORING AND MAINTENANCE APPROACH

Recommended monitoring programs measures are discussed in the following subsections for these phases of the project:

- **Pre-construction** – data and information baselines are established, initial monitoring infrastructure is installed and initialized, and repeat monitoring begins to establish groundwater trends and subsidence rates.
- **During construction** – construction activity limits subsidence monitoring to discrete points or smaller areas within construction zones. Repeat monitoring in the larger area updates groundwater trends and subsidence rates. During or towards end of construction, monitoring infrastructure for constructed facilities is installed and initialized. Potential significant problem areas may begin to be identified.
- **Post-construction** – may include two time periods: settlement period following completion of embankments and HSR structures, and the time between final track and appurtenance installation and start of train operations. Repeat monitoring updates groundwater trends and subsidence trends in the area and establishes subsidence trends at constructed HSR facilities. Potential problem areas may begin to be identified.
- **During train operations** – Monitoring focus may change as train-based monitoring systems (including on-board inertial monitoring) identifies developing problem areas, if present, from direct on-board measurements rather than having to infer potential problems from the external ground measurements. Continued subsidence monitoring updates groundwater level trends and subsidence magnitudes and rates.

Based on potential impact of subsidence on the HSR, these recommended programs are summarized in Table 10-1. Recommendations include:

1. **Methods whose availability, reliability, or applicability show promise** and that should be further investigated and discussed, and then possibly implemented.

2. **Additional methods considered valuable** which should be carefully considered, and implemented when practicable.
3. **Minimum monitoring programs considered essential** for understanding the hazards and risks of ongoing subsidence as it is developing.

A *Draft Conceptual Subsidence Monitoring Plan* is included in Appendix B. An actual monitoring plan for HSR subsidence will be developed at a future date.

10.4.1 Development of Final Instrumentation and Monitoring Plan

The instrumentation and monitoring recommendations presented here are tentative at this time. The actual instrumentation and monitoring plan will be developed based on these considerations and in coordination with the Authority.

10.4.2 Coordination with Existing Recording or Measuring Programs

During all phases of monitoring, efforts should be coordinated with other measurement, monitoring, and reporting programs, including:

1. Construction survey control for CP 2-3 (land-based and LiDAR)
2. California DWR groundwater levels
3. USGS subsidence studies
4. USGS groundwater modeling
5. JPL InSAR analyses
6. CGPS recordings for nearby stations in the Caltrans Scripps Orbit and Permanent Array Center (SOPAC) and University NAVSTAR Consortium (UNAVCO) networks

10.4.3 Preliminary Recommendations

We have the following preliminary recommendations; final recommendations will be developed later in collaboration with the Authority.

10.4.3.1 Pre-Construction

Preconstruction monitoring should be designed to establish baseline elevations, rates of historical and ongoing subsidence, and historical and current groundwater levels. It should include at least the following components:

- Site Reconnaissance
- L-band InSAR (and if available and feasible, X-band InSAR)
- Airborne LiDAR
- Control Point Survey (Static GPS/Optical)
- CGPS

In addition, the following components are recommended for serious consideration if or when needed, and where feasible:

- Trench or Test Pit (if other data suggests this is called for)
- C-band InSAR
- UAVSAR
- Land Survey (Optical or GPS)
- Borehole Tilt Meter (if other data suggests this is called for)
- Borehole Extensometer
- Monitoring well/piezometer

10.4.3.2 During Construction

Preconstruction monitoring should be designed to update the established baseline elevations, rates of historical and ongoing subsidence, historical and current groundwater levels and trends. It should include at least the following components:

- Site reconnaissance
- Trench or Test Pit (area of potential significant tensile strain)
- L-band InSAR (and if available and feasible, X-band InSAR at construction areas)
- Airborne LiDAR
- Control Point Survey (Static GPS/Optical)
- CGPS
- Borehole Extensometer (if possible, associate with water supply well)
- Monitoring well/piezometer

In addition, the following components are recommended for serious consideration and implementation if or when needed and where feasible:

- C-band InSAR
- UAVSAR
- Land Survey (Optical or Static GPS) (area of anomalous differential subsidence)
- Borehole Tilt Meter (area of significant tensile strain)
- Tape Extensometer (area of possible significant tensile strain)

10.4.3.3 Post-Construction

A post-construction period is where initial construction of facilities has been completed and design settlement is occurring. Post-construction monitoring should be designed to update the established baseline elevations, rates of historical and ongoing subsidence, historical and

current groundwater levels and trends, and re-establish differential subsidence monitoring at the constructed facilities. It should include at least the following components:

- Site reconnaissance
- L-band InSAR (and if available and feasible, X-band at construction areas)
- C-band InSAR
- Control Point Survey (Static GPS/Optical)
- CGPS
- Borehole Extensometer
- Monitoring well/piezometer

In addition, the following components are recommended for serious consideration and implementation if or when needed and where feasible:

- UAVSAR
- Airborne LiDAR
- Land Survey (Optical or GPS)
- Borehole Tilt Meter (area of significant tensile strain)
- Tape Extensometer (area of potential significant tensile strain)

In the post-construction period, ground-disturbing construction activities are anticipated to be minimal. C-band InSAR, with its' superior resolution of small differential movements, would replace the lower vertical accuracy airborne LiDAR as a primary area-wide differential subsidence monitoring tool.

10.4.3.4 Operational Period

During operations, monitoring should be designed to update baseline elevations, rates of historical and ongoing subsidence, and historical and current groundwater levels and trends. It should include at least the following components:

- Site reconnaissance
- L-band InSAR
- Control Point Survey (GPS/Optical)
- CGPS
- Borehole Extensometer
- Monitoring well/piezometer
- Instrumented Train
    - Vertical slope & curvature
    - Horizontal slope & curvature

- Superelevation
- Video

In addition, the following components are recommended for serious consideration and implementation if or when needed and where feasible:

- C-band InSAR
- X-band InSAR
- UAVSAR
- Land Survey (Optical or GPS)
- Borehole Tilt Meter (area of significant tensile strain)

10.4.4 Action Levels for Monitoring

Based on the results of the GSS, the following preliminary recommendations have been developed regarding action levels for subsidence, differential subsidence, ground curvature, on-board train accelerations, or other parameters. Final action levels will be developed in collaboration with the Authority and the design-build designers. In general, action levels should trigger more-detailed investigations and evaluations, which should develop recommendations regarding the need for mitigation actions.

10.4.4.1 Induced Change in Slope

In general, the design team (e.g., structural engineer or track engineer) should indicate the appropriate action levels for angular distortion. For preliminary purposes, we suggest action levels of 0.01% change in slope at viaducts, or 0.1% change in slope for guideways.

10.4.4.2 Induced Change in Vertical Curvature

An action level should be set that correspond with about half of the *Design Criteria* limits.

10.4.4.3 Induced Changes in Horizontal Curvature

An action levels should be set that correspond with about half of the *Design Criteria* limit.

10.4.4.4 Spatially-Abrupt Differential Subsidence

Although subsidence-induced faulting is not expected to occur across the HSR Alignment, such localized offset is possible, particularly in the vicinity of where the inactive Poso Creek Fault crosses the HSR Alignment.

An action level of about 0.25 inch of differential subsidence across a short length of track. Such as condition should be evaluated for the possibility of fault development. This development is likely to develop progressively over time, but could be more rapid; for instance, the observed differential movement of the Pond-Poso-Creek Fault was about 1 inch during one 4-month

period (i.e., an average of about 0.25 inches per month), but averaged more like 0.4 inches per year between the 1950s and about 1980 (Holzer 1980).

10.4.5 Data Repository

A system should be developed to maintain raw and processed data, and to evaluate that collected data for potential hazards that may be emerging and identified action levels for parameters such as rail performance, slope, vertical or horizontal curvature, and tensile ground strains.

Summary reports of the results of these evaluations should be these distributed to interested parties in a timely fashion, with flags to call attention to potential areas of concern.

In addition, all of the data should be reviewed for signs of changes in rail performance, slope, vertical or horizontal curvature, and tensile ground strains.

This will be designed during a future phase of the current GSS.

11.0 CLOSURE

This memo was prepared by the staff of Amec Foster Wheeler and our subconsultant GSI Environmental Inc., under the supervision of the engineers whose signatures appear hereon. We trust that this report meets the current project needs. If you have any questions or require additional information, please contact Jim French of Amec Foster Wheeler.

12.0 REFERENCES

AFW: See Amec Foster Wheeler Environment & Infrastructure.

ALSIG: See Arizona Land Subsidence Interest Group

AMEC Environment & Infrastructure, Inc., 2009. White Paper, in Procedural Documents for Land Subsidence and Earth Fissure Appraisals, for Flood Control District of Maricopa County, Phoenix, AZ, available at: ftp://ftp.mcdot.maricopa.gov/anonymous/FCD (last access: 22 October 2015), 2009.

AMEC Environment & Infrastructure, Inc., 2011a. Procedural Documents for Land Subsidence and Earth Fissure Appraisals. Prepared for the Flood Control District of Maricopa County. Contract FCD2008C016, Work Assignment No. 13. May.

AMEC Environment & Infrastructure, Inc., 2011b. Procedural Document: Geological Reconnaissance of Photolineaments and Terrestrial Search for Earth Fissures, May. Available at: ftp://ftp.mcdot.maricopa.gov/anonymous/FCD/Get_From%20FCD/Procedural%20Documents%20for%20Land%20Subsidence%20and%20Earth%20Fissure%20Appraisals/3.Geological%20Recon.%20of%20Photolineaments/Geolog.%20Recon.%20of%20Photolineaments%20&%20Terrestrial%20Search%20for%20Earth%20Fissures.pdf

AMEC Environment & Infrastructure, Inc., 2014a. Final Design-Level Subsidence and Earth Fissure Risk Zoning Report, Powerline, Vineyard Road and Rittenhouse Flood Retarding Structures On-Call Design Project, Pinal County, Arizona, for Flood Control District of Maricopa County, Phoenix, Arizona. AMEC Project No. 17-2013-4045, December 9.

AMEC Environment & Infrastructure, Inc., 2014b. Final Feasibility Study I&W Brine Cavern, Carlsbad, New Mexico, for NM Energy, Minerals and Natural Resources Department Oil Conservation Division, Santa Fe, NM. AMEC Project No. 1251700076, August. Available at: ftp://164.64.106.6/Public/OCD/Documents/I&W%20Brine%20Cavern%20Project/I&W%20Brine%20Cavern%20Project%20-%20Feasibility%20Study%20Final/

Arizona Land Subsidence Interest Group (ALSIG), 2011. Guidelines for Investigating Land-Subsidence and Earth Fissure Hazards in Arizona, Arizona Geological Survey Contributed Report No.CR-11-D, Arizona, August.

Austin, John T., 2012. Floods and Droughts in the Tulare Lake Basin. Sequoia Natural History Association, Three Rivers, California.

Authority. See California High-Speed Rail Authority.

Bartow, J.A., 1991. The Cenozoic evolution of the San Joaquin Valley, California. USGS Professional Paper 1501.

Bawden, G.W., Sneed, M., Stork, S.V. and Galloway, D.L., 2003. Measuring Human-Induced Land Subsidence from Space, Fact Sheet 069-03, US Geological Survey, December.

Bertoldi, G.L., Johnston, R.H., and Evenson, K.D., 1991. Ground Water in the Central Valley, California – A Summary Report, USGS Professional Paper 1401-A.

Bloch, R.B., 1991. Sheet 3 of 3, West Coast Regional Cross Section, San Andreas Fault to Sierra Nevada Range, Published by the American Association of Petroleum Geologists, Tulsa, Oklahoma.

Borchers, J.W. and Carpenter, M. 2014. Land Subsidence from Groundwater Use in California. Prepared by Luhdorff & Scalmanini Consulting Engineers. Prepared for the CA Water Plan Update 2013, Vol 4 Reference Guide.

Budhu, M., 2008. Mechanics of Earth Fissures Using the Mohr-Coulomb Failure Criterion. Environmental & Engineering Geoscience 14(4): 281-296.

Burbey, T.J., Warner, S.M., Blewitt, G., Bell, J.W., and Hill, E., 2006, Three-dimensional deformation and strain induced by municipal pumping, Part 1: Analysis of field data: Journal of Hydrology v. 319 p. 123-142.

California Department of Water Resources, 2011. *Groundwater Data & Monitoring*. South Central Region. http://www.water.ca.gov/groundwater/data_and_monitoring/south_central_region/GroundwaterLevel/gw_level_monitoring.cfm.

California Department of Conservation Division of Oil, Gas and Geothermal Resources (DOGGR), 2015-2017. Online data website www.conservation.ca.gov/dog

California Department of Water Resources, 2011. *Water Data Library*. http://www.water.ca.gov/waterdatalibrary/.

California Department of Water Resources, 2017. Estimated Subsidence in the San Joaquin Valley between 1949 – 2005. February 7.

California DOGGR, 2017. California Department of Conservation, Division of Oil, Gas and Geothermal Resources Website: https://secure.conservation.ca.gov/WellSearch/, accessed 2016 through June 30, 2017.

California High-Speed Rail Authority, 2012. California High-Speed Train Project, Agreement No.: HSR 13-06, Book 3, Part C, Subpart 1, Design Criteria, Execution Version, Rev. 0.1. Construction Package 1. December 2012.

California High-Speed Rail Authority, 2013. Agreement No.: HSR 13-06, Book 3, Part E, Subpart 3, Record of Survey and Control Monument Data. July 31.

California High-Speed Rail Authority, 2014a. RFP No.: HSR 13-57, Request for Proposals for Design-Build Services for Construction Package 2-3, Book IV, Part G.2 – Geotechnical Baseline Report. June 10.

California High-Speed Rail Authority, 2014b. RFP No.: HSR 13-57, Request for Proposals for Design-Build Services for Construction Package 2-3, Book IV, Part G.4 – Record of Survey and Control Monument Data. April 2.

California High-Speed Rail Authority, 2015. RFP No.: HSR 14-32, Request for Proposals for Design-Build Services for Construction Package 4, Book IV, Part G.2, Record of Survey and Control Monument Data. May 27.

Carpenter, M.C., 1994. Deformation Across and Near Earth Fissures: Measurement Techniques and Results. U.S. Geological Survey Subsidence Interest Group Conference, Edwards Air Force Base, Antelope Valley, California, November 18-19, 1992: Abstracts and Summary. Open-file Report 94-532.

Chirco & Lee, Oct 10, 2013: Draft Regional Land Subsidence along the California High-Speed Rail Alignment in the San Joaquin Valley.

CHSTP: California High-Speed Train Project: see California High-Speed Rail Authority.

City of Fresno, 2010. Water Quality Annual Report 2010.

Croft, M.G., 1972. Subsurface Geology of the Late Tertiary and Quaternary Water-Bearing Deposits of the Southern Part of the San Joaquin Valley, California. USGS Water-Supply Paper 1999-H.

Design Criteria: see California High-Speed Rail Authority, 2012.

DFJV. See Dragados/Flatiron Joint Venture.

Doherty, J., 2015. Calibration and Uncertainty Analysis for Complex Environmental Models. Watermark Numerical Computing, Brisbane, Australia. ISBN: 978-0-9943786-0-6.

Doherty, J., 2016a. PEST Model-Independent Parameter Estimation User Manual Part I: PEST, SENSAN and Global Optimizers, Watermark Numerical Computing.

Doherty, J., 2016b. PEST Model-Independent Parameter Estimation User Manual Part II: PEST Utility Support Software, Watermark Numerical Computing.

Dragados Flatiron Joint Venture, 2015a. LiDAR of CP 2-3 Alignment.

Dragados Flatiron Joint Venture, 2015b. *Long Term Deep Subsidence Influence on Project, Potential Design Delay, Change in Scope of Work.* Letter to Mr. Charlie Guess of the California High-Speed Rail Authority. September 11.

DWR: see California Department of Water Resources.

Farley, Greg, 2017. Personal communication between Greg Farley of the California Department of Water Resources and Jim French of Amec Foster Wheeler.

Farr, T.G., Jones, C.E., Liu, Z., 2015. *Progress Report: Subsidence in the Central Valley, California,* Jet Propulsion Laboratory, California Institute of Technology.

Farr, T.G., 2016. *PowerPoint file: San Joaquin Valley Subsidence May 7, 2015 – May 25, 2016.* Personal communication to Jim French of AFW.

Farr, T.G., Jones, C.E., Liu, Z., 2017. *Progress Report: Subsidence in California, March 2015 – September 2016*, Jet Propulsion Laboratory, California Institute of Technology.

Faunt, C.C., ed., 2009, *Groundwater Availability of the Central Valley Aquifer, California*: U.S. Geological Survey Professional Paper 1766, 225 p.

Faunt, Claudia C., Kenneth Belitz, and Randall T. Hanson, 2010. Development of a three-dimensional model of sedimentary texture in valley-fill deposits of Central Valley, California, USA, Hydrogeology Journal, 18:625-649.

Federal Emergency Management Agency (FEMA), 1985. Flood Insurance Study, Tulare County, California, July.

Federal Highway Administration: see FHWA.

Fergason, K.C., M. L. Rucker, and B. B. Panda, 2015. "Methods for monitoring land subsidence and earth fissures in the Western USA," in *Proc. IAHS*, 372, 361–366. doi:10.5194/piahs-372-361-2015

Fielding, E.J., Blom, R.G., and Goldstein, R.M. 1998. Rapid Subsidence over oil fields measured by SAR interferometry. Jet Propulsion Laboratory, California Institute of Technology, Pasadena, California. http://www-radar.jpl.nasa.gov/CrustalDef/oilfields/

Fresno Irrigation District et al., 2006. Fresno Area Regional Groundwater Management Plan.

Galloway, D.L., Jones, D.R, and Ingebritsen, E.S., 1999. Land Subsidence in the United States, USGS Circular 1182, 175 p.

GeoSlope International Ltd., 2012. *Seepage Modeling with Seep/W 2012, An Engineering Methodology*, Calgary, Alberta, Canada.

GeoSlope International Ltd., 2012. Stress and Deformation Modeling with Sigma/W 2012, An Engineering Methodology, Calgary, Alberta, Canada.

Gourmelen, N., Amelung, F., Casu, F., Manzo, M., and Lanari, R. 2007. Mining-related ground deformation in Crescent Valley, Nevada: Implications for sparse GPS networks. Geophysical Research Letters, Vol 34, L09309.

Grabowski, M., 2016. New analysis reveals large-scale motion around San Andreas Fault System, University of Hawai'i News, June 20. Accessed on June 21, 2016 at http://www.hawaii.edu/news/2016/06/20/new-analysis-reveals-large-scale-motion-around-san-andreas-fault-system/

Guacci, Gary, 1979. "The Pixley Fissure, San Joaquin Valley, California," Evaluation and Prediction of Subsidence, International Conference on Evaluation and Prediction of Subsidence held at Casino Hotel, Pensacola Beach, Florida. Edited by Surendra K. Saxena. ASCE Engineering Foundations Conferences. January.

Hanson, R.T., Boyce, S.E., Schmid, Wolfgang, Hughes, J.D., Mehl, S.M., Leake, S.A., Maddock, Thomas, III, and Niswonger, R.G., 2014, One-Water Hydrologic Flow Model (MODFLOW-OWHM): U.S. Geological Survey Techniques and Methods 6-A51, 120 p.

Holzer, Thomas L, 1980. "Faulting Caused by Groundwater Level Declines, San Joaquin Valley, California," Water Resources Research, Vol. 16, No. 6, Pages 1065-1070. December.

Holzer, Thomas L., 1984. "Ground Failure Induced by Ground-Water Withdrawal," in *Man-Induced Land Subsidence, Volume VI of Reviews in Engineering Geology,* Edited by Thomas L. Holzer. Geological Society of America.

Holzer, Thomas L., and Earl H. Pampeyan, 1981. “Earth Fissures and Localized Differential Subsidence,” in Water Resources Research, Vol. 17, No. 1, Pages 223-227. February.

Howell, S., Smith-Konter, B., Frazer, N. Tong, X., and Sandwell, D., 2016. The vertical fingerprint of earthquake cycle loading in southern California, Nature Geoscience, V9, p 611-614.

Hwang, Cheinway, Yuande Yang, Ricky Kao, Jiancheng Han, C. K. Shum, Michelle Sneed, Wei-Chia Hung, and Yung-Sheng Cheng, 2016. “Time-varying land subsidence detected by radar altimetry: California, Taiwan and north China.” In *Scientific Reports*: www.nature.com/scientificreports/.

Ireland, R.L., Poland, J.F. and Riley, F.S., 1984. *Land Subsidence in the San Joaquin Valley, California, as of 1980.* USGS Professional Paper 437-I.

Izett, G.A., Obradovich, J.D. and Mehnert, H.H., 1988. The Bishop Ash Bed (Middle Pleistocene) and some older (Pliocene and Pleistocene) Chemically and Mineralogically Similar Ash Beds in California, Nevada, and Utah. USGS Survey Bulletin 1675.

Jachens, R.C. and Holzer, T.L., 1979. “Geophysical Investigations of Ground Failure Related to Groundwater Withdrawal—Picacho Basin, Arizona,” in Groundwater, Vol. 17, No. 6. p. 574-585.

Jachens, R.C. and Holzer, T.L., 1982. “Differential Compaction Mechanisms for Earth Fissures Near Casa Grande, Arizona.” The Geological Society of America Bulletin, Vol. 93. p. 998-1012.

Johnson, A.I., Moston, R.P., and Morris, D.A., 1968. Physical and Hydrologic Properties of Water-Bearing Deposits in Subsiding Areas in Central California, USGS Professional Paper 497-A.

Ju, S.H, 2012. “Dynamic analysis of high-speed trains moving on bridges with foundation settlements,” in *Archives of Applied Mechanics*. DOI 10.1007/s00419-012-0653-1.

Keaton, J. R., M.L. Rucker, and S.S. Cheng, 1998. “Geomechanical Analysis of an Earth Fissure Induced by Ground-Water Withdrawal for Design of a Proposed Ash and Sludge Impoundment, Southeastern Arizona,” in: *Land Subsidence Case Studies and Current Research: Proceedings of the Dr. Joseph F. Poland Symposium on Land Subsidence*, edited by: Borchers, J. W., Association of Engineering Geologists, Star Publishing Company, Belmont, California, Special Publication No. 8, 217–226, 1998

Lisiecki, L. E., and M. E. Raymo, 2005. A Pliocene-Pleistocene stack of 57 globally distributed benthic δ18O records, Paleoceanography, 20, PA1003, doi:10.1029/2004PA001071.

Lofgren, B.E., 1975. Land Subsidence Due to Ground-Water Withdrawal, Arvin-Maricopa Area, California, USGS Professional Paper 437-D.

Lofgren, B.E., and R.L Klausing, 1969. Land Subsidence due to Ground-Water Withdrawal, Tulare-Wasco Area, California. USGS Professional Paper 437-B.

Marston, Landon, and Konar, Megan, 2017. “Drought impacts to water footprints and virtual water transfers of the Central Valley of California.” *Water Resources Research, Volume 53, Issue 7*, pages 5756–5773, American Geophysical Union. July 2017, Version of Record online: July 18, 2017.

Miller, D.D., 1999. Sequence Stratigraphy and Controls on Deposition of the Upper Cenozoic Tulare Formation, San Joaquin Valley, California. A dissertation submitted to the Department of Geological and Environmental Sciences and the Committee on Graduate Studies of Stanford University in Partial Fulfillment of the Requirements for the Degree of Doctor of Philosophy in Applied Earth Sciences, June.

Miller, R.E., Green J.H., and Davis, G.H. 1971. Geology of the Compacting Deposits in the Los Banos-Kettleman City Subsidence Area, California. USGS Professional Paper 497-E.

National Geodetic Survey (NGS), 2016. Website at http://www.ngs.noaa.gov/NGSDataExplorer/

National Oceanic & Atmospheric Administration (NOAA), 2009. Attachment Y Light Detection and Ranging (LIDAR) Requirements, Scope of Work for Shoreline Mapping under the NOAA Coastal Mapping Program. Remote Sensing Division, National Geodetic Survey, National Ocean Service, NOAA, U.S. Department of Commerce, December. Accessed on June 20, 2016 at http://www.ngs.noaa.gov/RSD/LIDAR_SOW_NGSDec2009.pdf

Page, R. W., 1986. Geology of the fresh ground-water basin of the Central Valley, California, with texture maps and sections: United States Geological Survey, Professional Paper 1401-C.

Panda, B. B., M.L. Rucker, and K.C. Fergason, 2015. “Modeling of earth fissures caused by land subsidence due to groundwater withdrawal,” in *Proc. IAHS*, 372, 69-72, doi:10.5194/piahs-372-69-2015, 2015.

Paul, Stephen, 2007. Historic Recreation: Tulare Lake, California. Available at: https://productforums.google.com/forum/#!topic/gec-nature-science/4laDZTIOHYc

Poland, J.F., Lofgren, B.E., Ireland, R.L., and Pugh, R.G., Land Subsidence in the San Joaquin Valley, California, As of 1972, U.S. Geological Survey Professional Paper 437-H.

Huang, Qiangbing, and Jianwei Qiao, 2015. *Ground Fissure: A Great Challenge to Metro Project in Xi'an, China.* NISOLS PowerPoint presentation on November 10.

Rail Delivery Partner, 2015. Personal communication from Tom Lee (Parsons Brinckerhoff under RDP contract with Authority) to Jim French (Amec Foster Wheeler). October 15.

Railway-Technology.com, accessed 2017. http://www.railway-technology.com/projects/xian-metro-shaanxi/.

RDP: See Rail Delivery Partner

Rucker, M.L., Fergason, K.C., Greenslade, M.D. and Hansen, L.A., 2013. Characterization of subsidence impacting flood control dams and levees, presented at the USSD Dam Conference, Phoenix, Arizona, March. Accessed on 6/9/2016 at: http://ussdams.com/proceedings/2013Proc/1269-1284.pdf

Rucker, M.L., K. C. Fergason, and B. B. Panda, 2015. “Subsidence Characterization and Modeling for Engineered Facilities in Arizona, USA,” in *Proc. IAHS*, 372, 361–366.

Rucker, M.L. and Holmquist, O.C.,2006, Surface Seismic Methods for Locating and Tracing Earth Fissures and other Significant Discontinuities in Cemented Unsaturated Soils and Earthen Structures, Unsaturated Soils 2006, Geotechnical Special Publication No. 147, Miller, G.A., Zapata, C.E., Houston, S.L. and D.G. Fredlund, eds., ASCE, Reston, Virginia, pp. 601-612.

Rucker, M.L. and Keaton, J.R. (1998) “Tracing an earth fissure using seismic refraction methods and physical verification.” Land Subsidence Case Studies and Current Research: Proceedings of the Dr. Joseph F. Poland Symposium on Land Subsidence, Spec. Publ. No. 8, AEG, Star Publishing Co., Belmont/CA: 207-216.

Saleeby, J. and Z. Foster, 2004. Topographic response to mantle lithospheric removal, southern Sierra Nevada region, California: Geology, v. 32, p. 245-248, doi:1130/G19958.1.

Saleeby, J., Le Pourhiet, L., Saleeby, Z., and Gurnis, M., 2012. Epeirogenic transients related to mantle lithosphere removal in the southern Sierra Nevada region, California: Part I. Implications of thermomechanical modeling. Geosphere; December 2012; v. 8, no. 6; p. 1286-1309; doi:10.1130/GES00746.1.

Saleeby, J., Z. Saleeby, and L. Le Pourhiet, 2013. Epeirogenic transients related to mantle lithosphere removal in the southern Sierra Nevada region, California: Part II. Implications of rock uplift and basin subsidence relations. Geosphere; June 2013; v. 9, no. 3; p. 394-425; doi:10.1130/GES00816.1.

Scheirer, A.H., Magoon, L.B., 2007. Age, Distribution, and Stratigraphic Relationship of Rock Units in the San Joaquin Basin Province, California, Chapter 5, Petroleum Systems and Geologic Assessment of Oil and Gas in the San Joaquin Basin Province, California. USGS Professional Paper 1713, Scheirer, A.H., ed.

Schmid, Wolfgang, and Hanson, R.T., 2009, The Farm Process Version 2 (FMP2) for MODFLOW-2005—Modifications and Upgrades to FMP1: U.S. Geological Survey Techniques and Methods 6-A-32, 102 p.

Smith, T.C., 1983. Pond Fault, Northern Kern County. California Division of Mines and Geology Fault Evaluation Report FER-144. April 12.

Sneed, M., Brandt, J., Solt, M., 2013. Land Subsidence along the Delta-Mendota Canal in the Northern Part of the San Joaquin Valley, California, 2003-10. USGS Scientific Investigation Report SCI2013-5142.

Soga, K., 2014. Understanding the real performance of geotechnical structures using an innovative fibre optic distributed strain measurement technology, Rivista Italiana di Geotechnica, No.4, Ottobre-Dicembre, p 7-48.

Soga, K., Mohamad, H. and Bennett, P.J., 2008. “Distributed Fiber Optics Strain Measurements for Monitoring Geotechnical Structures” (August 11, 2008). International Conference on Case Histories in Geotechnical Engineering, Paper 4. http://scholarsmine.mst.edu/icchge/6icchge/session14/4.

Summers Engineering, Inc., 1992. Tulare Lake Basin Topography. Originally based on survey by U.S.C. & G.S in June 1966. Revised May 1992 based on 1982-83 flood.

Tape, C., Muse, P., Simons, M., Dong, D. and Webb, F., 2009. Multiscale estimation of GPS velocity fields, Geophys. J. Int., 179, 945-971.

Thatcher, C., Danielson, J., Lim, S., Palaseanu-Lovejoy, M., Brock, J. and Kimbrow, D., 2013. Comparison of Airborne and Mobile Terrestrial Lidar to Map Louisiana Levees. Available at http://topotools.cr.usgs.gov/posters/levee_AAG_poster.pdf. Accessed on 6/22/2016.

Tsunashima, H. Naganuma,Y., Akira Matsumoto, Mizuma, T. and Mori, H. (2012). Condition Monitoring of Railway Track Using In-Service Vehicle, Reliability and Safety in Railway, Dr. Xavier Perpinya (Ed.), ISBN: 978-953-51-0451-3, InTech, Available from: http://www.intechopen.com/books/reliabilityand-safety-in-railway/condition-monitoring-of-railway-track-using-in-service-vehicle.U. S. Army Corps of Engineers (USACE), 2010. Success Dam Seismic Remediation, San Joaquin Valley, California, Floodplain Mapping Study for Economic Analysis (Redacted), August.

U.S. Geological Survey, 1928. Corcoran 7.5' Quadrangle Topographic Map. Topography by S.B. O'Hara; Control by U.S. Geological Survey; Surveyed in 1926.

U.S. Geological Survey (USGS), 2006. Quaternary Fault and Fold Database for the United States, Electronic document, available at: http//earthquakes.usgs.gov/regional/qfaults/

U.S. Geological Survey, 2016. The National Map, 2016, 3DEP products and services: The National Map, 3D Elevation Program Web page, accessed at http://nationalmap.gov/3DEP/3dep_prodserv.html.

USGS. See U.S. Geological Survey.

Weeks, R.E. and Panda, B.B. (2004) "Defining subsidence-induced earth fissure risk at McMicken Dam," Proceedings of the 24th Annual Conf. of the Assoc. State Dam Safety Officials, Phoenix, AZ, Sept 25-30.

Yudhbir, 1984. "Mechanics of Collapse Controlled Subsidence." In *Proc 3rd International Symposium on Land Subsidence*, Venice, 19–25 March, 1984, P467–477. Publ Wallingford: IAHS, 1986.

amec
foster
wheeler

TABLES

Table 9-1: Summary of Methods of Measurement and Monitoring for Subsidence and Related Parameters

Legend:
'+' directly applicable
' ~' secondary applicability
'?' possibly applicable
'-' not applicable

				Data Freq.		Period of Implementation				Automated Database Link Possible?		Parameters to Monitor For									
																		Fissures			
Category	**Method**	**Capabilities and Limitations**	**Method should be evaluated further**	Continuous	Intermittent/ Manual	Pre-construction	During construction	Post-construction	During Operations	Automated Data Acquisition	Link to Database?	Consolidation Settlement	Subsidence	Slope/Tilt	Curvature	Differential Horizontal Movement or Curvature	Groundwater Piezometric Head	Fissures	Sag	Flood Plain	Compaction Fault
	Tiltmeter			+						+				+							
InSAR	L-band	Good resolution of vertical deformation over broad areas; need to consider relative pros/cons of L-band (λ=24cm) or C-band (λ=6cm).			+	+	+	+	+		+	?	+	+	+	?		+		+	+
	C-band				+	+	+	+	+		+	~	+	+	+	?		+		+	+
	X-band				+	+	+	+	+		+	+	+	+	+	?		+		+	+
	Corner Reflectors				+	+	+	+	+		+	?	+			?				+	+
	Radar Transponders				+	+	+	+	+		+	?	+			?				+	+
Satellite	Satelite Altimetry	Data only along lines that occasionally cross HSR alignment, but data is continuous 1992 to present.			?	~	?	?	?		~		~							~	~
Satellite or Aircrafft	Gravity Meter	May show preseence of buried bedrocks highs, but this isn't likely a concern in SJV.			-	-	?	-	-		-	-	-	-	-						?
Aircraft	UAV-SAR	May be be able to give good vertical and horizontal resolution of movement, but requires frequent project-authorized flights.			+	~	~	~	~		~	+	+	+	+	?		+		~	~
Aircraft (or satellite)	LiDAR	Good vertical and horizontal resolution across fairly broad area; requires new flight, GPS check points curvey, and analyses each time information is wanted.			+							+	+					~		+	+
Survey	Optical / conventional	Good data for horizontal and best data for vertical movement for predetermined points; labor-intensive; based on benchmark reference, which may be moving; results also analysed as relative displacement / elevation change between monuments.			+	+	+	+	+			+	+	~	~						+

Table 9-1: Summary of Methods of Measurement and Monitoring for Subsidence and Related Parameters

Legend:
'+' directly applicable
' ~' secondary applicability
'?' possibly applicable
'-' not applicable

				Data Freq.		Period of Implementation				Automated Database Link Possible?		Parameters to Monitor For									
Category	**Method**	**Capabilities and Limitations**	Method should be evaluated further	Continuous	Intermittent/ Manual	Pre-construction	During construction	Post-construction	During Operations	Automated Data Acquisition	Link to Database?	Consolidation Settlement	Subsidence	Slope/Tilt	Curvature	Differential Horizontal Movement or Curvature	Groundwater Piezometric Head	Fissures	Sag	Flood Plain	Compaction Fault
	Static GPS	Best data for horizontal and vertical movement for predetermined points along recommended 1/4 mile spaing along alignment; moderately labor-intensive; based on absolute reference; results also analysed as relative displacement / elevation change between monuments.			+	?	+	+	+		+	+	+			+		+		+	+
CGPS	CGPS	Best continuous data for vertical and horizontal movement due to subsidence, but each instrument is only for a single point.		+		+	+	+	+	+	+	+	+			+				~	
Survey Monuments	Construction Control Points	Suggest at 1/4 mile intervals along alignment; should become backbone of monitoring system.			+	+	+	+	+			+	+							+	+
Borehole Extensometer	Standard nested	Requires large hole and/or several holes to get multiple tell-tail elevations; expensive installation		~	~	+	+	+	+		+	+	+							~	+
Tilt Meter	Borehole Tilt Meter	Shows angular rotation of rod in ground; relatively expensive but sensitive to very small rotations; Each one is limited to single preselected location. Continuous and/or remote data collection possible.		?	+	+	+	+	+	+	+			+		~					~
	Magnetic	Smaller boring diameter; quite a few depths can be read for each boring with good precision; may be limited to around 600 ft max. depth.			+	+	+	+	+		+	+	+							~	+

Table 9-1: Summary of Methods of Measurement and Monitoring for Subsidence and Related Parameters

Legend:
'+' directly applicable
' ~' secondary applicability
'?' possibly applicable
'-' not applicable

				Data Freq.		Period of Implementation				Automated Database Link Possible?		Parameters to Monitor For									
																		Fissures			
Category	**Method**	**Capabilities and Limitations**	Method should be evaluated further	Continuous	Intermittent/ Manual	Pre-construction	During construction	Post-construction	During Operations	Automated Data Acquisition	Link to Database?	Consolidation Settlement	Subsidence	Slope/Tilt	Curvature	Differential Horizontal Movement or Curvature	Groundwater Piezometric Head	Fissures	Sag	Flood Plain	Compaction Fault
Piezometer (new; or possibly re-purpose existing wells)	Stand Pipe	Simple technology, labor-intensive to read; single screen interval per boring.			+	+	+	+	+				~				+				+
	Vibrating Wire	Simpler to install; remote and/or continuous reading possible; can be nested.		~	~	+	+	+	+	+	+		~				+				+
	Pneumatic	Can be nested; labor-intensive to read.			~								~				+				+
	Surface Seismic Array	?	x	+	+	?	?	?	+	+	+										
	Fibre Bragg Grating sensors	?	x	+	+			+	+	+	+				?	+		+	?		+
	BOTDR	Distributed precise strain; significnt startup effort & cost	x	+	+			+	+	~	+	?			?			+			+
Misc.	Seismic Refraction	May identify crack presence (or, when repeated over time, initiation) at depth before visible at surface IF crack location is spanned by geophones. Labor intensive geophysical operation, usually applied when other evidence indicates potential or imminent earth fissure development.	x		+	+	+	+	+									+			+
	Passive Geophone	May identify crack initiation at depth before visible at surface IF crack location is spanned by phones and seismic energy propagation is properly oriented.		+				+	+	+	+										
	Precision electronic horizontal exte	Expensive / very expensive for measuring movement across known specific earth fissure location.Real-time monitoring capable.		+		+	+	+	+	+	+										
	Trench or test pit	Confirm presence or absence of earth fissuring by observing and mapping trench or pit sidewalls. Destructive test, OSHA regulations on work in trench	x		+	+	+	+	+									+			+
On-train	Accelerometer	Can report on	~	~	+				+	+	+	?			+						+
	GPS?			?	+				+	+	+	?	?								
	Camera			~	~	~	~	~	~			~	~	~	~	~	~	~	~	~	~
	Other?																				

Table 9-1: Summary of Methods of Measurement and Monitoring for Subsidence and Related Parameters

Legend:
'+' directly applicable
' ~' secondary applicability
'?' possibly applicable
'-' not applicable

				Data Freq.		Period of Implementation				Automated Database Link Possible?		Parameters to Monitor For									
																		Fissures			
Category	**Method**	**Capabilities and Limitations**	Method should be evaluated further	Continuous	Intermittent/ Manual	Pre-construction	During construction	Post-construction	During Operations	Automated Data Acquisition	Link to Database?	Consolidation Settlement	Subsidence	Slope/Tilt	Curvature	Differential Horizontal Movement or Curvature	Groundwater Piezometric Head	Fissures	Sag	Flood Plain	Compaction Fault
Extensometer	Tape Extensometer	Useful at location and in direction established. Primarily deployed as a monument array (typical 50-100 foot spacing) across feature when other evidence indicates imminent earth fissure development or after earth fissure is identified. Labor-intensive to read. Use with optical or GPS survey.			+	+	+	+	+		+					+		+			
	Fiber Optic BOTDR	Emerging technology for ground or concrete strain measurement	x	?	+		+	+	+	+	+	+				+		+			+
	Optic Interferometric Extensometer		x				+	+	+		+										
Contruction Water Well	Survey Monuments nearby (GPS or Total Station)			?	+	+	+	+	+				+								+
	Nearby Piezometers (25', 125', 500'?)			+		+	+	+				+									+
	Extensometer				+													+			
	Flow meter			+																	
	Tilt Meters			+										+	~						
	Barometric Pressures			?																	
	Ambient Tempurature			?																	

Legend: "+" = directly applicable; "~" = secondary applicability; "?" = possibly applicable; "-" - not applicable

Table 10-1: Recommended Monitoring Methods

	Pre-Construction			During Construction			Post-Construction			Operations			
Method	**Recommended Minimum Program**	**Preferred Program**	**To be Considered Further**	**Recommended Minimum Program**	**Preferred Program**	**To be Considered**	**Recommended Minimum Program**	**Preferred Program**	**To be Considered**	**Recommended Minimum Program**	**Preferred Program**	**To be Considered**	**Notes:** **'3' strongly recommended** **'2' recommended, less critical** **'1' consider in specific circumstances** **'?' may have value, consider** **Comments**
Site Reconnaissance	3	3		3	3		3	3		3	3		Look for evidence of fissures, faults, other modes of strain.
Trench or Test Pit		2		2	3				yes			yes	During construction, observe subgrade excavation in vicinity of Poso Creek Fault; post-construction and operations as needed if tensile ground displacement develops
L-band InSAR	3	3		2	2		3	3		3	3		Use JPL to the extent possible. Phase 2-4 consider automating acquisition.
C-band / X-band InSAR		2	yes		?	yes	3	3	yes	3	3		Where usable, C-band (Sentinel) or X-band provides superior resolution and frequent coverage if needed. Usefulness dependent upon coherent coverage; may not be usable in all areas.
Satellite Altimetry	2	2			1			1		?	?		Use existing data for baseline of history of subsidence rate/magnitude since 1992.
UAVSAR		?	yes		?	yes		?	yes	?	?	yes	Emerging availability, may be an effective future alternative.

Table 10-1: Recommended Monitoring Methods

	Pre-Construction			During Construction			Post-Construction			Operations			
Method	**Recommended Minimum Program**	**Preferred Program**	**To be Considered Further**	**Recommended Minimum Program**	**Preferred Program**	**To be Considered**	**Recommended Minimum Program**	**Preferred Program**	**To be Considered**	**Recommended Minimum Program**	**Preferred Program**	**To be Considered**	**Notes:** **'3' strongly recommended** **'2' recommended, less critical** **'1' consider in specific circumstances** **'?' may have value, consider** **Comments**
Airborne LiDAR	3	3		1	1			3	yes			yes	Confirm or modify existing topos; recommend future LiDAR during or end of construction, possibly after construction.
Terrestrial LiDAR							3	3	yes	3	3	yes	Monitoring viaduct & retained embankment movements
Land Survey (Optical or GPS)		2			2			2			2		Evaluate & monitor existing nearby structures and other features.
Control Point Survey (GPS/Optical)	3	3		3	3		3	3		3	3		GPS monuments at ~1/4 mile spacing may be backbone of horizontal ground movement / tensile strain / discrete displacement monitoring. Use construction control points during and post-construction for detail optical monitoring as needed.
CGPS	3	3		3	3		3	3		3	3		Pre-construction, use existing networks. Then select locations for permanent HSR sites. Priority is pairing with piezometers / compaction extensometers.

Table 10-1: Recommended Monitoring Methods

	Pre-Construction			During Construction			Post-Construction			Operations			
Method	**Recommended Minimum Program**	**Preferred Program**	**To be Considered Further**	**Recommended Minimum Program**	**Preferred Program**	**To be Considered**	**Recommended Minimum Program**	**Preferred Program**	**To be Considered**	**Recommended Minimum Program**	**Preferred Program**	**To be Considered**	**Notes:** **'3' strongly recommended** **'2' recommended, less critical** **'1' consider in specific circumstances** **'?' may have value, consider** **Comments**
Borehole Tilt Meter		1	yes		1	yes		1	yes		1	yes	Consider these in areas of critical ground displacement or differential subsidence and/or Poso Creek Fault crossing.
Borehole Extensometer		2	yes	2	2		2	2		2	2		Recommend 1 or 2 of these near areas of greatest subsidence. Existing wells within Alignment ROW may provide opportunity for cost-effective limited installs.
Tape Extensometer					?	yes		?	yes			yes	As needed if tensile ground strain is identified; may be first stage for close-spacing horizontal monitoring
Precision electronic horiz extensometer						yes			yes			yes	As needed if ground strain is identified; may be used for critical stage of close-spacing horizontal monitoring
Surface Seismic Array						yes			yes			yes	As needed if train-induced dynamic ground loading becomes an issue

Table 10-1: Recommended Monitoring Methods

	Pre-Construction			During Construction			Post-Construction			Operations			
Method	**Recommended Minimum Program**	**Preferred Program**	**To be Considered Further**	**Recommended Minimum Program**	**Preferred Program**	**To be Considered**	**Recommended Minimum Program**	**Preferred Program**	**To be Considered**	**Recommended Minimum Program**	**Preferred Program**	**To be Considered**	**Notes:** **'3' strongly recommended** **'2' recommended, less critical** **'1' consider in specific circumstances** **'?' may have value, consider** **Comments**
Fiber Optic BOTDR				1	1	yes	1	1	yes	1	1	yes	Emerging technology; monitor strain at viaducts & retained embankments; if successful, consider for general ground strain monitoring
Fiber Bragg Extensometers						yes			yes			yes	As needed if ground displacement is identified; critical level of close spacing horizontal monitoring
Seismic Refraction			yes			yes			yes			yes	As needed if reconnaissance or monitoring indicates possible ground displacement condition or feature
Passive Geophones						yes			yes			yes	Emerging technology; may be useful in areas suspected of fissure development
Monitoring well/piezometer		2		2	3		2	3		2	3		Recommend at least a few of these along alignment. Essential at compaction extensometer sites. Utilize existing wells within Alignment ROW.

Table 10-1: Recommended Monitoring Methods

	Pre-Construction			During Construction			Post-Construction			Operations			
Method	**Recommended Minimum Program**	**Preferred Program**	**To be Considered Further**	**Recommended Minimum Program**	**Preferred Program**	**To be Considered**	**Recommended Minimum Program**	**Preferred Program**	**To be Considered**	**Recommended Minimum Program**	**Preferred Program**	**To be Considered**	**Notes:** **'3' strongly recommended** **'2' recommended, less critical** **'1' consider in specific circumstances** **'?' may have value, consider** **Comments**
Instrumented Train													Emerging availability; provides complete coverage of rail geometry
Vertical slope & curvature										3	3	yes	
Horizontal slope & curvature										3	3	yes	
Superelevation										3	3	yes	
Video										3	3	yes	

Note: "3" means this method is strongly recommended; "2" means it is recommended but less critical than a 3; "1" means it seems appropriate and should be considered, but may not be necessary. "?" mean there may be some value in this mehtod and it should be considered further.

amec
foster
wheeler

PLATES

S:\OD15\8715180680\Plate_01-01_rev171108.mxd

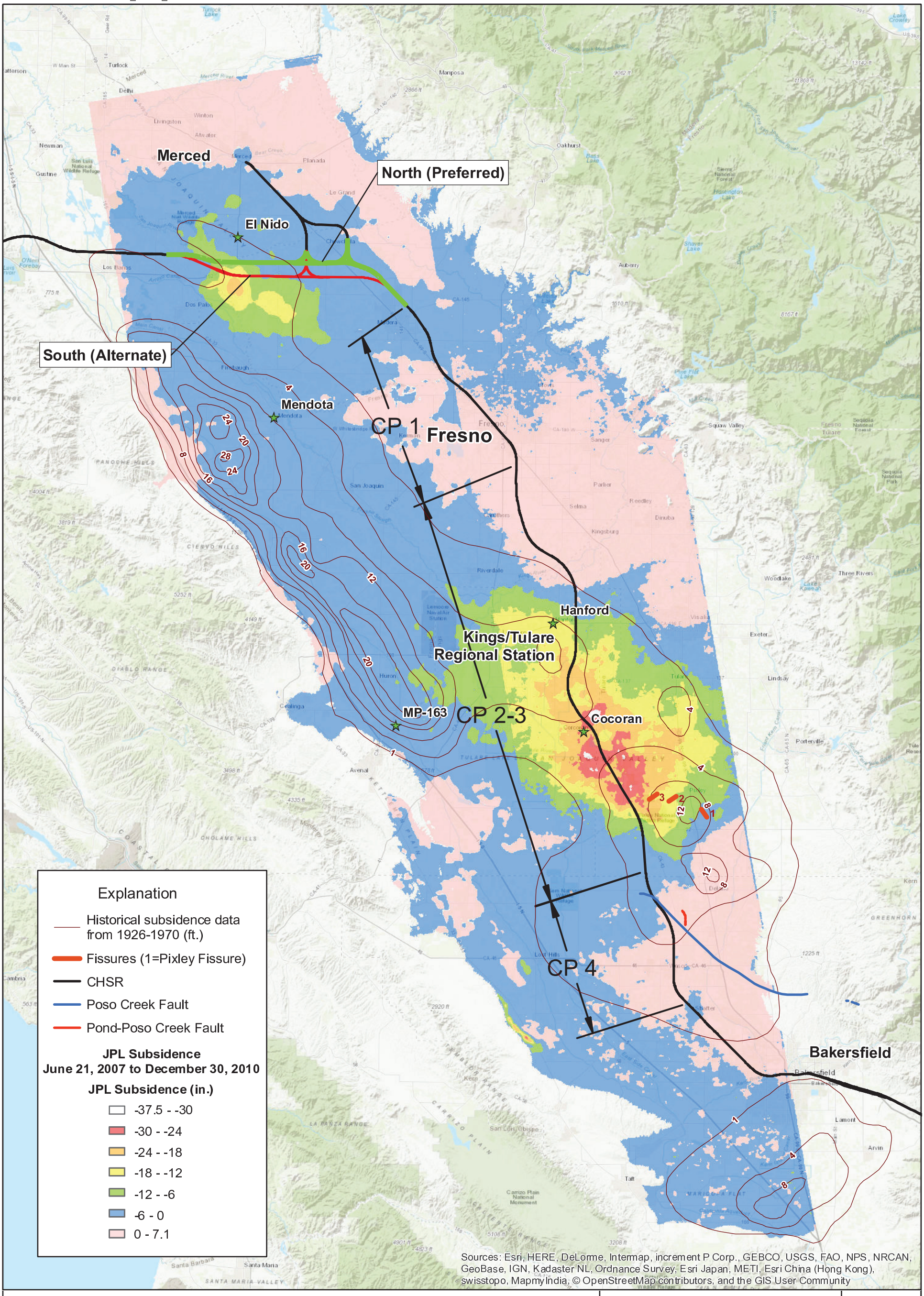

0 10 Miles

0 20 Kilometers

N

SAN JOAQUIN VALLEY
SUBSIDENCE MAP
San Joaquin Valley
HSR Ground Subsidence Study
California

amec foster wheeler

Date: 11/2017

Project No. 8715180680.04

Plate
ES-1

20180201

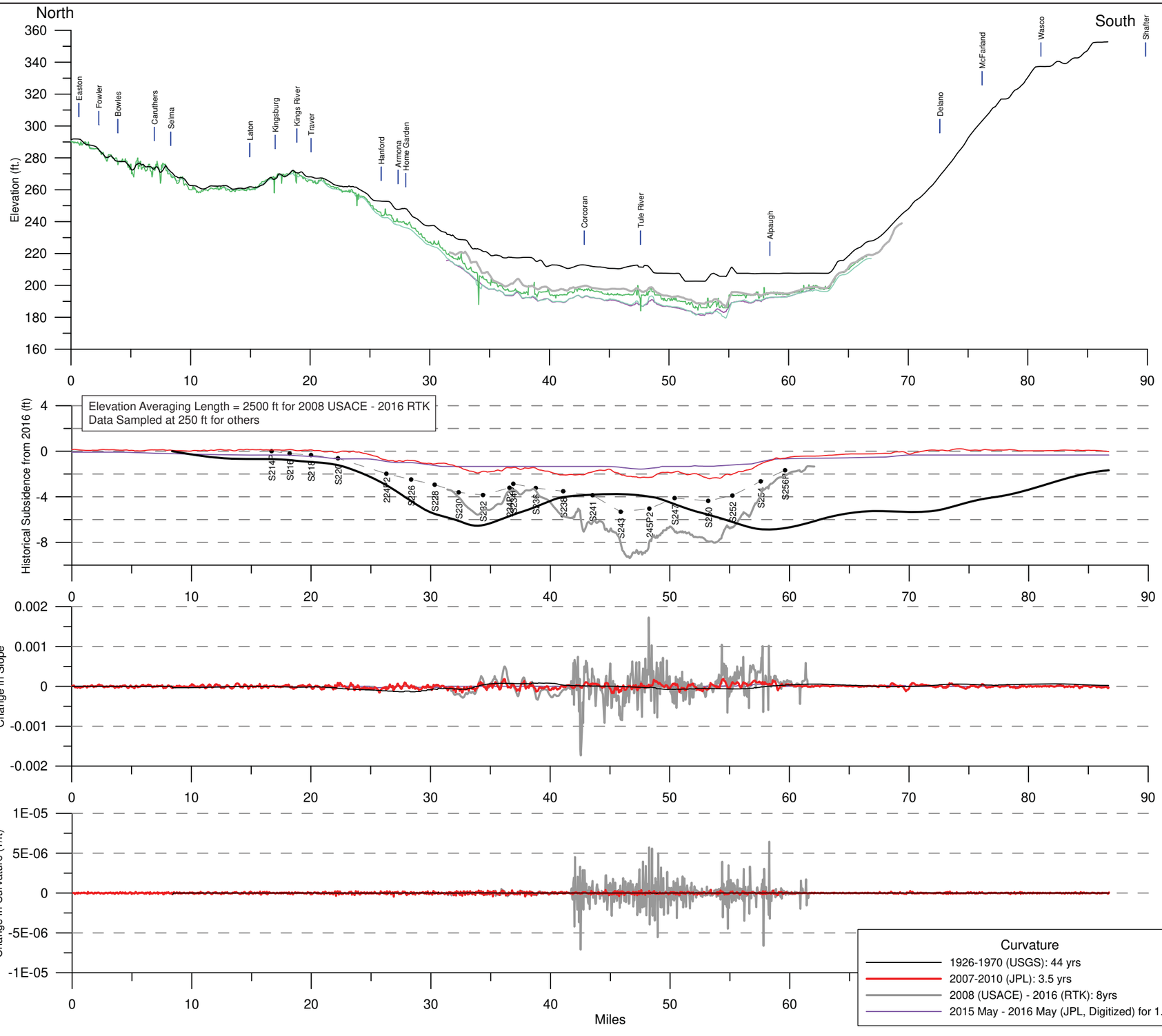

Ground Surface
- 1926 USGS
- 2008 (USACE)
- 2010 Baseline Report
- 2015 Dragados
- 2016 LM

Subsidence
- 1926-1970 (USGS): 44 yrs
- 2007-2010 (JPL): 3.5 yrs
- 2008 (USACE) - 2016 (RTK): 8yrs
- 2015 May - 2016 May (JPL, Digitized) for 1.04 yrs
- HSR Survey Monitoring Points

Slope
- 1926-1970 (USGS): 44 yrs
- 2007-2010 (JPL): 3.5 yrs
- 2008 (USACE) - 2016 (RTK): 8yrs
- 2015 May - 2016 May (JPL, Digitized) for 1.04 yrs

Curvature
- 1926-1970 (USGS): 44 yrs
- 2007-2010 (JPL): 3.5 yrs
- 2008 (USACE) - 2016 (RTK): 8yrs
- 2015 May - 2016 May (JPL, Digitized) for 1.04 yrs

PROFILES OF HISTORICAL SUBSIDENCE, SLOPES, AND CURVATURE IN SAN JOAQUIN VALLEY

San Joaquin Valley
HSR Ground Subsidence Study
California

Date: 08/08/2017

Project No. 8715180680.04

amec foster wheeler

Plate
ES-2

S:\OD15\8715180680\gis\profile\profiles_july2017\Plate_ES-02_historic.ai

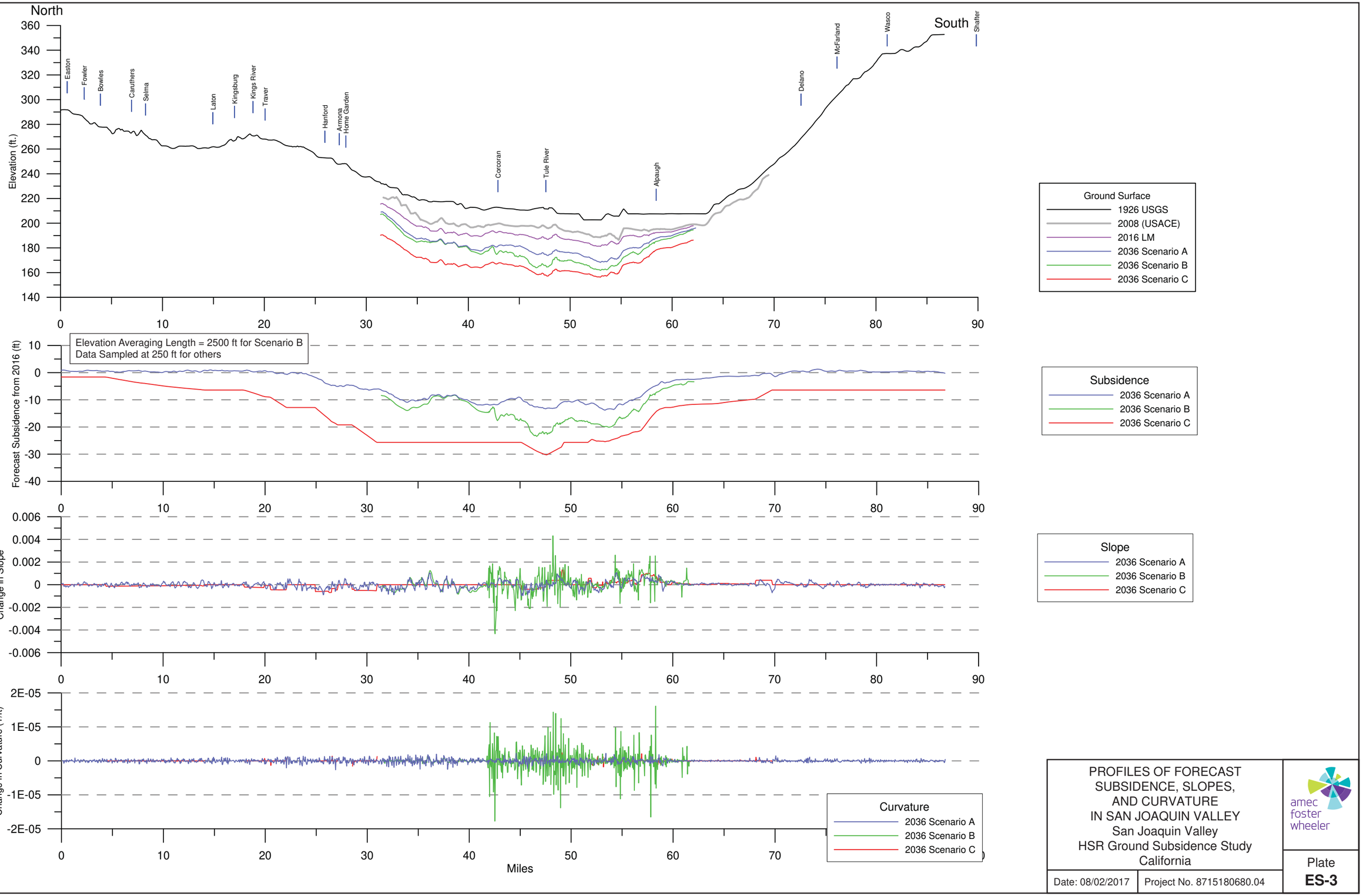

S:\OD15\8715180680\gis\profile\profiles_july2017\Plate_ES-03_forecast.ai

PROFILES OF FORECAST SUBSIDENCE, SLOPES, AND CURVATURE
IN SAN JOAQUIN VALLEY
San Joaquin Valley
HSR Ground Subsidence Study
California

Date: 08/02/2017 | Project No. 8715180680.04

amec foster wheeler

Plate
ES-3

S:\OD15\8715180680\Plate_01-01_rev171108.mxd

Merced

North (Preferred)

El Nido

South (Alternate)

Mendota

CP 1

Fresno

Hanford

Kings/Tulare
Regional Station

MP-163

CP 2-3

Cocoran

CP 4

Bakersfield

Explanation

Historical subsidence data from 1926-1970 (ft.)

Fissures (1=Pixley Fissure)

CHSR

Poso Creek Fault

Pond-Poso Creek Fault

JPL Subsidence
June 21, 2007 to December 30, 2010
JPL Subsidence (in.)

-37.5 - -30
-30 - -24
-24 - -18
-18 - -12
-12 - -6
-6 - 0
0 - 7.1

0 10 Miles
0 20 Kilometers

N

SAN JOAQUIN VALLEY
SUBSIDENCE MAP
San Joaquin Valley
HSR Ground Subsidence Study
California

amec foster wheeler

Date: 11/2017

Project No. 8715180680.04

Plate
1-1

20180201

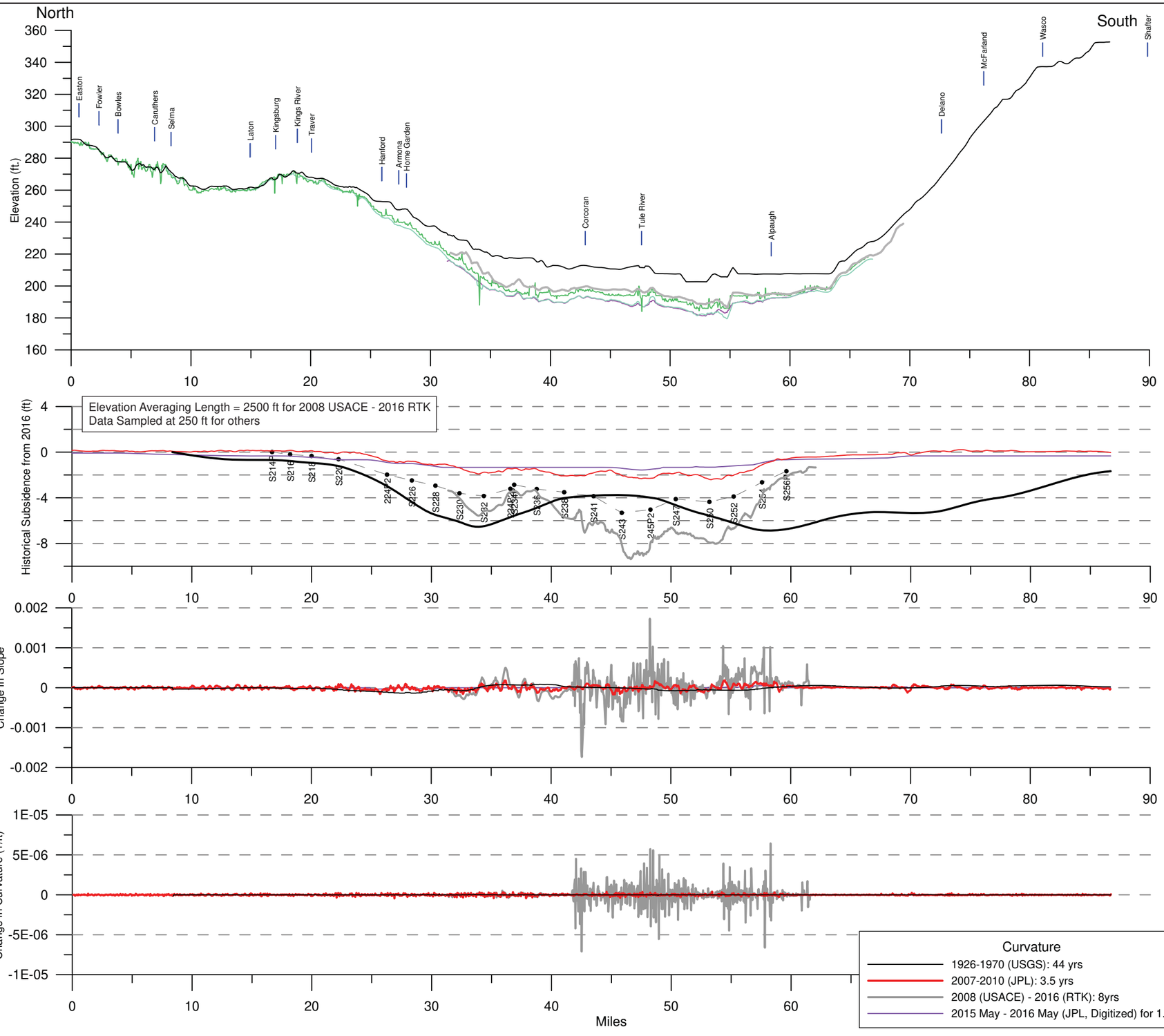

S:\OD15\8715180680\gis\profile\profiles_july2017\Plate_01-02_historic.ai

PROFILES OF HISTORICAL SUBSIDENCE, SLOPES, AND CURVATURE IN SAN JOAQUIN VALLEY

San Joaquin Valley
HSR Ground Subsidence Study
California

Date: 08/08/2017 | Project No. 8715180680.04

amec foster wheeler

Plate **1-2**

Pre-development of the central part of the San Joaquin Valley (modified from Faunt and others, 2009)

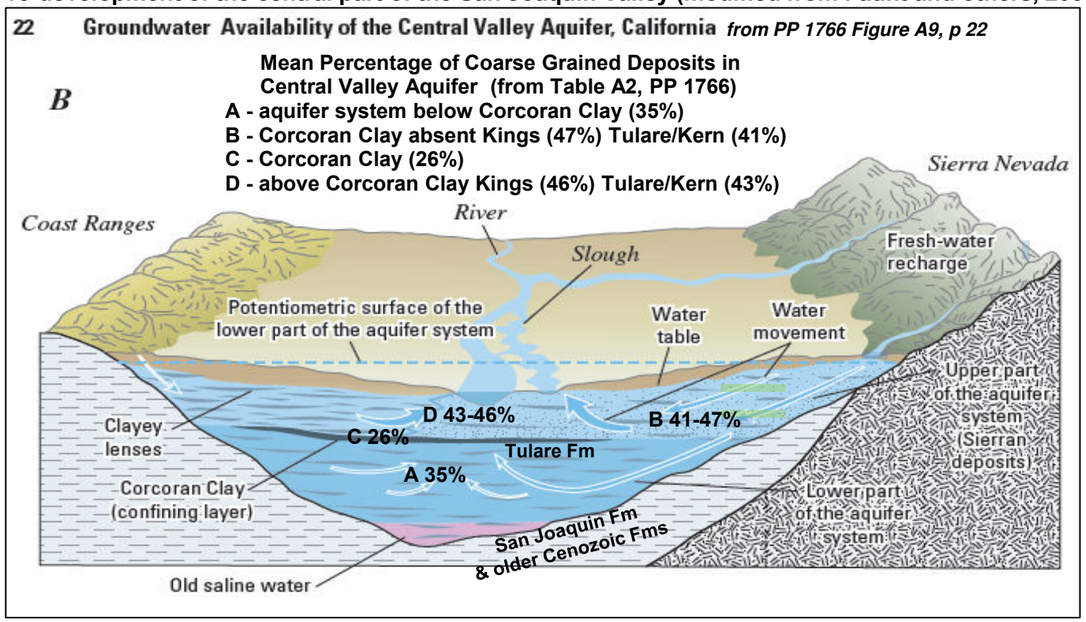

Above figure modified to reflect percentage of coarse-grained deposits fromTable A2 (PP 1766)

Notes: *from PP 1766 Figure A9, p 22*

'PP 1766' is USGS Professional Paper 1766 (Faunt and others, 2009)
Fine-grained deposits are shown as brown areas within aquifer system
Pattern of brown areas (fine-grained deposits with maximum subsidence potential) in aquifer system adapted from percolating matrix example in Rucker and others (2015)
Saline water pattern adapted from Figure 4 of Lofgren and Klausing (1969)

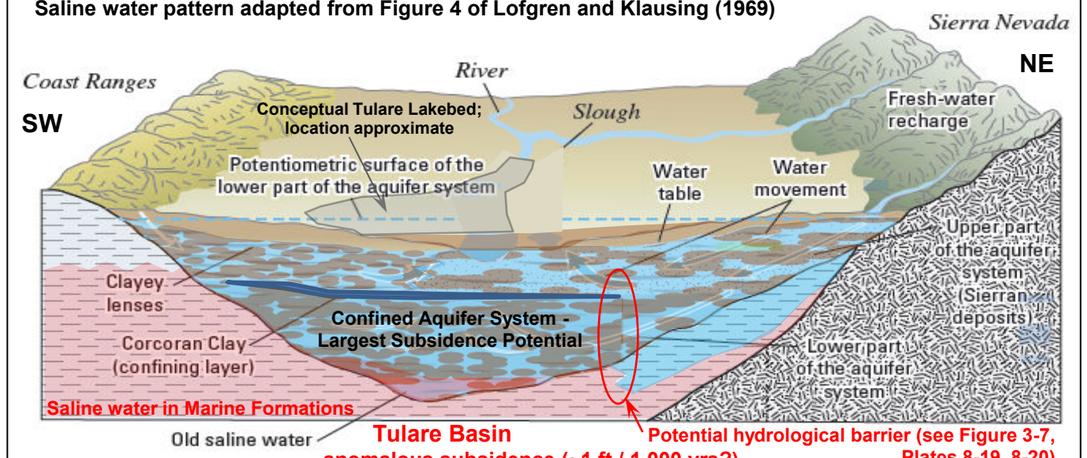

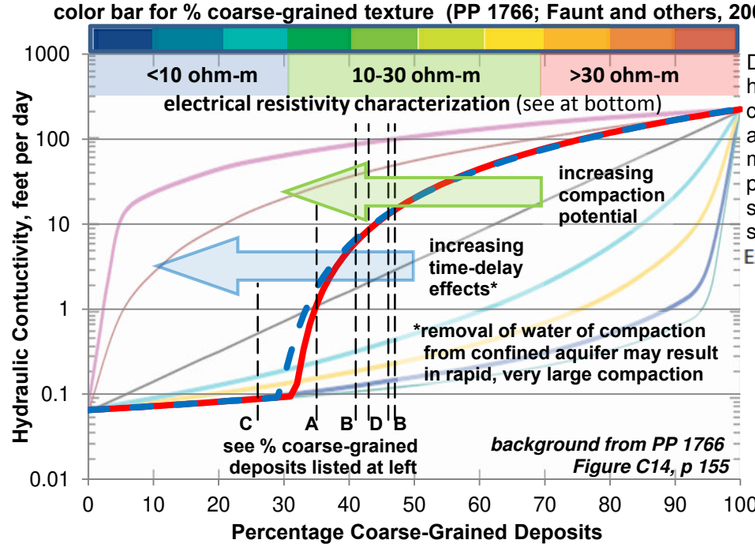

Determining a composite hydraulic conductivity in mixed coarse- and fine-grained alluvium is complex; various methods are discussed on pages 154-155 of PP 1766. A summary of averaging methods serves as the figure background:

Exponent of power mean—
−1.0 (Harmonic mean)
−0.8
−0.5
−0.3
0 (Geometric mean)
0.5
1.0 (Arithimetic mean

PT Approach to Estimate Hydraulic Conductivity

Pc =.3116, f =1.86
Pc = .289, f = 2
lithology averages

Estimating Hydraulic Conductivity from Percentage Coarse-grained Deposits

Another approach to assess behavior of a heterogeneous mixture of coarse- and fine-grained deposits utilizes concepts of connectivity from Percolation Theory (**PT**) as outlined by Rucker and others (2015). Various parameters may be modeled using **PT**, including permeability, electrical resistivity, and modulus. For this model of hydraulic conductivity (**K**), based on the fraction (not percentage) of coarse-grained deposits (**P**), the relation takes the form of

$$K_{aquifer\ system} = K_{fine} + C\,K_{coarse}\,(P - P_c)^f \quad \text{when} \quad P > P_c$$

where P_c is the threshold value where percolation begins, f is a power exponent (typically ~2 for permeability in 3-D) that may be empirically optimized, and **C** is a scaling constant. In the plot above, two 3-D PT cases are presented:

P_c = 31.16% (0.3116) assumes a face-centered cubic network matrix. f = 1.86 was empirically derived (Hunt 2004)

P_c = 28.9% (0.289) assumes a network of overlapping spheres and f = 2 to show parameter sensitivity.

In the context of modeling connectivity within a 3-D network, randomness is typically assumed for the distribution of low permeability cells in an otherwise high permeability matrix (or vice versa).

Tulare Formation Resistivity, Lithology & Compaction / Subsidence Potential

Fine-grained alluvium: very compressible silts and clays, but compaction is inhibited or delayed by very low permeabilities.
<~10 ohm-m resistivity

Heterogeneous alluvium: pathways of high permeability coarse-grained alluvium fraction provide drainage for the lenticular/ interlayered highly compressible fine-grained alluvium fraction.
~10 to ~25-30 ohm-m resistivity

Coarse-grained alluvium: sands and gravels with minor compaction which, due to high permeabilities is rapid.
>~25-30 ohm-m resistivity

HSR Ground Subsidence Study
California

OVERVIEW OF HYDRAULIC CONDUCTIVITY & COMPACTION / SUBSIDENCE POTENTIAL IN TULARE FORMATION (UNCONSOLIDATED TO SEMI-CONSOLIDATED ALLUVIUM)

PLATE **3-1**

Project 8715180680
PM : JF BY: MLR
Date 8/3/2017
Scale : n/a

amec foster wheeler

Example Lithological, Hydrological and Geotechnical Parameters Measurable from Oil/Gas Well Geophysical Logs

Well 102
(API 03920102)

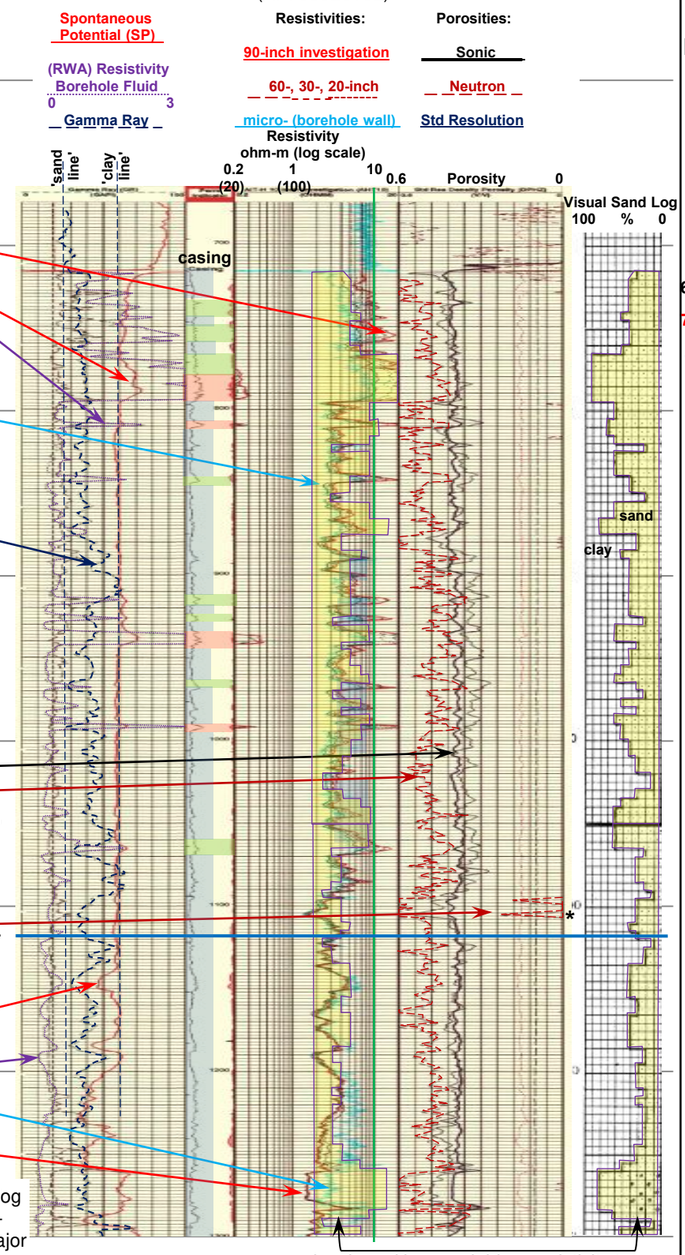

Moderate to high freshwater permeability zones are indicated by higher (90-inch) resistivities, SP trace trend to the right, and increase in borehole fluid resistivity at the zone producing fresh water. Borehole fluid is low resistivity, fresh water is high resistivity. Micro-resistivity is less than deep (90-inch) resistivity.

Gamma Ray log indicates varying percentage of clay content. Clays tend to contribute more gamma rays than sands; 'sand line' indicates minimal clays, 'clay line' indicates primarily clay.

Porosity logs indicate that alluvium porosity is typically ~0.36-0.42 per **Sonic log**, ~0.42-0.54 per Neutron log. Sonic log relevant for sand (?), (void ratio $e \simeq 0.56 - 0.72$), Neutron log for clay (?), (void ratio $e \simeq 0.72 - 1.17$) Highest porosities indicate ash deposits? (1,100 ft depth)*

Salt water in formation is indicated by SP trend to left, lower borehole fluid resistivity, and micro-resistivity greater than deep (90-inch investigation) resistivity.

* nearby well API 04720063 visual log description (mud log) depth 1,000-1,050 ft includes "volcanic ash major component w/ med brn bentonite"

Lithological, Geotechnical & Geophysical Measurements of the Pixley Corehole, 23/25-16N1, with Electrical Log (PP 437-B, Lofgren & Klausing 1969; PP 497-A, Johnson, Moston & Morris 1968)

Corehole is located ~1.6 miles west of Pixley Fissure No. 1

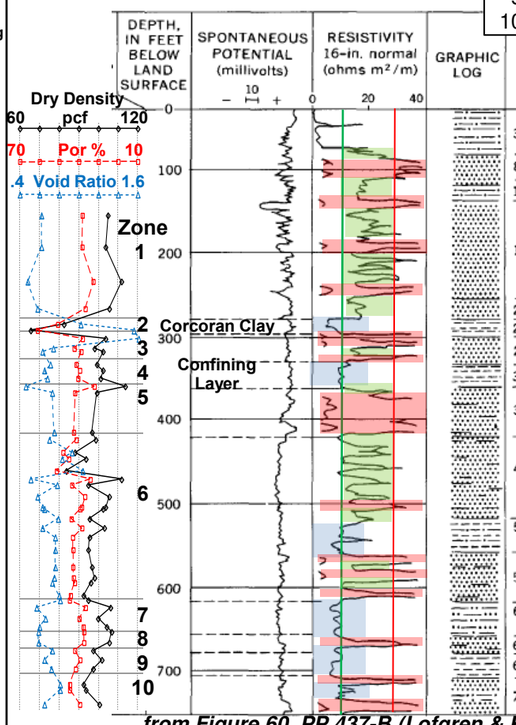

Zone	Depth feet	Average Spec Grav	Porosity n	Dry unit wt, pcf	Void Ratio	
1	0-280	2.68	0.36	108.7	0.54	
2	280-296	2.68	.56	73.6	1.27	Corcoran Clay
3	296-330	2.69	.40	100.7	.67	
4	330-360	2.70	.38	104.5	.61	principal confining layer
5	360-420	2.72	.42	98.4	.72	
6	420-620	2.70	.42	97.7	.72	
7	620-660	2.68	.41	98.7	.69	**Note:**
8	660-680	2.73	.37	107.3	.59	**data derived from**
9	680-710	2.69	.40	100.7	.67	**PP 437-B Table 13**
10	710-760	2.68	.43	95.3	.75	

GENERALIZED LITHOLOGIC DESCRIPTION
(from core descriptions and electric log)

30–80 Silt, sandy, loose to plastic, micaceous, yellowish-brown.

80–115 Sand, silty, loose to plastic, fine to coarse, yellowish brown.

115–138 Silt, sandy, loose to plastic, gravelly, calcareous, micaceous, yellowish-brown.

138–258 Sand, silty, loose to plastic, fine to coarse, micaceous, yellowish-brown.

258–280 Sand, silty, clayey, fine, some coarse, calcareous near bottom, micaceous, yellowish -brown.

280–296 Clay, plastic, silty, micaceous, pale brown to bluish-gray diatoms[1].

296–330 Sand, silty, loose to plastic, fine to coarse, micaceous pale olive to yellowish-brown.

330–360 Clay, sandy, silty, plastic, micaceous, calcareous streaks, yellowish-brown; thin sand interbeds[2].

360–420 Sand, silty, fine to coarse, gravelly, micaceous, yellowish-brown; thin clay interbeds.

420–520 Sand, silty, clayey, fine to coarse, some gravel, calcareous streaks, micaceous, yellowish-brown; clay, silt interbeds.

520–560 Clay, sandy, silty, plastic, gravelly, calcareous streaks, carbonaceous material, micaceous, yellowish-brown; thin sand interbeds.

560–620 Sand, silty, loose to friable, fine to coarse, gravelly some biotite, yellowish-brown; clay interbeds.

620–660 Silt, sandy, loose to plastic, some carbonaceous material calcareous nodules, micaceous, yellowish-brown; thin sand and clay interbeds.

660–680 Sand, silty, clayey, loose, fine to coarse, carbonaceous material brown to olive.

680–710 Clay, plastic, massive, calcareous nodules, micaceous, yellowish-brown.

710–752 Sand, loose, friable, massive, fine to coarse, micaceous.

from Figure 60, PP 437-B (Lofgren & Klausing 1969) and from Table 5, PP 497-A (Johnson, Moston & Morris 1968)

Legend - Tulare Formation Resistivity and Lithology

Fine-grained alluvium: very compressible silts and clays, but compaction is inhibited or delayed by very low permeabilities.
<~10 ohm-m resistivity

Heterogeneous alluvium: pathways of high permeability coarse-grained alluvium fraction provide drainage for the lenticular/ interlayered highly compressible fine-grained alluvium fraction.
~10 to ~25-30 ohm-m resistivity

Coarse-grained alluvium: sands and gravels with minor compaction which, due to high permeabilities is rapid.
>~25-30 ohm-m resistivity

HSR Ground Subsidence Study
California

EXAMPLE GEOTECHNICAL CHARACTERIZATION OF BASIN ALLUVIUM USING GEOPHYSICAL WELL LOGS

PLATE **3-2**

Project 8715180680
PM : JF BY: MLR
Date 7/12/2017
Scale : n/a

amec foster wheeler

site activity, well possibly being installed in August 2006?

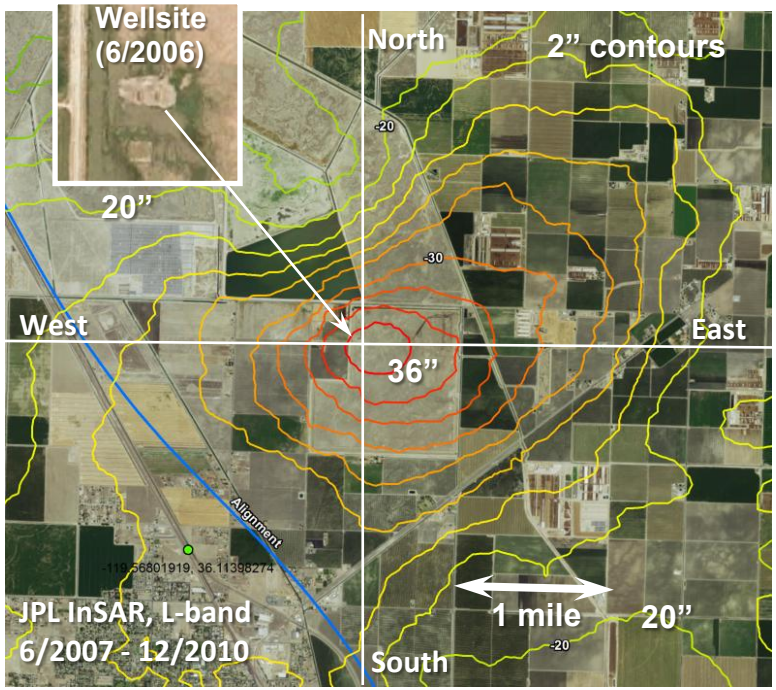

Same well location, different time periods

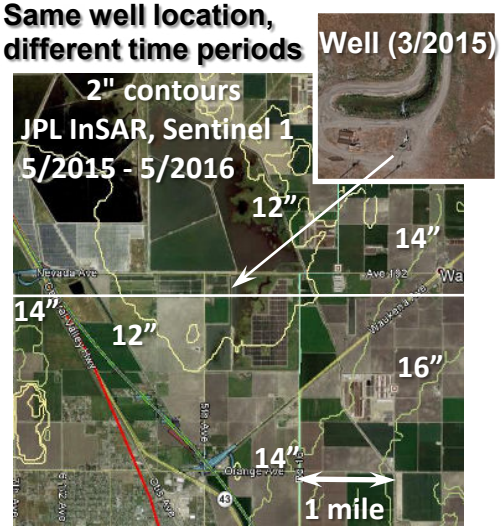

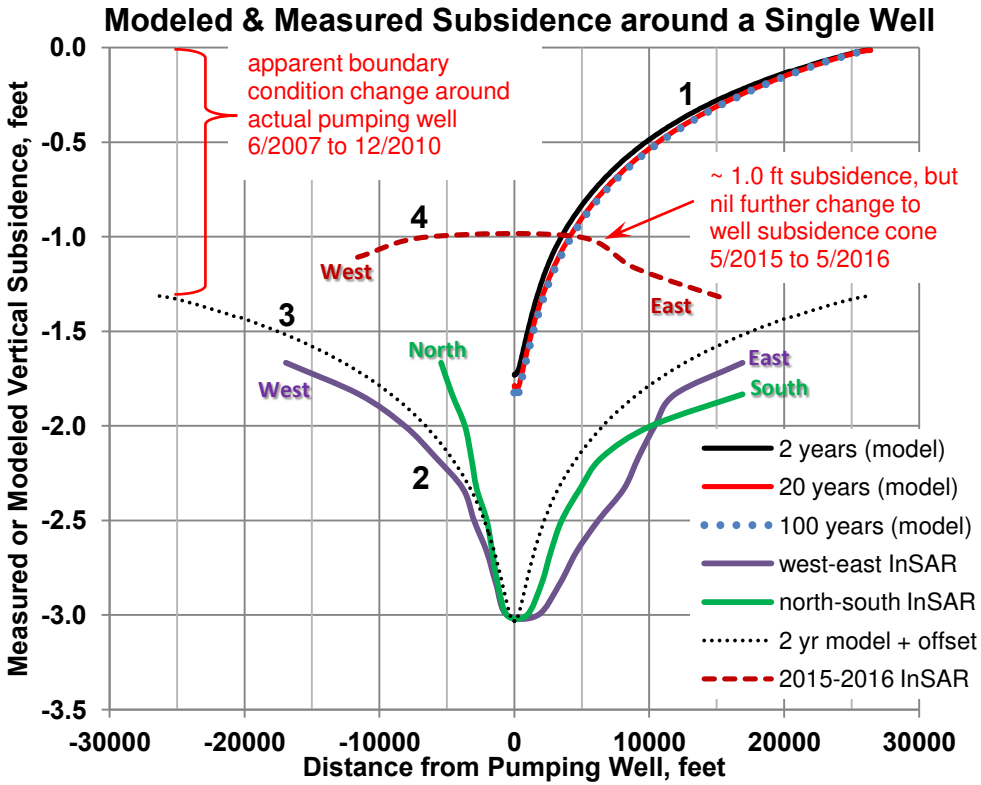

Notes on Modeled / Measured Subsidence Comparison:

1. Transient well model with constant head boundary condition. Note that the local well subsidence cone develops quickly, and is essentially complete in very few years.
2. Measured subsidence cone around an identified well appears within a few years of the wells installation.
3. Modeled well subsidence cone shape corresponds well to actual cone, but actual cone is likely influenced by variable subsurface conditions. Offset in total subsidence reflects changing actual well pumping boundary conditions; nearby wells and/or lack of connectivity cause no-flow boundaries.
4. Since local well subsidence cone developed in the first few years, well cone signature is absent in later subsidence profiling.

HSR Ground Subsidence Study
California

COMPARISON OF MODELED SINGLE WELL SUBSIDENCE WITH INSAR-DERIVED LOCAL SUBSIDENCE PATTERNS AROUND A LARGE PUMPING WELL NEAR CORCORAN, CA

PLATE
4-1

Project 8715180680
PM : JF BY: MLR
Date 7/12/2017
Scale : n/a

amec foster wheeler

Delamination Hinge
(Approximate per Saleeby & others 2013)

Tulare Basin Anomalous Subsidence
(Approximate per Saleeby & others, 2013)

Alos Palsar InSAR Colorband
June 2007 - December 2010

-38 inches 6

Legend

- Historic Oil/Gas Wells (HSR Vicinity)
- Oil/Gas Wells Referenced in Table 3-1
- CP2-3 Embankment
- CP2-3 Retained Embankment
- CP2-3 Viaduct
- HSR Alignment
- Pixley Fissure 1
- Pixley Fissures 2,3
- 2008-2016 LiDAR/RTK Subsidence Contours (ft)
- Profile Lines (Plates [8-] 6,7,20,21,22)
- 1926-1970 Subsidence Contours (ft)

Stationing

- UNAVCO CGPS Station
- CALTRANS (SOPAC) CGPS Station
- Miller (1999) Seismic Lines
- Clay Compaction Faults
- Pond Fault
- Poso Creek Fault

0 5 10 Miles

Job No.:	87-1518-0680
PM:	JF
Date:	8/3/2017
Scale:	1" = 10 miles

N

HSR Ground Subsidence Study
California

Central Valley Historic and Recent Subsidence, and Locations of Profiles Presented on Section 8 Plates

PLATE **8-1**

amec foster wheeler

S-N Profile 6th Ave - Dairy Ave to Corcoran - west of Hwy 43

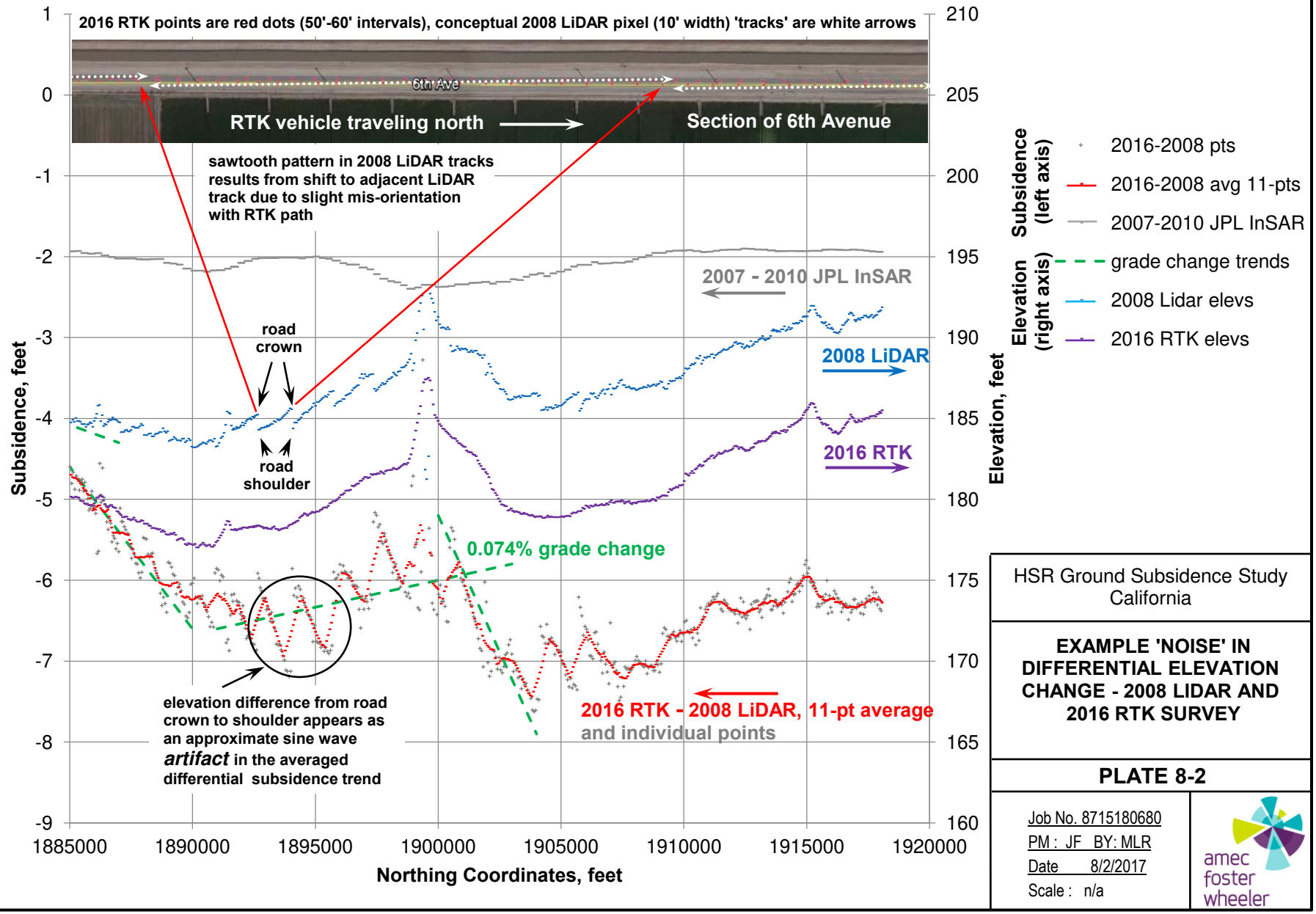

HSR Ground Subsidence Study
California

EXAMPLE 'NOISE' IN DIFFERENTIAL ELEVATION CHANGE - 2008 LIDAR AND 2016 RTK SURVEY

PLATE 8-2

Job No. 8715180680
PM : JF BY: MLR
Date 8/2/2017
Scale : n/a

amec foster wheeler

Google Earth Image of HSR Alignment CP2-3 area south of Hanford, CA

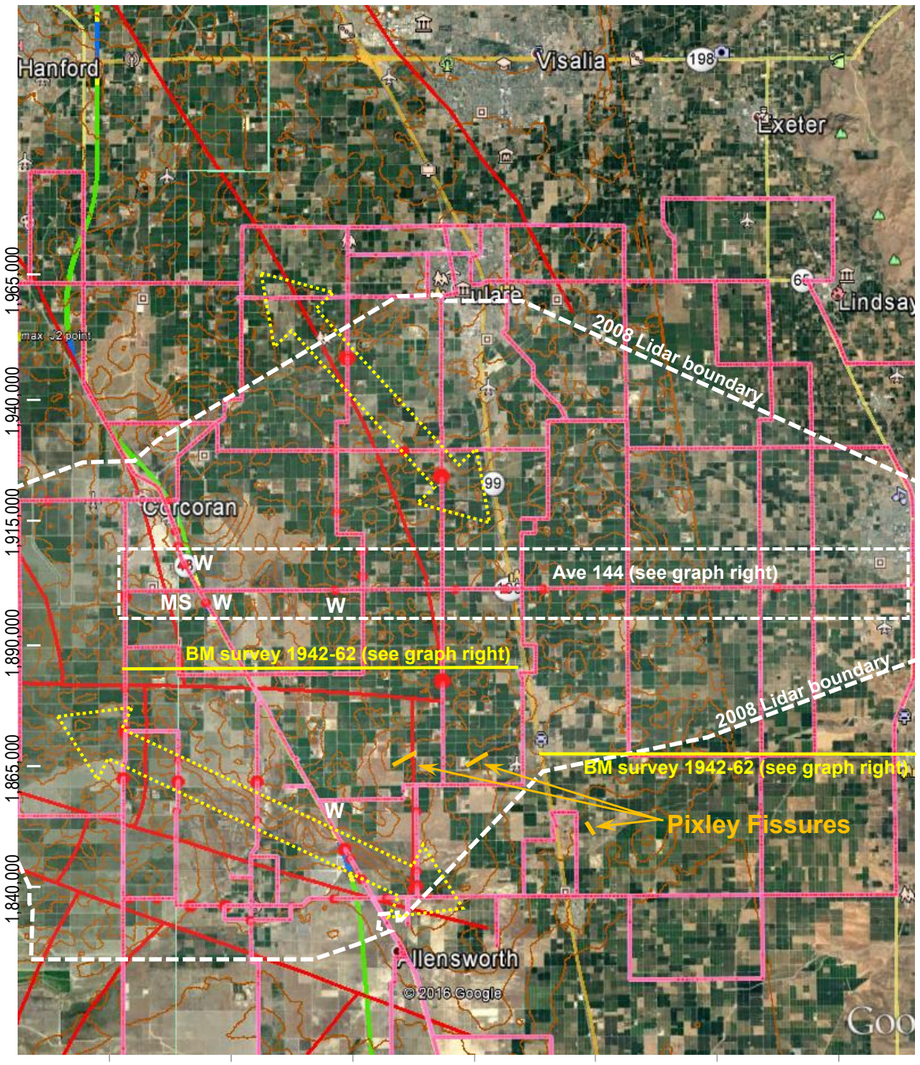

Vehicle-mounted **RTK** GPS routes
Conceptual **Compaction Faulting** (Saleeby and Foster, 2004)

Possible compaction faulting zone, as interpreted from patterns of apparent changes in slope from 2008 to 2016 coincident with anomalous elevation changes interpreted in 2008 LiDAR profiles
Change in slope point consistent with **ground strain concentration** due to interpreted differential subsidence from 2008 to 2016
Possible compaction fault as interpreted from 2008 to 2016 change in slope point coincident with anomalous 2008 ground elevation change

West to East Elevation and Subsidence Profiles along Quebec Avenue and Avenue 144, showing 2008 & 2016 elevations, subsidence profiles for 2008 to 2016 (LiDAR & RTK) and 2007 to 2010 (InSAR), and nearby 1942 to 1962 benchmark surveys

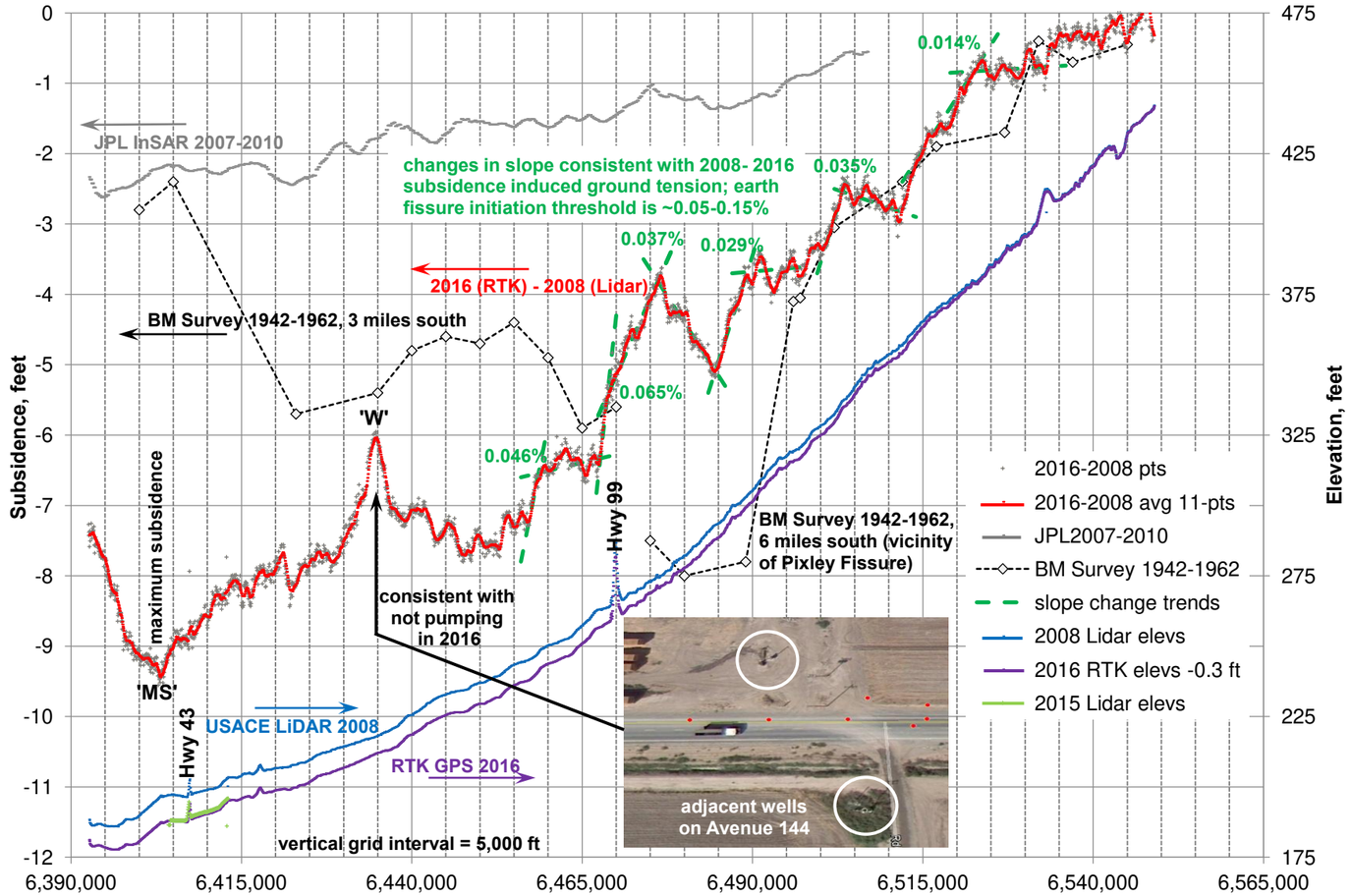

MS area of maximum interpreted subsidence
W Signature of local subsidence possibly associated with a single well or small group of wells

Differential elevations between LiDAR elevations obtained for the USACE in July 2008, and RTK GPS elevations obtained along selected roads in and around the project area in August 2016, provide details of local subsidence patterns to the east and in the vicinity of the Tulare Lakebed. Boundaries of the relevant portion of the 2008 LiDAR survey and roads used in the vehicle-mounted RTK survey are overlain on the image to the left. Approximate locations of the Pixley Fissures (circa 1969) east of the HSR alignment are also shown. A west to east profile of differential subsidence from 2008 to 2016 across the basin is plotted above. Although no current active earth fissuring has been reported in the area, the profile above indicates that areas of tensile ground strains due to current subsidence activity are developing. Similar patterns of differential subsidence may have been present during historic subsidence activity associated with the Pixley Fissures; the very limited subsidence monitoring technologies available at that time would not have detected the detail shown in the profile above. If current differential subsidence rates and associated ground tension continues, initiation of earth fissure activity can be anticipated in the near future.

HSR Ground Subsidence Study
California

2008 LIDAR AND 2016 RTK SURVEY SHOWING DISTRIBUTION OF POSSIBLE COMPACTION FAULTING, GROUND TENSION & DIFFERENTIAL ELEVATION CHANGE

PLATE **8-3**

Project 8715180680
PM : JF BY: MLR
Date 8/2/2017
Scale : n/a

amec foster wheeler

InSAR Subsidence 2007 to 2010, LiDAR 2008 Elevations, RTK 2016 Elevations, and Subsidence 2008 to 2016 Along HSR Alignment south of Corcoran

Profile Location

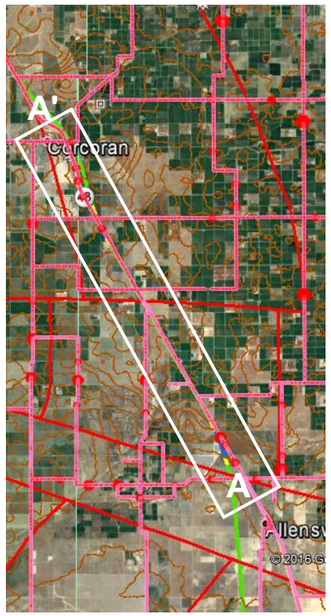

Subsidence points (+) are the differences of the 2008 & 2016 elevations at 2016 RTK points, collected at ~60 ft intervals on roads such as Hwy 43.
The subsidence trend (in red) is a running average of 11 adjacent points (or ~600 ft) to reduce variability ('noise') in the interpreted subsidence.

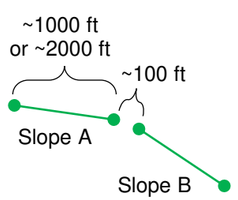

Slope is calculated from two trend points at ~1000 or ~2000 ft apart.

Slope Change = Slope B - Slope A

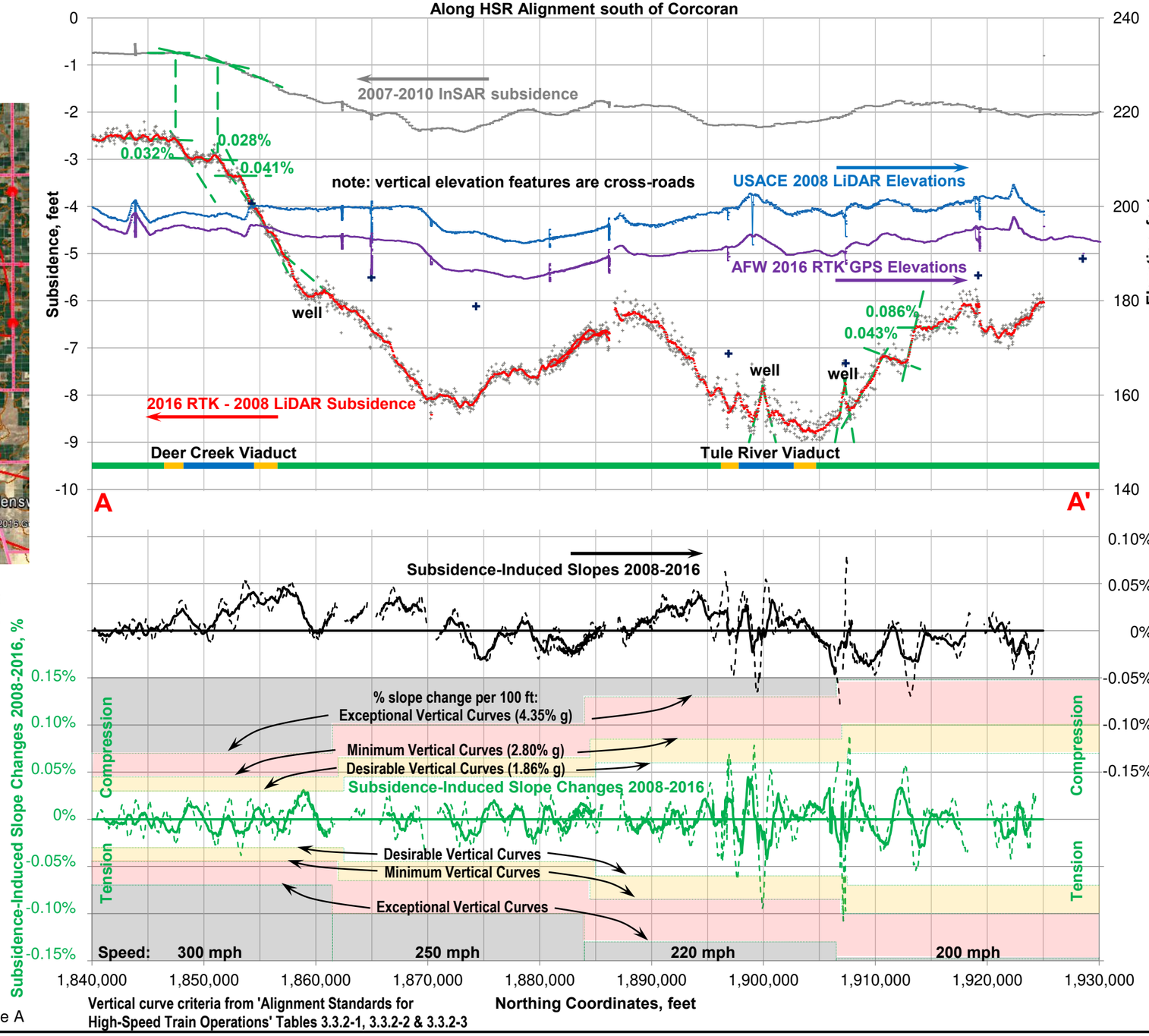

Legend

- 2016-2008 pts
- 2016-2008 avg 11-pts
- JPL InSAR 2007-2010
- 2016-2010 HSR benchmark (RTK elevation of benchmark in 2016)
- slope change trends
- 2008 Lidar elevs
- 2016 RTK elevs
- HSR embankment
- HSR retained embankment
- HSR Viaduct
- subsidence slope (2000 ft)
- subsidence slope (1000 ft)
- slope change (2000 ft)
- slope change (1000 ft)
- vertical curve criteria

Slopes and slope changes are approximations based on manual interpretations of the subsidence trends (upper plot) or calculations based on assumptions of line segment lengths (1000 or 2000 ft) as presented in the lower plot. Random variability or 'noise' are inherent in the measurement methods used.

Lengths of slope changes are difficult to assess from the data sets; 100-ft is assumed in the lower plot. Monitoring specific to the HSR alignment, such as repeat surveys of monument arrays in critical areas, can provide future measurements to a higher precision and reliability than these results.

HSR Ground Subsidence Study
California

2008 LIDAR AND 2016 RTK SURVEY SHOWING RECENT ELEVATIONS, SUBSIDENCE-INDUCED SLOPES & SLOPE CHANGES, HIGHWAY 43 ADJACENT TO HSR ALIGNMENT IN TULARE LAKE AREA

PLATE **8-4**

Project 8715180680
PM : JF BY: MLR
Date 8/2/2017
Scale : n/a

amec foster wheeler

Close-up of fault

photos provided by Thomas Holzer, USGS

Pond-Poso Creek Fault, 1978
Located near Peterson Road, east of HSR alignment

Poso Creek Fault Intersection along HSR Alignment Profile

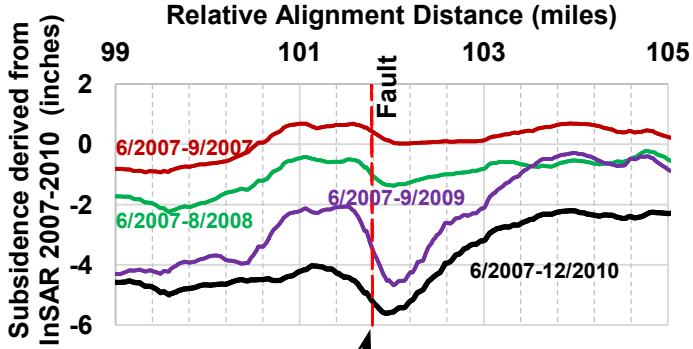

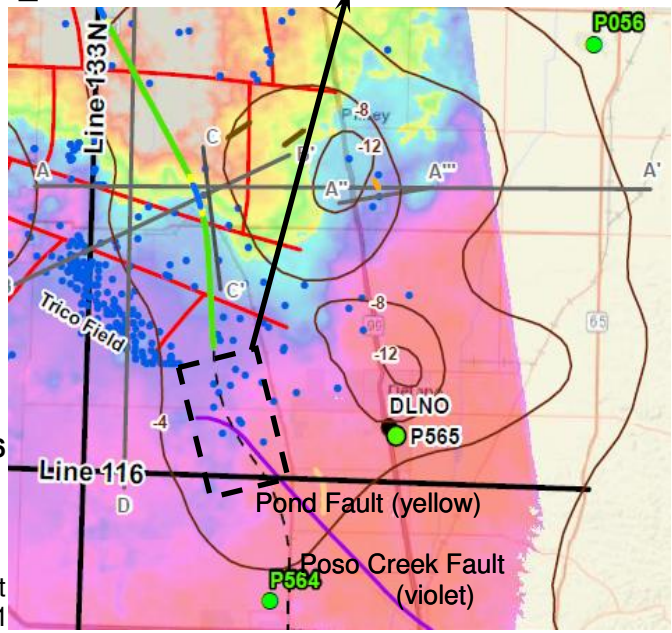

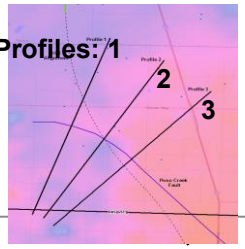

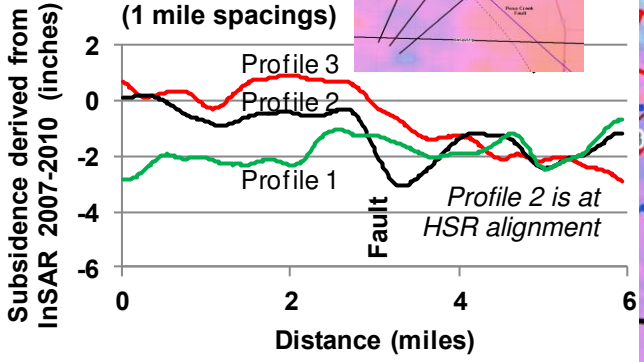

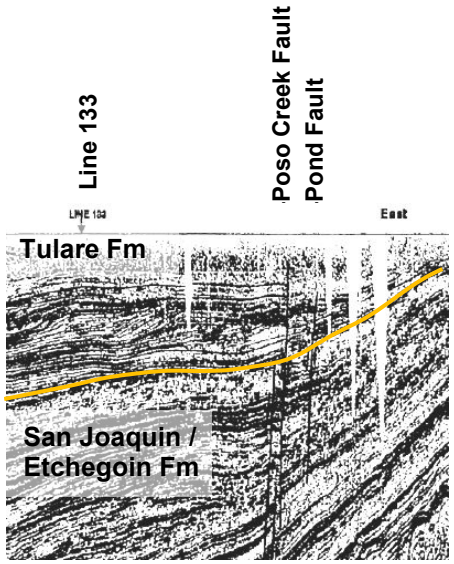

Part of Seismic Reflection Line 116 (Miller 1999)

Pond-Poso Creek Fault locations from Plate 8-1

HSR Alignment subsidence profile for 2007 to 2010 as derived from InSAR at fault intersection with alignment is shown at top.

HSR Ground Subsidence Study California	**PHOTOGRAPHS OF POND-POSO CREEK FAULT NEAR PETERSON ROAD & POSSIBLE FAULT SUBSIDENCE AT HSR ALIGNMENT**	PLATE **8-5**	Project 8715180680 PM : JF BY: MLR Date 8/2/2017 Scale : n/a amec foster wheeler

WSW

Profile B - B' Distance, miles

ENE

Compaction Fault?

HSR alignment

Corcoran Clay (0.6-0.7 Ma age) at top.

369 (API 10700369)

371 (API 10700371)

362 (API 10700362)

363 (API 10700363)

361 (API 10700361)

043 (API 10720043)

197 (API 10720197)

Spontaneous Potential 0 Resistivity ohm-m 60

Spontaneous Potential 0 Resistivity ohm-m 50

Depth, feet

~50 ft offset?

~100 ft offset?

Possible region of inhibited connectivity in aquifer system, where thick fine-grained strata (e.g. more than ~40 ft*) are interspersed with heterogeneous and coarse-grained strata

See Plate 8-15 for reflection seismic signatures of 'steeply dipping structure' that may be consistent with possible regions of inhibited connectivity in the Tulare Fm.

*The fine-grained confining layer in the USGS Pixley corehole (see Plates 3-2 and 8-20) is 30 feet thick.

Possible region of inhibited connectivity in aquifer system

Tulare Fm
This is the younger basin alluvium most susceptible to groundwater decline-induced compaction leading to subsidence. The **Corcoran Clay (0.6-0.7 Ma age)** is a major confining horizon for underlying good quality groundwater.

Depth of fresh water
Very low resistivities indicate fine grained materials and high TDS (>2,000 mgl) water. Reversal of Spontaneous Potential (SP) deflection relative to resistivity deflection also indicates presence of saline water in deep aquifer zones.

SP response and / or higher resistivity:

Top of San Joaquin Fm (2.2-3.4 Ma age?) @ First MyaSands. This is the last group of marine sequences in the basin alluvium. Very low resistivities indicate fine grained materials and salt water.

6/2007 to 12/2010 InSAR subsidence

6/2007 to 12/2010 InSAR subsidence

6/2007 to 12/2010 Subsidence, inches

see Plate 8-8 for Subsidence along B-B'

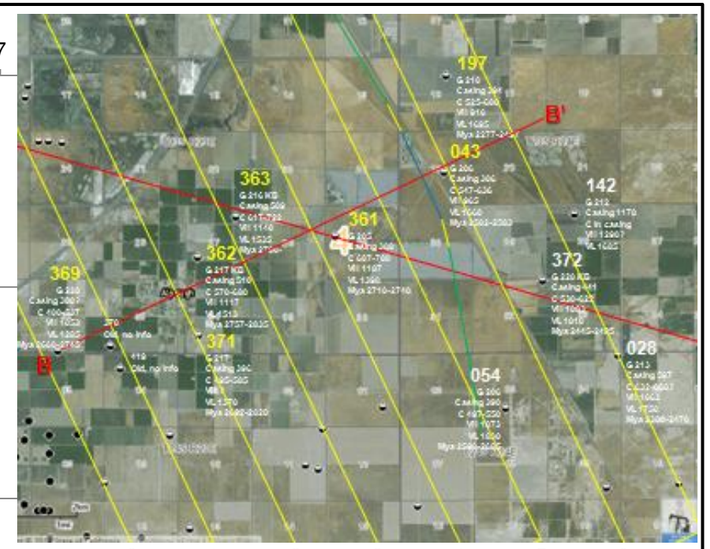

B - B' Profile Distance, miles

Fine-grained alluvium: very compressible silts and clays, but compaction is inhibited or delayed by very low permeabilities.
<~10 ohm-m resistivity

Heterogeneous alluvium: pathways of high permeability coarse-grained alluvium fraction provide drainage for the lenticular/ interlayered highly compressible fine-grained alluvium fraction.
~10 to ~25-30 ohm-m resistivity

Coarse-grained alluvium: sands and gravels with minor compaction which, due to high permeabilities is rapid.
>~25-30 ohm-m resistivity

bottom of fresh water (VL) very low resistivity

top of First Mya Sands, at well log where shaded

384 API well identification number, last 3 digits

Notes:
See **Plates 8-16** and **8-20** for description of e-log colors

Ma - million years ago

HSR Ground Subsidence Study
California

BASIN ALLUVIUM PROFILE & POSSIBLE PROFILE CHANGES, VICINITY OF HSR ALIGNMENT NEAR ALPAUGH & DEER CREEK - WEST TO EAST

PLATE **8-6**

Project 8715180680
PM : JF BY: MLR
Date 8/2/2017
Scale : n/a

amec foster wheeler

Profile C - C' Distance, miles

N

S

HSR alignment

Corcoran clay fault?

Corcoran Clay

Tulare Fm

Depth, feet

C - C' Profile Distance, miles

197 (API 10720197) Resistivity 0 ohm-m 50

043 (API 10720043) Resistivity 0 ohm-m 50

361 (API 10700361) 1.7 mi west Resistivity 0 ohm-m 50

372 (API 10700372) (1.2 mi east) Resistivity 0 ohm-m 50

177 (API 10720177) 1.4 mi west Resistivity 0 ohm-m 50

054 (API 10720054) Resistivity 0 ohm-m 50

239 (API 10720239) 1.2 mi west Resistivity 0 ohm-m 10

429 (API 10700429) 1.7 mi east Resistivity 0 ohm-m 50

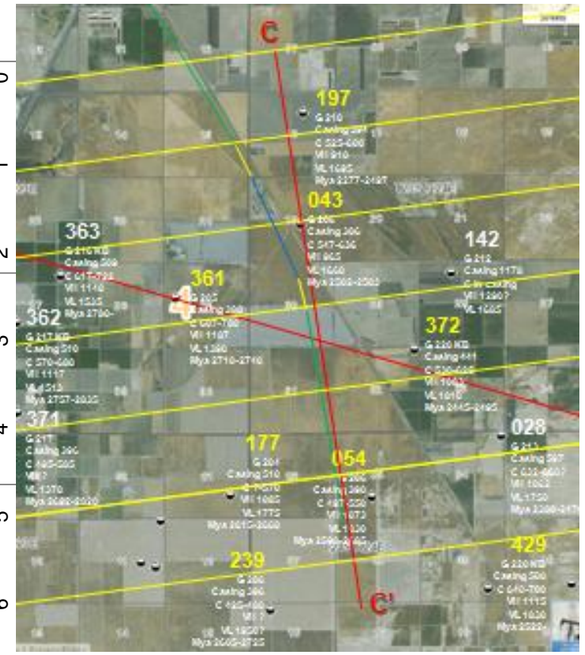

Depth of fresh water
Very low resistivities indicate fine grained materials and high TDS (>2,000 mgl) water. Spontaneous Potential deflection reversal indicates saline water.

Top of San Joaquin Fm (2.2-3.4 Ma age?) @ First Mya Sands
This is the youngest group of marine sequences in the basin alluvium. Very low resistivities indicate fine grained materials and salt water.

SP response and / or higher resistivity:

east of HSR

near HSR

First Mya Sands

east of HSR

west of HSR

west of HSR

near HSR

west of HSR

east of HSR

Fine-grained alluvium: very compressible silts and clays, but compaction is inhibited or delayed by very low permeabilities.
<~10 ohm-m resistivity

Heterogeneous alluvium: pathways of high permeability coarse-grained alluvium fraction provide drainage for the lenticular/ interlayered highly compressible fine-grained alluvium fraction.
~10 to ~25-30 ohm-m resistivity

Coarse-grained alluvium: sands and gravels with minor compaction which, due to high permeabilities is rapid.
>~25-30 ohm-m resistivity

bottom of fresh water (VL) very low resistivity

First Mya Sands - higher resistivity and / or SP response

384 API well identification number, last 3 digits

Notes:
See **Plates 8-16** and **8-20** for description of e-log colors.
Ma - million years ago

HSR Ground Subsidence Study
California

DEEP BASIN ALLUVIUM PROFILE & POSSIBLE PROFILE CHANGES IN VICINITY OF HSR ALIGNMENT NEAR ALPAUGH & DEER CREEK, NORTH TO SOUTH

PLATE **8-7**

Project 8715180680
PM : JF BY: MLR
Date 8/2/2017
Scale : n/a

amec foster wheeler

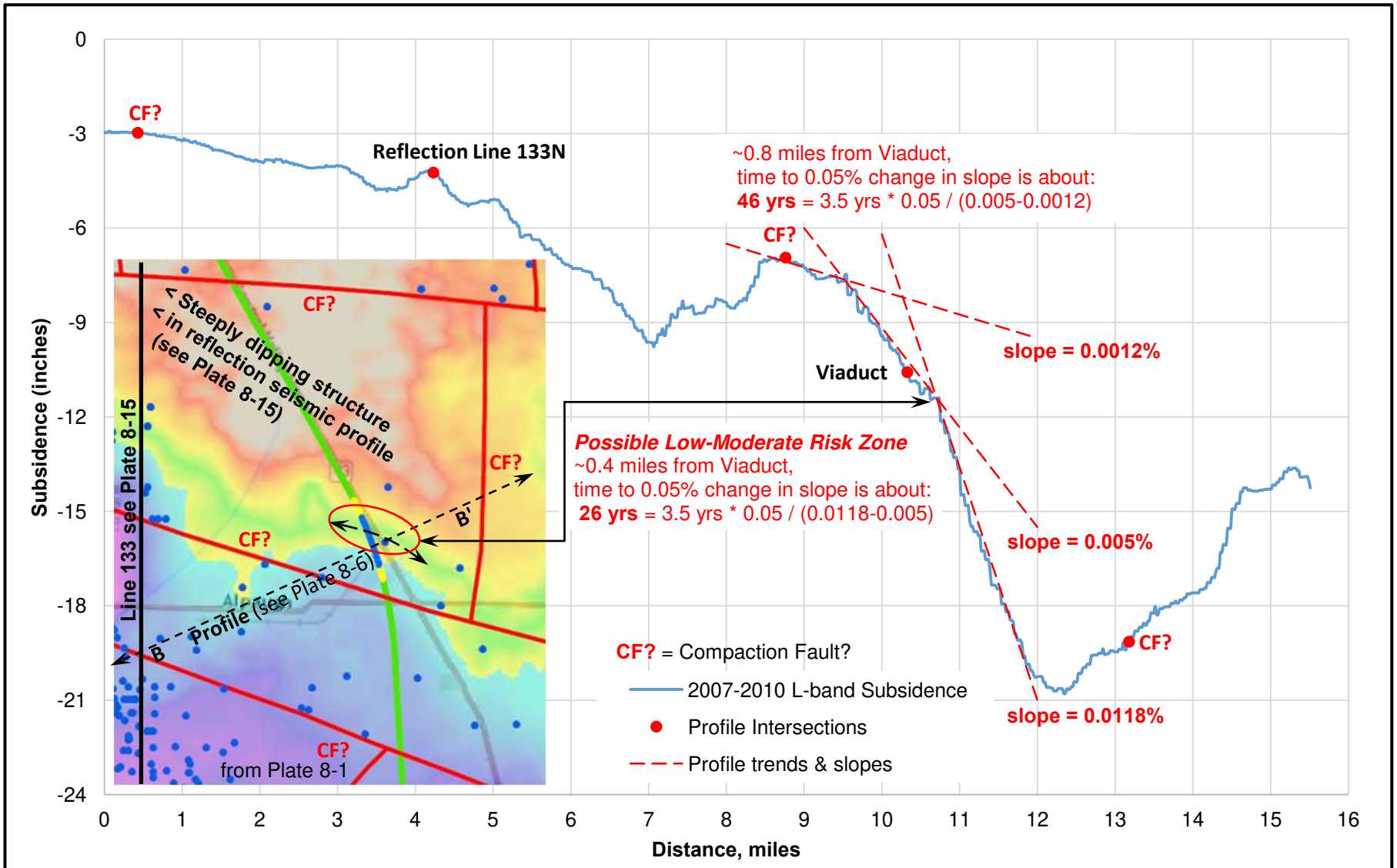

HSR Ground Subsidence Study California	**POSSIBLE FUTURE LOW-MODERATE RISK CONDITION BASED ON JUN 2007 - DEC 2010 (3.5 YRS) JPL INSAR PROFILE AT DEER CREEK VIADUCT, WEST TO EAST PROFILE B - B'**	PLATE **8-8**	Project 8715180680 PM : JF BY: MLR Date 8/2/2017 Scale : n/a

amec foster wheeler

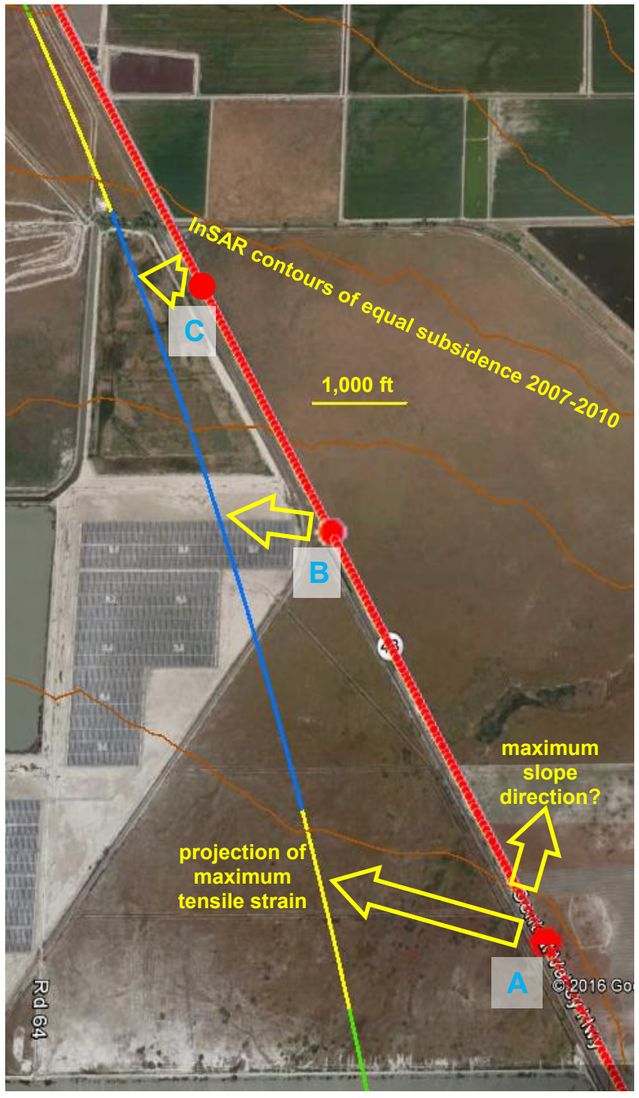

Deer Creek Viaduct Area
Approximate Locations of Tensile Ground Strains Interpreted at Hwy 43 Projected towards Viaduct and Retained Embankment

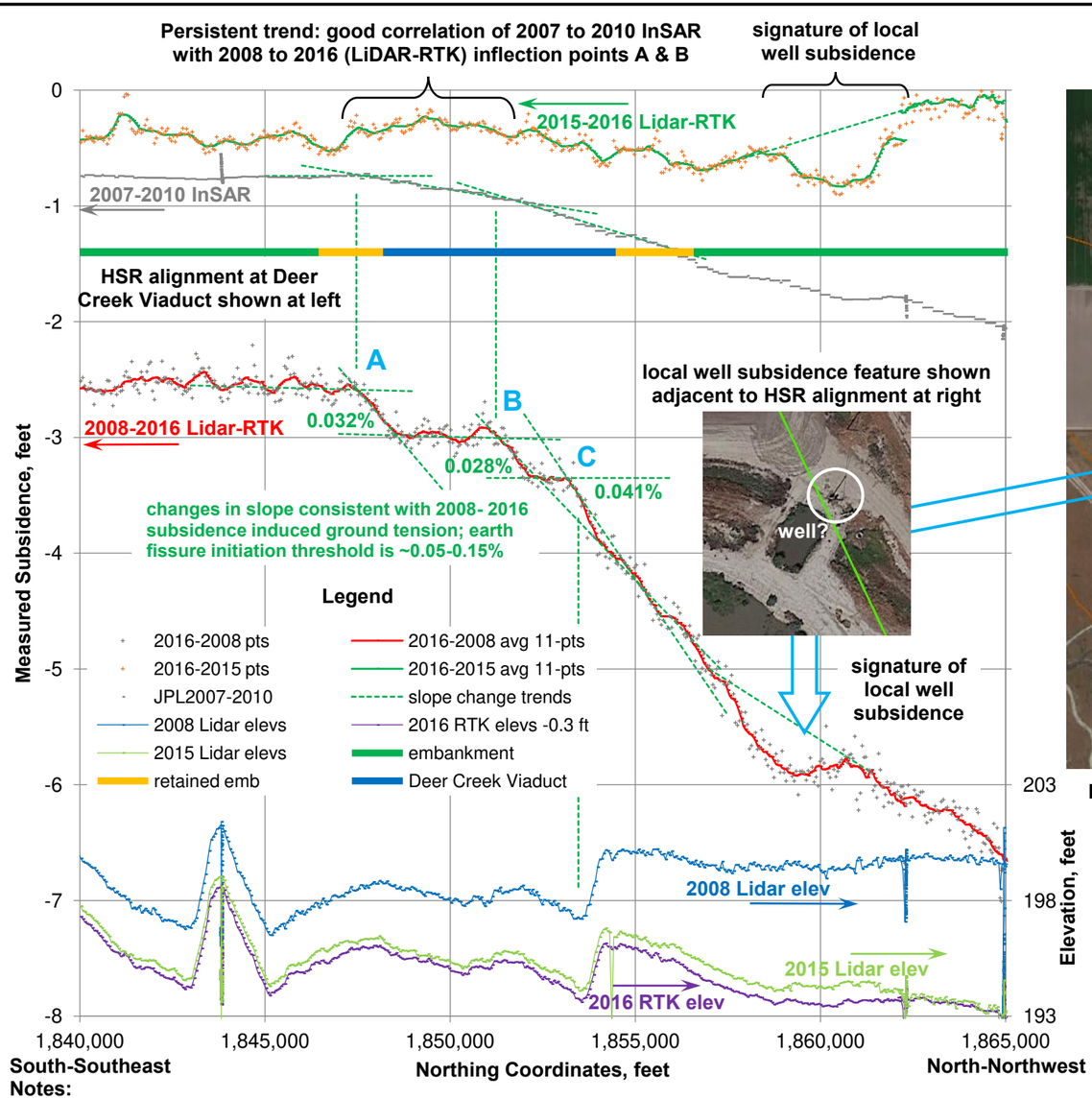

Probable Local Well Subsidence Feature North of Deer Creek Viaduct

Notes:

HSR alignment is ~30° west of north; where the alignment is parallel to Highway 43, a 1,000-foot change in northing coordinate distance represents 1,158 feet of alignment distance.

Changes in slope rate at **Points A & B** are approximately **0.03%** (estimated range ~0.028%-0.032%) along the alignment. However, if 2008 to 2016 slope dip is about perpendicular to subsidence contours (strike) derived from 2007 to 2010 InSAR results, the actual change in slope rate from 2008 to 2016 may be about double the alignment rate at **~0.06%.**

Elevation data points (RTK and corresponding LiDAR) are spaced at approximate 50-foot intervals along Highway 43; horizontal positions are derived from RTK results.

Elevation trends along Highway 43 are running averages of 11 adjacent elevation data points (about 500-foot sample intervals). The **standard deviation** of the difference of each elevation data point and the 11-point running average is about **0.13 feet** for the 2008 to 2016 data sets and about **0.09 feet** for the 2015 to 2016 data sets.

HSR Ground Subsidence Study
California

DIFFERENTIAL ELEVATION CHANGE BETWEEN 2008 (LIDAR) & 2016 (RTK) VICINITY OF HSR AT DEER CREEK VIADUCT

PLATE
8-9

Project 8715180680
PM : JF BY: MLR
Date 8/2/2017
Scale : n/a

amec foster wheeler

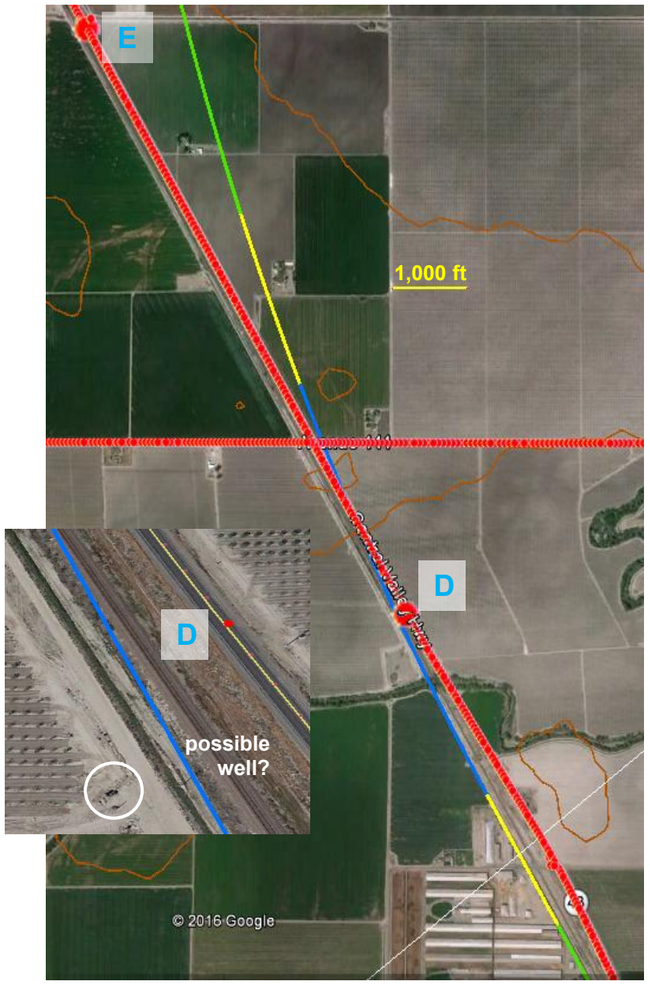

Tule River Viaduct Area
Approximate location of anomalous elevation change consistent with historic (but not current) well pumping at point 'D.' There is a possible indication of a well being present in the vicinity of point 'D.' However, point 'D' is not the nearest RTK point to the feature.

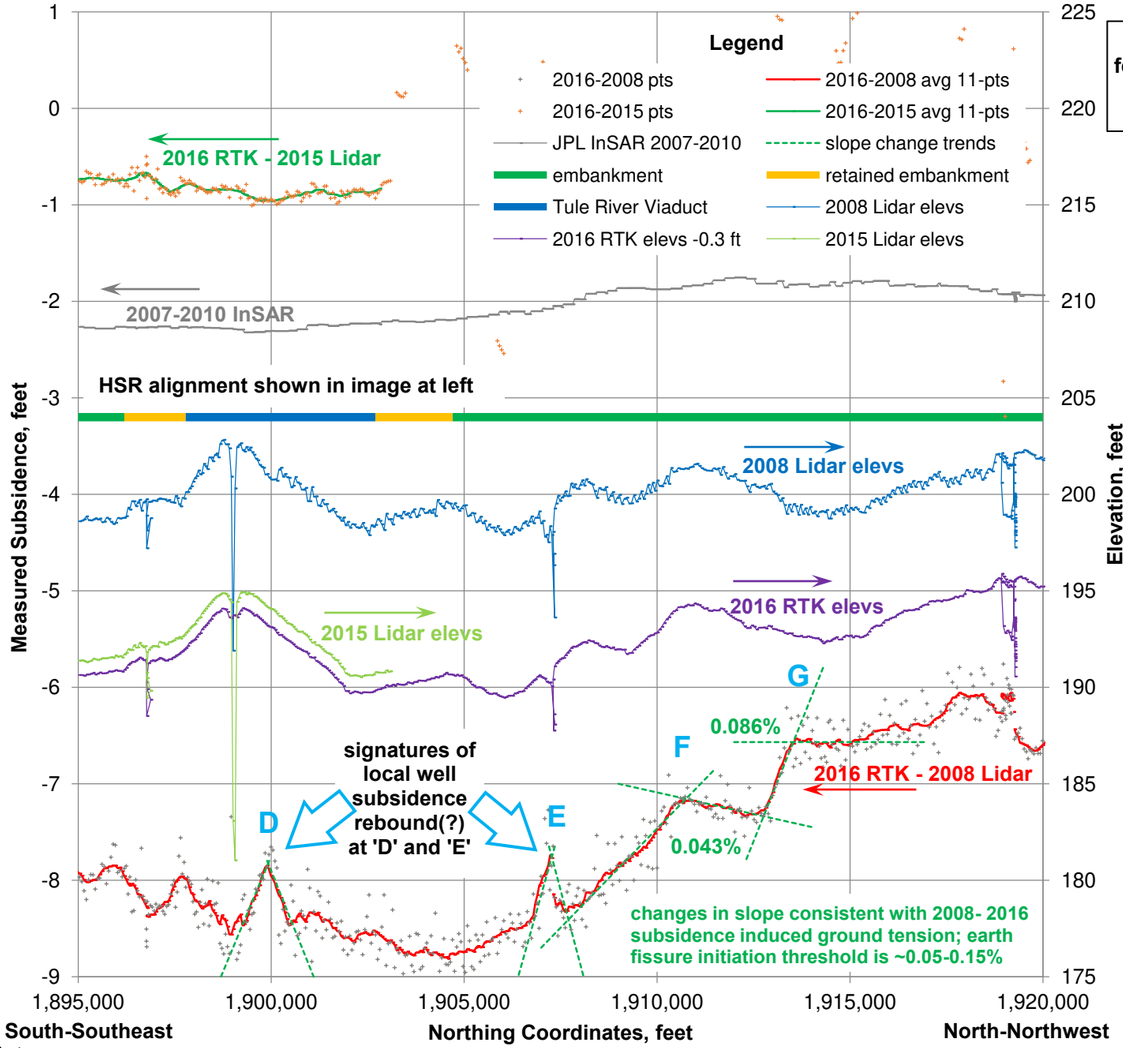

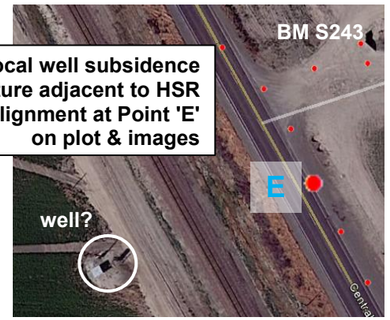

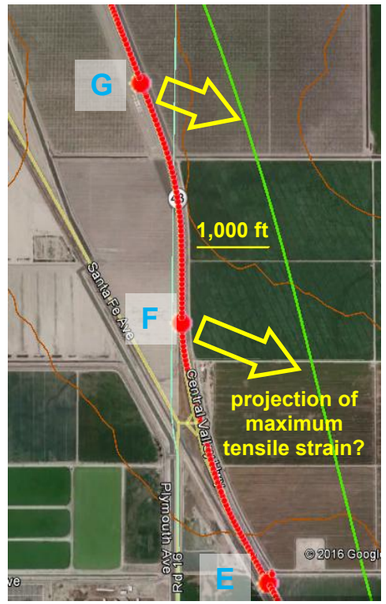

Notes:

HSR alignment is ~30º west of north; where the alignment is parallel to Highway 43, a 1,000-foot change in northing coordinate distance represents 1,158 feet of alignment distance.

Changes in slope rate are approximately **0.04%** at **Point F** and **0.09%** at **Point G** along the alignment. The strike of the 2008 to 2016 slope dip relative to the RTK point alignment is anticipated to result in a somewhat higher true slope change.

Apparent **Local Well Features D & E** may be elastic rebound (?) in 2016 from 2008 pumping. These features are about 1,050 feet ('D') and 830 feet ('E') long and 0.5 feet high; the ground may have been compressed prior to current tension.

Elevation data points (RTK and corresponding LiDAR) are spaced at approximate 50-foot intervals along Highway 43; horizontal positions are derived from RTK results.

Elevation trends along Highway 43 are running averages of 11 adjacent elevation data points (about 500-foot sample intervals). The **standard deviation** of the difference of each elevation data point and the 11-point running average is about **0.13 feet** for the 2008 to 2016 data sets and about **0.09 feet** for the 2015 to 2016 data sets.

HSR Ground Subsidence Study
California

DIFFERENTIAL ELEVATION CHANGE BETWEEN 2008 (LIDAR) AND 2016 (RTK) VICINITY OF HSR AT TULE RIVER VIADUCT

PLATE
8-10

Project 8715180680
PM : JF BY: MLR
Date 8/2/2017
Scale : n/a

amec foster wheeler

DIFFERENTIAL SUBSIDENCE FEATURES

See Plate 8-	CA coordinates, Feet Northing	Easting	Distance from HSR	Feature Type	Slope Change	Vertical offset (ft)	Lateral dist (ft)	Compaction fault? 2008 topo relief (ft)	Relevance to HSR
South to North - Highway 43 Project Alignment (18.3 miles)					**characterize subsidence features along HSR alignment**				
8-9 'A'	1,847,472	6,439,471	~2,000 ft	offset - CF?	**0.032**	0.4		minor	south CF zone delineation
8-9 'B'	1,851,242	6,437,256	~1,000 ft	offset - CF?	**0.028**	0.3		minor	south CF zone delineation
8-9 'C'	1,853,169	6,436,121	~670 ft	offset - CF?	**0.041**	0.7		2.8	south CF zone delineation
8-9	1,859,455	6,432,427	~250 ft	well	--	0.4	3400 / 2	--	well activity in 2016, not in 2008?
8-10 'D'	1,899,797	6,408,756	~120 ft	well	--	0.5	1100 / 2	--	well activity in 2008, not in 2016?
8-10 'E'	1,907,136	6,404,463	~1,300 ft	well	--	0.5	830 / 2	--	well activity in 2008, not in 2016?
8-10 'F'	1,910,544	6,403,247	~1,500 ft	offset	**0.043**	--	--	--	vicinity of 2007-2010 InSAR well feature
8-10 'G'	1,913,419	6,402,782	~1,100 ft	offset	**0.086**	0.6	900	--	vicinity of 2007-2010 InSAR well feature
South to North - Alpaugh to Angiola Road 38 / Road 40 (9.2 miles)									**characterize possible CF zones**
	1,839,836	6,417,275	4.1 mi	offset	**0.018**	0.5	2600	--	
	1,858,733	6,418,727	2.3 mi	offset - CF?	**0.031**	0.8	2400	0.9	south CF zone delineation
	1,866,032	6,418,748	1.6 mi	offset - CF?	**0.035**	0.7	1800	1.3	south CF zone delineation
South to North - Road 16 (6.2 miles)									**characterize possible CF zones**
	1,860,485	6,402,608	4.8 mi	offset	**0.030**	0.8	2700	--	south CF zone delineation
	1,866,143	6,402,947	4.1 mi	offset - CF?	**0.101**	1.9	1800	2.7	south CF zone delineation
	1,870,161	6,402,989	3.7 mi	offset	**0.045**	1.1	2200	--	south CF zone delineation
South to North - 6th Avenue / Dairy Avenue (16.6 miles)									**characterize possible CF zones**
	1,866,808	6,392,038	5.9 mi	offset - CF?	**0.059**	2.0	3400	2.1	south CF zone delineation
	1,875,509	6,392,437	4.9 mi	offset - CF?	**0.054**	1.6	3100	2.2	south CF zone delineation
	1,883,636	6,392,460	4.1 mi	rotation	**0.029**	--	--	--	
8-2	1,901,117	6,392,580	2.8 mi	offset - CF?	**0.074**	1.2	2100	2.6	
South to North - Pratt Ave / Road 96 (22.5 miles)									**characterize possible CF zones**
	1,846,052	6,450,416	2.4 mi	offset - CF?	**0.028**	0.2	600	0.8	south CF zone delineation
	1,848,838	6,450,431	2.5 mi	offset	**0.038**	0.3	790	--	south CF zone delineation
	1,860,094	6,450,416	3.1 mi	offset - CF?	**0.034**	0.5	990	1.0	~2 miles south of Pixley Fissure #3
	1,884,786	6,455,865	6.3 mi	offset - CF?	**0.028**	0.6	2700	7.3	at conceptual arcuate mapped CF
	1,923,474	6,455,981	9.9 mi	offset - CF?	**0.037**	1.6	3800	2.2	north CF zone delineation
South to North Road 72 / Road 64 / Road 68 (12.2 miles)									**characterize possible CF zones**
	1,904,499	6,440,093	5.6 mi	offset	**0.050**	0.3	670	--	
	1,909,451	6,440,085	6.1 mi	rotation	**0.043**	--	--	--	
	1,916,717	6,434,944	5.9 mi	rotation	**0.018**	--	--	--	
	1,946,056	6,437,301	8.4 mi	offset - CF?	**0.027**	0.5	2100	1.3	north CF zone delineation
West to East Quebec Ave / Avenue 144 (29.8 miles)					**characterize subsidence behavior / distribution near area of Pixley Fissures**				
8-3	1,901,971	6,434,625	4.4 mi	wells	--	0.9	3800 / 2		well activity in 2008, not in 2016?
8-3	1,901,941	6,458,508	8.4 mi	offset	**0.046**	0.7	1300	n/d	
8-3	1,901,935	6,468,511	10.1 mi	offset	**0.065**	0.7	1000	n/d	
8-3	1,901,918	6,476,053	11.3 mi	rotation	**0.037**	--	--	--	
8-3	1,901,897	6,489,151	13.4 mi	offset	**0.029**	1.3	4400	n/d	
8-3	1,901,831	6,502,961	15.6 mi	offset	**0.035**	1.1	3000	n/d	
8-3	1,901,801	6,522,943	19.0 mi	rotation	**0.014**	--	--	--	
West to East Whitley Ave / (Waukena) / Octal Avenue (20.0 miles)									**characterize possible CF zones**
	1,919,385	6,377,269	3.5 mi	offset - CF?	**0.024**	0.5	2200	0.6	
	1,919,231	6,401,541	~230 feet	rotation	**0.030**	--	--	--	
	1,928,398	6,434,708	6.3 mi	offset	**0.042**	1.7	4400		
	1,928,255	6,448,561	8.9 mi	offset	**0.035**	1.0	2900		north CF zone delineation
West to East - Virginia Ave / Ave 54 / Ave 56 (11.5 miles)									**characterize possible CF zones**
	1,844,035	6,393,140	7.9 mi	offset	**0.067**	0.3	530		
	1,844,045	6,398,635	7.0 mi	offset	**0.080**	0.5	580		
	1,842,680	6,405,392	5.9 mi	offset - CF?	**0.055**	0.4	600	1.4	
	1,842,623	6,412,297	4.7 mi	rotation - CF?	**0.010**	--	--	2.5	
	1,842,514	6,425,602	2.4 mi	rotation - CF?	**0.012**	--	--	2.2	
	1,843,774	6,434,000	0.8 mi		**0.057**	0.4	720		
	1,843,840	6,444,513	1.2 mi		**0.044**	0.6	1300		
									CF = Compaction Fault

Note:
see Plate 8-4
for explanation of
% slope change

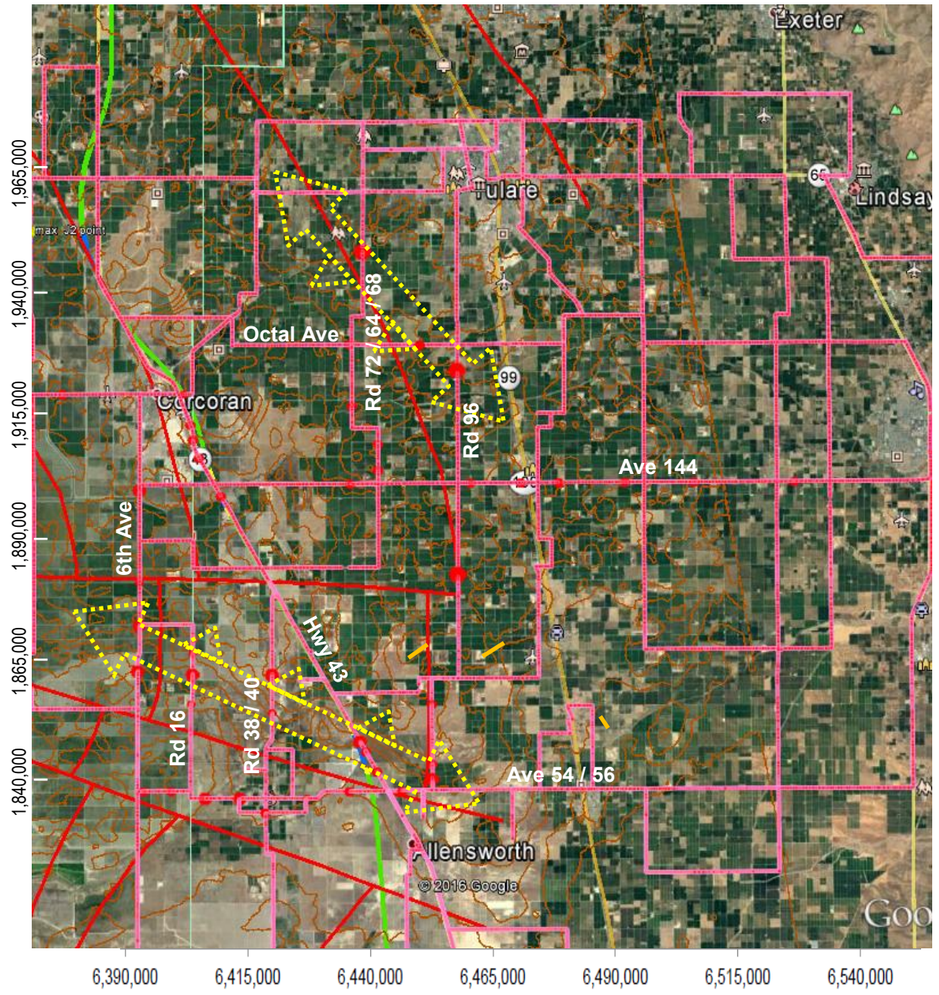

down-dip direction

Possible compaction faulting zone, as interpreted from patterns of apparent changes in slope from 2008 to 2016 coincident with anomalous elevation changes interpreted in 2008 LiDAR profiles

- **Change in slope point** consistent with **ground strain concentration** due to interpreted differential subsidence from 2008 to 2016
- **Possible compaction fault** as interpreted from 2008 to 2016 change in slope point coincident with anomalous 2008 ground elevation change

Vehicle-mounted **RTK** GPS routes

Conceptual **Compaction Faulting** (Saleeby and Foster, 2004)

HSR Ground Subsidence Study
California

TABLE 8-1
DIFFERENTIAL SUBSIDENCE FEATURES INTERPRETED BY COMPARISON OF 2008 LIDAR & 2016 RTK SURVEY

PLATE **8-11**

Project 8715180680
PM : JF BY: MLR
Date 8/2/2017
Scale : n/a

amec foster wheeler

Pixley Fissure No. 3, 1969
Located in Section 1 of
Township T23S R24E

Pixley Fissure No. 2, 1969
Located in Section 15 of
Township T23S R25E

photos provided by Thomas Holzer, USGS

Pixley Fissure No. 1, 1969
Located in Section 15 of
Township T23S R25E,
aerial view

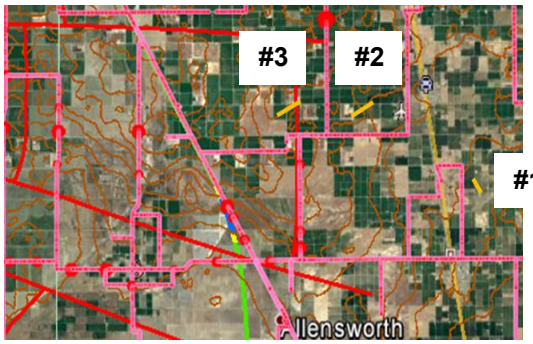

Pixley Fissures locations from Plate 8-3; see also related Plates 8-1, 8-14, 8-18 through 8-20

HSR Ground Subsidence Study California	**PHOTOGRAPHS OF PIXLEY FISSURES 1, 2 AND 3**	PLATE **8-12**	Project 8715180680 PM : JF BY: MLR Date 8/2/2017 Scale : n/a	amec foster wheeler

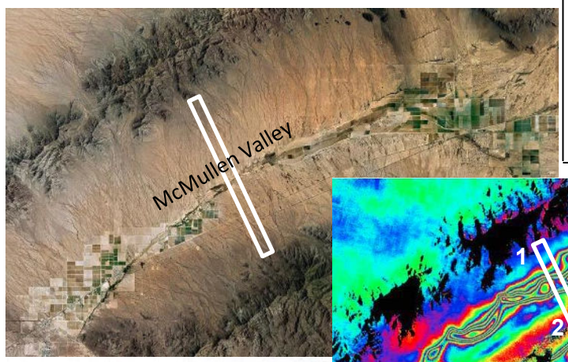


track offset at earth fissure southwest of Willcox, AZ

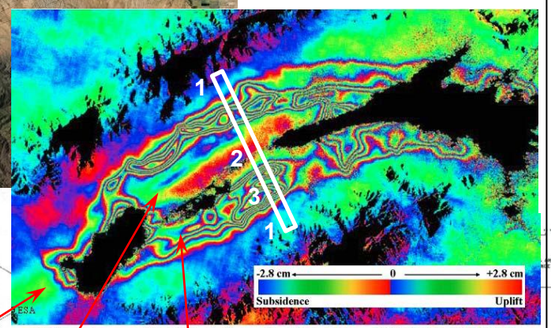

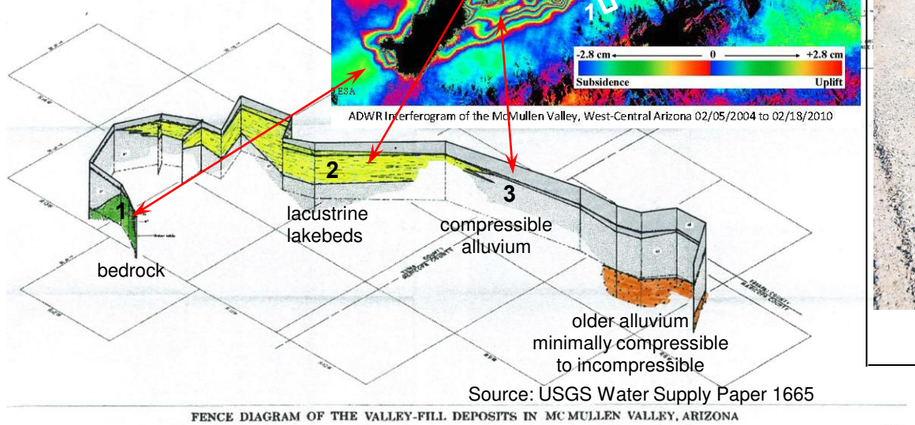

Source: USGS Water Supply Paper 1665

McMullen Valley, Western Arizona

InSAR (C-band from 2004 through 2010) of this largely undeveloped basin provides a clear example of typical basin subsidence behaviors and patterns. Agriculture at the valley ends has been driving groundwater decline throughout the basin since the 1960s; InSAR is decorrelated at agricultural fields. Subsidence patterns indicated by InSAR include:

1. Subsidence does not occur in bedrock and is none to minimal in the coarse alluvium around the basin edges. This is consistent with the Plate 8-1 pattern of no subsidence at mountains and hills surrounding the SJV, and none to minimal subsidence at the HSR alignment around Fresno and to the northeast of the HSR alignment in the Corcoran area.
2. Subsidence is minimal at the ancient lakebeds forming continuous lacustrine deposits (fine-grained deposits described in Plate 8-16) in the center of the basin. This is consistent with the Plate 8-1 pattern of minimal subsidence to the southwest of the HSR alignment in the Corcoran area. Plate 8-15 shows this subsidence pattern in profile at the 'Lake Tulare Trough'.
3. Subsidence is concentrated in the heterogenuous alluvium (described in Plate 8-16) surrounding the continuous lacustrine deposits. This is consistent with the Plate 8-1 subsidence bowl through the Corcoran area.

Relevant Subsidence & Earth Fissure Experience in Arizona

Although many of the earth fissures found in Arizona are associated with differential subsidence due to shallowing of bedrock at basin edges, several fissures are located away from mountain fronts where bedrock shallowing is not relevant. Holzer (1980; Jachens & Holzer, 1979) utilized studies at the Picacho Fissure system near Eloy, AZ as an analogue for earth fissuring at the Pond-Poso Creek Fault. Some earth fissuring in the Willcox Basin (Keaton & others, 1998) has resulted from differential subsidence across facies changes in the basin alluvium. Mid-basin earth fissuring has occurred in the West Salt River Valley where total subsidence has approached 20 feet; bedrock in that mid-basin area is at depths of several thousand feet. That fissuring occurred as subsidence of 2.2 feet in 7 years (~0.3 feet/year) in the upper 1,000 feet of alluvium was measured at a nearby compaction extensometer.

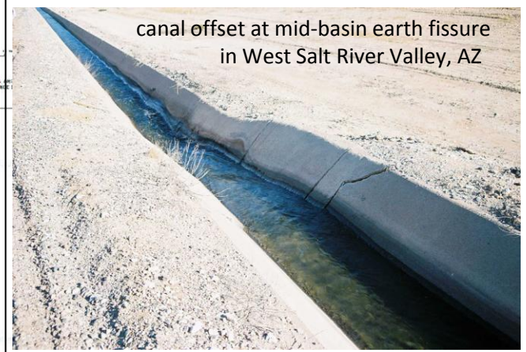
canal offset at mid-basin earth fissure in West Salt River Valley, AZ

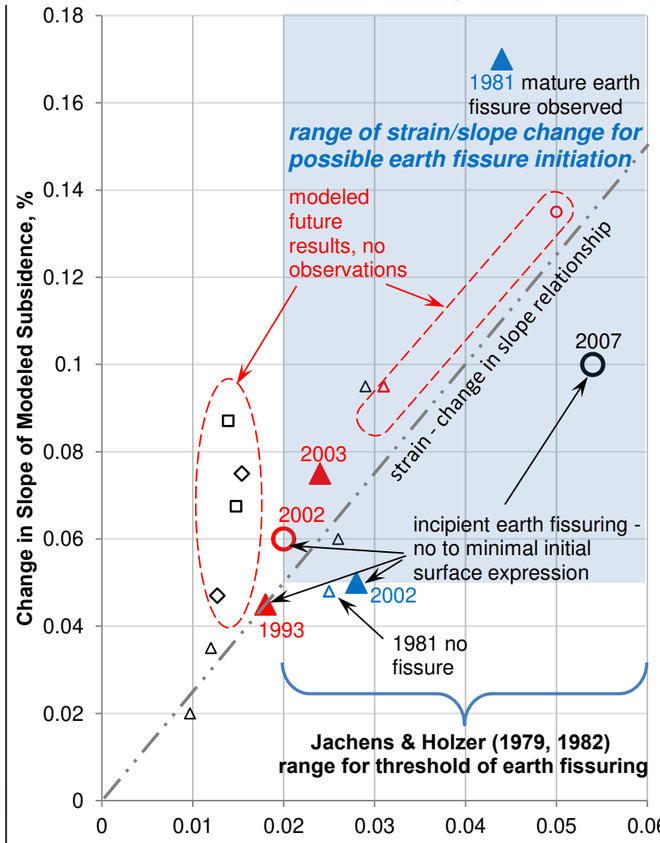

Various 2-d stress-strain model results:

- ◇ 'southern-AZ' Profile 3
- □ 'southern-AZ' Profile 2
- ▲ AEPCO fissure 1993, 2003
- △ AEPCO modeled future
- O Powerline FRS A-A'
- ▲ McMicken Dam A-A'
- △ McMicken Dam modeled A-A' 1981
- △ McMicken Dam 2006
- O N Nevada site
- O N Nevada site modeled future

Notes:
Observed earth fissures are presented as large symbols with year of discovery.

Modeled concentrations of strain and associated slope change with no observed earth fissures, or modeling of future scenarios, are presented as small symbols.

2-D finite element stress-strain modeling performed using SEEPW/SIGM/W programs

If differential subsidence trend continues ~20 years, then total change in slope would be ~0.05%, ***'Approximate threshold to anticipate Earth Fissuring'***

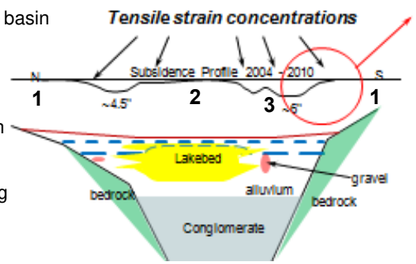

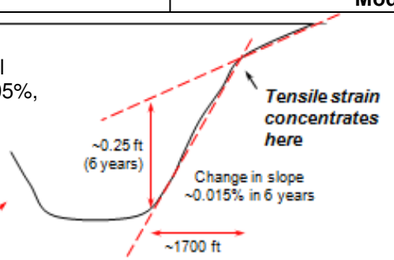

Pending further empirical observations, studies and analyses, the ***Approximate Threshold to anticipate Earth Fissuring*** seems to be reached at the subsidence edge (hinge point) once subsidence has reached a rate of about 1 foot differential subsidence per 2000 feet of ground distance (change in slope ~0.05%)

HSR Ground Subsidence Study
California

CONCEPTUAL CHARACTERIZATION OF SUBSIDENCE PROFILE CHANGES THAT MAY LEAD TO EARTH FISSURING

PLATE **8-13**

Project 8715180680
PM : JF BY: MLR
Date 8/2/2017
Scale : n/a

amec foster wheeler

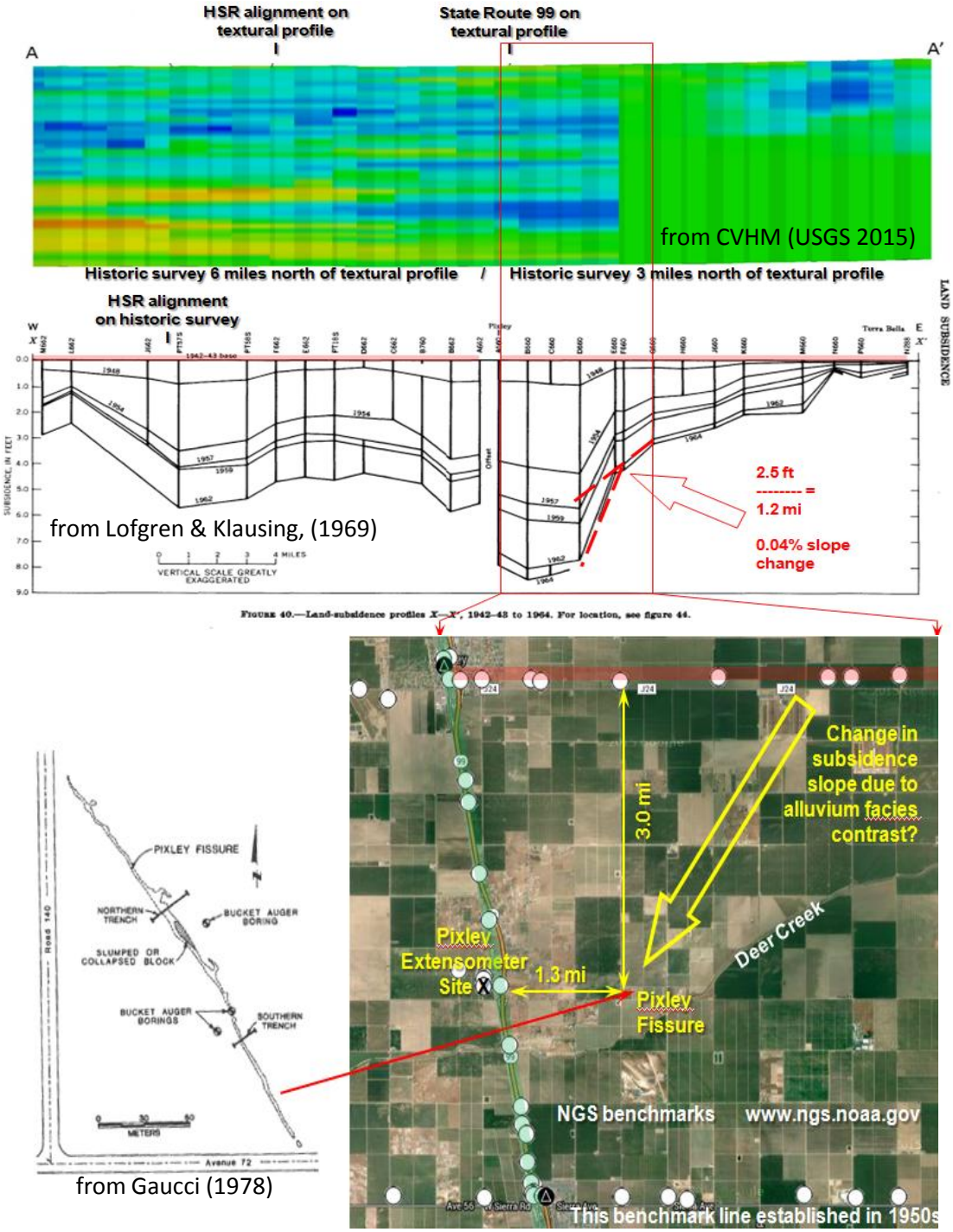

The Textural Model (top) from USGS CVHM running west to east through the Pixley Extensometer Site and the Pixley Fissure No. 1. The historic survey profile (center) is 3 miles to the north. Note that the subsidence slope change correlates well with the conceptualized alluvium texture change in the CVHM Textural Model. Local geological/lithological changes, such as that associated with Deer Creek, may have contributed to localized variability in the alluvium texture near the fissure site.

HSR Ground Subsidence Study California	**PIXLEY FISSURE No. 1 AREA**	PLATE **8-14**	Project 8715180680 PM : JF BY: MLR Date 8/2/2017 Scale : n/a amec foster wheeler

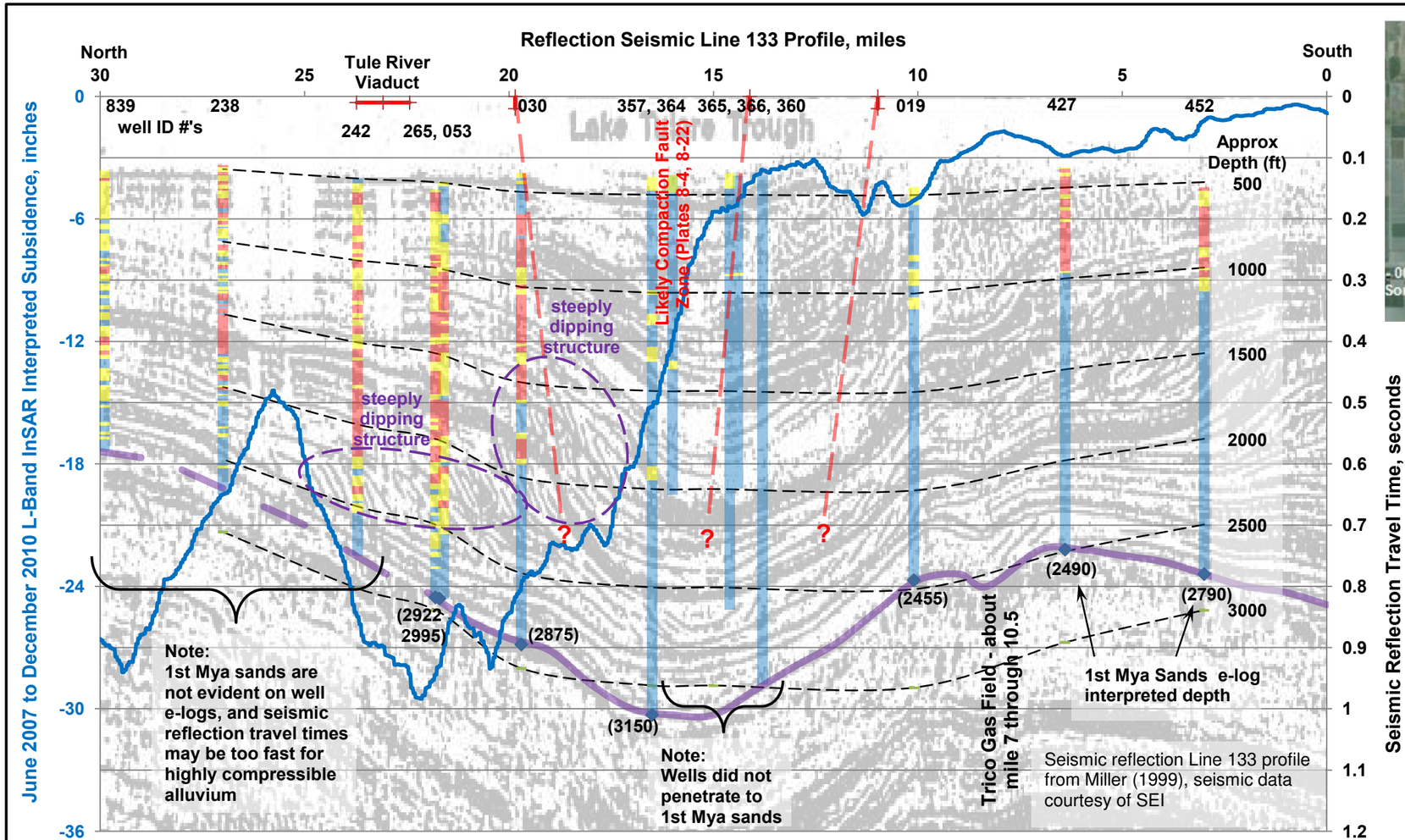

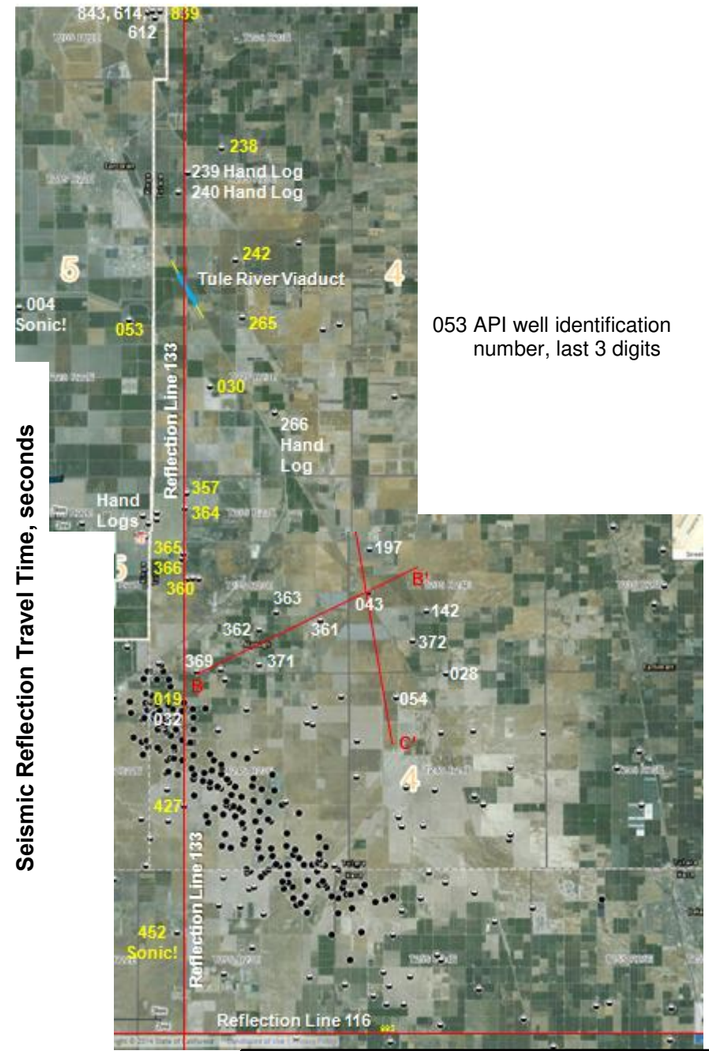

053 API well identification number, last 3 digits

E-log Compaction (leading to Subsidence) Characteristics from Selected Wells and 2007 to 2010 InSAR Subsidence Profile Overlay on Seismic Reflection Line 133 (Miller 1999), Including Profile at HSR Tule River Viaduct

Notes:
Seismic reflection profile background is part of Seismic Line 133 from Miller (1999).

- 1st Mya Sands marker bed is interpreted in the seismic profile by Miller (1999). Using 1st Mya Sands interpretation in the e-logs (shown at wells), average p-wave velocities of about 6,200 to 6,400 feet/sec are interpreted in the Lake Tulare Trough area, and about 7,100 to 7,500 feet/sec are interpreted to the north and south.
- Approximate depths in the alluvium based on average p-wave travel times and known depth of 1st Mya Sands from selected well e-logs. Seismic travel times north of the Tule River Viaduct appear to be too fast (indicating relatively higher strength, less compressible alluvium) for the documented subsidence north of the Viaduct.
- Geo-referenced subsidence (in inches) profile along Seismic Line 133 interpreted from June 2007 to December 2010 L-band InSAR provided by JPL.
- Possible projections of Corcoran clay faulting based on seismic reflection patterns, using fault surface locations presented in Saleeby and Foster (2004).

- Fine-grained alluvium as described in Plates 8-16 and 8-20. This alluvium is very compressible, but compaction is inhibited or delayed by very low mass permeabilities.
- Heterogeneous alluvium as described in Plates 8-16 and 8-20. The high permeability coarse-grained fraction provides drainage to the highly compressible fine-grained fraction.
- Coarse-grained alluvium as described in Plates 8-16 and 8-20. Coarse-grained compaction tends to be minor and, due to high permeabilities, rapid.

HSR Ground Subsidence Study
California

ALLUVIUM PROFILE & SUSCEPTIBILITY TO SUBSIDENCE SEISMIC REFLECTION LINE 133 THROUGH TULE RIVER VIADUCT

PLATE **8-15**

Project 8715180680
PM : JF BY: MLR
Date 8/2/2017
Scale : n/a

amec foster wheeler

Well 10720043, drilled in 1972, is located near the east side of the Deer Creek Viaduct in the vicinity of Alpaugh

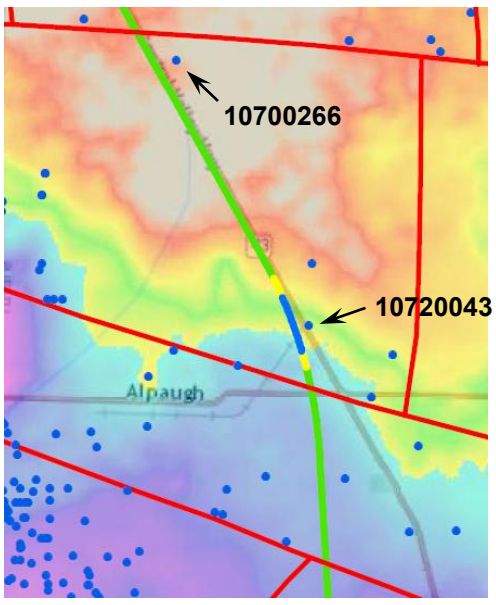

Well 043 is located near the Deer Creek Viaduct in the vicinity of inferred Corcoran clay faulting (red lines). Blue dots are oil and gas well locations with data available online.

Historic geophysical borehole logs from oil and gas exploration provide the best available dataset of quantitative information concerning deeper alluvium relevant to understanding and characterizing subsidence. Data for many wells (e.g. blue dots in the figure above) are now available online at http://www.conservation.ca.gov/dog/Pages/Index.aspx For subsidence behavior, the primary characterization tool is the electrical log. In fresh water aquifer systems (where subsidence due to groundwater withdrawal is focused), the alluvium behavior can be simplified into three primary groups.

Fine-grained alluvium, composed primarily of clays and silts, has low resistivity (typically <10 ohm-m) and is very compressible. Having very low permeability, it has very slow compaction (leading to subsidence) occurring, perhaps over decades to centuries.

Heterogeneous alluvium has moderate resistivity (typically 10 to ~25-30 ohm-m) and is composed of inter-lensing and/or inter-fingering of fine-grained and coarse grained alluvium. The high permeability coarse-grained alluvium fraction provides drainage to the highly compressible fine-grained alluvium fraction. Although total compaction (leading to subsidence) for a given thickness of heterogeneous alluvium may be less than fine-grained alluvium, it occurs much more rapidly, perhaps over years to decades.

Coarse-grained alluvium has high resistivity (typically greater than ~25 to 30 ohm-m) and is composed primarily of sands and gravels. The high energy needed to transport coarse particles may provide densification during the deposition process so that coarse-grained alluvium is relatively incompressible. Coarse-grained compaction (leading to subsidence) tends to be minor and, due to high permeabilities, rapid.

Subsidence behavior of alluvium is discussed in greater detail by Rucker and others (2015).

1981 Depth-to-Corcoran contouring places top of Corcoran clay between 500 and 550 feet here, while Saleeby & Foster (2004) place it at about 300 feet.

Well 10700266, drilled 6 miles to the NNW in 1929, had a visual descriptive log.

Fine-grained alluvium:
'sticky blue clay (shale),'
'blue clay and boulders'

Heterogeneous alluvium:
'sandy shale…,'
'sand, streaks shale (clay)'

Coarse-grained alluvium:
'hard...sand, streaks clay (shale)
'…sand [no clay/shale streaks]'

555'

An (approx) 80-foot zone of very low resistivity (typical 5 ohm-m) is present at 555 to 635 feet.
Interpreted as Corcoran Clay

Alluvium between 635 and 700 feet may track with Corcoran Clay or the underlying aquifer system. 700'

The principal compressible alluvium section is from 700 to 1010 feet. This section is dominated by measured resistivity values between 10 to 30 ohm-m that occur due to the heterogeneous inter-lensing and inter-fingering of fine-grained alluvium (<10 ohm-m) and coarse grained alluvium (>30 ohm-m) at relatively vertical scales of a few feet or less. Resistivity tools are several feet in length so that the measurements are an average of the heterogeneous material volume.

1030'

The deeper, coarse grained alluvium (typically 50 to 100 ohm-m) makes relatively little contribution to the total subsidence magnitude. The overall modulus for this (red) alluvium >30 ohm-m is anticipated to be about 10x the modulus of the heterogeneous (green) alluvium; conversely, the compressibility of the red alluvium is about one-tenth the compressibility of the green alluvium.

On this e-log presentation, when the measurement is >50 ohm-m, a 2nd scale of 0 to 500 ohm-m traces the very high resistivity data. These portions of the resistivity trace are highlighted in red.

A significant drop in the resistivity at greater depth may be an indicator of saline water below the usable aquifer, as well as an increase in the fine-grained portion of the deeper alluvium.

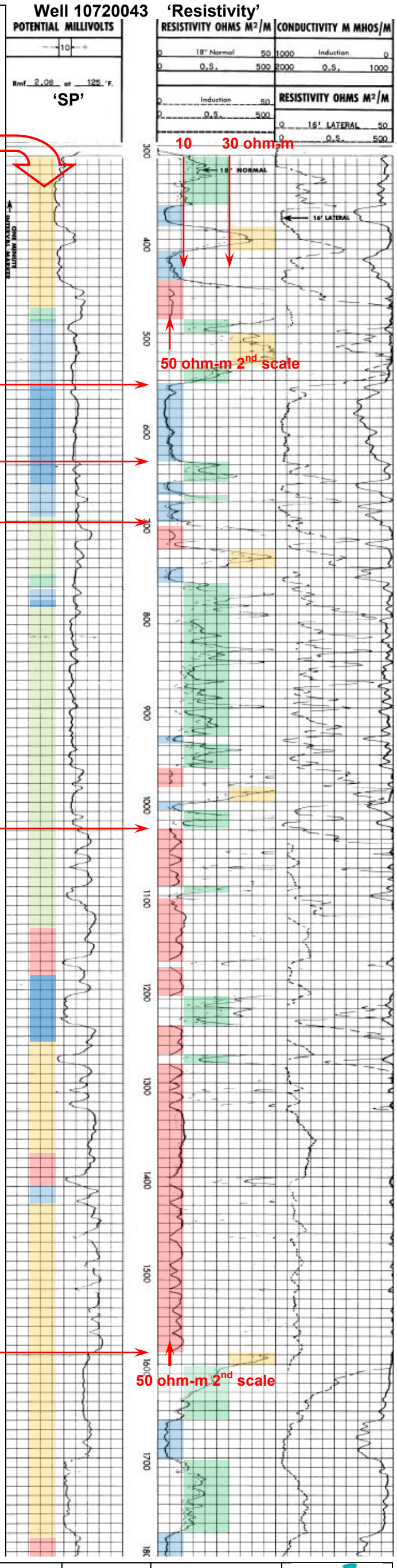

HSR Ground Subsidence Study California	**COMPONENTS OF COMPRESSIBLE BASIN ALLUVIUM CONTRIBUTING TO SUBSIDENCE – HSR ALIGNMENT NEAR ALPAUGH**	PLATE **8-16**	Project 8715180680 PM: JF BY: MLR Date 8/2/2017 Scale: n/a	amec foster wheeler

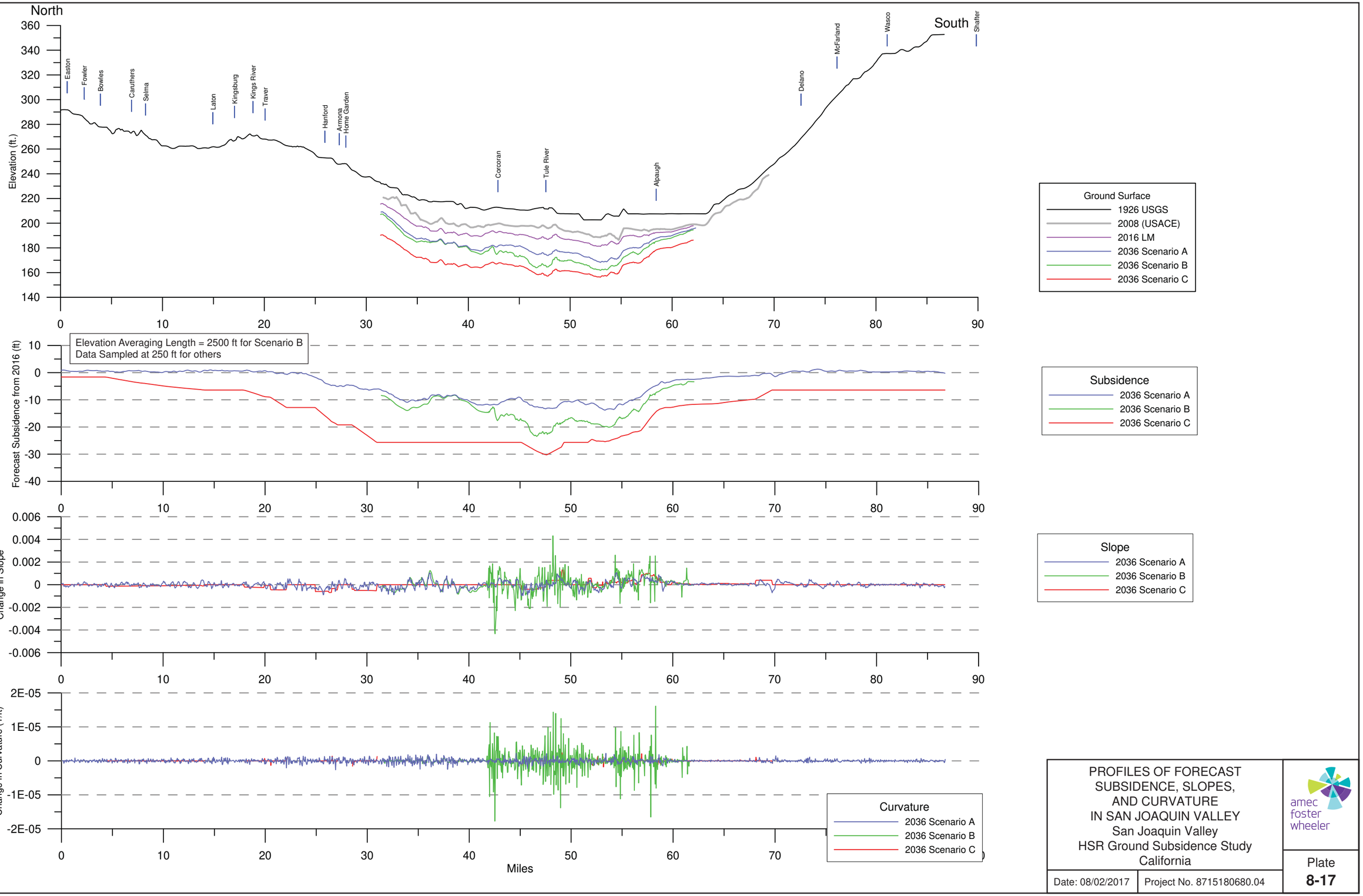

PROFILES OF FORECAST SUBSIDENCE, SLOPES, AND CURVATURE
IN SAN JOAQUIN VALLEY
San Joaquin Valley
HSR Ground Subsidence Study
California

Date: 08/02/2017 | Project No. 8715180680.04

amec foster wheeler

Plate
8-17

S:\OD15\8715180680\gis\profile\profiles_july2017\Plate_08-17_forecast.ai

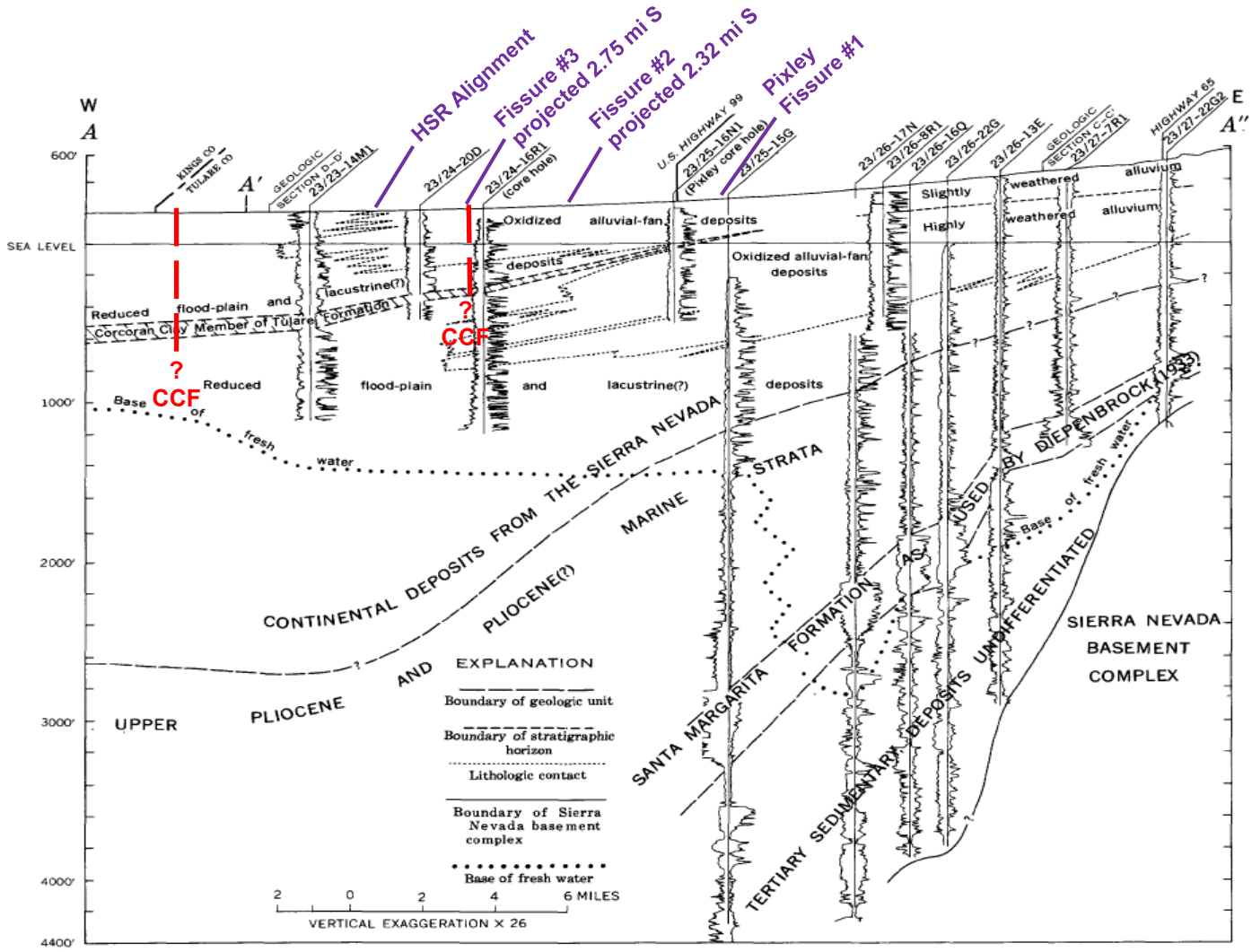

from Lofgren & Klausing, 1969

FIGURE 4.—Geologic section A–A'' through the Pixley core hole. See figure 6 for well locations.

see Plate 8-1 for Profile A-A' location in SJV — — — (CCF) Corcoran Compaction Fault (Saleeby & Foster, 2004)

HSR Ground Subsidence Study California	**WEST TO EAST GEOLOGIC SECTION A-A' FROM LOFGREN & KLAUSING, 1969**	PLATE **8-18**	Project 8715180680 PM : JF BY: MLR Date 8/2/2017 Scale : n/a

amec foster wheeler

Profile A"- A"' Distance, miles

0 1 2 3 4 5 6 7

Corcoran Clay (0.6-0.7 Ma age) may pinch out in the vicinity of the Pixley Fissure.

Pixley Fissure

PP 437-B

374 (API 10700374)

024 (API 10720024)

375 (API 10700375)

373 (API 10700373)

384 (API 10700384)

377 (API 10700377)

381 (API 10700381)

Tulare Fm
This is the younger basin alluvium most susceptible to groundwater decline-induced compaction leading to subsidence.
The **Corcoran Clay (0.6-0.7 Ma age)** is a major confining horizon for underlying good quality groundwater. The Corcoran Clay is too shallow to be identified in these oil /gas wells in the eastern portion of the Central Valley where well casings typically extend to depths of 400 to 600 ft.

~150 ft offset

Top of San Joaquin Fm (2.2-3.4 Ma age?)
This is the youngest group of marine sequences in the basin alluvium. Very low resistivities indicate fine grained materials and salt water. Possible ~150 ft offset in vicinity of Pixley Fissure No. 1?

Top of Santa Margarita Fm (7 Ma age)
This marker formation (with correlating higher resistivities) shows possible ~400 ft offset over 7 million years

~400 ft offset

Spontaneous Potential | Resistivity 0 ohm-m 30

~2-3 ohm-m

top of Santa Margarita Fm ~15-20 ohm-m

Spontaneous Potential | Resistivity 0 ohm-m 30

~7-9 ohm-m (lowest)

top of San Joaquin Fm ~2-3 ohm-m (lowest)

Depth, feet

0 500 1000 1500 2000 2500 3000 3500 4000

0 1 2 3 4 5 6

A"- A"' Profile Distance, miles

- top of San Joaquin Fm (VL) very low resistivity
- top of Santa Margarita Fm (SM), at well log where shaded
- 384 API well identification number, last 3 digits

Notes:
Ma - million years ago

HSR Ground Subsidence Study
California

DEEP BASIN ALLUVIUM PROFILE & POSSIBLE 'COMPACTION FAULT' OFFSET VICINITY OF PIXLEY FISSURE NO. 1

PLATE **8-19**

Project 8715180680
PM : JF BY: MLR
Date 8/2/2017
Scale : n/a

amec foster wheeler

Profile A"- A"' Distance, miles

Depth, feet

confining clays (Corcoran clay?)

Pixley Fissure

Oil / gas well surface casings typically extend 400 to 600 ft into the basin alluvium.

374 (API 10700374)

024 (API 10720024)

375 (API 10700375)

373 (API 10700373)

384 (API 10700384)

377 (API 10700377)

381 (API 10700381)

3

22

75

% total subsidence at Pixley compaction extenso-meters, 1960-1963

(1.9 ft total subsidence 1960-1963) USGS

possible ~150 ft offset

Alluvium in Principal Depths of Subsidence in Confined Aquifers below Corcoran Clay Horizon

<31% coarse*

Fine-grained alluvium composed primarily of clays and silts has low resistivity (typically <10 ohm-m) and is very compressible. Having very low permeability, it has very slow compaction, occurring perhaps over decades or centuries.

69-31% coarse-grained*

Heterogeneous alluvium has moderate resistivity (typically 10 to ~25-30 ohm-m) and is composed of inter-lensing and/or inter-fingering of fine-grained and coarse grained alluvium. The high permeability coarse-grained alluvium fraction provides drainage to the highly compressible fine-grained alluvium fraction. Although total compaction for a given thickness of heterogen-eous alluvium may be less than fine-grained alluvium, it occurs much more rapidly, perhaps over years or decades.

> 69% coarse-grained*

Coarse-grained alluvium has high resistivity (typically greater than ~25 to 30 ohm-m) and is composed primarily of sands and gravels. The high energy needed to transport coarse particles may provide densification during the deposition process so that coarse-grained alluvium is relatively incompressible. Coarse-grained compaction tends to be minor and, due to high permeabilities, rapid.

Possible hydrological barrier in compressible basin alluvium in proximity to Pixley Fissure - Hydrological barrier is a result of differential movement at 'compaction fault' disrupting permeable alluvium lateral connectivity in heterogeneous alluvium.

- compaction extensometer depths
- top of San Joaquin Fm very low resistivity, at well log where shaded
- San Joaquin Fm interpreted top
- Approximate 10 ohm-m line
- Approximate 30 ohm-m line

373 (10700373) API well identification number

* Principal compressible alluvium is color coded by resistivity. Influencing horizons are typically >20 feet thick. Conceptual % coarse-grained to resistivity is discussed in Rucker, Fergason & Panda (2015).

HSR Ground Subsidence Study
California

ALLUVIUM PROFILE & SUSCEPTIBILITY TO SUBSIDENCE VICINITY OF PIXLEY FISSURE NO. 1

PLATE **8-20**

Project 8715180680
PM : JF BY: MLR
Date 8/2/2017
Scale : n/a

amec foster wheeler

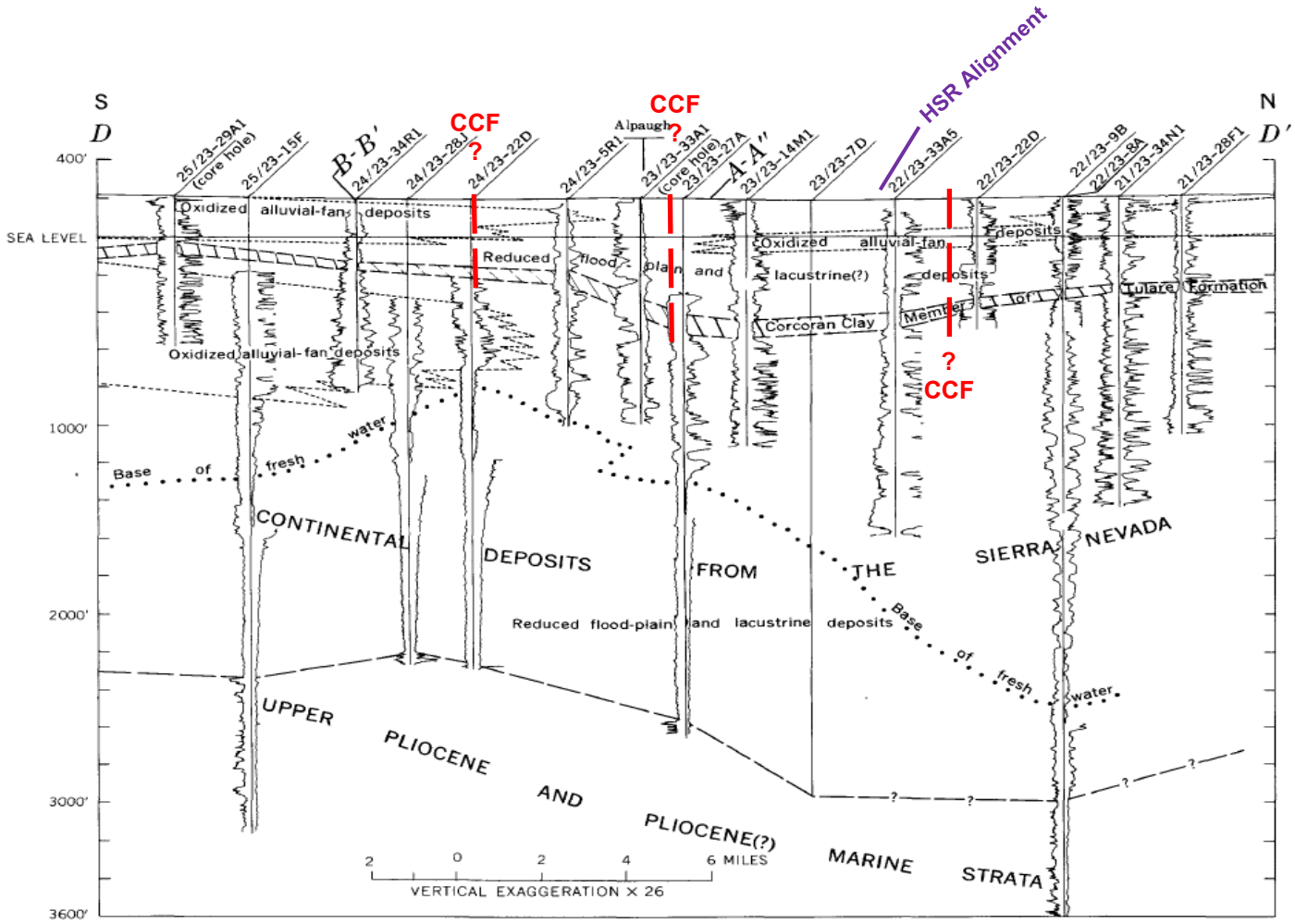

FIGURE 10.—Geologic section *D–D'* through Alpaugh. See figure 6 for location of wells and figure 4 for explanation.

from Lofgren & Klausing, 1969

see Plate 8-1 for Profile D-D' location in SJV

— — (CCF) Corcoran Compaction Fault (Saleeby & Foster, 2004)

HSR Ground Subsidence Study California	**SOUTH TO NORTH GEOLOGIC SECTION D-D' FROM LOFGREN & KLAUSING (1969)**	PLATE **8-21**	Project 8715180680 PM : JF BY: MLR Date 8/2/2017 Scale : n/a

amec foster wheeler

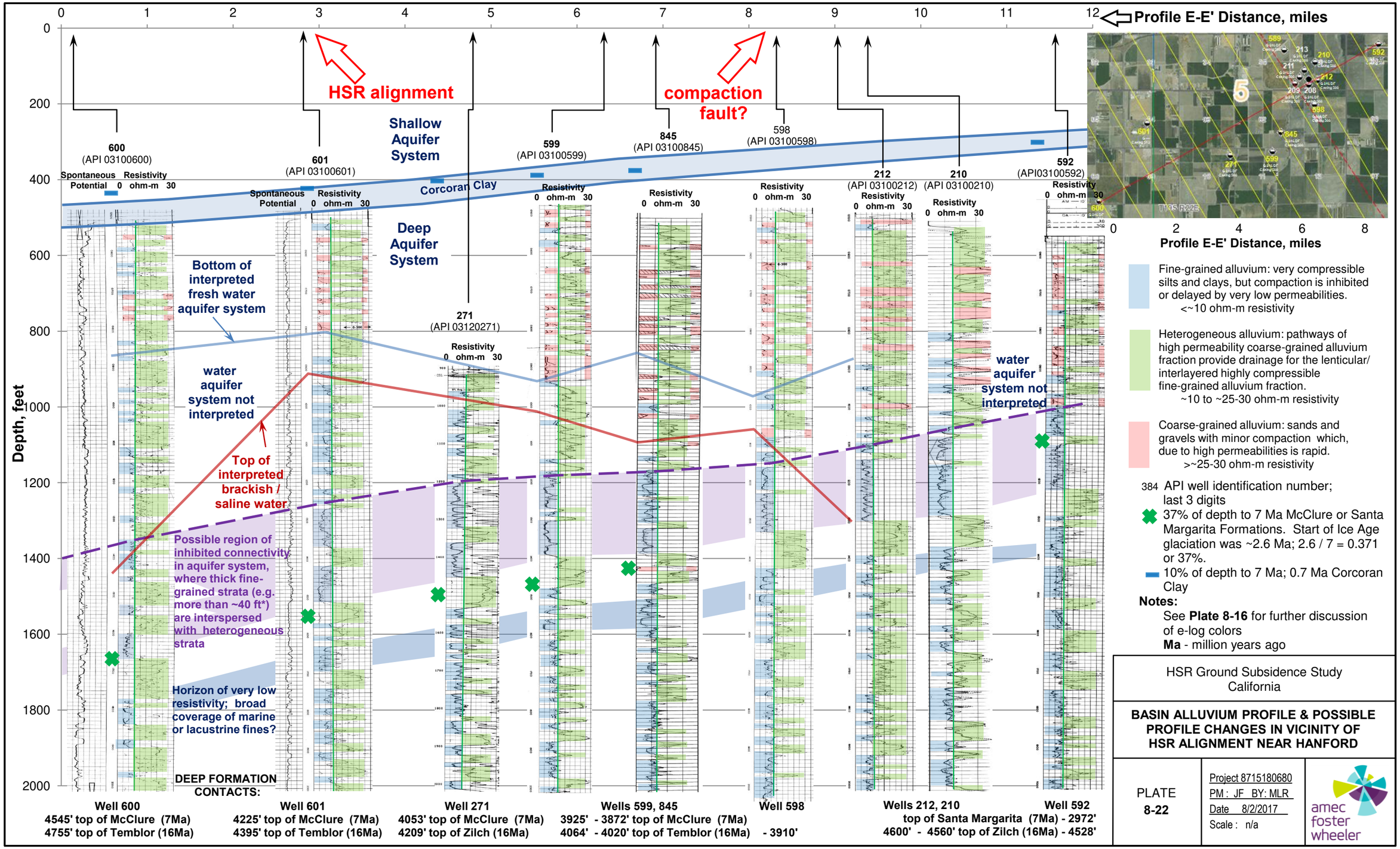
Profile E-E' Distance, miles
HSR alignment
compaction fault?
Shallow Aquifer System
Deep Aquifer System
Corcoran Clay
600 (API 03100600)
601 (API 03100601)
599 (API 03100599)
845 (API 03100845)
598 (API 03100598)
271 (API 03120271)
212 (API 03100212)
210 (API 03100210)
592 (API03100592)
Spontaneous Potential
Resistivity 0 ohm-m 30
Depth, feet
Bottom of interpreted fresh water aquifer system
water aquifer system not interpreted
Top of interpreted brackish / saline water
Possible region of inhibited connectivity in aquifer system, where thick fine-grained strata (e.g. more than ~40 ft*) are interspersed with heterogeneous strata
Horizon of very low resistivity; broad coverage of marine or lacustrine fines?
DEEP FORMATION CONTACTS:
Well 600
4545' top of McClure (7Ma)
4755' top of Temblor (16Ma)
Well 601
4225' top of McClure (7Ma)
4395' top of Temblor (16Ma)
Well 271
4053' top of McClure (7Ma)
4209' top of Zilch (16Ma)
Wells 599, 845
3925' - 3872' top of McClure (7Ma)
4064' - 4020' top of Temblor (16Ma)
Well 598
- 3910'
Wells 212, 210
top of Santa Margarita (7Ma) - 2972'
4600' - 4560' top of Zilch (16Ma) - 4528'
Well 592
T19S R22E
Profile E-E' Distance, miles
Fine-grained alluvium: very compressible silts and clays, but compaction is inhibited or delayed by very low permeabilities.
<~10 ohm-m resistivity
Heterogeneous alluvium: pathways of high permeability coarse-grained alluvium fraction provide drainage for the lenticular/ interlayered highly compressible fine-grained alluvium fraction.
~10 to ~25-30 ohm-m resistivity
Coarse-grained alluvium: sands and gravels with minor compaction which, due to high permeabilities is rapid.
>~25-30 ohm-m resistivity
384 API well identification number; last 3 digits
37% of depth to 7 Ma McClure or Santa Margarita Formations. Start of Ice Age glaciation was ~2.6 Ma; 2.6 / 7 = 0.371 or 37%.
10% of depth to 7 Ma; 0.7 Ma Corcoran Clay
Notes:
See Plate 8-16 for further discussion of e-log colors
Ma - million years ago
HSR Ground Subsidence Study
California
BASIN ALLUVIUM PROFILE & POSSIBLE PROFILE CHANGES IN VICINITY OF HSR ALIGNMENT NEAR HANFORD
PLATE 8-22
Project 8715180680
PM : JF BY: MLR
Date 8/2/2017
Scale : n/a
amec foster wheeler

Measured Subsidence Above and Below Corcoran Clay - Pixley Extensometers Site

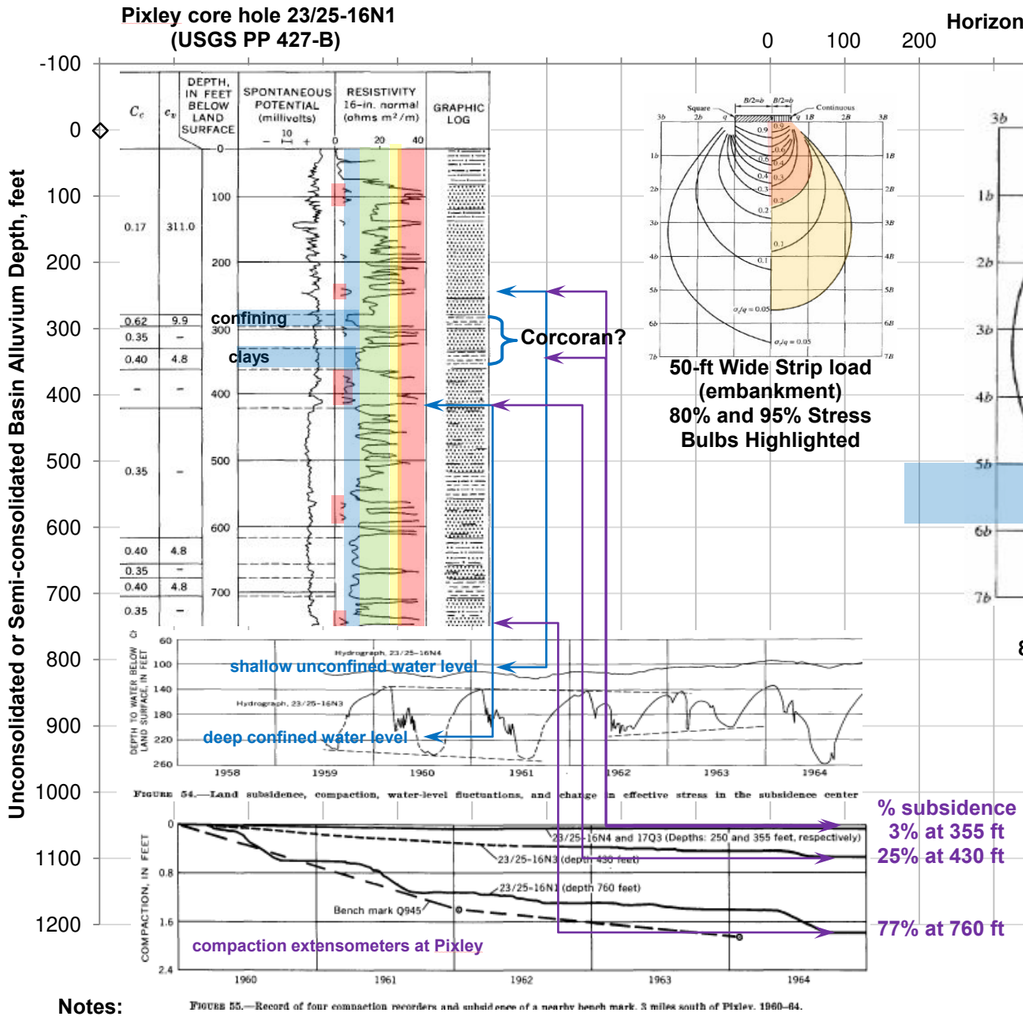

% subsidence
3% at 355 ft
25% at 430 ft
77% at 760 ft

Notes:
Data and information from the Pixley Compaction Extensometers Site through 1964 is presented in USGS Professional Paper 437-B.

Depth to the bottom of confining clays (presumed to be the Corcoran Clay) at the Pixley Site is about 360 feet at the corehole 23/25-16N1 shown. Pixley is located near the inferred edge of Corcoran Clay. Pumped aquifers in the Pixley area were below the confining clays; about 97% of the measured subsidence from 1960 through 1964 was below the confining clays.

The Pixley area is more throughly discussed in Section 8.5 of this report.

Boussinesq Stress Distribution under Square and Continuous (Strip) Loadings, Isotropic Soil Conditions Assumed

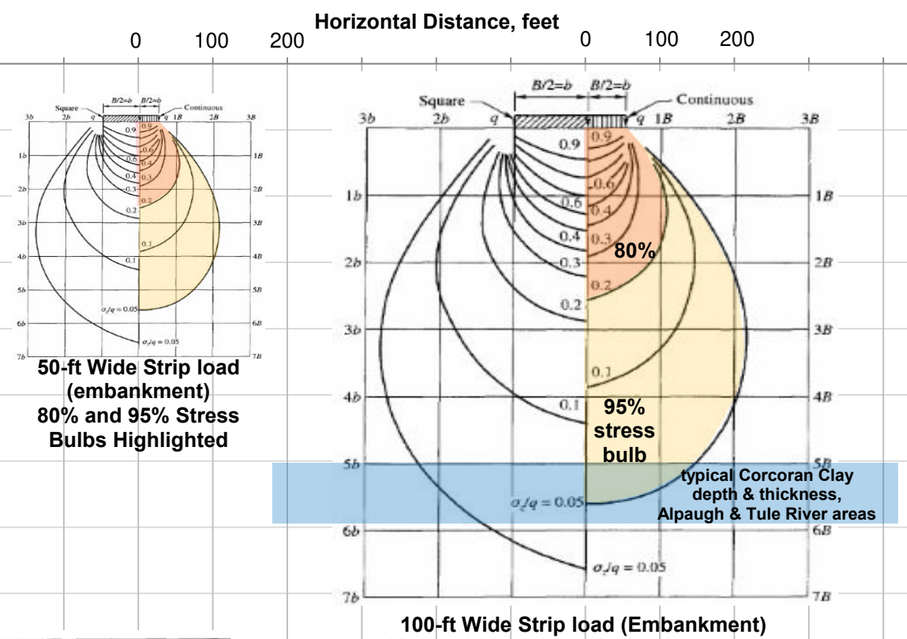

Notes:
The theoretical distribution of stress shown above assumes that the soil mass is uniform and isotropic. Given that assumption, for an embankment width of 100 feet and a depth to bottom of the Corcoran Clay (top of productive confined aquifers) at a depth about 600 feet, 95% of the embankment settlement stress can be anticipated to be distributed above the top of productive aquifers; subsidence is anticipated to be concentrated within the productive aquifers.

Given these assumptions, 95% of the embankment settlement stress can be anticipated to be distributed within a horizontal distance of twice the embankment width and centered at the embankment centerline.

Modeled Typical Horizontal and Vertical Subsidence Pattern around a Single 500-foot Deep Well, Unconfined Aquifer

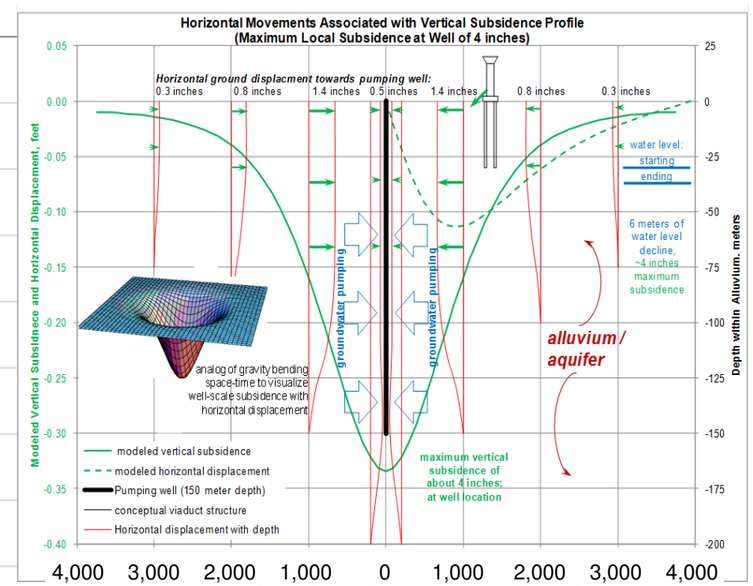

Notes:
Distances of subsidence impact from a deep pumping well are significantly greater than distances of settlement impact from an embankment loading due to a shallow foundation.

Subsidence due to pumping in shallow aquifers (unconfined or confined) will result from compression within the shallow aquifer system.

HSR Ground Subsidence Study
California

SETTLEMENT AND SUBSIDENCE IN UNCONSOLIDATED AND SEMI-CONSOLIDATED BASIN MATERIALS

PLATE **9-1**

Project 8715180680
PM : JF BY: MLR
Date 7/12/2017
Scale : n/a

amec foster wheeler

NGS Survey Data obtained from website http://www.ngs.noaa.gov/NGSDataExplorer/
CGS - Coast and Geodetic Survey
NGS - National Geodetic Survey

Elevations shown are the most recent in the NGS database, adjusted to current NAVD88 elevation. Some locations have been visited recently by geocaching to confirm their condition; reported informal geocach elevations, not measured by survey-grade methods, do not appear to be credible. Original CGS or NGS point names or designations (Q963, K458, TURNBULL 2, etc.) are also shown.

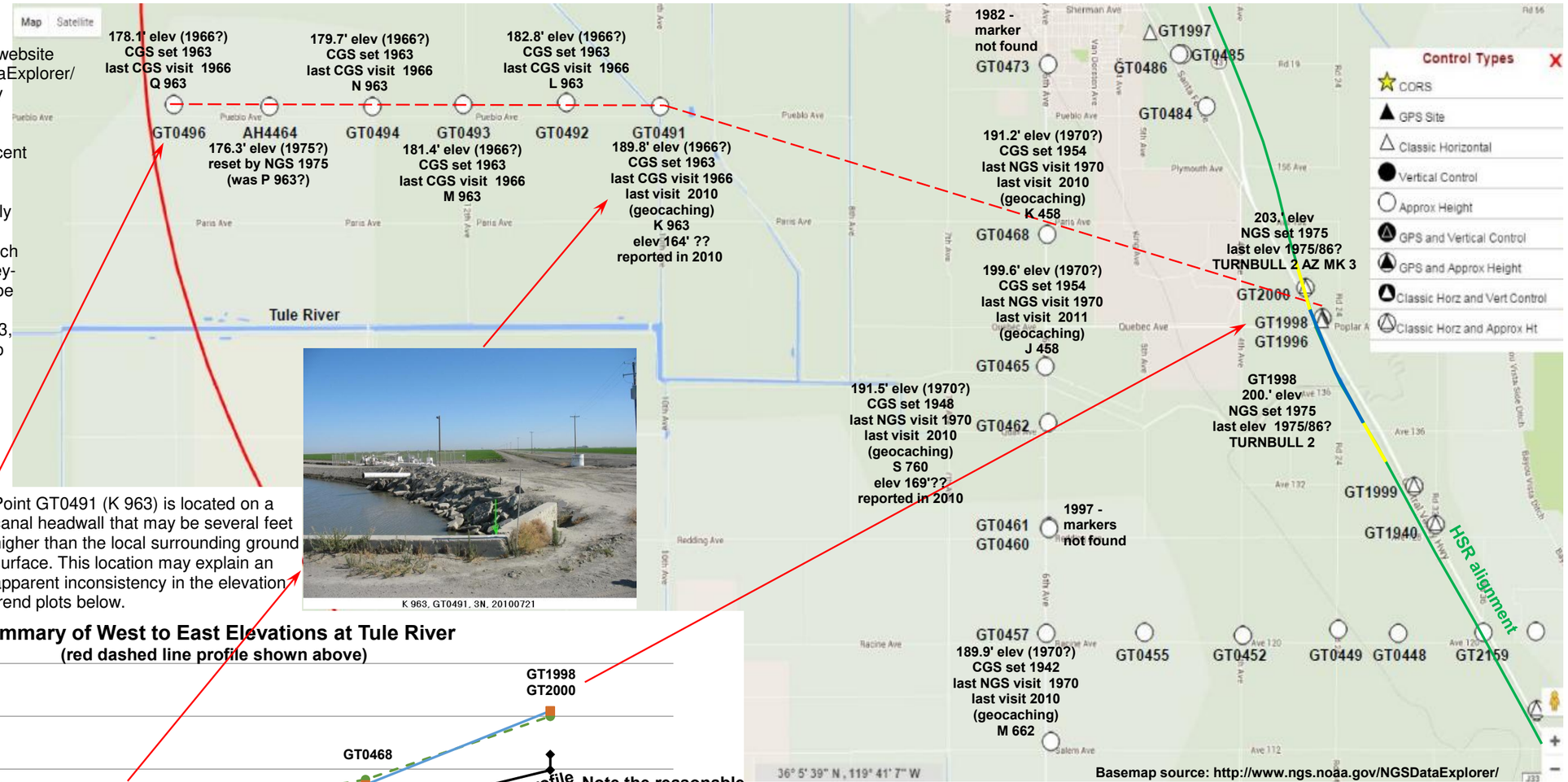

Point GT0491 (K 963) is located on a canal headwall that may be several feet higher than the local surrounding ground surface. This location may explain an apparent inconsistency in the elevation trend plots below.

K 963, GT0491, 3N, 20100721

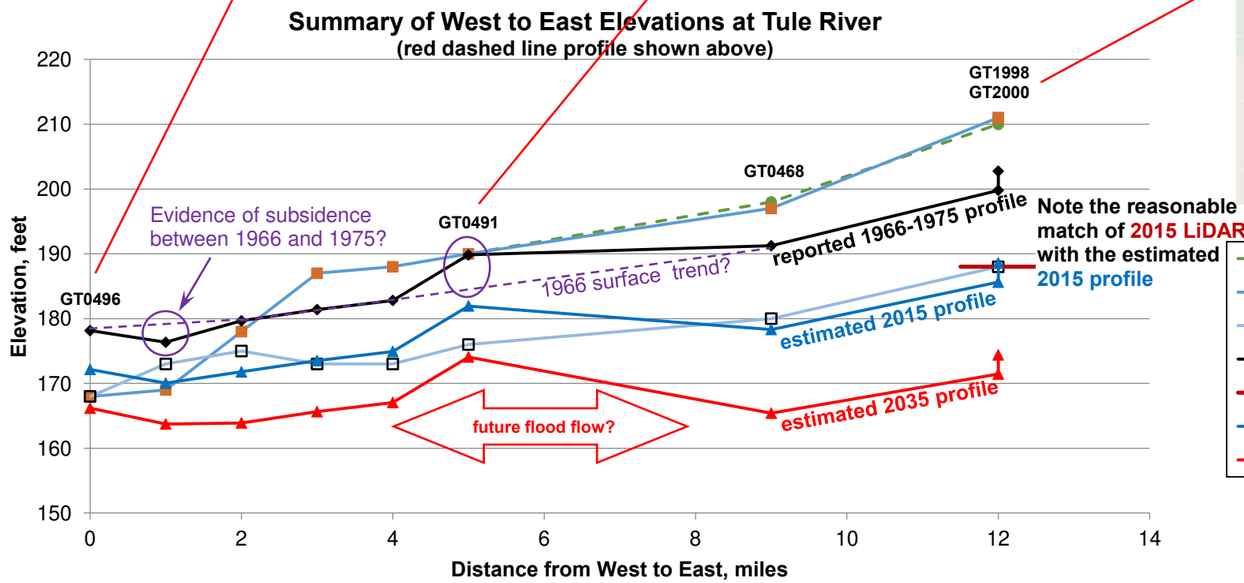

Note the reasonable match of 2015 LiDAR with the estimated 2015 profile

LEGEND

- elevations interpolated from published (in 2013) 10-ft contours
- (June 2016*) Google elevations per Google Earth
- (checked 5/8/2017) Google elevations per Google Earth
- Benchmark (BM) elevations (1960s-70s?)
- 2015 Lidar at Tule River
- BM elevs - (20 years subsidence at L-band InSAR rate)
- BM elevs - (40 years subsidence at L-band InSAR rate)

L-band InSAR subsidence rates are derived from ALOS satellite data (6-21-2007 to 12-30-2010) processed by JPL; see Plates 1-1 and 8-1 for graphical presentations of that subsidence.
* Google elevations revised when checked May 8, 2017

HSR Ground Subsidence Study
California

EXISTING TULE RIVER AREA BENCHMARKS IN NGS DATABASE

PLATE
9-2

Project 8715180680
PM : JF BY: MLR
Date 7/12/2017
Scale : n/a

amec foster wheeler

amec foster wheeler

APPENDIX A

Ground Movement Rates at Existing CGPS Sites

APPENDIX A

GROUND MOVEMENT RATES AT EXISTING CGPS SITES

Ground Subsidence Study
California High-Speed Rail Project
San Joaquin Valley, California

This attachment discusses available Global Position Survey (GPS) information relevant to the HSR alignment in the Central Valley. GPS information includes Continuous GPS (CGPS) stations operated by UNAVCO (www.unavco.org) for the Plate Boundary Observatory (PBO), and CGPS stations operated by Caltrans (http://sopac.ucsd.edu/sector.shtml). CGPS stations associated with the PBO are assumed to be referenced and checked on a frequent basis by the various scientific entities that utilize the PBO in their ongoing seismological and geological / geophysical research. Repeat GPS survey performed by Caltrans has also been provided at several Caltrans CGPS sites. Caltrans CGPS sites designations are on Figure A-1, and consist of four letters (CHOW, CRCN, DLNO, LEMA, MULN, RBRU) commonly related to the closest town.

Multiple frames of reference are included in the databases. The UNAVCO database includes CGPS site change from the date of startup in the NAM08 (North American 2008) reference frame, which is tied to the North American plate. Caltrans data from the SOPAC website is presented in several reference frames, including ITRF (International Terrestrial Reference Frame), WGS (World Geodetic System) and NAD (North American Datum). To date, Amec Foster Wheeler has had difficulty reconciling the horizontal portion of the Caltrans ITRF data, and the WGS coordinates do not appear to have sufficient decimal places to provide useful horizontal change information. Provided NAD coordinates appear to have better resolution than WGS coordinates, but do not result in the detail presented in UNAVCO data in NAM08 coordinates. Thus, Caltrans CGPS results are not plotted in the following figures.

Locations of CGPS stations utilized in this Attachment are shown on Attachment Figure 1. PBO stations closest to the Corcoran area of the HSR alignment with CGPS records are located around the perimeter of the Central Valley where subsidence in the time of GPS has been minimal. Station P565 at Delano is a reasonable reference point. Being part of the PBO, it may be assumed that this point (and other CGPS points with designations of P###) is checked and re-assessed on a frequent basis by seismological specialists and geological/geophysical researchers. Station P564 is located to the southwest near the HSR alignment, and P545 and P544 are located farther to the southwest and west. PBO stations farther north than P565 (such as P056 and P566) are outside the area for which JPL has provided InSAR results. Station P300 is at the basin edge to the west, and Stations P304, P305 and P307 are in the vicinity of El Nido, but outside of the local subsidence feature near El Nido. Finally, P537 is located outside the San Joaquin Valley, and is southwest of the San Andreas Fault. Data files of daily elevations for PBO stations are available for download starting at the UNAVCO website www.unavco.org.

Caltrans maintains the Central valley Spatial Reference Network (CVSRN) with some coverage at or in the vicinity of the HSR. CGPS Stations (from southeast to northwest) DLNO, CRCN, LEMA, MULN and CHOW are located through the region of greatest subsidence. Station RBRU near Fresno provides a reference with little active subsidence. Station DLNO is located near PBO Station P565. Station CRCN is located in the area of greatest apparent subsidence along

the alignment around Corcoran, CA. Historical CGPS daily elevations for Caltrans CVSRN stations are available through the SOPAC website at http://sopac.ucsd.edu/sector.shtml.

For comparing CGPS data with InSAR results, Caltrans has also provided a history of GPS repeat surveys at relevant points, including DLNO, CRCN, LEMA, MULN and CHOW. Dates of these surveys were 5/3/2010, 1/14/2011, 1/9/2012, 9/21/2013, 7/1/2014, 3/3/2015 and 3/3/2015. Points LEMA and MULN were initially surveyed on an earlier date of 2/12/2008. There is overlap between these two GPS survey / CGPS points and L-band InSAR for the time period of 2008 through 2010. The 1/14/2011 GPS survey was performed just two weeks after the last L-band InSAR was acquired.

JPL (Farr and others 2015) provided L-band InSAR classical interferometry for the Central Valley. This work was performed for the California Department of Water Resources (DWR), and appears to have been focused on DWR infrastructure. Starting with the 6/21/2007 scene, classical interferometric results were obtained for the following dates: 9/21/2007, 11/6/2007, 12/22/2007, 2/6/2008, 3/23/2008, 5/8/2008, 8/8/2008, 6/26/2009, 9/26/2009, 12/27/2009, 3/29/2010, 5/14/2010, and 12/30/2010. Two L-band scenes were needed to provide coverage for the Central Valley. As shown in Figure 1, the western scene, which includes points MULN and CHOW, covers the California Aqueduct and areas with extensive historical subsidence measurements and studies. The scene appears to have relatively 'smooth' results (Figure 1) which may, at least in part, be the result of extensive post-processing smoothing or other operations having been applied to the classical interferometric information. The eastern scene, which includes points RBRU, LEMA, CRCN, DLNO and P565, has interferometric results that exhibit considerable small-scale roughness relative to the western scene. This implies that the classical interferometric results may be less smoothed by post-processing operations.

Subsidence rates for these CGPS sites are summarized in the table below.

Summary of Ground Movements as Recorded at Existing CGPS Sites

					Ground Movement, feet				Est. Horizontal Non-Tectonic Movement, feet		Elastic Movement, feet		Annual Subsidence Rate feet/year	
SITE	Database	Reference Frame	Data Begin Date	Data End Date	Total Vertical	Total Horizontal	Vertical 2013-	Horizontal 2013-	Total Data Set	2013-	Vertical (typical)	Horizontal (typical)	1/1/2007 to 1/1/2011	1/1/2013 to 1/1/2016
P056	unavco	NAM08	11/17/2005	3/1/2016	-1.34	0.54	-0.77	0.18	0.05	0.03	0.06	0.03	0.09	**0.25**
P300	unavco	NAM08	12/15/2004	3/1/2016	0.03	0.52	0.01	0.14	0.16	0.09	nil	0.03	0.00	0.00
P304	unavco	NAM08	4/30/2004	3/1/2016	-0.64	0.53	-0.35	0.13	0.07	nil	nil	0.02	0.05	0.12
P305	unavco	NAM08	7/22/2005	3/1/2016	0.04	0.46	0.04	0.32			nil	nil	0.00	0.00
P307	unavco	NAM08	10/18/2005	3/1/2016	-0.89	0.57	-0.39	0.18	0.08	0.02	0.05	0.01	0.07	0.13
P537	unavco	NAM08	5/3/2006	3/1/2016	0.07	1.08	-0.03	0.36	Southwest of San Andreas Fault				0.00	0.00
P544	unavco	NAM08	12/15/2005	3/1/2016	-0.10	0.53	-0.04	0.16	0.07	0.02	0.05	nil	0.02	0.02
P545	unavco	NAM08	10/30/2007	3/1/2016	-0.22	0.48	-0.14	0.17	0.09	0.03	nil	0.01	0.02	0.05
P564	unavco	NAM08	11/2/2006	3/1/2016	-1.15	0.54	-0.65	0.19	0.12	0.07	0.18	0.04	0.08	**0.22**
P565	unavco	NAM08	11/17/2005	10/21/2015	-0.95	0.53	-0.74	0.15	0.07	0.03	0.08	0.02	0.04	**0.25**
P566	unavco	NAM08	11/16/2005	3/1/2016	-0.38	0.47	-0.26	0.13	0.03	0.01	0.03	0.00	0.03	0.05
CRCN	sopac	NAD	1/1/2013	2/26/2016			-3.10							**0.99**
DLNO	sopac	NAD	1/1/2013	2/26/2016			-0.93							**0.31**
LEMA	sopac	NAD	1/1/2013	2/26/2016			-2.27							**0.73**
MULN	sopac	NAD	1/1/2013	2/26/2016			-0.63							**0.21**
RBRU	sopac	NAD	1/1/2013	2/26/2016			-0.06							0.02
CHOW	sopac	NAD	1/1/2013	2/26/2016			-1.17							**0.38**

CGPS sites with current subsidence rates greater than 0.2 feet per year are in bold in the rightmost column. Site P537 was assessed to verify that apparent background ('tectonic') horizontal movements of about 14 millimeters per year are consistent with relative plate boundary movements in this area where the San Andreas Fault (SAF) movement at the North American and Pacific Plates boundary is creeping rather than locked.

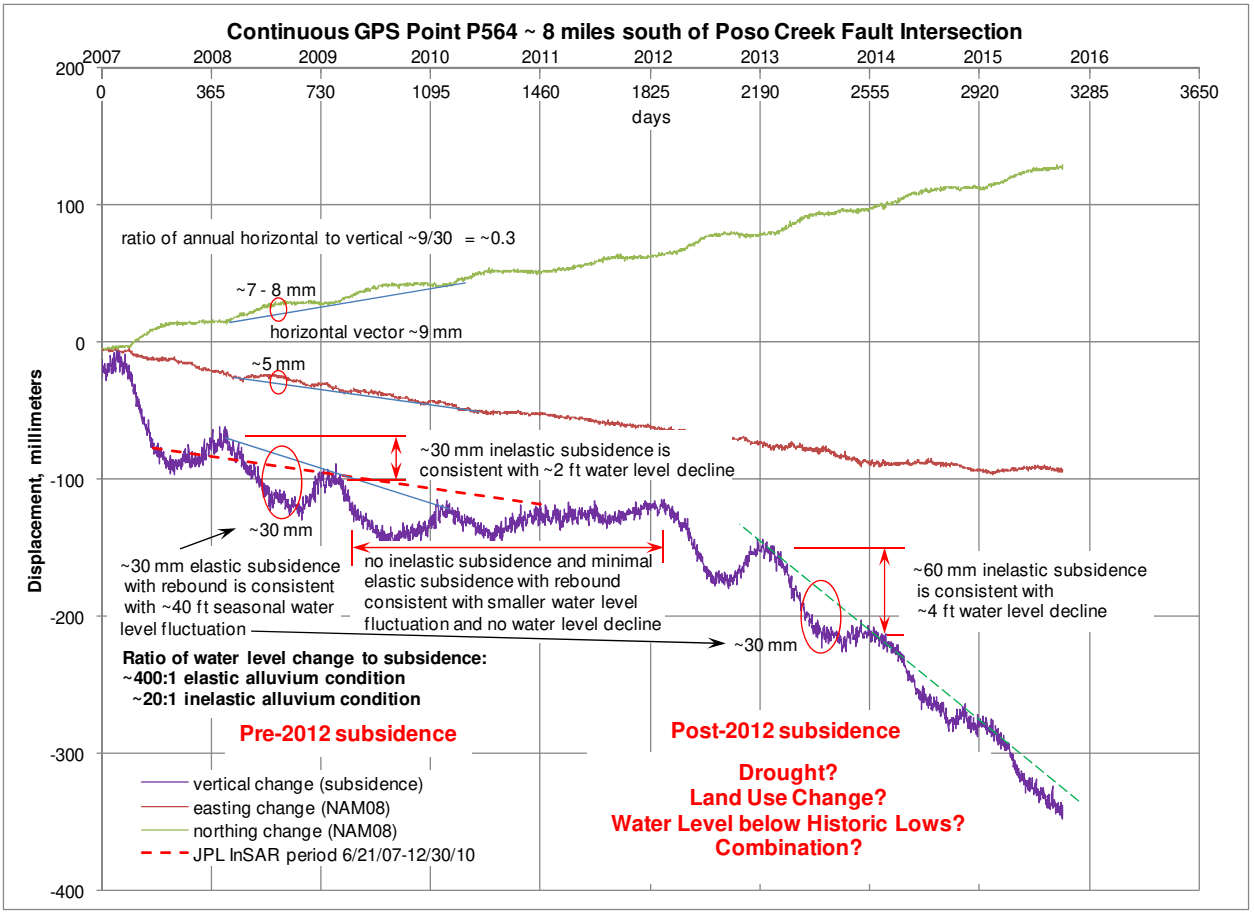

CGPS movements can begin to provide insights into subsidence behavior and details that have traditionally been accomplished using compaction extensometers. As is shown in the figure above, vertical movements at CGPS Site P564 are consistent with a combination of elastic ground compression and inelastic ground consolidation over time. These movements are consistent with and appear to be synchronized with seasonal pumping patterns. Whereas classic compaction extensometers had multiple measurement points at various depths to provide (using mid-20th century strip chart-type technology; continuous surface survey monitoring was not feasible) continuous soil compression (or compaction) data at depth below the Corcoran Clay Unit, the surface mounted CGPS site monitors total subsidence continuously. If little pumping is occurring above the Corcoran Clay, it can be assumed that soil compression is occurring primarily in the deeper confined aquifers below the clay. Subsurface aspects of the overall monitoring program may be focused on differences in pumping between the upper aquifers and the confined lower aquifers. The total subsidence may then be 'distributed' between deeper and shallower aquifers.

Following are plots of the ground movements at various CGPS Sites:

The following plots are intended to present recent ground movement directions, magnitudes, and trends or changes in movement trends at these CGPS sites. Combined south-north and east-west horizontal movement is plotted in black with west to the left, east to the right, north up and south down. Since tectonic movement is causing these sites to be moving to the northwest (in GPS space), time in years is plotted from right to left to allow consolidation of the horizontal and vertical movements and their component parts. (It should be noted that future calculations using GPS-based survey for subsidence monitoring and HSR construction control, will have to account for both subsidence and tectonic movements.) Vertical movement is plotted in purple.

Seasonal patterns of agricultural groundwater pumping are commonly seen reflected in both vertical and horizontal movement at the sites. Some of these movements are elastic in nature, with maximum subsidence (downward) occurring through the summer into autumn that then rebound taking place in winter into early spring. Some of these movements continue throughout each year, but typically at an accelerated rate through the summer into autumn and a decelerated rate through the winter into early spring. Because most soil consolidation is non-linear and inelastic (and hence non-reversible), it should be anticipated that most of the observed subsidence will be non-reversible.

Observed horizontal movement in the San Joaquin Valley includes a component of relatively steady-state tectonic movement, and can include horizontal components of groundwater pumping induced subsidence. The anticipated tectonic movement trend has been plotted in such a manner as to facilitate the ability to distinguish likely subsidence-induced horizontal movement from tectonic movement. For each CGPS site plotted, a calculated difference between the tectonic trend and total horizontal movement has been included at the upper left corner of the horizontal movement plot.

Relationships between horizontal and vertical movements are further explored at CGPS Station P564. Based on an interpretation of observed movement, it appears there is at least one active pumping well in the vicinity of P564; vertical and horizontal movements at P564 may include effects of that nearby pumping.

Data for these plots was downloaded from the UNAVCO website. The data is also available on the SOPAC database. Horizontal coordinate data in monthly intervals was downloaded and plotted with the UNAVCO data. Without further processing, much the SOPAC coordinate data matched poorly against the UNAVCO data. This indicates that data issues may need to be addressed before available SOPAC CGPS can be effectively utilized for subsidence monitoring.

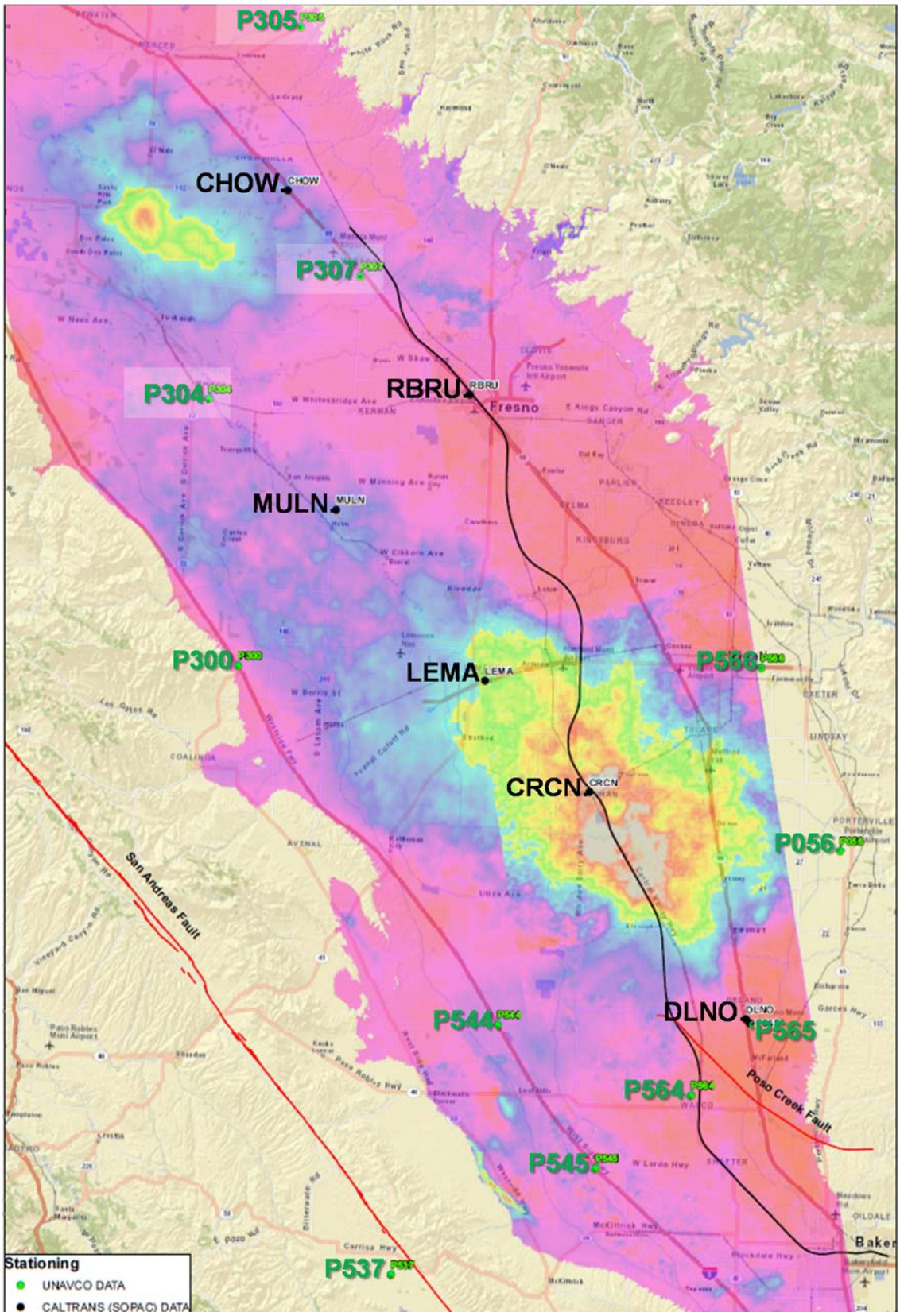

Figure A-1 SITE PLAN showing locations of CGPS sites

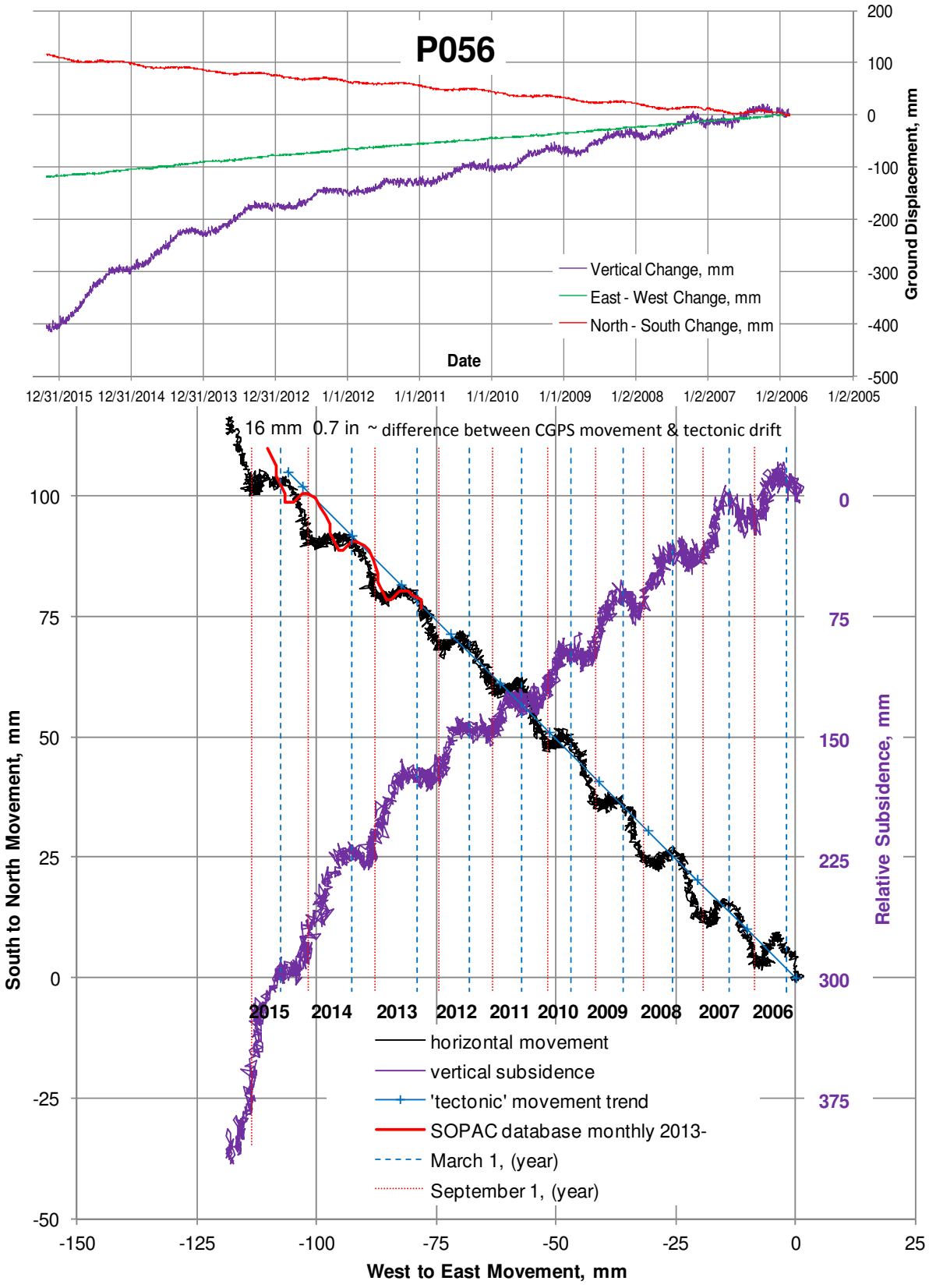
P056
Ground Displacement, mm
Vertical Change, mm
East - West Change, mm
North - South Change, mm
Date
16 mm 0.7 in ~ difference between CGPS movement & tectonic drift
South to North Movement, mm
West to East Movement, mm
Relative Subsidence, mm
horizontal movement
vertical subsidence
'tectonic' movement trend
SOPAC database monthly 2013-
March 1, (year)
September 1, (year)

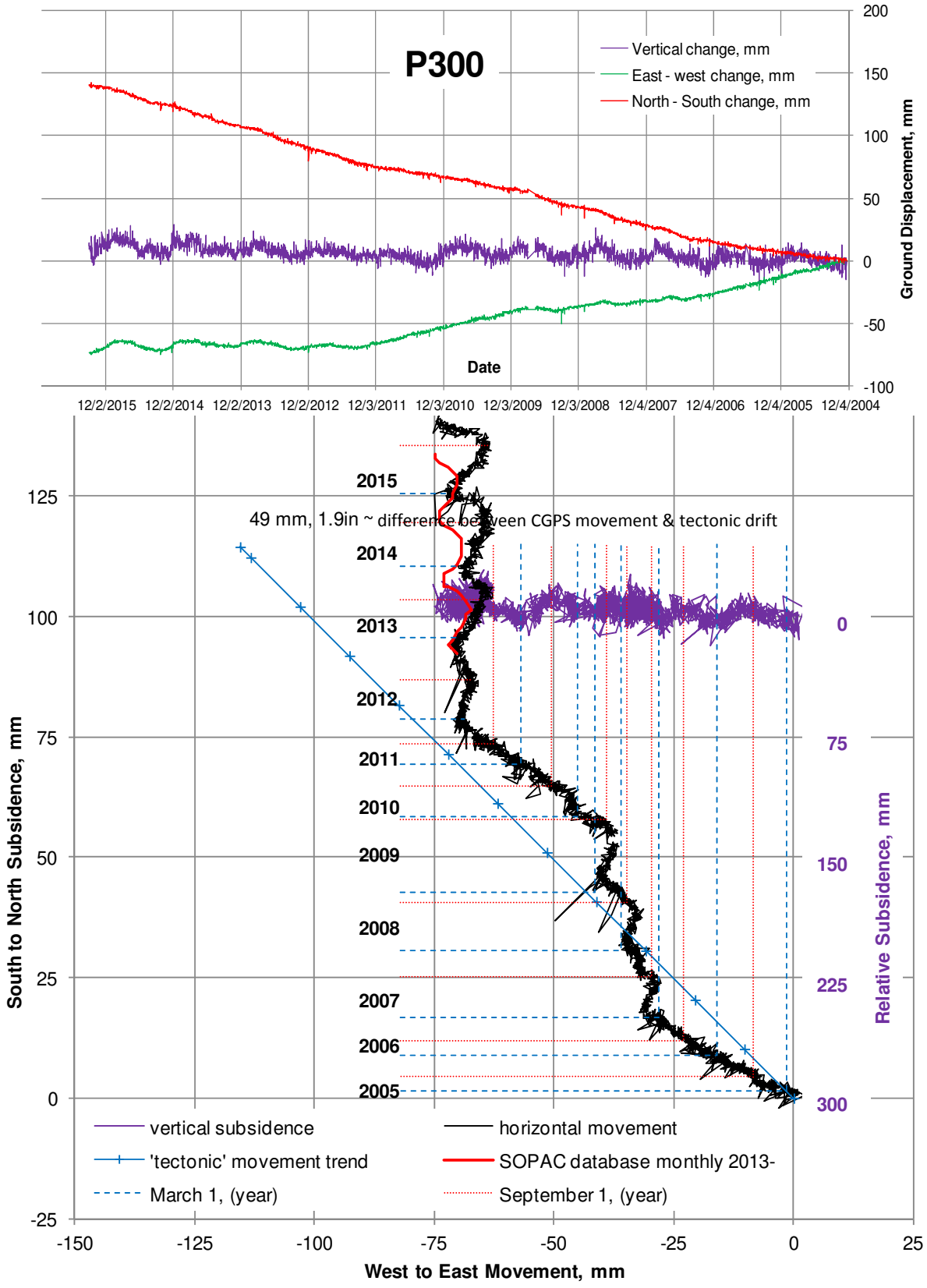
P300
Vertical change, mm
East - west change, mm
North - South change, mm
Ground Displacement, mm
Date
12/2/2015 12/2/2014 12/2/2013 12/2/2012 12/3/2011 12/3/2010 12/3/2009 12/3/2008 12/4/2007 12/4/2006 12/4/2005 12/4/2004
49 mm, 1.9in ~ difference between CGPS movement & tectonic drift
2015
2014
2013
2012
2011
2010
2009
2008
2007
2006
2005
South to North Subsidence, mm
Relative Subsidence, mm
West to East Movement, mm
vertical subsidence
horizontal movement
'tectonic' movement trend
SOPAC database monthly 2013-
March 1, (year)
September 1, (year)

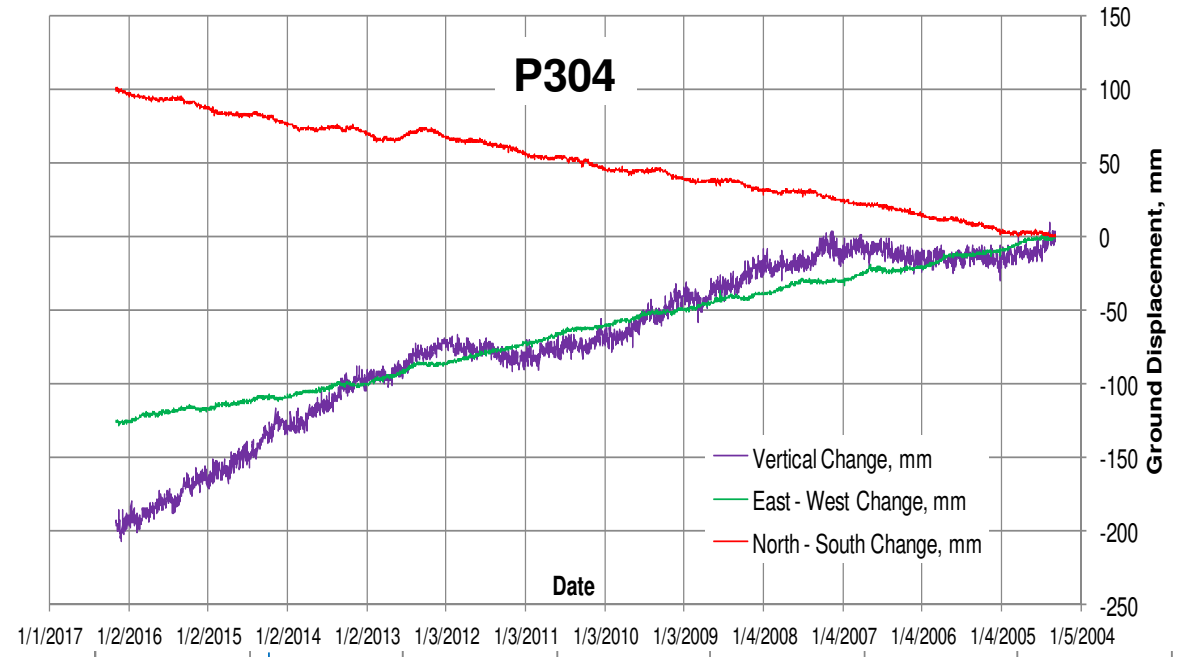
P304
Ground Displacement, mm
150
100
50
0
-50
-100
-150
-200
-250
Vertical Change, mm
East - West Change, mm
North - South Change, mm
Date
1/1/2017 1/2/2016 1/2/2015 1/2/2014 1/2/2013 1/3/2012 1/3/2011 1/3/2010 1/3/2009 1/4/2008 1/4/2007 1/4/2006 1/4/2005 1/5/2004

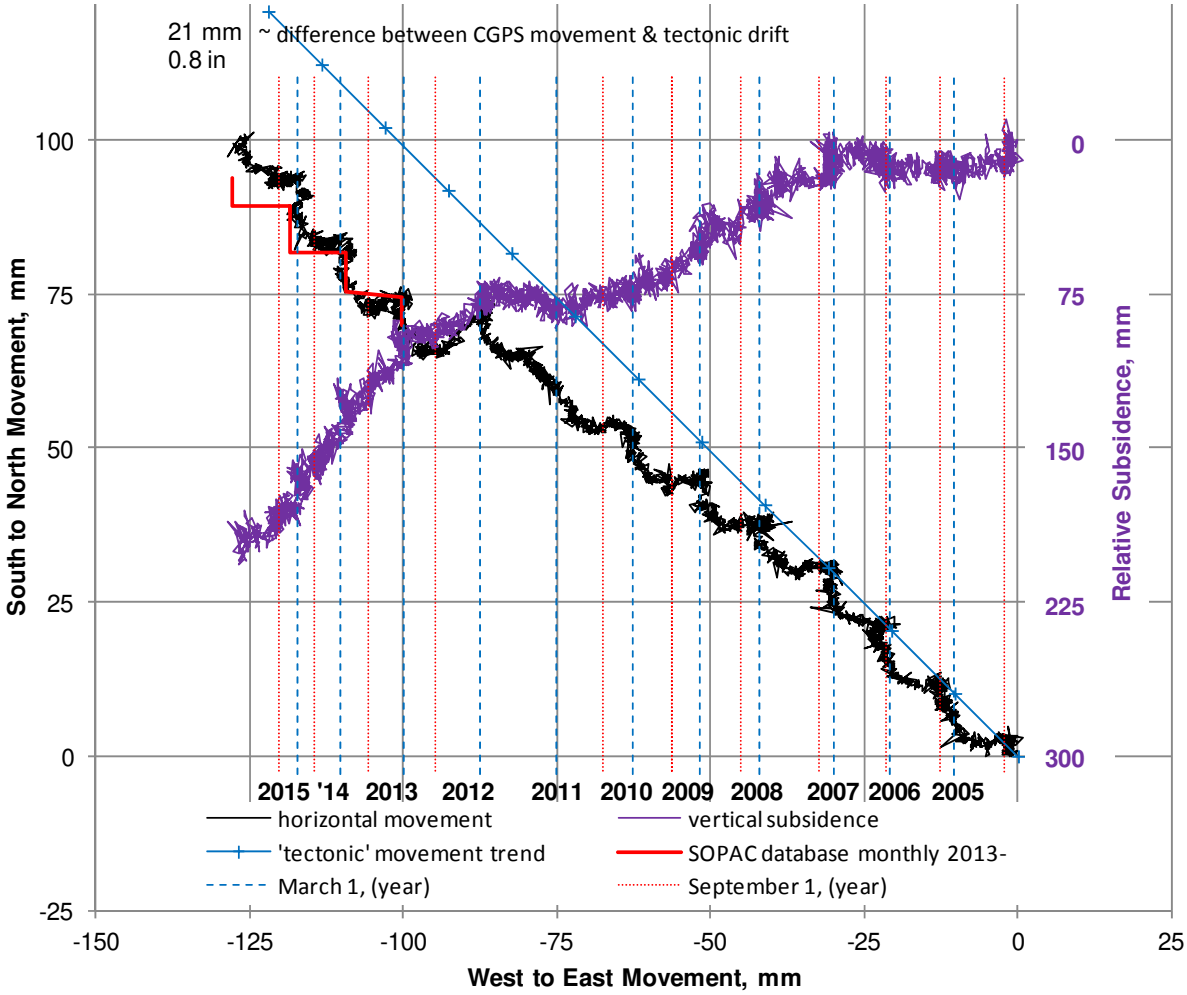
21 mm
0.8 in
~ difference between CGPS movement & tectonic drift
South to North Movement, mm
Relative Subsidence, mm
100
75
50
25
0
-25
0
75
150
225
300
2015 '14 2013 2012 2011 2010 2009 2008 2007 2006 2005
horizontal movement
vertical subsidence
'tectonic' movement trend
SOPAC database monthly 2013-
March 1, (year)
September 1, (year)
-150 -125 -100 -75 -50 -25 0 25
West to East Movement, mm

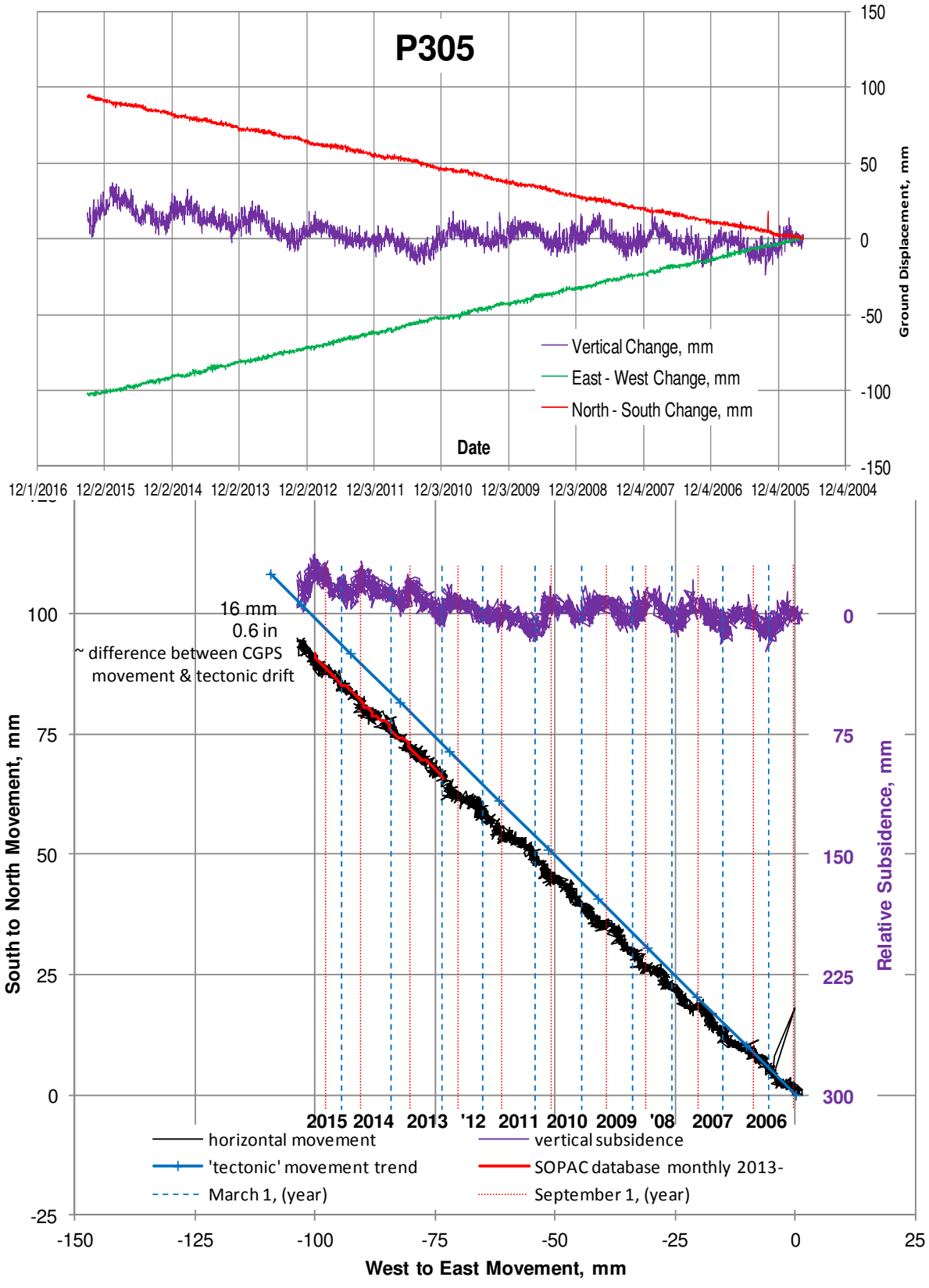
P305
150
100
50
0
-50
-100
-150
Ground Displacement, mm
Vertical Change, mm
East - West Change, mm
North - South Change, mm
Date
12/1/2016 12/2/2015 12/2/2014 12/2/2013 12/2/2012 12/3/2011 12/3/2010 12/3/2009 12/3/2008 12/4/2007 12/4/2006 12/4/2005 12/4/2004
16 mm
0.6 in
~ difference between CGPS
movement & tectonic drift
South to North Movement, mm
Relative Subsidence, mm
2015 2014 2013 '12 2011 2010 2009 '08 2007 2006
horizontal movement
vertical subsidence
'tectonic' movement trend
SOPAC database monthly 2013-
March 1, (year)
September 1, (year)
West to East Movement, mm

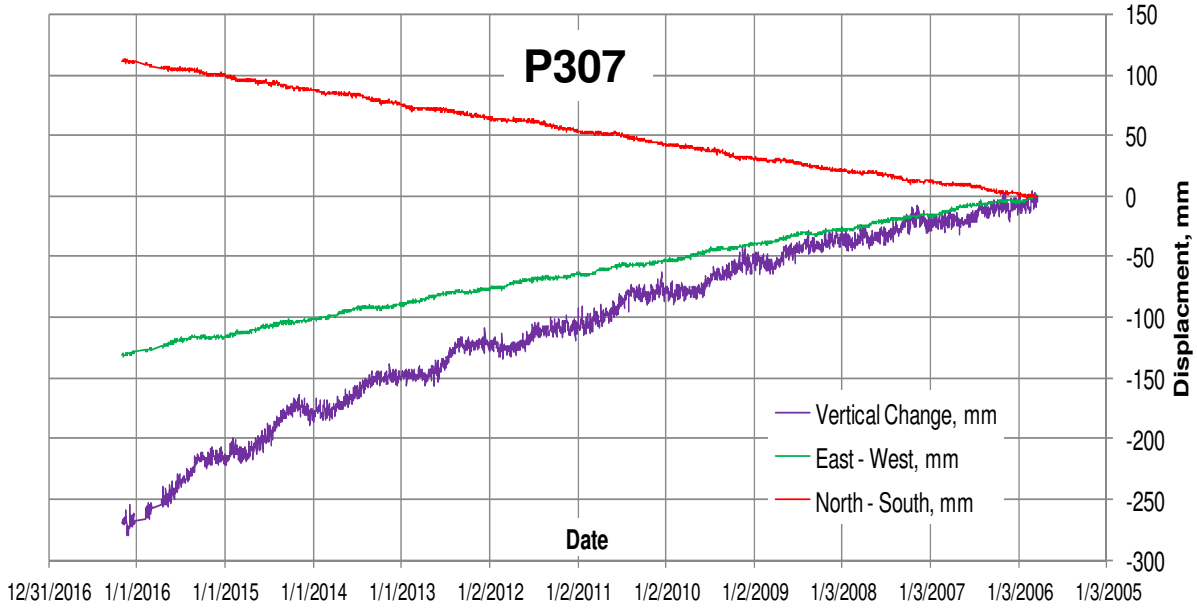
P307
Vertical Change, mm
East - West, mm
North - South, mm
Displacment, mm
Date
150
100
50
0
-50
-100
-150
-200
-250
-300
12/31/2016
1/1/2016
1/1/2015
1/1/2014
1/1/2013
1/2/2012
1/2/2011
1/2/2010
1/2/2009
1/3/2008
1/3/2007
1/3/2006
1/3/2005

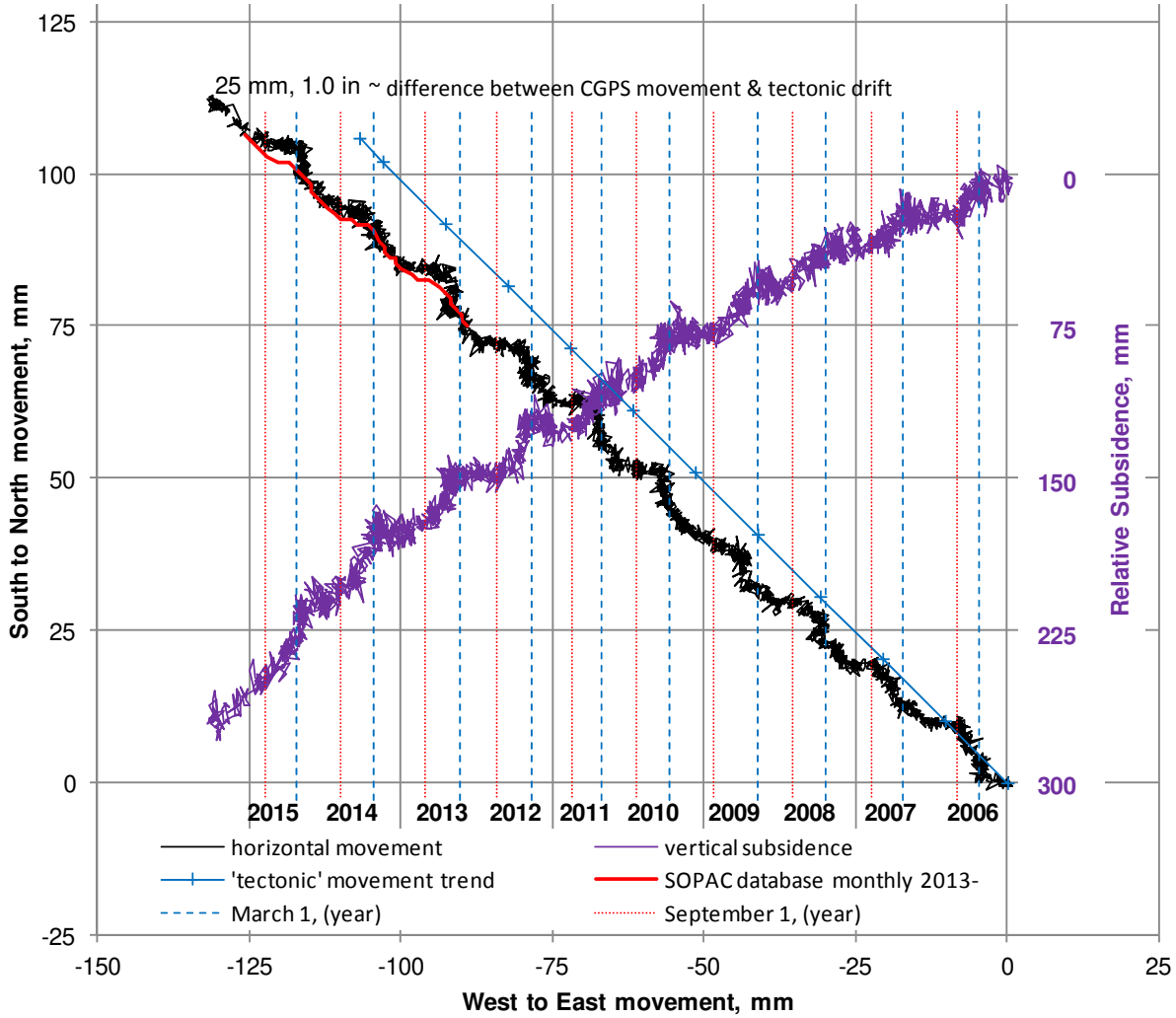
25 mm, 1.0 in ~ difference between CGPS movement & tectonic drift
South to North movement, mm
West to East movement, mm
Relative Subsidence, mm
2015
2014
2013
2012
2011
2010
2009
2008
2007
2006
horizontal movement
vertical subsidence
'tectonic' movement trend
SOPAC database monthly 2013-
March 1, (year)
September 1, (year)

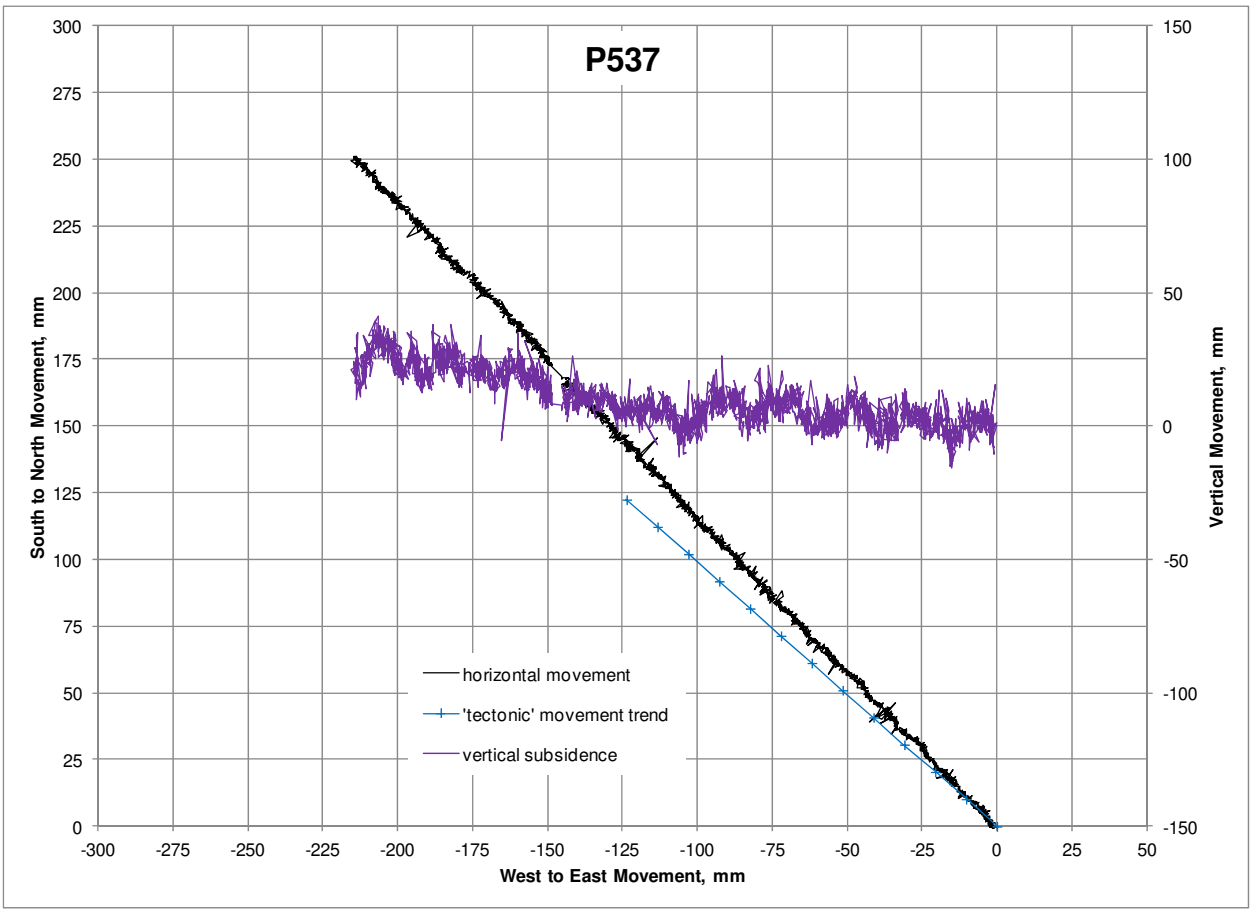
P537
South to North Movement, mm
Vertical Movement, mm
West to East Movement, mm
horizontal movement
'tectonic' movement trend
vertical subsidence
300
275
250
225
200
175
150
125
100
75
50
25
0
150
100
50
0
-50
-100
-150
-300
-275
-250
-225
-200
-175
-150
-125
-100
-75
-50
-25
0
25
50

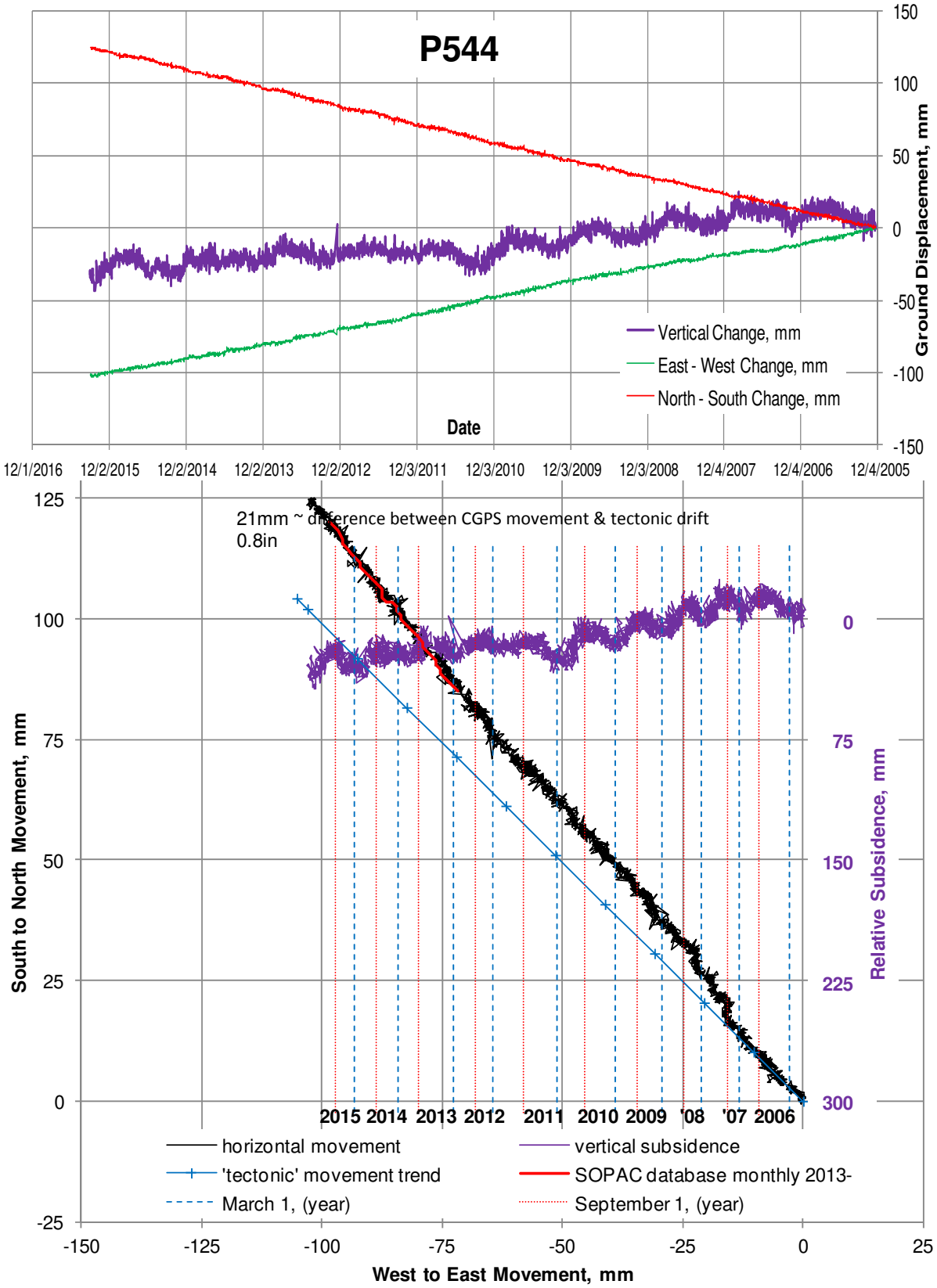
P544
Ground Displacement, mm
Date
Vertical Change, mm
East - West Change, mm
North - South Change, mm
21mm ~ difference between CGPS movement & tectonic drift
0.8in
South to North Movement, mm
West to East Movement, mm
Relative Subsidence, mm
2015 2014 2013 2012 2011 2010 2009 '08 '07 2006
horizontal movement
vertical subsidence
'tectonic' movement trend
SOPAC database monthly 2013-
March 1, (year)
September 1, (year)

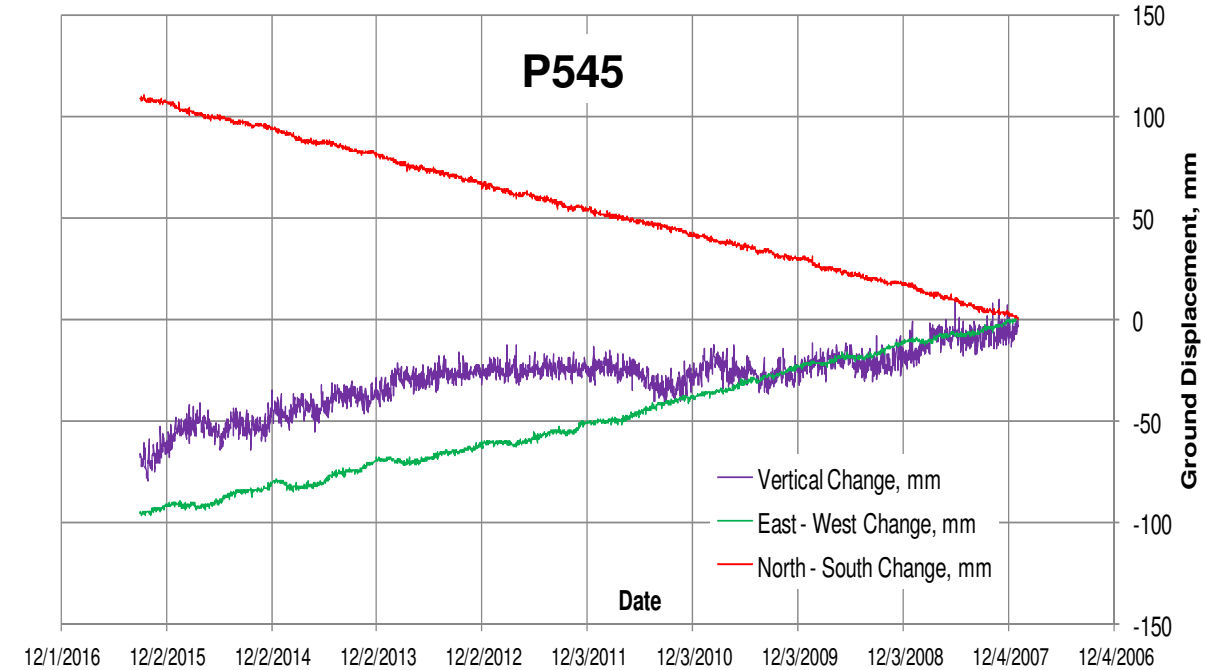
P545
150
100
50
0
-50
-100
-150
Ground Displacement, mm
Vertical Change, mm
East - West Change, mm
North - South Change, mm
Date
12/1/2016
12/2/2015
12/2/2014
12/2/2013
12/2/2012
12/3/2011
12/3/2010
12/3/2009
12/3/2008
12/4/2007
12/4/2006

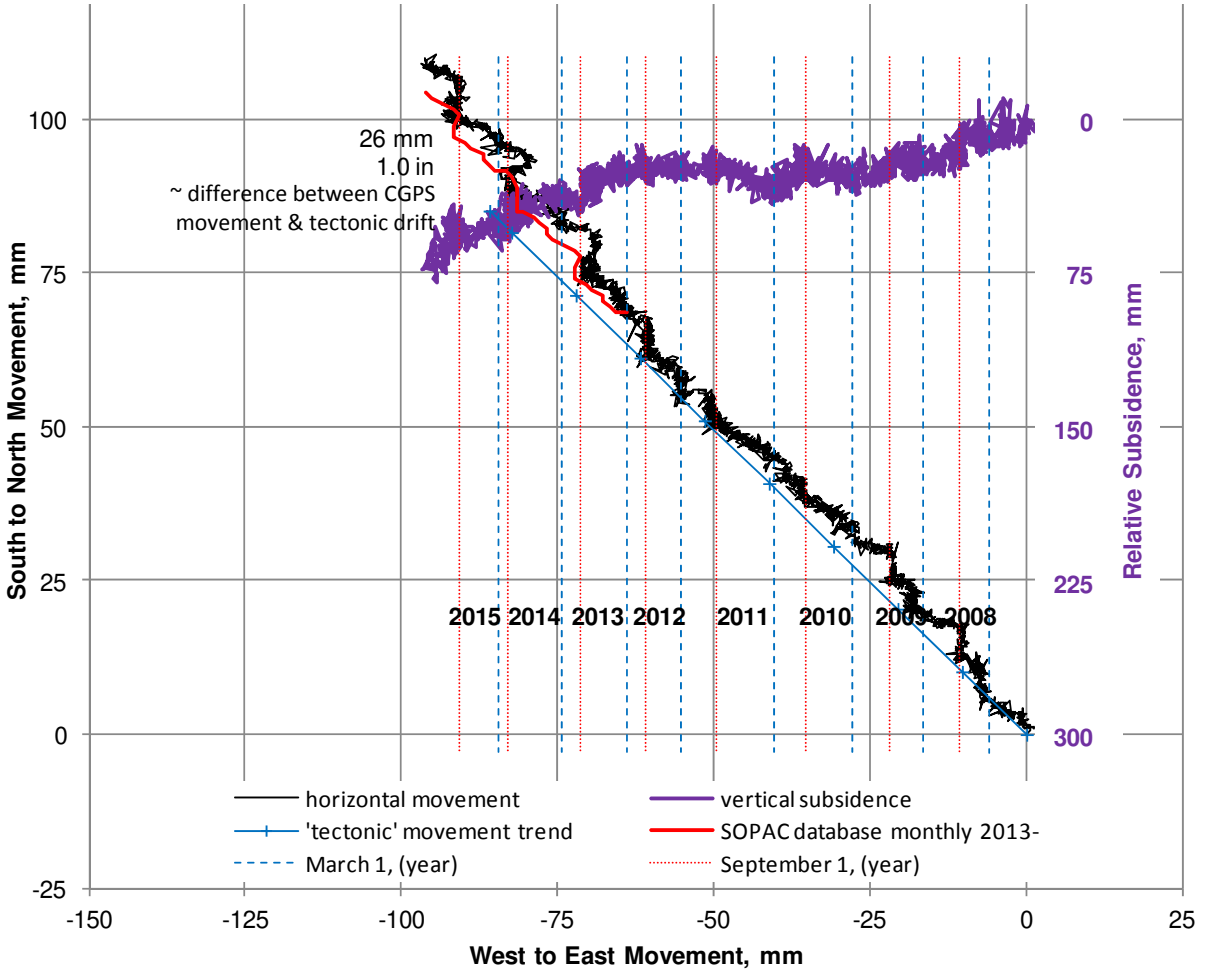
26 mm
1.0 in
~ difference between CGPS movement & tectonic drift
2015
2014
2013
2012
2011
2010
2009
2008
South to North Movement, mm
Relative Subsidence, mm
West to East Movement, mm
horizontal movement
'tectonic' movement trend
March 1, (year)
vertical subsidence
SOPAC database monthly 2013-
September 1, (year)

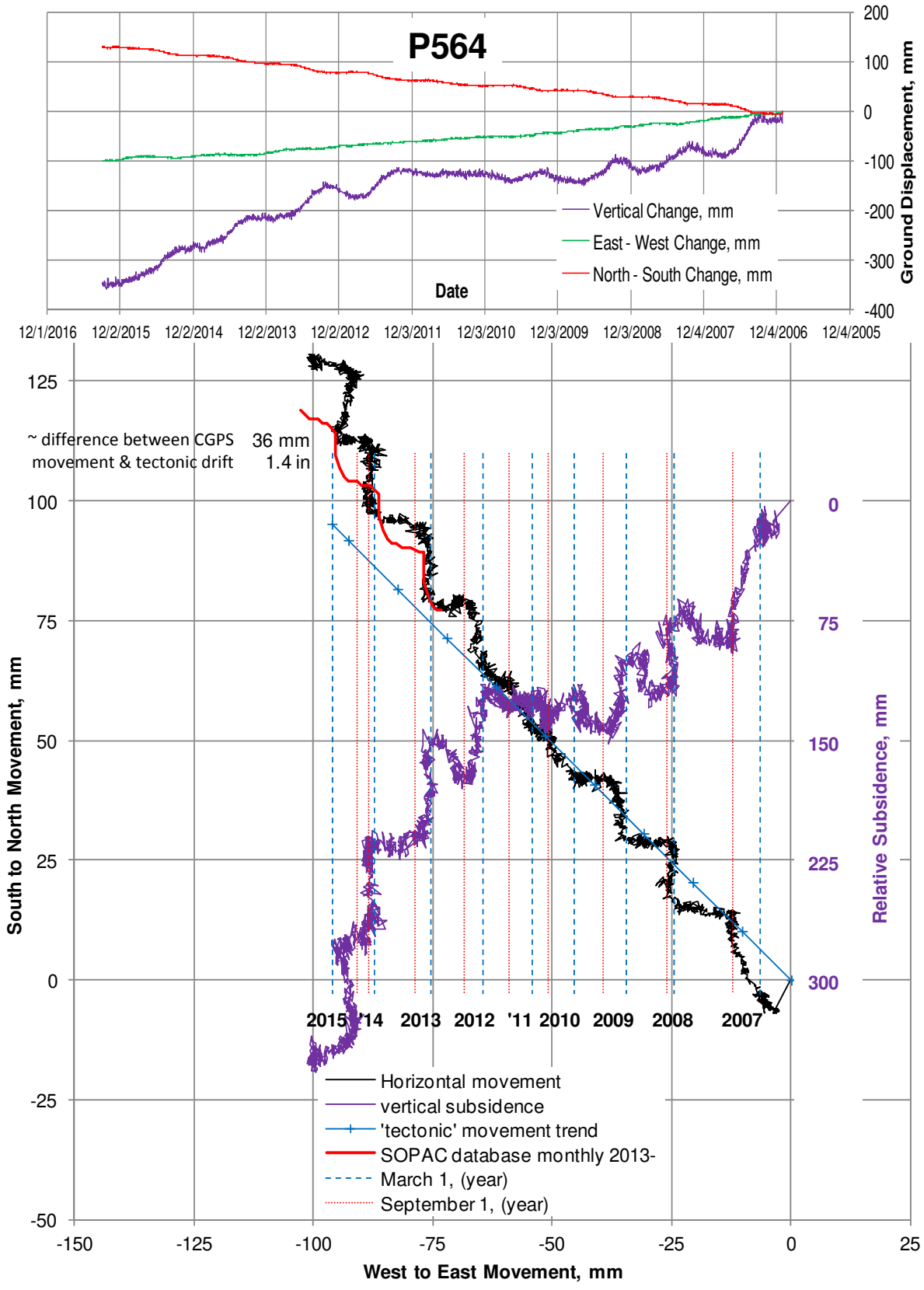
P564
Vertical Change, mm
East - West Change, mm
North - South Change, mm
Date
Ground Displacement, mm
200
100
0
-100
-200
-300
-400
12/1/2016
12/2/2015
12/2/2014
12/2/2013
12/2/2012
12/3/2011
12/3/2010
12/3/2009
12/3/2008
12/4/2007
12/4/2006
12/4/2005
~ difference between CGPS movement & tectonic drift
36 mm
1.4 in
South to North Movement, mm
Relative Subsidence, mm
West to East Movement, mm
2015
'14
2013
2012
'11
2010
2009
2008
2007
Horizontal movement
vertical subsidence
'tectonic' movement trend
SOPAC database monthly 2013-
March 1, (year)
September 1, (year)

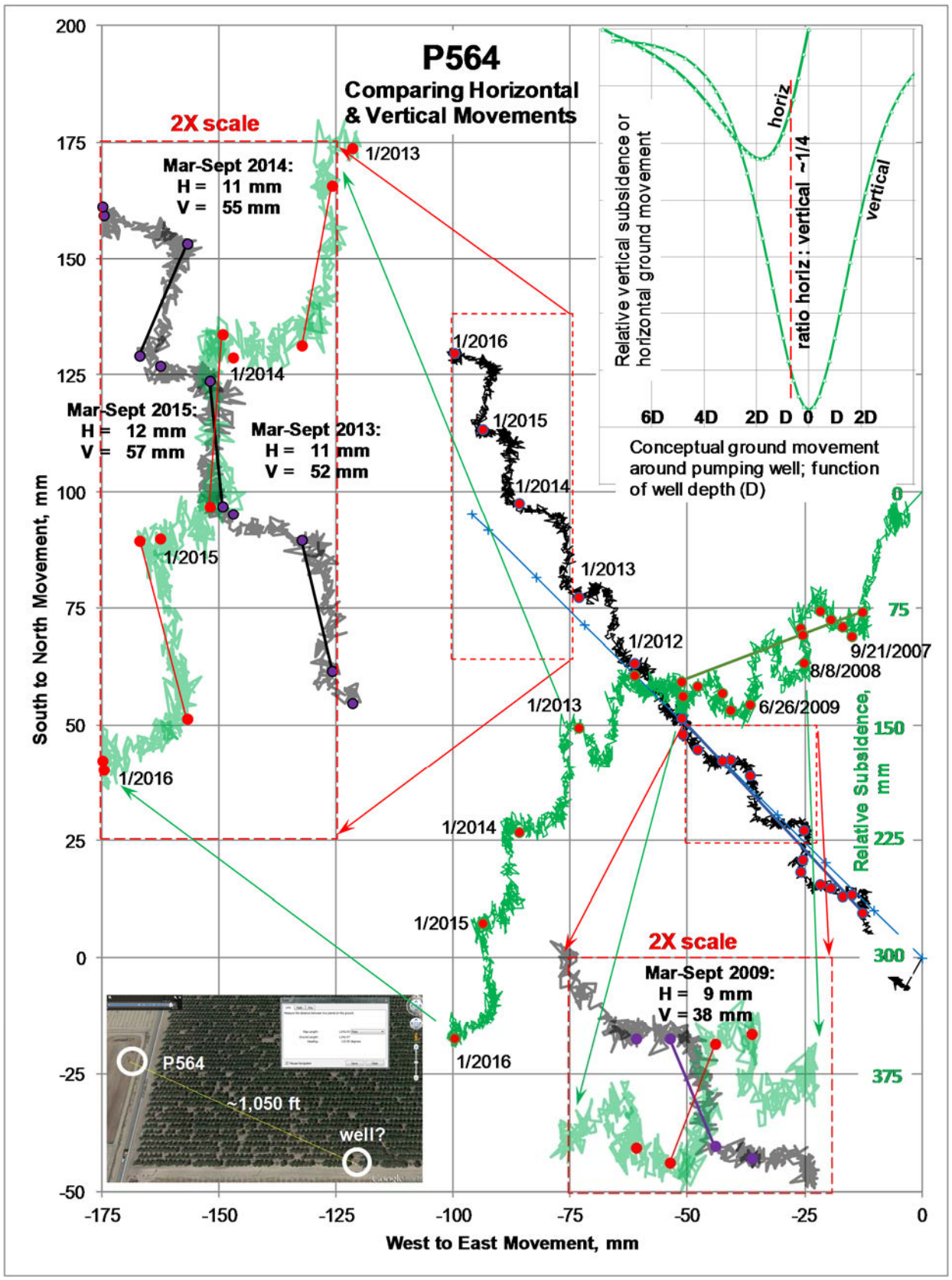
P564
Comparing Horizontal & Vertical Movements
2X scale
Mar-Sept 2014:
H = 11 mm
V = 55 mm
Mar-Sept 2015:
H = 12 mm
V = 57 mm
Mar-Sept 2013:
H = 11 mm
V = 52 mm
1/2013
1/2014
1/2015
1/2016
1/2012
9/21/2007
8/8/2008
6/26/2009
2X scale
Mar-Sept 2009:
H = 9 mm
V = 38 mm
Relative vertical subsidence or horizontal ground movement
horiz
vertical
ratio horiz : vertical ~1/4
6D 4D 2D D 0 D 2D
Conceptual ground movement around pumping well; function of well depth (D)
P564
~1,050 ft
well?
South to North Movement, mm
West to East Movement, mm
Relative Subsidence, mm
200
175
150
125
100
75
50
25
0
-25
-50
-175
-150
-125
-100
-75
-50
-25
0
75
150
225
300
375

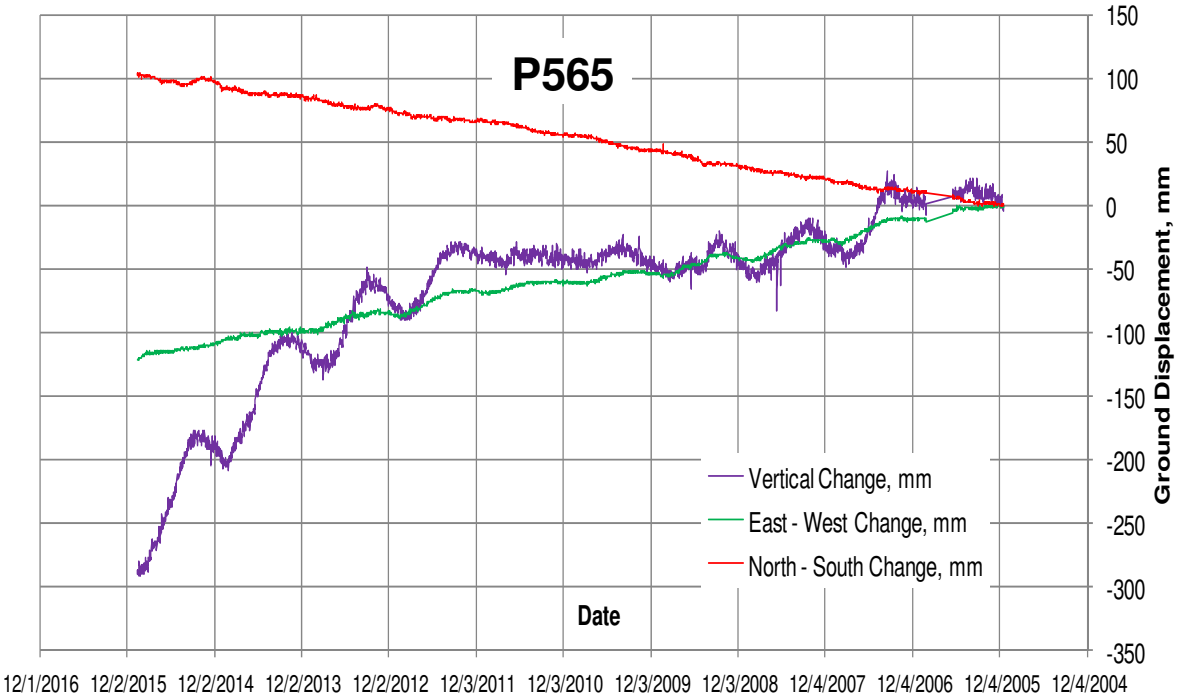
P565
Vertical Change, mm
East - West Change, mm
North - South Change, mm
Date
Ground Displacement, mm
150
100
50
0
-50
-100
-150
-200
-250
-300
-350
12/1/2016 12/2/2015 12/2/2014 12/2/2013 12/2/2012 12/3/2011 12/3/2010 12/3/2009 12/3/2008 12/4/2007 12/4/2006 12/4/2005 12/4/2004

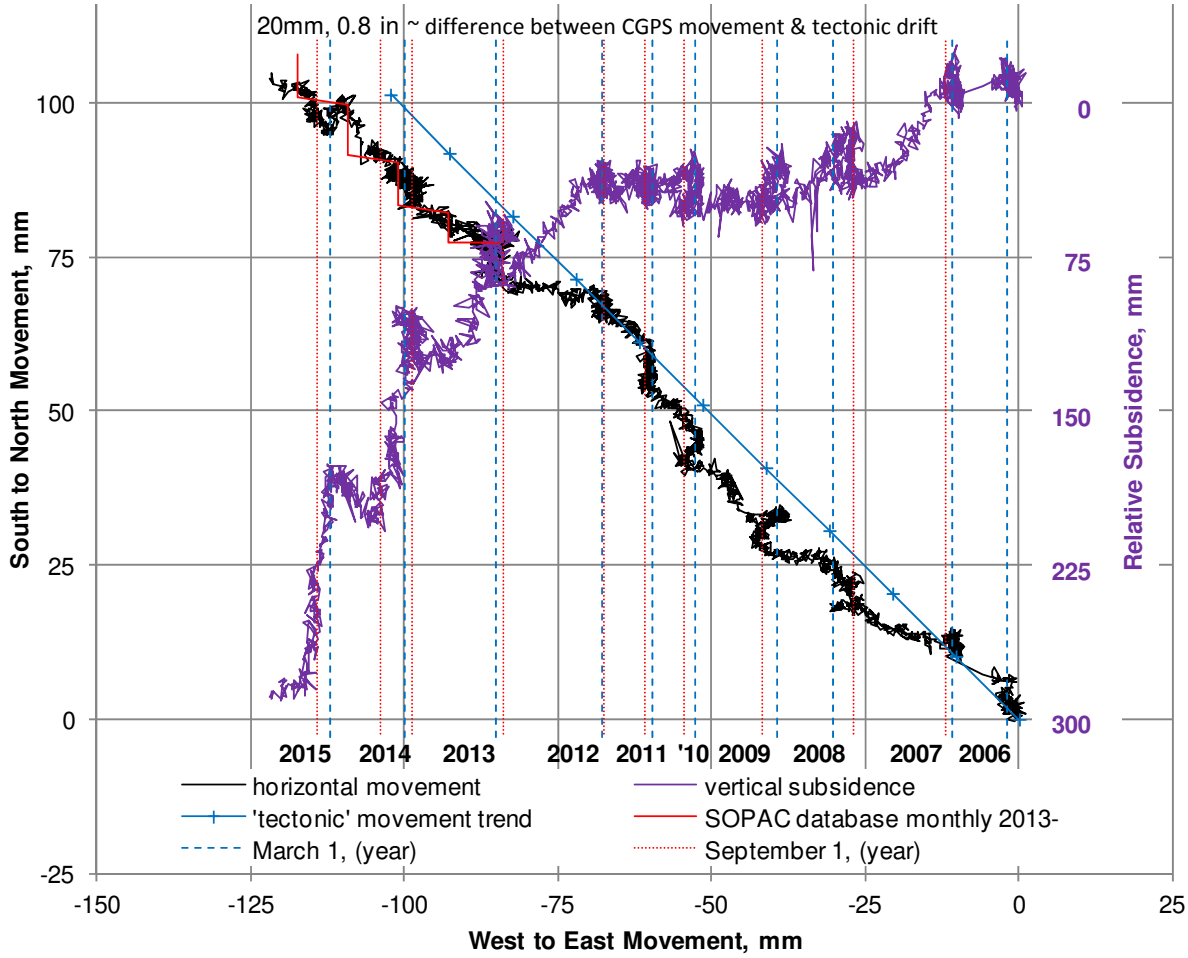
20mm, 0.8 in ~ difference between CGPS movement & tectonic drift
South to North Movement, mm
West to East Movement, mm
Relative Subsidence, mm
100
75
50
25
0
-25
-150
-125
-100
-75
-50
-25
0
25
0
75
150
225
300
2015 2014 2013 2012 2011 '10 2009 2008 2007 2006
horizontal movement
'tectonic' movement trend
March 1, (year)
vertical subsidence
SOPAC database monthly 2013-
September 1, (year)

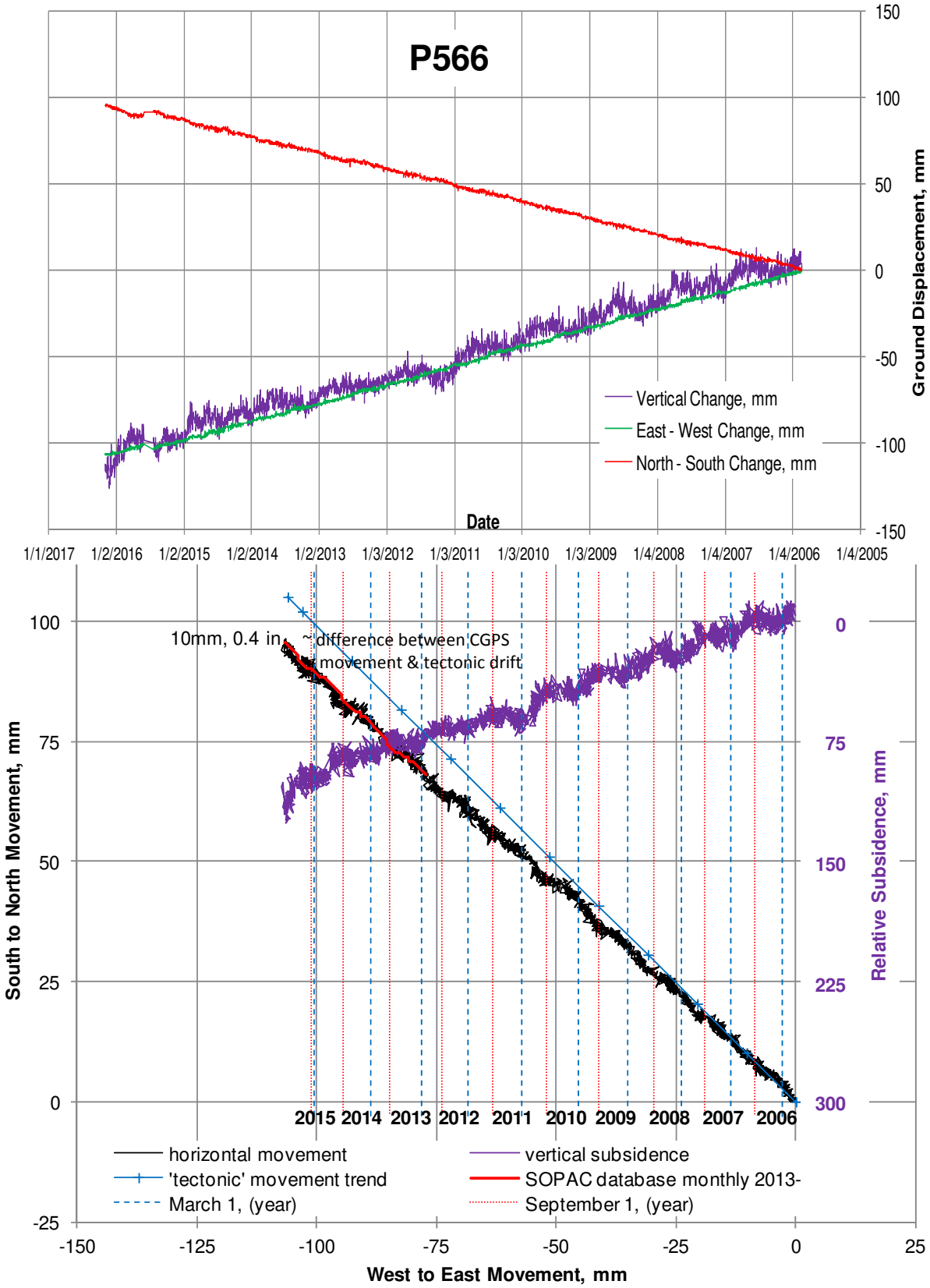
P566
Ground Displacement, mm
Date
Vertical Change, mm
East - West Change, mm
North - South Change, mm
10mm, 0.4 in ~difference between CGPS movement & tectonic drift
South to North Movement, mm
West to East Movement, mm
Relative Subsidence, mm
2015 2014 2013 2012 2011 2010 2009 2008 2007 2006
horizontal movement
'tectonic' movement trend
March 1, (year)
vertical subsidence
SOPAC database monthly 2013-
September 1, (year)

APPENDIX B

Draft HSR Alignment Conceptual Initial Subsidence Instrumentation and Monitoring Plan

APPENDIX B

DRAFT HSR ALIGNMENT CONCEPTUAL INITIAL SUBSIDENCE INSTRUMENTATION AND MONITORING PLAN

Ground Subsidence Study
California High-Speed Rail Project
San Joaquin and Antelope Valleys, California

Submitted to:

California High Speed Rail Authority

Prepared by:
Amec Foster Wheeler
Environment & Infrastructure, Inc.

TABLE OF CONTENTS

LIST OF FIGURES
(NOT DEVELOPED IN THIS CONCEPTUAL PLAN)

LIST OF APPENDICES
(NOT DEVELOPED IN THIS CONCEPTUAL PLAN)

1.0 INTRODUCTION

This version of this Subsidence Instrumentation and Monitoring Plan (the Plan) is presented as a conceptual plan. A final plan will be developed after discussions with the High Speed Rail (HSR) Authority regarding what should be included in the final plan.

The Subsidence Instrumentation and Monitoring Plan (the Plan) presented herein includes discussions of the design, installation and operation of an initial land subsidence and ground deformation monitoring and detection system at the California High-Speed Rail System (System). This plan was developed by Amec Foster Wheeler Environment & Infrastructure, Inc. (Amec Foster Wheeler), for the California High-Speed Rail Authority (Authority). The purpose of the monitoring system is to provide a means of reducing the risk of potential adverse impacts related to the undetected development of subsidence-induced ground distress at the HSR alignment. This risk reduction will be realized by quantifying the rate and distribution of ground deformation in the vicinity of the System, coupled with the ability to detect ground rupture along the HSR alignment.

The various methods of monitoring include conventional instrumented in-ground systems and methods, as well as advanced techniques. The conventional systems include the use of Global Positioning System (GPS) survey, ground reconnaissance and photo-geological analysis. Advanced techniques include the processing and interpretation of differential interferograms of repeat-pass, satellite-based synthetic aperture radar (InSAR), Uninhabited Aerial Vehicle-Based Synthetic Aperture Radar (UAVSAR), and other remote-acquisition data, and advanced geotechnical instrumentation as needed.

This Conceptual Plan contains detailed discussions regarding potential location and design of the initial subsidence monitoring instrumentation, and procedural components of the monitoring system including methods of measurement, monitoring frequency and levels of precision.

2.0 PROJECT DESCRIPTION

The Authority is responsible for the planning, design, construction and operation of the first high-speed rail system in the nation. The System will connect the mega-regions of the State of California, contribute to economic development and a cleaner environment, create jobs and preserve agricultural and protected lands. Phase 1 service will connect San Francisco to the Los Angeles basin in less than three hours at speeds of over 200 miles per hour. The System will eventually extend to Sacramento and San Diego, totaling 800 miles with up to 24 stations. In addition, the Authority is working with regional partners to implement a statewide rail modernization plan that will invest billions of dollars in local and regional rail lines to meet the State's 21st century transportation needs.

Due to historical land subsidence, the Authority is in the process of developing a program wide approach to address the impacts of land subsidence on high-speed rail infrastructure in the San Joaquin and Antelope Valleys. This conceptual preliminary monitoring and instrumentation plan proposes instrumentation and methodologies for monitoring the effect of land subsidence on the System.

The immediate reason for monitoring subsidence and associated horizontal movement will be to better understand the causes, rates, magnitudes, and areal distribution of past and ongoing subsidence, in order to better forecast future subsidence and how this may impact the HSR. An additional purpose of the monitoring system is to provide a means of reducing the risk of potential adverse impacts related to hazard associated with changes in floodplains, the undetected development of an earth fissure, compaction fault, or other discrete subsidence-related feature in the vicinity of the HSR. This risk reduction will be realized by quantifying the rate and distribution of ground deformation in the vicinity of the system, coupled with the ability to detect ground rupture along the alignment.

In addition, future monitoring will inform operators of any potential developing conditions where changes in track geometry or subsurface conditions may call for increased monitoring and/or mitigation measures.

Monitoring will include evaluations of pre-construction (including past records such as survey data archived satellite InSAR imagery, etc.), during-construction, and post-construction and operation phases.

3.0 MONITORING SYSTEM DESIGN

In light of the current understanding of subsidence in the vicinity of the HSR system alignment (the Alignment), monitoring will provide the means to measure ground displacements and strains to anticipate and assess the potential for detrimental geometrical changes to the Alignment and compaction fault or earth fissure development. Employing multiple methods, the monitoring strategy will utilize an integrated approach, including both regional and local measurements. The entire length of the Alignment will be instrumented, as well as utilizing measurements from other relevant locations in the Central Valley, to monitor land subsidence along the Alignment and to detect possible future ground rupture along the Alignment.

Monitoring methods, instrument locations and design specifications for initial subsidence monitoring are detailed in the following sections. The monitoring system should periodically be evaluated for effectiveness and, as appropriate, could be augmented with additional methods or coverage in the future. Advanced instrumentation and monitoring focused on geotechnical performance of HSR structures will be integrated into the process of subsidence monitoring.

3.1 Instrumentation Coverage

GPS/Optical monuments located at approximate 1,000–foot to ¼ mile intervals along the Alignment will form the framework of the initial monitoring system. The monument network is suggested to be divided into six (6) mile Monitoring Zones (MZ) to facilitate local adjustments, calculations, and possible variations in monitoring needs along the Alignment. For calculation purposes, one mile of each zone will overlap into the adjacent zone so that monitoring results at zone ends will be smooth and not abrupt. Existing continuous GPS (CGPS) stations scattered through the Central Valley in the general vicinity of the Alignment will provide subsidence data beyond the Alignment. Currently, fifteen (15) such stations with accessible historic ground coordinate data have been reviewed; usable historic data from these monuments ranges from

2013 to the present to as far as 2005 to the present. Availability of these CGPS stations may change in the future.

An additional floodplain Monitoring Zone (FMZ) will address potential differential subsidence impact on potential flooding conditions along the Alignment. The lowest elevation portion of the alignment appears to be in the vicinity of the Tule River around the eastern edge of the former Tulare Lake. If subsidence continues at faster rates near the Alignment compared to downstream portions of the Tule River in the former lakebed, then ground surface grades available to transport floodwaters to the west may become reduced, or in a worst case, reverse back towards the Alignment vicinity. A series of existing benchmarks in the Tule River vicinity west of the Alignment will be selected for elevation monitoring. These existing benchmarks, at spacing of about 1 mile, will be monitored to verify that sufficient downstream grade continues to be available to pass floodwaters to the west of the alignment. If appropriate, feasible, and not already present, protection should be provided for these monuments.

Other instrumentation that may be incorporated into the monitoring system on an as-needed basis will be discussed in later sections.

3.1.1 Continuous GPS (CGPS) Stations

CGPS stations provide real-time monitoring capability of specific points on the ground for the duration of the project. It is recommended that a CGPS station under the administrative control of the Authority be established in each MZ for purposes of HSR monitoring. Cooperation and coordination with other agencies on sharing CGPS sites may be feasible and may have benefits. Station location, and the purpose of station location, may vary for each CGPS station. For MZs with relatively little subsidence, a CGPS station might be located to monitor regional tectonic drift. For MZs with significant subsidence, a CGPS station might be located at a critical subsidence point to provide continuous data coverage at that critical location. A CGPS station should be co-located with real-time water level and/or compaction extensometer monitoring, if such real-time monitoring is performed. Final CGPS station locations may be determined after completion and evaluation of the project Baseline monitoring. Relevant existing CGPS stations will be incorporated into the subsidence monitoring system; these stations may or may not be available in the future, depending on the purposes for which they are in operation.

3.1.2 Static GPS Survey

Static GPS survey of the monument network will be performed to provide basic horizontal and vertical displacement data on a scheduled basis. Relative displacement between adjacent monuments using static GPS is the foundation of horizontal ground tension monitoring which will identify zones of potential compaction faulting or earth fissure development. Static GPS provides monitoring of relative horizontal ground displacement perpendicular to the Alignment that may impact HSR operations. Cooperation and coordination with other agencies on shared static GPS surveys may be feasible and may have benefits.

3.1.3 Optical Survey

Optical survey of additional monuments and benchmarks will provide high precision vertical monitoring over shorter distances between or in the near vicinity of the GPS Monuments. Such benchmarks may be installed on an as-needed basis for specific local subsidence features identified through monitoring, or may be part of the construction control benchmark system.

3.1.4 Other Instrumentation

Other instrumentation may include water levels at wells or piezometers for groundwater monitoring, and, if available, compaction extensometers or other displacement instrumentation. A CGPS station should be co-located with any compaction extensometer installation.

3.2 Monitoring Modes

The ground deformation monitoring program for the System is comprised of two basic data modes. The first of these data modes includes two remote techniques: InSAR (and/or UAVSAR) and aerial photography/imagery. The second mode includes terrestrial means of collecting relevant data including direct measurements of elevation and/or horizontal position, ground reconnaissance, collection of site-specific groundwater levels and review of regional groundwater levels. As monitoring progresses, specific situations requiring additional and different measuring methods and technologies may occur. Appropriate monitoring strategies and methods will be applied for such specific situations. Attributes and constraints of the basic initial data collection methods are discussed below.

3.2.1 Monitoring by Survey

The use of survey techniques provides a means of forming a network for the various instrumentation systems. This approach is an effective method of monitoring deformation along the HSR alignment. As shown on **(to be developed)**, a network of **(insert number)** proposed GPS/Optical monuments will be installed along the alignment. The GPS/Optical monuments will be constructed in accordance with Type B Survey Benchmark Deep Rod (Drawing No. DD-SV-101) or equivalent. GPS/Optical monuments located along the System alignment will be placed at a spacing of approximately 1/4 mile at alternating right and left edges of the alignment right-of-way. Due to the gradual and small relative movements to be measured, verification of accuracy is a critical aspect of this portion of the monitoring program. Registered land surveyors with appropriate experience in the complex local tectonic conditions, as well as subsidence conditions, should be contracted to perform data collection via static GPS observations and when specified by conventional or digital leveling techniques, process and evaluate data for quality assurance purposes, and provide reporting of the results.

Horizontal and Vertical Positions by Static GPS Survey – Horizontal and vertical positions by survey of the proposed alignment GPS/Optical monuments, other specified existing benchmarks, benchmarks on bedrock (or off-site reference points such as CGPS sites) should be performed using appropriate GPS survey equipment and techniques. Results of the GPS survey should be reported in northing, easting and elevation. The survey reference frame is to be determined. Maximum care in setup on monuments and measuring height of the

instruments, including measuring in both feet and meters, should be observed. Accuracy of plus or minus 0.016 foot (5 mm) horizontal and plus or minus 0.033 foot (10 mm) vertical should be achieved. Achieving such accuracy using GPS may require that each point, including bedrock or off-site reference points, be occupied for 0.5 to 4 hours with a minimum of 5 visible satellites. The northing and easting results will be used to monitor horizontal movement of the GPS/Optical monuments at the site. National Geodetic Guidelines (NGS-58) should be followed to attempt to achieve a vertical accuracy of +/- 2 cm (local network); see

https://www.ngs.noaa.gov/PUBS_LIB/NGS-58.html.

Vertical Position by Digital/Optical Leveling – Relational elevation differences between brass caps or monitoring points and adjacent or nearby GPS/Optical monuments should be determined through the use of differential digital level loops, or conventional level techniques. These measurements should incorporate the closest GPS/Optical monuments that are tied to bedrock (or off-site reference points such as CGPS sites) elevations using GPS or conventional optical methods for each survey event. Accuracy for relative vertical elevations obtained by this method is primarily controlled by the amount necessary for loop closure. The expected error of elevation for each point measured along the loop is equal to the loop closure error divided by the number of points. Elevations measured by leveling should be required to meet an accuracy of at least 0.01 foot.

3.2.2 Satellite-based InSAR

InSAR has proven to be a valuable tool in detecting differential subsidence due to groundwater withdrawal within the System study area. Interferometry has the capability to detect and quantify minute changes in terrain elevation by comparing phase variances of satellite-based, side-looking radar data between satellite orbits of a similar trajectory. InSAR data for this area was initially processed by the Jet Propulsion Laboratory for the California Department of Water Resources (DWR), and was then made available to the Authority and Amec Foster Wheeler. The continued use of InSAR is recommended, since it provides a regional means of delineating subsidence behavior. Two principal methods of InSAR processing are currently available; classical interferometry and persistent scatter. Each has advantages and limitations for subsidence monitoring. As new InSAR technologies become available, they should be considered for use in future monitoring. The following are currently relevant guidelines for acquiring and analyzing classical InSAR data for this project.

As made available by an agency or vendor, all InSAR products produced for ground deformation monitoring at the FRS should first be produced in a GeoTIFF format, accompanied by a metadata text file describing in detail the various parameters and source information for the image. The detailed metadata format should initially be structured considering the Federal Geographic Data Committee (FGDC) standards for geospatial metadata. Once ISO/Technical Committee 211 prepares Remote Sensing Extensions for ISO metadata standard ISO 19115, the metadata format should be adjusted to conform with the standard. For differential interferometric products, the following information should be documented, at a minimum:

- General product description;
- Status (preliminary, draft, final);

- Date of submission;
- Spatial domain;
- Spatial reference data;
- Description of software used to process data;
- Source of SAR data (identify satellite);
- Identity of processor, including contact, phone and address;
- Data acquisition times;
- Duration, in both months and days;
- Dimension of full fringe of interferometric display;
- Pixel size;
- Trajectory of satellite acquisitions, including directions, incident angles and ascension/dissension mode;
- Quality control information, including comparison with independent data (primarily CGPS or static GPS survey), and anticipated error; and
- Description of post-processing actions such as smoothing, unwrapping, stacking, etc.

Subsequent to an analysis of preliminary detection imagery, xyz files of the unwrapped differential interferograms should be obtained. The most convenient and readily usable format for this information appears to be ESRI grid. Each SAR image and differential interferogram should be formatted accordingly and included in the deliverable, with both xyz files in ESRI grids and companion GeoTIFF image files.

Regions of decorrelation in processed differential interferograms should be presented in both masked and unmasked formats. At present, a full-fringe parameter equal to ½ of the C-band, L-band or X-band wavelength and a color spectrum of blue-green-yellow-orange-red are most desirable for GeoTIFF differential interferogram images.

A signal track (z-dimension) accuracy as established by current best-practice is acceptable for ground subsidence monitoring. The issue of resolution appears to be far more problematic, given past experience with rather coarse pixel dimensions and extensive smoothing of InSAR results, and interpolation in areas lacking coherent or correlated InSAR data. Subtle variations in the shape of ground deformation lend considerable insight regarding the influence of local geologic conditions on the distribution of resultant horizontal strains. In turn, this aids the investigator in predicting the location and timing of potential future ground rupture.

InSAR data can be analyzed by direct observation of interferograms and cross-sectional presentation of vertical elevation changes. These analyses can be utilized in a variety of ways, such as to support lineament analysis and reconnaissance, to compare with survey data and for use as a calibration tool for subsidence modeling. InSAR data analysis is particularly useful for assessing changes in the locations and rates of regional ground deformation.

3.2.3 UAVSAR

JPL currently operates a UAVSAR program that is providing repeat interferometry for subsidence monitoring of the California Aqueduct for DWR. This program is demonstrating effectiveness for monitoring subsidence along linear infrastructure in the California Central Valley. It has the potential to provide much better spatial and measurement resolution than satellite-based InSAR and it therefore can offer a viable and potentially valuable supplement to satellite interferometry, as long as satellite information is available for comparison. However, it would require contracting with JPL to perform a series of location-specific data-gathering flights and data processing to cover an area and a time period of interest.

3.2.4 Aerial Imagery

High resolution rectified color aerial imagery for the region encompassing the HSR Alignment should be obtained and analyzed at least once every three years. The imagery should be acquired as color orthographic imagery with a minimum resolution of 0.33 feet. The aerial imagery should provide geodetic coordinates in feet in accordance with the appropriate project reference frame or frames **(currently not determined**). Ground truthing of the photo-geologic interpretations should be performed during ground reconnaissance.

3.2.5 Ground Reconnaissance

When applicable and appropriate, visual ground reconnaissance should be performed by an experienced person walking the site looking for cracks, potholes or other features which may indicate earth fissuring in the alignment area roads and ground, the HSR embankments and/or native soils. Areas where measurements indicate the potential development of large tensile strains should be visually inspected. Visual inspections should be performed as close in time as practicable to the other field measurements included in the monitoring program. Locations and descriptions of cracks, potholes and other erosional features should be documented with sketches, maps and photographs, as appropriate, and should include information regarding locations, dimensions and orientations. Features identified during reconnaissance should be marked with stakes, small flags or whiskers nailed into the ground and the locations of the features should be determined using a handheld GPS instrument. Ground reconnaissance also provides an opportunity to observe and assess the condition of survey monuments. Any disturbances by vandalism, traffic, flooding or other causes should be noted.

3.2.6 Groundwater Levels

Since the early 20th Century, groundwater in the study area has declined due to withdrawal of groundwater by wells. Local ground subsidence has resulted from the consolidation of dewatered sediments. Regional groundwater level changes may correlate to potential shifts in subsidence trends. Groundwater level information from System monitoring wells will be incorporated into the System database. Groundwater level data from regional-registered wells will be obtained from California DWR and used to develop hydrographs of groundwater levels. These data will be incorporated into the System database and included in the annual reporting.

4.0 MONITORING SYSTEM INSTRUMENTATION INSTALLATION

Instrumentation employed in the ground deformation monitoring program is comprised of an array of survey monuments. This set of instrumentation will provide the basic components necessary to monitor ground movement and to identify specific areas of elevated risk of ground fissure rupture. Existing and proposed locations of the monitoring system components are shown on **Figure 1 (not developed in this conceptual plan)**.

4.1 GPS/Optical Monuments

(Number to be determined) GPS/Optical monuments are proposed to be established. The GPS/Optical monuments will be placed at a spacing of approximately 1,250 feet along the System alignment as described in Section 3.2.3 of this Plan. The monuments will be placed near the right-of way edge and extend a minimum depth of 5 feet into stable and/or cemented soils in native ground. The anticipated embedment depths required to found the GPS/Optical monuments within stable soils are presented in **Table 1 (Example only)** below.

EXAMPLE ONLY

Table 1 – GPS/Optical Monument Locations

Monitoring Zone-Monument	Approximate Station-Left/Right	Estimated Final Depth Below Natural Grade (ft.)
A-GPS-01	100+00 L	15
A-GPS-02	1350+00 R	7
A-GPS-03	2600+00 L	7
A-GPS-04	3850+00 R	12
A-GPS-05	5100+00 L	15
A-GPS-06	6350+00 R	15
A-GPS-07	7600+00 L	18
A-GPS-08	8850+00 R	12
A-GPS-09… through …A-GPS-24	continue increasing Station distance by 1,250 feet per monument, alternate side	…
A-GPS-25	30100+00 R	15
A-GPS-26	31350+00 L	15
B-GPS-01	32600+00 R	15
B-GPS-02	33850+00 L	15
B-GPS-03	35100+00 R	15
B-GPS-04	36350+00 L	18

Each GPS/Optical monument will be provided with suitable protection. Steel fence posts or other protective barriers may be installed at each monument to prevent damage to the monument by vehicles and other equipment, depending upon the location of the monument. Installation of the GPS/Optical monuments will likely occur as soon as feasible as part of baseline monitoring. When completed, as-built details of the monuments will be presented in **Appendix A (not developed in this conceptual plan)** of this Plan. The monuments shall be installed in accordance with **Appendix B (not developed in this conceptual plan)** of this Plan.

4.2 Brass Caps Monuments

Brass cap construction control monuments are assumed to be part of the elevation control for project construction and acceptance criteria specified in the *Design Criteria* (Authority 2012) in Table 10-5 (Page 10-27). The brass caps (or other settlement monuments) should be protected during and following construction activities. The use of brass cap (or other) settlement monuments provides a cost effective means by which to observe developing data trends that could necessitate additional instrumentation in the future. As the monitoring is implemented into the future, the frequency that each of the brass cap monuments (or other elevation control monuments) is surveyed can be adjusted to most effectively meet monitoring needs.

Where existing off-project monuments are utilized for monitoring (such as for floodplain monitoring), it is assumed that additional monument protection will not be feasible. If it is feasible, appropriate, and not already present, protection should be provided for these monuments.

4.3 Monument Naming Convention

(A monument naming convention will be developed and implemented) Example of a naming convention: The following naming convention was selected for establishing reference names for existing and proposed instruments. For proposed GPS/Optical monuments, “A-GPS-##” was utilized. The Monitoring Zone (MZ) is identified by an alpha letter. For the conceptual example shown in Table 1, consecutive numbering was established for the GPS/Optical monuments resulting in the establishment of GPS-01 through GPS-25 for distance of approximately 6 miles at spacing of approximately 1,250 feet in a hypothetical MZ ‘A’. The first four monuments of hypothetical adjacent MZ ‘B’ are included in Table 1 to indicate the overlap at MZ boundaries for continuity in measurements. Locations of the monuments on the left or right of Alignment centerline is indicated by “L” or “R” following the Stationing.

See **Appendix C (not developed in this conceptual plan)** for a complete listing of monuments and associated stationing.

5.0 MONITORING SCHEDULES

As detailed in this **(initial conceptual)** plan, the ground movement portion of the monitoring strategy for the HSR alignment involves the application of remote sensing technologies, ground reconnaissance and determinations of vertical and horizontal position by static GPS survey and digital leveling survey. An initial schedule for data acquisition and periodic data analysis has been established for each component of the monitoring system. Other aspects of the monitoring, including project-specific CGPS stations and water level instrumentation, will be incorporated into the program as they become available. After each phase of construction to operation, and after every four years of data collection, these schedules should be reevaluated, with an opportunity to adjust, should the measured rate of deformation merit either an increase or decrease in the frequency of data acquisition. The following summarizes the recommended schedules.

5.1 Monitoring Baseline

A baseline monitoring period of one year with multiple survey measurement cycles to assess seasonal variations is recommended. Quarterly measurements will be made of all survey monuments in the monitoring system. Data analysis will be performed to identify areas with preliminary indications of possible problems. Identified possible problem areas will receive additional monitoring; monitoring will be designed and implemented based on identified conditions and concerns.

InSAR and/or other available remote sensing data will be collected, processed and analyzed. Analysis will be in the context of the results from the other baseline monitoring to refine understanding and utilization of this information for monitoring.

5.2 Monitoring During Construction and Post-Construction

Except in areas of previously identified possible problems, semi-annual survey measurement cycles to assess maximum (pumping season) and minimum (non-pumping season) conditions. Data analysis will be performed to identify areas with preliminary indications of possible problems. Identified problem areas will receive additional monitoring; monitoring will be designed and implemented based on identified conditions and concerns.

InSAR and/or other available remote sensing data will be collected, processed and analyzed. Analysis of data coincident in time with other monitoring will be in the context of the results from the other monitoring to continue to refine understanding and utilization of this information for monitoring. Analysis of data obtained between other monitoring events will be in a context of early warning of possible impending problems developing between other monitoring events.

Geotechnical monitoring performed during and following construction is not addressed in this conceptual initial subsidence instrumentation and monitoring plan. Extensive geotechnical instrumentation and monitoring is anticipated as part of the construction and post-construction program. Results of geotechnical monitoring will be essential to separating magnitudes of settlements from subsidence. Results of geotechnical monitoring must be made available and integrated into the subsidence monitoring program. Results of the subsidence monitoring program must be made available and integrated into the geotechnical monitoring program.

5.3 Monitoring During HSR Operation

The addition of train-mounted inertial-based dynamic monitoring systems and other instrumentation will provide detailed location-specific information to identify geometric problem areas on the alignment. The availability of this information will change the focus of subsidence and ground displacement monitoring; it is anticipated that the Monitoring Plan and it's implementation will be significantly revised.

Except in areas of previously identified possible problems, annual survey measurement cycles will continue, especially for horizontal displacement monitoring and floodplain monitoring. Data analysis will be performed to identify areas with indications of possible problems. Identified

problem areas will receive additional monitoring; monitoring will be designed and implemented based on identified conditions and concerns.

InSAR and/or other available remote sensing data will be collected, processed and analyzed. Analysis of data obtained between other monitoring events will be in a context of early warning of possible impending problems developing between other monitoring events.

EXAMPLE SCHEDULE

Activity	Data Acquisition	Data Analysis
InSAR Imagery	Initial – monthly to quarterly thereafter	Initial – monthly to quarterly thereafter
Groundwater Levels	Coordinate with InSAR acquisition	Coordinate with InSAR analysis
Aerial Imagery	Initial – annually thereafter	Initial – every three years thereafter
Ground Inspection	Initial – annually thereafter and after major storm events	Initial – annually thereafter and after major storm events
Static GPS Survey	**Baseline** – quarterly for 1 year. **Const & Post-Const** – semi-annual except as problems require increased frequency, **Operation** – annual except at problems where / when they develop **Floodplain Monitoring** annual, may be performed using RTK survey	Each survey cycle
Digital Leveling Survey	**Baseline** – quarterly for 1 year. **Const & Post-Const** – semi-annual except at problems, **Operation** – annual except at problems	Each survey cycle

6.0 DATA COLLECTION, ANALYSIS AND REPORTING

Data collected in the field shall be checked and compiled into the information database. Quality assurance checks should include verification that no transposition, calculation or accuracy errors occurred during data collection and compilation. The information shall then be analyzed and interpreted to verify conditions and trends concerning vertical elevation changes and horizontal strain accumulation. All data, along with reports from previous years, shall be reviewed and assessed as a whole. A report presenting, detailing and interpreting the data along with any potential recommendations should be prepared annually. The reporting procedures for each monitoring method are described in the following subsections.

6.1 Survey Points

All benchmarks and monuments surveyed as part of the HSR System Alignment Instrumentation and Monitoring Plan shall be surveyed by registered land surveyors with appropriate experience in the complex local tectonic conditions, as well as subsidence conditions. Benchmarks and monuments shall be surveyed per the recommended monitoring schedules listed above using the techniques discussed within this Plan.

6.1.1 Vertical Readings

The land surveyor shall provide a data report for the digital leveling survey used to obtain elevation readings for each monument. The report shall include a discussion of techniques used to collect, convert and check the readings. Reporting of vertical measurements shall state when the measurement readings were taken, who performed the readings, what equipment was used, the measurement error of the equipment and anticipated measurement error of the technique, what procedures were employed to ensure accurate readings, and any other information pertinent to data acquisition. The surveyor shall provide a summary data table that clearly lists the elevation in feet for each GPS/Optical monument, brass cap monument and benchmark surveyed. The elevation data shall be transferred to summary tables (see example in **Appendix C**). Also, figures that plot elevation and stationing for all the data should be created.

Note: an example Appendix C is not developed in this conceptual plan.

6.1.2 Horizontal Readings

The land surveyor shall provide a data report for the static GPS observations used to obtain northing and easting readings for each GPS/Optical monument. The report shall include a discussion of techniques used to collect, convert and check the readings. Reporting of GPS/Optical monument readings shall state when the measurement readings were taken, who performed the readings, what equipment was used, the measurement error of the equipment and anticipated measurement error of the technique, what procedures were employed to ensure for accurate readings, and any other information pertinent to the data acquisition. The surveyor shall provide a summary data table that clearly lists the northing and easting in feet for each GPS/Optical monument. The data shall be transferred to a summary table (see example in **Appendix D**). Also, figures with subplots for each monument showing spatial position, as easting versus northing, through time, for each sequential survey reading, shall be created.

Note: an example Appendix D is not developed in this conceptual plan.

6.1.3 Horizontal Distance and Strain Calculations between GPS/Optical Monuments

Strain accumulation can be determined by monitoring the change in horizontal distance between GPS/Optical monuments. In order to resolve areas of horizontal ground strain within the instrumented MZs on the Alignment, calculations of horizontal distances between GPS/Optical monuments shall be performed following each static GPS data acquisition. Horizontal distance calculations shall be performed between monuments within approximately

6,000 feet of each other. Additional calculations within the system are possible and should be considered as deemed appropriate.

Following each static GPS observation survey, the northing and easting coordinates **(according to the reference frame to be determined)**, which are provided by the land surveyor for each GPS/Optical monument, shall be used to calculate the distance between monuments. The distance between monuments is calculated in a spreadsheet following each data acquisition (see example spreadsheet in **Appendix E**). The horizontal distance in feet (x) between two monuments (with northing and easting values of N1, E1 and N2, E2) is calculated using trigonometric relationships as follows:

$$x = \sqrt{\left|N_1 - N_2\right|^2 + \left|E_1 - E_2\right|^2}$$

Both the northing and easting coordinates have an accuracy of plus or minus 0.016 feet (5 mm). Therefore, the maximum error for the distance between two points is 0.045 feet according to the following:

$$error_{\max} = \sqrt{\left|0.016ft. + 0.016ft.\right|^2 + \left|0.016ft. + 0.016ft.\right|^2}$$

However, a more representative value of error between two points may be 0.023 feet, calculated by the following:

$$error = \sqrt{\left|0.016ft.\right|^2 + \left|0.016ft.\right|^2}$$

Due to the low probability that the maximum error will frequently occur, plots of the reference line data should be shown with an error of 0.023 feet.

The spreadsheet shall also serve as a data summary table that lists the historical and current horizontal distance between GPS/Optical monuments, change in feet and percent strain accumulation since the last data collection, and comparisons to baseline readings presented as change in feet and percent strain accumulation.

Note: an example Appendix E is not developed in this conceptual plan.

6.2 InSAR

Newly acquired InSAR scenes shall be included in each annual report and historical data should be included in the initial monitoring report. The report shall include interpretations concerning locations and rates of subsidence. The subsidence data obtained from InSAR shall also be plotted against differential elevation data obtained through survey methods (survey results may also be used as QA/QC during InSAR processing). A comparison of these data sets shall be included as part of the structure evaluation, with the caveat that each data set has a different level of precision and accuracy. An analysis shall be made showing the deformation between the oldest available data and the newly acquired data. **(Example only)** Figures will illustrate the

location of Profile Lines used for this analysis. Example profiles of plots for Profile Lines # through ## are presented as **Figures F-#** through **F-## in Appendix F**, respectively.

Note: an example Appendix F is not developed in this conceptual plan.

6.3 High-Resolution Aerial Imagery

High-resolution, rectified, color aerial imagery shall be acquired and reviewed every three years. Photo-geologic interpretations of the acquired imagery shall be completed by experienced personnel following the investigative guidelines developed in concert with the Authority (for example, see AMEC 2011). All lineaments observed on the imagery shall be plotted and compared to previous interpretations regarding the presence of identified lineaments and the presence of fissuring in the study area.

6.4 Ground Reconnaissance

Reporting of ground inspection shall state when the site visit was conducted and who performed the reconnaissance. Any changes to existing earth fissure features or the inception of a new earth fissure shall be described in detail. Observable disturbances to survey monuments shall also be noted. Selected ground inspection photographs documenting identified features should be included in the report. When the ground reconnaissance includes ground truth activities of photo-geologic interpretations, investigative guidelines developed in concert with the Authority (for example, see AMEC 2011) shall be followed.

6.5 Regional Groundwater Levels

Regional groundwater levels from well data shall be included in the report. Hydrograph data for relevant California DWR-registered wells in the vicinity of the alignment shall be presented. The report shall describe changes in groundwater levels and the rates of change. **Appendix G** provides an example sheet displaying groundwater levels and the wells that should be included in the monitoring activities.

Note: an example Appendix G is not developed in this conceptual plan.

7.0 BASELINE ESTABLISHMENT OF DATA

All measurements from newly-installed instrumentation at the HSR alignment should be considered preliminary during the first year of data collection; an initial data set (or sets) is required to develop a baseline for future interpretations. Therefore, the first year of readings for surveying should be considered initial measurements. Where possible, initial readings from this monitoring program should be compared to any available historical readings to assess consistency. Once consistent readings have been achieved, future data may be used with greater confidence for displacement and ground strain interpretations. Frequencies of surveys may also be adjusted in the future to best economize the survey events while meeting project monitoring goals and objectives. For construction control brass cap monuments, the independently purposed record of survey measurements can continue.

8.0 ALERT LEVELS AND RESPONSE ACTIONS

(These are suggestions only; actual alert levels and responses remain to be determined.): Current subsidence rates and magnitudes are significant to very significant along portions of the Alignment. The potential for settlement independent of subsidence may influence the setting of alert levels. Table 10-5: Maximum Residual Settlement Limits (California High-Speed Train Project Design Criteria, Page 10-27 [Authority 2012]) limits uniform residual settlement of embankments, after track installation, to 1-1/8 inch (0.094 feet) for ballasted track. Annual subsidence rates exceed that uniform residual settlement limit over a significant portion of the CP2/3 Alignment. It will be necessary to separate out the components of subsidence versus settlement where subsidence is occurring. Once trains are in operation, on-board acceleration monitoring will better assess where areas of developing adverse accelerations that are approaching or exceeding 0.05g may be located. It should be noted that published allowable settlement criteria for Chinese HSR criteria limits allowable post-construction subsidence for embankments (Huang and others 2015) to 5 cm (2 inches), and per Wang and others (2015) for ballasted track, uniform pier settlement to 30 mm (1.2 inches) and adjacent pier differential settlement to 15 mm (0.6 inches).

Suggested initial Alert Levels include:

1) Differential elevation change between adjacent GPS monuments greater than 0.09 feet.

2) Indication of possible increasing tensile ground strain from visual inspection or InSAR signatures.

2) On-board acceleration exceeding 0.05g in horizontal or vertical direction.

3) On-board acceleration at a specific location increasing over time from initial level and approaching 0.05g. **(criteria to be developed during operation)**

It should be understood that, because of current subsidence rates and magnitudes, significant portions of the CP2/3 Alignment will be in at least an initial ‘Alert Level’ condition from the start of monitoring. That ‘Alert Level’ condition may remain in effect until after groundwater decline ceases.

Response actions will be a function of the magnitude of subsidence-induced ground movements on serviceability or other impacts on the Alignment. If there are no noticeable increases of measured on-train accelerations in the area of an alert level, no action may be necessary. Response may range from vigilance in that area to increase in monitoring density and frequency if changes in subsidence behavior are being noted. If measured on-train accelerations increase in an alert level area, but maximum allowable train accelerations are not exceeded, response might be to resolve subsidence-related track geometric issues within the context of increased monitoring density and frequency with maintenance. If subsidence-related movements results in exceedances of measured on-train maximum allowable accelerations, mitigation procedures to address Operability Performance Levels (OPL) similar to response to seismic fault movement may need to be implemented. Such response could include reduced train speeds at the subsidence feature, reduced train service to that area, to temporary closure for repairs.

9.0 REFERENCES

AMEC Earth & Environmental, Inc. (AMEC). 2011. Procedural Documents for Land Subsidence and Earth Fissure Appraisals. FCD2008C016 Work Assignment No. 13, May.

California High-Speed Train Project Design Criteria, Page 10-27, dated December 7, 2012.

Huang, L., Xiao, H., Yang, S., Han, Y. 2015. Effects of Groundwater Exploitation on Embankment for High-speed Railway Lines. The Open Civil Engineering Journal, 2015, Volume 9, 417-422.

Wang, X., Wu, L., Zhou, Y., Wang, Y. 2015. The Long-Term Settlement Deformation Automatic Monitoring System for the Chinese High-Speed Railway. Hindawi Publishing Company, Shock and Vibration, Volume 2015, Article ID 147972.

FIGURES

APPENDIX A

MONITORING SYSTEM INSTALLATION AS-BUILTS (TO BE COMPLETED ONCE INSTALLED)

(NOT DEVELOPED IN THIS CONCEPTUAL PLAN)

APPENDIX B

MONITORING SYSTEM INSTALLATION GUIDELINES

(Not developed in this conceptual plan)

APPENDIX C

EXAMPLE SURVEY DATA ENTRY TABLES AND SCOPE OF WORK

(Not developed in this conceptual plan)

APPENDIX D

EXAMPLE VERTICAL LEVELING SURVEY DATA TABLES AND PLOTS

(Not developed in this conceptual plan)

APPENDIX E

EXAMPLE HORIZONTAL MONUMENT MEASUREMENT NETWORK AND VERTICAL DISPLACEMENT

(Not developed in this conceptual plan)

APPENDIX F

EXAMPLE INSAR DATA PROFILE FIGURES AND PLOTS

(Not developed in this conceptual plan)

APPENDIX G

EXAMPLE HYDROGRAPHS OF SELECTED WELLS

(Not developed in this conceptual plan)

amec foster wheeler

APPENDIX C

RTK Survey Statement

APPENDIX C

RTK SURVEY STATEMENT

Ground Subsidence Study
California High-Speed Rail Project
San Joaquin Valley, California

CORCORAN SURVEY

SURVEY METHOD

This survey was performed using Real Time Kinematic (RTK) methods. GPS corrections were obtained for all survey data points utilizing Caltrans Real Time Network (CRTN) Stations CRCN (RTCM0011) and P298 (RTCM0003). National Geodetic Survey (NGS) monument KT 200 (PID AC6136) was held for elevation. Continuous collection RTK surveying was performed across the project area using a truck mounted GPS receiver. The data point collection interval was set at 50 foot along the paths that the truck was driven along roads within the project area. Survey data processing was performed using Trimble Business Center software. The CRTN generated elevations for each collected point were adjusted based on a mean elevation difference in the survey ties to KT 200.

DATUM

NAD 83 (2011) California State Plane Coordinate System Zone 4 (0404)

Geoid 09 NAVD88 Elevation

Survey was performed in August 2016.

BENCHMARK

NGS monument

Designation: KT 200

PID: AC3136

Found US Army Corps of Engineers brass disk set in concrete 1.3 feet southeast of a fiberglass witness post, 36.2 feet northwest of the centerline of highway 190, 46.0 feet southwest of the centerline of Success dam projected to the southeast.

NAVD88 Elevation = 699.6 feet

VERTICAL ACCURACY

The vertical accuracy for the survey is based on an approximation of the longest GPS vector for the project, 50 KM. Based on this length of baseline, the mathematical vertical accuracy is calculated to be +/- 7 centimeters or +/- 0.23 feet. The accuracy calculation is based on the manufacturer and NGS formula of 2 centimeters + 1 ppm. Due to the methodology and uncertainty of the vertical accuracy of the CRTN stations in this area, the actual accuracy of any single survey data point is estimated to be +/- 0.5 feet.

EL NIDO SURVEY

SURVEY METHOD

Survey was performed by RTK method utilizing GPS corrections from Caltrans RTN stations CHOW (RTCM0014), ALTH (RTCM0013), and P305 (RTCM0005). Continuous collection RTK surveying was performed across the project area using a truck mounted GPS receiver. The data point collection interval was set at 50 foot along the paths that the truck was driven along roads within the project area. Survey data processing was performed using Trimble Business Center software. Elevation checks were made to NGS monuments K 361 (PID HS2341), 1 JD 365 (PID AA4255), HPGN D CA 10 FP (PID AA4259) and v 1070 USBR (HS1999).

Survey was performed in December 2016.

DATUM

NAD 83 (2011) California State Plane Coordinate System Zone 3 (0403) (Grid Coordinates)
Geoid 09, NAVD88 Elevation

VERTICAL ACCURACY

The maximum vertical accuracy for the survey is based on an approximation of the longest Vector for the project (80 km). Based on this length of baseline the vertical accuracy was calculated to be +/- 10 cm or +/- 0.34' per manufacturer equipment capabilities only. Due to the methodology and uncertainty of the vertical accuracy of the CRTN stations in this area, the actual accuracy of any single survey data point is estimated to be +/- 0.5 feet.

POSO CREEK SURVEY

SURVEY METHOD

Survey was performed by RTK method utilizing GPS corrections from Caltrans RTN Station DLNO (RTCM0016). Continuous collection RTK surveying was performed across the project area using a truck mounted GPS receiver. The data point collection interval was set at 50 foot along the paths that the truck was driven along roads within the project area. Survey data processing was performed using Trimble Business Center software. Elevation checks were made to NGS Monuments K T 200 (PID AC6136). Additional elevation checks were made to High Speed Rail Monuments S254, S260, S267 and S277, all of which had been surveyed during the Corcoran area survey in August of 2016.

Survey was performed in December 2016.

DATUM

NAD 83 (2011) California State Plane Coordinate System Zone 5 (0405)(Grid Coordinates)
Geoid 09, NAVD88 Elevation

VERTICAL ACCURACY

The maximum vertical accuracy for the survey is based on an approximation of the longest vector for the project (63.5 km). Based on this length of baseline the vertical accuracy was calculated to be +/- 8.35 cm or +/- 0.27' per manufacturer equipment capabilities only. Due to the methodology and uncertainty of the vertical accuracy of the CRTN stations in this area, the actual accuracy of any single survey data point is estimated to be +/- 0.5 feet.

amec foster wheeler

APPENDIX D

El Nido Subsidence Bowl

APPENDIX D

EL NIDO SUBSIDENCE BOWL

California High Speed Rail Project
San Joaquin Valley, California
Final Report (Draft for Review)

TABLE OF CONTENTS

Page

TABLE OF CONTENTS
(Continued)

TABLES EMBEDDED WITHIN TEXT

FIGURES

LIST OF PLATES

APPENDIX D

EL NIDO SUBSIDENCE BOWL

California High Speed Rail Project
San Joaquin Valley, California
Final Report (Draft for Review)

1.0 INTRODUCTION

As a supplement to the main Ground Subsidence Study (GSS) report titled *Ground Subsidence Study, California High Speed Rail Project, Corcoran Subsidence Bowl, San Joaquin Valley, California*, this appendix presents a similar evaluation of the potential impacts of subsidence on future High-Speed Rail (HSR) infrastructure and train performance in the El Nido Subsidence Bowl (ENSB) area. The ENSB is centered just south of the High-Speed Rail (HSR) Alignment where it parallels Highway 152, and roughly midway between Interstate 5 and Highway 99, as seen on Plate D1-1. Although subsidence rates in the San Joaquin Valley (SJV) for the past 10 or more years have generally been fastest in the Corcoran Subsidence Bowl, subsidence in the ENSB has been nearly as fast. Observed subsidence as well as subsidence-induced changes to slope and curvature are shown on Plate D1-2, which show these values are noticeably less than for the Corcoran Subsidence Bowl. The discussions in the main GSS report are generally applicable to the ENSB area also, unless supplemented or otherwise stated herein.

2.0 SOURCES OF INFORMATION

Most sources of information are presented in the body of this report and are relevant to the ENSB also. The following summary is repeated here for its high relevance to the ENSB.

2.1 PERSONAL COMMUNICATION: JEANINE JONES AND GREG FARLEY OF THE CALIFORNIA DEPARTMENT OF WATER RESOURCES

Ms. Jeanine Jones indicated that DWR flood management personnel believe subsidence has been responsible for recent scour areas at the Avenue 21 bridge along the Eastside Bypass, which they are currently concerned about. Mr. Farley indicated this is an area where subsidence has resulted in loss of freeboard for the Eastside Bypass Canal, which means that floodwaters flow deeper and wider than originally designed (actually, this means that floodwaters could overtop the embankment if high flows occur). At the bridge, the abutment appears to constrict the flow, resulting in turbulence and consequent erosion of the levees just down steam from the bridge (see Figure D2-1).

Figure D2-1: Eastside Bypass Flood Flows at Avenue 21 Bridge

2.2 TOPOGRAPHIC AND SUBSIDENCE DATA

Most of the primary sources of topographic and subsidence data in the El Nido Area are described in the body of the main GSS report, including:

1. InSAR results provided by the Jet Propulsion Laboratory for May 2007 to December 2010, and May 2015 to August 2016.
2. The National Map (2016) for elevation data.

In addition:

3. Digital topographic data is available from by the California Department of Water Resources (DWR 2008) for the ENSB area.
4. The California Department of Transportation (Caltrans) has been performing an ongoing elevation survey of Highway 152.
5. We have conducted a Global Positioning System GPS) survey enhanced with Real Time Kinematic Satellite Navigation (RTK) in the vicinity of the ENSB.

3.0 MECHANISMS OF SUBSIDENCE

3.1 INTRODUCTION

In general, geology, hydrogeology, and mechanisms of subsidence in the ENSB area thought to be similar to those in the Corcoran area, and we anticipate there will be similar contractual considerations regarding the distinguishing of subsidence and settlement.

3.2 REVIEW OF LOCAL RELEVANT GEOLOGY AND HISTORIC LAND USE (MIKE)

Historic oil and gas well geophysical logs indicate (GSS Report Table 3-1) that the top of the Santa Margarita Formation (7 Ma) at the ENSB is at a depth of about 2,200 feet; this is much shallower than the depth to contemporaneous sediments in the Tulare Basin to the south. (This may be because, as Saleeby et al. (2012, 2013) posit, in Pliocene-Quaternary time, the eastern portion of the SJV north of the Tulare Basin and the central foothills of the Sierra Nevadas (as well as the Sierra Nevadas proper) have undergone anomalous tectonic uplift.) Scheirer and Magoon (2007) report that Pliocene and Quaternary formations in this area (younger than the Santa Margarita Formation) are unnamed and undifferentiated. The mid-Pleistocene Corcoran Clay has been mapped at typical depths of about 200 feet to 260 feet in this area. Historic oil and gas wells are cased to below the Corcoran Clay, but geophysical logs (Plate D3-1) indicate that fresh water aquifers are present at depths shallower than about 1,100 feet. A large suite of geophysical logs at Well API 03920102 (in the northwest corner of the ENSB) presented in the main GSS Report Plate 3-2 includes an anomalous high porosity at a depth of about 1,100 feet consistent with a discrete volcanic ash deposit. Izett and others (1988) report volcanic activity in the region at about 2.1 to 2.2 Ma, in the early Pleistocene; relative depths to the overlying Corcoran Clay and underlying Santa Maria Formation are consistent with the bottom of Pleistocene sediments correlating to the Tulare Formation to be at a depth of about 1,100 feet the ENSB area.

The confined fresh water aquifer system in the ENSB appears to extend from just below the Corcoran Clay (i.e., below about 250 feet) to a typical depth of about 1,100 feet. Geophysical log resistivities indicate that the aquifer system predominantly consists of fine-grained aquitards (less than 10 ohm-meters resistivity). Of eight evaluated electrical logs through the ENSB presented in Plate D3-1, only one log is indicated to be more than about 30% (32.3%) heterogeneous or coarse grained alluvium. The other seven logs in Plate D3-1 range from about 12% to 28% heterogeneous or coarse-grained alluvium. As indicated in the GSS Report Plate 3-1, such high percentages of fine-grained alluvium is consistent with low aquifer system permeabilities. Relatively small zones of likely good connectivity within the aquifer system, based on alluvium zone thicknesses and depths, are labeled in Plate D3-1.

**As new farmlands began to be cultivated in this area, they were likely irrigated by pumping groundwater from new wells in each area, and the underlying predominantly fine-grained aquifer system would have responded by compressing, leading to subsidence of the ground surface. Being a predominantly fine-grained aquifer system (Plate D3-1), overall aquifer connectivity is assumed to be impeded, such that groundwater drawdown cones might not spread as far laterally as they might be in a higher-permeability aquifer. Once groundwater pumping has been established for a few years, the localized subsidence pattern would have been established (e.g., around the 2007-2010 timeframe), subsequent years (e.g., around the 2015-2016 timeframe) might not display such a pronounced localized bowl of subsidence. This pattern is consistent with the single well model presented in Section 4.1 and depicted on Plate 4-1 of the GSS Report.

4.0 NUMERICAL MODELING

The results of numerical modeling performed for a representative single well in the Corcoran Subsidence Bowl are generally applicable to the ENSB area (see Section 4.1 of the main GSS report for details).

The main GSS report has a discussion on the potential application of the upcoming second version of the USGS's Central Valley Hydrogeological Model (CVHM2, currently under revision) to HSR's use (Section 4.2 of the main GSS report). After our review of an interim version of the model and discussion with the USGS, the project team concluded that the interim version of the model is not ready for use in forecasting subsidence for the HSR at this time. The discussions and conclusions are also generally applicable to the ENSB area.

5.0 PAST SUBSIDENCE MAGNITUDES, RATES & PATTERNS IN EL NIDO AREA

Historic USGS subsidence mapping (GSS Report Plate 1-1) indicates that only about 1 foot of subsidence occurred in the ENSB area occurred between 1926 and 1970. Sneed and others (2013) have documented a maximum of about 5.3 feet of subsidence (at Benchmark F982 shown in Plate D5-1 as the dashed blue line) on a 1972 to 2004 subsidence profile along Highway 152 to the north of the ENSB. The average subsidence rate at this location was about 0.17 feet per year from 1972 to 2004. Subsidence from 1972 to 2004 decreased to about 2 feet at about 5 miles west and about 11 miles east of the maximum location. The north HSR Alignment alternative runs very close to a part of this Highway 152 profile, as shown in Plate D5-1.

The ENSB was a prominent feature in the JPL L-band InSAR covering June 2007 through December 2010. Contours of that subsidence are shown on Plate D5-1. The south HSR Alignment alternative crosses part of the ENSB with a maximum local subsidence of 1.4 feet in the center of this 7-mile-wide bowl. The north HSR Alignment passes near the northern edge of the ENSB, with a maximum local subsidence of about 0.8 feet in the center of a 5-mile-wide bowl. Average maximum subsidence rates were about 0.56 feet per year at the south alternative and about 0.32 feet per year at the north alternative. Beyond the edges of both of these subsidence bowls, there was about 0.5 feet of "local area" subsidence along the HSR Alignment alternatives; the local area subsidence rate was about 0.2 feet per year. The spatial pattern of the 2007-2010 subsidence is likely due to land use changes, i.e., infilling of farming activities can be seen in air photos taken between 2007 and 2008 or 2009 in the areas that would become the ENSB in the years between 2007 and 2010 (see Plate D5-1); presumably these newly-cultivated areas resulted in new irrigation wells being drilled, which likely resulted in new areas of groundwater drawdown, which presumably resulted in the accelerated subsidence rates observed.

As shown on Plate D5-1 lower right and Figure D5-1, by 2015-2016 the center of the ENSB appears to have shifted slightly toward the south and east (compare with Plate D1-1 upper right, for 2007-2010 subsidence). Also in the 2015-2016 subsidence profiles along the HSR Alignments, the ENSB does not appear to be as pronounced a feature as it appears in the 2007-2010 profiles, although the maximum rates have increased from about 0.5 feet per year from 2007 to 2010, to about 1 foot per year from May 2015 to May 2016. In other words, both the rates, location, and the shape of the "subsidence bowl" appear to be changing with time, and it should be expected that they will continue to change in the future. These changes will likely be a function of a number of factors, including land use and pumping rates.

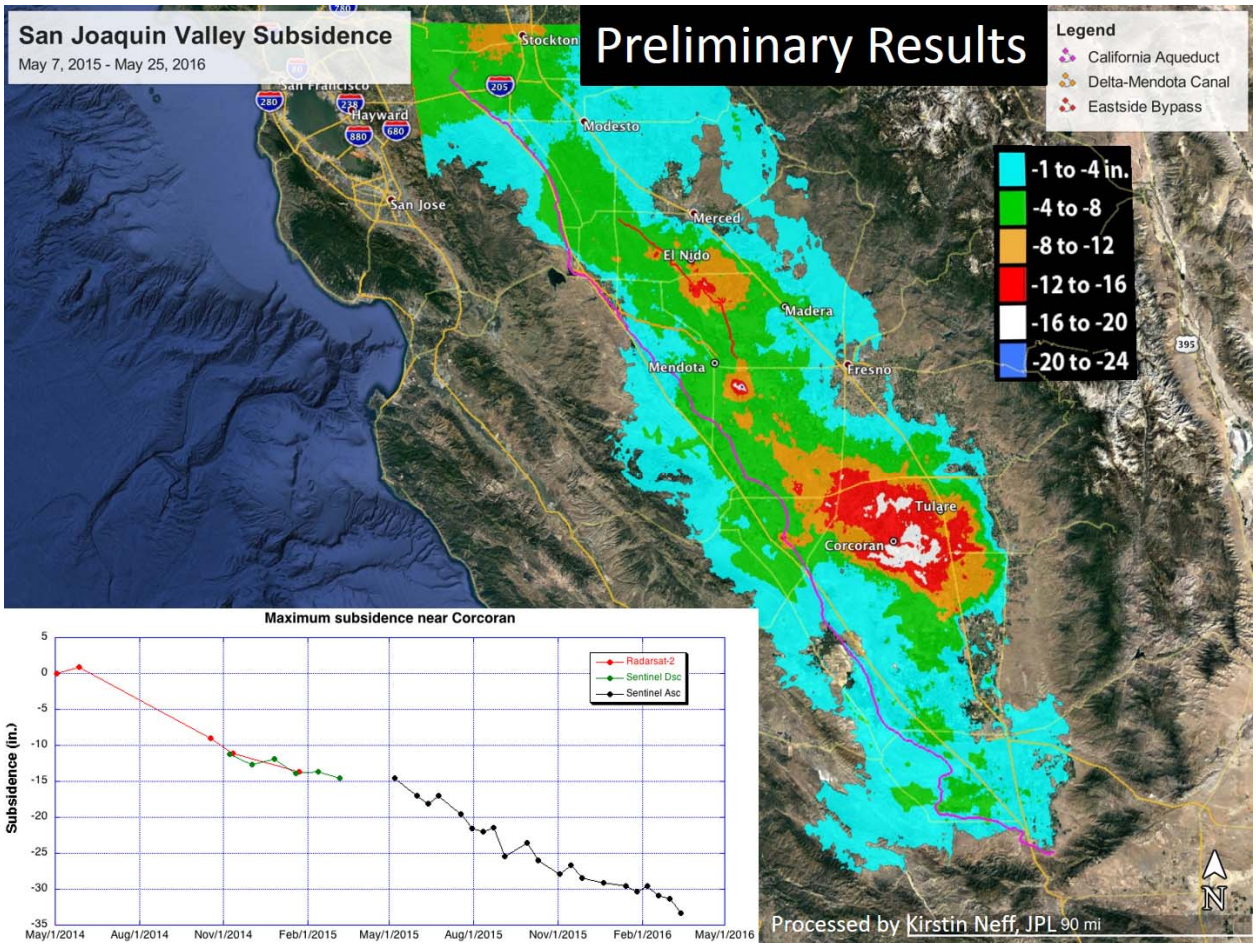

Figure D5-1: San Joaquin Valley Subsidence May 7, 2015 – May 25, 2016 (JPL). Also shows a plot of maximum subsidence near Corcoran for the period May 2014 through March 2016.

Recent survey-based subsidence monitoring for the San Joaquin River Restoration Project began in December 2011. Survey monitoring is continuing on a semi-annual basis. Survey benchmarks H1235, E158 and F158 in the National Geodetic Survey online database, are in the ENSB area. Semi-annual subsidence measurements at these benchmarks are shown on Plate D5-1. Annual subsidence rates starting from either December 2011 or July 2012, through December 2016 at these benchmarks range from about 0.44 to 0.56 feet per year; these rates are generally consistent with the recent InSAR-derived rates described above.

6.0 FORECASTING FUTURE SUBSIDENCE

As described in the main GSS report, we have assumed groundwater drawdown will continue for a number of years. The California Sustainable Groundwater Management Act (SGMA), passed by the State legislature in 2014, requires groundwater use to become sustainable toward the end of the 2030s, with a target date for full sustainability of 2040. Based on this, we have assumed that current or ongoing subsidence rates may continue for about 20 years, and

we have estimated future subsidence on this basis. Although some subsidence may continue beyond this time, we anticipate it will be slowing, and more significantly, it will be approaching a more spatially-uniform condition such that rates of differential subsidence will be much less than they currently are. This assumption is applicable to the ENSB area as well as the Corcoran area.

We have created profiles along the HSR Alignment in this area using two subsidence rates: (1) by extrapolating the 2007-2010 InSAR subsidence rates forward 20 years, and (2) doing the same for the 2015-2016 InSAR subsidence rates. Profiles have been developed along the north HSR Alignment (which is currently the Authority's preferred route), and for the south HSR alignment, which passes closer to the center of the ENSB such that subsidence magnitudes and rates are greater than along the north HSR Alignment.

Plate D6-1 presents 20-year forecasts for profiles of subsidence, induced changes in slope, and induced changes in vertical curvature. As can be seen, the maximum magnitudes of forecast subsidence are slightly less than for the Corcoran Subsidence Bowl (e.g., compare with Plate 8-17 of the main GSS report), as are the forecasts of induced changes in slopes and curvature. Based on this, we consider the evaluations and recommendations in the main GSS report are applicable here, namely, similar design considerations should be addressed, and a similar monitoring and maintain plan should be implemented.

6.1 RECOMMENDATIONS FOR FUTURE MONITORING & INSTRUMENTATION

Because forecasts using the above-described approach contains many uncertainties and may not be conservative, we recommend that future subsidence be monitored. Preliminary and conceptual recommendations for monitoring current and future land subsidence for the project are presented in Sections 8.6.5 and 10.0 of the main GSS report. GPS survey methods should be utilized to provide reliable and precise elevations at specific points along the HSR Alignment. Satellite-based InSAR technologies and procedures are rapidly developing and could provide invaluable information regarding rates and patterns of subsidence. The UAVSAR program operated by JPL for DWR (Farr et al. 2015, 2017) is beginning to demonstrate effective corridor subsidence monitoring capabilities. Finally, once the HSR is operational, inertial and other continuous on-train monitoring methods should be implemented and utilized to provide critical information concerning changing track geometries resulting from continuing subsidence.

7.0 POTENTIAL IMPACTS TO HSR SYSTEM

7.1 TECHNICAL CONSIDERATIONS

There are several ways in which subsidence could adversely impact the HSR. Each has been evaluated as discussed in the main body of the GSS report. In general, because subsidence, differential subsidence, and changes in slope and curvature are expected to be similar to but somewhat less than in the Corcoran Subsidence Bowl area, a similar approach may be taken for the ENSB area.

7.2 SUBSIDENCE-INDUCED CHANGES TO FLOODPLAINS

7.2.1 Drainage Network Evaluation

We used the ArcHydro package on ESRI's ArcGIS platform to delineate the predominant drainage network within the Areas of Interest (AOIs) presently and in the future. An area is of interest for this evaluation if (1) it is in in or near the flood zones delineated by FEMA, (2) in the ENSB area, and (3) in the HSR Alignment neighborhood. The floodplain shown in

Figure D7-1 encompasses the San Joaquin River and the confluences of the Eastside Bypass Channel, a side arm of Chowchilla River, Berenda Slough and Fresno River. The same figure shows the present and future drainage networks delineated by ArcHydro. Small changes in drainage paths indicate that the associated floodplains are not expected to be significantly impacted by ground subsidence.

Figure D7-2 shows the observed subsidence measured by the JPL, extrapolated from a 3.5-year period to a 20-year period, and the projected changes along selected slopes in the floodplain. Both subsidence bowls are anticipated to increase the gradient of the ground surface of the floodplain side arms and in the main channel, southeast of the evaluated area (see profile locations on Figure D7-2) by a maximum of about 14% (e.g., changing a 1% slope to 1.14% slope), which would lead to a discharge increase to up to 7%. Closer to the HSR Alignment, the present ground surface in the main channel becomes very flat. The future subsidence might reverse the present slope locally (see profile locations 4,7,8 on Figure D7-2) which would impound the drainage water and cause an increased flow depth in the floodplain. For this reason, we conducted a simplified one-dimensional flow channel analysis in the vicinity of these sections.

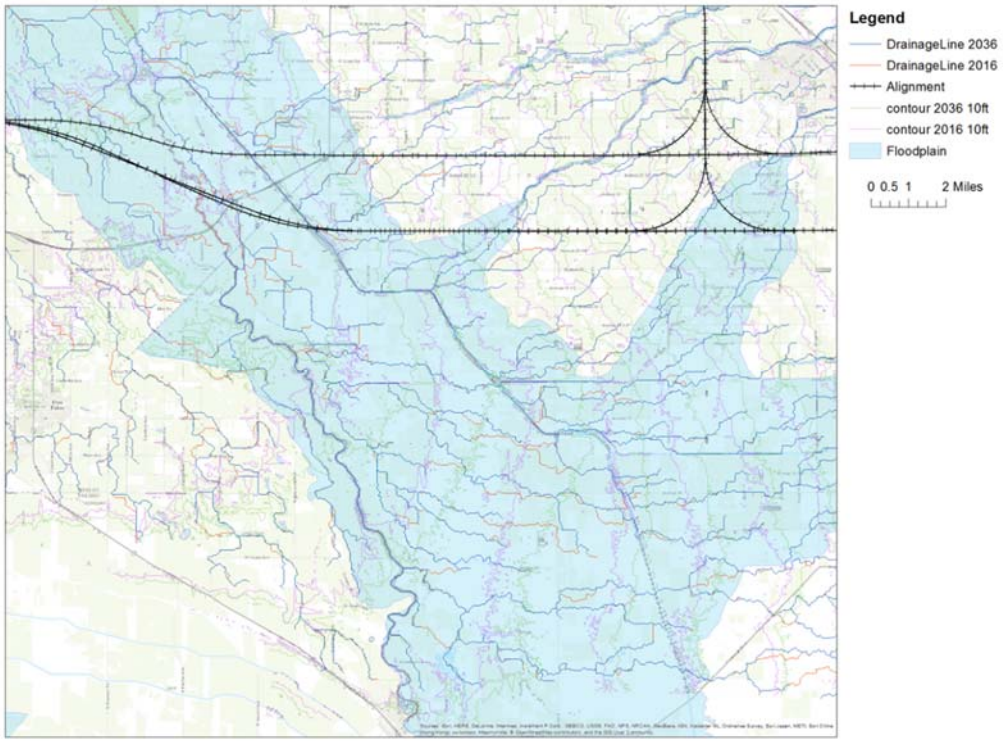

Figure D7-1. Drainage characteristics delineated by ArcHydro

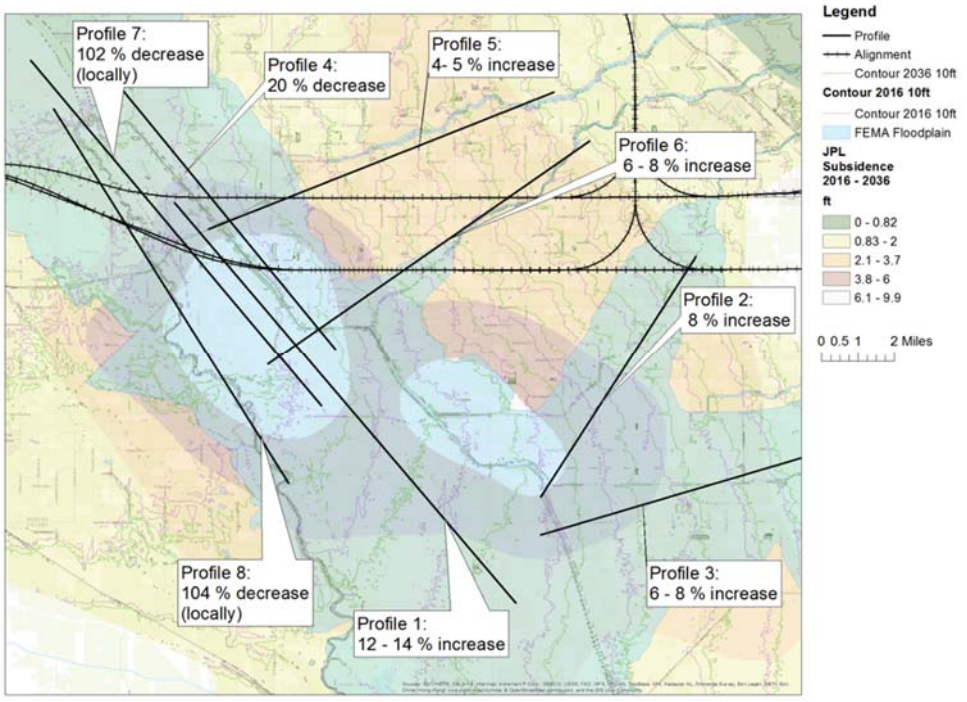

Figure D7-2: Changes in surface slope due to subsidence

7.2.2 1D Flow Analysis

From the identified sections with the critical slope changes, we generated simplified flow channels with triangular or trapezoidal cross-sections. We conducted one-dimensional channel flow simulations with HEC-RAS, developed by the US Army Corps of Engineers, to estimate the increase in flood depth due to the slope change. Two channels were modeled, the location of these channels and their cross-sections are shown in Figure D7-3.

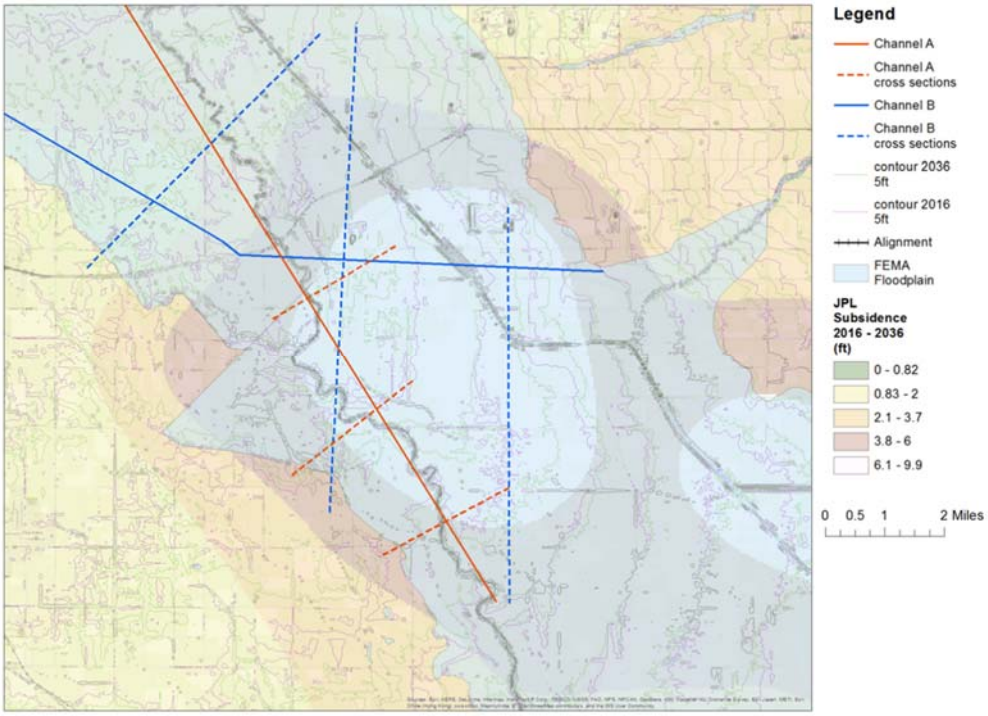

Figure D7-3: One-dimensional flow channels simulated with HEC-RAS

7.2.2.1 Channel A

Channel A follows the San Joaquin River. The three cross-sections were selected based on topography and location relative to the observed subsidence bowl and for modeling were simplified to triangular or trapezoidal shapes. The discharge through each channel was calibrated to a flow depth of around a 1/7 to 1/2 foot. Both width and shape of the cross-sections change with the forecast subsidence, which generally results in a wider channel. However, the slope between the second and the third cross-section is anticipated to become flatter, causing an increase of the flow depth of about half a foot at the second from the northernmost cross-section of the channel. This increase is quite small and is judged to be within an acceptable range and does not require further evaluation.

7.2.2.2 Channel B

Channel B follows the larger-scale topography across both Chowchilla Canal and San Joaquin River from east to west. As was done for Channel A, we selected the cross-sections based on both topography and on location relative to the observed subsidence. The cross-sections were simplified to nearly triangular shapes. The flood discharge was calibrated to a flow depth of approximately 1 foot in the uppermost cross-section for the existing surface conditions.

The stations along the cross-sections in a west-to-east direction intersecting with the northern and the southern HSR Alignment options and the corresponding flood depths are shown in Table D7-1 for the center cross-section and in Table D7-2 for the furthest downstream cross-section along the channel. (The stationing of the HSR Alignment crossings do not remain the same for the different years because of the subsidence shape.)

As a sensitivity analysis, the channel flow simulation was repeated assuming a subsidence rate which is one and a half times the forecast subsidence rates for the 20-year period. At this larger subsidence rate, the ground surface slope would be reversed locally, causing a damming. The flow depth at the southern HSR Alignment alternative at the second cross-section would be around 4 feet for the southern HSR Alignment option and 0.1 at the northern option. The flow depths at the furthest from downstream cross-section would be 0.4 feet and 2.5 feet for the southern and northern options, respectively.

Table D7-1: Channel B: Stations and flood depths at HSR Alignment at second from northernmost cross-section.

Year	**2016**		**2036**		**2036 – 1.5 x Subsidence Rate**	
Alignment Option	Station (ft)	Flood Depth (ft)	Station (ft)	Flood Depth (ft)	Station (ft)	Flood Depth (ft)
Southern	15,000	2.5	22,000	3	23,000	4

Table D7-2: Channel B: Stations and flood depths at HSR Alignment at furthest downstream cross-section.

Year	**2016**		**2036**		**2036 – 1.5 x Subsidence Rate**	
Alignment Option	Station (ft)	Flood Depth (ft)	Station (ft)	Flood Depth (ft)	Station (ft)	Flood Depth (ft)
Southern	0	0.5	0	0.1	8,400	0.4
Northern	5,500	2.5	5,500	2	14,400	2.5

In summary, we anticipate that the potential maximum impact of subsidence on flood depth is likely to be on the order of 1.5 feet along the southern HSR Alignment. The impact on the northern HSR Alignment is anticipated to be minimal.

8.0 REMAINING UNCERTAINTIES

There are remaining uncertainties in the ENSB area. Most are similar to the uncertainties in the Corcoran Subsidence Bowl Area:

- Paucity of Quantitative Data for Localized Differential Subsidence: This is similar to the Corcoran area.
- Lack of Thorough Hydrogeological Data & Model: This is similar to the Corcoran area.
- Uncertainties Regarding Future Groundwater Drawdown and Subsidence: This is similar to the Corcoran area. Forecast rates and magnitudes of subsidence, as well as forecast differential subsidence and induced changes in slopes and curvature, are discussed above in Section 6.0.

Uncertainties regarding subsidence-induced fissures and compaction faults, and regarding other subsidence mechanisms, are discussed in the following subsections.

8.1 POTENTIAL FOR SUBSIDENCE-INDUCED FISSURES & COMPACTION FAULTS (MIKE)

Potential for subsidence-induced compaction faults or earth fissures are anticipated to be lower in the El Nido area than in the Tulare Basin. Subsidence rates in the El Nido area, though still very large at about 0.5 feet per year, are lower than in the Tulare Basin. InSAR-derived patterns of subsidence in the ENSB do not show edges that are as abrupt as the edges appear in the Corcoran subsidence bowl. Slope changes at the edge of the ENSB appear to not be continuing to develop and increase as shown by comparing the 2007 to 2010 InSAR patterns with the 2015 to 2016 InSAR patterns (see profile plots on Plate D5-1). The compressible freshwater aquifer system underlying the ENSB area appears to be thinner than aquifer systems in the Tulare Basin; this is expected to limit the ultimate subsidence magnitudes around El Nido compared to the Corcoran vicinity. Continued subsidence monitoring is expected to provide information useful for refining characterization of the compressible and adjacent less-compressible to incompressible basin alluvium, and enable refined understanding of potential for earth fissuring or compaction faulting.

8.2 OTHER SUBSIDENCE MECHANISMS

Although this ground subsidence study (GSS) has focused on subsidence induced by groundwater extraction, other forms of subsidence may be present within the SJV, as discussed in the main body of the GSS report. The way each other mechanism relates to the El Nido area is described as follows.

8.2.1 Hydrocompaction

The potential for hydrocompaction of dry fills should be addressed by each Design-Build Contractor.

The potential for hydrocompaction of loose debris flow deposits should be investigated by the Design-Build Contractor, particularly where the HSR Alignment is near to the toe of the coast range near Interstate 5.

8.2.2 Oil and Gas Extraction

Along the Highway 152 corridor, there is not expected to be more than minor subsidence due to extraction of oil and gas. The online California Division of Oil, Gas, & Geothermal Resources (DOGGR) database indicates that the Chowchilla Gas Field, located primarily in Township 10S-14E through which Highway 152 passes, includes 54 primarily gas wells. One of these wells is listed as active, two wells are listed as inactive, and the other 51 wells are listed as having been plugged. With current activity being a small fraction of historic activity, subsidence in this area due to oil and gas extraction is anticipated to be, for practical purposes, essentially complete.

8.2.3 Tectonic Subsidence

Tectonic subsidence is not expected to be a significant concern along the Highway 152 corridor.

8.2.4 Organic Soils and Peat

Peat and other organic soils are not likely to be present in any broad areas of the HSR Alignment. However, the design-build contractors should evaluate the possibility of their presence, particularly near river crossings, ponds, or marshy areas, and develop recommendations to mitigate any potential hazards that if they are identified.

9.0 INSTRUMENTATION AND MONITORING OPTIONS

In general, the approach to instrumentation and monitoring should follow an approach similar to what will be implemented in the Corcoran Subsidence Bowl area.

Potential erosion or changes in FEMA or project-based floodplain limits or depths should be tracked and coordinated with the owners/operators of any canals or waterways that the HSR will cross.

The San Joaquin River Restoration Project survey network provides regional coverage so that the HSR may utilize this network of benchmarks as ground truth for verification of InSAR-based subsidence along the HSR Alignment. We expect there will be opportunities for coordination and data sharing for subsidence monitoring.

10.0 EVALUATIONS AND RECOMMENDATIONS

In most locations, subsidence is not expected to result in significant impact to the HSR performance. However, several potential risks remain, and therefore our recommendations for the following are the same as for the Corcoran Subsidence Bowl as described in the main body of the GSS report:

- Subsidence-Induced Curvature, Faults, and Fissures: see Section 10.2 of the main GSS report
- Monitoring & Maintenance Approach: see Section 10.3 of the main GSS report

Potential flood or erosion impacts should be anticipated within existing FEMA or other floodplains, and these floodplains may grow and increase in depth slightly if the southern HSR Alignment is selected, as discussed above.

11.0 CLOSURE

This report appendix was prepared by the staff of Amec Foster Wheeler and our subconsultant GSI Environmental Inc., under the supervision of the engineers whose signatures appear hereon. We trust that this report meets the current project needs. If you have any questions or require additional information, please contact Jim French of Amec Foster Wheeler.

12.0 ADDITIONAL REFERENCES

California Department of Water Resources, Secondary Post-Processed LiDAR topography Data, Task Order 20, CVFED program.

DWR: See California Department of Water Resources.

Izett, G.A., Obradovich, J.D. and Mehnert, H.H., 1988. The Bishop Ash Bed (Middle Pleistocene) and some older (Pliocene and Pleistocene) Chemically and Mineralogically Similar Ash Beds in California, Nevada, and Utah. USGS Survey Bulletin 1675.

S:\OD15\8715180680\Plate_D01-01_rev171108.mxd

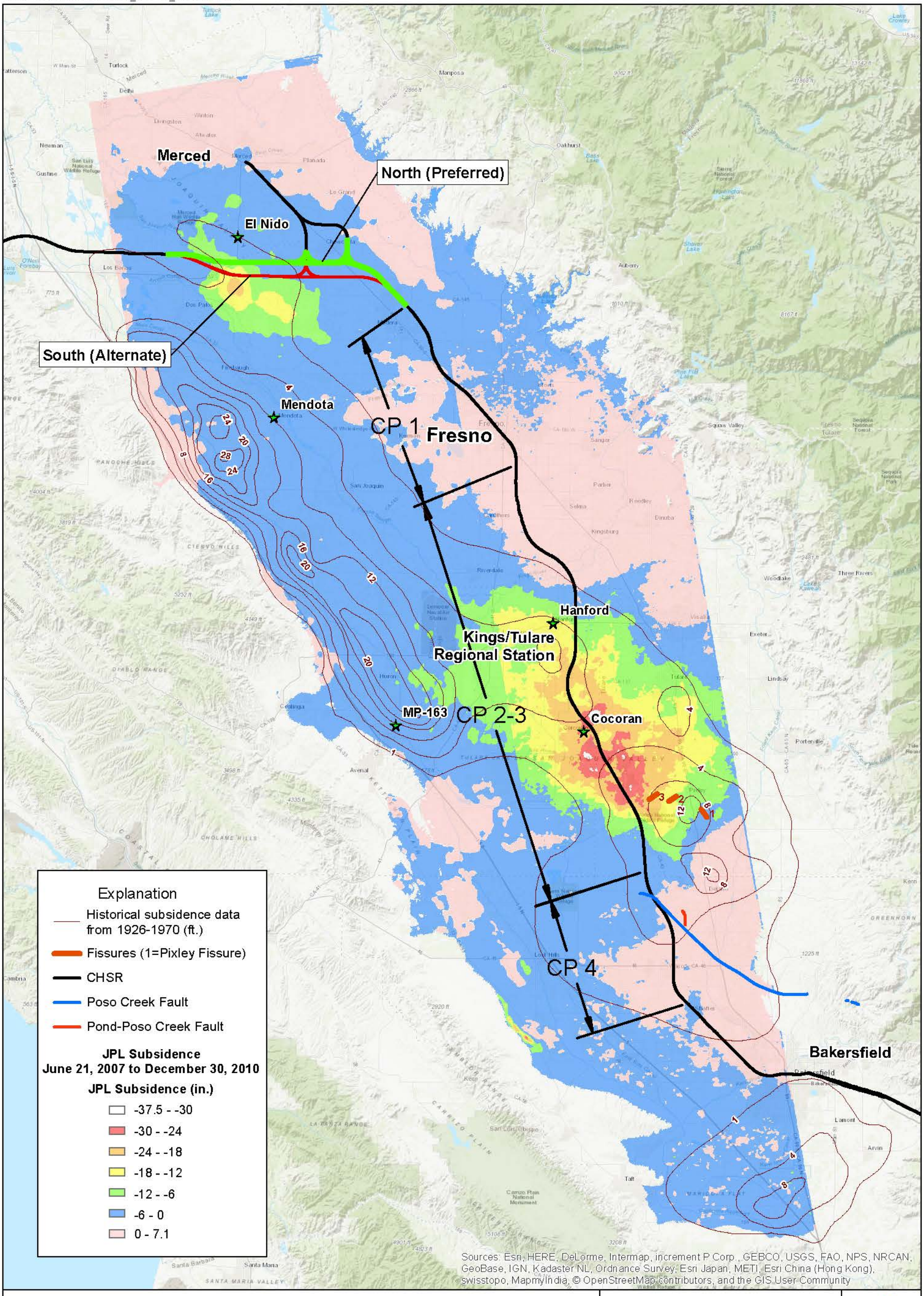

0 10 Miles
0 20 Kilometers

SAN JOAQUIN VALLEY
SUBSIDENCE MAP
San Joaquin Valley
HSR Ground Subsidence Study
California

amec foster wheeler

Date: 11/2017 | Project No. 8715180680.04

Plate
D1-1

West/North

East/South

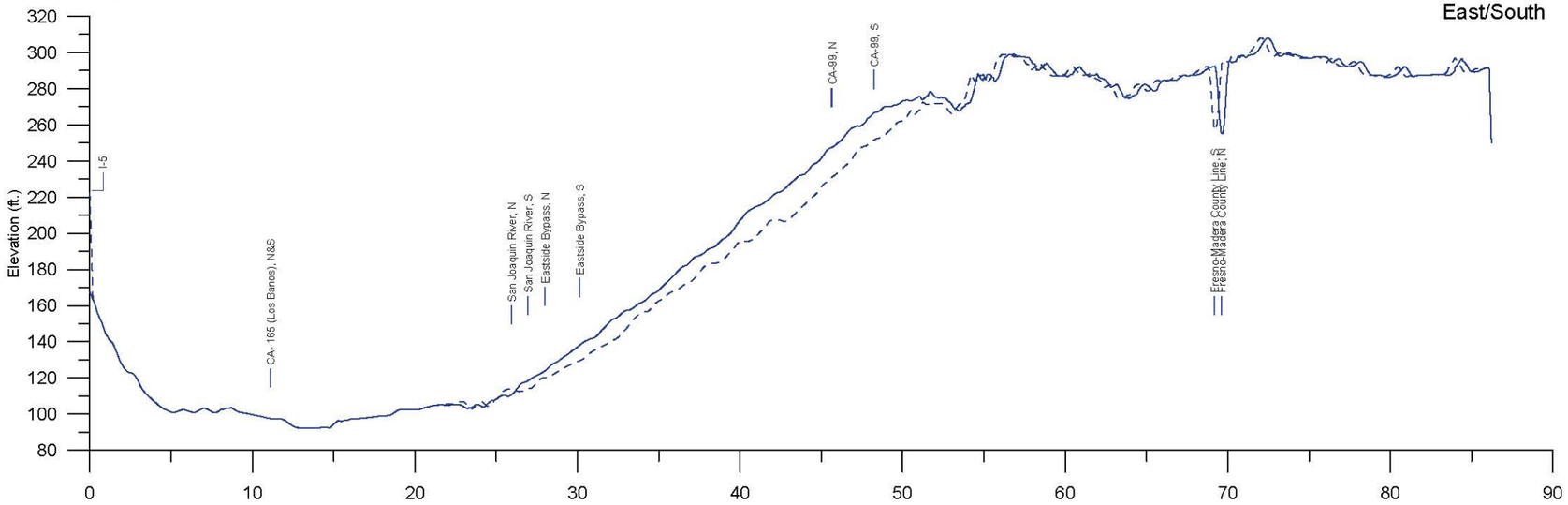

Ground Surface
1926 USGS, North Alignment
1926 USGS, South Alignment

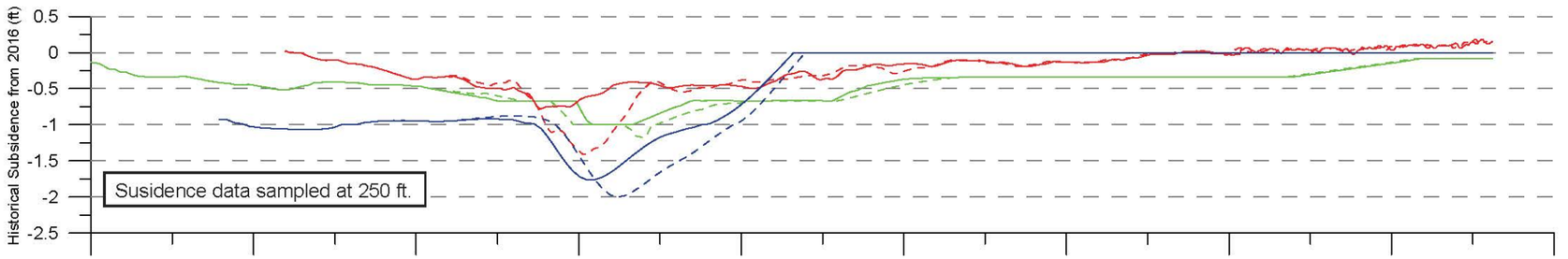

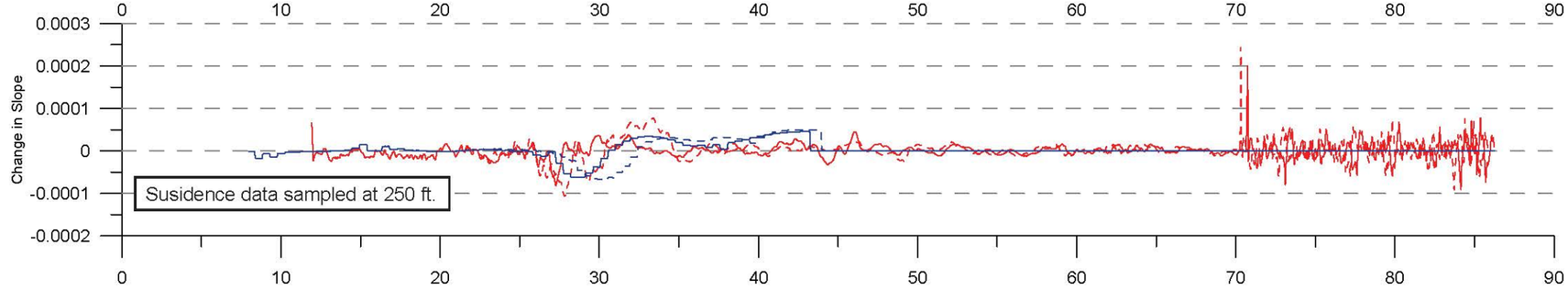

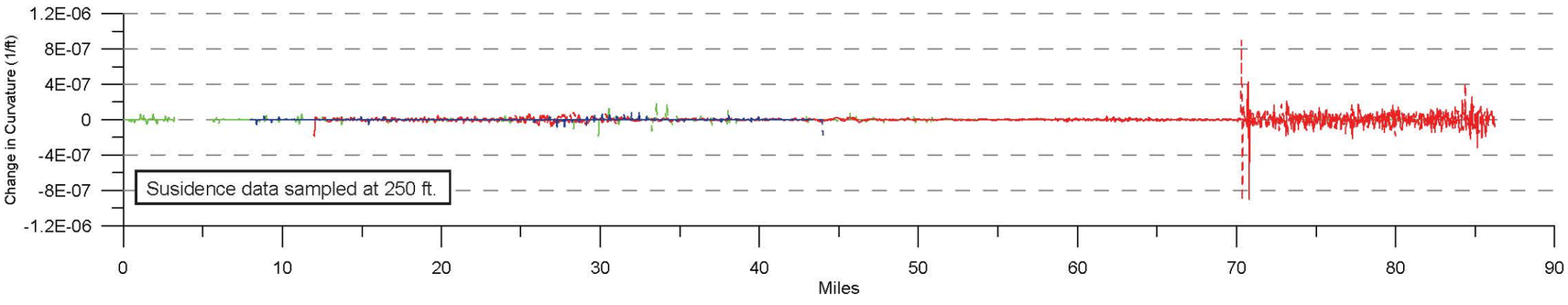

Subsidence, Slope, and Curvature
1926-1970 (USGS) for 44 yrs, North Alignment
1926-1970 (USGS) for 44 yrs, South Alignment
2007-2010 (JPL) for 3.5 yrs, North Alignment
2007-2010 (JPL) for 3.5 yrs, South Alignment
2015 May - 2016 May (JPL, Digitized) for 1.04 yrs, North Alignment
2015 May - 2016 May (JPL, Digitized) for 1.04 yrs, South Alignment

PROFILES OF HISTORICAL SUBSIDENCE, SLOPES, AND CURVATURE
IN SAN JOAQUIN VALLEY
San Joaquin Valley
HSR Ground Subsidence Study
California

amec foster wheeler

Date: 08/16/2017 | Project No. 8715180680.04

Plate
D1-2

S:\OD15\8715180680\gis\profile\profiles_aug2017\Plate_D1-02_historic_el_nido.ai

~0.62 Ma Friant Pumice

Corcoran Clay

~0.74 Ma Bishop Ash

Some extensive confining clay horizons may correspond to major ashfall events (see USGS Bulletin 1675). The most significant, the Corcoran clay, is bounded by two such events; the Bishop Ash and Friant pumice. Two earlier periods of eruptive activity may be represented within or at the bottom of the fresh water aquifer as shown below.

~0.8-1.2 Ma (?) Glass Mountain U, T, D, G ash bed(s) possible? (Izett & others 1988)

~2.1-2.2 Ma ash bed(s) possible?*

Profile Distance, miles

033 (API 03900033)
067 (API 04700067)
102 (API 03920102)
098 (API 03920098)
091 (API 03900091)
014 (API 03900014)
019 (API 03900019)
017 (API 03900017)

Resistivity ohm-m 0 10 50 100

RESISTIVITY -ohms. m²/m

Resistivity, ohm-m 0 10 20 0 20 100 200

~35-40 ft offset?

~65-70 ft offset?

good lateral connectivity likely

poor to minimal lateral connectivity likely

good lateral connectivity likely

Depth, feet

6/2007 - 12/2010 Subsidence, feet

-0.5
-1.0
-1.5

% log wth resistivity type classification

033	067	102	098	091	014	019	017
6.3%	4.3%	5.9%	0.0%	6.3%	6.7%	0.0%	0.0%
11.7%	8.4%	21.6%	32.3%	11.7%	18.1%	27.5%	19.0%
82.0%	87.3%	72.5%	67.7%	82.0%	75.2%	72.5%	81.0%

*(?) Taylor Canyon U, C, P; Waucoba Road 1, 2 ash beds in this time; see neutron porosity log for Well 102 at 1,100 ft depth (Plate 3-2)

Profile Distance, miles

384 API well identification number, last 3 digits

Fine-grained alluvium; very compressible silts and clays, but compaction is inhibited or delayed by very low permeabilities.
<~10 ohm-m resistivity

Heterogeneous alluvium; pathways of high permeability coarse-grained alluvium fraction provides drainage for the lenticular/ interlayered highly compressible fine-grained alluvium fraction.
~10 to ~25-30 ohm-m resistivity

Coarse-grained alluvium; sands and gravels with minor compaction which, due to high permeabilities,is rapid.
>~25-30 ohm-m resistivity

Notes: top of Santa Margarita Fm (7 Ma) at depth of 2218 ft in Well 017.
Ma - million years ago

HSR Ground Subsidence Study
California

BASIN COMPRESSIBLE ALLUVIUM PROFILE & POSSIBLE PROFILE CHANGES IN VICINITY OF SOUTHERN HSR ALIGNMENT NEAR EL NIDO

PLATE **D3-1**

Project 8715180680
PM : JF BY: MLR
Date 7/3/2017
Scale : n/a

amec foster wheeler

HSR alignment alternatives

Minimal historic local agricultural activity in 2007-2010 subsidence maximum area through 2007 (*June 2007 through December 2010 subsidence contours shown for reference*)

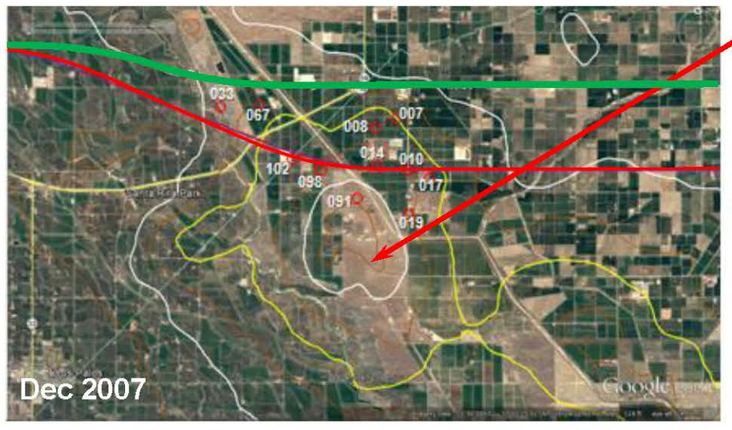

O[019] Locations of historic oil well logs with identifier numbers used for Plate EN-1 Subsurface Profile

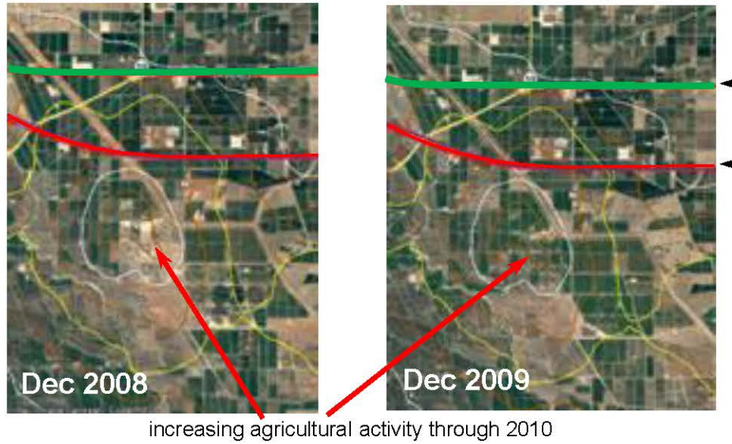

HSR alignment alternatives

increasing agricultural activity through 2010

InSAR-derived subsidence contours for June 2007 through December 2010, feet

Measured Subsidence along HSR Alignment Alternatives; Several Time Periods

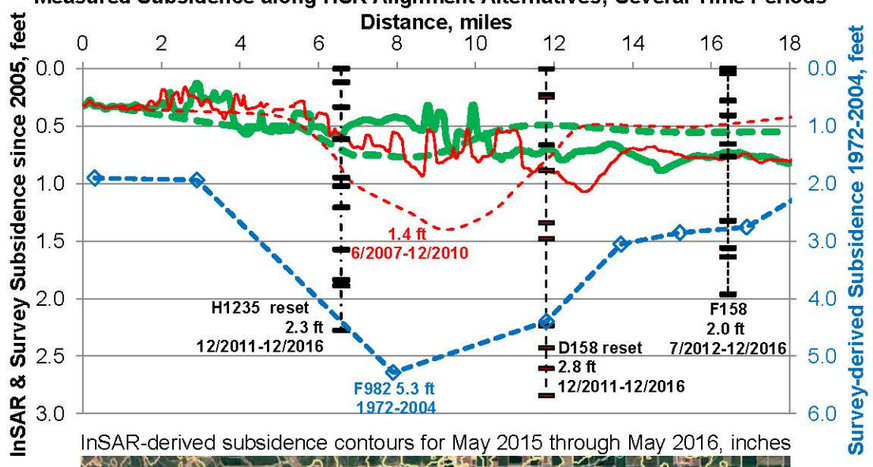

InSAR-derived subsidence contours for May 2015 through May 2016, inches

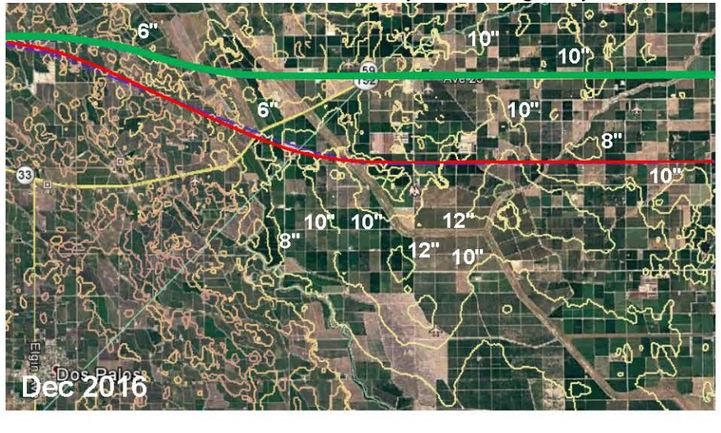

Maximum Annual Subsidence Rates Estimated on Northern HSR Alignment

1972 - 2004	0.17 ft/yr	survey
2007 - 2010	0.30 ft/yr	InSAR
2015 - 2016	0.88 ft/yr	InSAR
2011 - 2016	0.56 ft/yr	survey

Comparison of Survey Monuments with Nearest 5/2015-5/2016 InSAR Points, feet

Survey Monument	12/14-12/15	12/15-12/16	Annual Average	InSAR 5/15-5/16
H1235 reset	-0.63	-0.44	-0.54	-0.58
D158 reset	-0.95	-0.42	-0.68	-0.70
F158 reset	-0.79	-0.40	-0.60	-0.73

Subsidence Profiles Legend

InSAR
- Northern Jun 2007 - Dec 2010
- Northern May 2015 - May 2016
- Southern Jun 2007 - Dec 2010
- Southern May 2015 - May 2016

Survey
- D158 reset Dec 2011 - Dec 2016
- F158 reset Jul 2012 - Dec 2016
- H1235 reset Dec 2011 - Dec 2016
- Hwy 152 Survey 1972 - 2004

Legend Notes:

6/2007 through 12/2010 InSAR is Palsar L-band provided by JPL.

5/2015 through 5/2016 InSAR is Sentinel C-band provided by JPL

D158, F158 & H1235 survey results from http://www.restoresjr.net/monitoring-data/subsidence-monitoring/

Hwy 152 survey results from Figure 17, USGS SIR 2013-5142 (Sneed, Brandt, and Solt, 2013)

HSR Ground Subsidence Study
California

RECENT LAND-USE AND SUBSIDENCE HISTORY AT SUBSIDENCE FEATURE SOUTH OF EL NIDO

PLATE
D5-1

Project 8715180680
PM: JF BY: MLR
Date 11/8/2017
Scale : n/a

amec foster wheeler

West/North

East/South

Elevation (ft.)

I-5

CA- 165 (Los Banos), N&S

San Joaquin River, N

San Joaquin River, S

Eastside Bypass, N

Eastside Bypass, S

CA-99, N

CA-99, S

Fresno-Madera County Line, N

Fresno-Madera County Line, S

Ground Surface
1926 USGS, North Alignment
1926 USGS, South Alignment

Forecast Subsidence from 2016 (ft)

Susidence data sampled at 250 ft.

Subsidence, Slope, and Curvature
2036 Scenario A, North Alignment
2036 Scenario A, South Alignment
2036 Scenario C, North Alignment
2036 Scenario C, South Alignment

Change in Slope

Susidence data sampled at 250 ft.

Change in Curvature (1/ft)

Susidence data sampled at 250 ft.

Miles

PROFILES OF 20-YEAR FORECAST SUBSIDENCE, SLOPES, AND CURVATURE
IN SAN JOAQUIN VALLEY
San Joaquin Valley
HSR Ground Subsidence Study
California

Date: 08/16/2017

Project No. 8715180680.04

amec foster wheeler

Plate
D6-1

S:\VOD15\8715180680\gis\profile\profiles_aug2017\Plate_D6-01_forecast.ai

APPENDIX E

Antelope Valley Subsidence

APPENDIX E

ANTELOPE VALLEY

Ground Subsidence Study Report
California High Speed Rail Project
Kern and Los Angeles Counties, California

TABLE OF CONTENTS

Page

TABLE EMBEDDED WITHIN TEXT

FIGURES EMBEDDED WITHIN TEXT

PLATE

APPENDIX E

ANTELOPE VALLEY

Ground Subsidence Study Report
California High Speed Rail Project
Kern and Los Angeles Counties, California

1.0 INTRODUCTION

As a supplement to the main Ground Subsidence Study (GSS) report titled *Ground Subsidence Study, California High Speed Rail Project, Corcoran Subsidence Bowl, San Joaquin Valley, California*, this appendix presents a supplementary evaluation of subsidence and the potential impact subsidence could have on future High-Speed Rail (HSR) infrastructure and train performance in the Antelope Valley (AV). The discussions in the main GSS report are generally applicable within Antelope Valley, unless supplemented or otherwise stated herein. Similar to the San Joaquin Valley (SJV), subsidence has been occurring along the future HSR Alignment within the AV since the last century. However, the maximum observed subsidence between about 1915 and 2015 is about 9.4 feet, for an average of about 1.25 inches/yr; 1993-1995 InSAR data indicates similar maximum rates, on the order of 2 inches (50 mm) over this 26-month period (see Section 5.2.1 below). These are all far less than the maximum rates of up to about 20 inches per year recently observed in the SJV.

2.0 SOURCES OF INFORMATION

Most sources of data are summarized in Section 2.0 of the main GSS report. The following discussion pertains specifically to the AV subsidence bowl area.

2.1 TOPOGRAPHIC AND SUBSIDENCE DATA

The primary sources of available historical subsidence data in the AV are based on older survey data published by the U.S. Geographical Survey (USGS), interferometric synthetic aperture radar (InSAR) data processed and published by the USGS, and continuous geographic position system (CGPS) records, as summarized in the in this section. The USGS (Siade et al., 2014) report has summarized the historical subsidence data, including the inSAR data, as discussed in Section 5.1. Elevation data is shown in a National Map (2016). In addition, LiDAR data (2016) is available from the University of California, San Diego.

2.2 CALTRANS OFFICE OF STRUCTURE INVESTIGATIONS - SOUTH

Caltrans Office of Structure Investigations – South is responsible for the investigation, evaluation, work recommendations, and documentation of all city, county, state, and federal bridges in northern California, including the Antelope Valley. In November 2017, Mr. Ching Chao, PE (Chief, Structures Investigations – South) indicated that the Office was not aware of

subsidence being an issue in Antelope Valley, nor was he aware of subsidence having had any impact to structures within his area of jurisdiction.

Also in November 2017, Ms. Deborah Wong, Deputy District 7 Director of Maintenance, indicated that she was not aware of subsidence having caused any problems within her area of jurisdiction, which includes Langcaster and Palmdale.

3.0 MECHANISMS OF SUBSIDENCE

3.1 INTRODUCTION

In general, mechanisms of subsidence in the AV are similar to those in the Corcoran area. We anticipate the High Speed Rail Authority (Authority) may implement similar contractual considerations regarding the distinguishing of subsidence and settlement as has been done for Construction Package 2-3 (CP 2-3) in the area of the Corcoran Subsidence Bowl.

3.2 REVIEW OF LOCAL RELEVANT GEOLOGY

The USGS Scientific Investigation Report 2014-5166 titled *Groundwater-Flow and Land-Subsidence Model of Antelope Valley, California* (Siade et al., 2014) summarizes historical water utilization in the valley, and measured historical groundwater levels and land subsidence resulting from historical groundwater consumption. Although the general background information and findings of Siade et al. (2014) are not repeated here, discussion of items pertaining specifically to the HSR Alignment is described below.

Siade et al. (2014) divide the AV into sub-basins that are typically bounded or separated by faults and/or mountain fronts. Their organization of Antelope Valley is shown on Plate E3-1, with our addition of the HSR Alignment. Because groundwater pumpage, groundwater recharge, and subsurface conditions are not spatially uniform across the AV, differential subsidence will occur, with greater subsidence occurring where pumpage is greater, recharge is slower, and subsurface conditions are more compressible. Differential subsidence can lead to induced changes in ground slope and curvature, and if these induced changes are great enough, it will result in induced accelerations for high speed trains running on the tracks, and there is a potential it could result in development of earth fissures or compaction faults, as discussed below in Sections 5.1 and 8.1. Relatively low-permeability fault zones can behave as aquitards, or “leaky” hydraulic barriers, that slow horizontal migration of groundwater, which can result in relatively abrupt changes in drawdown and compressibility from one side of the fault to another, which, in turn, can result in relatively abrupt differential subsidence. Near mountain fronts, where the top of bedrock commonly slopes down from the toe of the mountain and continuing beneath the alluvial surfaces, the thickness of potentially compressible soils can vary fairly rapidly with horizontal distance from the toe of the mountain. Thus, differential effects are often greatest near such faults or mountain fronts.

Entering Antelope Valley from the north at the Oak Creek sub-basin, the HSR Alignment crosses the Randsberg-Mohave Fault, passes through the northeastern edge of the Willow Springs groundwater sub-basin, crosses the Willow Springs Fault, catches perhaps the extreme eastern corner of the Neenach sub-basin and crosses the Neenach Fault before entering the Lancaster sub-basin. Subsurface data in the form of historical geophysical logs is largely absent for Antelope Valley; Siade et al. (2014) discuss using the few available resistivity logs, mostly in the Lancaster Basin, to assist in basin characterization.

Figure 4 in Siade et al. (2014, page 8) indicates that bedrock is less than 500 feet deep at the Randsberg-Mohave Fault crossing (Plate E3-1). The Oak Creek sub-basin is anticipated to have a thinner basin alluvium section, so that basin alluvium compaction is more likely to be greater on the Willow Springs side of the fault crossing.

Groundwater measurements (DWR 2017) in the northeastern portion of Willow Springs sub-basin indicate depths to groundwater are typically greater than 300 feet. The thickness of saturated basin alluvium may be small, or saturated alluvium may be absent, at this fault crossing. With a resulting small potential for subsidence and for differential subsidence, the risk of earth fissuring may be minimal at this location.

HSR crossings at the Willow Springs and Neenach Faults (Plate E3-1), however, may be at basin boundaries where the basin alluvium separated by low-permeability sub-basin boundary faulting is interpreted to be 500 to 1,000 feet in thickness. Total historical groundwater level decline in this area has been more than 100 feet, and recent depths to groundwater have been less than about 200 feet. Historical subsidence in the Neenach Fault vicinity of the HSR Alignment near Rosamond is estimated to have been about 1 foot (Siade et al., 2014, page 24).

The area where the HSR Alignment passes through the Lancaster sub-basin (Plate E3-1), and exits the valley at Palmdale, is the area within Antelope Valley that is most likely to be subject to significant land subsidence. The overall compressible basin alluvium aquifer system as described by Siade et al. (2014) is more than 1,000 feet in thickness, and in some places the depth to basement rock is several thousand feet. Historical subsidence up to 6 feet has been documented. Saide et al. (2014) also report that, starting by the 1980s, groundwater levels seem to have generally stabilized or partially recovered. However, as Saide et al. (2014) note, adjudication in 2011 concluded that groundwater use in the Antelope Valley was still in overdraft and that groundwater withdrawals should be limited to 60,000 acre-ft/yr to be sustainable. Potential implications of land subsidence modeling results will be discussed below.

The HSR Alignment crosses the San Andreas Fault System as it exits the Antelope Valley to the south.

4.0 NUMERICAL MODELING OF SUBSIDENCE AND GROUNDWATER DRAWDOWN

4.1 MODELING OF SUBSIDENCE FROM DRAWDOWN AROUND SINGLE WELL

Numerical modeling was performed for a representative single well in the Corcoran Subsidence Bowl (see Section 4.1 of the main GSS report). A similar study was performed for ground and groundwater extraction conditions representative of the area along the HSR Alignment in AV. The follow table summarizes the site profile assumed in the model. It is based information provided in the USGS ground water model of the AV (Table E4-1). The groundwater extraction rate was assumed to be 1500 gallons per minute, which is a representative common total pumping rate within a 1-mile square area.

Table E4-1: Idealized site profile assumed in single-well modeling

Layer	Top (ft)	Bottom (ft)	Thickness (ft)	Kh (f/d)	Kv (f/d)	Mv (1/psf)
1	2312	2194	118	21.1	2.113	5.0E-07
2	2194	1948	246	6.2	0.309	1.0E-06
3	1948	1548	400	4.2	0.211	4.5E-07
4	1548	1000	548	0.98	0.020	6.0E-07

The resulting vertical and transverse displacement profiles along a linear alignment at 1000 ft from the well are shown in Figure E4-1. A profile of the resulting vertical slope is depicted in Figure E4-2. The resulting horizontal and vertical acceleration profiles along the alignment for a training travelling at 250 miles per hour are shown in Figure E4-3.

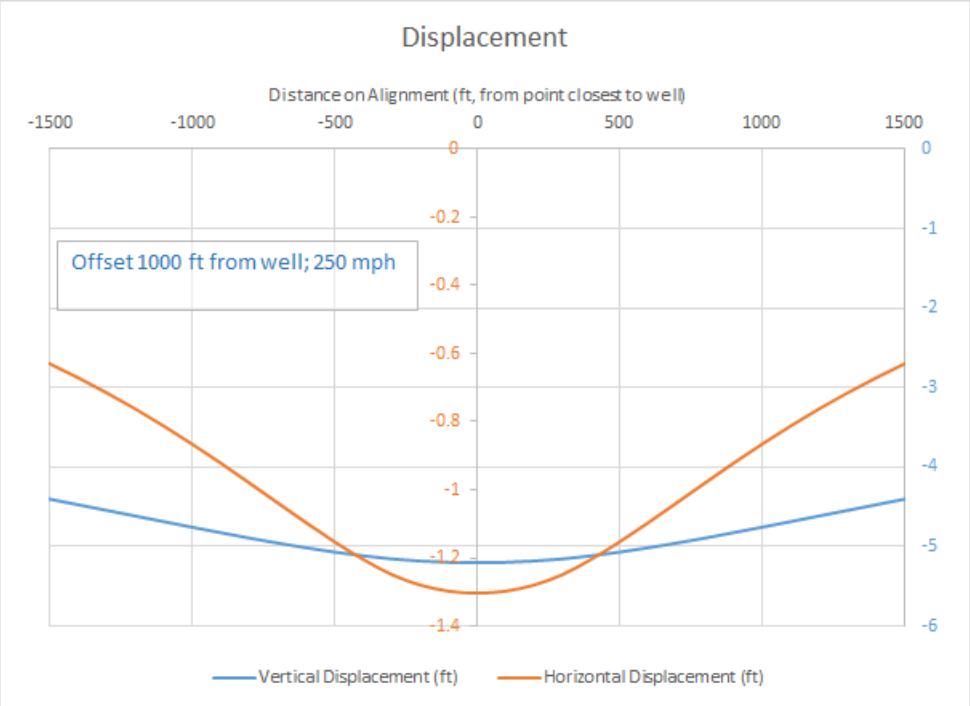

Figure E4-1: Vertical and transverse displacement profiles along alignment

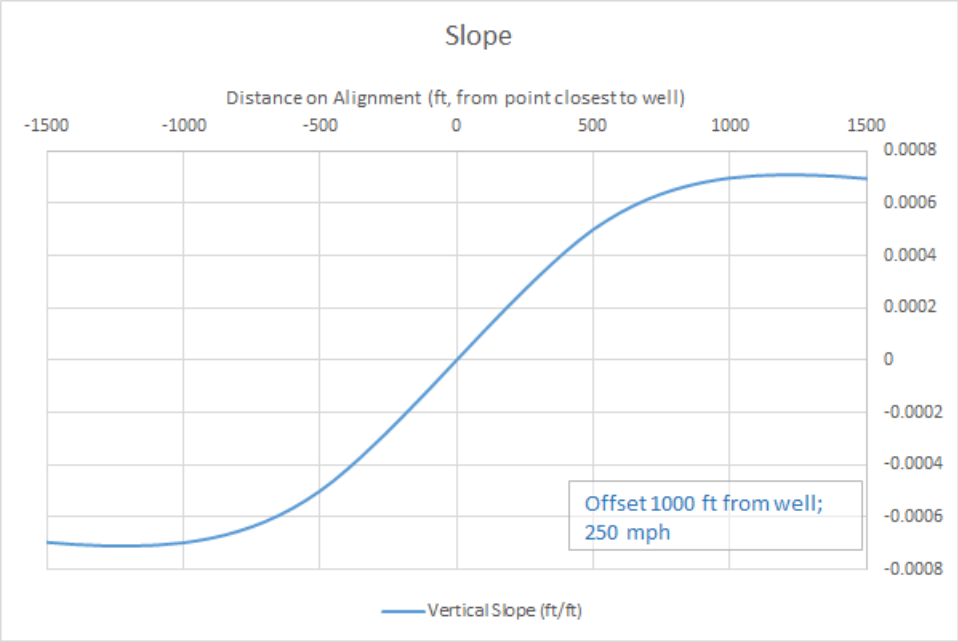

Figure E4-2: Vertical slope profile along alignment

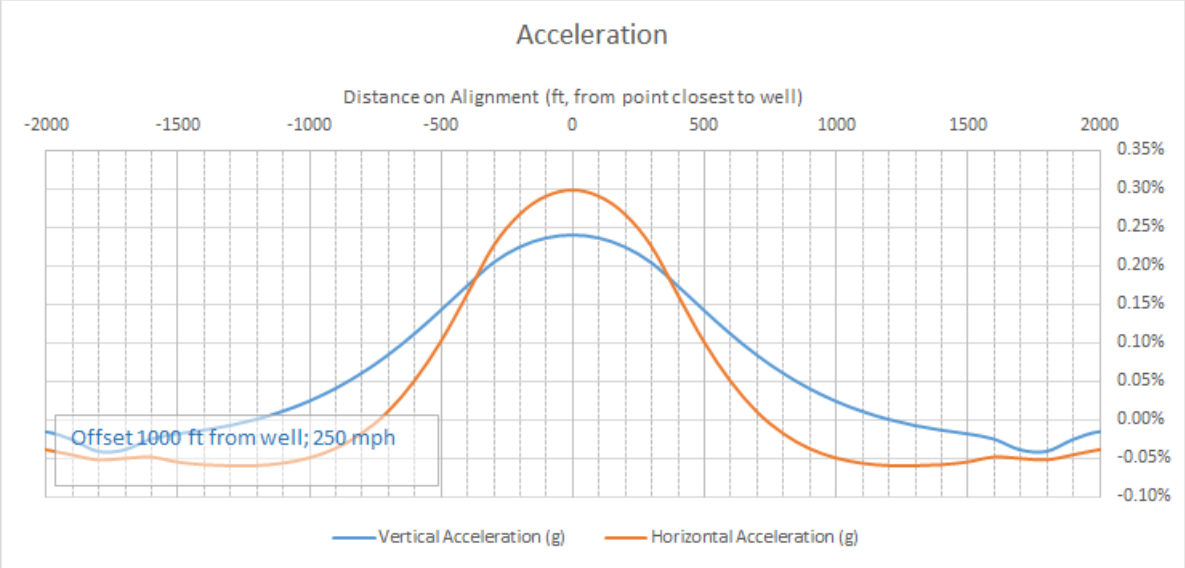

Figure E4-3: Horizontal and vertical acceleration profiles along alignment

The induced changes in vertical or horizontal acceleration are all far less than the allowable limits in the *Design Criteria* (0.05g). In conclusion, we anticipate that unless a large pumping well, screened in the upper aquifer and drawing groundwater down from within this aquifer, is located quite close to the HSR Alignment, the induced curvatures are expected to be relatively

small, with induced accelerations well below the *Design Criteria* limits. The results from parameter/sensitivity analysis support the conclusion.

4.2 ANTELOPE VALLEY HYDROGEOLOGIC MODEL FOR HSR APPLICATION

The USGS recently released the latest version of an Antelope Valley Hydrogeologic Model (AVHM) to evaluate the hydrologic impacts of regional-scale pumping and the resulting subsidence using a 1 km (3,281 ft) spatial resolution (Siade et al., 2014). It is the third model developed by the USGS for the AV. It updated and refined the second USGS model (2003) of the AV by incorporating new hydrogeological data and converting the units into metric system. The AVHM was calibrated to a steady-state condition representative of an average 1915 condition and then the transient conditions for the period from 1915 through 2005.

As described in Saide et al. (2014), the AVHM consists of 130 rows, 118 columns, and 4 layers. Layer 1 represents a shallow portion of the upper aquifer in the Lancaster subbasin coincident with the area of former Lake Thompson. This layer represents a confining unit, which is partially disconnected from the remainder of the upper aquifer system due to the presence of laterally extensive, shallow clay interbeds throughout the region just beneath Layer 1. Layer 2 represents the remainder of the upper aquifer. The bottom elevation of Layer 2 is constant at Elevation 1,950 feet above sea level, except where bedrock is higher. Model Layer 3 represents the middle aquifer. It extends from the base of the upper aquifer to the top of the lower aquifer (Elevation 1,550 ft) at all locations where bedrock is below Elevation 1,550 ft. Layer 4 represents the lower aquifer. It extends from the base of the middle aquifer to the top of the basement complex, or Elevation 1,000 ft if the top of the basement complex is lower. The sediments encountered beneath this elevation are usually older continental deposits. They are anticipated to have negligible yield and are ignored.

Natural recharge is applied along intermittent streams including Littlerock Creek and in the model boundary vicinity. An average of about 30,000 acre-feet per year is applied uniformly to all stress periods. No infiltration of precipitation falling on the valley floor is assumed to occur because the reference evapotranspiration rate is much greater than the estimated average annual precipitation rate. Treated wastewater from reclamation plants is modeled as recharge in the AVHM. Irrigation and urban return flows are simulated in the AVHM with an account of the delays associated with travel time through the unsaturated zone. Irrigation return flows were estimated based on an assumption of 30 percent of the agricultural pumpage. An urban return flow rate of 7.2 inches per year was applied to urban areas. Public water supply and agricultural well locations and pumpage rates were specified annually.

Siade et al. (2014) consider three scenarios of potential future pumping and aquifer recharge conditions over a 50-year period (2006 to 2055), including:

- Scenario 1 - no change in the distribution of pumpage;
- Scenario 2 - redistribution of pumpage; and

- Scenario 3 - artificial recharge.

All three scenarios consider a total pumpage of 110,000 acre-feet per year according to the safe yield value ruled by the Los Angeles County Superior Court of California (Siade et al., 2014). Natural recharge is uniform over the 50-year period using long-term average conditions. The specified head boundaries are held constant. The results from the model were considered in this study.

Modeled future land subsidence is focused in a conical shape several miles wide on the north side of Lancaster. The maximum predicted future subsidence ranges from about 3.2 feet to 2.8 feet for the three modeled scenarios (Plate E3-1). The HSR Alignment passes through the modeled subsidence cone. The steepest portion of the modeled subsidence cone has a change in slope of 1.6 feet in about 1.2 miles (2 kilometers) or about 0.025 percent. That change in slope is about half of the change in slope threshold (about 0.05 to 0.15%) anticipated to initiate earth fissuring.

5.0 PAST SUBSIDENCE MAGNITUDES, RATES & PATTERNS IN ANTELOPE VALLEY

5.1 HISTORICAL REPORTS OF SUBSIDENCE ALONG THE HSR ALIGNMENT IN ANTELOPE VALLEY

The USGS (Siade et al., 2014) has reported subsidence in the northern Antelope Valley from 1930 to 1992 on the order of up to 6.6 feet near Lancaster (and along the HSR Alignment, as shown in Figure E5-1), and up to about 3 feet to the west of Rosamond.

The USGS also simulated this historical subsidence in the calibration of their AVHM. The simulated subsidence values for the period from 1930 through 1951, and in 2005 are shown on Figure E5-2. It is noted that the mapped historical induced changes in slope, and the simulated historical induced changes in slope, appear to be on the order of 0.05 to 0.08 percent (see Figure E5-1 for mapped historical subsidence, and Figure E5-2 for simulated historical subsidence).

Earth fissures, polygonal cracks, and sink-like depressions have been identified and evaluated on Rogers Lake Bed; this playa surface (i.e., dry lake bed) was used as aircraft runways and so the ground has been regularly and carefully monitored (Prince et al., 1995). Holzer (1984) reported an earth fissure about 11 km east-northeast of Lancaster that was first noticed in 1978. These earth fissures developed at a time of significant land subsidence prior to groundwater adjudication. However, we are not aware of any subsidence-induced fissures or faults along or immediately adjacent to the HSR Alignment.

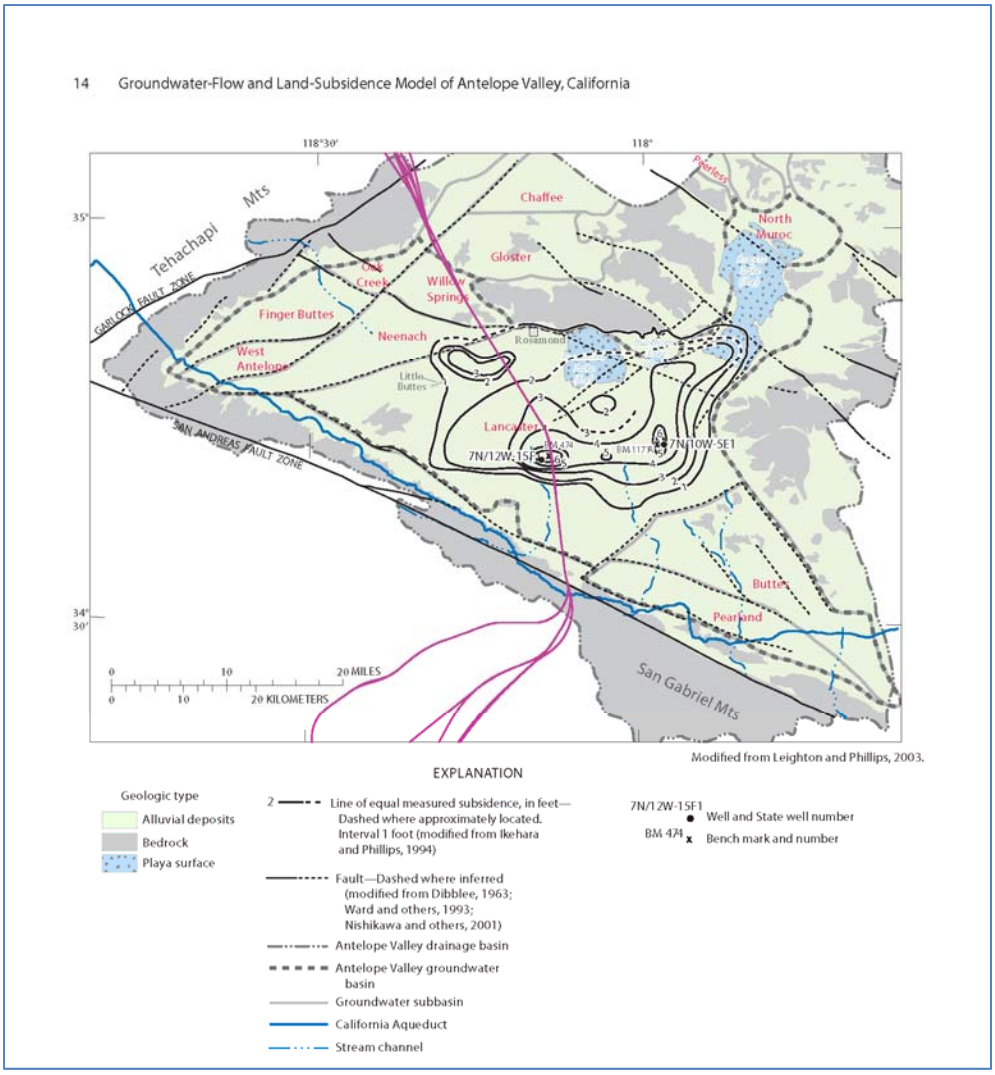

Figure E5-1: Land subsidence contours in the Antelope Valley groundwater basin by measurements, interpoloation, and extrapolation. From Siade et al., 2014.

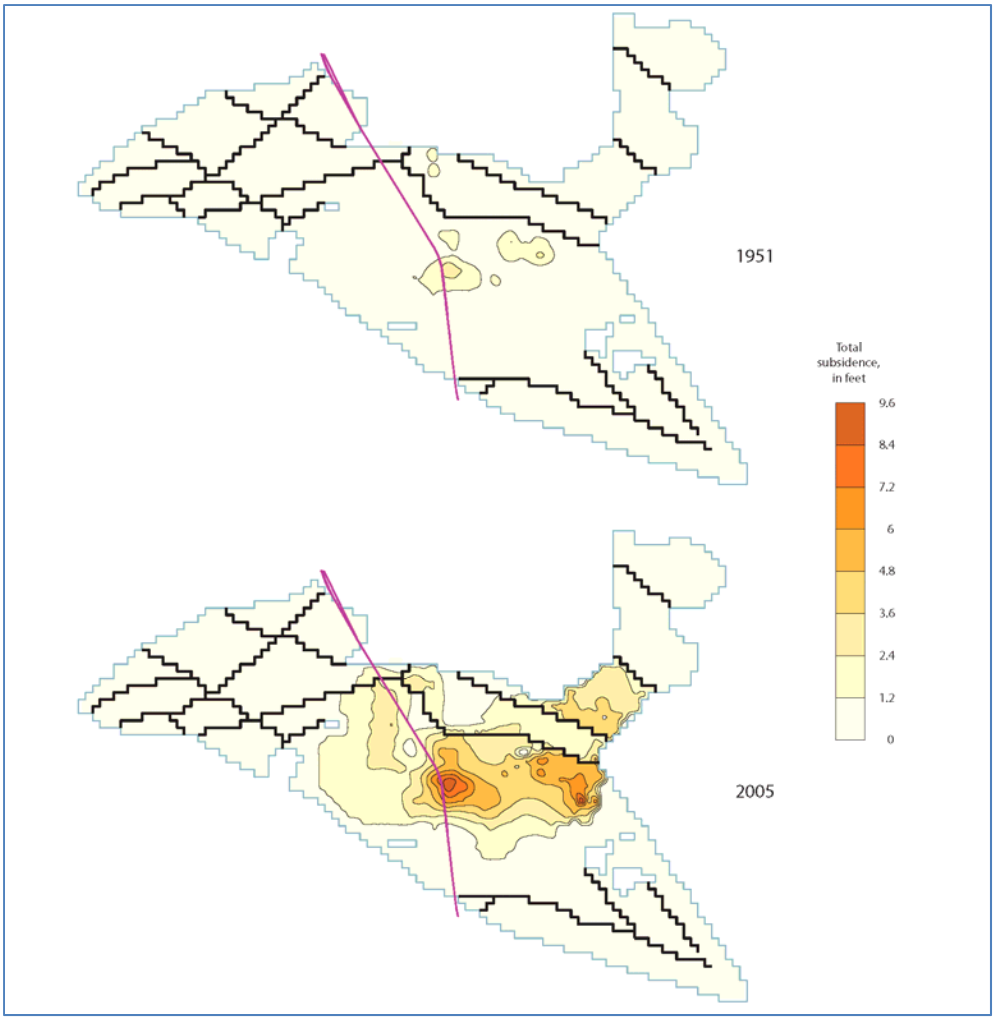

Figure E5-2: Areal distribution of simulated total land subsidence from 1930 to 1951 and 2005 for the Antelope Valley groundwater model. From Siade et al., 2014.

5.2 RECENT SUBSIDENCE ALONG THE HSR ALIGNMENT IN ANTELOPE VALLEY

5.2.1 InSAR Data

In the early 1990s, subsidence appears to have been relatively slow, on the order of an inch per year (see Figure E5-3). It appears that efforts to curtail groundwater drawdown and associated subsidence in this area may have been partially successful, and adjudication in 2011 (Siade et al., 2014) will likely shift groundwater use further toward sustainability (i.e., reduced groundwater drawdown), as will the Sustainable Groundwater Management Act (SGMA) passed by the California Legislature in 2014. Unless future groundwater drawdown increases in the future, based on Siade et al. (2014) we anticipate that future subsidence will also be slower than the rate of 1 inch per year observed in the 1990s.

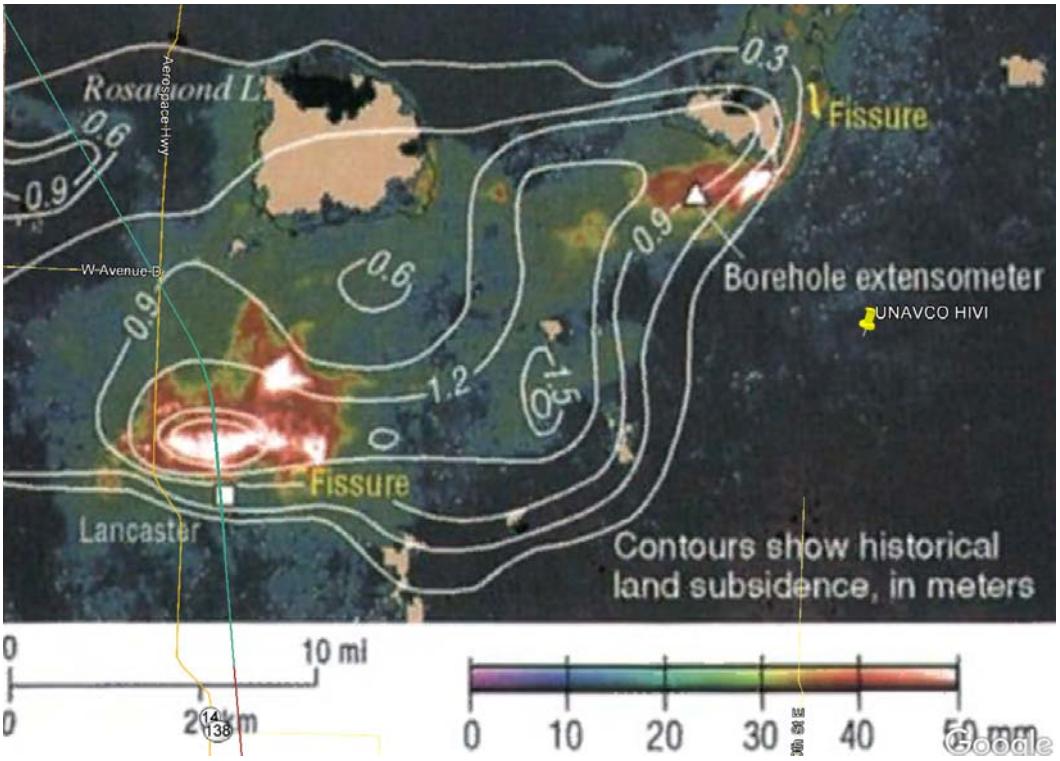

Figure E5-3: InSAR-detected subsidence (October 1993 to December 1995) and historical (1930–92) subsidence (Beige-colored areas signify regions of decorrelation of the radar; black-colored areas signify regions of small-magnitude uplift). From Galloway et al., 2014. Green line is HSR Alignment.

5.2.2 Continuous GPS Data

CGPS recordings are available for nearby stations in the Caltrans Scripps Orbit and Permanent Array Center (SOPAC) and University NAVSTAR Consortium (UNAVCO) networks. These systems are further discussed in Appendix A of the main GSS report. Figure E5-4 shows the locations of four nearby UNAVCO CGPS locations. Figure E5-5 shows a monthly running average of the vertical change readings for each of these four UNAVCO sites; there is up to about 10 to 20 mm of seasonal undulation, but less than about 10 mm in overall trend over the 12 to 17 years of available data. However, it should be noted that these available CGPS locations do not appear to capture the zones of greatest subsidence (i.e., near the center of the subsidence bowl or cone visible in Figures E6-1 through E6-3 above), so these observed trends should not be interpreted to represent the maximum rates within Antelope Valley.

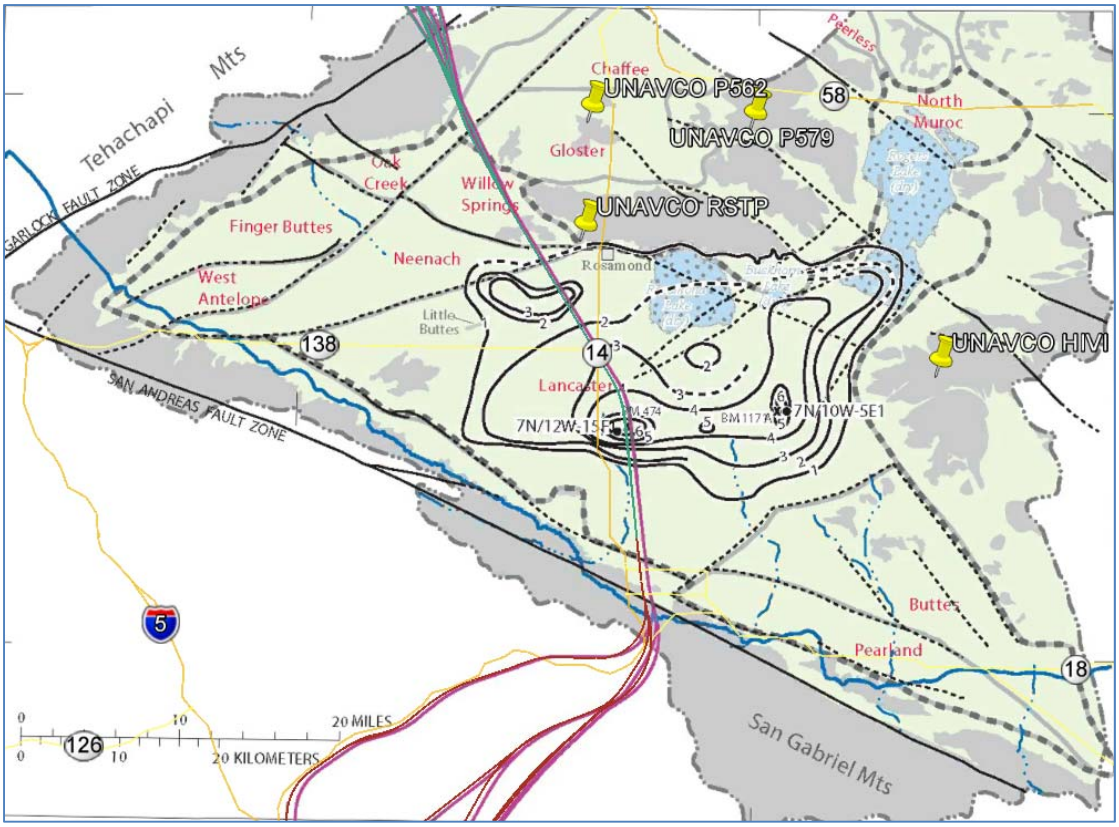

Figure E5-4: Nearby UNAVCO CGPS locations, shown with land subsidence contours in the Antelope Valley groundwater basin by measurements, interpoloation, and extrapolation from Siade et al., 2014.

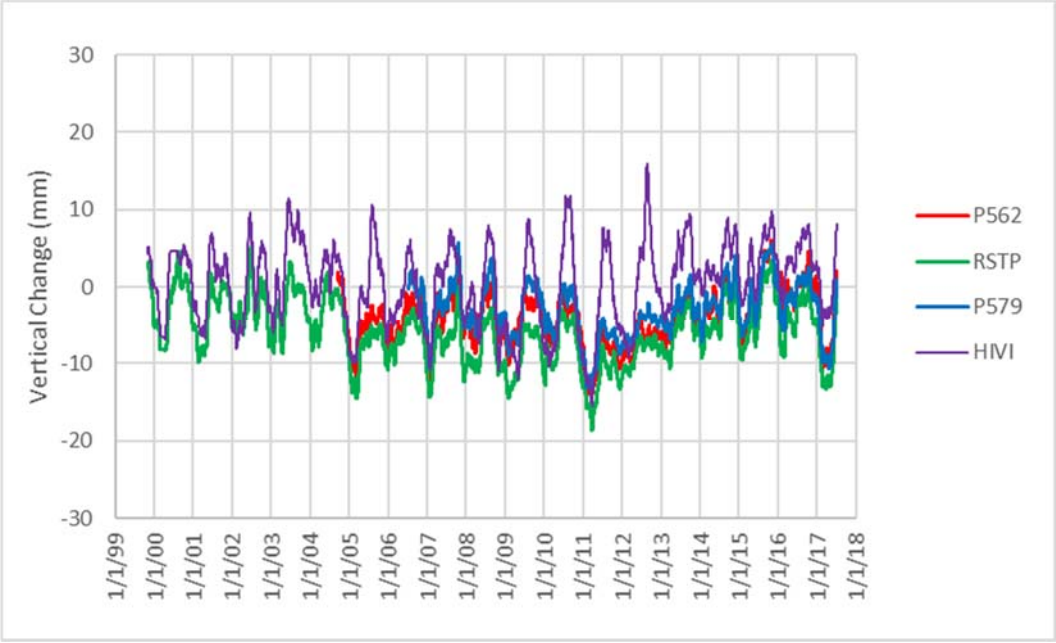

Figure E5-5: UNAVCO CGPS Vertical Monthly Averages

6.0 FORECASTS OF FUTURE SUBSIDENCE

For this GSS, we considered two approaches to estimate forecasts of future subsidence in the AV over a 20-year period. One approach is based on proportionating the forecasts of 50-year subsidence (2005-2055) by the AVHM (Section 6.1) to a 20-year period (i.e., scaling by a factor of 20/50 = 0.4). Another approach is based on subsidence rates estimated from available topographic data (Section 6.2). Along the HSR Alignment, the latter approach results in larger predicted subsidence. It is more conservative and is considered in this study. The changes to the HSR Alignment over this period is discussed in Section 6.2.

6.1 50-YEAR FORECASTS BY THE USGS

Forecasts of subsidence from 2005 through 2055 were made by the USGS (Siade et al., 2014). Three scenarios were prepared, which are presented in Figures E6-1 through E6-3 below, with maximum total forecast subsidence for the three scenarios ranging from about 2.8 to 3.2 feet, which amounts to an average rate of up to about ¾ inch per year.

In the vicinity of the HSR Alignment, the maximum forecast induced changes in slopes are on the order of 0.03 percent in a horizontal direction (i.e., not necessarily in the direction along or perpendicular to the HSR Alignment). It may be noted that this is less than either the mapped or the simulated historical induced changes in slope, which were on the order of 0.05 to 0.08 percent (see Figure E5-1 for mapped historical subsidence, and Figure E5-2 for simulated historical subsidence).

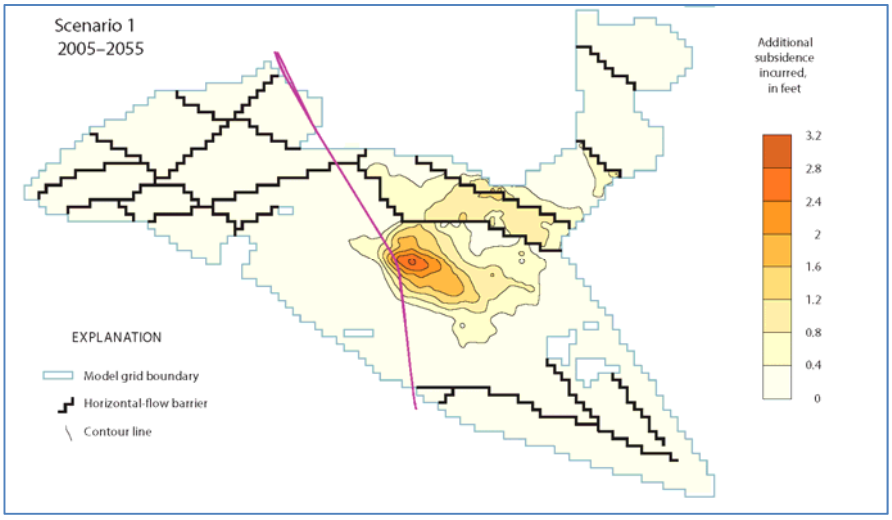

Figure E6-1: Contours of simulated 2005 to 2055 subsidence associated with a spatial and temporal uniform reduction in total groundwater pumpage to 110,000 acre-feet per year (acre-ft/yr) for the Antelope Valley groundwater model, California. After Siade et al., 2014.

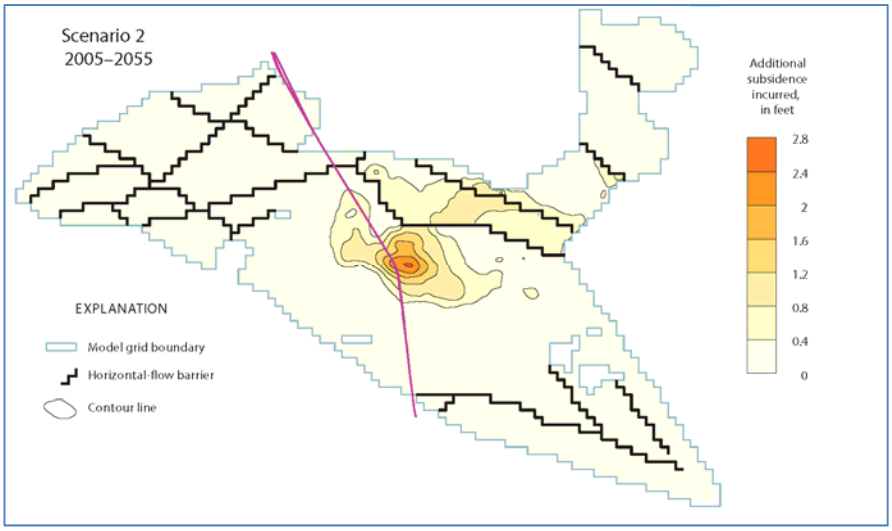

Figure E6-2: Contours of simulated 2005 to 2055 subsidence associated with a redistribution of groundwater pumpage in the Lancaster Subbasin of the Antelope Valley groundwater model, California. After Siade et al., 2014.

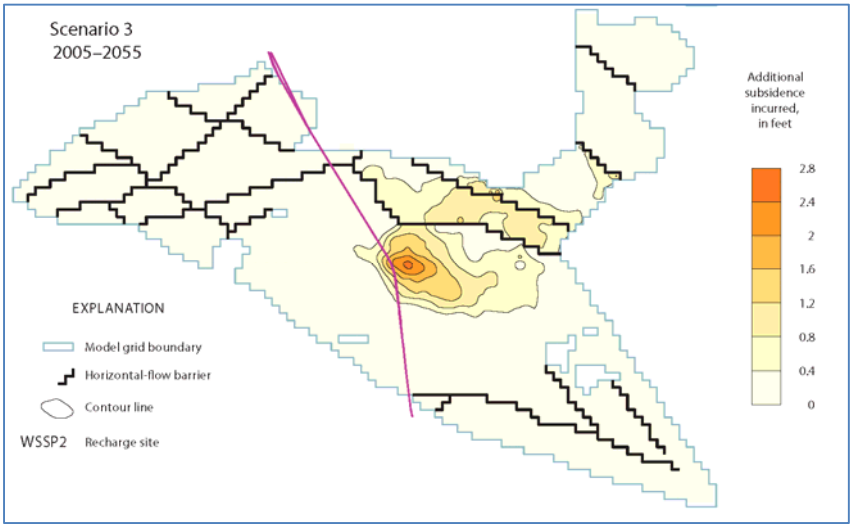

Figure E6-3: Contours of simulated 2055 total additional land subsidence associated with two artificial recharge operations in the Antelope Valley groundwater model; plot shows additional subsidence incurred from 2006 to 2055. After Siade et al., 2014.

6.2 FORECASTING BASED ON COMPARING HISTORICAL AND RECENT TOPOGRAPHIC DATA

The topography shown by the Digital Elevation Model (DEM) provided by USGS originates, according to the topography information of the USGS Quadmaps, from around 1930. The University of California, San Diego (UCSD) conducted a LiDAR survey for the Authority for a 2-

mile-wide strip along the HSR Alignment in 2016. The approximate average rate of subsidence from 1930 (the USGS DEM) to 2016 (the LiDAR data) was calculated as the difference between the 1930 and 2016 elevations, divided by 86 years; this rate was extrapolated forward within the major hydraulic pathways for the hydraulic analysis, which are discussed below in Section 7.2. (We assumed that future ground subsidence over 20 years could be approximated by 0.2 times the amount of ground subsidence between 1930 and 2016.) The resulting maximum subsidence along the HSR Alignment is approximately 2 feet. The subsidence profile along the planned HSR Alignment is shown in Figure E6-4.

This estimated magnitude of forecast ground subsidence was subtracted from the present DEM to compute the estimated future DEM. The elevation profile along the HSR Alignment is shown in Figure E6-5. The elevation changes are marginal and do not seem to affect the overall topography to a significant degree.

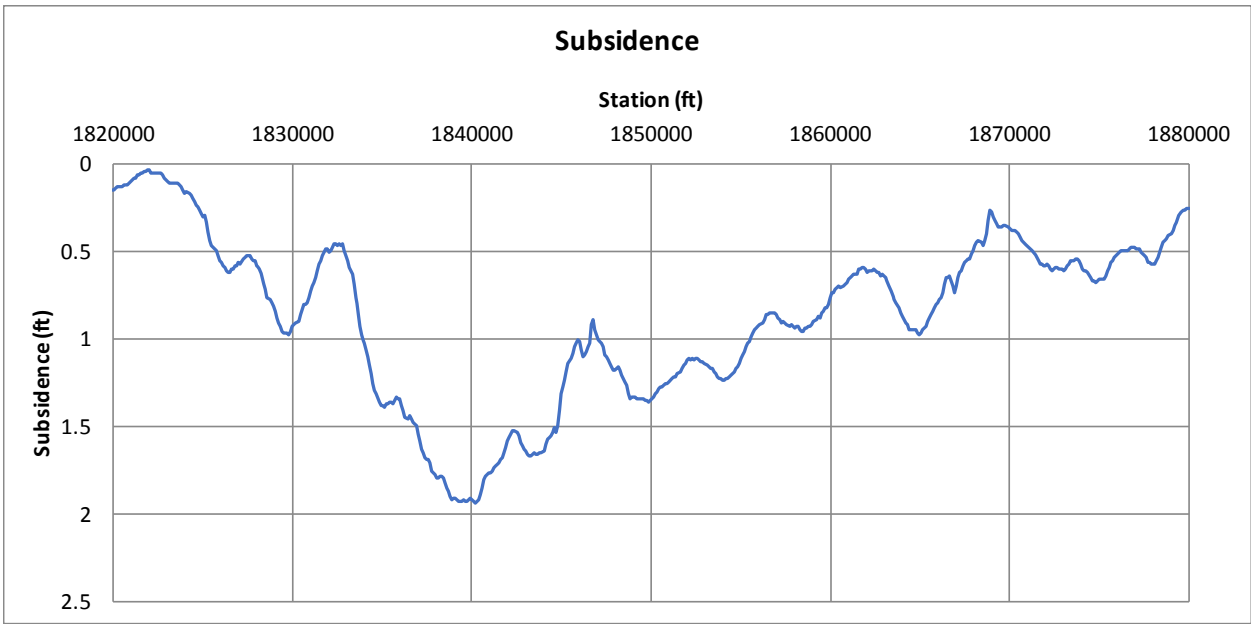

Figure E6-4: Forecast Subsidence Profile, 20 years

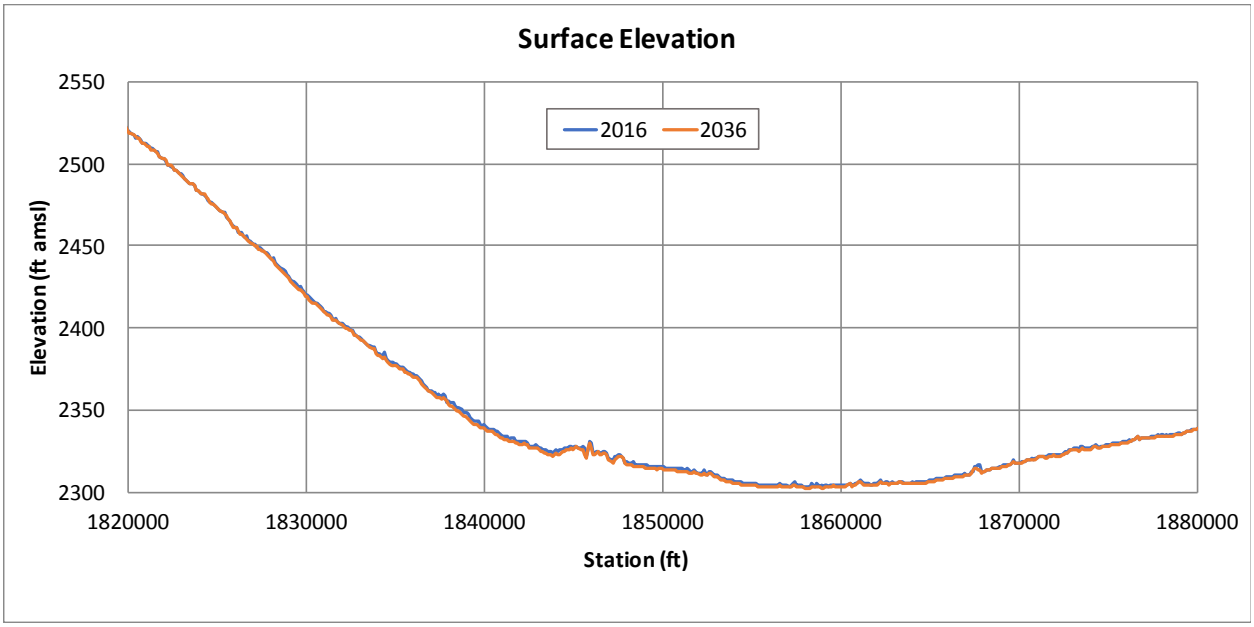

Figure E6-5: Forecast Subsided Profile

6.3 RECOMMENDATIONS FOR FUTURE MONITORING & INSTRUMENTATION

Because forecasts are inherently uncertain, we recommend that future subsidence be monitored. Preliminary and conceptual recommendations for monitoring current and future land subsidence for the project are presented in Sections 8.6.5, 8.6.6, and 10.4 of the body of the GSS report.

GPS survey methods should be utilized to provide reliable and precise elevations at specific points along the project Alignment. Satellite-based InSAR technologies and procedures are rapidly developing and could provide invaluable information regarding rates and patterns of subsidence. The UAVSAR program operated by JPL for DWR (Farr et al., 2015, 2017) is beginning to demonstrate effective corridor subsidence monitoring capabilities. Finally, once the HSR is operational, inertial and other continuous on-train monitoring methods should be implemented and utilized to provide critical information concerning changing track geometries resulting from continuing subsidence.

7.0 POTENTIAL IMPACTS TO HSR SYSTEM

7.1 TECHNICAL CONSIDERATIONS

There are several ways in which subsidence could adversely impact the HSR. Each has been evaluated as discussed in the main body of the GSS report. In general, because in Antelope Valley the subsidence, differential subsidence, and changes in slope and curvature are expected to be significantly less than in the Corcoran Subsidence Bowl, potential impacts to the HSR system are anticipated to also be significantly less. In addition, there are no significant

floodwater storage feature floodplains along the HSR Alignment in Antelope Valley, so any future subsidence is not expected to have a significant adverse impact on flood hazards along the HSR Alignment.

7.2 SUBSIDENCE-INDUCED CHANGES TO FLOODPLAINS

We examined the HSR Alignment in regard to its proximity to (1) the forecasted subsidence is relatively larger (Section 6) and (2) the floodplains delineated on FEMA floodplain map. This comprises the some areas of interest (AOI) along the HSR Alignment crossing of the valley.

We used the ArcHydro package on ESRI's ArcGIS platform to delineate the predominant drainage network within the AOI presently and in the future. Figure E7-1 shows the present and future drainage networks delineated by ArcHydro. Small changes in drainage paths are observed in the two major floodplains crossing the HSR Alignment in the AV, but do not indicate a change of the overall floodplain delineation. The changes in the smaller southern floodplain crossing the HSR Alignment were evaluated in a higher DEM resolution as shown on Figure E7-2.

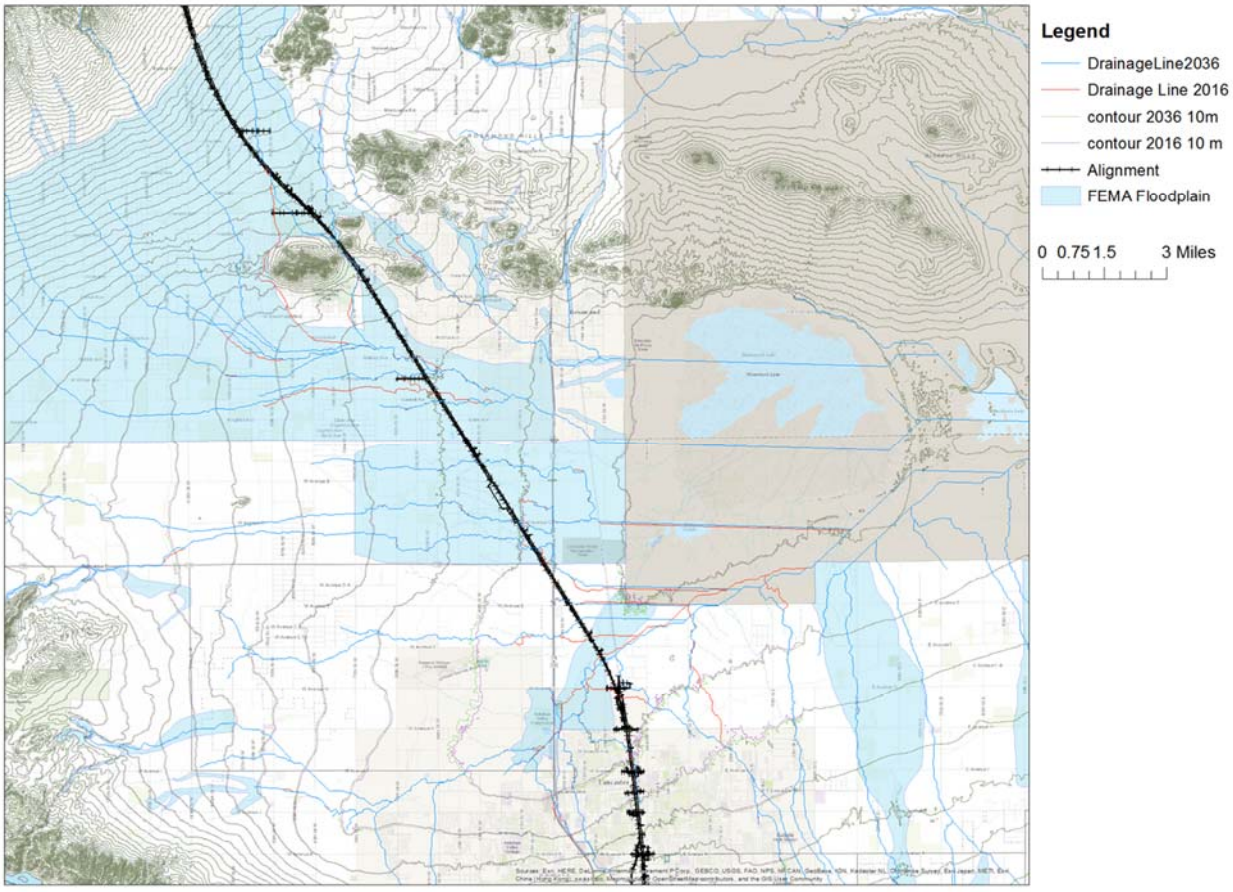

Figure E7-1: Drainage characteristics delineated by ArcHydro

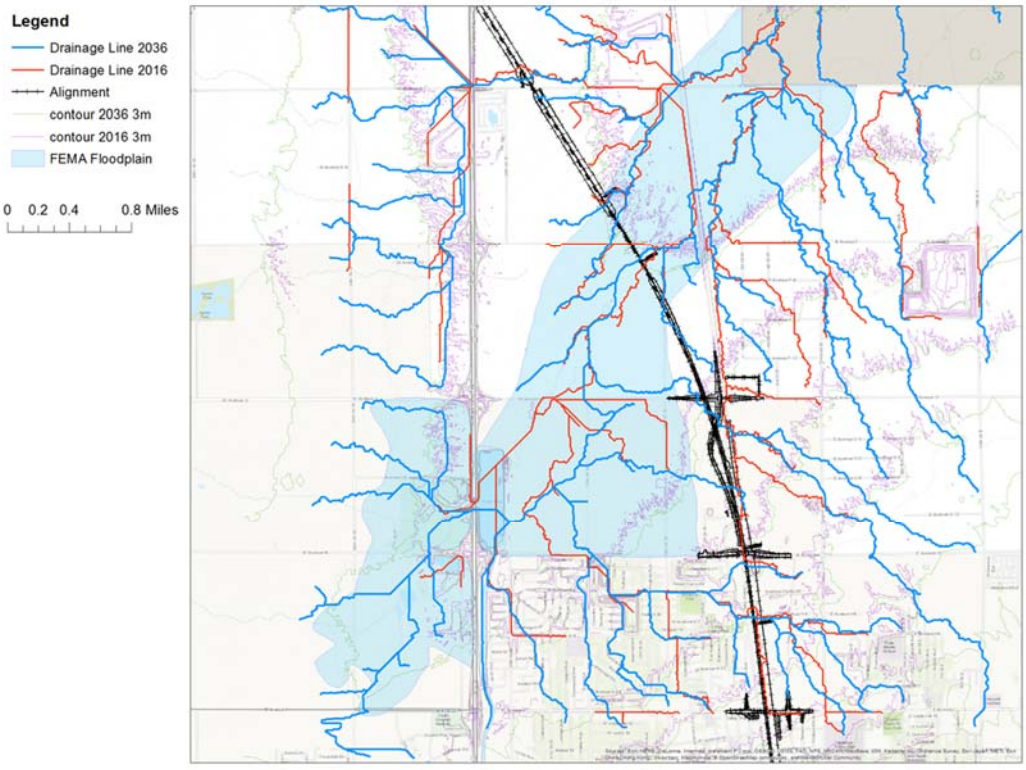

Figure E7-2: Drainage characteristics delineated by ArcHydro in southern floodplain

One section was developed along the major drainage pathway in the southern floodplain to evaluate the potential slope changes. The location of the section is shown on Figure E7-3. The USGS DEM was used as a reference; because the projected subsidence between 2016 and 2036 is small, the results of the analysis will not be highly sensitive to potential imprecision in the reference elevations and topography of the USGS DEM. The percentage change in the averaged projected slope is expected to decrease by around 15%, potentially slowing down the flood water by around 8%.

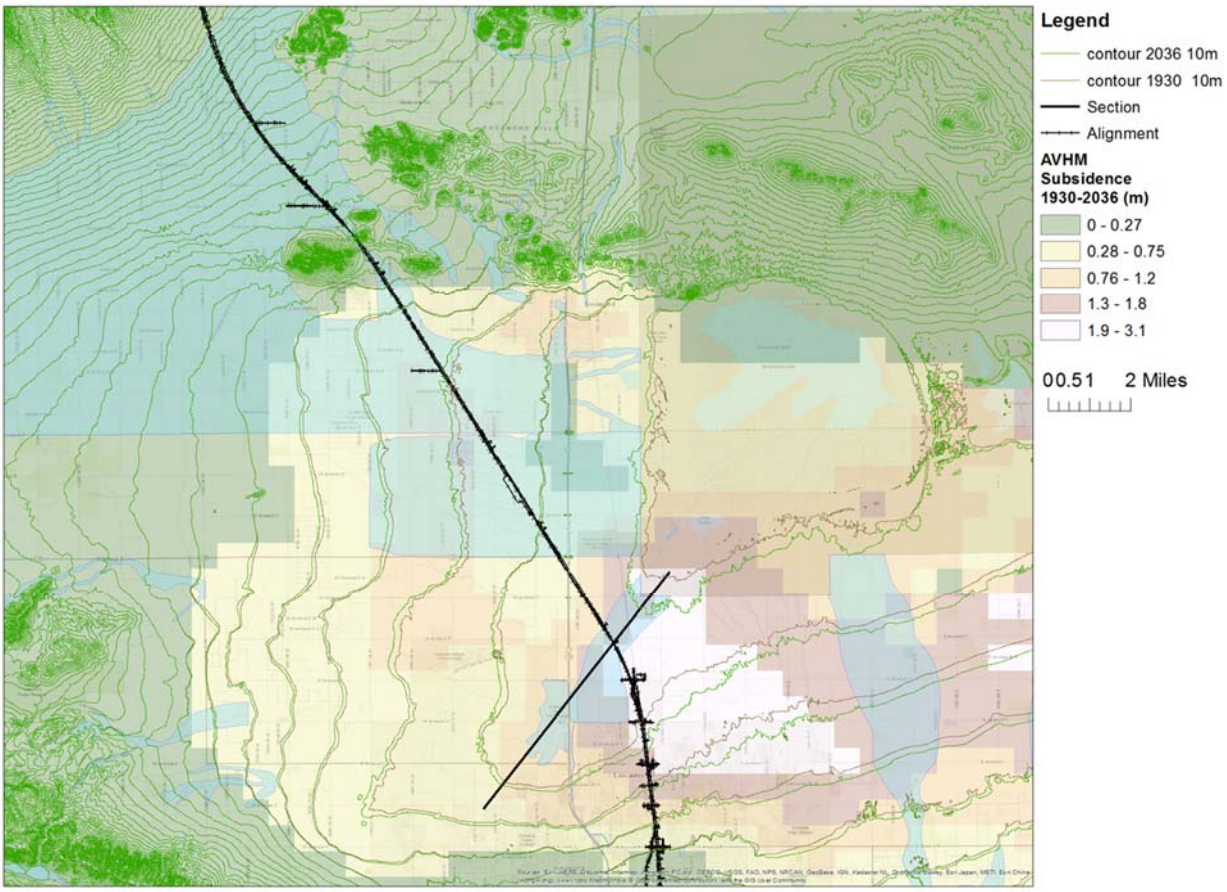

Figure E7-3: Location of examined slope

Although the forecast subsidence in the Antelope Valley is noticeable, the impacts on the HSR are expected to be relatively small. According to our analysis, the drainage pathways are not expected to change significantly. In addition, the floodplains close to the HSR Alignment are not flood water storage features, but only areas along major runoff pathways, so the sensitivity of floodplains to the elevation changes is expected to be relatively small.

8.0 REMAINING UNCERTAINTIES

There are remaining uncertainties along the HSR Alignment in the Antelope Valley. Most are similar to the uncertainties in the SJV:

- Paucity of Quantitative Data for Localized Differential Subsidence.
- Uncertainties within the AVHM Hydrogeological Data & Model.
- Uncertainties Regarding Future Groundwater Drawdown.

8.1 POTENTIAL FOR SUBSIDENCE-INDUCED FISSURES & COMPACTION FAULTS?

Potential for subsidence-induced compaction faults or earth fissures are anticipated to be lower in the Antelope Valley than in the Corcoran Subsidence Bowl, to a large extent because subsidence rates in the Antelope Valley are much slower and forecast magnitudes are much lower.

Relevant potential subsidence rates and magnitudes are presented by Siade et al. (2014) for three future groundwater utilization scenarios, with modeled resulting land subsidence, for the time period of 2005 to 2055. Modeled land subsidence is focused in a conical shape several miles wide on the north side of Lancaster. The maximum subsidence ranges from about 3.2 feet to 2.8 feet for the three modeled scenarios (Plate E3-1). The HSR Alignment passes through the modeled subsidence cone. The steepest portion of the modeled subsidence cone has a change in slope of 1.6 feet in about 1.2 miles (2 kilometers) or about 0.025 percent. That change in slope is about half of the change in slope threshold (about 0.05 to 0.15%) anticipated to initiate earth fissuring.

8.2 OTHER SUBSIDENCE MECHANISMS

Although this ground subsidence study (GSS) has focused on subsidence induced by groundwater extraction, other forms of subsidence may be present within the SJV, as discussed in the main body of the GSS report. The way each other mechanism relates to the El Nido area is described as follows.

8.2.1 Hydrocompaction

Wind-deposited or debris-flow soils that could be highly susceptible to hydrocompaction are not expected to be present along the HSR Alignment within Antelope Valley. However, the potential for hydrocompaction of dry soils should be addressed by each Design-Build Contractor.

8.2.2 Oil and Gas Extraction

Subsidence due to extraction of oil and gas is not expected along the HSR Aligment within Antelope Valley. Review of the California DOGGR (2017) website indicates that there has been minimal historical oil and gas exploration in Antelope Valley. Only a few historical oil or gas wildcat wells are reported to have been drilled within a few miles of the HSR Alignment, and no concentrated drilling activity is indicated on the DOGGR website in the vicinity of the Alignment.

8.2.3 Tectonic Subsidence

Tectonic fault offset could affect the HSR Alignment at the north edge of the Antelope Valley (at the Garlock Fault crossing) and the southwest edge the Antelope Valley (at the of San Andreas Fault crossing). A portion of future fault offset could be vertical, which could result in “tectonic subsidence.” However, a fault displacement hazard study is being performed under a separate contract to the Authority, and this topic is not further addressed in this GSS.

8.2.4 Organic Soils and Peat

Peat and other organic soils are not expected to be present along the HSR Alignment within Antelope Valley. However, the design-build contractors should evaluate the possibility of their presence, particularly near river crossings, ponds, or marshy areas, and develop recommendations to mitigate any potential hazards that if they are identified.

9.0 INSTRUMENTATION AND MONITORING OPTIONS

In general, the approach to instrumentation and monitoring should follow an approach similar to what will be implemented in the Corcoran Subsidence Bowl area. Specific recommendations for Antelope Valley are presented in Section 10.0 below.

Relevant portions of the network of benchmarks used to calibrate the SIR 2014-5166 modeling effort (Figure 11, Siade et al., 2014) may serve as an initial reference for subsidence monitoring along the HSR Alignment; we suggest that subsidence monitoring for the HSR be coordinated with any ongoing subsidence monitoring that may be continuing in the Antelope Valley.

10.0 EVALUATIONS AND RECOMMENDATIONS

In most locations, subsidence is not expected to cause a significant impact to the HSR performance. The induced change to the flood and erosion conditions already present along the HSR Alignment is anticipated to be minimal. However, several potential risks remain, and therefore our recommendations for the following are similar to those for the Corcoran Subsidence Bowl as described in the main body of the GSS report:

- Subsidence-Induced Curvature, Faults, and Fissures (see Section 10.1 of the main GSS report).
- Monitoring & Maintenance Approach (see Section 10.3 of the main GSS report).

11.0 CLOSURE

This appendix report was prepared by the staff of Amec Foster Wheeler and our subconsultant GSI Environmental Inc., under the supervision of the engineers whose signatures appear hereon. We trust that this report meets the current project needs. If you have any questions or require additional information, please contact Jim French of Amec Foster Wheeler.

12.0 ADDITIONAL REFERENCES

California Department of Water Resources (DWR), 2017. Water Data Library. Accessed at http://www.water.ca .gov/waterdatalibrary/ on July 10, 2017.

DWR: See California Department of Water Resources.

Galloway, D. L., Hudnut, K. W., Ingebritsen, S. E., Phillips, S. P., Peltzer, G., Rogez, and Rosen, P. A., 1998. "Detection of aquifer system compaction and land subsidence using interferometric synthetic aperture radar, Antelope Valley, Mojave Desert, California." *Water Resources Research, Vol. 34, No. 10*, pages 2573-2585. October.

Prince, K.R., Galloway, D.L., Leake, S.A., editors, 1995. U.S. Geological Survey Subsidence Interest Group Conference, Edwards Air Force base, Antelope Valley, California, November 18-19, 1992: Abstracts and Summary, U.S. Geological Survey Open-File Report 94-532.

Siade, Adam J., Nishikawa, Tracy, Rewis, Diane L., Martin, Peter, and Phillips, Steven P., 2014. *Groundwater-Flow and Land-Subsidence Model of Antelope Valley, California.* Prepared by the U.S. Geological Survey in cooperation with the Los Angeles County Department of Public Works, Antelope Valley-East Kern Water Agency, Palmdale Water District, and Edwards Air Force Base. Scientific Investigations Report 2014–5166.

HSR Alignment fault crossing, minimal differential subsidence potential

HSR Alignment fault crossing, differential subsidence potential *if* large future groundwater pumping

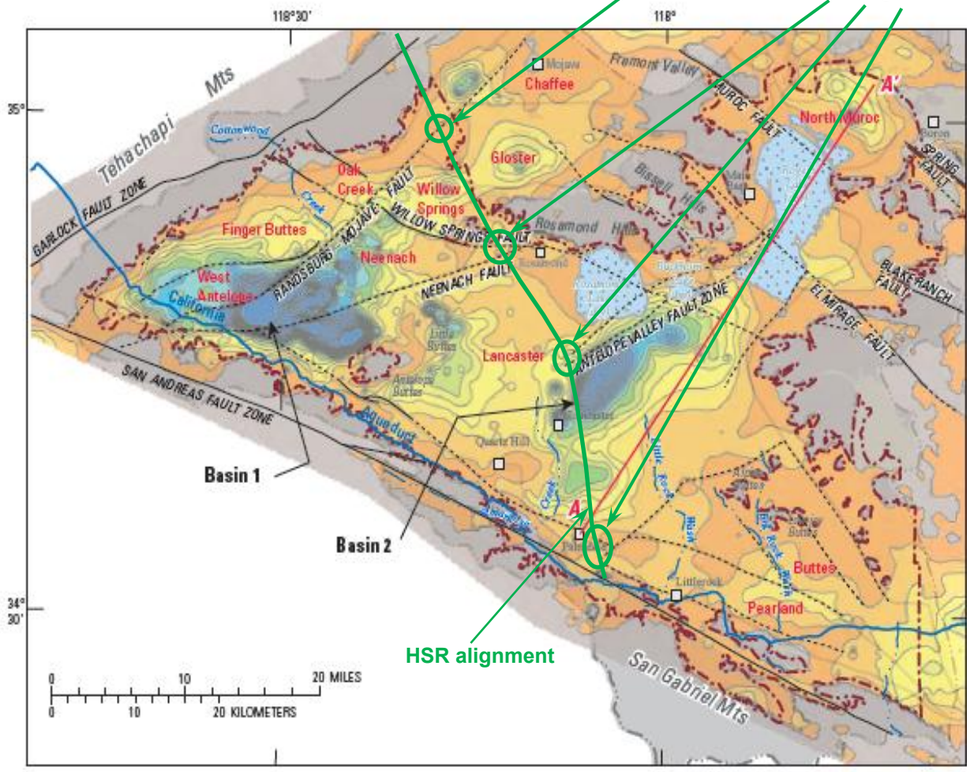

EXPLANATION

Geologic type
- Alluvial deposits
- Bedrock
- Playa surface

- Fault—Dashed where inferred (modified from Dibblee, 1963; Ward and others, 1993; Nishikawa and others, 2001)
- Antelope Valley drainage basin
- Antelope Valley adjudicated basin
- A — A' Line of section
- Pearland — Groundwater subbasin and name

Depth to basement, in feet
−1
−501
−1001
−1501
−2001
−2501
−3001
−3501
−4001
−4501
−5001

Summary of relevant basin hydro-geology - depth of alluvium, groundwater basins and sub-basin bounding faults in relation to HSR alignment

Figure 4. Depth to the basement complex below land surface, derived from gravity data for the Antelope Valley groundwater basin and surrounding area, California. Since the basement complex probably does not transmit groundwater, this map describes the likely extent and depth of the aquifer system. ***from Siade and others (2014), SIR 2014-5166 p 8.***

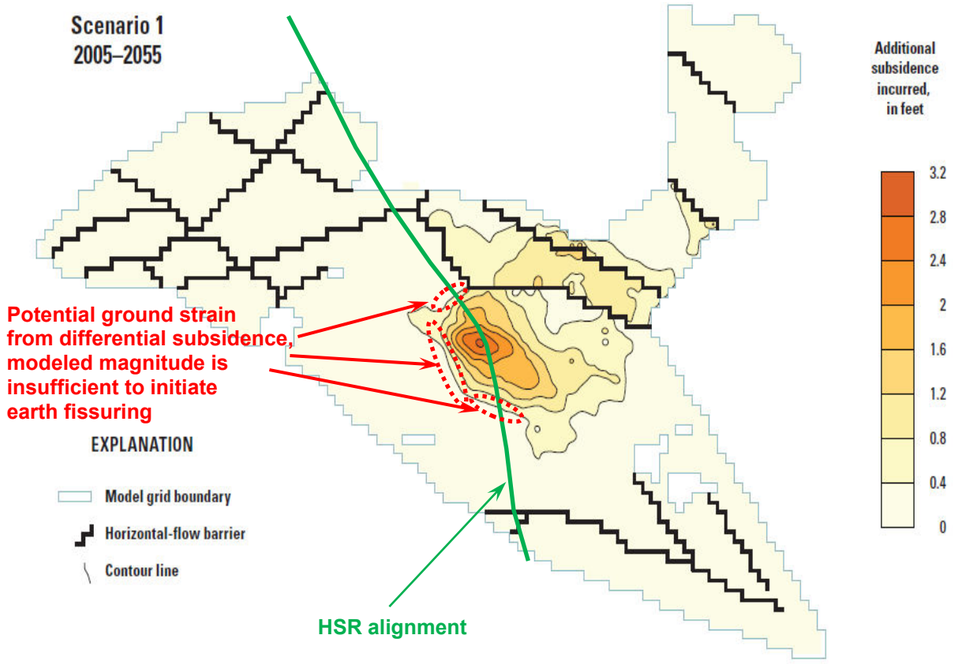

Additional land subsidence associated with a spatial and temporal uniform reduction in total groundwater pumpage to 110,000 acre-feet per year (acre-ft/yr) for the Antelope Valley groundwater model, California. Note that the subsidence illustrated in this plot represents additional subsidence incurred from 2006 to 2055. From Siade et al. (2014), SIR 2014-5166, p. 78 (Figure 46).

Summary of modeled future subsidence in adjudicated basin, in relation to HSR alignment

HSR Ground Subsidence Study
California

SUB-BASINS, FAULTS, DEPTH TO BEDROCK AND MODELED FUTURE SUBSIDENCE, ANTELOPE VALLEY

PLATE
E3-1

Project 8715180680
PM : JF BY: MLR
Date 7/11/2017
Scale : n/a

amec foster wheeler